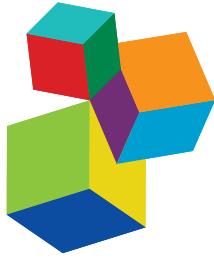


EXPLORING THE FRONTIERS OF REGENERATIVE CARDIOVASCULAR MEDICINE

EDITED BY: Joshua D. Hutcheson, Julie A. Phillippi and Elena Aikawa
PUBLISHED IN: *Frontiers in Cardiovascular Medicine*





frontiers

Frontiers Copyright Statement

© Copyright 2007-2019 Frontiers Media SA. All rights reserved.

All content included on this site, such as text, graphics, logos, button icons, images, video/audio clips, downloads, data compilations and software, is the property of or is licensed to Frontiers Media SA ("Frontiers") or its licensees and/or subcontractors. The copyright in the text of individual articles is the property of their respective authors, subject to a license granted to Frontiers.

The compilation of articles constituting this e-book, wherever published, as well as the compilation of all other content on this site, is the exclusive property of Frontiers. For the conditions for downloading and copying of e-books from Frontiers' website, please see the Terms for Website Use. If purchasing Frontiers e-books from other websites or sources, the conditions of the website concerned apply.

Images and graphics not forming part of user-contributed materials may not be downloaded or copied without permission.

Individual articles may be downloaded and reproduced in accordance with the principles of the CC-BY licence subject to any copyright or other notices. They may not be re-sold as an e-book.

As author or other contributor you grant a CC-BY licence to others to reproduce your articles, including any graphics and third-party materials supplied by you, in accordance with the Conditions for Website Use and subject to any copyright notices which you include in connection with your articles and materials.

All copyright, and all rights therein, are protected by national and international copyright laws.

The above represents a summary only. For the full conditions see the Conditions for Authors and the Conditions for Website Use.

ISSN 1664-8714
ISBN 978-2-88945-818-9
DOI 10.3389/978-2-88945-818-9

About Frontiers

Frontiers is more than just an open-access publisher of scholarly articles: it is a pioneering approach to the world of academia, radically improving the way scholarly research is managed. The grand vision of Frontiers is a world where all people have an equal opportunity to seek, share and generate knowledge. Frontiers provides immediate and permanent online open access to all its publications, but this alone is not enough to realize our grand goals.

Frontiers Journal Series

The Frontiers Journal Series is a multi-tier and interdisciplinary set of open-access, online journals, promising a paradigm shift from the current review, selection and dissemination processes in academic publishing. All Frontiers journals are driven by researchers for researchers; therefore, they constitute a service to the scholarly community. At the same time, the Frontiers Journal Series operates on a revolutionary invention, the tiered publishing system, initially addressing specific communities of scholars, and gradually climbing up to broader public understanding, thus serving the interests of the lay society, too.

Dedication to Quality

Each Frontiers article is a landmark of the highest quality, thanks to genuinely collaborative interactions between authors and review editors, who include some of the world's best academicians. Research must be certified by peers before entering a stream of knowledge that may eventually reach the public - and shape society; therefore, Frontiers only applies the most rigorous and unbiased reviews.

Frontiers revolutionizes research publishing by freely delivering the most outstanding research, evaluated with no bias from both the academic and social point of view. By applying the most advanced information technologies, Frontiers is catapulting scholarly publishing into a new generation.

What are Frontiers Research Topics?

Frontiers Research Topics are very popular trademarks of the Frontiers Journals Series: they are collections of at least ten articles, all centered on a particular subject. With their unique mix of varied contributions from Original Research to Review Articles, Frontiers Research Topics unify the most influential researchers, the latest key findings and historical advances in a hot research area! Find out more on how to host your own Frontiers Research Topic or contribute to one as an author by contacting the Frontiers Editorial Office: researchtopics@frontiersin.org

EXPLORING THE FRONTIERS OF REGENERATIVE CARDIOVASCULAR MEDICINE

Topic Editors:

Joshua D. Hutcheson, Florida International University, United States

Julie A. Phillippi, University of Pittsburgh, United States

Elena Aikawa, Brigham and Women's Hospital, United States



Christiaan Barnard, the surgeon who performed the first heart transplant, shown with a small child.

Courtesy of the Chris Barnard Division of Cardiothoracic Surgery, University of Cape Town.

This Research Topic celebrates the 50th anniversary of the first heart transplant performed in December of 1967 in Cape Town, South Africa. Cardiovascular researchers met in South Africa in December 2017 to commemorate this event, presenting an opportune time to reflect on the achievements of applied cardiovascular research and highlight forthcoming technology developments that will shape the future of cardiovascular medicine. The clinical breakthrough in 1967 offered hope to many patients suffering with cardiac complications, and these life-saving surgeries continue

to have a tremendous impact. Tissue shortages, surgical risks, and complications due to improper host-transplant tissue interactions, however, limit the utility of heart transplants to the most severe cases of cardiac morbidity. Recent advances have yielded mechanistic insight into the factors that control cardiovascular tissue maintenance and remodeling. The field of regenerative medicine seeks to control these factors to promote in situ tissue regeneration or engineered tissue replacement. These exciting new technologies could lead to a renaissance in the treatment of many cardiovascular diseases, just as the realization of heart transplantation 50 years ago. In this Research Topic, researchers and clinicians from regenerative medicine and applied cardiovascular biology provide literature reviews and original manuscripts to demonstrate the trajectory of cardiovascular medicine. The contributions vertically integrate advances by clinicians, engineers, and basic scientists, all researching similar topics from different angles and with complementary perspectives. Taken together, these contributions demonstrate the process of applied cardiovascular research from basic science discoveries to implementation in clinical practice.

Citation: Hutcheson, J. D., Phillippi, J. A., Aikawa, E., eds. (2019). Exploring the Frontiers of Regenerative Cardiovascular Medicine. Lausanne: Frontiers Media. doi: 10.3389/978-2-88945-818-9

Table of Contents

SECTION 1

RESEARCH TOPIC OVERVIEW

- 06** *Editorial: Exploring the Frontiers of Regenerative Cardiovascular Medicine*
Julie A. Phillippi, Elena Aikawa and Josh Hutcheson
- 11** *After 50 Years of Heart Transplants: What Does the Next 50 Years Hold for Cardiovascular Medicine? A Perspective From the International Society for Applied Cardiovascular Biology*
Joshua D. Hutcheson, Craig J. Goergen, Frederick J. Schoen, Masanori Aikawa, Peter Zilla, Elena Aikawa and Glenn R. Gaudette

SECTION 2

CARDIAC REGENERATION

- 21** *Using Acellular Bioactive Extracellular Matrix Scaffolds to Enhance Endogenous Cardiac Repair*
Danyil A. Svystonyuk, Holly E. M. Mewhort and Paul W. M. Fedak
- 29** *Development of a Contractile Cardiac Fiber From Pluripotent Stem Cell Derived Cardiomyocytes*
Katrina J. Hansen, Michael A. Laflamme and Glenn R. Gaudette

SECTION 3

HEART VALVE DISEASE AND REGENERATION

- 40** *Sheep-Specific Immunohistochemical Panel for the Evaluation of Regenerative and Inflammatory Processes in Tissue-Engineered Heart Valves*
Sylvia Dekker, Daphne van Geemen, Antoon J. van den Bogaardt, Anita Driessen-Mol, Elena Aikawa and Anthal I. P. M. Smits
- 59** *Stem Cell Cytoskeletal Responses to Pulsatile Flow in Heart Valve Tissue Engineering Studies*
Glenda Castellanos, Sana Nasim, Denise M. Almora, Sasmita Rath and Sharan Ramaswamy
- 68** *Mechanotransduction Mechanisms in Mitral Valve Physiology and Disease Pathogenesis*
Leah A. Pagnozzi and Jonathan T. Butcher
- 82** *Cell Sources for Tissue Engineering Strategies to Treat Calcific Valve Disease*
Eva Jover, Marco Fagnano, Gianni Angelini and Paolo Madeddu
- 109** *Can we Grow Valves Inside the Heart? Perspective on Material-Based in Situ Heart Valve Tissue Engineering*
Carlijn V. C. Bouten, Anthal I. P. M. Smits and Frank P. T. Baaijens

SECTION 4

VASCULAR REMODELING AND REGENERATION

- 119** *Case Study: Intra-Patient Heterogeneity of Aneurysmal Tissue Properties*
Giampaolo Martufi, Arianna Forneris, Samaneh Nobakht, Kristina D. Rinker, Randy D. Moore and Elena S. Di Martino

129 *Medial Hypoxia and Adventitial Vasa Vasorum Remodeling in Human Ascending Aortic Aneurysm*

Marie Billaud, Jennifer C. Hill, Tara D. Richards, Thomas G. Gleason and Julie A. Phillippi

144 *Cell Phenotype Transitions in Cardiovascular Calcification*

Luis Hortells, Swastika Sur and Cynthia St. Hilaire

153 *Future Perspectives on the Role of Stem Cells and Extracellular Vesicles in Vascular Tissue Regeneration*

Eoghan M. Cunnane, Justin S. Weinbaum, Fergal J. O'Brien and David A. Vorp



Editorial: Exploring the Frontiers of Regenerative Cardiovascular Medicine

Julie A. Phillippi¹, Elena Aikawa^{2*} and Josh Hutcheson³

¹ Departments of Cardiothoracic Surgery and Bioengineering, University of Pittsburgh, Pittsburgh, PA, United States,

² Brigham and Women's Hospital, Harvard Medical School, Boston, MA, United States, ³ Florida International University, Miami, FL, United States

Keywords: cardiovascular disease, regenerative medicine, calcific aortic valve, cardiovascular calcification, aneurysm, stem cells, extracellular matrix

Editorial on the Research Topic

Exploring the Frontiers of Regenerative Cardiovascular Medicine

In this special issue of Frontiers in Cardiovascular Medicine, we assembled a collection of original research articles (4), reviews (6), a case report and a perspective within an over-arching theme of “Exploring the Frontiers of Regenerative Cardiovascular Medicine.” This collection of work engaged multiple disciplines. From this set of articles, we identified two emerging themes representing current knowledge and active progress within research domains related to regenerative medicine in the cardiovascular space. The first theme explores recent basic science efforts in uncovering new disease mechanisms, addresses challenges of working in human pathologic tissue and cell culture models and identifies novel theories in cardiovascular pathophysiology. The second theme encompasses recent translational strides. In this issue, a perspective article from investigators of the International Society for Applied Cardiovascular Biology (ISACB) by Hutcheson et al. details significant progress in applying cardiovascular biology in translational directions. A comprehensive retrospective first takes us through the work of international experts since the first human heart transplant in Cape Town, South Africa. This benchmark event in 1967 was commemorated 20 years later when this society was born and then 50 years later in 2017 when scientists reconvened in Cape Town for a celebration and international convention on cardiovascular disease. Motivated by the topics discussed at this commemorative assembly, this comprehensive perspective takes us through the past 50 years, highlighting the pioneering and innovative efforts of the scientific community of clinician, engineer, biologist and industry thought leaders to meet the critical needs of yesterday through interdisciplinary and international cooperation and to address today's unmet clinical needs for patients with cardiovascular disease. This published Research Topic represents a curated collection of articles that uniquely attack cardiovascular disease from multiple directions, and uniformly embrace a reaffirmed interdisciplinary mission to understand and treat cardiovascular disease through regenerative medicine.

OPEN ACCESS

Edited and reviewed by:

Paul H. A. Quax,
Leiden University, Netherlands

*Correspondence:

Elena Aikawa
eaikawa@bwh.harvard.edu

Specialty section:

This article was submitted to
Atherosclerosis and Vascular
Medicine,
a section of the journal
Frontiers in Cardiovascular Medicine

Received: 28 January 2019

Accepted: 06 February 2019

Published: 26 February 2019

Citation:

Phillippi JA, Aikawa E and
Hutcheson J (2019) Editorial:
Exploring the Frontiers of Regenerative
Cardiovascular Medicine.
Front. Cardiovasc. Med. 6:13.
doi: 10.3389/fcvm.2019.00013

ON THE BASIC SCIENCE FRONT: CARDIOVASCULAR DISEASE MECHANISMS AND MODEL SYSTEMS

In abdominal aortic aneurysm (AAA), an inflammatory process drives medial degeneration, whereas in the ascending thoracic aorta, non-inflammatory smooth muscle cell loss accompanies

accumulation of proteoglycans amidst elastin fragmentation (1). Martufi et al. authored a case report detailing the intra-patient heterogeneity in simulated wall stress and histopathological features of an unruptured aneurysmal specimen of human aorta from a single patient. Using finite element analysis and computational fluid dynamic simulations, mechanical wall stress, and shear stress field were estimated from computed tomographic angiography captured 2 weeks prior to elective aortic replacement. Tensile strength testing and histological analyses of resected aortic specimens from multiple regions were compared with predicted stresses. Using geometric values (e.g., wall thickness and thrombus thickness), the constitutive model exhibited good predicative value of resected specimen tensile testing. Post-operative assessment revealed appreciative regional variability in both mechanical testing and histological evaluation of elastin and collagen content and organization. The study findings are consistent with an emerging contemporary opinion that aortic size alone is an insufficient predictor of rupture risk (2, 3) and vessel heterogeneity at the tissue level in association with local biological factors could better inform on wall vulnerability.

The epi-center of human aneurysmal disease of the aorta has traditionally been the aortic media where the histopathologic hallmarks of aneurysm in both the thoracic and abdominal aorta include elastin degradation. Though the adventitia is known to provide a majority of the biomechanical support to the vessel (4), and local cell populations influence medial biology (5), there is much less known about the role of the adventitia in aneurysmal disease. Furthermore, there resides within the adventitia, several population of progenitor-like cells associated with a microvascular network known as the vasa vasorum (6) that penetrate the outer two-thirds of the medial layer in vessels of at least 29 layers of elastic lamellae (7). Focusing on specimens of human aorta, Billaud et al. made detailed morphometric analyses of the adventitial vasa vasorum and revealed several features of microvascular remodeling including reduced density of vessel, thicker walls, and increased lumen area. In accordance with these microvascular abnormalities in the adventitia, evidence of hypoxia was noted in the aortic media by detection of increased protein expression of glucose transporter 1. In a finding consistent with prior work from the same group of decreased angiogenesis-related factors in the adventitial ECM of aneurysmal human aorta (8), decrease of pro-angiogenic gene expression was associated with increased expression of the anti-angiogenic factor thrombospondin 1 (TSP-1), supporting the notion that angiogenic signaling is deficient in aneurysmal aorta. Taken together, the data bolster a theory that vasa vasorum dysfunction leads to a malperfused aortic media in aneurysmal patients. A more complete understanding in how the adventitia biologically and biomechanically influences aortic medial homeostasis may pave the way for novel therapeutic interventions that have the potential to be not only preventative, but also less invasive than the standard of care of surgical aortic replacement.

Critical to the translation of novel therapies for valvular and vascular pathologies is the development of new clinically relevant animal models. The ovine model currently serves

as the gold standard for testing tissue engineered heart valves (TEHVs). Post-implantation remodeling processes *in vivo* have been largely under-studied and constitute a gap in knowledge impeding progress in TEHV optimization. In this issue, Dekker et al. comprehensively tested a sheep-specific immunohistochemical panel and validated several antibodies that detect ECM composition, cellular phenotype, and inflammatory status in ovine tissues. Inspired by the ECM composition and cellular profile of human native aortic and pulmonary valves and working specifically with formalin-fixed paraffin-embedded sections, the immunological panel was validated using the aortic valve, spleen, and kidney from normal juvenile sheep and one juvenile sheep diagnosed with endocarditis. The authors concluded that use of the immunohistological panel to evaluate ovine models will inform the researcher of ECM remodeling, cellular composition and inflammatory processes post-implantation of TEHVs.

Indeed, an understanding of native cellular composition is key to unraveling how phenotype transitions contribute to cardiovascular pathologies. From the laboratory of Hortells et al. reviewed current knowledge in the role of phenotypic changes in cardiovascular calcification. Previously thought to be a passive process, ectopic calcification exhibit features similar to biological processes of bone formation and remodeling. Focusing on the contribution of cellular phenotype, plasticity and their ability to transition to osteoblast-like cells, this review shares evidence from studies of animal disease models and human cell culture systems. Phenotypic transitions to osteoblast-like cells can occur due to fibroblast to myofibroblast conversion, EndoMT processes, and smooth muscle cells phenotypic switching. The authors raise several provocative questions pertaining to the theory that de-differentiation of a lineage-specific cell to an immature state may permit up-regulation of genes that contribute to calcium deposition and remodeling, a common denominator among these cellular transitions in cardiovascular calcification. Because cells in areas of pathological cardiovascular calcification have exhibited the ability to produce calcifying extracellular vesicles (9), the role of cell phenotype in production of extracellular vesicles whose contents either inhibit or promote mineral imbalance will be of high importance (10).

Tissue biomechanics can also influence cellular phenotype and understanding how different forces affect cell behavior is critical to developing clinically relevant cardiovascular disease models. Castellanos et al. explored changes in the cytoskeleton of bone marrow-derived stem cells (HBMSCs) under conditions mimicking fluid-induced shear stresses relevant to heart valves. Using a microfluidic channel device, HBMSCs were exposed to pulsatile shear stress (PSS) or steady shear stress (SS). When compared with no flow controls and SS exposed cells, PSS caused an increase in the number of actin filaments, filament density, and the filament angle in HBMSCs. PSS also resulted in up-regulation of *klf2*, a key gene involved in valvulogenesis. These findings add to our understanding in how mechanical stress affects stem cell behavior and this knowledge could help fine tune stem cell-mediated approaches to heart valve tissue engineering.

Likewise, understanding what biomechanics are at play in native valves will help to direct tissue regeneration efforts. In the case of mitral valve disease, several mechano-sensitive genes are thought to play a role and uncovering mechanisms of regulation could offer new insight into novel targeting therapeutics. Pagnozzi et al. reviewed the current literature in native mitral valve physiology and how valvular cells interpret environmental cues and interact with one another. These cell-cell and cell-environment relationships change with developmental stage and are mediated by a variety of cell surface receptors, ion channels, and structures such as cilia. Cells are also influenced by the extracellular matrix, the glycocalyx, and cell responses can be modulated by the presence of various serotonergic drugs. The authors put forth a theory of pathway integration as a likely explanation for the interplay of multiple mechanotransducing signals. Keeping the concept of dynamic reciprocity at the forefront of translational efforts, they suggest that therapeutic restoration of mechano-sensing pathway balance might be a promising direction through manipulation of the environment, modulation of how cells experience the environment or by directly altering cell-environment communication.

TRANSLATIONAL HORIZONS: UNDERSTANDING AND CONTROLLING CELL BEHAVIOR FOR HEART VALVE ENGINEERING AND CARDIAC REPAIR

For heart valve tissue engineering, technological advances in materials-based approaches still require pursuit of unanswered questions. An incomplete understanding in how pathological mechanisms influence the body's response to implanted material is among the biggest obstacles. Bouten et al. shares a perspective on the state of the art in materials-based approaches for heart valve tissue engineering. In highlighting small-scale clinical trials, the authors raise the important, yet unanswered questions pertaining to *in situ* tissue growth and remodeling. Materials-based approaches leverage the rapid repopulation of scaffold material by endogenous cells, thus making the strategy clinically attractive and the regulatory path less complex than those dependent on inclusion of *ex vivo* cells. However, a path to translation may be limited at least in part by an incomplete understanding in how neo-tissue responds under (patho) physiological hemodynamics. The authors identified three thematic areas of outstanding challenges. First, understanding materials-driven regeneration will require new knowledge in how endogenous cells respond to implanted material. New disease models that account for inter-patient variability and enable co-culture of multiple cell types, immune cells in particular, will be highly valuable. Secondly, smart biomaterial development and rational scaffold design should recapitulate native valve function, instruct healthy tissue remodeling, and have durability across the lifespan. Lastly, predicting tissue development and growth will benefit from sophistication of computational modeling methodologies that account for material degradation and neo-tissue formation profiles, ongoing growth and remodeling, tissue

architecture and signaling. Basic science inquiry remains an ongoing and integral part of the translational process for heart valve tissue engineering. A widespread skepticism of whether heart valve tissue engineering will ever come to fruition is acknowledged. The authors propose a roadmap to successful translation- one that includes integrated byways through *in vitro* and *in silico* studies, extensive pre-clinical trials and optimization en route to randomized clinical trials and cost-effectiveness evaluations amidst current valvular replacement approaches.

For any TEHV to be truly efficacious, it must resist and withstand factors and forces driving cardiovascular calcification. For example, in the setting of calcific aortic valve disease, how does one consider the cellular contribution to disease pathophysiology when designing a TEHV therapy? Jover et al. complementarily echoes Hortells et al to describe mechanisms involved in calcific aortic valve disease. The authors also highlight the pluses and minuses of various cell sources in the context of *in vitro* development of TEHVs. They encourage scaffold design with cell behavior and tissue source close in mind. Inclusion of *ex vivo* cultured mesenchymal stem cells, endothelial progenitor cells, or induced pluripotential stem cells might prevail; however, other approaches could ignore stem cells in favor of native valvular interstitial cells, valvular endothelial cells, and other native cells types. The decision-making process of choosing a cell type and source should consider several aspects including cell-graft interactions, accessibility and scalability, tissue specificity, paracrine signaling capacity, and retention on/within scaffolding biomaterials.

Recent progress in the development of biomaterials for valve, cardiac and vascular repair have shown new promise for the treatment of associated cardiovascular disease, in particular for *in vivo* delivery of exogenous cells, as expertly reviewed elsewhere (11). Understanding how biomaterials affect cell behavior is an essential component in translating new biomaterials to patients. Fibrin microthreads have recently emerged as a potential native biomaterial substrate to support stem cell growth and preserve differentiative potential. In this issue, Hansen et al. reported use of fibrin microthreads to culture human iPSC-derived cardiomyocytes (CM). Using a digital speckle tracking algorithm, the team calculated beating frequency, average and maximum contractile strain, and angle of contraction of beating iPSC-CM on fibrin microthreads and detected changes in these parameters from 7 to 21 days of culture. Seeded cells exhibited increased beating frequency, higher calcium conduction velocities, and were positive for connexin 43 expression between cells and aligned with microthread orientation. Study findings profiled seeding conditions and demonstrate temporal control of obtaining contractile behavior of cardiomyocytes. Suture needles can be threaded with fibrin microthreads, thus a regenerative approach is envisaged, where these scaffolds might effectively serve as an *in vivo* delivery system for iPSC-CM to injured or diseased myocardium.

Whether or not cells (i.e., stem/progenitor) are required for cardiovascular repair is a hotly debated topic in the field of cardiovascular regenerative medicine. Cunnane et al. addresses this controversy in the context of developing and testing of

tissue-engineered vascular grafts (TEVGs). Use of an autologous stem cell population is desirable due to reduced immunologic response. However, some patient populations (e.g., the elderly, diabetic, or immunocompromized) likely possess limited stores of stem cell populations that exhibit adequate regenerative responses. Therefore, allogeneic stem cell sources are actively under consideration, with the new challenge of identifying what stem cell-derived products or functions are necessary to elicit the desired regenerative response. Excitement for stem cell therapy approach in TEVGs might be diminished in light of realization that stem cell survival post-implantation for cardiac repair was found to be relatively short-lived and the promise of successful pre-clinical studies have not translated well in clinical trials for heart failure (12). The authors share examples from the literature demonstrating the bioactivity of stem cell-derived components (e.g., secreted factors, extracellular vesicles) in TEVG studies that could be harnessed and applied to tubular scaffolds in new cell-free strategies for vascular tissue engineering.

Delivery of ECM alone, in the absence of seeded *ex vivo* cultured cells, is another viable strategy for cardiovascular regenerative medicine. This acellular approach is attractive because ECM biomaterials exhibit little no rejection *in vivo*, and it circumvents numerous obstacles related to cell procurement, propagation and cell-biomaterial interaction. A review by Svystonyuk et al. shares early strategies in cardiac regeneration and provides the rationale for acellular bioactive ECM biomaterials as an important research thrust. The epicardium appears to be a viable niche to encourage cardiac regeneration by targeting the prevalent resident fibroblast population, which comprises 20% of the myocardium and are thought to serve as active mediators of ECM-derived signaling. Prior work from the authors demonstrated reduction of scar in basic fibroblast growth factor enhanced ECM-treated rat epicardial infarcts (13). The authors suggest that acellular bioactive ECMs offer fewer translational hurdles than cell therapy-based approaches. The authors are encouraged by knowledge that ECMs represent tunable biomaterials that contain numerous bioactive signaling molecules (14) and suggest that they might potentiate endogenous repair mechanisms in the heart and are attractive biomaterials for repair of injured or diseased myocardium and perhaps other cardiovascular tissues.

REFERENCES

1. Lopez-Candales A, Holmes DR, Liao S, Scott MJ, Wickline SA, Thompson RW. Decreased vascular smooth muscle cell density in medial degeneration of human abdominal aortic aneurysms. *Am J Pathol.* (1997) 150:993–1007.
2. Hiratzka LF, Creager MA, Isselbacher EM, Svensson LG, Nishimura RA, Bonow RO, et al. Surgery for aortic dilatation in patients with bicuspid aortic valves: a statement of clarification from the American College of Cardiology/American Heart Association Task Force on clinical practice guidelines. *J Am College Cardiol.* (2016) 67:724–31. doi: 10.1016/j.jacc.2015.11.006

FINAL PERSPECTIVES ON AN ERA OF TRANSPLANTATION, UNCOVERING DISEASE MECHANISMS, AND TISSUE ENGINEERING

What lies beyond the horizon in the current frontier of regenerative cardiovascular medicine? While great strides have been made in understanding stem cell populations and observational studies of human disease give rise to clinically-relevant and hypothesis-driven work, substantial gaps in knowledge remain regarding what pathways should be targeted for interventional therapies. Among the largest obstacles to traversing the translational divide or so-called “valley of death” to clinical application, is the tedious and tenuous pathway of commercialization and regulatory hurdles. As modern communities of academic medicine continue to cultivate fertile ecosystems that foster interdisciplinary collaboration, facilitate international cooperation, and encourage entrepreneurship, we expect these translational barriers will diminish. Ongoing basic science and translational efforts in the development of efficacious engineered tissues and organs quite possibly could help to alleviate the exceedingly high demand for donor replacement organs or ultimately eliminate the need altogether. A goal should also be to bring these future therapies to developed and non-developed regions worldwide Hutcherson et al. Given the tremendous advancements since Dr. Christiaan Barnard made the first incision in the first successful heart transplantation, the next half century should reap the fruits of the advancements in the prior 50 years.

AUTHOR CONTRIBUTIONS

JP drafted the editorial in consultation with JH and EA. JH, and EA edited the editorial.

FUNDING

JP is supported by the National Heart, Lung and Blood Institute under Award #R01HL131632. EA laboratory is supported by NIH grants R01 HL114805, R01 HL136431, and R01 HL141917. JH is supported by a Scientist Development Grant from the American Heart Association (17SDG633670259).

3. Parish LM, Gorman JH III, Kahn S, Plappert T, St John-Stutton MG, et al. Aortic size in acute type A dissection: implications for preventive ascending aortic replacement. *Eur J Cardiothorac Surg.* (2009) 35:941–5; discussion 5–6. doi: 10.1016/j.ejcts.2008.12.047
4. Deveja RP, Iliopoulos DC, Kritharis EP, Angouras DC, Sfyris D, Papadodima SA, et al. Effect of aneurysm and bicuspid aortic valve on layer-specific ascending aorta mechanics. *Ann Thorac Surg.* (2018) 106:1692–1701. doi: 10.1016/j.athoracsur.2018.05.071
5. Majesky MW, Dong XR, Hoglund V, Mahoney WM Jr., Daum G. The adventitia: a dynamic interface containing resident progenitor cells. *Arterioscler Thromb Vasc Biol.* (2011) 31:1530–9. doi: 10.1161/ATVBAHA.110.221549

6. Billaud M, Donnenberg VS, Ellis BW, Meyer EM, Donnenberg AD, Hill JC, et al. Classification and functional characterization of vasa vasorum-associated perivascular progenitor cells in human aorta. *Stem Cell Rep.* (2017) 9:292–303. doi: 10.1016/j.stemcr.2017.04.028
7. Wolinsky H, Glagov S. Nature of species differences in the medial distribution of aortic vasa vasorum in mammals. *Circ Res.* (1967) 20:409–21. doi: 10.1161/01.RES.20.4.409
8. Fercana GR, Yerneni S, Billaud M, Hill JC, VanRyzin P, Richards TD, et al. Perivascular extracellular matrix hydrogels mimic native matrix microarchitecture and promote angiogenesis via basic fibroblast growth factor. *Biomaterials* (2017) 123:142–54. doi: 10.1016/j.biomaterials.2017.01.037
9. Bakhshian Nik A, Hutcheson JD, Aikawa E. Extracellular vesicles as mediators of cardiovascular calcification. *Front Cardiovasc Med.* (2017) 4:78. doi: 10.3389/fcvm.2017.00078
10. Hutcheson JD, Aikawa E. Extracellular vesicles in cardiovascular homeostasis and disease. *Curr Opin Cardiol.* (2018) 33:290–7. doi: 10.1097/HCO.0000000000000510
11. Ogle BM, Bursac N, Domian I, Huang NF, Menasche P, Murry CE, et al. Distilling complexity to advance cardiac tissue engineering. *Sci Transl Med.* (2016) 8:342ps13. doi: 10.1126/scitranslmed.aad2304
12. Nguyen PK, Rhee JW, Wu JC. Adult stem cell therapy and heart failure, 2000 to 2016: a systematic review. *JAMA Cardiol.* (2016) 1:831–41. doi: 10.1001/jamacardio.2016.2225
13. Mewhort HE, Turnbull JD, Meijndert HC, Ngu JM, Fedak PW. Epicardial infarct repair with basic fibroblast growth factor-enhanced CorMatrix-ECM biomaterial attenuates postischemic cardiac remodeling. *J Thorac Cardiovasc Surg.* (2014) 147:1650–9. doi: 10.1016/j.jtcvs.2013.08.005
14. Reing JE, Zhang L, Myers-Irvin J, Cordero KE, Freytes DO, Heber-Katz E, et al. Degradation products of extracellular matrix affect cell migration and proliferation. *Tissue Eng Part A.* (2009) 15:605–14. doi: 10.1089/ten.tea.2007.0425

Conflict of Interest Statement: The authors declare that the research was conducted in the absence of any commercial or financial relationships that could be construed as a potential conflict of interest.

Copyright © 2019 Phillippi, Aikawa and Hutcheson. This is an open-access article distributed under the terms of the Creative Commons Attribution License (CC BY). The use, distribution or reproduction in other forums is permitted, provided the original author(s) and the copyright owner(s) are credited and that the original publication in this journal is cited, in accordance with accepted academic practice. No use, distribution or reproduction is permitted which does not comply with these terms.



After 50 Years of Heart Transplants: What Does the Next 50 Years Hold for Cardiovascular Medicine? A Perspective From the International Society for Applied Cardiovascular Biology

Joshua D. Hutcheson^{1*}, Craig J. Goergen², Frederick J. Schoen³, Masanori Aikawa³, Peter Zilla⁴, Elena Aikawa³ and Glenn R. Gaudette⁵

¹ Department of Biomedical Engineering, Florida International University, Miami, FL, United States, ² Weldon School of Biomedical Engineering, Purdue University, West Lafayette, IN, United States, ³ Brigham and Women's Hospital, Harvard Medical School, Boston, MA, United States, ⁴ Chris Barnard Division of Cardiothoracic Surgery, University of Cape Town, Cape Town, South Africa, ⁵ Worcester Polytechnic Institute, Worcester, MA, United States

OPEN ACCESS

Edited by:

Hendrik Tevæarai Stahel,
Universitätsspital Bern, Switzerland

Reviewed by:

Rhys David Evans,
University of Oxford, United Kingdom
Steven Clive Greenway,
University of Calgary, Canada

*Correspondence:

Joshua D. Hutcheson
jhutches@fiu.edu

Specialty section:

This article was submitted to
Atherosclerosis and Vascular
Medicine,
a section of the journal
Frontiers in Cardiovascular Medicine

Received: 16 November 2018

Accepted: 24 January 2019

Published: 14 February 2019

Citation:

Hutcheson JD, Goergen CJ,
Schoen FJ, Aikawa M, Zilla P,
Aikawa E and Gaudette GR (2019)
After 50 Years of Heart Transplants:
What Does the Next 50 Years Hold for
Cardiovascular Medicine? A
Perspective From the International
Society for Applied Cardiovascular
Biology. *Front. Cardiovasc. Med.* 6:8.
doi: 10.3389/fcvm.2019.00008

The first successful heart transplant 50 years ago by Dr. Christiaan Barnard in Cape Town, South Africa revolutionized cardiovascular medicine and research. Following this procedure, numerous other advances have reduced many contributors to cardiovascular morbidity and mortality; yet, cardiovascular disease remains the leading cause of death globally. Various unmet needs in cardiovascular medicine affect developing and underserved communities, where access to state-of-the-art advances remain out of reach. Addressing the remaining challenges in cardiovascular medicine in both developed and developing nations will require collaborative efforts from basic science researchers, engineers, industry, and clinicians. In this perspective, we discuss the advancements made in cardiovascular medicine since Dr. Barnard's groundbreaking procedure and ongoing research efforts to address these medical issues. Particular focus is given to the mission of the International Society for Applied Cardiovascular Biology (ISACB), which was founded in Cape Town during the 20th celebration of the first heart transplant in order to promote collaborative and translational research in the field of cardiovascular medicine.

Keywords: cardiovascular medicine, heart transplant, arterial disease, aortic valve, myocardial regeneration, tissue engineering, interdisciplinary/multidisciplinary

INTRODUCTION

Christiaan Barnard, an innovative surgeon, transplanted the world's first human heart on December 3, 1967 in Cape Town, South Africa (**Figures 1A,B**). Soon after, surgeons across the world started transplanting hearts into patients with end-stage heart disease. The potential of rejection required immunosuppression, which left patients susceptible to infection. The approval of cyclosporine use for transplant recipients allowed for better post-transplant patient care and improved patient survival. In 2016, 3,209 hearts were transplanted in the U.S. alone and over 5,000 worldwide (1). However, the availability of transplantable hearts and their function once implanted is still far

from optimal. To help overcome issues in the field of cardiac and vascular diseases more broadly, a collaborative group of cardiac surgeons, cardiologists, engineers and biologists founded the International Society for Applied Cardiovascular Biology (ISACB) in Cape Town during the 20th celebration of the first heart transplant in 1987. Now after more than 30 years, ISACB has nurtured an alliance among academic scientists and engineers, clinicians, and industry-based scientists to understand, prevent, and manage cardiovascular disease.

While scientists, engineers and clinicians have a long history of cooperation, with strong academic roots and participation in professional societies, the participation of industry in professional society meetings and has been dominated by marketing considerations. Proprietary concerns have further isolated many corporate scientists from open forums of communication. As stated by founding member and former ISACB President Peter Zilla, these “traditional roles and stereotypes must rapidly wane in light of the complexity that is required for any biologically “conscientious” product of today or tomorrow... and... industry scientists must be better integrated within the academic and medical communities.” Dr. Zilla (**Figure 1C**), a surgeon scientist and Head of the Christiaan Barnard Department of Cardiothoracic Surgery of the Groote Schuur Hospital and the University of Cape Town, emphasizes the importance of understanding relevant science and corporate considerations while providing the surgeon with a usable solution as essential in developing better treatments for cardiovascular diseases. Collaborations between scientists, surgeons, engineers and investigators from other fields stimulates new opportunities to develop translatable solutions to significant cardiovascular issues. Thirty years later, and now 50 years after the world’s first heart transplant, ISACB continues to foster a multidisciplinary convergence of professional expertise and experiences, through the *application* of biology to clinical medicine in order to prevent and overcome cardiovascular disease. Moreover, ISACB has also fostered collaboration among professional societies focused on cardiovascular biology, cardiology, surgery, pathology, and bioengineering, including joint meetings with the Society for Cardiovascular Pathology (SCVP), the North American Vascular Biology Organization (NAVBO), Heart Valve Tissue Engineering (HVTE), and others.

In this perspective, we summarize developments in the restoration of cardiac function, including improved blood flow, valvular repair, replacement and tissue engineering, regeneration of myocardial tissue, mechanisms for vascular and valvular diseases, and other related areas. Particular attention will be paid to the practical application of potential therapies, as was discussed at the scientific sessions during the 30th anniversary of ISACB, which was held in Cape Town in December of 2017 to coincide with the celebration of the world’s first heart transplant (**Figure 2**). More specifically, ISACB members have made important (and largely ongoing) advances and contributions to:

1. Unraveling *the mechanisms of atherosclerosis and its complications* (such as myocardial infarction), coupled with imaging technologies that reveal dynamic vascular and cardiac structures, atherosclerotic risk factors, and improved diagnostic strategies. This mechanistic understanding has immense clinical benefit. Recent major areas in atherosclerosis research that have made remarkable progress include the biology of vascular inflammation, assessment of vulnerable plaque, and advancements in lipid lowering statins.
2. Leading a virtual explosion in the number and scope of *cardiovascular surgical and interventional diagnostic and therapeutic procedures and devices used to manage heart disease*. Four developments are noteworthy in this regard: (1) the emergence of pediatric and adult cardiac surgery as routine therapies, including repairs for congenital cardiac abnormalities and acquired valvular heart disease, and valve replacement and coronary artery bypass surgery, (2) the growth of cardiac transplantation as a clinically-important therapeutic modality, beginning in 1967, and enabled by the development of endomyocardial biopsy as a primary and invaluable diagnostic tool, and the widespread use of this technology in patients with diverse pathologies of the myocardium; (3) the development and use of a broad array of prosthetic and adjunctive medical devices (including heart valves, vascular grafts and stents, and cardiac assist devices), demonstration of their complications, and improved generations of these devices, often through collaborations with industry; and (4) the recognition of the central importance of myocardial protection in cardiac surgery and intervention, which permitted the above to occur.
3. *Elucidating the impact of genetic abnormalities on many specific subsets of cardiovascular disease*, including the single-gene mutation etiologies of congenital abnormalities, (hypertrophic, dilated, and arrhythmogenic right ventricular) cardiomyopathies, channelopathies, and connective tissue disorders such as Marfan, Loeys–Dietz, and Williams syndromes, as well as complex multi-gene phenotypes and gene-environment interactions.

We describe below selected areas of current interest and active contribution of ISACB members that were discussed at the Cape Town 50th Anniversary meeting that are likely to yield considerable clinical benefit over the next several decades.

VASCULAR DISEASE, ARTERIAL REMODELING, AND VASCULAR REPLACEMENT

Vascular disease encompasses a broad range of pathologies, extending from the cerebral vasculature to vessels in the lower limbs. While there is a broad range of arterial and venous diseases with varying risk factors, symptoms, and complications, this section focuses on two of major current clinical issues: atherosclerosis and aneurysms. Several recent studies and findings provide an overview of current efforts and areas for future work.



FIGURE 1 | (A) Wax figures of the cardiac surgeon Christiaan Barnard, his team, and the patient Louis Washkansky during the first human heart transplantation at the Heart of Cape Town Museum in Grootte Schuur Hospital that took place in 1967. **(B)** Grootte Schuur Hospital where the first human heart transplantation was performed by Christiaan Barnard. This beautiful hospital is located on the slope of Devil's Peak shown in the background. **(C)** Peter Zella, MD, PD, Ph.D., FCs, Head of the Christiaan Barnard Department of Cardiothoracic Surgery at Grootte Schuur Hospital of the University of Cape Town. He co-founded the ISACB and was a past president of the society. Dr. Zella organized the 50th Anniversary Heart Transplant Celebration in Cape Town, "Courage and Innovation: 50 Years of transplantation" at Grootte Schuur Hospital in December, 2017.



FIGURE 2 | (A) ISACB Meeting in 2017 took place as part of the 50th Anniversary Heart Transplant Celebration in Cape Town, "Courage and Innovation: 50 Years of transplantation" at Grootte Schuur Hospital. **(B)** ISACB members at the reception of the 50th Anniversary Heart Transplant Celebration in Cape Town, "Courage and Innovation: 50 Years of transplantation".

Atherosclerosis and Tissue Engineered Vascular Grafts

Coronary artery atherosclerosis is associated with an inflammatory process (2) and contributes to significant morbidity and mortality (3). Surgeons often implant bypass grafts to deliver oxygenated blood around a stenosis to distal coronary beds. Current gold standard treatments use vessels harvested from other parts of the body since this autologous approach outperforms synthetic grafts. Unfortunately, these vessels require surgical harvesting and are prone to restenosis due to intimal hyperplasia. A current clinical focus is the development of a long-lasting tissue-engineered vascular graft (TEVG) (4). Despite significant efforts, ideal TEVGs have remained elusive. Many groups are working on developing TEVGs with appropriate mechanical properties, bioactivity, and biocompatibility (4, 5). Protein-coated polytetrafluoroethylene (ePTFE) grafts lined with autologous endothelial cells have shown long-term patency in almost 500 patients. The complexity of the cell sourcing and seeding procedures, however, does not make this technique amenable to routine use in vascular surgery. Yet, the clinical successes indicate the potential at this early stage of tissue engineering efforts. Ongoing efforts *in vitro* and *in vivo* seek to optimize long-term patency, mechanical properties, and reendothelialization (6). Recent advancements suggest continued improvements are possible and continued development could eliminate many of the issues associated with current synthetic grafts.

Atherosclerosis can also be present in peripheral arteries, and peripheral artery disease (PAD) can lead to intermittent claudication and critical limb ischemia in later stages of disease progression (7). The risk of developing lower-limb PAD increases with obesity, a history of atherosclerosis, high triglycerides, low high-density lipoprotein, and aging (8). Ongoing efforts seek to develop non-invasive interventions to treat atherosclerosis and prevent deleterious remodeling of the vascular wall. A recent study showed an association between serum levels of sortilin, a glycoprotein involved in glucose and lipid metabolism, with aortic calcification and general cardiovascular disease risk (9). Carotid artery atherosclerosis revealed PCSK6 as a novel protease, possibly making these lesions prone to rupture (10). The development of a novel platelet lysate hydrogel has shown promise to promote angiogenic activity of mesenchymal stem cells (MSC) that can also be delivered concomitantly (11). While each of these individual findings may lead to a therapeutic breakthrough, the combination of multiple studies over the next 50 years has the potential to improve our mechanistic insight into atherosclerosis and PAD, providing unique treatment solutions.

Emerging Evidence for Monocyte/Macrophage Heterogeneity

Accumulating evidence from basic science and clinical medicine suggests that inflammation plays critical roles in the pathogenesis of atherosclerotic vascular diseases and their clinical complications (12). Emerging evidence indicates that macrophages are a heterogeneous population (13). Similarly, we know that monocytes, generally considered as

macrophage precursors, are also heterogeneous (14). Changes in macrophage behavior and attributes in response to systemic or local environmental cues may help execute specific functions during the disease process. Traditionally macrophages were thought to adopt a pro-inflammatory or anti/non-inflammatory phenotype in response to stimuli (M1 vs. M2 polarization), but new evidence suggest that macrophage heterogeneity is more multi-dimensional (15–17). Studies using single cell analyses have demonstrated the dynamic and complex nature of human primary monocytes and macrophages heterogeneity (18–20). Understanding the underlying mechanisms of monocyte/macrophage heterogeneity and related therapeutic implications may require innovative approaches such as machine learning from large clinical studies.

Aneurysms: Imaging, Biomechanics, and Novel Therapies

Abdominal aortic aneurysm (AAA) is an inflammatory disease of the aorta resulting in pathologic dilation of the vessel wall. Clinically, an aortic diameter 50% larger than normal is considered aneurysmal, and only surgical treatment options currently exist (21). Between 5 and 10% of people in the industrialized world over the age of 65 suffer from AAAs (22, 23), accounting for roughly 16,000 deaths and 150,000 inpatient hospitalizations per year in the U.S (24, 25). Although recent studies have provided insight into the pathogenesis of AAA, a detailed understanding of the underlying mechanisms that lead to AAA expansion remains incomplete.

Development of novel therapies that will interrupt development of an AAA or halt aneurysm progression remains a challenge (26). Efforts are focusing on investigating the association between genetic variants and aneurysm formation (27) and the role of enzyme activity in extracellular matrix (ECM) changes within the aortic wall (28). Further work has focused on the role of the inflammasome, including both innate immunity and inflammation, in aneurysm formation and progression (29). Recent studies have shown that serum amyloid A, a protein that associates with high-density lipoprotein when in circulation, exacerbates acute vascular events by activating the inflammasome (30, 31). Others have investigated the correlation between circulating biomarkers and aortic disease, showing that elevated circulating levels of the soluble receptor for advanced glycation end products is associated with a variety of aortopathies, independent of aortic diameter (32). Identifying patients at increased risk for aneurysm development and then increasing aortic wall strength through pharmacologic means could slow growth of AAAs to large diameters where rupture is more likely.

Beyond aortic wall research, blood flow hemodynamics have been shown to be critical to the formation and growth of aneurysms, dissections, and thrombus (33). This provides strong motivation to develop sophisticated data-driven models of blood flow, pressure, and wall elasticity associated with AAAs. Recent work focused on implementing a multi-modality imaging approach that combined high frequency ultrasound (US) and optical coherence tomography (OCT) as inputs for a murine

computational modeling study (34). The results showed that differences in final lesion size and compositions correlated with vortical structures obtained through mouse-specific fluid dynamic simulations, suggesting that differences in morphology and hemodynamics play crucial roles in AAA formation. These data agree with a large amount of previous work where imaging-based computational findings have suggested a link between hemodynamic perturbations and aneurysmal disease heterogeneity (35). The combination of imaging, hemodynamic simulations, and biomechanical analysis is proving to be useful for exploring potential translational strategies that could soon be useful to predict possible aneurysm expansion and rupture (36, 37). Taken together, these recent advancements suggest a bright future for multi-disciplinary cardiovascular research in clinical medicine, genetics, biology, and engineering to address unmet clinical need associated with AAA.

VALVE DISEASE AND VALVE REPAIR AND REPLACEMENT TECHNOLOGIES

Valve diseases constitute a global health burden. In developed countries, age-related calcific aortic valve disease (CAVD) eventuates in aortic stenosis, whereas in developing countries, rheumatic heart disease remains the leading cause of valvular structural abnormalities (38). Other key causes of valvular dysfunction include mitral valve prolapse (myxomatous valve disease) and functional mitral regurgitation owing to ischemic heart disease. High rates of congenital valve abnormalities present complications in pediatric patients without regard to environmental conditions. Each of these causes of valve dysfunction represent unique challenges in the management of valve disease, but appropriate solutions hinge on understanding the factors that govern valve homeostasis and function.

Although decades of basic and clinical research and the advent of lipid lowering therapies (especially statins) have markedly reduced morbidity and mortality associated with atherosclerotic cardiovascular diseases, clinical trials have shown that statins have no effect on progression of existing CAVD, and thus no effective therapy is available. As a result, clinical options for patients with CAVD are limited to invasive open heart surgery or transcatheter valve implantation (39).

Pathological remodeling most commonly affects the aortic and mitral valves, likely a consequence of higher systemic pressures, underscoring the importance of biomechanical function and sensitivity. Given the relatively high incidence and severity, we focus our discussion here on aortic valve disease and replacement, an area of tremendous clinical need.

Aortic Valve, Function, Structure, Biology, and Target Discovery

Unidirectional blood flow from the left ventricle to the aorta for systemic distribution normally occurs through coordinated action of three leaflets. Leaflet action is controlled by a layered and highly organized ECM microarchitecture (40–43). The ECM structure is maintained by two cell populations: valvular endothelial cells (VECs) and valvular interstitial cells (VICs).

VECs appear phenotypically distinct from other endothelial cell populations in vascular tissues and exhibit regional heterogeneity with side-specific differences in gene expression (44–46). VICs are a poorly defined population of cells with subpopulations of fibroblasts, myofibroblasts, smooth muscle cells, and neuron-like cells previously identified within the leaflets (47, 48). Phenotypic changes in VECs and VICs have been associated with aortic valve remodeling (49), but the relative contributions of these cells and associated subpopulations remain unknown. The role of inflammation in valve remodeling (50, 51) is especially relevant when considering approaches to valve disease in developing countries, where rheumatic heart disease is a major contributor. VECs and VICs also display mechanosensitivity and readily respond to changes in the mechanical environment (52–55). The complex cellular and biomechanical environment is difficult to recapitulate *in vitro* and animal models of aortic valve disease are lacking (56), making mechanistic studies on the biomechanical and biochemical initiators of disease difficult to perform.

Recent studies have sought to overcome this limitation by using large, unbiased proteomic and transcriptomic approaches to characterize molecular changes in aortic valve leaflets obtained from patients undergoing replacement surgeries (57). Combining pathological characterization of the leaflets following resection with network-based analysis of the proteomic and transcriptomic data has yielded new insight into the potential molecular drivers of aortic valve disease. Coupled with new genome wide association studies that have revealed new lipid associations with aortic valve disease, these big data approaches may provide new clues about points of non-invasive therapeutic intervention and the development of drug-based therapies (58, 59). However, challenges remain in identification of patients during the early stages of disease before gross remodeling of the aortic valve leaflets necessitate replacement.

Synthetic and Bioprosthetic Approaches to Aortic Valve Replacement

Given the lack of non-invasive treatment or suitable options for CAVD, the traditional clinical approach has been surgical valve replacement. First introduced in 1960, early iterations of devices for aortic valve replacement utilized mechanical valves consisting of caged-ball or tilting disk designs surgically implanted into the aortic orifice following removal of the diseased valve (60). These devices provided the first viable clinical solution for patients with aortic valve abnormalities and offered extraordinary reduction in mortality associated with CAVD. Of note, inoperable patients with CAVD have a 2–3 year mortality of <50% (61, 62). Though these devices helped correct valve dysfunction, nearly all patients who received mechanical valves suffered valve-related complications within 10 years, and many died of these complications (63).

To enhance biocompatibility and create a more normal geometry, bioprosthetic valves were introduced in the clinic in the late 1960s as an alternative to mechanical valves (64). Bioprosthetic valves are fabricated from glutaraldehyde treated (and hence non-viable) porcine aortic valve or bovine pericardial

tissue formed into a tri-leaflet structure. Bovine pericardium is used most frequently today. These valves do not require lifelong anticoagulation therapy, and bioprosthetic valves more adequately recapitulate the biomechanics and hemodynamics of native aortic valves. Nevertheless, bioprosthetic valves frequently undergo calcification, leading to stenosis or tearing with regurgitation. After ~15–20 years, bioprosthetic valves often must be replaced, requiring the patient to undergo an additional invasive surgical procedure. The mineral forms due to phosphorus in devitalized cell remnants and possibly residual aldehyde affinity for mineral. Newer versions of bioprosthetic valves overcome this limitation through detergent-based treatments that reduce cell-based material and inhibit mineral deposition (65). To avoid multiple surgeries, modern mechanical valves have been deemed more suitable for younger patients who need aortic valve replacement. Clinicians must weigh the relative risks of reoperation to replace bioprosthetic valves vs. the risks associated with anticoagulant therapy in patients with mechanical valves (66).

The advent of transcatheter aortic valve implantation (TAVI) has begun to revolutionize aortic valve replacement. Synthetic or bovine pericardial-based aortic valves are placed into the aortic annulus using an endovascular catheter. The catheter is most often introduced through the femoral artery and guided to the annulus whereupon the replacement aortic valve is deployed, displacing the diseased aortic valve (67). First introduced for elderly patients and those deemed unfit for surgical-based replacements, TAVI is becoming standard care for many patients with CAVD (68). Patients undergoing TAVI procedures have similar outcomes as those who receive surgical aortic valves (69). Early analyses indicated that TAVI may induce stroke, paravalvular leak, and vascular wall damage during catheterization; however, subsequent studies have shown that other complications may be less of a concern than those arising from surgery (70, 71). TAVI “valve-in-valve” approaches also obviate the need for open surgical procedures for patients with degeneration of a previously implanted bioprosthetic valve. After the initial bioprosthetic valve deteriorates, a TAVI procedure can introduce a new valve that is likely to exceed the expected lifespan of the patient.

The leading cause of aortic valve disease in developing countries is rheumatic heart disease, but the local infrastructure is not generally well-suited for open heart procedures. TAVI may provide a more appropriate option for patients in these regions (72); however, two specific limitations must be overcome. Typically, aortic valve disease and bioprosthetic degeneration are associated with the deposition of calcific mineral on the leaflets. This mineral provides a structure to anchor TAVI valves, but rheumatic-induced aortic valve remodeling does not usually involve heavy calcification. Positioning the catheter during TAVI also requires imaging modalities not commonly available in developing countries. Recently developed TAVI strategies designed specifically for low resource settings may help overcome these limitations (73). The new design employs a supra-annular anchoring technique that latches to the non-calcified valve structure and provides tactile feedback that allows the clinician to locate the correct annular position without the

need for fluoroscopic imaging. This technique could address a major unmet clinical need in developing countries.

Engineering Living Aortic Valve Tissue

Since the first replacement aortic valves were introduced, advancements in both valve design and replacement techniques have provided lifesaving options for many patients. However, issues remain, particularly for pediatric patients who require aortic valve replacement due to congenital valvular abnormalities. These children often require multiple procedures to replace valves that do not adapt to somatic growth, and calcification of valves and conduits is accelerated in young recipients. These patients would benefit from engineered aortic valve constructs that fully integrate with native host tissues, do not degenerate, and adapt to size and pressure changes in the cardiovascular system. Efforts to develop tissue engineered aortic valves should integrate knowledge of the complex biological environment, dynamic biomechanics, material durability, and delivery/implantation methods discussed in the previous sections. Early attempts to engineer living aortic valve tissues employed biodegradable scaffolds seeded with mixed populations of arterial-derived endothelial cells and fibroblasts (74). These constructs yielded ECM deposition consistent with native valve structure after 2 months in an ovine model, demonstrating the potential utility of a living engineered tissue that can actively remodel appropriately after implantation (75).

Translation of these proof-of-concept techniques to clinical practice for human patients remains elusive, however. Questions persist on the appropriate cell source, the most appropriate material for the scaffolds, the minimum biomechanical functionality required for implantation, and the methods to assess remodeling *in situ* following implantation (76). In the early 2000s, the first tissue engineered aortic valve replacement surgeries were performed in neonates with severe congenital malformations (77). These valves exhibited beneficial early remodeling in an ovine model, and gross long-term ECM remodeling was attributed to a problem with the animal model. The outcomes from initial clinical trials, however, were largely poor. Many of the valves exhibited remodeling concomitant with inflammation, including fibrosis and deterioration, comparable to the observations made in the ovine endpoints (77).

These early outcomes reduced enthusiasm for aortic valve tissue engineering, but the clinical need for pediatric patients with aortic valve dysfunction remains. Early clinical successes have been noted in pediatric mitral valve repair using constructs of porcine small intestinal submucosa handmade in the clinic to resemble valve leaflets (78). The *ad hoc* use of this material in patients with few other clinical options has yielded promising results in short-term clinical follow-ups and work by recruiting endogenous cells that stimulate leaflet remodeling and growth (79, 80). Similar strategies are being developed for aortic valve replacement. Many approaches currently in pre-clinical development seek to recruit host cells after implantation of a polymer matrix without cells or other biological adjuncts. In such an approach, proper ECM development and leaflet maturation takes cues from and depends on processes that occur in native valve development (so-called “*in situ* tissue engineering”) (81).

This strategy enables off-the-shelf availability of constructs without the need for maintenance of cellular viability, and could provide a clinically feasible solution that avoids cell sourcing complications (82).

Whether these tissue engineered constructs can adequately recapitulate the function of native aortic valves remains to be seen. Perhaps the complete recapitulation of the complex biological structure and biomechanical properties of native valve are not required to produce adequate and lasting function. Imperfect strategies that offer new life to a patient with no other options provide clinical value, and knowledge gained through iterations of incremental improvement will help fill gaps in our current understanding of aortic valve biology and function. Ultimately, non-invasive therapeutics may prevent or reverse adult-onset aortic valve remodeling, and minimally invasive implantation of tissue engineered valves may fix congenital abnormalities in pediatric patients. Achieving these goals will require concerted interdisciplinary efforts of basic scientists, engineers, and clinicians. All are well-represented within ISACB.

CARDIAC REGENERATION

Unlike other tissues in the body, the heart does not possess significant regenerative capacity. The adult heart responds to infarction by creating a collagen dense scar. While this may strengthen the mechanical properties of the wall to help eliminate ventricular rupture, it decreases the overall pump capacity of the heart. In many cases, this decreased function leads to congestive heart failure. While a heart transplant is currently the only “tried and true” means to restore mechanical pump function in these patients, the lack of organ donors calls for additional solutions.

Engineered cardiac tissues offer a potential solution. Rapid advances in cell therapy, including induced pluripotent stem cells, have demonstrated that cells can be grown in the laboratory and differentiated into cardiac muscle cells. In order to restore contractile function in the heart, these cells need to form an aligned and synchronized dense network, and a vascular supply will be needed to maintain viability. Thus, tissue engineered cardiac scaffolds should provide for cell attachment and survival while allowing the scaffold to contract in sync with the rest of the heart.

Engineering Cardiac Scaffolds

When considering scaffolds for cardiac tissue engineering, many factors must be considered for the vast applicability of these materials (83). Cost, sustainability, and labor skill requirements must all be considered for widespread use. A potential starting point for engineered cardiac tissue is an acellular scaffold (84). Investigators have used a master bank of human cells to produce the ECM for these scaffolds. This allows for a controlled initial material source, which helps bring costs down and maintain quality control over the product. Decellularization leaves an ECM that is attractive for native cells to adhere and proliferate (85–87). Lyophilization and sterilization yields an “off the shelf” product, which also helps bring down costs. These scaffolds can be produced in a Good Manufacturing Practices (GMP) facility with appropriate quality controls, allowing for consistent

production of scaffolds with the same properties. Most pre-clinical work to date with this scaffold has been in a congenital model, showing that the scaffold grows with the animal. The Emmert/Hoerstrup group is currently working to develop the scaffold as a cardiac patch.

Difficulties remain in vascularizing scaffolds to maintain cell viability. Instead of using mammalian cells to produce a scaffold, investigators are looking toward the plant kingdom, specifically spinach leaves (88). After the decellularizing process, the vascular network inherent to the plant remains and can be used to perfuse fluid. Microspheres, of similar size to red blood cells, were also able to pass through the plant vasculature, and the scaffold is able to serve as a basement membrane for contracting cardiac myocytes. Further work, however, is required for clinical realization of this technique.

Cells for Cardiac Regeneration

Clinical trials on cell therapy for heart disease have demonstrated only limited success (89). This may be due in part to the variability in the cells used in cardiac cell therapy. Most cardiac clinical trials have utilized MSC. While this cell type has not demonstrated deleterious effects, improvement in cardiac function appears to be limited.

Embryonic stem cells (ESCs) and induced pluripotent stem cells (iPS cells) have demonstrated the potential to form contractile myocytes. ESCs can proliferate to provide a plentiful source of cells. They are also able to differentiate into contracting cells with many properties similar to adult cardiac myocytes. ESCs, however, remain a topic of controversy. An exciting discovery in 2006 introduced a new cell type—iPS cells that can be produced from adult differentiated cells (e.g., fibroblast) through genetic engineering (90). By inserting specific genes regulating transcription factors, the adult cells can be induced to becoming an embryonic-like stem cell. These cells can then be differentiated into contractile cells with properties similar to cardiac myocytes. Thus, a patient’s own cells can potentially yield cardiac myocytes that restore cardiac function, eliminating any immune rejection response from the recipient. However, significant concerns still remain for both ESCs and iPS cells prior to their use in the clinic. Cell sorting and validation is essential to moving the field forward. Incorporation of the wrong cell type in the heart can lead to fatal arrhythmias or worse, and proliferation of these cells must be regulated.

THE NEXT 50 YEARS

Despite decades of active research efforts in cardiovascular biology, few basic science discoveries have arrived in the clinic as efficient drugs or devices. Indeed, many preclinical breakthroughs have failed to survive clinical translation. Because of insufficient expertise and tight funding, academic investigators often struggle to translate findings into clinical development (91, 92). This gap also results from strategies in industry to avoid investing in early, high-risk targets (93, 94). Clearing such roadblocks requires new paradigms for translational research. As ISACB has consistently promoted since it was founded, close collaboration between academic investigators and industry

scientists, who can share clear goals and understand potential mutual benefits, will facilitate exchange of ideas, resources, and expertise and lead to innovative therapies for cardiovascular diseases (15, 95).

Looking back on the improvements made in treating cardiovascular diseases over the past 50 years, one cannot help but wonder: what key advances will occur in the next 50 years? In addition to the areas discussed above, endovascular therapies, valve repair and replacement technologies, arrhythmia ablation, xenotransplantation, and long-term cardiac support (both mechanical and biological) will almost certainly continue to improve. Additionally, it is probable that significant strides will be made toward directed prevention of a broad range of cardiovascular conditions. New discoveries require innovative technologies. Considering the accelerated speed of technological development, courage and innovation are important values, as suggested during the 50th Anniversary Heart Transplant Celebration. With effective collaboration fostered by the ISACB and similar cross-disciplinary societies, the next 50 years will

likely lead to many more life-saving treatments that will hopefully be extended to ALL patients around the world.

AUTHOR CONTRIBUTIONS

JH, CG, FS, MA, PZ, EA, and GG all contributed to the text and editing of the manuscript.

FUNDING

EA is supported by National Institutes of Health (NIH) grants R01HL 136431 and R01HL 141917. Scientist Development Grants from the American Heart Association support JH (17SDG633670259) and CG (14SDG18220010). MA's research described here is supported by the grants from the NIH (R01HL107550 and R01HL126901) and Kowa Company, Ltd., Nagoya, Japan. GG's research described here is supported by NIH grant R01 HL115282 and National Science Foundation grant NSF IGERT DGE 1144804.

REFERENCES

- Colvin M, Smith JM, Hadley N, Skeans MA, Carrico R, Uccellini K, et al. OPTN/SRTR 2016 Annual Data Report: Heart. *Am J Transplant.* (2018) 18(Suppl. 1):291–362. doi: 10.1111/ajt.14561
- Fung E, Tang SM, Canner JB, Morishige K, Arboleda-Velasquez JF, Cardoso AA, et al. Delta-like 4 induces notch signaling in macrophages: implications for inflammation. *Circulation* (2007) 115:2948–56. doi: 10.1161/CIRCULATIONAHA.106.675462
- Hansson GK. Inflammation, atherosclerosis, and coronary artery disease. *N Engl J Med.* (2005) 352:1685–95. doi: 10.1056/NEJMra043430
- Pashneh-Tala S, MacNeil S, Claeysens F. The tissue-engineered vascular graft—past, present, and future. *Tissue Eng Part B Rev.* (2015) 22:68–100. doi: 10.1089/ten.teb.2015.0100
- Best C, Strouse R, Hor K, Pepper V, Tipton A, Kelly J, et al. Toward a patient-specific tissue engineered vascular graft. *J Tissue Eng.* (2018) 9:2041731418764709. doi: 10.1177/2041731418764709
- de Valence S, Tille JC, Mugnai D, Mrowczynski W, Gurny R, Moller M, et al. Long term performance of polycaprolactone vascular grafts in a rat abdominal aorta replacement model. *Biomaterials* (2012) 33:38–47. doi: 10.1016/j.biomaterials.2011.09.024
- Lin JB, Phillips EH, Riggins TE, Sangha GS, Chakraborty S, Lee JY, et al. Imaging of small animal peripheral artery disease models: recent advancements and translational potential. *Int J Mol Sci.* (2015) 16:11131–77. doi: 10.3390/ijms160511131
- Diehm C, Schuster A, Allenberg JR, Darius H, Haberl R, Lange S, et al. High prevalence of peripheral arterial disease and co-morbidity in 6880 primary care patients: cross-sectional study. *Atherosclerosis* (2004) 172:95–105. doi: 10.1016/S0021-9150(03)00204-1
- Goettsch C, Iwata H, Hutcheson JD, O'Donnell CJ, Chapurlat R, Cook NR, et al. Serum sortilin associates with aortic calcification and cardiovascular risk in men. *Arterioscler Thromb Vasc Biol.* (2017) 37:1005–1011. doi: 10.1161/ATVBAHA.116.308932
- Perisic L, Hedin E, Razuvaev A, Lengquist M, Osterholm C, Folkersen L, et al. Profiling of atherosclerotic lesions by gene and tissue microarrays reveals PCSK6 as a novel protease in unstable carotid atherosclerosis. *Arterioscler Thromb Vasc Biol.* (2013) 33:2432–43. doi: 10.1161/ATVBAHA.113.301743
- Robinson ST, Douglas AM, Chadid T, Kuo K, Rajabalan A, Li H, et al. A novel platelet lysate hydrogel for endothelial cell and mesenchymal stem cell-directed neovascularization. *Acta Biomater.* (2016) 36:86–98. doi: 10.1016/j.actbio.2016.03.002
- Tabas I, Lichtman AH. Monocyte-macrophages and T cells in atherosclerosis. *Immunity* (2017) 47:621–34. doi: 10.1016/j.immuni.2017.09.008
- Martinez FO, Gordon S. The evolution of our understanding of macrophages and translation of findings toward the clinic. *Expert Rev Clin Immunol.* (2015) 11:5–13. doi: 10.1586/1744666X.2015.985658
- Buscher K, Marcovecchio P, Hedrick CC, Ley K. Patrolling mechanics of non-classical monocytes in vascular inflammation. *Front Cardiovasc Med.* (2017) 4:80. doi: 10.3389/fcvm.2017.00080
- Decano JL, Aikawa M. Dynamic macrophages: understanding mechanisms of activation as guide to therapy for atherosclerotic vascular disease. *Front Cardiovasc Med.* (2018) 5:97. doi: 10.3389/fcvm.2018.00097
- Murray PJ, Allen JE, Biswas SK, Fisher EA, Gilroy DW, Goerdt S, et al. Macrophage activation and polarization: nomenclature and experimental guidelines. *Immunity* (2014) 41:14–20. doi: 10.1016/j.immuni.2014.06.008
- Nahrendorf M, Swirski FK. Abandoning M1/M2 for a network model of macrophage function. *Circ Res.* (2016) 119:414–7. doi: 10.1161/CIRCRESAHA.116.309194
- Iwata H, Goettsch C, Sharma A, Ricchiuto P, Goh WW, Halu A, et al. PARP9 and PARP14 cross-regulate macrophage activation via STAT1 ADP-ribosylation. *Nat Commun.* (2016) 7:12849. doi: 10.1038/ncomms12849
- Thomas GD, A.Hamers AJ, Nakao C, Marcovecchio P, Taylor AM, McSkimming C, et al. Human blood monocyte subsets: a new gating strategy defined using cell surface markers identified by mass cytometry. *Arterioscler Thromb Vasc Biol.* (2017) 37:1548–1558. doi: 10.1161/ATVBAHA.117.309145
- Nakano T, Katsuki S, Chen M, Decano JL, Halu A, Lee LH et al. Uremic toxin indoxyl sulfate promotes pro-inflammatory macrophage activation via the interplay of OATB2B1 and DLL4-Notch signaling: potential mechanism for accelerated atherogenesis in chronic kidney disease. *Circulation* 139:78–96. doi: 10.1161/CIRCULATIONAHA.118.034588
- Goergen CJ, Johnson BL, Greve JM, Taylor CA, Zarins CK. Increased anterior abdominal aortic wall motion: possible role in aneurysm pathogenesis and design of endovascular devices. *J Endovasc Ther.* (2007) 14:574–84. doi: 10.1177/152660280701400421
- Scott RA, Bridgewater SG, Ashton HA. Randomized clinical trial of screening for abdominal aortic aneurysm in women. *Br J Surg.* (2002) 89:283–5. doi: 10.1046/j.0007-1323.2001.02014.x
- Silverstein MD, Pitts SR, Chaikof EL, Ballard DJ. Abdominal aortic aneurysm (AAA): cost-effectiveness of screening, surveillance of intermediate-sized AAA, and management of symptomatic AAA. *Proc(Bayl Univ Med Cent)* (2005) 18:345–67. doi: 10.1080/08998280.2005.11928095
- Ailawadi G, Eliason JL, Upchurch GR Jr. Current concepts in the pathogenesis of abdominal aortic aneurysm. *J Vasc Surg.* (2003) 38:584–8. doi: 10.1016/S0741-5214(03)00324-0

25. Fleming C, Whitlock EP, Beil TL, Lederle FA. Screening for abdominal aortic aneurysm: a best-evidence systematic review for the U.S. Preventive Services Task Force. *Ann Intern Med.* (2005) 142:203–11. doi: 10.7326/0003-4819-142-3-20050210-00012
26. Norman PE, Curci JA. Understanding the effects of tobacco smoke on the pathogenesis of aortic aneurysm. *Arterioscler Thromb Vasc Biol.* (2013) 33:1473–7. doi: 10.1161/ATVBAHA.112.300158
27. Helgadottir A, Thorleifsson G, Magnusson KP, Gretarsdottir S, Steinthorsdottir V, Manolescu A, et al. The same sequence variant on 9p21 associates with myocardial infarction, abdominal aortic aneurysm and intracranial aneurysm. *Nat Genet.* (2008) 40:217–24. doi: 10.1038/ng.72
28. Curci JA, Liao S, Huffman MD, Shapiro SD, Thompson RW. Expression and localization of macrophage elastase (matrix metalloproteinase-12) in abdominal aortic aneurysms. *J Clin Invest.* (1998) 102:1900–10. doi: 10.1172/JCI2182
29. Zack M, Boyanovsky BB, Shridas P, Bailey W, Forrest K, Howatt DA, et al. Group X secretory phospholipase A(2) augments angiotensin II-induced inflammatory responses and abdominal aortic aneurysm formation in apoE-deficient mice. *Atherosclerosis* (2011) 214:58–64. doi: 10.1016/j.atherosclerosis.2010.08.054
30. Webb NR, De Beer MC, Wroblewski JM, Ji A, Bailey W, Shridas P, et al. Deficiency of endogenous acute-phase serum amyloid A protects apoE^{-/-} mice from angiotensin II-induced abdominal aortic aneurysm formation. *Arterioscler Thromb Vasc Biol.* (2015) 35:1156–65. doi: 10.1161/ATVBAHA.114.304776
31. Thompson JC, Wilson PG, Shridas P, Ji A, de Beer M, de Beer FC, et al. Serum amyloid A3 is pro-atherogenic. *Atherosclerosis* (2018) 268:32–35. doi: 10.1016/j.atherosclerosis.2017.11.011
32. Branchetti E, Bavaria JE, Grau JB, Shaw RE, Poggio P, Lai EK, et al. Circulating soluble receptor for advanced glycation end product identifies patients with bicuspid aortic valve and associated aortopathies. *Arterioscler Thromb Vasc Biol.* (2014) 34:2349–57. doi: 10.1161/ATVBAHA.114.303784
33. Di Achille P, Tellides G, Figueroa CA, Humphrey JD. A haemodynamic predictor of intraluminal thrombus formation in abdominal aortic aneurysms. *Proc R Soc A* (2014) 470:20140163. doi: 10.1098/rspa.2014.0163
34. Phillips EH, DiAchille P, Bersi MR, Humphrey JD, Goergen CJ. Multimodality imaging enables detailed hemodynamic simulations in dissecting aneurysms in mice. *IEEE Trans Med Imaging* (2017) 36:1297–305. doi: 10.1109/TMI.2017.2664799
35. Humphrey JD, Taylor CA. Intracranial and abdominal aortic aneurysms: similarities, differences, and need for a new class of computational models. *Annu Rev Biomed Eng.* (2008) 10:221–46. doi: 10.1146/annurev.bioeng.10.061807.160439
36. Vorp DA. Biomechanics of abdominal aortic aneurysm. *J Biomech.* (2007) 40:1887–902. doi: 10.1016/j.jbiomech.2006.09.003
37. Vande Geest JP, Di Martino ES, Bohra A, Makaroun MS, Vorp DA. A biomechanics-based rupture potential index for abdominal aortic aneurysm risk assessment: demonstrative application. *Ann N Y Acad Sci.* (2006) 1085:11–21. doi: 10.1196/annals.1383.046
38. Zuhlke LJ, Beaton A, Engel ME, Hugo-Hamman CT, Karthikeyan G, Katzenellenbogen JM, et al. Group A streptococcus, acute rheumatic fever and rheumatic heart disease: epidemiology and clinical considerations. *Curr Treat Options Cardiovasc Med.* (2017) 19:15. doi: 10.1007/s11936-017-0513-y
39. Yutzey KE, Demer LL, Body SC, Huggins GS, Towler DA, Giachelli CM, et al. Calcific aortic valve disease: a consensus summary from the Alliance of Investigators on Calcific Aortic Valve Disease. *Arterioscler Thromb Vasc Biol.* (2014) 34:2387–93. doi: 10.1161/ATVBAHA.114.302523
40. Tseng H, Grande-Allen KJ. Elastic fibers in the aortic valve spongiosa: a fresh perspective on its structure and role in overall tissue function. *Acta Biomater.* (2011) 7:2101–8. doi: 10.1016/j.actbio.2011.01.022
41. Buchanan RM, Sacks MS. Interlayer micromechanics of the aortic heart valve leaflet. *Biomech Model Mechanobiol.* (2014) 13:813–26. doi: 10.1007/s10237-013-0536-6
42. Ayoub S, Ferrari G, Gorman RC, Gorman JH, Schoen FJ, Sacks MS. Heart valve biomechanics and underlying mechanobiology. *Compr Physiol.* (2016) 6:1743–80. doi: 10.1002/cphy.c150048
43. Bakhty AA, Govindjee S, Mofrad MRK. Consistent trilayer biomechanical modeling of aortic valve leaflet tissue. *J Biomech.* (2017) 61:1–10. doi: 10.1016/j.jbiomech.2017.06.014
44. Holliday CJ, Ankeny RF, Jo H, Nerem RM. Discovery of shear- and side-specific mRNAs and miRNAs in human aortic valvular endothelial cells. *Am J Physiol Heart Circ Physiol.* (2011) 301:H856–67. doi: 10.1152/ajpheart.00117.2011
45. Miragoli M, Yacoub MH, El-Hamamsy I, Sanchez-Alonso JL, Moshkov A, Mongkoldhumrongkul N, et al. Side-specific mechanical properties of valve endothelial cells. *Am J Physiol Heart Circ Physiol.* (2014) 307:H15–24. doi: 10.1152/ajpheart.00228.2013
46. Simmons CA, Grant GR, Manduchi E, Davies PF. Spatial heterogeneity of endothelial phenotypes correlates with side-specific vulnerability to calcification in normal porcine aortic valves. *Circ Res.* (2005) 96:792–9. doi: 10.1161/01.RES.0000161998.92009.64
47. El-Hamamsy I, Yacoub MH, Chester AH. Neuronal regulation of aortic valve cusps. *Curr Vasc Pharmacol.* (2009) 7:40–6. doi: 10.2174/157016109787354088
48. Mulholland DL, Gotlieb AI. Cell biology of valvular interstitial cells. *Can J Cardiol.* (1996) 12:231–6.
49. Aikawa E, Whittaker P, Farber M, Mendelson K, Padera RF, Aikawa M, et al. Human semilunar cardiac valve remodeling by activated cells from fetus to adult: implications for postnatal adaptation, pathology, and tissue engineering. *Circulation* (2006) 113:1344–52. doi: 10.1161/CIRCULATIONAHA.105.591768
50. New SE, Aikawa E. Molecular imaging insights into early inflammatory stages of arterial and aortic valve calcification. *Circ Res.* (2011) 108:1381–91. doi: 10.1161/CIRCRESAHA.110.234146
51. Aikawa E, Nahrendorf M, Sosnovik D, Lok VM, Jaffer FA, Aikawa M, et al. Multimodality molecular imaging identifies proteolytic and osteogenic activities in early aortic valve disease. *Circulation* (2007) 115:377–86. doi: 10.1161/CIRCULATIONAHA.106.654913
52. Hutcheson JD, Chen J, Sewell-Loftin MK, Ryzhova LM, Fisher CI, Su YR, et al. Cadherin-11 regulates cell-cell tension necessary for calcific nodule formation by valvular myofibroblasts. *Arterioscler Thromb Vasc Biol.* (2013) 33:114–20. doi: 10.1161/ATVBAHA.112.300278
53. Hutcheson JD, Venkataraman R, Baudenbacher FJ, Merryman WD. Intracellular Ca(2+) accumulation is strain-dependent and correlates with apoptosis in aortic valve fibroblasts. *J Biomech.* (2012) 45:888–94. doi: 10.1016/j.jbiomech.2011.11.031
54. Richards J, El-Hamamsy I, Chen S, Sarang Z, Sarathchandra P, Yacoub MH, et al. Side-specific endothelial-dependent regulation of aortic valve calcification: interplay of hemodynamics and nitric oxide signaling. *Am J Pathol.* (2013) 182:1922–31. doi: 10.1016/j.ajpath.2013.01.037
55. Yip CY, Chen JH, Zhao R, Simmons CA. Calcification by valve interstitial cells is regulated by the stiffness of the extracellular matrix. *Arterioscler Thromb Vasc Biol.* (2009) 29:936–42. doi: 10.1161/ATVBAHA.108.182394
56. Bowler MA, Merryman WD. *In vitro* models of aortic valve calcification: solidifying a system. *Cardiovasc Pathol.* (2015) 24:1–10. doi: 10.1016/j.carpath.2014.08.003
57. Schlotter F, Halu A, Goto S, Blaser MC, Body SC, Lee LH, et al. Spatiotemporal multi-omics mapping generates a molecular atlas of the aortic valve and reveals networks driving disease. *Circulation* (2018) 138:377–93. doi: 10.1161/CIRCULATIONAHA.117.032291
58. Koenig SN, Lincoln J, Garg V. Genetic basis of aortic valvular disease. *Curr Opin Cardiol.* (2017) 32:239–45. doi: 10.1097/HCO.0000000000000384
59. Thanassoulis G, Campbell CY, Owens DS, Smith JG, Smith AV, Peloso GM, et al. Genetic associations with valvular calcification and aortic stenosis. *N Engl J Med.* (2013) 368:503–12. doi: 10.1056/NEJMoa1109034
60. Fiedler AG, Tolis G Jr. Surgical treatment of valvular heart disease: overview of mechanical and tissue prostheses, advantages, disadvantages, and implications for clinical use. *Curr Treat Options Cardiovasc Med.* (2018) 20:7. doi: 10.1007/s11936-018-0601-7
61. Mozaffarian D, Benjamin EJ, Go AS, Arnett DK, Blaha MJ, Cushman M, et al. Heart disease and stroke statistics-2016 update: a report from the American Heart Association. *Circulation* (2016) 133:e38–360. doi: 10.1161/CIR.0000000000000350

62. Otto CM, Burwash IG, Legget ME, Munt BI, Fujioka M, Healy NL, et al. Prospective study of asymptomatic valvular aortic stenosis. Clinical, echocardiographic, and exercise predictors of outcome. *Circulation* (1997) 95:2262–70. doi: 10.1161/01.CIR.95.9.2262
63. Kortland NM, Etnel JRG, Arabkhan B, Mokhles MM, Mohamad A, Roos-Hesselink JW, et al. Mechanical aortic valve replacement in non-elderly adults: meta-analysis and microsimulation. *Eur Heart J*. (2017) 38:3370–7. doi: 10.1093/eurheartj/ehx199
64. Schoen FJ, Levy RJ. Bioprosthetic heart valve failure: pathology and pathogenesis. *Cardiol Clin*. (1984) 2:717–39. doi: 10.1016/S0733-8651(18)30720-3
65. Schoen FJ, Levy RJ. Calcification of tissue heart valve substitutes: progress toward understanding and prevention. *Ann Thorac Surg*. (2005) 79:1072–80. doi: 10.1016/j.athoracsur.2004.06.033
66. Zhao DF, Seco M, Wu JJ, Edelman JB, Wilson MK, Valley MP, et al. Mechanical versus bioprosthetic aortic valve replacement in middle-aged adults: a systematic review and meta-analysis. *Ann Thorac Surg*. (2016) 102:315–27. doi: 10.1016/j.athoracsur.2015.10.092
67. Van Hemelrijck M, Taramasso M, De Carlo C, Kuwata S, Regar E, Nietlispach F, et al. Recent advances in understanding and managing aortic stenosis. *F1000Res* (2018) 7:58. doi: 10.12688/f1000research.11906.1
68. Sondergaard L, Steinbruchel DA, Ihlemann N, Nissen H, Kjeldsen BJ, Petursson P, et al. Two-year outcomes in patients with severe aortic valve stenosis randomized to transcatheter versus surgical aortic valve replacement: the all-comers nordic aortic valve intervention randomized clinical trial. *Circ Cardiovasc Interv*. (2016) 9:e003665. doi: 10.1161/CIRCINTERVENTIONS.115.003665
69. Reardon MJ, Van Mieghem NM, Popma JJ, Kleiman NS, Sondergaard L, Mumtaz M, et al. Surgical or transcatheter aortic-valve replacement in intermediate-risk patients. *N Engl J Med*. (2017) 376:1321–31. doi: 10.1056/NEJMoa1700456
70. Kapadia SR, Leon MB, Makkar RR, Tuzcu EM, Svensson LG, Kodali S, et al. 5-year outcomes of transcatheter aortic valve replacement compared with standard treatment for patients with inoperable aortic stenosis (PARTNER 1): a randomised controlled trial. *Lancet* (2015) 385:2485–91. doi: 10.1016/S0140-6736(15)60290-2
71. Lindman BR, Pibarot P, Arnold SV, Suri RM, McAndrew TC, Maniar HS, et al. Transcatheter versus surgical aortic valve replacement in patients with diabetes and severe aortic stenosis at high risk for surgery: an analysis of the PARTNER Trial (Placement of Aortic Transcatheter Valve). *J Am Coll Cardiol*. (2014) 63:1090–9. doi: 10.1016/j.jacc.2013.10.057
72. Bezuidenhout D, Williams DF, Zilla P. Polymeric heart valves for surgical implantation, catheter-based technologies and heart assist devices. *Biomaterials* (2015) 36:6–25. doi: 10.1016/j.biomaterials.2014.09.013
73. Scherman J, van Breda B, Appa H, Heerden C, Ofoegbu C, Bezuidenhout D, et al. Transcatheter valve with a hollow balloon for aortic valve insufficiency. *Multimed Man Cardiothorac Surg*. (2018) doi: 10.1510/mmcts.2018.012. [Epub ahead of print].
74. Shinoka T, Breuer CK, Tanel RE, Zund G, Miura T, Ma PX, et al. Tissue engineering heart valves: valve leaflet replacement study in a lamb model. *Ann Thorac Surg*. (1995) 60:S513–6. doi: 10.1016/0003-4975(95)00733-4
75. Shinoka T, Ma PX, Shum-Tim D, Breuer CK, Cusick RA, Zund G, et al. Tissue-engineered heart valves. Autologous valve leaflet replacement study in a lamb model. *Circulation* (1996) 94:II164–8.
76. Hjortnaes J, Bouten CV, Van Herwerden LA, Grundeman PF, Kluin J. Translating autologous heart valve tissue engineering from bench to bed. *Tissue Eng Part B Rev*. (2009) 15:307–17. doi: 10.1089/ten.teb.2008.0565
77. Simon P, Kasimir MT, Seebacher G, Weigel G, Ullrich R, Salzer-Muhar U, et al. Early failure of the tissue engineered porcine heart valve SYNERGRAFT in pediatric patients. *Eur J Cardiothorac Surg*. (2003) 23:1002–6, Discussion 1006. doi: 10.1016/S1010-7940(03)00094-0
78. Bibevski S, Scholl FG. Feasibility and early effectiveness of a custom, hand-made systemic atrioventricular valve using porcine extracellular matrix (CorMatrix) in a 4-month-old infant. *Ann Thorac Surg*. (2015) 99:710–2. doi: 10.1016/j.athoracsur.2014.04.140
79. Bibevski S, Levy A, Scholl FG. Mitral valve replacement using a handmade construct in an infant. *Interact Cardiovasc Thorac Surg*. (2017) 24:639–40. doi: 10.1093/icvts/ivw406
80. Ramaswamy S, Lordeus M, Mankame OV, Valdes-Cruz L, Bibevski S, Bell SM, et al. Hydrodynamic assessment of aortic valves prepared from porcine small intestinal submucosa. *Cardiovasc Eng Technol*. (2017) 8:30–40. doi: 10.1007/s13239-016-0290-x
81. Riem Vis PW, Kluin J, Sluijter JP, van Herwerden LA, Bouten CV. Environmental regulation of valvulogenesis: implications for tissue engineering. *Eur J Cardiothorac Surg*. (2011) 39:8–17. doi: 10.1016/j.ejcts.2010.05.032
82. Motta SE, Lintas V, Fioretta ES, Hoerstrup SP, Emmert MY. Off-the-shelf tissue engineered heart valves for in situ regeneration: current state, challenges and future directions. *Expert Rev Med Devices* (2018) 15:35–45. doi: 10.1080/17434440.2018.1419865
83. Emmert MY, Fioretta ES, Hoerstrup SP. Translational challenges in cardiovascular tissue engineering. *J Cardiovasc Transl Res*. (2017) 10:139–49. doi: 10.1007/s12265-017-9728-2
84. Weber B, Emmert MY, Schoenauer R, Brokopp C, Baumgartner L, Hoerstrup SP. Tissue engineering on matrix: future of autologous tissue replacement. *Semin Immunopathol*. (2011) 33:307–15. doi: 10.1007/s00281-011-0258-8
85. Kochupura PV, Azeloglu EU, Kelly DJ, Doronin SV, Badylak SF, Krukenkamp IB, et al. Tissue-engineered myocardial patch derived from extracellular matrix provides regional mechanical function. *Circulation* (2005) 112(9 Suppl.):I144–9. doi: 10.1161/CIRCULATIONAHA.104.524355
86. Badylak S, Obermiller J, Geddes L, Matheny R. Extracellular matrix for myocardial repair. *Heart Surg Forum* (2003) 6:E20–6.
87. Scholl FG, Boucek MM, Chan KC, Valdes-Cruz L, Perryman R. Preliminary experience with cardiac reconstruction using decellularized porcine extracellular matrix scaffold: human applications in congenital heart disease. *World J Pediatr Congenit Heart Surg*. (2010) 1:132–6. doi: 10.1177/2150135110362092
88. Gershlag JR, Hernandez S, Fontana G, Perreault LR, Hansen KJ, Larson SA, et al. Crossing kingdoms: using decellularized plants as perfusable tissue engineering scaffolds. *Biomaterials* (2017) 125:13–22. doi: 10.1016/j.biomaterials.2017.02.011
89. Pavo N, Charwat S, Nyolczas N, Jakab A, Murlasits Z, Bergler-Klein J, et al. Cell therapy for human ischemic heart diseases: critical review and summary of the clinical experiences. *J Mol Cell Cardiol*. (2014) 75:12–24. doi: 10.1016/j.yjmcc.2014.06.016
90. Takahashi K, Yamanaka S. Induction of pluripotent stem cells from mouse embryonic and adult fibroblast cultures by defined factors. *Cell* (2006) 126:663–76. doi: 10.1016/j.cell.2006.07.024
91. Bjerrum OJ. New safe medicines faster: a proposal for a key action within the European union's 6th framework programme. *Pharmacol Toxicol*. (2000) 86(Suppl. 1):23–6. doi: 10.1034/j.1600-0773.86.s1.7.x
92. Petsko GA. When failure should be the option. *BMC Biol*. (2010) 8:61. doi: 10.1186/1741-7007-8-61
93. Gaspar R, Aksu B, Cuine A, Danhof M, Takac MJ, Linden HH, et al. Towards a European strategy for medicines research (2014–2020): the EUEPS position paper on Horizon 2020. *Eur J Pharm Sci*. (2012) 47:979–87. doi: 10.1016/j.ejps.2012.09.020
94. Munro TP, Mahler SM, Huang EP, Chin DY, Gray PP. Bridging the gap: facilities and technologies for development of early stage therapeutic mAb candidates. *MAbs* (2011) 3:440–52. doi: 10.4161/mabs.3.5.16968
95. Schuhmacher A, Gassmann O, Hinder M. Changing R&D models in research-based pharmaceutical companies. *J Transl Med*. (2016) 14:105. doi: 10.1186/s12967-016-0838-4

Conflict of Interest Statement: The authors declare that the research was conducted in the absence of any commercial or financial relationships that could be construed as a potential conflict of interest.

Copyright © 2019 Hutcheson, Goergen, Schoen, Aikawa, Zilla, Aikawa and Gaudette. This is an open-access article distributed under the terms of the Creative Commons Attribution License (CC BY). The use, distribution or reproduction in other forums is permitted, provided the original author(s) and the copyright owner(s) are credited and that the original publication in this journal is cited, in accordance with accepted academic practice. No use, distribution or reproduction is permitted which does not comply with these terms.



Using Acellular Bioactive Extracellular Matrix Scaffolds to Enhance Endogenous Cardiac Repair

Daniyil A. Svystonyuk, Holly E. M. Mewhort and Paul W. M. Fedak*

Section of Cardiac Surgery, Department of Cardiac Sciences, Cumming School of Medicine, Libin Cardiovascular Institute of Alberta, University of Calgary, Calgary, AB, Canada

OPEN ACCESS

Edited by:

Joshua D. Hutcheson,
Florida International University,
United States

Reviewed by:

Glenn Gaudette,
Worcester Polytechnic Institute,
United States
Willi Jahnen-Dechent,
RWTH Aachen Universität, Germany

*Correspondence:

Paul W. M. Fedak
paul.fedak@gmail.com

Specialty section:

This article was submitted to
Atherosclerosis and
Vascular Medicine,
a section of the journal
Frontiers in Cardiovascular Medicine

Received: 04 January 2018

Accepted: 22 March 2018

Published: 11 April 2018

Citation:

Svystonyuk DA., Mewhort HEM. and
Fedak PWM.
(2018) Using Acellular Bioactive
Extracellular Matrix Scaffolds to
Enhance Endogenous Cardiac
Repair.
Front. Cardiovasc. Med. 5:35.
doi: 10.3389/fcvm.2018.00035

An inability to recover lost cardiac muscle following acute ischemic injury remains the biggest shortcoming of current therapies to prevent heart failure. As compared to standard medical and surgical treatments, tissue engineering strategies offer the promise of improved heart function by inducing regeneration of functional heart muscle. Tissue engineering approaches that use stem cells and genetic manipulation have shown promise in preclinical studies but have also been challenged by numerous critical barriers preventing effective clinical translational. We believe that surgical intervention using acellular bioactive ECM scaffolds may yield similar therapeutic benefits with minimal translational hurdles. In this review, we outline the limitations of cellular-based tissue engineering strategies and the advantages of using acellular biomaterials with bioinductive properties. We highlight key anatomic targets enriched with cellular niches that can be uniquely activated using bioactive scaffold therapy. Finally, we review the evolving cardiovascular tissue engineering landscape and provide critical insights into the potential therapeutic benefits of acellular scaffold therapy.

Keywords: extracellular matrix, biomaterials science, cardiovascular diseases, regeneration mechanisms, cardiovascular surgery

INTRODUCTION

Heart failure is a growing epidemic that is predicted to disable 1 in 5 Americans in their life time (1). Despite the prevalence of heart failure, effective treatment options remain limited. Pharmacological interventions can improve symptoms and prolong survival, but are unable to promote functional recovery of cardiomyocytes lost to injury (2). Organ transplantation remains the only curative option but a disparity between donor heart supply and patient demand coupled with the need for immunosuppressive therapy makes this an ineffective solution to address the growing needs of the heart failure population (3). Durable mechanical support therapies continue to evolve and improve but complications for destination therapy patients are a concern.

As our understanding of the factors and mechanisms that regulate heart structure and function have improved, the concept of engineering cardiovascular tissues to restore heart function has rapidly advanced (4, 5). Whole organ regeneration is the ultimate goal of tissue engineering but at present exists only as a futuristic possibility. Early tissue engineering approaches using stem cell and gene therapy have shown promise, but remain fraught with translational hurdles. As such, there has been an increasing shift in focus towards utilizing tissue engineering strategies that can stimulate repair by modulating the host-substrate microenvironment and enhancing endogenous tissue repair processes (6).

In this review, we focus on the translational limitations of contemporary cardiac regenerative approaches and describe how acellular bioactive ECM scaffolds may provide an effective solution. Specifically, we outline important anatomical and cellular targets that may benefit from bioactive scaffold therapy and provide insights into the future of cardiovascular tissue engineering and its translation into viable clinical applications.

EARLY TISSUE ENGINEERING STRATEGIES TOWARDS CARDIAC REGENERATION

The field of cardiovascular tissue engineering was born out of a need to design functional substitutes for tissue that was presumed irreversibly damaged. Leveraging the plasticity of stem cells and direct genetic manipulation became popular options to achieve this goal.

The ability to effectively isolate and expand endogenous stem cells offered the exciting promise of leveraging the cells' inherent regenerative capacity to treat cardiovascular disease (7). Over the past decades there has been significant enthusiasm within the scientific community for cell-therapies based on a foundation of encouraging preclinical evidence. Why is it that cell-mediated regeneration remains absent from conventional treatment modalities? Part of the problem lies in the biology surrounding exogenous cell delivery to the microenvironment of a failing heart. Damaged myocardium lacks the necessary structural and biological microenvironment to support proper cell health and function. Accordingly, it is no surprise that stem cell survival and engraftment is poor and this remains a dominant issue preventing effective clinical translation (8). Interestingly, the benefits of cell therapy are well documented in preclinical animal models despite the fact that cells are delivered to similar hostile microenvironments in the heart. Long term donor cell engraftment and survival is poor yet functional myocardial recovery is readily observed. These findings represent a paradigm shift in our understanding of the cell-mediated therapeutic effect, indicating that the benefits of cell therapy may lie in their ability to act as source of regenerative and reparative paracrine factors (9, 10).

Gene therapy allows targeted control of specific molecular pathways, typically through adenoviral vectors, that can restore lost functionality or enhance endogenous cardiac repair processes (11). Contemporary gene therapy approaches have targeted a number of cardiovascular systems, including: cell metabolic activity, calcium regulation, vasculogenesis, and stem cell activation (12). The concept of targeting single genes to drive critical repair pathways toward functional recovery is exciting but clinical outcomes of gene therapy have been mostly unsuccessful. Of the five cardiac gene therapy clinical trials published to date, all five have shown safety but failed to meet primary efficacy endpoints (13–17). Indeed, targeting a single gene in a pathway that involves multiple complex molecular mechanisms is unlikely to yield appreciable clinical benefit. Interestingly, trials that aimed to genetically bolster stem cell recruitment to the myocardium showed benefit in a cohort of patients with advanced ischemic cardiomyopathy (16).

The lessons learned from attempts at gene therapy for heart failure are important: enhancing targeted molecular pathways and signalling mechanisms in failing myocardium can have substantial therapeutic benefits (18). This challenged the notion that tissue engineering must necessarily be an “outside-in” approach and instead, argued that tissue engineering can occur from within by rescuing and/or stimulating endogenous repair pathways.

LEVERAGING ACELLULAR BIOACTIVE SCAFFOLDS TOWARDS CARDIAC REGENERATION

The paracrine hypothesis of cell therapy and direct genetic manipulation of endogenous repair mechanisms highlights that a failing heart can be primed toward tissue regeneration and repair by altering the signalling environment of the host cells. Acellular bioactive scaffolds serve as niche signalling microenvironments that may be used toward driving cardiac repair (19). While such scaffolds can be synthetic or semi-synthetic and injectable or non-injectable, this report will focus on extracellular matrix (ECM)-based patch biomaterials.

The mainstay of acellular bioactive materials is the extracellular matrix, a structural scaffold that has all of the necessary cues and signals to support proper cell health, function and tissue repair processes (4). Some studies have utilized a simple ECM scaffold consisting of either type I collagen or gelatin as a vessel to deliver a single protein or cell type (20, 21). Conversely, more complex ECM scaffolds may be derived through the decellularization of biological tissue. These scaffolds may exert bioactive effects by way of growth factor reservoirs, matricellular proteins and complex ultrastructural compositions (22, 23).

Early studies characterizing acellular biological tissues have shown that the decellularization process does not disrupt native bioactive constituents present in the ECM scaffolds, such as FGF-2 and VEGF (24). Additionally, degradation products produced by the remodeling of the ECM materials by the host tissue has been shown to affect endogenous cell activity (25). As such, decellularized ECM scaffolds from highly regenerative organs, like the gastrointestinal system, may be used to circumvent the limited regenerative capacity of the heart (26). Following decellularization, the bioactive properties of the ECM can be leveraged without the underlying safety concern of an adverse immunogenic response (22, 24). In fact, Dziki and colleagues demonstrated that acellular bioactive scaffolds may influence macrophage polarization away from a pro-inflammatory M1 phenotype towards a pro-reparative M2 phenotype (27). To date, there have been an abundance of convincing preclinical studies that outline the cardioprotective benefits of ECM biomaterials in the heart (28–32).

Our group has explored epicardially implanted acellular bioactive scaffolds across a number of clinically relevant models of ischemic injury. We first established efficacy in a rodent chronic heart failure model where we demonstrated that surgically implanted ECM scaffolds can attenuate infarct expansion

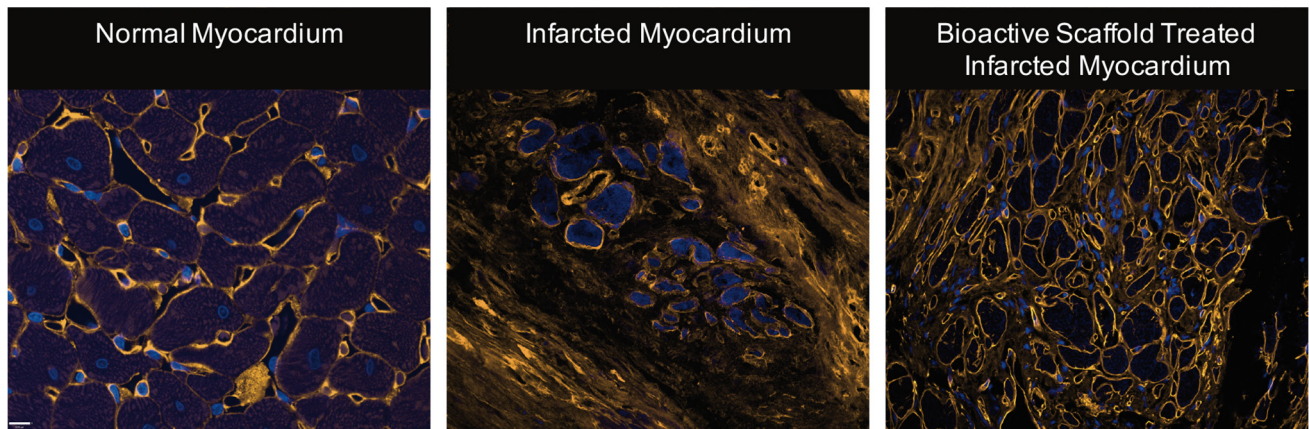


FIGURE 1 | Representative images of normal myocardium, infarcted myocardium from a sham, and infarcted myocardium following surgical implantation of bioactive scaffold on the epicardial surface (blue = nucleus, orange = collagen). The infarct area of bioactive scaffold-treated animals showed less collagen density and ECM architecture more consistent with normal cardiac tissue (Reprinted from *The Journal of Thoracic and Cardiovascular Surgery*, Vol 147/Issue 5, Holly EM Mewhort, Jeannine D Turnbull, Christopher Meijndert, Janet MC Ngu, Paul WM Fedak, Epicardial infarct repair with basic fibroblast growth factor-enhanced CorMatrix-ECM biomaterial attenuates postischemic cardiac remodeling, 1650–1659., Copyright 2014, with permission from Elsevier) (28).

and LV remodeling while simultaneously improving cardiac function (**Figure 1**). Importantly, we demonstrated that bioactive scaffolds can be further enhanced with exogenous growth factors highlighting its capacity as a platform therapy (28, 33). Using a large preclinical porcine model of ischemia-reperfusion, we were able to observe regional myocardial improvements by serial cardiac MRI following surgical implantation of bioactive scaffolds during the acute stage post-MI (**Figure 2**). Interestingly, histological examination of the infarct area in bioactive scaffold-

treated animals showed small arteriole formation next to islands of surviving cardiomyocytes (29). We later confirmed that these beneficial effects are due to bioactive constituents present within the scaffolds and were not the result of a passive myocardial restraint effect (34). Collectively, these findings have given us insight into the optimal therapeutic window for bioactive scaffold therapy and suggest that the greatest benefit may be as an adjunct to surgical macroscopic revascularization where hibernating myocardium is perfused by bioactive scaffold-

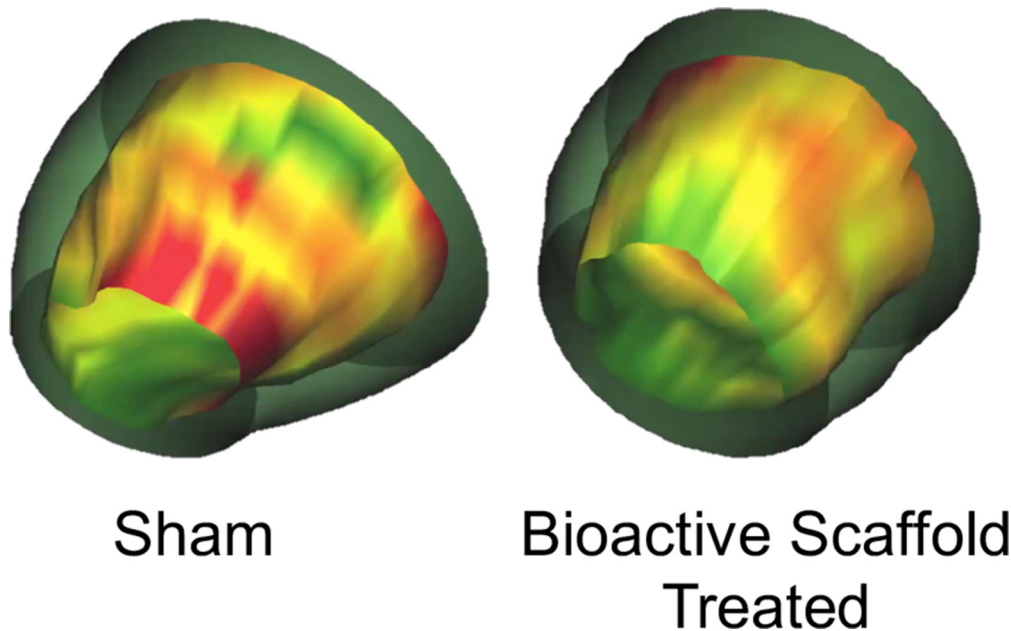


FIGURE 2 | 3-D images of the LV reconstructed from MRI data depicting wall thickening in sham versus bioactive scaffold-treated animals 6 weeks after the initial ischemic event (green = normal, yellow = hypokinetic, red = akinetic). Bioactive scaffold treatment resulted in regional improvement in myocardial function (29).

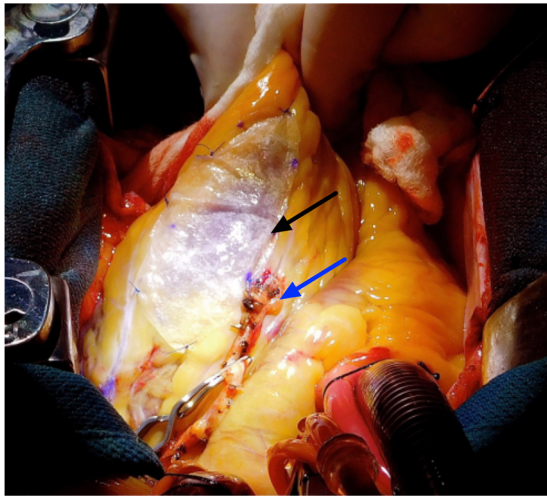


FIGURE 3 | Representative image of surgical implantation of a bioactive scaffold at the time of revascularization surgery. Patients were selected for bioactive scaffold therapy in adjunct with CABG and followed by serial cardiac MRI up to six months following surgery. Black arrow indicates acellular bioactive scaffold. Blue arrow indicates bypass graft.

mediated microvascular formation. At present, we are completing a first-in-man pilot clinical feasibility trial (ClinicalTrials.gov ID: NCT02887768) where acellular bioactive scaffolds are surgically implanted at the time of CABG surgery (**Figure 3**).

Although passive mechanical restraint has been shown to benefit functional recovery of the failing heart, this was not the primary mechanism observed in our studies as scaffold implants did not alter ventricular compliance and vasculogenesis was observed (35, 36). How is it then that acellular bioactive scaffolds can induce adaptive tissue remodeling and improve function? Emerging evidence has identified the plasticity and regenerative capacity of endogenous cells and anatomic structures of the heart (34, 37). Surgically implanted bioactive scaffolds introduce a new signalling microenvironment in the heart that may potentiate these innate regeneration processes. Specifically, altering the function of the epicardium and matrix-modulating cardiac fibroblasts may demonstrate how nature's own platform can be leveraged to promote endogenous cardiac regeneration.

The Epicardium as an Anatomic Niche for Endogenous Repair

Over the past decade, insights from vertebrate studies have identified the epicardium as the key structure responsible for their high cardiac regenerative capacity (38). Understandably, targeting the epicardium for tissue regeneration has been the subject of great therapeutic interest.

The epicardium is the outermost mesothelial layer of the heart surrounding the myocardium (39). In early development, the epicardium is a source of progenitor cells that undergo epithelial to mesenchymal (EMT) transition to yield vascular smooth muscle cells and fibroblasts, with a few studies showing their differentiation into cardiomyocytes and endothelial cells

as well (40–43). Collectively, it is the progenitor cell migration from the pro-epicardial layer that dictates and coordinates cardiomyocyte proliferation and organization, electro-conduction, coronary vasculature assembly, and structural valve and chamber development (44).

While the epicardium plays an active role in the development of the embryonic heart, it exists as a dormant cell layer in the adult uninjured heart (44). However, studies have demonstrated that the genetic programme that drives epicardial-derived cell migration during development is rapidly reactivated in the adult heart in response to ischemic injury (45). Interestingly, the reactivation of the epicardium appears to occur globally throughout the heart and is not localized exclusive to the site of the injury. It was hypothesized that epicardial activation can occur due to external factors present in the pericardial fluid following myocardial infarction (46, 47).

The ability of the epicardium to orchestrate cardiac regeneration versus cardiac repair remains a highly debated topic. Studies in zebrafish and fetal non-vertebrates have identified the epicardium as source of key paracrine factors that are capable of restoring lost cardiac muscle and rescuing heart function after injury (38, 48). Conversely, epicardial activation in adult non-vertebrates following ischemic injury is limited by the number of activated progenitor cells that then differentiate exclusively to non-myocyte cells of the heart (21, 45). The mechanisms that limit regeneration despite preservation of the same embryonic gene programme are not well understood. However, if the epicardium is reactivated through an extra-cardiac paracrine milieu, perhaps modifying the paracrine microenvironment can dictate a more regenerative pathway.

Acellular scaffolds rich in cytokines and growth factors may hold the key to epicardial-driven cardiac regeneration. Using a surgically implanted epicardial patch enriched with human follistatin-like1 protein in preclinical animal models of ischemic injury, Wei and colleagues were able to document evidence of significant cardiogenesis, vasculogenesis and functional recovery in the post-MI hearts (20). Similarly, Wang et al. used a mesenchymal stem cell-loaded epicardial patch implanted one week post-MI and showed preliminary evidence of epicardial-derived progenitor cell activation and differentiation into smooth muscle cells, endothelial cells and cardiomyocytes. Here, the synthetic patch preserved MSC survival and enhanced their expression of key cardioprotective proteins that activated the epicardium toward regeneration (21).

In addition to simple-ECM materials, more complex ECM materials derived from decellularized tissues may be leveraged towards enhanced epicardial activation. As previously discussed, the ECM serves as a natural reservoir of various growth factors and matricellular proteins that can promote tissue regeneration processes (23, 29, 49). In a preclinical porcine model of ischemia-reperfusion injury, our group has shown that the surgical implantation of an intestinal ECM scaffold on the epicardial surface of ischemic tissue resulted in increased epicardial activation (29). These findings were confirmed in a separate study where ECM scaffold therapy resulted in enhanced beta-catenin nuclear localization in the infarct area indicative of epicardial progenitor cell mobilization (34). Interestingly, both models showed evidence

of enhanced vascularity in the infarct region. Since the epicardium is a known source vascular smooth muscle cells and vasculogenic paracrine factors, it is conceivable that epicardial activation following bioactive scaffold implantation can result in new blood vessel formation.

The epicardium serves as an important and necessary structure for endogenous tissue regeneration processes. Most contemporary tissue engineering strategies deliver via an intramyocardial approach and may be incapable of epicardial activation. Conversely, surgically implanted acellular scaffolds can target the epicardium directly and have been shown to enhance cardiac repair and regeneration by way of bioactive constituents that bolster epicardial activation.

Targeting Cardiac Fibroblasts as Mediators of the Cardiac Microenvironment

Cardiac fibroblasts represent approximately 20% of the non-myocyte cell population in the heart and are directly involved in maintaining cardiac structure and remodeling (50, 51). Cardiac fibroblasts regulate the extracellular matrix microenvironment, which in turn influences surrounding cell behavior and tissue processes (52). Under normal physiological conditions, the cardiac fibroblasts are responsible for regulating ECM biology by maintaining a highly coordinated rate of turn over via specialized matrix degrading enzymes and their endogenous inhibitors (53). Due to their close association with the ECM, cardiac fibroblasts are often regarded as sentinel cells that respond to environmental stimuli and modify their behavior accordingly (54).

Under pathophysiological conditions following acute ischemic injury, cardiac fibroblasts have an important role in preserving the heart's mechanical function through the deposition of scar tissue (50, 55). Following the initial inflammatory event that clears the ischemic area of necrotic myocytes, cardiac fibroblasts are chemically recruited to the site of granulation tissue formation and differentiate into a more contractile and secretory phenotype known as myofibroblasts (56, 57). Through a process known as reparative fibrosis, myofibroblasts contribute to wound healing by replacing lost cardiac tissue with a collagenous scar that is able to sustain ventricular load and prevent mechanical rupture (58). Although scar deposition is a necessary and adaptive reparative process, it is the continued activation of cardiac fibroblasts in the injured heart that yield more deleterious consequences to global cardiac structure and function. Understandably, therapies that mitigate scarring in the post-MI heart have been the subject of therapeutic interest.

Although activated fibroblasts have traditionally been considered a terminally differentiated cell type, there is an emerging body of evidence that suggests they are more plastic than previously appreciated. Indeed, Nobel prize winning work has shown mature dermal fibroblasts can be reprogrammed into pluripotent stem cells through invasive genetic manipulation (59). However, can cellular reprogramming or redirection of fibroblast behaviour be also achieved by changing the host-substrate environment, such as using bioactive ECM scaffolds? In a landmark study, Plikus et al. demonstrated that the fate of dermal myofibroblasts can be changed

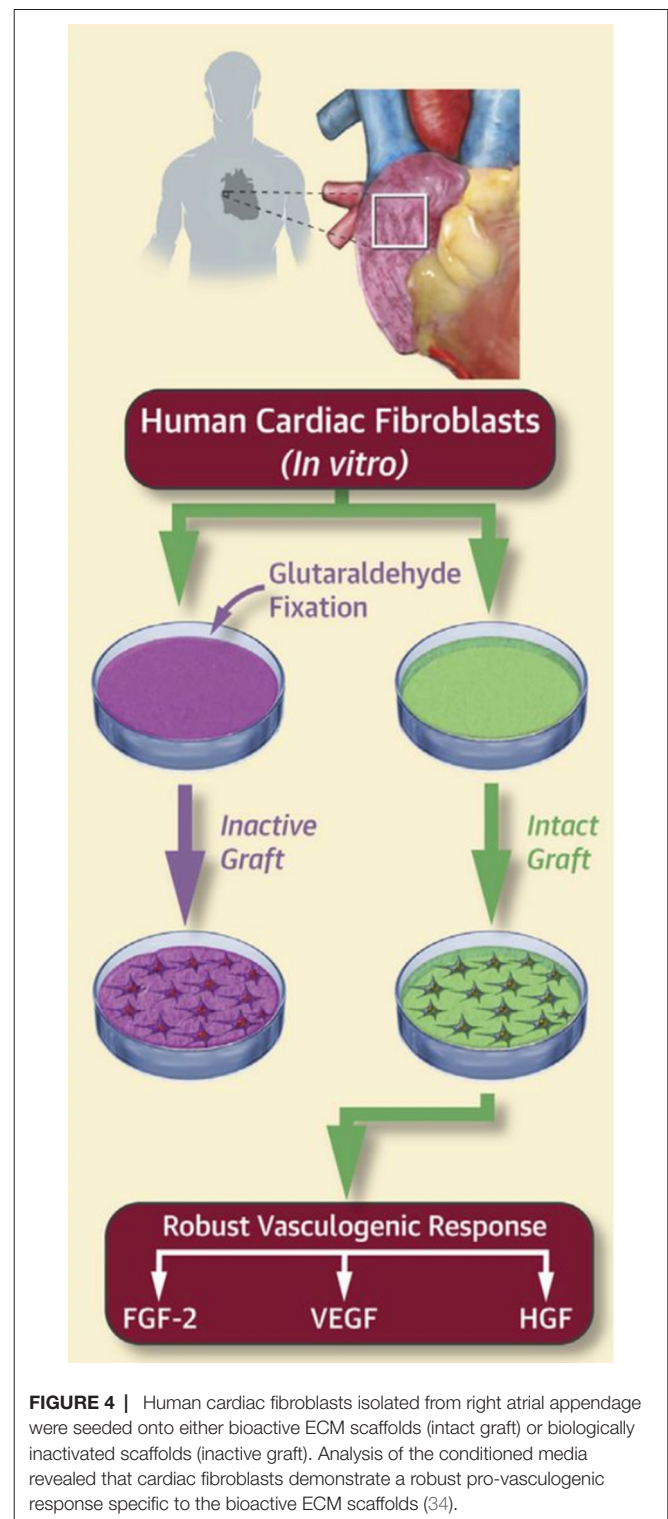


FIGURE 4 | Human cardiac fibroblasts isolated from right atrial appendage were seeded onto either bioactive ECM scaffolds (intact graft) or biologically inactivated scaffolds (inactive graft). Analysis of the conditioned media revealed that cardiac fibroblasts demonstrate a robust pro-vasculogenic response specific to the bioactive ECM scaffolds (34).

towards a regenerative adipocyte lineage by exposing cells to a new signaling microenvironment. Interestingly, these findings were replicated in myofibroblasts isolated from patients with keloids, which are characterized as pathologic scars formed by persistent myofibroblast activity (60).

Similar to keloids, the cardiac myofibroblasts in the injured heart remain continuously activated, resulting in infarct scar expansion, thinning and stiffening of the remote myocardium (53, 61–63). Here, sustained myofibroblast activity is the product of the physiologically distinct microenvironment of a healing wound characterized by complex chemical and mechanical stimuli (64, 65). Surgically implanted bioactive scaffolds may therefore target cardiac myofibroblasts directly by way of instructive paracrine and structural mediators, changing their phenotype to restore tissue homeostasis and regeneration.

Our group has recently explored this idea using cardiac myofibroblasts derived from human atria. We have shown that human cardiac myofibroblasts increase expression of key vasculogenic proteins when seeded on acellular ECM scaffolds rich with bioactive constituents (**Figure 4**) (34). In a rodent infarct model, we documented neovascularization with elevated concentrations of pro-vasculogenic factors in the infarcted myocardium as late as 14 weeks following ECM scaffold implantation. In a separate study, we show that ECM scaffold therapy attenuates infarct scar expansion and restores ECM homeostasis (28). Since cardiac myofibroblasts are the most abundant cell type in the infarct area (66), our collective results suggest the bioactive scaffolds may be driving the cells towards a pro-vasculogenic phenotype that create a paracrine microenvironment favoring new blood vessel formation and mitigating excessive scar deposition.

Although fibroblasts are a distinctly heterogeneous cell type, one thing that remains constant regardless of cell origin is their ability to change their behaviour and phenotype in response to different biochemical and biomechanical cues (67). Further studies characterizing the plasticity of cardiac fibroblasts to new signalling microenvironments introduced by biomaterials are warranted.

CHANGING LANDSCAPE OF TISSUE ENGINEERING

The future of tissue engineering will require synergy among conventional approaches that have been classically studied in a mutually exclusive manner. Combining bioactive scaffolds with other established tissue engineering strategies may hold the key to catalyzing endogenous cardiac repair mechanisms and promoting true cardiovascular tissue regeneration (68).

The strengths of bioactive scaffolds are realized not only as an effective standalone therapy, but also as a platform to deliver therapeutic agents directly to the heart. Our group has demonstrated that bioactive scaffolds can be loaded with exogenous growth factors beyond what is naturally present in the scaffolds alone (28, 33). Targeting the epicardial space may improve myocardial uptake while limiting systemic recirculation as compared to the traditional intramyocardial approach. This can mean more targeted delivery of pharmacologic therapeutics specific to cardiovascular processes.

Additionally, bioactive scaffolds may be used in conjunction with cell therapy and resolve cell engraftment and survival issues associated

with intracoronary or intramuscular delivery (69). Preliminary studies have shown improved stem cell survival when tethered to ECM-based patches as well as enhanced tolerance for the hostile post-MI microenvironment (21, 70–73). The preserved biochemical and biomechanical signature of acellular bioactive scaffolds has been shown to drive cardiogenesis from seeded stem cells and augment pro-regenerative signalling (72, 74, 75). Evidence from early clinical trials support the feasibility and safety of the cell-scaffold approach (76, 77). Results from the ongoing ESCORT trial (ClinicalTrials.gov ID: NCT02057900) will provide valuable insight into the therapeutic efficacy of epicardially implanted bioactive scaffolds seeded with cardiac-committed stem cells.

Regardless of the approach, bioactive scaffolds represent a tunable platform that can be further engineered towards the specific clinical characteristics of the recipient patient. In this way, the use of acellular bioactive scaffolds complements the changing clinical landscape that is becoming increasingly focused on personalized and precise therapies.

CONCLUSION

Standard therapy for ischemic heart disease patients fails to restore functional cardiac tissue. The heart contains a number of intrinsic repair processes and cell types that may be manipulated or bolstered to promote adaptive repair and regeneration. The use of acellular bioactive scaffolds for cardiac repair and regeneration is rationalized by two key points. First, bioactive scaffolds represent a unique signalling microenvironment that can target niche anatomic structures, like the epicardium, to activate endogenous repair mechanisms. Additionally, they may redirect the activity of native cardiac fibroblasts, whose fate and function is closely associated with their microenvironment, towards a more regenerative phenotype. Second, bioactive scaffolds can be leveraged as a platform for exogenous growth factors and stem cells, further maximizing their therapeutic efficacy by eliminating the common hurdles of associated with delivery. Collectively, acellular bioactive scaffolds represent a unique frontier in cardiovascular tissue engineering that may yield promising clinical outcomes.

AUTHOR CONTRIBUTIONS

DS, HM, and PF designed, drafted and revised the manuscript.

FUNDING

Project funding was provided to Dr. Fedak by Heart and Stroke Foundation of Canada. Salary support for Dr. Mewhort was provided by Alberta Innovates Health Solutions. Salary support for Mr. Svystonyuk was provided by Alberta Innovates Health Solutions and the Killam Trusts. Funding for clinical translation (phase 1 feasibility trial) was provided by CorMatrix Cardiovascular Inc.

REFERENCES

- Benjamin EJ, Blaha MJ, Chiuve SE, Cushman M, Das SR, Deo R, et al. Heart disease and stroke statistics-2017 update: A report from the American Heart Association. *Circulation* (2017) 135(10):e146–603. doi: 10.1161/CIR.0000000000000485
- Yancy CW, Jessup M, Bozkurt B, Butler J, Casey DE, Colvin MM, et al. 2017 ACC/AHA/HFSA focused update of the 2013 ACCF/AHA guideline for the management of heart failure: A report of the American College of Cardiology/American Heart Association Task Force on Clinical Practice Guidelines and the Heart Failure Society of America. *Circulation* (2017) 136(6):e137–61. doi: 10.1161/CIR.0000000000000509
- Garbade J, Barten MJ, Bittner HB, Mohr FW. Heart transplantation and left ventricular assist device therapy: two comparable options in end-stage heart failure? *Clin Cardiol* (2013) 36(7):378–82. doi: 10.1002/clc.22124
- Akhyari P, Kamiya H, Haverich A, Karck M, Lichtenberg A. Myocardial tissue engineering: the extracellular matrix. *Eur J Cardiothorac Surg* (2008) 34(2):229–41. doi: 10.1016/j.ejcts.2008.03.062
- Ogle BM, Bursac N, Domian I, Huang NF, Menasché P, Murry CE, et al. Distilling complexity to advance cardiac tissue engineering. *Sci Transl Med* (2016) 8(342):342ps13. doi: 10.1126/scitranslmed.aad2304
- Mcdonald MA, Ashley EA, Fedak PWM, Hawkins N, Januzzi JL, McMurray JJV, et al. Mind the gap: current challenges and future state of heart failure care. *Can J Cardiol* (2017) 33(11):1434–49. doi: 10.1016/j.cjca.2017.08.023
- Matsa E, Sallam K, Wu JC, Jc W. Cardiac stem cell biology: glimpse of the past, present, and future. *Circ Res* (2014) 114(1):21–7. doi: 10.1161/CIRCRESAHA.113.302895
- Nguyen PK, Neofytou E, Rhee JW, Wu JC, Jc W. Potential strategies to address the major clinical barriers facing stem cell regenerative therapy for cardiovascular disease: a review. *JAMA Cardiol* (2016) 1(8):953–10. doi: 10.1001/jamacardio.2016.2750
- Menasché P. The future of stem cells: Should we keep the "stem" and skip the "cells"? *J Thorac Cardiovasc Surg* (2016) 152(2):345–9. doi: 10.1016/j.jtcvs.2016.02.058
- Menasché P, Vanneau V. Stem cells for the treatment of heart failure. *Curr Res Transl Med* (2016) 64(2):97–106. doi: 10.1016/j.retram.2016.04.003
- Matkar PN, Leong-Poi H, Singh KK. Cardiac gene therapy: are we there yet? *Gene Ther* (2016) 23(8–9):635–48. doi: 10.1038/gt.2016.43
- Kawase Y, Ladage D, Hajjar RJ. Rescuing the failing heart by targeted gene transfer. *J Am Coll Cardiol* (2011) 57(10):1169–80. doi: 10.1016/j.jacc.2010.11.023
- Jessup M, Greenberg B, Mancini D, Cappola T, Pauly DF, Jaski B, et al. Calcium Upregulation by Percutaneous Administration of Gene Therapy in Cardiac Disease (CUPID): a phase 2 trial of intracoronary gene therapy of sarcoplasmic reticulum Ca²⁺-ATPase in patients with advanced heart failure. *Circulation* (2011) 124(3):304–13. doi: 10.1161/CIRCULATIONAHA.111.022889
- Greenberg B, Butler J, Felker GM, Pomikowski P, Voors AA, Desai AS, et al. Calcium upregulation by percutaneous administration of gene therapy in patients with cardiac disease (CUPID 2): a randomised, multinational, double-blind, placebo-controlled, phase 2b trial. *Lancet* (2016) 387(10024):1178–86. doi: 10.1016/S0140-6736(16)00082-9
- Hulot J-S, Salem J-E, Redheuil A, Collet J-P, Varnous S, Jourdain P. Effect of intracoronary administration of AAV 1 / SERCA2a on ventricular remodelling in patients with advanced systolic heart failure : results from the AGENT-HF randomized phase 2 trial. *Eur J Heart Fail* (2017):1–8.
- Chung ES, Miller L, Patel AN, Anderson RD, Mendelsohn FO, Traverse J, et al. Changes in ventricular remodelling and clinical status during the year following a single administration of stromal cell-derived factor-1 non-viral gene therapy in chronic ischaemic heart failure patients: the STOP-HF randomized Phase II trial. *Eur Heart J* (2015) 36(33):2228–38. doi: 10.1093/eurheartj/ehv254
- Hammond HK, Penny WF, Traverse JH, Henry TD, Watkins MW, Yancy CW, et al. Intracoronary gene transfer of adenylyl cyclase 6 in patients with heart failure: a randomized clinical trial. *JAMA Cardiol* (2016) 1(2):1–9. doi: 10.1001/jamacardio.2016.0008
- Chaanine AH, Kalman J, Hajjar RJ. Cardiac gene therapy. *Semin Thorac Cardiovasc Surg* (2010) 22(2):127–39. doi: 10.1053/j.semtcvs.2010.09.009
- Burdick JA, Mauck RL, Gorman JH, Gorman RC. Acellular biomaterials: an evolving alternative to cell-based therapies. *Sci Transl Med* (2013) 5(176):176ps4–9. doi: 10.1126/scitranslmed.3003997
- Wei K, Serpooshan V, Hurtado C, Diez-Cuñado M, Zhao M, Maruyama S, et al. Epicardial FSTL1 reconstitution regenerates the adult mammalian heart. *Nature* (2015) 525(7570):479–85. doi: 10.1038/nature15372
- Wang QL, Wang HJ, Li ZH, Wang YL, Wu XP, Tan YZ. Mesenchymal stem cell-loaded cardiac patch promotes epicardial activation and repair of the infarcted myocardium. *J Cell Mol Med* (2017) 21(9):1751–66. doi: 10.1111/jcmm.13097
- Badylak SF, Freytes DO, Gilbert TW. Extracellular matrix as a biological scaffold material: Structure and function. *Acta Biomater* (2009) 5(1):1–13. doi: 10.1016/j.actbio.2008.09.013
- Robinson KA, Li J, Mathison M, Redkar A, Cui J, Chronos NA, et al. Extracellular matrix scaffold for cardiac repair. *Circulation* (2005) 112(9 Suppl):I-135–43. doi: 10.1161/CIRCULATIONAHA.104.525436
- Voytik-Harbin SL, Brightman AO, Kraine MR, Waisner B, Badylak SF. Identification of extractable growth factors from small intestinal submucosa. *J Cell Biochem* (1997) 67(4):478–91. doi: 10.1002/(SICI)1097-4644(19971215)67:4<478::AID-JCB6>3.0.CO;2-P
- Sicari BM, Dziki JL, Siu BF, Medberry CJ, Dearth CL, Badylak SF. The promotion of a constructive macrophage phenotype by solubilized extracellular matrix. *Biomaterials* (2014) 35(30):8605–12. doi: 10.1016/j.biomaterials.2014.06.060
- Hussey GS, Keane TJ, Badylak SF. The extracellular matrix of the gastrointestinal tract: a regenerative medicine platform. *Nat Rev Gastroenterol Hepatol* (2017) 14(9):540–52. doi: 10.1038/nrgastro.2017.76
- Dziki JL, Sicari BM, Wolf MT, Cramer MC, Badylak SF. Immunomodulation and mobilization of progenitor cells by extracellular matrix bioscaffolds for volumetric muscle loss treatment. *Tissue Eng Part A* (2016) 22(19–20):1129–39. doi: 10.1089/ten.tea.2016.0340
- Mewhort HE, Turnbull JD, Meijndert HC, Ngu JM, Fedak PW. Epicardial infarct repair with basic fibroblast growth factor-enhanced CorMatrix-ECM biomaterial attenuates postischemic cardiac remodeling. *J Thorac Cardiovasc Surg* (2014) 147(5):1650–9. doi: 10.1016/j.jtcvs.2013.08.005
- Mewhort HE, Turnbull JD, Satriano A, Chow K, Flewitt JA, Andrei AC, et al. Epicardial infarct repair with bioinductive extracellular matrix promotes vasculogenesis and myocardial recovery. *J Heart Lung Transplant* (2016) 35(5):661–70. doi: 10.1016/j.healun.2016.01.012
- Efraim Y, Sarig H, Cohen AN, Sarig U, de Berardinis E, Chaw SY, et al. Biohybrid cardiac ECM-based hydrogels improve long term cardiac function post myocardial infarction. *Acta Biomater* (2017) 50:220–33. doi: 10.1016/j.actbio.2016.12.015
- Sarig U, Sarig H, de-Berardinis E, Chaw SY, Nguyen EB, Ramanujam VS, et al. Natural myocardial ECM patch drives cardiac progenitor based restoration even after scarring. *Acta Biomater* (2016) 44:209–20. doi: 10.1016/j.actbio.2016.08.031
- Seif-Naraghi SB, Singelyn JM, Salvatore MA, Osborn KG, Wang JJ, Sampat U, et al. Safety and efficacy of an injectable extracellular matrix hydrogel for treating myocardial infarction. *Sci Transl Med* (2013) 5(173):173ra25–10. doi: 10.1126/scitranslmed.3005503
- Park DSJ, Mewhort HEM, Teng G, Belke D, Turnbull J, Svystonyuk D, et al. Heparin augmentation enhances bioactive properties of acellular extracellular matrix scaffold. *Tissue Eng Part A* (2018) 24(1–2):128–34. doi: 10.1089/ten.tea.2017.0004
- Mewhort HEM, Svystonyuk DA, Turnbull JD, Teng G, Belke DD, Guzzardi DG, et al. Bioactive extracellular matrix scaffold promotes adaptive cardiac remodeling and repair. *JACC: Basic to Translational Science* (2017) 2(4):450–64. doi: 10.1016/j.jacbs.2017.05.005
- Costanzo MR, Ivanhoe RJ, Kao A, Anand IS, Bank A, Boehmer J, et al. Prospective evaluation of elastic restraint to lessen the effects of heart failure (PEERLESS-HF) trial. *J Card Fail* (2012) 18(6):446–58. doi: 10.1016/j.cardfail.2012.04.004
- Abraham WT, Anand I, Aranda JM, Boehmer J, Costanzo MR, Demarco T, et al. Randomized controlled trial of ventricular elastic support therapy in the treatment of symptomatic heart failure: rationale and design. *Am Heart J* (2012) 164(5):638–45. doi: 10.1016/j.ahj.2012.07.015
- Smart N, Riley PR. The epicardium as a candidate for heart regeneration. *Future Cardiol* (2012) 8(1):53–69. doi: 10.2217/fca.11.87
- Lepilina A, Coon AN, Kikuchi K, Holdway JE, Roberts RW, Burns CG, et al. A dynamic epicardial injury response supports progenitor cell activity during zebrafish heart regeneration. *Cell* (2006) 127(3):607–19. doi: 10.1016/j.cell.2006.08.052

39. van Wijk B, Gunst QD, Moorman AF, van den Hoff MJ. Cardiac regeneration from activated epicardium. *PLoS ONE* (2012) 7(9):e44692. doi: 10.1371/journal.pone.0044692
40. Katz TC, Singh MK, Degenhardt K, Rivera-Feliciano J, Johnson RL, Epstein JA, et al. Distinct compartments of the proepicardial organ give rise to coronary vascular endothelial cells. *Dev Cell* (2012) 22(3):639–50. doi: 10.1016/j.devcel.2012.01.012
41. Zhou B, Ma Q, Rajagopal S, Sm W, Domian I, Rivera-Feliciano J. Epicardial progenitors contribute to the cardiomyocyte lineage in the developing heart. *Cardiovasc Res* (2009) 454:109–13.
42. Gittenberger-de Groot AC, Vrancken Peeters MP, Mentink MM, Gourdie RG, Poelmann RE. Epicardium-derived cells contribute a novel population to the myocardial wall and the atrioventricular cushions. *Circ Res* (1998) 82(10):1043–52. doi: 10.1161/01.RES.82.10.1043
43. Cai CL, Martin JC, Sun Y, Cui L, Wang L, Ouyang K, et al. A myocardial lineage derives from Tbx18 epicardial cells. *Nature* (2008) 454(7200):104–8. doi: 10.1038/nature06969
44. Smits AM, Dronkers E, Goumans MJ. The epicardium as a source of multipotent adult cardiac progenitor cells: their origin, role and fate. *Pharmacol Res* (2018) 127:129–40. doi: 10.1016/j.phrs.2017.07.020
45. Zhou B, Honor LB, He H, Ma Q, Oh JH, Butterfield C, et al. Adult mouse epicardium modulates myocardial injury by secreting paracrine factors. *J Clin Invest* (2011) 121(5):1894–904. doi: 10.1172/JCI45529
46. Foglio E, Puddighinu G, Fasanaro P, D'Arcangelo D, Perrone GA, Mocini D, et al. Exosomal clusterin, identified in the pericardial fluid, improves myocardial performance following MI through epicardial activation, enhanced arteriogenesis and reduced apoptosis. *Int J Cardiol* (2015) 197:333–47. doi: 10.1016/j.ijcard.2015.06.008
47. Limana F, Bertolami C, Mangoni A, di Carlo A, Avitabile D, Mocini D, et al. Myocardial infarction induces embryonic reprogramming of epicardial c-kit(+) cells: role of the pericardial fluid. *J Mol Cell Cardiol* (2010) 48(4):609–18. doi: 10.1016/j.yjmcc.2009.11.008
48. Chen T, Chang TC, Kang JO, Choudhary B, Makita T, Tran CM, et al. Epicardial induction of fetal cardiomyocyte proliferation via a retinoic acid-inducible trophic factor. *Dev Biol* (2002) 250(1):198–207. doi: 10.1006/dbio.2002.0796
49. Faulk DM, Johnson SA, Zhang L, Badylak SF. Role of the extracellular matrix in whole organ engineering. *J Cell Physiol* (2014) 229(8):984–9. doi: 10.1002/jcp.24532
50. Baudino TA, Carver W, Giles W, Borg TK. Cardiac fibroblasts: friend or foe? *Am J Physiol Heart Circ Physiol* (2006) 291(3):H1015–H1026. doi: 10.1152/ajpheart.00023.2006
51. Pinto AR, Ilinykh A, Ivey MJ, Kuwabara JT, D'Antoni ML, Debuque R, et al. Revisiting cardiac cellular composition. *Circ Res* (2016) 118(3):400–9. doi: 10.1161/CIRCRESAHA.115.307778
52. Tallquist MD, Molkenin JD. Redefining the identity of cardiac fibroblasts. *Nat Rev Cardiol* (2017) 14(8):484–. doi: 10.1038/nrcardio.2017.57
53. Fedak PWM, Verma S, Weisel RD, Li R-K. Cardiac remodeling and failure. *Cardiovascular Pathology* (2005) 14(2):49–60. doi: 10.1016/j.carpath.2005.01.005
54. Diaz-Araya G, Vivar R, Humeres C, Boza P, Bolivar S, Muñoz C. Cardiac fibroblasts as sentinel cells in cardiac tissue: receptors, signaling pathways and cellular functions. *Pharmacol Res* (2015) 101:30–40. doi: 10.1016/j.phrs.2015.07.001
55. Camelliti P, Borg TK, Kohl P. Structural and functional characterisation of cardiac fibroblasts. *Cardiovasc Res* (2005) 65(1):40–51. doi: 10.1016/j.cardiores.2004.08.020
56. Willems IE, Havenith MG, de Mey JG, Daemen MJ. The alpha-smooth muscle actin-positive cells in healing human myocardial scars. *Am J Pathol* (1994) 145(4):868–75.
57. Talman V, Ruskoaho H. Cardiac fibrosis in myocardial infarction—from repair and remodeling to regeneration. *Cell Tissue Res* (2016) 365(3):563–81. doi: 10.1007/s00441-016-2431-9
58. Bassat E, Mutlak YE, Genzelinakh A, Shadrin IY, Baruch Umansky K, Yifa O, et al. The extracellular matrix protein agrin promotes heart regeneration in mice. *Nature* (2017) 547(7662):179–84. doi: 10.1038/nature22978
59. Takahashi K, Tanabe K, Ohnuki M, Narita M, Ichisaka T, Tomoda K, et al. Induction of pluripotent stem cells from adult human fibroblasts by defined factors. *Cell* (2007) 131(5):861–72. doi: 10.1016/j.cell.2007.11.019
60. Plikus MV, Guerrero-Juarez CF, Ito M, Li YR, Dedhia PH, Zheng Y, et al. Regeneration of fat cells from myofibroblasts during wound healing. *Science* (2017) 355(6326):748–52. doi: 10.1126/science.aai8792
61. Czubryt MP. Common threads in cardiac fibrosis, infarct scar formation, and wound healing. *Fibrogenesis Tissue Repair* (2012) 5(1):19. doi: 10.1186/1755-1536-5-19
62. Burstein B, Nattel S. Atrial fibrosis: mechanisms and clinical relevance in atrial fibrillation. *J Am Coll Cardiol* (2008) 51(8):802–9. doi: 10.1016/j.jacc.2007.09.064
63. Krenning G, Zeisberg EM, Kalluri R. The origin of fibroblasts and mechanism of cardiac fibrosis. *J Cell Physiol* (2010) 225(3):631–7. doi: 10.1002/jcp.22322
64. Yong KW, Li Y, Huang G, Lu TJ, Safwani WK, Pinguan-Murphy B, et al. Mechanoregulation of cardiac myofibroblast differentiation: implications for cardiac fibrosis and therapy. *Am J Physiol Heart Circ Physiol* (2015) 309(4):H532–H542. doi: 10.1152/ajpheart.00299.2015
65. Moore-Morris T, Guimarães-Camboia N, Yutzey KE, Pucéat M, Evans SM. Cardiac fibroblasts: from development to heart failure. *J Mol Med* (2015) 93(8):823–30. doi: 10.1007/s00109-015-1314-y
66. Ma Y, Iyer RP, Jung M, Czubryt MP, Lindsey ML. Cardiac fibroblast activation post-myocardial infarction: current knowledge gaps. *Trends Pharmacol Sci* (2017) 38(5):448–58. doi: 10.1016/j.tips.2017.03.001
67. Hannan RT, Peirce SM, Barker TH. Fibroblasts: diverse cells critical to biomaterials integration. *ACS Biomater Sci Eng* (2017). doi: 10.1021/acsbomaterials.7b00244
68. Rafatian G, Davis DR. The frustration and futility of intracoronary stem cell therapy. *Can J Cardiol* (2017) 33(12):1510–2. doi: 10.1016/j.cjca.2017.09.023
69. Lakshmanan R, Krishnan UM, Sethuraman S. Living cardiac patch: the elixir for cardiac regeneration. *Expert Opin Biol Ther* (2012) 12(12):1623–40. doi: 10.1517/14712598.2012.721770
70. Miyagi Y, Chiu LL, Cimini M, Weisel RD, Radisic M, Li RK. Biodegradable collagen patch with covalently immobilized VEGF for myocardial repair. *Biomaterials* (2011) 32(5):1280–90. doi: 10.1016/j.biomaterials.2010.10.007
71. Blondiaux E, Pidal L, Autret G, Rahmi G, Balvy D, Audureau E, et al. Bone marrow-derived mesenchymal stem cell-loaded fibrin patches act as a reservoir of paracrine factors in chronic myocardial infarction. *J Tissue Eng Regen Med* (2017) 11(12):3417–27. doi: 10.1002/term.2255
72. Wang L, Meier EM, Tian S, Lei I, Liu L, Xian S, et al. Transplantation of Isl1⁺ cardiac progenitor cells in small intestinal submucosa improves infarcted heart function. *Stem Cell Res Ther* (2017) 8(1):230. doi: 10.1186/s13287-017-0675-2
73. Simpson D, Liu H, Fan TH, Nerem R, Dudley SC. A tissue engineering approach to progenitor cell delivery results in significant cell engraftment and improved myocardial remodeling. *Stem Cells* (2007) 25(9):2350–7. doi: 10.1634/stemcells.2007-0132
74. Ott HC, Matthies TS, Goh SK, Black LD, Kren SM, Netoff TI, et al. Perfusion-decellularized matrix: using nature's platform to engineer a bioartificial heart. *Nat Med* (2008) 14(2):213–21. doi: 10.1038/nm1684
75. Chang CW, Petrie T, Clark A, Lin X, Sondergaard CS, Griffiths LG. Mesenchymal stem cell seeding of porcine small intestinal submucosal extracellular matrix for cardiovascular applications. *PLoS ONE* (2016) 11(4):e0153412–9. doi: 10.1371/journal.pone.0153412
76. Miyagawa S, Domae K, Yoshikawa Y, Fukushima S, Nakamura T, Saito A, et al. Phase I clinical trial of autologous stem cell-sheet transplantation therapy for treating cardiomyopathy. *J Am Heart Assoc* (2017) 6(4):e003918–13. doi: 10.1161/JAHA.116.003918
77. Chachques JC, Trainini JC, Lago N, Masoli OH, Barisani JL, Cortes-Morichetti M, et al. Myocardial assistance by grafting a new bioartificial upgraded myocardium (MAGNUM clinical trial): one year follow-up. *Cell Transplant* (2007) 16(9):927–34. doi: 10.3727/096368907783338217

Conflict of Interest Statement: The authors declare that the research was conducted in the absence of any commercial or financial relationships that could be construed as a potential conflict of interest.

Copyright © 2018 Svystonyuk, Mewhort and Fedak. This is an open-access article distributed under the terms of the Creative Commons Attribution License (CC BY). The use, distribution or reproduction in other forums is permitted, provided the original author(s) and the copyright owner are credited and that the original publication in this journal is cited, in accordance with accepted academic practice. No use, distribution or reproduction is permitted which does not comply with these terms.



Development of a Contractile Cardiac Fiber From Pluripotent Stem Cell Derived Cardiomyocytes

Katrina J. Hansen¹, Michael A. Laflamme² and Glenn R. Gaudette^{1*}

¹ Department of Biomedical Engineering, Worcester Polytechnic Institute, Worcester, MA, United States, ² Toronto General Hospital Research Institute, McEwen Centre for Regenerative Medicine, University Health Network, Toronto, ON, Canada

OPEN ACCESS

Edited by:

Julie A. Phillippi,
University of Pittsburgh,
United States

Reviewed by:

Mahmood Khan,
The Ohio State University,
United States
Philipp Diehl,
Universitäts-Herzzentrum Freiburg,
Germany

*Correspondence:

Glenn R. Gaudette
gaudette@wpi.edu

Specialty section:

This article was submitted to
Atherosclerosis and
Vascular Medicine,
a section of the journal
Frontiers in Cardiovascular Medicine

Received: 27 December 2017

Accepted: 04 May 2018

Published: 11 June 2018

Citation:

Hansen KJ, Laflamme MA and
Gaudette GR
(2018) Development of a Contractile
Cardiac Fiber From Pluripotent Stem
Cell Derived Cardiomyocytes.
Front. Cardiovasc. Med. 5:52.
doi: 10.3389/fcvm.2018.00052

Stem cell therapy has the potential to regenerate cardiac function after myocardial infarction. In this study, we sought to examine if fibrin microthread technology could be leveraged to develop a contractile fiber from human pluripotent stem cell derived cardiomyocytes (hPS-CM). hPS-CM seeded onto fibrin microthreads were able to adhere to the microthread and began to contract seven days after initial seeding. A digital speckle tracking algorithm was applied to high speed video data (>60 fps) to determine contraction behaviour including beat frequency, average and maximum contractile strain, and the principal angle of contraction of hPS-CM contracting on the microthreads over 21 days. At day 7, cells seeded on tissue culture plastic beat at 0.83 ± 0.25 beats/sec with an average contractile strain of $4.23 \pm 0.23\%$, which was significantly different from a beat frequency of 1.11 ± 0.45 beats/sec and an average contractile strain of $3.08 \pm 0.19\%$ at day 21 ($n = 18$, $p < 0.05$). hPS-CM seeded on microthreads beat at 0.84 ± 0.15 beats/sec with an average contractile strain of $3.56 \pm 0.22\%$, which significantly increased to 1.03 ± 0.19 beats/sec and $4.47 \pm 0.29\%$, respectively, at 21 days ($n = 18$, $p < 0.05$). At day 7, 27% of the cells had a principle angle of contraction within 20 degrees of the microthread, whereas at day 21, 65% of hPS-CM were contracting within 20 degrees of the microthread ($n = 17$). Utilizing high speed calcium transient data (>300 fps) of Fluo-4AM loaded hPS-CM seeded microthreads, conduction velocities significantly increased from 3.69 ± 1.76 cm/s at day 7 to 24.26 ± 8.42 cm/s at day 21 ($n = 5-6$, $p < 0.05$). hPS-CM seeded microthreads exhibited positive expression for connexin 43, a gap junction protein, between cells. These data suggest that the fibrin microthread is a suitable scaffold for hPS-CM attachment and contraction. In addition, extended culture allows cells to contract in the direction of the thread, suggesting alignment of the cells in the microthread direction.

Keywords: pluripotent stem cell derived cardiomyocytes, high density mapping, contractile strain, fibrin microthreads, cardiovascular regeneration

INTRODUCTION

Cardiovascular disease (CVD) continues to be one of the leading causes of death worldwide (1). Myocardial infarction, a type of CVD, can develop into heart failure due to the inability for the heart to regenerate itself after a massive loss of contractile myocytes. Treatment for heart failure is limited with the only clinically acceptable method to regenerate contractile function being a heart

transplant. However, due to limited donor availability and the potential for immune rejection, a heart transplant is not an ideal treatment option (2). Consequently, researchers have investigated other therapeutic options for heart failure, such as cellular therapy. Many studies have delivered hMSCs (human mesenchymal stem cells) to animal infarct models as well as human patients in clinical trials; however, there has only been minimal improvement in left ventricular function (2, 3). Studies of pluripotent stem cell derived cardiomyocytes have shown promise in small animal models to improve function via attenuated left ventricular remodeling by paracrine effects and improvements in neovascularization (4–7). More recent studies using larger animal models have delivered human pluripotent stem cell derived cardiomyocytes (hPS-CM) to guinea pig (8) and macaque monkey (9) models of infarction and have demonstrated the ability to electrically couple to the host myocardium and remuscularize portions of the ischemic tissue. To deliver the cells to the infarcted tissue, groups traditionally use an intramyocardial injections which suffers from low engraftment rates (<10%) (10). Many valuable cells are being lost in the delivery process and are never able to reach the intended ischemic tissue.

Cardiac tissue engineering has allowed for the creation of a large mass of muscle to be used in myocardial regeneration strategies (11, 12). Many of the scaffolds used in cardiac tissue engineering allow for directed orientation to align cardiomyocytes and improve contractility and electrical conduction (13–16). Scaffold free techniques using cell sheet technology have the added advantage of allowing tissue formations without the use of exogenous materials (17, 18). However, many of the structural advantages of transplanting hPS-CM in infarct models using a cardiac patch or cell sheet are lost due to the formation of collagen interfaces between the host and graft tissue which limit the ability for the graft cells to migrate into the host tissue (13, 19).

Previously, we have developed a fibrin microthread suture that can be used for efficient cell delivery directly to the myocardium (20). These fibrin microthreads have been shown to support hMSC

and C2C12 myoblast attachment and survival as well as direct cellular alignment for myoblasts (21). Additionally, previous studies have indicated that fibrin is a suitable biomaterial to support hPS-CM attachment and contraction (13, 22). However, it is unknown whether fibrin microthreads are capable of supporting hPS-CM attachment and directing cell functionality. The aim of this study is to develop and characterize an hPS-CM seeded fibrin suture for future use as a delivery platform for cardiac repair. Here we implement strategies to seed hPS-CM onto fibrin microthreads and characterize how these cells function on the microthreads and understand how their contractile properties may change over time in culture.

MATERIALS AND METHODS

Seeding Platform for hPS-CM Attachment to Fibrin Microthreads

Fibrin microthreads were produced as described previously (23). Briefly, fibrinogen (70 mg/ml; MP Biomedical) and thrombin (8 U/ml; Sigma) were coextruded using a blending tip connector in a 10 mM HEPES (Calbiochem) buffered bath (pH 7.4). A custom built extrusion system was used to extrude microthreads at a flow rate of 0.23 mL/min through 0.38 mm polyethylene tubing. After extrusion, the microthreads were allowed to polymerize before being removed and air dried.

hPS-CM were generated using a previously described directed differentiation protocol using activin-A and bone morphogenetic protein-4 (4, 24). Cells were cryopreserved as previously reported (25), and all cell preparations contained >70% cardiac troponin T + cardiomyocytes by flow cytometry. To facilitate hPS-CM seeding individual fibrin microthreads were used and adhered in groups of three to custom polydimethylsiloxane (PDMS) washers (inner diameter: 1.2 cm) using medical grade silicone adhesive

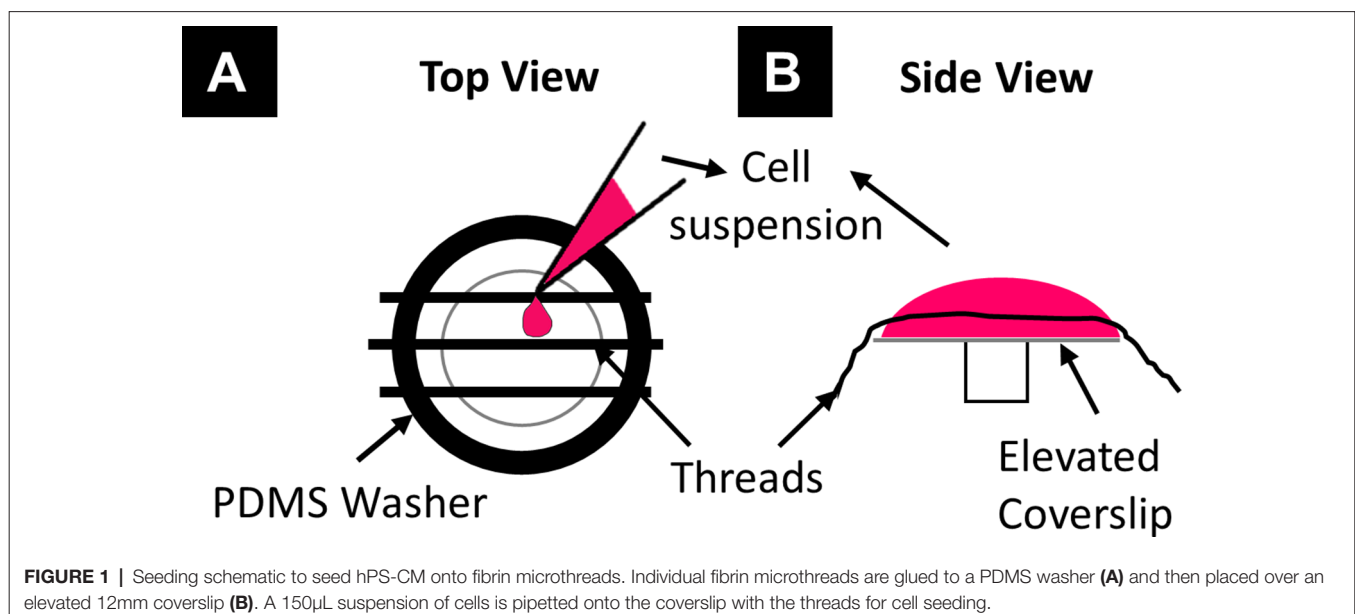


(**Figure 1A**). PDMS constructs with microthreads were placed in a six well plate for ethylene oxide (EtO) sterilization. Constructs were allowed to de-gas for 24 h after EtO sterilization. Immediately before seeding, microthreads were allowed to rehydrate for 20 min in dPBS. Thread constructs were then placed over an elevated 12 mm glass coverslip and coated with ECM protein (fibronectin or collagen IV, 10 $\mu\text{g}/\text{ml}$) for 2 h. For hPS-CM seeding, constructs were moved to new 12 mm glass coverslip platforms and a 150 μL cell suspension (1.33×10^6 cells/ml) in aprotinin (50 $\mu\text{g}/\text{ml}$) supplemented RPMI-B27 medium was added to the coverslip (**Figure 1B**). Control TCP plates were coated with 0.1% gelatin, collagen IV, or fibronectin and were seeded with hPS-CM at a density of 150,000 cells/cm². Cells were allowed to attach for 18 h in an incubator at 37°C, after which cell seeded microthreads were moved to a six well plate with fresh RPMI-B27 medium supplemented with aprotinin, medium was changed every 2–3 days.

Effect of ECM Surface Coatings on hPS-CM Attachment

To examine the effect of different surface coatings on hPS-CM attachment to fibrin microthreads, ECM proteins collagen IV and fibronectin were used. After the threads were hydrated and moved to an elevated 12 mm coverslip, threads were coated with ECM proteins for 2 h after which constructs were moved to another elevated 12 mm coverslip for final cell seeding. Cells were seeded as described previously. 48 h after seeding, constructs were moved to new wells with fresh medium for continued culture, or microthreads were prepared for a CyQuant assay. All threads from one construct were cut and placed in an eppendorf tube containing 1 ml of dPBS and the CyQuant assay was run according to the manufactures specifications.

Viability of hPS-CM Attachment on Fibrin Microthreads

To characterize cell viability a LIVE/DEAD assay (Life Technologies) was conducted, according to manufactures recommendations, 48 h after hPS-CM constructs were seeded. Briefly, medium was aspirated and replaced with 1 ml of sterile RPMI containing a 4 μM ethidium homodimer-1 and 2 μM calcein-AM working solution and plates were incubated at 37C for 15 min. The RPMI solution was aspirated and replaced with a 4 μM ethidium homodimer-1 and 2 μM calcein-AM working solution with Hoechst 33342 (0.5 $\mu\text{g}/\text{mL}$; Life Technologies) and plates were incubated for an additional 15 min at 37C. Calcein-AM (green Ex/em 495 nm/515 nm) is retained within the cytoplasm of living cells, while ethidium homodimer-1 (red, Ex/em 495 nm/635 nm) enters dead cells and binds nuclear DNA, but is excluded from living cells with intact plasma membrane activity. Microthreads were imaged using a Leica DMIL inverted microscope.

Capturing Contraction of hPS-CM Seeded Microthreads

To record the contraction produced by seeded sutures a LEICA DMIL inverted microscope with a Fastec HiSpec4 camera mounted

to record video at high magnifications. Video was recorded at 60 frames per second for 25 s at a magnification level of 200x at 4 different locations along the length of the thread. To determine the time course of contraction, microthreads were recorded at days 7, 14, and 21 post seeding. Collagen IV, fibronectin, and fibrin only hPS-CM seeded sutures were analyzed. Parallel control experiments were run with hPS-CM plated on fibronectin (10 $\mu\text{g}/\text{ml}$) and collagen IV (10 $\mu\text{g}/\text{ml}$) coated TCP at a density of 150,000 cells/cm². The data was analyzed to calculate average contractile strain, maximum contractile strain, and beat frequency using high density mapping (HDM), a speckle tracking algorithm, as previously described (26). For contractility alignment, the values of the principal angle were calculated for zero to peak of E2, for each contraction cycle, and were compared to the angle of the microthread and the difference between the two was determined. Aligned cells were defined as those with an angle differences between +/-0–20 degrees. The percent of cells contracting in alignment with the microthread was reported for days 7, 14, and 21.

Conduction Velocity Measurements

To measure conduction velocity hPS-CM seeded sutures were loaded with Fluo-4 AM (5 μM dissolved in Pluronic F-127 (20% solution in DMSO); Invitrogen) and recorded at days 7, 14, and 21 using a previously defined system (26), within 2 h of dye addition. Briefly, a Zeiss AcioObserver.A1 inverted microscope with a Hamamatsu Orca Flash 4.0sCMOS camera was used to obtain fluorescent videos at greater than 70 frames per second. Calcium transient analysis of the individual frames was applied to 2–3 regions along the thread using a custom MATLAB code that determined the average fluorescence intensity change with respect to baseline intensity and was reported as $\Delta F/F_0$. Calcium transients for each region were then plotted together and the frame difference between the start frames of each calcium transient cycle for the different regions was recorded and the time delay was calculated. Next, the distance between the center points of each region was calculated using ImageJ. Conduction velocity was then calculated by dividing the distance between the regions by the time delay between the initiations of the calcium transients and is reported in cm/s.

Immunocytochemistry

At day 1, 4, 7, 14, and 21 hPS-CM seeded microthreads were fixed in 4% paraformaldehyde for 10 min, rinsed with PBS and blocked in 5% goat serum or 1.5% rabbit serum in PBS for 45 min. Primary antibodies were applied at a dilution of 1:100 (mouse-anti-alpha actinin, Abcam; rabbit-anti-connexin-43, Cell Signaling Technologies) at 4°C overnight. Cells were incubated for an hour in the appropriate secondary antibodies (AF488 anti-mouse 1:400, AF568 anti-rabbit 1:400, Invitrogen). Cells were counterstained using Hoechst 33342 (0.5 $\mu\text{g}/\text{mL}$, Life Technologies) for 5 min. Images were obtained using a Leica laser scanning confocal microscope.

Alpha-Actinin Fiber Alignment

Confocal images of alpha-actinin stained hPS-CM seed on microthreads and TCP were uploaded to ImageJ (NIH) for actinin

fiber alignment using OrientationJ. Briefly, each image was split into its green channel and each section of fibers were outlined and analyzed. Output angle data for each image was averaged and compared to the angle of the thread and reported as the difference between the thread angle and the average fiber angle.

Statistical Analysis

Statistical analyses were performed using GraphPad Prism 6 (GraphPad Software, Inc.). Comparisons between seeding conditions, alignment data, and conduction velocities were analyzed using a one-way ANOVA, with a post-hoc Tukey test for multiple comparisons. Comparisons for contractile parameters of hPS-CM seeded on different surface coatings (threads and TCP) between time points were done using a two-way ANOVA with a Tukey post-hoc analysis for multiple comparisons. Comparisons were done including all data from threads and TCP, and separately with data from just plates groups and just threads groups to elucidate differences washed out when all groups across time and culture substrates were compared. A Pearson linear correlation coefficient was calculated in excel using the PEARSON function to assess the strength of correlation between contractile alignment and average contractile strain. Cell attachment number, average and maximum contractile strain, actinin alignment, and conduction velocity are reported as mean \pm SEM, frequency data is reported as mean \pm SD. Significance was considered at $p < 0.05$.

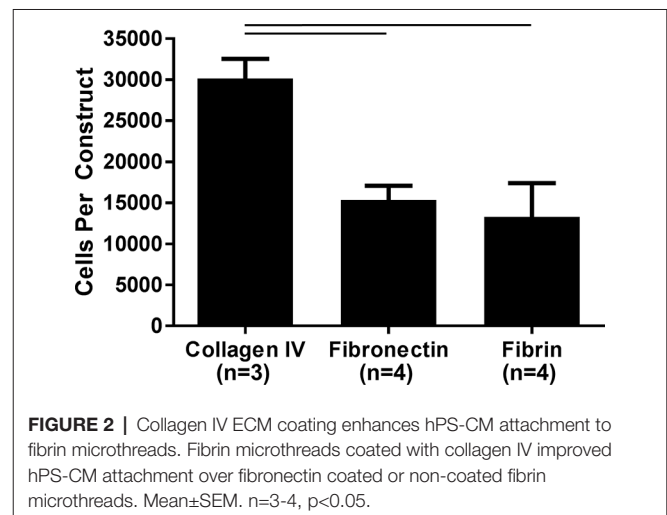
RESULTS

Collagen IV Coating Improves hPS-CM Attachment to Fibrin Microthreads

Fibronectin and collagen IV ECM protein coatings were evaluated against fibrin only to determine how ECM protein coating would affect hPS-CM attachment. Immunohistochemistry confirmed that both fibronectin and collagen IV proteins coatings resulted in positive expression of fibronectin and collagen IV on the surface of the microthread. Cell attachment was measured and quantified 2 days post seeding using a CyQuant DNA assay. hPS-CM attachment was observed for all conditions, with significantly higher cells attached on the collagen IV coated microthreads ($n = 3-4$, $p < 0.05$, **Figure 2**). Increases in cell attachment and using different protein coatings did not appear to affect cell viability as indicated qualitatively by a LIVE/DEAD stain (**Figure S1**).

hPS-CM Exhibit Opposite Temporal Trends in Contractile and Maximum Strains When Cultured on TCP and Fibrin Microthreads

To examine contractile behavior, average contractile strain and maximum contractile strains were evaluated from hPS-CM seeded TCP (0.1% gelatin, collagen IV, and fibronectin coated) and microthreads (fibrin, fibronectin and collagen IV coated) at days 7, 14, and 21 post seeding. On TCP both average contractile strains and maximum contractile strains followed similar trends such that cells cultured on TCP produced decreased strains over 21 days. Cells on TCP exhibit a significant decrease in average contractile strain over time, beginning at $4.23 \pm 0.23\%$ on day 7

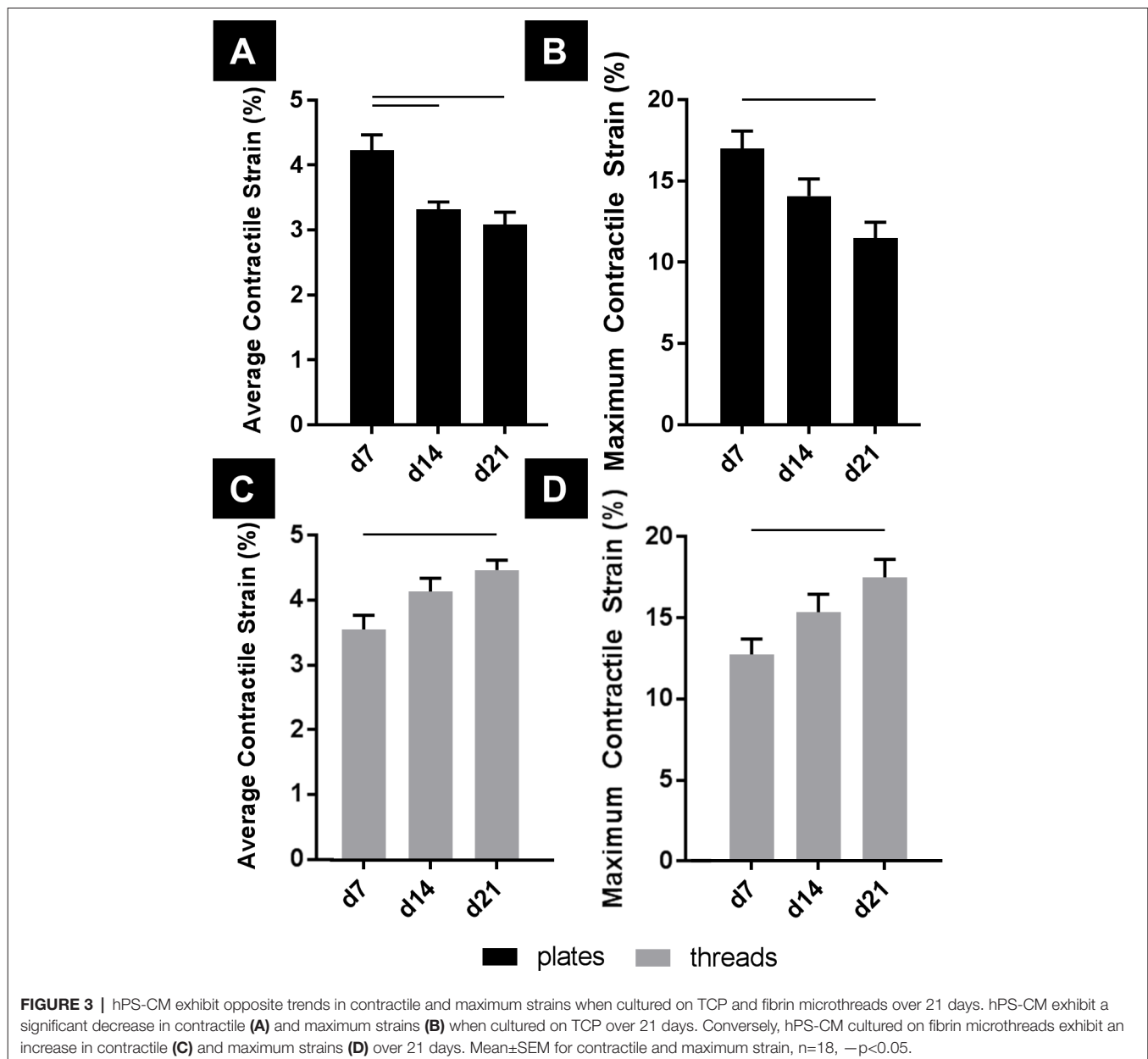


and ending at $3.08 \pm 0.19\%$ on day 21 (**Figure 3A**, $n = 18$, $p < 0.05$). Maximum contractile strain followed a similar trend; cells on TCP had a maximum contractile strain of $17.01 \pm 1.07\%$ on day 7, which significantly decreased to $11.48 \pm 0.99\%$ on day 21 (**Figure 3B**, $n = 18$, $p < 0.05$). hPS-CM seeded on microthreads increased average contractile strain and maximum contractile strain over 21 days. At day 7, hPS-CM seeded on microthreads begin at an average contractile strain of $3.56 \pm 0.22\%$ and increased average contractile strain to $4.47 \pm 0.29\%$ on day 21 (**Figure 3C**, $n = 18$, $p < 0.05$). In terms of maximum contractile strain, hPS-CM seeded on microthreads produced a maximum contractile strain on day 7 of $12.70 \pm 0.94\%$ which significantly increased to a maximum contractile strain of $17.44 \pm 1.09\%$ on day 21 (**Figure 3D**, $n = 18$, $p < 0.05$).

Looking between culture substrate and over time, cells cultured on TCP and microthreads exhibited significantly different average contractile strains on days 7, 14, and 21, and significantly different maximum contractile strains on days 7 and 21 (**Figure 4A,B**, $n = 18$, $p < 0.05$). Both average contractile strain and maximum contractile strain were higher at day 21 for hPS-CM cultured on fibrin microthreads than the strains produced by hPS-CM cultured on TCP at day 7. Average contractile strain and maximum contractile strain followed similar trends between coating groups, on TCP and on microthreads over 21 days (**Figure S2**).

Contractile Frequency Increases Over 21 Days for hPS-CM Cultured on TCP and Microthreads

Beat frequency was examined to determine if there were any changes in beat rate for hPS-CM seeded on microthreads or TCP over 21 days (**Figure 4C**). Frequency significantly increased from day 7 to day 21 for both TCP and microthread groups; from 0.83 ± 0.25 Hz to 1.11 ± 0.45 Hz for the TCP group and from 0.84 ± 0.15 Hz to 1.03 ± 0.19 Hz for the microthread group ($n = 18$, $p < 0.05$). No differences were found between TCP and microthread groups for any time points. Frequency was found to increase over time for all surface coatings, on microthreads and TCP, with the



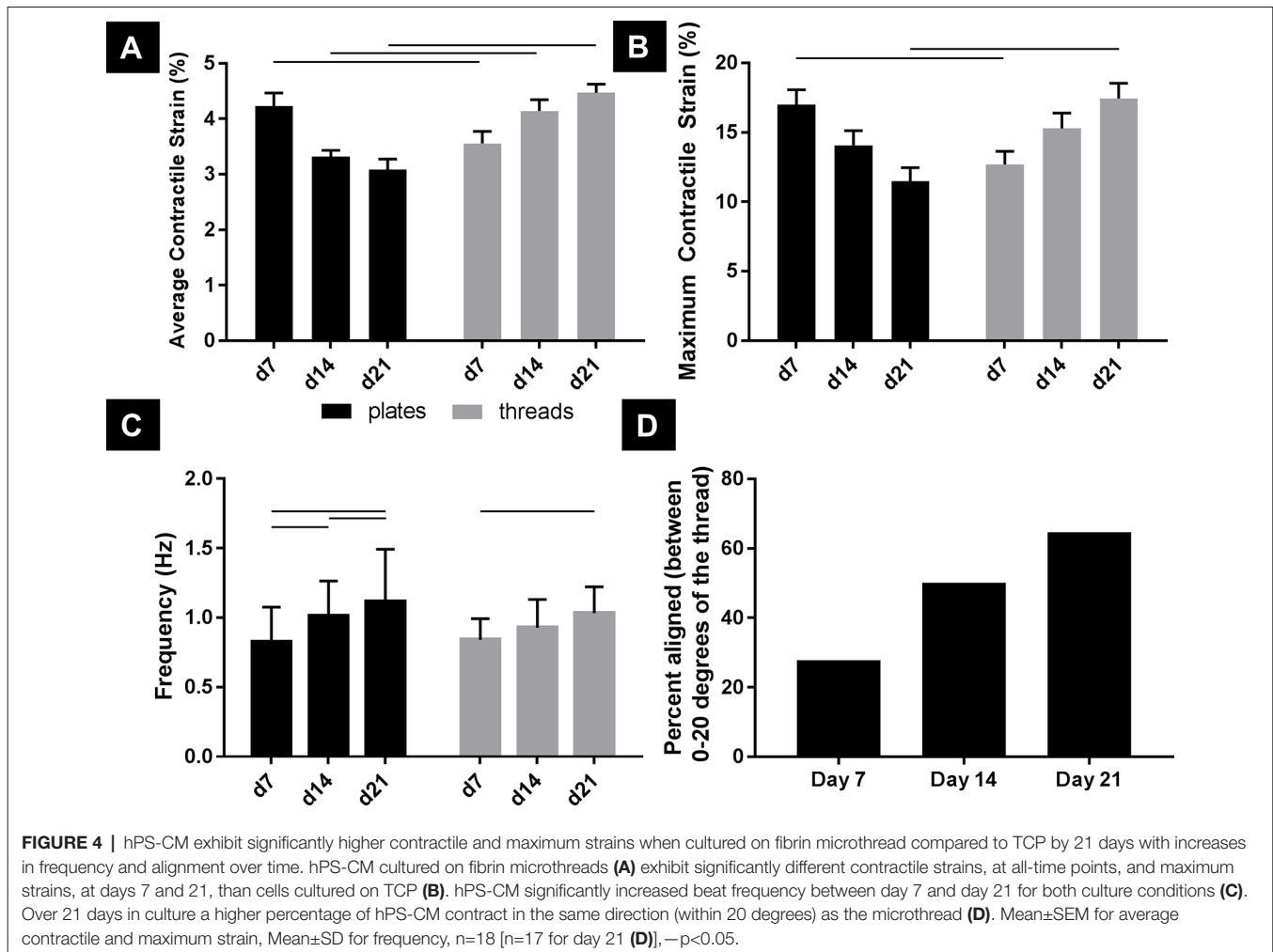
exception for the gelatin coated group which decreased between day 14 and 21 (Figure S2).

hPS-CM contraction direction becomes more aligned with the thread over 21 days in culture

hPS-CM seeded on non-coated, collagen IV and fibronectin coated fibrin microthreads were used to examine changes in cellular alignment to the fibrin microthreads in terms of direction of principal contraction ($n = 17-18$, Figure 4D). Values reported are the percentage of cells that contracted within 0–20 degrees of the direction of the fibrin microthread. At day 7 only 27% of cells contracted within 20 degrees of the direction the fibrin microthread,

this increased to 65% by day 21. Additionally, hPS-CM seeded on TCP did not exhibit the same trend over 21 days in culture as cells had wide ranges of principal contraction angles at all-time points indicating that they remained unaligned over 21 days (data not shown).

When contractile alignment was plotted together with changes in average contractile strain over 21 days there appeared to be a linear relationship between contractile alignment and average contractile strain for hPS-CM seeded on sutures (Figure S3). A Pearson linear correlation coefficient of 0.99 between variables was found indicating a strong correlation between increases in contractile alignment and average contractile strain. For hPS-CM cultured on TCP average contractile strain decreased over 21 days



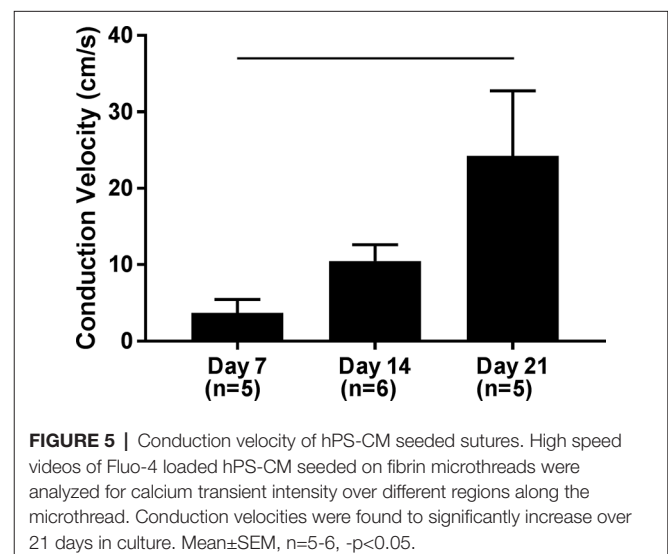
with no major change in alignment as indicated by the flat orange trendline in Figure S3 and a Pearson linear correlation coefficient of -0.20 .

hPS-CM Seeded on Microthreads Increase Conduction Velocity Over 21 Days in Culture

Using the system previously developed (26) we examined calcium transients in terms of conduction velocity of hPS-CM seeded on fibrin microthreads. High speed videos of hPS-CM seeded on microthreads loaded with Fluo-4 AM dye were analyzed for calcium transient intensity over 2–3 regions along the microthread to determine conduction velocity at days 7, 14, and 21. Conduction velocities significantly increased from 3.69 ± 1.76 cm/s at day 7 to 24.26 ± 8.42 cm/s at day 21 (Figure 5, $n = 5-6$, $p < 0.05$).

hPS-CM Seeded Microthreads Express Alpha-Actinin and Connexin 43

Alpha-actinin and connexin 43 staining were utilized to determine hPS-CM morphology up to 21 days in culture. hPS-CM were readily attached to microthreads at all-time points and exhibited positive



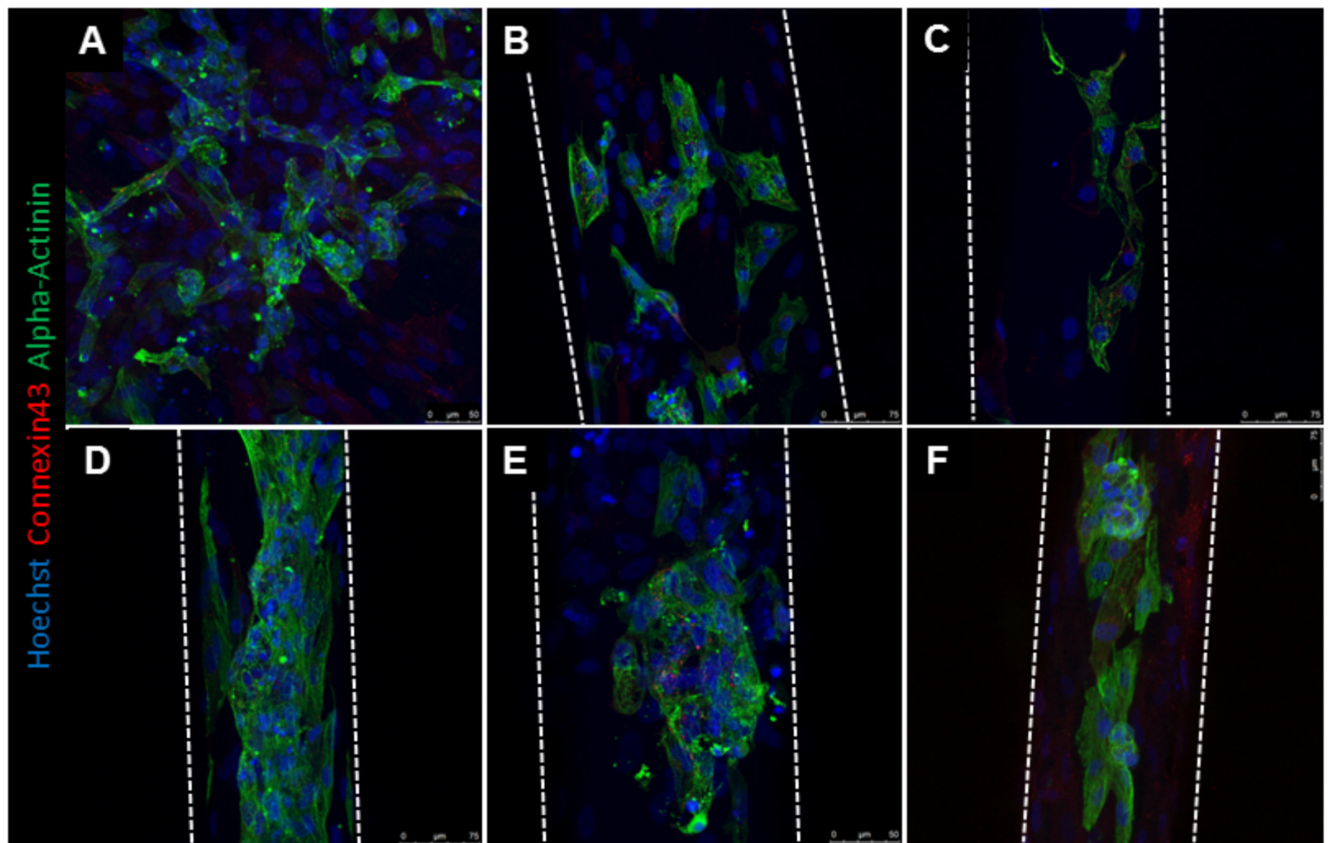


FIGURE 6 | hPS-CM seeded onto fibrin microthreads express alpha-actinin and connexin 43. hPS-CM seeded onto tissue culture plastic (A) and collagen IV coated fibrin microthreads express alpha-actinin and connexin 43 proteins at days 1 (B), 4 (C), 7 (D), 14 (E), and 21 (F) in culture. Cells seeded on tissue culture plastic exhibit no dominant alignment. Cells at later time points are more aligned along the length of the fibrin microthread.

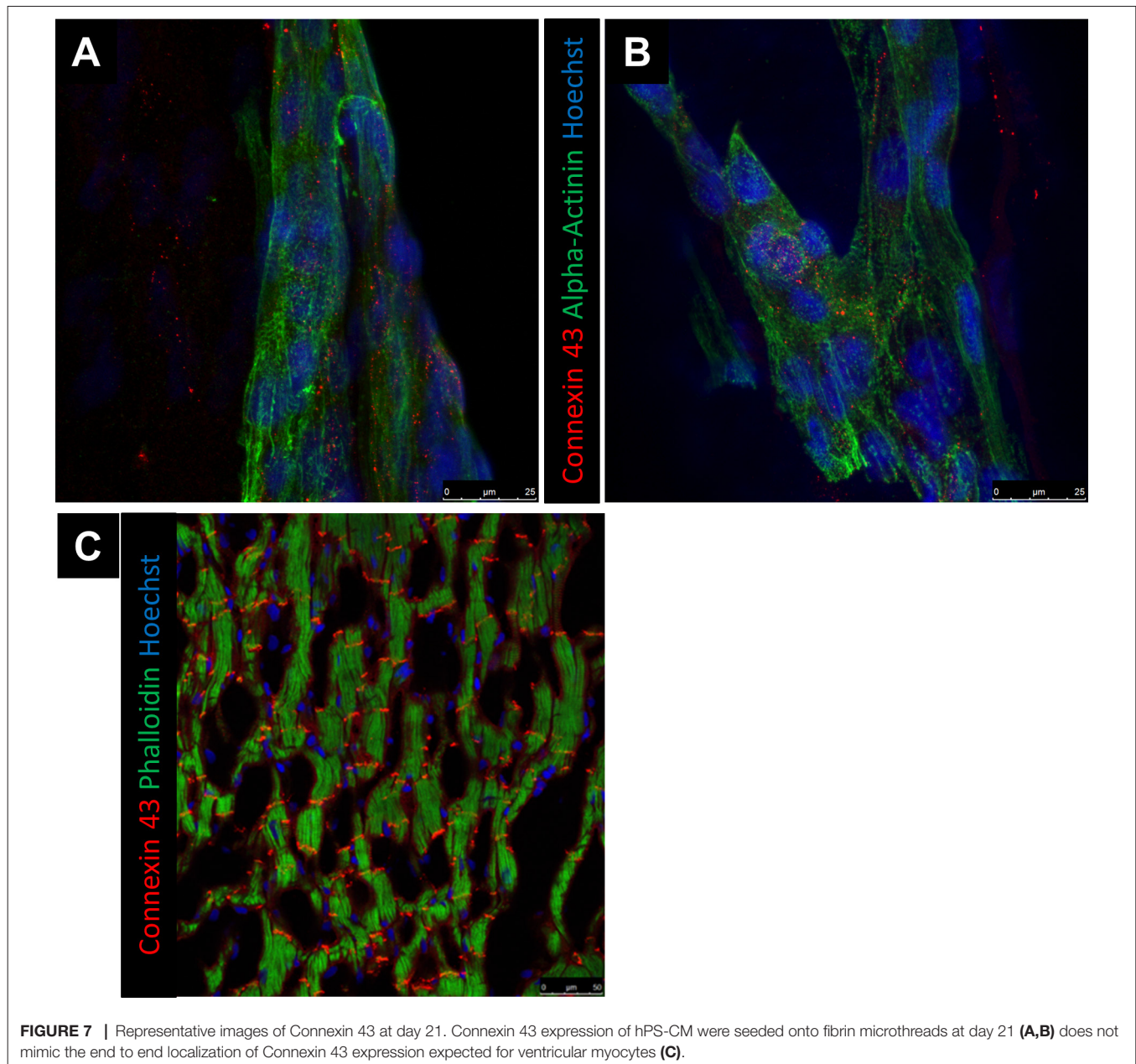
alpha-actinin and connexin 43 staining (Figure 6). Cells were less elongated at the earlier time points (1 and 4 days). By day 7 cells had begun to elongate along the direction of the microthread and exhibited more organized sarcomere structure. Quantifying alignment demonstrated that hPS-CM at day 7 were aligned within 13.7 ± 6.2 degrees to the thread, compared to 11.7 ± 5.8 and 8.0 ± 1.1 degrees on days 14 and 21, respectively ($n = 4-27$ images, NS, Figure S4). Cells on TCP exhibited no dominant fiber alignment as indicated by a range of fiber angles from -86.6 to 86.4 degrees ($n = 43$ cell regions, data not shown). Cells demonstrated positive connexin 43 staining; however, at all-time points the staining was diffuse through the cells with no evidence of organization and polarization to the intercalated disks (Figure 7).

DISCUSSION

The goals of this study were to define the seeding conditions and time to obtain a contractile hPS-CM seeded microthread and characterize the cells contractile behavior when seeded on the microthreads. By obtaining a contractile cardiomyocyte microthread the microthreads can be attached to a suture needle in such a way that allows for targeted cell delivery to cardiac tissue. This study did not examine cell delivery

to cardiac tissue via the microthreads, however previous work in our lab has suggested the feasibility of efficient and directed microthread based cell delivery (20). This cell delivery platform could provide an improved cell delivery method for regenerative medicine strategies seeking to treat heart failure. In this work, different ECM surface coatings were used to improve cell attachment. Fibronectin and collagen IV were chosen due to their presence in cardiac basement membrane. Additionally, other studies seeding hPS-CM on various substrates have demonstrated successful hPS-CM attachment using fibronectin and collagen IV coatings (27, 28). hPS-CM attached with higher quantities to collagen IV coated microthreads two days after seeding. All conditions did allow hPS-CM attachment, suggesting that hPS-CM preferentially attached to collagen IV coated microthreads, but a protein coating is not necessary to obtain hPS-CM attachment on fibrin microthreads. Qualitatively, protein coatings did not affect cell viability as the majority of cells attached were found to be viable for all conditions.

In regards to contractility, hPS-CM seeded on microthreads began to contract within 7 days after seeding and cell contraction was observed for all conditions. Beat frequency increased over 21 days for hPS-CM seeded on microthreads and on TCP to above 1 Hz, a similar finding to other groups (29, 30). Average contractile strain and maximum contractile strain was found to increase over 21 days



for hPS-CM seeded on microthreads. These values, at all-time points, were significantly different than the average contractile strain and maximum contractile strain produced by hPS-CM on TCP, which were found to decrease over 21 days. Maximum contractile strains produced by hPS-CM on the microthreads near the 19% strain that is produced by adult human myocardium (31). Other tissue engineered constructs, such as the engineered heart tissue created by Eng et al. have demonstrated strains upwards of 17%, although these tissues needed to be electrically stimulated to produce higher strains where the unstimulated controls only produced strains of 10% (30).

Cardiomyocytes exist in an environment that requires them to be highly aligned and organized to produce efficient contractions. Previous studies have suggested the ability for fibrin microthreads to direct cell orientation along the microthread (21). In order to

investigate the relationship of alignment with strain changes over time we sought to quantify cell alignment to determine the effect cell alignment may have had on changes in strain. Within a given layer of healthy myocardium, cardiomyocytes are aligned within 13 degrees of each other (32). The same would be expected of hPS derived cardiomyocytes for efficient contraction of the heart.

We demonstrated that over 21 days in culture the direction of cell contraction was more aligned along thread. Additionally, alignment was confirmed by immunohistochemical stains as cells aligned more closely to the thread over 21 days with a final alignment within 8 degrees of the thread. Studies in two and three dimensions have demonstrated the importance of cardiomyocyte alignment on improving contractility compared to unaligned controls (15, 33). As average contractile strains and maximum contractile strains increased

over 21 days for hPS-CM seeded on microthreads, this would suggest that these cells are able to produce higher strains because they are contracting in a direction more aligned with the microthreads. No principal contraction alignment was found for cells cultured on TCP, which may explain the decrease in strains produced by these cells over time. A study by Khan et al. demonstrated that hPS-CM cultured on a polylactide-co-glycolide nanofiber scaffold improved alignment and function compared to hPS-CM cultured on tissue culture plastic. These results supports the findings here where hPS-CM cultured on a fibrin microthread scaffold also influenced and improved cell alignment and function (34).

Conduction velocity in ventricular myocardial tissue is approximately 50cm/s (35, 36). Here, using calcium transient analysis we demonstrated conduction velocities that began at 3.7 cm/s on day 7, increasing by day 21 to a mean of 24.2 cm/s with some microthreads demonstrating conduction velocities reaching 46.3 cm/s. Not only do these conduction velocities near that of human myocardium, but increasing conduction velocities over time would suggest that this increase may be due to the higher alignment of hPS-CM over time. Other studies have indicated a similar trend in conduction velocities where aligned cultures of cardiomyocytes demonstrated a 1.6 increase in conduction velocity (37).

Alignment may not be the only contribution to changes in strain over time; substrate stiffness may also play a role in how much strain the cells can produce. While alignment may be driving an increase in contractile strain it is possible that substrate stiffness plays a role. Hydrated fibrin microthreads have a modulus value around 2.2 MPa (21) whereas tissue culture plastic has a modulus value on the gigapascal range (38) which is significantly stiffer than human myocardial tissue, which can range in stiffness from 20 to 500kPa (39). It has been demonstrated that increased cell functionality may be a function of both substrate stiffness and alignment (40–43). McDevitt et al. demonstrated that cardiomyocytes patterned on glass coverslips lost their alignment over 10 days in culture suggesting that the stiff glass substrate is unfavorable to cardiomyocytes even though they had originally been patterned in an aligned manner (42). Ribeiro et al. used matrigel micropatterns on physiologically relevant degrees of stiffness to constrain hPS-CMs into rectangular shapes that follow a physiological 7:1 aspect ratio (33). These patterned hPS-CM were capable of producing higher contractile forces and improved myofibril alignment. The studies by McDevitt and Ribeiro were done on glass coverslips, however cardiomyocytes exist in a 3D environment and thus it is important to consider the effects of alignment and stiffness in an environment that better mimics myocardium. Chrobak et al. examined cardiomyocyte function using an unaligned fibrin gel with a modulus of approximately 0.25 kPa (44). They demonstrated contractile strains decreased over time suggesting that in a soft unaligned environment cardiomyocytes are unable to increase strains over time. Black et al. demonstrated that an aligned cardiomyocyte populated fibrin gel was capable of increased twitch forces at 2 weeks in culture over unaligned controls (45). These results, in conjunction with the data presented here, suggest that neither an unaligned soft substrate or an aligned stiff substrate are enough to improve cardiomyocyte function, but that a soft substrate that promotes alignment may be ideal for cardiomyocyte function.

When hPS-CM were seeded onto collagen IV coated tissue TCP, cells retained their contractile nature, but lacked a rod like phenotype with the organized sarcomere structure expected of mature cardiomyocyte. Connexin 43 is a protein found in cardiac connexons, which make up gap junctions that connect cardiomyocytes. To facilitate cardiac conduction, gap junctions are organized end-to-end at the intercalated disks within cardiac tissue. Qualitatively, no organizational differences in connexin 43 staining was found for hPS-CM seeded on TCP or fibrin microthreads at any time points. However, we demonstrated that conduction velocity increased over 21 days, yet connexin 43 expression did not appear to be more localized by 21 days. Studies have shown that increases in conduction velocity may not be solely connexin 43 dependent. Cardiac conduction can be determined by several factors including membrane excitability, intercellular coupling, as well as the size, shape and orientation of the cardiomyocytes (46, 47). de Boer et al. utilized a geometrically defined culture of immature cardiomyocytes and demonstrated that β -adrenergic induced increases in conduction velocity were due to changes in the intrinsic excitability of the cardiomyocytes and not alterations in gap junctional coupling. In adult mice with induced deletion of connexin 43, a 50% decrease in connexin 43 protein did not have any impact on conduction velocity (48). In a similar study, a 50% decrease in *Scn5a*, a gene that encodes sodium channel $Na_v1.5$, demonstrated reduction in conduction velocity (49). To examine this phenomenon at the cellular level strands of neonatal cardiac myocytes with a 43% reduction in connexin 43 levels demonstrated no significant decrease in conduction velocity, but did demonstrate a significant increase in the action potential upstroke suggesting an increase in sodium channels. The data presented in these studies suggest that an increase in membrane excitability, plays an important role in conduction velocity. While not directly explored here, it is possible that connexin 43 localization was not the main driver for the increase in conduction velocity and that increases in membrane excitability and alignment have a role.

However, it is still important to note that many of these differences in alpha-actinin and connexin 43 organization and localization can be attributed to the immature phenotype of hPS-CM (50). This suggests that further steps will be necessary for enhanced maturation of connexin 43 localization and sarcomere organization of hPS-CM even given a substrate that promotes cell alignment. Others have shown that extended culture, as well incorporating electrical and mechanical stimulation can provide the cues necessary to impart maturation leading to improvements in cardiomyocytes functionality (50–53).

These findings suggest that hPS-CM are capable of attaching to fibrin microthreads, however a collagen IV protein coating improves hPS-CM attachment to fibrin microthreads. Additionally, hPS-CM were able to contract and align to the microthreads over 21 days in culture. By day 14 cell seeded microthreads were contracting at a frequency approaching that of a human heart and were producing strains nearing those produced by human myocardium. One of the limiting factors regenerative therapies for cardiac disease face is the inability to efficiently deliver cells to the area of damage. Many studies transplanting hPS-CM to diseased cardiac tissue have done so using a cardiac patch or cell

sheet in order to improve cell retention (13, 54). However, these cell delivery methods have limited success due to the formation of collagen interfaces between the host and graft tissue, which limits the ability for graft cells to migrate into host tissue, thus limiting the potential for functional and electrical integration. This cell seeded microthread platform could influence cardiac cell therapy by utilizing the microthread as a delivery method by attaching a suture needle to the microthreads, as had been done previously (20, 55, 56). Doing so would provide a contractile fiber of cardiomyocytes that are able to be directly delivered to the damaged cardiac tissue to aid in regeneration of function in infarcted ventricular myocardium.

AUTHOR CONTRIBUTIONS

KH designed the study, collected, analyzed and interpreted data, and wrote the manuscript. ML provided the hPS-CM and

contributed to study design, data interpretation, and manuscript editing. GG contributed to study design, data interpretation, manuscript writing, and provided financial support. All authors read and approved the final manuscript.

FUNDING

This study was supported by National Institutes of Health grants RO1-HL115282 (GG), P01-HL094374 and RO1-HL117991 (ML) and National Science Foundation grants DGE 1144804 (KH, GG).

SUPPLEMENTARY MATERIAL

The Supplementary Material for this article can be found online at: <http://journal.frontiersin.org/article/10.3389/fcvm.2018.00052/full#supplementary-material>

REFERENCES

- Go AS, Mozaffarian D, Roger VL, Benjamin EJ, Berry JD, Borden WB, et al. Heart disease and stroke statistics-2013 update: a report from the American Heart Association. *Circulation* (2013) 127(1):e6-e245. doi: 10.1161/CIR.0b013e31828124ad
- Jakob P, Landmesser U. Current status of cell-based therapy for heart failure. *Curr Heart Fail Rep* (2013) 10(2):165–76. doi: 10.1007/s11897-013-0134-z
- Russo V, Young S, Hamilton A, Amsden BG, Flynn LE. Mesenchymal stem cell delivery strategies to promote cardiac regeneration following ischemic injury. *Biomaterials* (2014) 35(13):3956–74. doi: 10.1016/j.biomaterials.2014.01.075
- Laflamme MA, Chen KY, Naumova AV, Muskheli V, Fugate JA, Dupras SK, et al. Cardiomyocytes derived from human embryonic stem cells in pro-survival factors enhance function of infarcted rat hearts. *Nat Biotechnol* (2007) 25(9):1015–24. doi: 10.1038/nbt1327
- Caspi O, Huber I, Kehat I, Habib M, Arbel G, Gepstein A, et al. Transplantation of human embryonic stem cell-derived cardiomyocytes improves myocardial performance in infarcted rat hearts. *J Am Coll Cardiol* (2007) 50(19):1884–93. doi: 10.1016/j.jacc.2007.07.054
- van Laake LW, Passier R, Monshouwer-Kloots J, Verkleij AJ, Lips DJ, Freund C, et al. Human embryonic stem cell-derived cardiomyocytes survive and mature in the mouse heart and transiently improve function after myocardial infarction. *Stem Cell Res* (2007) 1(1):9–24. doi: 10.1016/j.scr.2007.06.001
- Fernandes S, Naumova AV, Zhu WZ, Laflamme MA, Gold J, Murry CE. Human embryonic stem cell-derived cardiomyocytes engraft but do not alter cardiac remodeling after chronic infarction in rats. *J Mol Cell Cardiol* (2010) 49(6):941–9. doi: 10.1016/j.yjmcc.2010.09.008
- Shiba Y, Fernandes S, Zhu WZ, Filice D, Muskheli V, Kim J, et al. Human ES-cell-derived cardiomyocytes electrically couple and suppress arrhythmias in injured hearts. *Nature* (2012) 489(7415):322–5. doi: 10.1038/nature11317
- Chong JJ, Yang X, don CW, Minami E, Liu YW, Weyers JJ, et al. Human embryonic-stem-cell-derived cardiomyocytes regenerate non-human primate hearts. *Nature* (2014) 510(7504):273–7. doi: 10.1038/nature13233
- Hou D, Youssef EA, Brinton TJ, Zhang P, Rogers P, Price ET, et al. Radiolabeled cell distribution after intramyocardial, intracoronary, and interstitial retrograde coronary venous delivery: implications for current clinical trials. *Circulation* (2005) 112(9 Suppl):150–6. doi: 10.1161/CIRCULATIONAHA.104.526749
- Masuda S, Shimizu T. Three-dimensional cardiac tissue fabrication based on cell sheet technology. *Adv Drug Deliv Rev* (2016) 96:103–9. doi: 10.1016/j.addr.2015.05.002
- Hirt MN, Hansen A, Eschenhagen T. Cardiac Tissue Engineering. *State of the Art* (2014) 114:354–67.
- Wendel JS, Ye L, Tao R, Zhang J, Zhang J, Kamp TJ, et al. Functional effects of a tissue-engineered cardiac patch from human induced pluripotent stem cell-derived cardiomyocytes in a rat infarct model. *Stem Cells Transl Med* (2015) 4(11):1324–32. doi: 10.5966/sctm.2015-0044
- Zhang D, Shadrin IY, Lam J, Xian HQ, Snodgrass HR, Bursac N. Tissue-engineered cardiac patch for advanced functional maturation of human ESC-derived cardiomyocytes. *Biomaterials* (2013) 34(23):5813–20. doi: 10.1016/j.biomaterials.2013.04.026
- Bian W, Jackman CP, Bursac N. Controlling the structural and functional anisotropy of engineered cardiac tissues. *Biofabrication* (2014) 6(2):024109. doi: 10.1088/1758-5082/6/2/024109
- Fleischer S, Feiner R, Shapira A, Ji J, Sui X, Daniel Wagner H, et al. Spring-like fibers for cardiac tissue engineering. *Biomaterials* (2013) 34(34):8599–606. doi: 10.1016/j.biomaterials.2013.07.054
- Matsuura K, Wada M, Shimizu T, Haraguchi Y, Sato F, Sugiyama K, et al. Creation of human cardiac cell sheets using pluripotent stem cells. *Biochem Biophys Res Commun* (2012) 425(2):321–7. doi: 10.1016/j.bbrc.2012.07.089
- Masumoto H, Matsuo T, Yamamizu K, Uosaki H, Narazaki G, Katayama S, et al. Pluripotent stem cell-engineered cell sheets reassembled with defined cardiovascular populations ameliorate reduction in infarct heart function through cardiomyocyte-mediated neovascularization. *Stem Cells* (2012) 30(6):1196–205. doi: 10.1002/stem.1089
- Gerbin KA, Yang X, Murry CE, Coulombe KL. Enhanced electrical integration of engineered human myocardium via intramyocardial versus epicardial delivery in infarcted rat hearts. *PLoS One* (2015) 10(7):e0131446. doi: 10.1371/journal.pone.0131446
- Guyette JP, Fakhrazadeh M, Burford EJ, Tao ZW, Pins GD, Rolle MW, et al. A novel suture-based method for efficient transplantation of stem cells. *J Biomed Mater Res A* (2013) 101(3):809–18. doi: 10.1002/jbm.a.34386
- Grasman JM, Pumphrey LM, Dunphy M, Perez-Rogers J, Pins GD. Static axial stretching enhances the mechanical properties and cellular responses of fibrin microthreads. *Acta Biomater* (2014) 10(10):4367–76. doi: 10.1016/j.actbio.2014.06.021
- Christoforou N, Liau B, Chakraborty S, Chellapan M, Bursac N, Leong KW. Induced pluripotent stem cell-derived cardiac progenitors differentiate to cardiomyocytes and form biosynthetic tissues. *PLoS One* (2013) 8(6):e65963. doi: 10.1371/journal.pone.0065963
- Proulx MK, Carey SP, Ditroia LM, Jones CM, Fakhrazadeh M, Guyette JP, et al. Fibrin microthreads support mesenchymal stem cell growth while maintaining differentiation potential. *J Biomed Mater Res A* (2011) 96(2):301–12. doi: 10.1002/jbm.a.32978
- Zhu WZ, van Biber B, Laflamme MA. Methods for the derivation and use of cardiomyocytes from human pluripotent stem cells. *Methods Mol Biol* (2011) 767:419–31. doi: 10.1007/978-1-61779-201-4_31

25. Xu C, Police S, Hassanipour M, Li Y, Chen Y, Priest C, et al. Efficient generation and cryopreservation of cardiomyocytes derived from human embryonic stem cells. *Regen Med* (2011) 6(1):53–66. doi: 10.2217/rme.10.91
26. Hansen KJ, Favreau JT, Gershlag JR, Laflamme MA, Albrecht DR, Gaudette GR. Optical method to quantify mechanical contraction and calcium transients of human pluripotent stem cell-derived cardiomyocytes. *Tissue Eng Part C Methods* (2017) 23(8):445–54. doi: 10.1089/ten.tec.2017.0190
27. Rodriguez ML, Graham BT, Pabon LM, Han SJ, Murry CE, Sniadecki NJ. Measuring the contractile forces of human induced pluripotent stem cell-derived cardiomyocytes with arrays of microposts. *J Biomech Eng* (2014) 136(5):051005. doi: 10.1115/1.4027145
28. Moyes KW, Sip CG, Obenza W, Yang E, Horst C, Welikson RE, et al. Human embryonic stem cell-derived cardiomyocytes migrate in response to gradients of fibronectin and Wnt5a. *Stem Cells Dev* (2013) 22(16):2315–25. doi: 10.1089/scd.2012.0586
29. Hescheler J, Halbach M, Egert U, Lu ZJ, Bohlen H, Fleischmann BK, et al. Determination of electrical properties of ES cell-derived cardiomyocytes using MEAs. *J Electrocardiol* (2004) 37(Suppl):110–6. doi: 10.1016/j.jelectrocard.2004.08.034
30. Eng G, Lee BW, Protas L, Gagliardi M, Brown K, Kass RS, et al. Autonomous beating rate adaptation in human stem cell-derived cardiomyocytes. *Nat Commun* (2016) 7:10312. doi: 10.1038/ncomms10312
31. Taylor RJ, Moody WE, Umar F, Edwards NC, Taylor TJ, Stegemann B, et al. Myocardial strain measurement with feature-tracking cardiovascular magnetic resonance: normal values. *Eur Heart J Cardiovasc Imaging* (2015) 16(8):871–81. doi: 10.1093/ehjci/jev006
32. Lee WN, Pernot M, Couade M, Messas E, Bruneval P, Bel A, et al. Mapping myocardial fiber orientation using echocardiography-based shear wave imaging. *IEEE Trans Med Imaging* (2012) 31(3):554–62. doi: 10.1109/TMI.2011.2172690
33. Ribeiro AJ, Ang YS, Fu JD, Rivas RN, Mohamed TM, Higgs GC, et al. Contractility of single cardiomyocytes differentiated from pluripotent stem cells depends on physiological shape and substrate stiffness. *Proc Natl Acad Sci U S A* (2015) 112(41):12705–10. doi: 10.1073/pnas.1508073112
34. Khan M, Xu Y, Hua S, Johnson J, Belevych A, Janssen PM, et al. Evaluation of changes in morphology and function of human induced pluripotent stem cell derived cardiomyocytes (hipsc-cms) cultured on an aligned-nanofiber cardiac patch. *PLoS One* (2015) 10(5):e0126338. doi: 10.1371/journal.pone.0126338
35. Dhillon PS, Gray R, Kojodjojo P, Jabr R, Chowdhury R, Fry CH, et al. Relationship between gap-junctional conductance and conduction velocity in mammalian myocardium. *Circ Arrhythm Electrophysiol* (2013) 6(6):1208–14. doi: 10.1161/CIRCEP.113.000848
36. Durrer D, van Dam RT, Freud GE, Janse MJ, Meijler FL, Arzbaecher RC. Total excitation of the isolated human heart. *Circulation* (1970) 41(6):899–912. doi: 10.1161/01.CIR.41.6.899
37. Bursac N, Parker KK, Iravanian S, Tung L. Cardiomyocyte Cultures With Controlled Macroscopic Anisotropy. *A Model for Functional Electrophysiological Studies of Cardiac Muscle* (2002) 91:e45–54.
38. Wells RG. The role of matrix stiffness in regulating cell behavior. *Hepatology* (2008) 47(4):1394–400. doi: 10.1002/hep.22193
39. Radisic M, Christman KL, Science M, and Tissue Engineering: Repairing the Heart. *Mayo Clinic proceedings Mayo Clinic* (2013) 88:884–98.
40. Jacot JG, McCulloch AD, Omens JH. Substrate stiffness affects the functional maturation of neonatal rat ventricular myocytes. *Biophys J* (2008) 95(7):3479–87. doi: 10.1529/biophysj.107.124545
41. Mcdevitt TC, Angello JC, Whitney ML, Reinecke H, Hauschka SD, Murry CE, et al. In vitro generation of differentiated cardiac myofibers on micropatterned laminin surfaces. *J Biomed Mater Res* (2002) 60(3):472–9. doi: 10.1002/jbm.1292
42. Mcdevitt TC, Woodhouse KA, Hauschka SD, Murry CE, Stayton PS. Spatially organized layers of cardiomyocytes on biodegradable polyurethane films for myocardial repair. *J Biomed Mater Res A* (2003) 66(3):586–95. doi: 10.1002/jbm.a.10504
43. Ribeiro AJ, Ang YS, Fu JD, Rivas RN, Mohamed TM, Higgs GC, et al. Contractility of single cardiomyocytes differentiated from pluripotent stem cells depends on physiological shape and substrate stiffness. *Proc Natl Acad Sci U S A* (2015) 112(41):12705–10. doi: 10.1073/pnas.1508073112
44. Chrobak MO, Hansen KJ, Gershlag JR, Vratsanos M, Kanellias M, Gaudette GR, et al. Design of a Fibrin Microthread-Based Composite Layer for Use in a Cardiac Patch. *ACS Biomater Sci Eng* (2017) 3(7):1394–403. doi: 10.1021/acsbomaterials.6b00547
45. Black LD, Meyers JD, Weinbaum JS, Shvelidze YA, Tranquillo RT. Cell-induced alignment augments twitch force in fibrin gel-based engineered myocardium via gap junction modification. *Tissue Eng Part A* (2009) 15(10):3099–108. doi: 10.1089/ten.tea.2008.0502
46. de Boer TP, van Rijen HVM, van der Heyden MAG, de Bakker JMT and van Veen TAB. Adrenergic regulation of conduction velocity in cultures of immature cardiomyocytes. *Netherlands Heart Journal* (2008) 16:106–9.
47. Stein M, van Veen TA, Hauer RN, de Bakker JM, van Rijen HV. A 50% reduction of excitability but not of intercellular coupling affects conduction velocity restitution and activation delay in the mouse heart. *PLoS One* (2011) 6(6):e20310. doi: 10.1371/journal.pone.0020310
48. van Rijen HV, Eckardt D, Degen J, Theis M, Ott T, Willecke K, et al. Slow conduction and enhanced anisotropy increase the propensity for ventricular tachyarrhythmias in adult mice with induced deletion of connexin43. *Circulation* (2004) 109(8):1048–55. doi: 10.1161/01.CIR.0000117402.70689.75
49. van Veen TAB, Stein M, Royer A, Le Quang K, Charpentier F, Colledge WH. Impaired Impulse Propagation in Scn5a-Knockout Mice. *Combined Contribution of Excitability, Connexin Expression, and Tissue Architecture in Relation to Aging* (2005) 112:1927–35.
50. Lundy SD, Zhu WZ, Regnier M, Laflamme MA. Structural and functional maturation of cardiomyocytes derived from human pluripotent stem cells. *Stem Cells Dev* (2013) 22(14):1991–2002. doi: 10.1089/scd.2012.0490
51. Lluçia-Valldeperas A, Soler-Botija C, Gálvez-Montón C, Roura S, Prat-Vidal C, Perea-Gil I, et al. Electromechanical conditioning of adult progenitor cells improves recovery of cardiac function after myocardial infarction. *Stem Cells Transl Med* (2017) 6(3):970–81. doi: 10.5966/sctm.2016-0079
52. Kroll K, Chabria M, Wang K, Häusermann F, Schuler F, Polonchuk L. Electro-mechanical conditioning of human iPSC-derived cardiomyocytes for translational research. *Prog Biophys Mol Biol* (2017) 130(Pt B):212–22. doi: 10.1016/j.pbiomolbio.2017.07.003
53. Ruan JL, Tulloch NL, Razumova MV, Saiget M, Muskheli V, Pabon L, et al. Mechanical stress conditioning and electrical stimulation promote contractility and force maturation of induced pluripotent stem cell-derived human cardiac tissue. *Circulation* (2016) 134(20):1557–67. doi: 10.1161/CIRCULATIONAHA.114.014998
54. Masumoto H, Ikuno T, Takeda M, Fukushima H, Marui A, Katayama S, et al. Human iPSC cell-engineered cardiac tissue sheets with cardiomyocytes and vascular cells for cardiac regeneration. *Sci Rep* (2014) 4:6716. doi: 10.1038/srep06716
55. Tao ZW, Favreau JT, Guyette JP, Hansen KJ, Lessard J, Burford E, et al. Delivering stem cells to the healthy heart on biological sutures: effects on regional mechanical function. *J Tissue Eng Regen Med* (2017) 11(1):220–30. doi: 10.1002/term.1904
56. Hansen KJ, Favreau JT, Guyette JP, Tao ZW, Coffin ST, Cunha-Gavidia A, et al. Functional Effects of Delivering Human Mesenchymal Stem Cell-Seeded Biological Sutures to an Infarcted Heart. *Biores Open Access* (2016) 5(1):249–60. doi: 10.1089/biores.2016.0026

Conflict of Interest Statement: The authors declare that the research was conducted in the absence of any commercial or financial relationships that could be construed as a potential conflict of interest.

Copyright © 2018 Hansen, Laflamme and Gaudette. This is an open-access article distributed under the terms of the Creative Commons Attribution License (CC BY). The use, distribution or reproduction in other forums is permitted, provided the original author(s) and the copyright owner are credited and that the original publication in this journal is cited, in accordance with accepted academic practice. No use, distribution or reproduction is permitted which does not comply with these terms.



Sheep-Specific Immunohistochemical Panel for the Evaluation of Regenerative and Inflammatory Processes in Tissue-Engineered Heart Valves

Sylvia Dekker¹, Daphne van Geemen¹, Antoon J. van den Bogaerdt², Anita Driessen-Mol^{1,3}, Elena Aikawa⁴ and Anthal I. P. M. Smits^{1,3*}

¹ Soft Tissue Engineering & Mechanobiology Division, Department of Biomedical Engineering, Eindhoven University of Technology, Eindhoven, Netherlands, ² Division Heart Valve Bank, ETB-BISLIFE, Beverwijk, Netherlands, ³ Institute for Complex Molecular Systems (ICMS), Eindhoven University of Technology, Eindhoven, Netherlands, ⁴ Division of Cardiovascular Medicine, Department of Medicine, Center for Excellence in Cardiovascular Medicine, Brigham and Women's Hospital, Boston, MA, United States

OPEN ACCESS

Edited by:

Simon W. Rabkin,
University of British Columbia, Canada

Reviewed by:

Daniel Duerschmied,
Albert Ludwigs Universität Freiburg,
Germany

Valery Bochkov,
University of Graz, Austria

*Correspondence:

Anthal I. P. M. Smits
a.i.p.m.smits@tue.nl

Specialty section:

This article was submitted to
Atherosclerosis and Vascular
Medicine,
a section of the journal
Frontiers in Cardiovascular Medicine

Received: 17 March 2018

Accepted: 13 July 2018

Published: 15 August 2018

Citation:

Dekker S, van Geemen D, van den Bogaerdt AJ, Driessen-Mol A, Aikawa E and Smits AIPM (2018) Sheep-Specific Immunohistochemical Panel for the Evaluation of Regenerative and Inflammatory Processes in Tissue-Engineered Heart Valves.
Front. Cardiovasc. Med. 5:105.
doi: 10.3389/fcvm.2018.00105

The creation of living heart valve replacements via tissue engineering is actively being pursued by many research groups. Numerous strategies have been described, aimed either at culturing autologous living valves in a bioreactor (*in vitro*) or inducing endogenous regeneration by the host via resorbable scaffolds (*in situ*). Whereas a lot of effort is being invested in the optimization of heart valve scaffold parameters and culturing conditions, the pathophysiological *in vivo* remodeling processes to which tissue-engineered heart valves are subjected upon implantation have been largely under-investigated. This is partly due to the unavailability of suitable immunohistochemical tools specific to sheep, which serves as the gold standard animal model in translational research on heart valve replacements. Therefore, the goal of this study was to comprise and validate a comprehensive sheep-specific panel of antibodies for the immunohistochemical analysis of tissue-engineered heart valve explants. For the selection of our panel we took inspiration from previous histopathological studies describing the morphology, extracellular matrix composition and cellular composition of native human heart valves throughout development and adult stages. Moreover, we included a range of immunological markers, which are particularly relevant to assess the host inflammatory response evoked by the implanted heart valve. The markers specifically identifying extracellular matrix components and cell phenotypes were tested on formalin-fixed paraffin-embedded sections of native sheep aortic valves. Markers for inflammation and apoptosis were tested on ovine spleen and kidney tissues. Taken together, this panel of antibodies could serve as a tool to study the spatiotemporal expression of proteins in remodeling tissue-engineered heart valves after implantation in a sheep model, thereby contributing to our understanding of the *in vivo* processes which ultimately determine long-term success or failure of tissue-engineered heart valves.

Keywords: immunohistochemistry, ovine antibodies, cardiovascular tissue engineering, elastogenesis, inflammation, macrophages, valvular interstitial cells, extracellular matrix

INTRODUCTION

Valvular heart disease is a major health problem. Heart valve tissue engineering (TE) strategies aim to create autologous, living heart valves with the potential for growth and remodeling to replace the malfunctioning heart valve. Since approximately two decades ago, several TE strategies have been actively pursued to create living heart valve replacements *in vitro*, using a variety of cell sources, scaffold types and fabrication methods (1–11). Alternative to the traditional *in vitro* TE paradigm, *in situ* TE strategies are being developed, using acellular, readily-available scaffolds which are designed to induce endogenous tissue regeneration directly at the valve's functional site (12–14). *In situ* TE scaffolds include natural matrices, such as decellularized allografts (15–18) or *de novo* engineered and decellularized heart valves (19–23), or resorbable synthetic heart valves (24, 25).

For all heart valve TE strategies, the main challenge lies in the functional, and eventually homeostatic integration of the TE valve into the body. In particular, mimicking the sophisticated tri-layered structure of the native valve, including a well-organized anisotropic collagen and elastin network populated with quiescent valvular interstitial cells (VICs), requires a thorough understanding of valvular developmental and biomechanical remodeling processes (26, 27). Moreover, the host immune response evoked by a TE heart valve after implantation is perhaps the most crucial determinant of successful valve integration. This is even more important for *in situ* TE strategies, which rely on triggering a favorable inflammatory response upon implantation in order to induce a regenerative cascade (13, 28, 29).

In general, any implanted device (whether or not cellular) will induce an inflammatory response by the host. This response occurs as a cascade of events, ignited by disruption of the tissue structure and cell damage due to the implantation procedure (30). At the very early stages of implantation, blood-biomaterial interactions lead to the adsorption of endogenous proteins from blood to the biomaterial surface. Following this provisional matrix formation and within the first days after implantation, acute inflammation occurs with an immediate influx of innate immune cells, mostly neutrophils and monocytes. In later stages, chronic inflammation develops as inflammatory stimuli persist at the implant side, with phagocytic macrophages and multinucleated giant cells controlling the microenvironment in cross-talk with lymphocytes. Tissue producing cells such as endothelial cells, fibroblasts, and various (circulating) stem and progenitor cells of both mesenchymal and hematopoietic origin, produce an extracellular matrix (ECM) and account for remodeling as in the cascade of normal wound healing. Depending on the implant properties and the host's immune tissue responses, these may lead to either functional regenerated tissue or pathological fibrotic repair (13, 28). In addition, in case of a TE heart valve prosthesis, healing outcome is influenced by the direct exposure to the blood stream and the resulting hemodynamic loads. However, although some of these immunological events have been experimentally demonstrated for *in situ* TE blood vessel prostheses (31, 32), specific information regarding these immunological processes for TE heart valves is sparse.

Heart valve TE research has predominantly focused on optimizing valvular graft design and *in vitro* culture protocols (6–11, 33), and relatively little mechanistic data is available regarding the *in vivo* biological events that drive remodeling and integration of TE valves after implantation (34). *In vivo* testing of heart valves is typically performed in sheep, as this is the FDA-approved animal model for preclinical evaluation of heart valves. The heart valves of sheep resemble those of humans in terms of mechanical properties and hemodynamic flow parameters (35). Furthermore, sheep develop relatively rapidly, thus the growth and remodeling processes to which heart valves are subjected within several months in juvenile sheep, take several years to develop in patients (36). Finally, due to the enhanced calcium metabolism in sheep, the sheep represent the “worst-case-scenario” in terms of valvular calcification (37, 38). For the bulk of *in vivo* studies using TE heart valves, explant analysis is focused on valve functionality, overall tissue composition and mechanical properties. However, there is an imminent need for mechanistic studies to unravel the biological processes underlying *in vivo* valve integration and remodeling in terms of cellular infiltration and phenotypical characterization, immunological processes, tissue formation/organization, and valve development (34).

So far, a detailed spatiotemporal characterization of cellular phenotypes and tissue remodeling is lacking due to the limited commercially available sheep-specific antibodies for immunohistochemistry. Therefore, the goal of this study was to develop a comprehensive sheep-(cross) reactive marker panel of antibodies to assess the inflammatory and regenerative processes in TE heart valves. Based on previous studies on the composition of native human heart valves throughout development and adult stages (39–42), the panel includes antibodies to study ECM composition, elastogenesis, VIC phenotypes, endothelial cells (ECs), proliferation/apoptosis, and inflammation. These antibodies were tested against paraffin sections of native ovine aortic valve tissue. Markers for inflammatory cells and apoptosis were tested on ovine spleen and kidney tissue.

METHODS

Sheep Tissue

The desired control tissues (aortic heart valve, kidney) were collected from two juvenile sheep (female, Swifter, 1 year old). Additionally, the spleen of a juvenile sheep (female, Swifter, 1 year old) diagnosed with endocarditis was collected to study the inflammatory markers. The ovine tissues from these three sheep were discarded tissues from synthetic pulmonary heart valve replacement experiments. This study was carried out in accordance with local and national regulations, approved by the animal ethics committee of the University Medical Center Utrecht. Also, ovine pulmonary valves were obtained from the slaughterhouse. All tissues were immediately fixed in 4% paraformaldehyde for 24 h at 4°C. After fixation the tissues were embedded in paraffin, sectioned with a thickness of 5 µm, applied to a poly-lysine coated slide (Thermo Scientific), and dried overnight in a 37°C incubator.

All antibodies for valve-related proteins (i.e., ECM-related proteins, proteins involved in elastogenesis, and VIC markers) were validated on the ovine aortic valves ($n = 2$) and ovine pulmonary valve leaflets ($n = 2$). The antibodies for inflammatory proteins were validated on the ovine spleen tissue, representing a tissue with a well-known composition of immune cells.

Human Tissue

Cryopreserved human aortic and pulmonary valves were obtained from a Dutch postmortem donor (male; 38 years old), giving permission for research according to national ethical and regulatory guidelines. This study was carried out in accordance with the recommendations of ETB-BISLIFE, division Heart Valve Bank (Beverwijk, the Netherlands), and was conducted conform the principles outlined in the Declaration of Helsinki. The valves were obtained from ETB-BISLIFE, division Heart Valve Bank and were used in a previous study by our research group, aimed at investigating the histopathological and mechanical properties of human heart valves during various stages of life (40). The valves were assessed to be unfit for implantation due to findings that contra-indicated implantation, consisting among others of positive bacteriological sampling, serological findings in the donor and other procedural non-conformities that caused rejection of the donor (e.g., sexual risk behavior and/or risk in drug abuse). The cause of death was not related to valvular disease or condition known to precede valvular disease and both valves were structurally and mechanically unaffected. After thawing, the tissue was fixed overnight in 4% paraformaldehyde, processed, and subsequently embedded in paraffin to prepare sections with a thickness of 10 μm .

Histology

Tissue slides were deparaffinized in xylene and rehydrated in a graded series of ethanol. A modified Russell-Movat pentachrome stain (43) was performed to visualize overall tissue composition and organization (American MasterTech). ECM components, including collagen (yellow), elastin (black) and glycosaminoglycan/proteoglycans (GAGs; green-blue) were detected as well as cell nuclei (dark-blue/purple) and fibrin (red). Weigert's Iron Hematoxylin (Sigma) and Eosin (Sigma) staining was performed to reveal distinct compartments of spleen tissue.

Immunohistochemistry

After deparaffinization, antigen retrieval was performed, depending on the used primary antibody (Table 1). For heat-mediated antigen retrieval, the tissue slides were heated in a 96°C water bath for 20 min in modified citrate buffer (pH 6.1, DAKO) or TRIS-EDTA buffer (pH 9.0, DAKO). After heating, slides were slowly cooled down to room temperature (45 min). For enzymatic antigen retrieval, 0.05% pepsin (Sigma) in 10 mM HCl or 0.6 U/ml Proteinase K (Sigma, in 50 mM Tris Base, 1 mM EDTA, 0.5% Triton X-100, pH 8.0) was applied to the tissue slides for 12 min at 37°C. Nonspecific binding was blocked by either goat serum (Invitrogen) or horse serum (Life Technologies) in 1% bovine serum albumin (BSA; Sigma)

in phosphate-buffered saline (PBS; Sigma)/0.05% Tween-20 (Merck) for 2 h at room temperature. Primary antibodies were prepared in the optimized concentrations (see Table 1) in 1:10 diluted blocking solution. Tissue slides were incubated overnight at 4°C and thereafter washed with PBS/tween-20. The applied secondary antibodies were either goat-anti-rabbit antibody (DAKO) or horse-anti-mouse antibody (DAKO), both labeled with biotin and diluted 1:500 in PBS/Tween-20. After 2 h of incubation at room temperature the sections were washed with TRIS-buffered saline (TBS)/tween-20. To enhance staining, an ABC-alkaline phosphatase kit (Vector laboratories, VECTASTAIN® ABC-AP Staining Kit) was used for 1 h at room temperature, according to the manufacturer's guidelines. After washing with TBS/tween-20, the slides were exposed to SIGMA FAST™ BCIP/NBT (5-Bromo-4-chloro-3-indolyl phosphate/Nitro blue tetrazolium, pH 9.5; Sigma) for 5–30 min (depending on the intensity of the staining, which was assessed by light microscopy). For counterstaining of cells, nuclear fast red (Sigma) was applied for 3 min. The sections then were dehydrated and mounted in Entellan (Merck). Negative controls were generated with the same procedure omitting the primary antibody during the first incubation.

Imaging and Representation

Light microscopy images and tile scans were acquired and documented with a Zeiss Axio Observer Z1 microscope using Zeiss ZEN software. The tile scans of one of the ovine aortic valves are displayed as representative samples for all valves tested. To provide a concise semi-quantitative overview of protein expression in the ovine valves, the protein expression was scored (scale 0–4; no expression—high expression, respectively) per region in the valve (arterial wall, hinge region, belly, and free edge of the leaflet) and per valvular layer (fibrosa, spongiosa, and ventricularis).

RESULTS

Human and Sheep Heart Valve Histopathology

Russell-Movat pentachrome staining reveals comparable structure and gross morphology for human and ovine aortic and pulmonary heart valve leaflets, with collagen on the outflow side (fibrosa), elastin on the inflow side (ventricularis) and soluble proteoglycans and glycoproteins in the interstitial layer (spongiosa) (Figure 1). In the sheep valves, the transition from one tissue layer to the other is highly delineated, while in human the layers merge into each other. Toward the free edge of the leaflet, the stratification in the both human and ovine leaflets becomes less pronounced and is no longer observable at the leaflet tip. For both the pulmonary and aortic valves, the ovine leaflets are visibly more cellularized when compared to the human leaflets. Elastin expression shows a remarkable difference in amount and network organization, with a distinct, multi-layered elastic network in the human leaflets, compared to only a few fibers in the sheep leaflets.

TABLE 1 | Antibodies used for immunohistochemistry.

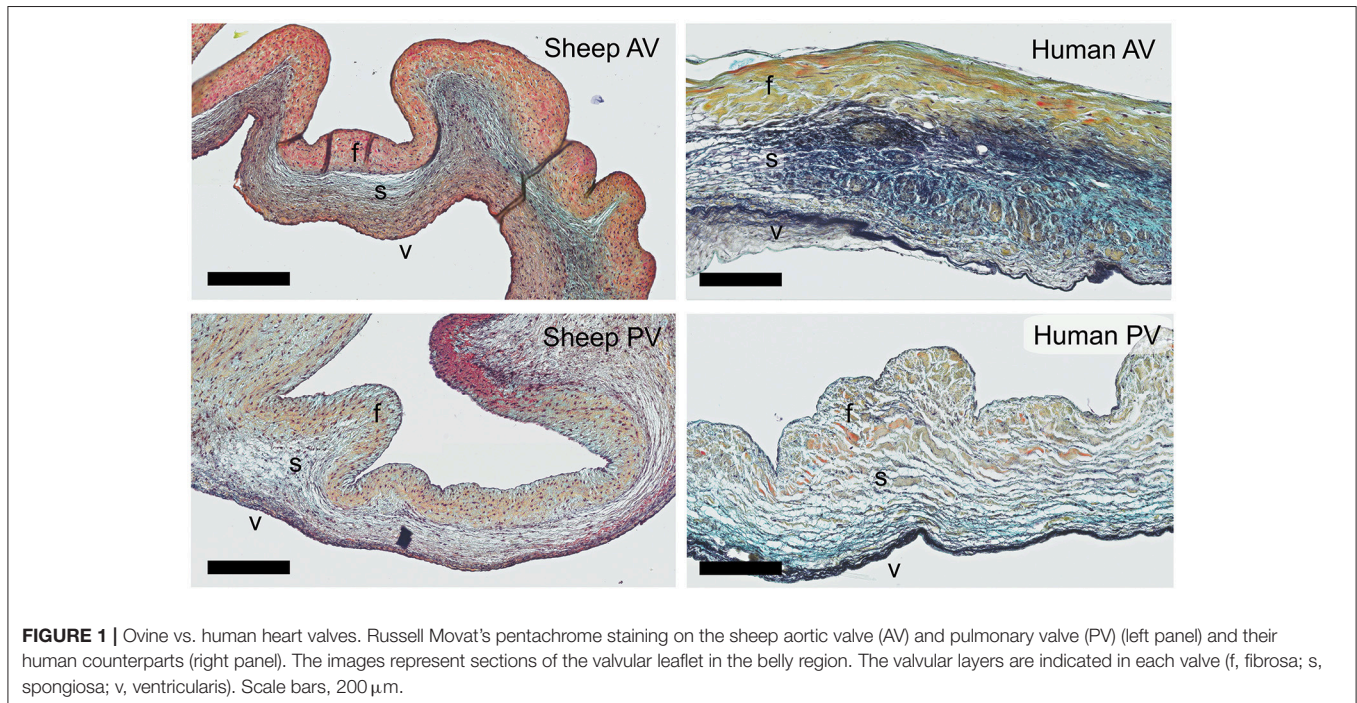
Antibody	Host	Clone	Distributor	Cat. No.	Antigen retrieval	Dilution
ECM						
Collagen type 1	Mouse	Col-1, IgG1	Sigma	C2456	Citrate	200
Collagen type 3	Rabbit	Polyclonal	Abcam	Ab7778	Pepsin	250
Periostin	Rabbit	Polyclonal	n.a.	n.a.	Citrate	500
Versican	Rabbit	Polyclonal	Abcam	Ab6994	Proteinase K	200
Biglycan	Rabbit	Polyclonal	Biorbyt	orb100396	Pepsin	150
Decorin	Rabbit	Polyclonal	Biorbyt	orb10520	Tris/EDTA	150
MMP-1	Rabbit	EP1247Y, IgG	Abcam	ab52631	Citrate	200
MMP-2	Mouse	6E3F8, IgG2b	Abcam	ab86607	Proteinase K	400
MMP-9	Rabbit	Polyclonal	Abcam	ab38898	Citrate	200
MMP-13	Rabbit	Polyclonal	Abcam	ab39012	Citrate	200
TGF- β 1	Rabbit	Polyclonal	Abcam	ab9758	Citrate	500
TGF- β 3	Rabbit	Polyclonal	Novus Biologicals	NB600-1531	Citrate	400
ELASTOGENESIS						
(Tropo)elastin	Rabbit	Polyclonal	Abcam	ab21610	Pepsin	400
Fibronectin	Rabbit	Polyclonal	Sigma	F3648	Pepsin	300
Fibrillin-1	Rabbit	Polyclonal	Sigma	HPA017759	Pepsin	100
Fibrillin-2	Rabbit	Polyclonal	Sigma	HPA012853	Pepsin	100
Lysil oxidase (LOX)	Rabbit	Polyclonal	Novus Biologicals	NB100-2530	Tris/EDTA	200
Fibulin-4	Rabbit	Polyclonal	Abonline	abin1701235	Pepsin	200
Fibulin-5	Mouse	3F10A5, IgG1	Abonline	abin1107239	Proteinase K	100
EMILIN-1	Rabbit	Polyclonal	Biorbyt	orb183385	Pepsin	200
VICs						
α -SMA	Rabbit	Polyclonal	Abcam	ab5694	Pepsin/citrate	600
Vimentin	Rabbit	D21H3, IgG	Cell Signalling	5741	Citrate	300
SM22	Rabbit	Polyclonal	Abcam	ab14106	Citrate	200
Calponin	Rabbit	Polyclonal	Abcam	ab46794	Pepsin	150
Cadherin-11	Rabbit	Polyclonal	Thermo Scientific	71-7600	Citrate	100
SMemB	Mouse	3H2, IgG2b	Abcam	ab684	Tris/EDTA	200
VECs						
CD31 (PECAM-1)	Mouse	CO.3E-1D4, IgG2a	Novus Biologicals	NB100-65900	Pepsin	100
CD34	Rabbit	EP373Y, IgG	Abcam	ab81289	Tris/EDTA	200
VE-Cadherin	Rabbit	Polyclonal	Abcam	ab33168	Citrate	200
von Willebrand factor	Rabbit	Polyclonal	Abcam	ab6994	Citrate	1200
PROLIFERATION/APOPTOSIS						
Ki-67	Rabbit	Polyclonal	Thermo Scientific	rb1510-PO	Citrate	200
Cleaved Caspase-3	Rabbit	Polyclonal	Cell Signalling	9661	Citrate	200
CALCIFICATION						
Osteocalcin	Rabbit	Polyclonal	Abcam	ab93876	Tris/EDTA	200
INFLAMMATION						
CD45	Mouse	1.11.32, IgG1	AbD-serotec	MCA2220GA	None	1000
CD3	Rabbit	Polyclonal	DAKO	A0452	Tris/EDTA	200
CD64	Mouse	3D3, IgG1	Abcam	ab140779	Citrate	200
CSF-1R (CD115)	Rabbit	Polyclonal	Abonline	abin498117	Citrate	200
EMR-1	Rabbit	Polyclonal	Gene Tex	GTX101895	Tris/EDTA	500
iNOS	Rabbit	Polyclonal	Abcam	ab3523	Citrate	400

(Continued)

TABLE 1 | Continued

Antibody	Host	Clone	Distributor	Cat. No.	Antigen retrieval	Dilution
CCR7 (CD197)	Rabbit	Polyclonal	Abcam	ab32527	Citrate	1200
TNF- α	Rabbit	Polyclonal	Acris	AP20373PU-n	Citrate	300
CD163	Mouse	EdHu-1, IgG1	AbD-serotec	mca1853	Citrate	250
CD200R	Rabbit	Polyclonal	Abonline	Abin737586	Citrate	200
Arginase-1	Rabbit	Polyclonal	Bioss	bs-8585R-Biotin	Citrate	500
IL-10	Rabbit	Polyclonal	Biorbyt	orb221323	Citrate	200
CXCR4 (CD184)	Mouse	44716, IgG2b	RnD systems	MAB172	Citrate	500
CD44	Rabbit	Polyclonal	Abcam	ab24504	Citrate	250

MMP, matrix metalloproteinase; TGF- β , transforming growth factor- β ; EMILIN-1, elastin microfibril interfacier 1; α -SMA, α -smooth muscle actin; CSF-1R, colony stimulating factor-1 receptor; EMR-1, EGF-like module-containing mucin-like hormone receptor-like 1; iNOS, inducible nitric oxide synthase; TNF- α , tumor necrosis factor- α ; IL-10, interleukin-10; VE-cadherin, vascular endothelial cadherin



ECM Remodeling

The staining patterns of the major ECM (-related) proteins, including collagen type I and III and proteoglycans as well as matrix metalloproteinases (MMPs) and transforming growth factor- β (TGF- β) was analyzed in the ovine aortic valve leaflets ($n = 2$) and pulmonary valve leaflets ($n = 2$). All valves displayed similar staining patterns. **Figures 2, 3** display the representative tile scans of protein expression in one of the aortic valves. Negative control sections for all tested antibodies, in which the primary antibody was omitted, revealed no background signal (not shown).

Collagen type I is mainly present in the fibrosal layer in a punctuated pattern indicative of the circumferential orientation of the fibers (**Figure 2**, top panel). It is also present within the loose connective tissue. Collagen type III expression is overlapping with collagen type I in the fibrosa, but is also present in the spongiosa, endothelial layer, and microvasculature.

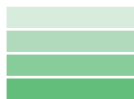
Periostin is observed in the hinge region, fibrosa, aortic wall, and microvasculature, and is increasingly expressed by interstitial cells toward the free edge of the valve leaflet. Expression of the tested proteoglycans reveals a dispersed distribution of versican throughout the leaflet, as well as connective tissue, microvasculature and cardiac muscle (**Figure 2**, bottom panel). Biglycan shows an overall weak staining, mainly in the ventricularis. Decorin is predominantly expressed in the spongiosa, with most pronounced expression in the tip and hinge regions.

Matrix metalloproteinases-1 (MMP-1) is predominantly distributed through the spongiosa and is expressed in the microvasculature of the base of the leaflet (**Figure 3**). MMP-13 is highly present in the spongiosa and ventricularis, the hinge region and the connective tissue. MMP-2 is expressed as an abundant cellular staining throughout the leaflet layers, aorta and microvasculature. MMP-9 is observed in hinge cells

TABLE 2 | Summary of protein expression in the ovine aortic valve; categorized per region (aorta, leaflet hinge, belly, and free edge), or per leaflet layer (fibrosa, spongiosa, ventricularis).

		Aorta	Hinge	Belly	Free edge	Fibr.	Spon.	Ventr.
Extracellular matrix	Collagen I							
	Collagen III							
	Periostin							
	Decorin							
	Biglycan							
	Versican							
	MMP-1							
	MMP-13							
	MMP-2							
	MMP-9							
TGF-β1								
TGF-β3								
Elastogenesis	Elastin							
	Fibronectin							
	Fibrillin-1							
	Fibrillin-2							
	Fibulin-4							
	Fibulin-5							
	EMILIN-1							
	LOX							
VICs	α-SMA							
	Vimentin							
	SM22							
	Calponin							
	Cadherin-11							
	SMemB							
	Ki-67							
	Osteocalcin							

No expression



High expression

and sparsely in cells within the ventricularis. TGFβ1 is strongly expressed in the smooth muscle cell layer of the aortic wall and microvasculature, but not in the valve leaflet, while TGFβ3 shows only a weak staining in the aortic wall (Figure 3).

Elastic Network

Movat's shows abundant deposition of elastin in the aortic wall and a weaker staining in the leaflet ventricularis. Selected antibodies to assess elastin-related proteins include (tropo)elastin, fibrillins, fibulins, and cross-linking proteins (Figure 4). (Tropo)elastin is abundant in the ventricularis, but also the endothelial layers and spongiosa are positively stained. Fibronectin is present in all leaflet layers cells, with the most pronounced expression in the fibrosa and ventricularis. Fibrillins (FBN)–1 and–2 are expressed in the spongiosa and

the ventricularis. These patterns are mostly overlapping, except for the strong FBN-2 staining in the tip of the leaflet. FBN-2 staining is restricted to the leaflet, while for FBN-1 the heart connective tissue is positive as well. Lysyl oxidase (LOX) exhibits only a mild expression in the ventricularis, while an overall strong staining pattern in the aorta and cardiac muscle tissue is found. Fibulin-4 exhibits strong staining of the ventricularis, as well as the aortic wall, heart tissue, and endothelial cells. For fibulin-5, on the other hand, a mild staining of the spongiosa and ventricularis is observed, in addition to positive staining of VICs in the tip of the leaflet and the endothelial cells of mainly the aorta. Elastin microfibril interfacier 1 (EMILIN-1) is very weakly present in the ventricularis and spongiosa, as compared to a stronger expression in the heart muscle tissue.

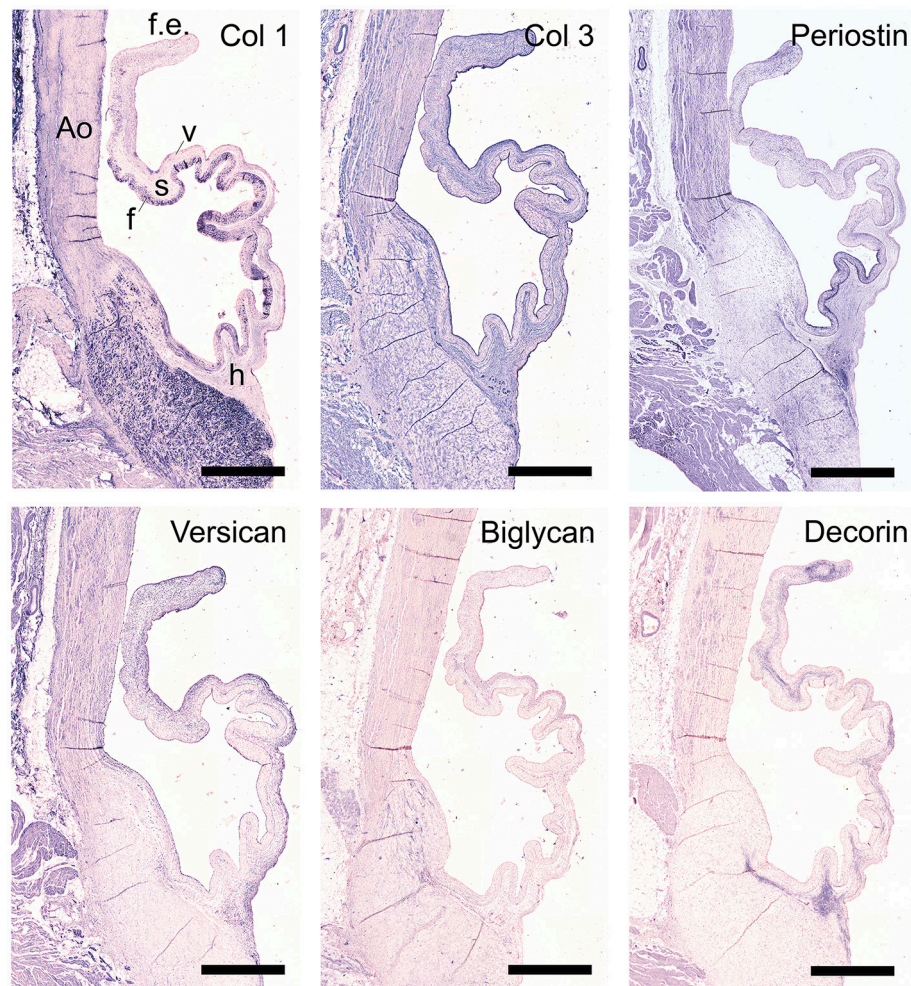


FIGURE 2 | Collagens and proteoglycans. Tile scans of sheep aortic valve sections with the leaflet hinge (h), the free edge (f.e.), the aorta (Ao), and the three valvular layers (f, fibrosa; s, spongiosa; v, ventricularis) as indicated (top left). Valves were stained with antibodies against collagen type 1 (Col 1), collagen type 3 (Col 3), and periostin (top panel), and the proteoglycans versican, biglycan, and decorin (bottom panel). Scale bars, 1 mm.

Valvular Interstitial Cells

To characterize VIC phenotypes, several smooth muscle and mesenchymal markers are included in the antibody panel (Figure 5). The intermediate filament vimentin shows extensive staining in almost all cells in the leaflet, with particularly abundant presence of vimentin-positive cell in the tip of the leaflet. On the other hand, the valve leaflet contains only a very limited number of alpha-smooth muscle actin (α -SMA) positive cells below the endothelial layer on the ventricularis side of the leaflet. In contrast, the smooth muscle cells (SMCs) of the aortic wall and microvasculature are highly positive for α -SMA. Another marker for mature differentiated SMCs, SM22, strongly stains the aortic wall, heart muscle cells, microvasculature, and connective tissue. In the leaflet, SM22 displays a similar staining pattern as vimentin. The calponin antibody stains mainly the aortic SMCs, the microvasculature, and the cells in the fibrosa and tip of the leaflet. Cadherin-11 (as mesenchymal marker for VICs) is expressed in VICs throughout the leaflet, but especially

in the ventricularis. Additionally, this antibody stains cells of the aorta and microvasculature and shows expression in the heart muscle. Non-muscle myosin heavy chain (SMemB), produced by activated mesenchymal cells, stains the VICs throughout the leaflet, the endothelial lining, as well as the cells of the aorta.

Endothelial Cells

CD31, CD34, von Willebrand factor (vWF), and vascular endothelial cadherin (VE-cadherin; CD144) were used to assess the endothelial cell function (Figure 6). All studied markers show expression in the aortic endothelial cells. CD31 specifically stains all endothelial cells of the valvular leaflet, while CD34, VE-cadherin, and vWF have differential expression in the endothelial cells on the ventricular side of the leaflet. CD34 is also present in VICs (more abundant in the ventricularis) and the aortic wall. VE-cadherin and vWF also show some modest staining of individual VICs and SMCs within the aortic wall.

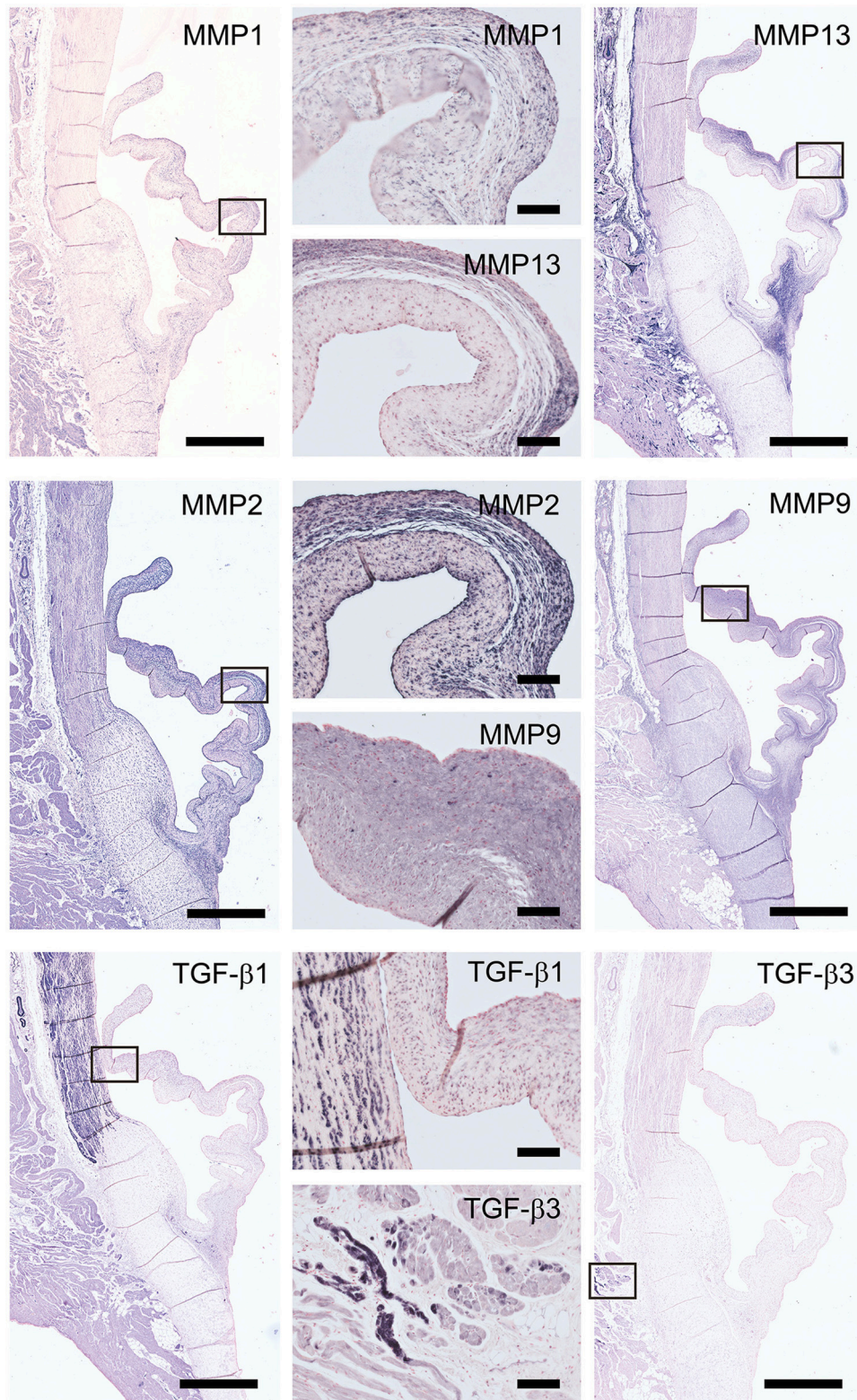


FIGURE 3 | Matrix remodeling and synthesis-related proteins. Tile scans of sheep aortic valve sections (left and right columns), with high magnification zooms (middle column) as indicated. Valves were stained with antibodies against matrix metalloproteinases (MMPs; collagenases MMP1, MMP13, and gelatinases MMP2, MMP9) and transforming growth factor- β , isoforms 1 and 3 (TGF- β 1 and TGF- β 3, respectively). Scale bars, 1 mm (tile scans) or 100 μ m (zooms).

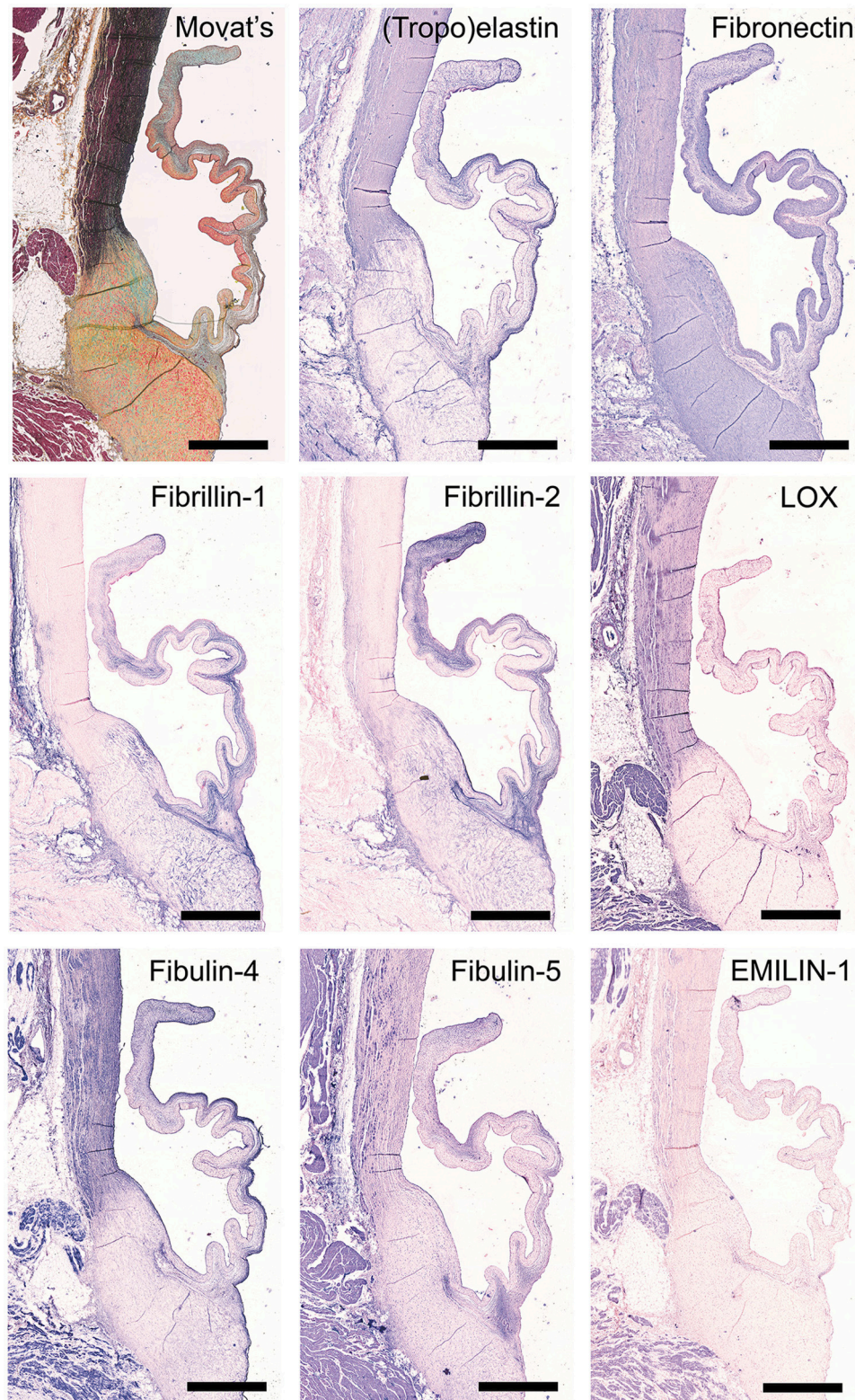


FIGURE 4 | Elastin and elastin-related proteins. Tile scans of sheep aortic valve sections stained with Russell Movat's pentachrome (mature elastic fibers in black) and antibodies against proteins involved in elastic fiber formation, including the core protein (tropo)elastin, fibronectin, the microfibrillar proteins fibrillin-1 and fibrillin-2, and cross-linking proteins fibulin-4, fibulin-5, lysyl oxidase (LOX), and Elastin microfibril interfacier 1 (EMILIN-1). Scale bars, 1 mm.

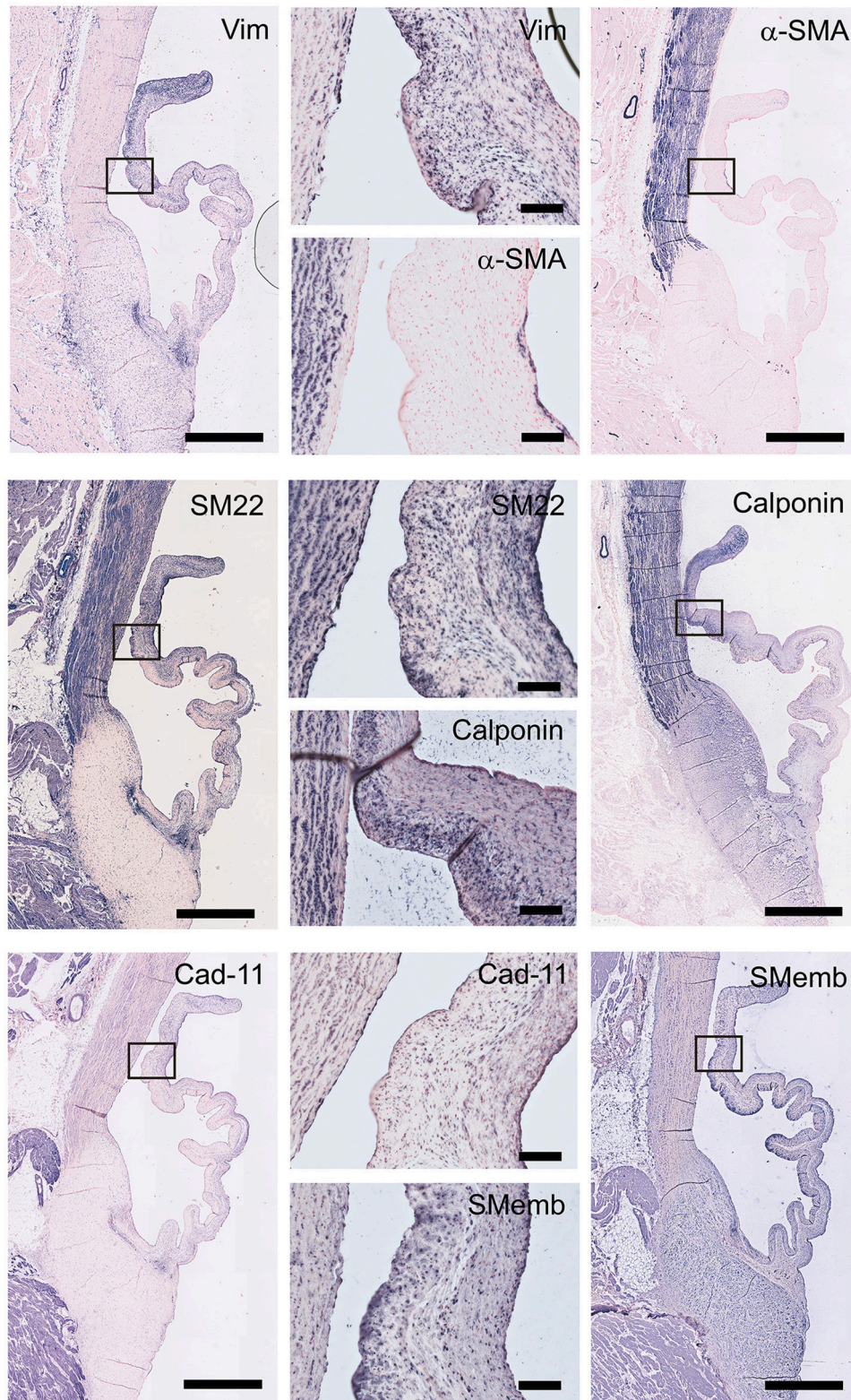


FIGURE 5 | Valvular interstitial cell (VIC) markers. Tile scans of sheep aortic valve sections (left and right columns), with high magnification zooms (middle column) as indicated. Valves were stained with antibodies against vimentin, α -smooth muscle actin (α -SMA), SM22, calponin, cadherin-11 (Cad-11), and the embryonic form of myosin heavy chain (SMemb). Scale bars, 1 mm (tile scans) or 100 μ m (zooms).

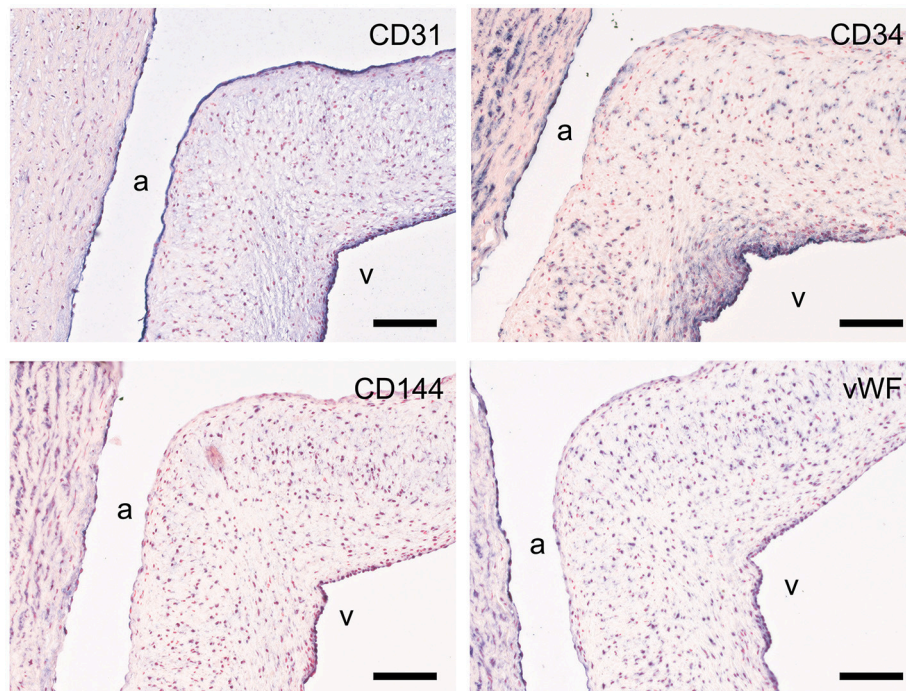


FIGURE 6 | Valvular endothelial cell (VEC) markers. Sections of the sheep aortic valve leaflet stained with antibodies against the endothelial cell markers CD31, CD34, VE-Cadherin (CD144), or von Willebrand Factor (vWF). Represented are the aortic wall and a section of the valvular leaflet (near the free edge), with “a” and “v” indicating the aortic and ventricular sides of the leaflet, respectively. Scale bars, 100 μ m.

Proliferation and Apoptosis

The proliferation marker Ki67 is abundantly expressed throughout the valve leaflet, predominantly staining VICs at the hinge and the tip of the leaflet (Figure 7). Apoptosis is evaluated using an antibody against cleaved caspase-3 (Cas3). Using this antibody, apoptosis was not observed in the valvular leaflet, but was detected in localized sections of the ovine renal tubuli (Figure 7).

Calcification

Osteocalcin expression was detected in chondrocyte-like cells in a section of an ovine pulmonary leaflet in which the onset of calcification was observed (Figure 8). Although no calcium was detected in this region using alizarin red staining (data not shown), osteocalcin expression in this portion of the valve colocalized with strong proteoglycan presence, indicative of cartilage-like tissue, as evident from Russell-Movat pentachrome staining.

Inflammatory Cells

The signs of inflammation are not observed in our non-diseased ovine valves. We therefore validated inflammatory markers using the spleen from a sheep with endocarditis (Figure 9). CD45 is abundantly expressed by all leukocyte cells, but not erythrocytes or the mesenchymal cells in the trabeculae and arterioles. CD3 staining is mainly observed in the germinal centers of the white pulp, with positive cells scattered in the mantle and marginal zones. CD64 and EGF-like module-containing

mucin-like hormone receptor-like 1 (EMR-1) stain macrophages in both the red and white pulp, whereas colony stimulating factor-1 receptor (CSF-1R) displays a sparse staining of specific subpopulations of macrophages in both red and white pulp. IL-10, iNOS, and CD163 predominantly stain positive for the splenic tissue macrophages in the red pulp. Additionally, some isolated CD163- and iNOS-positive cells are noted in the white pulp. CD200R displays a specific staining in the marginal zone of the white pulp, whereas CD44 stains lymphocytes and myeloid cells predominantly in the red pulp. Excessive immune reactivity was observed for arginase-1 (Arg-1), CCR-7, and tumor necrosis factor-alpha (TNF- α).

DISCUSSION

Limited data is available on the *in vivo* processes that determine the regeneration and long-term functional integration of TE heart valves upon implantation. These require incorporation of inflammatory and developmental processes that drive neotissue formation toward functional regeneration or fibrotic repair. Since histochemical evaluation of explants is typically limited to basic histology, due to a lack of commercially available sheep-specific antibodies, the aim of this study was to establish, validate, and optimize a comprehensive immunohistochemical panel of antibodies for ovine tissues to study TE heart valves. This panel includes antibodies against structural ECM proteins (e.g., collagens, proteoglycans), ECM-related proteins (e.g.,

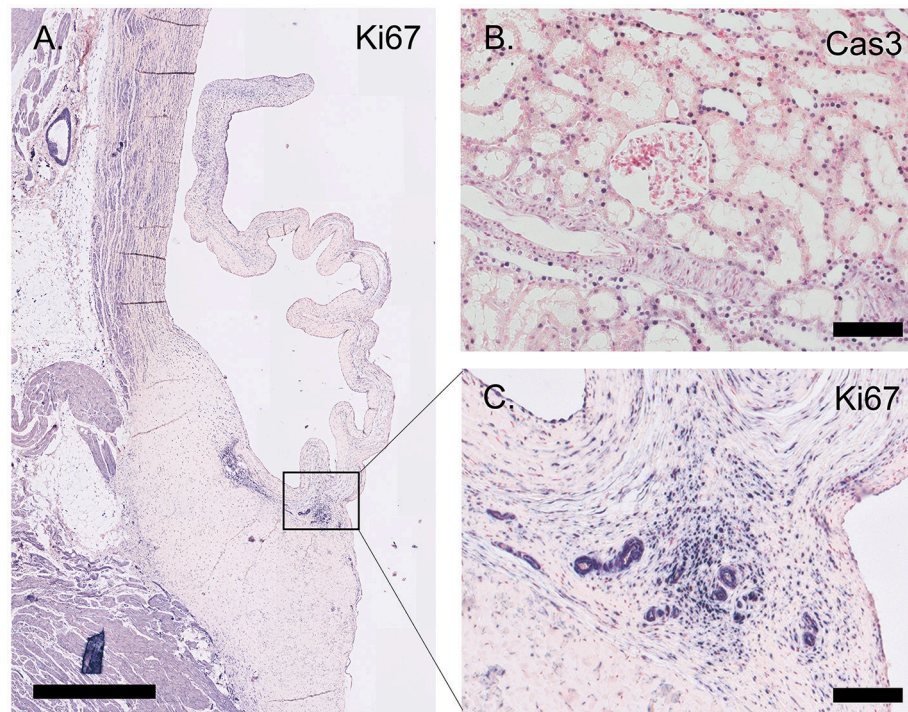


FIGURE 7 | Proliferation and apoptosis markers. **(A)** Tile scan of an ovine aortic valve stained with the proliferation marker Ki67. **(B)** Section of the ovine kidney stained against the apoptosis marker cleaved caspase-3 (Cas3). **(C)** Zoom of the Ki67-labeled aortic valve demonstrating abundant Ki67 expression in the vascularized hinge region. Scale bars, 1 mm **(A)** and 100 μm **(B, C)**.

periostin, MMPs, TGF- β isoforms), and proteins responsible for elastogenesis, as well as cell phenotypic markers for VICs, ECs, inflammatory cells, and relevant cell function markers (e.g., proliferation, apoptosis, calcification).

The immunohistochemical analysis of explanted TE heart valves in preclinical studies is typically limited to a few antibody stainings assessing VIC activation and endothelial coverage (e.g., α -SMA and CD31). Nevertheless, several recent studies concerning *in situ* cardiovascular TE have employed antibodies to characterize more specific functions, for example the regenerative processes in decellularized allogeneic heart valves (15), the occurrence of elastogenesis in synthetic *in situ* TE heart valves (24), and the somatic growth of an *in situ* TE pulmonary artery in lambs (44). The need for a sheep-specific antibody panel for cardiovascular research has previously been proposed by De Visscher et al. who reported on a panel of immunohistochemical and immunofluorescent stains for sheep (45). Although highly relevant, the selected antibodies were tested on formalin-fixed frozen sections of various ovine tissues, such as artery and skin, but not on native ovine heart valves. Building on these previous reports, to the best of our knowledge, the described panel is the first comprehensive panel of 47 antibodies, validated against native ovine heart valves, which enables a complete and detailed evaluation of TE heart valve explants from sheep studies.

In the selection of antibodies for our panel, we took inspiration from various studies describing the morphology,

ECM composition and cellularity of native human heart valves throughout development and adult stages (39–42, 46). As anticipated, we observed several clear differences between human and ovine valves. Most strikingly, the ovine leaflets, both pulmonary and aortic, displayed a much more defined transition between the valvular layers, higher cellularity and less elastin expression when compared to the human valves. Human valves instead often demonstrate incorporation of collagen fibers and elastin network within the other layers (47). These differences observed between human and ovine valves could partly be caused by disease (48) and a discrepancy in age, since recent studies have shown that human valves continuously develop (40, 49) and degenerate throughout life. The ovine aortic valves used in this study were derived from 1 year old sheep, which translates to human adolescence (15–19 years of age), while the human valves were derived from a 38-year old human donor. The human valves were cryopreserved before further processing, which may have introduced freezing artifacts. Moreover, the sections of the human valves were thicker compared to the sections of the ovine valves (10 μm and 5 μm , respectively), which could lead to variations in intensity of the pentachrome staining and antibody expression. Previous research demonstrated significant differences between human- and sheep-derived VIC-like cells, in terms of ECM synthesis and cellular proliferation (50). Similarly, here we observed a notably high amount of proliferating VICs in the ovine aortic leaflet, as determined by Ki67 staining. In contrast, proliferation and overall cell turnover were very low

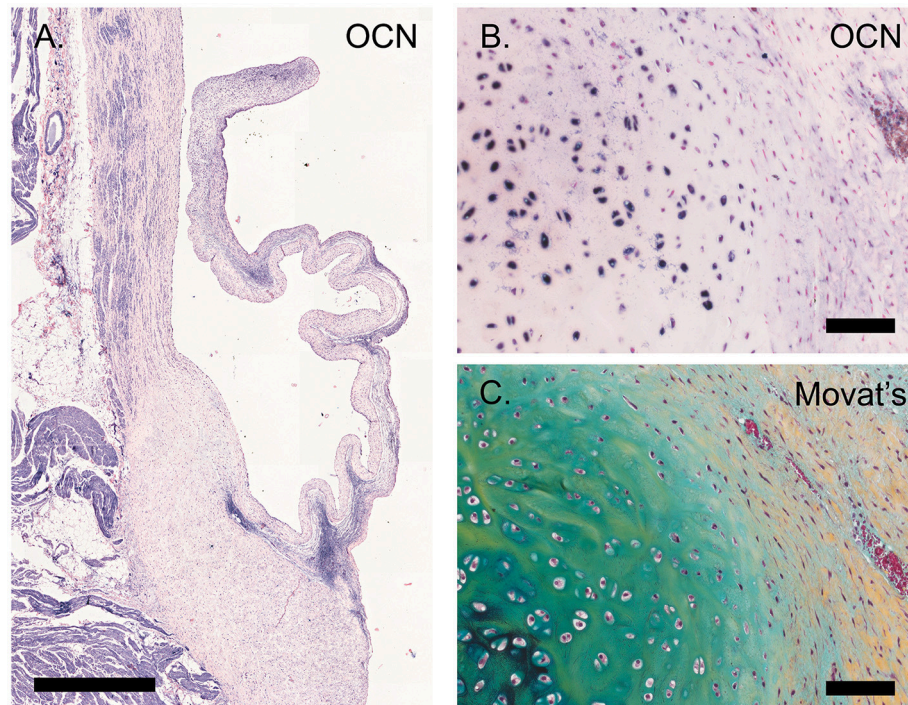


FIGURE 8 | Calcification. **(A)** Tile scan of a healthy ovine aortic valve stained with osteocalcin (OCN). **(B)** Section of the ovine pulmonary wall in which the onset of calcification was detected, stained against OCN. **(C)** Russell Movat's pentachrome staining of the same section of pulmonary wall revealed abundant presence of proteoglycans (in blue-green), colocalizing with OCN expression. Scale bars, 1 mm **(A)** and 100 μ m **(B, C)**.

in human adults as compared to fetal valves (39). Notably, the observed protein expression was remarkably similar between the various ovine leaflets (both aortic and pulmonary) that were included in the validation.

All tested structural proteins exhibit specific staining patterns, as summarized in **Table 2**. Collagen is an essential load-bearing component of valvular ECM that contributes significantly to the mechanical strength of the tissue. As previously reported, collagen type I is mainly observed in the fibrosa, while collagen type III expression is more diffused throughout the leaflet (40, 42). Periostin co-localizes with collagen type I as described before (51), supporting its role in collagen deposition and maturation (52–54). Glycoaminoglycans are found throughout the heart valves (55). As both decorin (56) and biglycan (57) are involved in collagen fiber formation, and collagen type III has a critical role in fibrillogenesis (58), it is not surprising that the expression patterns of these proteins are mostly overlapping. Versican is mainly observed in the ventricularis, which supports the important role of this protein in the assembly and organization of elastin (59). Complementary to the matrix proteins, our panel includes collagenases (MMP1, MMP13) and gelatinases (MMP2, MMP9) as important proteolytic enzymes involved in physiological matrix turnover and remodeling. Human heart valves display specific expression patterns of MMPs and tissue inhibitors of metalloproteinases (TIMPs), which differ between the four different heart valve (60). In this respect, it would be relevant to expand the current panel with antibodies

against various TIMPs, which have not been validated in our study.

One of the hallmarks of functional regeneration of heart valves is the formation of an elastic network, or elastogenesis. Elastin is mainly found in the ventricularis layer of healthy adult valves. It has been demonstrated that Verhoeff's method does not stain immature fibers, and thus, it is not efficient for evaluating the process of elastogenesis during valve development and remodeling. As delineated by Wagenseil and Mecham (61), the processes underlying elastic fiber formation are highly complex and require the interplay of various molecules. These include the core protein (tropo)elastin, microfibrillar proteins (fibrillin-1 and fibrillin-2) and various linking proteins, including EMILIN-1 and LOX. Other proteins involved include fibulin-4, which links the enzyme LOX to tropoelastin (62) and fibulin-5, which acts as a bridge between microfibrils and tropoelastin (63, 64). In addition, a fibronectin network is needed for the assembly of fibrillins, and consequently of microfibrils, that provides a microenvironment that controls tropoelastin/elastin arrangement and cross-linking processes (65). In addition to their essential role in elastogenesis, many of these proteins have been reported to have important signaling roles in pathophysiological tissue remodeling processes, relevant to TE (66, 67). In the present study, validation of the antibodies revealed specific expression patterns of elastogenesis-related proteins in the ovine heart valve leaflet (see **Table 2**). Fibrillin-1, for example, is not exclusively located in the ventricularis, but also spreads into the spongiosa, which is in

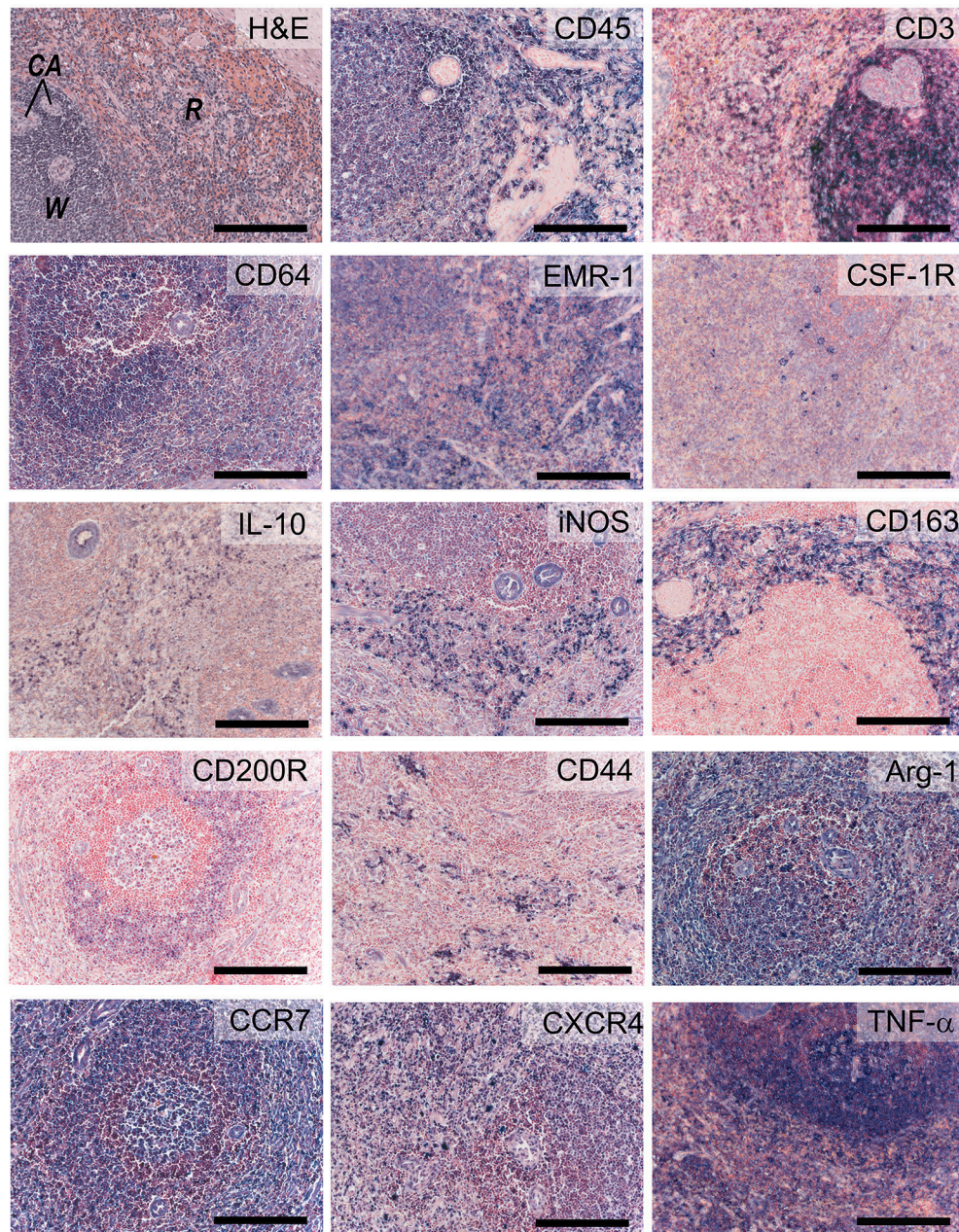


FIGURE 9 | Inflammatory markers. Sections of activated ovine spleen, isolated from a sheep with endocarditis. Hematoxylin and eosin (H&E, top left) staining reveals the characteristic splenic red pulp (R) and white pulp (W), with the central arterioles (CA). Sections are stained with antibodies against CD45, CD3, CD64, EGF-like module-containing mucin-like hormone receptor-like 1 (EMR-1), colony stimulating factor-1 receptor (CSF-1R), interleukin-10 (IL-10), inducible nitric oxide synthase (iNOS), CD163, CD200R, CD44, Arginase-1 (Arg-1), CCR-7, CXCR4, and tumor necrosis factor- α (TNF- α). Scale bars, 200 μ m.

accordance with previous findings by Votteler et al. for mature human heart valves (41). Similarly, although EMILIN-1 only shows weak staining, it is detectable in both the ventricularis and the spongiosa, which was also reported for human valves. One notable difference however, is the abundant expression of fibrillin-2 in the ovine leaflet, and particularly in the leaflet tip, compared to undetectable levels of fibrillin-2 in adolescent and adult human valves, as reported in the study by Votteler et al. This

points to species-differences in fibrillin-2 expression, which may be attributed to the aforementioned differences in ECM synthesis and activity of ovine VICs when compared to human VICs.

Healthy adult heart valve leaflets contain mainly a quiescent population of VICs of fibroblast-like phenotypes that maintain valve homeostasis and structural leaflet integrity (39, 48, 68). In addition, SMCs and activated myofibroblasts are interspersed between the ECM layers (39, 69). α -SMA expressing

myofibroblasts are present throughout the entire leaflet mostly during disease and development (39, 48). Myofibroblasts produce and secrete most of the surrounding ECM, particularly collagen, whereas a small subpopulation of mature SMCs (marked by SM22, Calponin) and dedifferentiated SMCs (marked by SMemb) secrete MMPs and TIMPs. Fibroblast-like VICs express general mesenchymal markers, such as vimentin and CD44, the latter being required to remodel ECM (70). Quiescent VICs can be activated by environmental cues and stimulated by valvular endothelial cells (VECs) (71), leading to differentiation into myofibroblast-like α -SMA-positive VICs. These activated VICs are important for valve remodeling. However, continuous and uncontrolled VIC activation in adult valves is associated with valve diseases resulting in fibrosis and calcification. For heart valve TE, the VIC phenotypic state can reflect the current remodeling demands of the valvular tissue at a particular stage of the process of heart valve formation. In a comparative study of native and TE heart valves, TE valves displayed persistent expression of VIC activation markers when compared to quiescent VICs in native valves (69). Hence, to account for the complex and dynamic phenotypic manifestations of VICs, a range of SMC- and fibroblast-associated markers has been included in our panel of antibodies.

The ovine valve analyzed in our study displayed a notably high expression of SMC markers (see **Table 2**). Given that the aortic valve we used for antibody validation was derived from a sheep that had undergone pulmonary valve replacement with a synthetic valve, the observed expression of SMC markers may be indicative of VIC activation as a side-effect of that intervention. Moreover, pronounced osteocalcin expression was detected in the leaflet, which may be indicative of the presence of osteoblast-like VICs as a result of persistent VIC activation and dysregulated apoptosis, as previously reported (72). Correspondingly, in human valves, expression of SMC markers and co-activators has been correlated to valve calcification (73), suggesting that markers such SM22 and calponin could be expressed by other cell types within heterogeneous VIC populations. In addition, recent studies demonstrated that cadherin-11 is not only involved in embryonic heart development and valve maturation (74, 75), but also associated with calcification of aortic valves (76). Another useful marker for cardiovascular (micro)calcifications, not included in our antibody panel, could be sortilin, a sorting protein and a key regulator of SMC calcification via its recruitment to extracellular vesicles (77).

With respect to VECs, of the markers we tested, CD31 demonstrates the most specific endothelial staining on the ovine leaflet. Apart from VECs, CD34 is a well-known marker for hematopoietic progenitor cells, and when combined with other markers such as CD45 and collagen type I, can be used to identify fibrocytes (78). Of note, CD34, vWF and VE-Cadherin were mostly expressed in VECs on the ventricular side of the leaflet, the side exposed to high flow, but not the aortic side of the leaflet. Importantly, although not validated here, the selected VIC and VEC antibodies (e.g., α -SMA and CD31) do allow for double-label immunofluorescent staining to assess endothelial-to-mesenchymal transition (EndMT). This is highly relevant for evaluating heart valve TE, as basal levels of

EndMT may contribute to the replenishment of VICs as part of physiologic valve remodeling throughout postnatal life (79, 80), and VEC-VIC interactions are important for maintaining valve homeostasis and the prevention of osteogenesis (72).

In addition to the valve-associated markers that constitute our panel of antibodies, we selected antibodies to characterize immune cells and the inflammatory state of a tissue, such as the pan-leukocyte marker CD45, lymphocyte marker CD3, and pro- and anti-inflammatory cytokines (e.g., TNF- α and IL-10, respectively). Inflammation is well-established to be a critical regulator of pathophysiological valvular remodeling (81). For TE approaches, the host immune response and the inflammation induced by the implanted heart valve graft is one of the most critical determinants of successful and functional valve integration. In fact, recent *in situ* cardiovascular TE approaches rely on the notion that the host inflammatory response can be used as the driver of endogenous tissue regeneration when harnessed properly [reviewed in (13)].

The primary target cells we focused on in the current study were macrophages. As in normal wound healing, macrophages play an important role in regeneration, via the cross-talk with (myo)fibroblasts and other immune cells, such as T cells. Depending on their polarization state, macrophages mediate the formation and remodeling of new tissue by secreting essential growth factors and cytokines that either inhibit or promote functional tissue formation. Pro-inflammatory (M1) macrophages (characterized by iNOS, CCR-7) maintain inflammation state via the secretion of e.g., TNF- α , while alternatively activated (M2) macrophages (characterized by CD163, Arg-1, CD200R) secrete high levels of IL-10 and TGF- β to suppress the inflammation, and contribute to tissue repair, remodeling, vasculogenesis and retain homeostasis (82). Previous studies suggest that the M2/M1 macrophage ratio in early phases after implantation can be used as a predictor for long-term tissue outcome in natural biomaterials (83). Albeit practical, the M1-M2 paradigm is highly simplified. More realistically, macrophages form a very heterogeneous cell population with a broad range of (overlapping) M1–M2 characteristics (84). As a consequence, macrophage characterization is not straightforward and marker expression of macrophages specific for sheep has not yet been described. Of interest, Griebel et al previously reported cross-reactivity of a range of CD antigens for sheep lymphoid and myeloid cells (85). However, that study was focused on flow cytometry and it has to be tested whether those antibodies are suitable for use as immunohistological staining on paraffin or frozen sections. In our study, the spleen samples were obtained from a sheep with endocarditis, and thus represented an activated inflammatory state. The spleen tissue contained heterogeneous pools of macrophages, where M2-like macrophages were positive for CD163 and CD200R, whereas M1 macrophages expressed iNOS. Arginase and CCR7, reported as M2 and M1 markers, respectively, in different species, were abundantly expressed in spleen samples. None of the markers we tested represented a suitable pan-macrophage marker for sheep, for example analog to human CD68. Multiple anti-CD68 clones were tested on inflamed lung and spleen tissues under different antigen retrieval conditions, leading to unsatisfactory

results (data not shown). EMR-1, the human homolog to F4/80 in mouse, could serve as a general marker. Although in humans expression of EMR-1 is restricted to eosinophils (86), we observed a less specific expression pattern in the ovine spleen. CSF-1R was tested as an alternative macrophage marker, being previously described as a marker committed to the mononuclear phagocytic lineage (87). In our panel, CSF-1R displays a highly specific expression pattern restricted to a small number of individual cells in the spleen. CD64, a classical monocyte- and macrophage-associated marker, was identified to be the most reliable pan-macrophage marker in sheep. To further discriminate between monocytes and macrophages, various CD14 antibodies were tested, but no positive immune reaction was observed in the ovine tissues (data not shown). Of note, CD44 is known to be highly induced in macrophages at the onset of fusion and, as such, can serve as an excellent marker for multinucleated giant cells (88). Taken together, there are very few unique macrophage markers and a combination of markers is required to identify the specific macrophage phenotype. For TE constructs, combinations of different anti-macrophage antibodies could give a spatiotemporal indication of the status of inflammation and wound healing. Moreover, macrophage polarization state is governed via the cross-talk with other immune cells, such as T helper cells, which have been reported to play an essential role in tissue regeneration as well (89). Consequently, markers to distinguish T helper 1 and T helper 2 cells (e.g., CXCR3 and CCR8, respectively) would be valuable additions to the antibody panel as described in our study.

From a translational point of view, our results indicate substantial differences between human and ovine valves that should be taken into account in the preclinical testing of valve replacements (e.g., tissue-engineered heart valves) using the sheep model. Particularly, whereas the expression of activated VIC markers (e.g., SM22, calponin, periostin, osteocalcin) are typically associated with pathological events in human valves, the abundant expression of these markers in the native ovine valves as observed in this study, suggests that these markers are not necessarily representative of adverse remodeling in TE heart valves when evaluated in sheep. On the other hand, the observed continuous expression of these same markers may be one of the factors that underlie the increased tendency for calcification of sheep. All in all, while the sheep still represents the animal model of choice for the preclinical evaluation of heart valve substitutes, our findings imply that data obtained from preclinical studies in sheep, particularly in terms of tissue organization and remodeling and VIC activation, should be interpreted in the correct context and with the appropriate

caution, as data may not translate directly to the human situation.

CONCLUSION

The field of heart valve TE has made great progress over the last decades. However, little mechanistic data is available on the *in vivo* inflammatory and remodeling processes underlying functional tissue regeneration of TE heart valves. The comprehensive sheep-specific panel of antibodies described in this study could serve for the detailed evaluation of the regenerative processes including ECM formation/remodeling, elastogenesis, VIC, and VEC phenotyping, and inflammation, when assessing TE heart valves implanted in sheep, the designated preclinical model.

AUTHOR CONTRIBUTIONS

SD, DvG, EA, AvdB, and AS contributed to the investigation, methodology, and validation of the study. SD, DvG, and AS contributed to visualization of the data. AD-M and AS conceptualized and supervised the study, and AS acquired the funding. SD, DvG, and AS prepared the original draft. EA critically read and edited the final version of the manuscript. All authors reviewed and edited the manuscript and agreed to be accountable for all aspects of the work involved in preparing this manuscript.

FUNDING

AS is supported by an Acceleration and Career Development Grant within the 1Valve Program, funded by the Netherlands Cardio Vascular Research Initiative (CVON): The Dutch Heart Foundation, Dutch Federation of University Medical Centres, the Netherlands Organisation for Health Research and Development and the Royal Netherlands Academy of Sciences. EA is supported by the National Institutes of Health (NIH) grants R01HL 114805 and 136431.

ACKNOWLEDGMENTS

The authors would like to thank Dr. Jolanda Kluin and Marcelle Uiterwijk for their help in providing the ovine control tissues, discarded from synthetic pulmonary heart valve replacement experiments. The antibody against periostin was kindly provided by Prof. Roger Markwald, Charleston, SC, USA. Finally, we gratefully acknowledge Prof. Carlijn Bouten and Prof. Frank Baaijens for plentiful useful discussions.

REFERENCES

- Hoerstrup SP, Sodani R, Daebritz S, Wang J, Bacha EA, Martin DP, et al. Functional living trileaflet heart valves grown *in vitro*. *Circulation* (2000) 102:III44–9. doi: 10.1161/01.CIR.102.suppl_3.III-44
- Shin'oka T, Ma PX, Shum-Tim D, Breuer CK, Cusick RA, Zund G, et al. Tissue-engineered heart valves. Autologous valve leaflet replacement study in a lamb model. *Circulation* (1996) 94:III164–8. doi: 10.1016/0003-4975(95)00733-4
- Schmidt D, Achermann J, Odermatt B, Breymann C, Mol A, Genoni M, et al. Prenatally fabricated autologous human living heart valves based on amniotic fluid derived progenitor cells as single cell source. *Circulation* (2007) 116:164–70. doi: 10.1161/CIRCULATIONAHA.106.681494

4. Mol A, Rutten MCM, Driessen NJB, Bouten CVC, Zünd G, Baaijens FPT, et al. Autologous human tissue-engineered heart valves: prospects for systemic application. *Circulation* (2006) 114:1152–8. doi: 10.1161/CIRCULATIONAHA.105.001123
5. Schmidt D, Dijkman PE, Driessen-Mol A, Stenger R, Mariani C, Puolakka A, et al. Minimally-invasive implantation of living tissue engineered heart valves: a comprehensive approach from autologous vascular cells to stem cells. *J Am Coll Cardiol*. (2010) 56:510–20. doi: 10.1016/j.jacc.2010.04.024
6. Hurtado-Aguilar LG, Mulderrig S, Moreira R, Hatam N, Spillner J, Schmitz-Rode T, et al. Ultrasound for *in vitro*, noninvasive real-time monitoring and evaluation of tissue-engineered heart valves. *Tissue Eng Part C Methods* (2016) 22:974–81. doi: 10.1089/ten.tec.2016.0300
7. Capulli AK, Emmert MY, Pasqualini FS, Kehl D, Caliskan E, Lind JU, et al. JetValve: Rapid manufacturing of biohybrid scaffolds for biomimetic heart valve replacement. *Biomaterials* (2017) 133:229–41. doi: 10.1016/j.biomaterials.2017.04.033
8. Duan B, Kapetanovic E, Hockaday LA, Butcher JT. Three-dimensional printed trileaflet valve conduits using biological hydrogels and human valve interstitial cells. *Acta Biomater* (2014) 10:1836–46. doi: 10.1016/j.actbio.2013.12.005
9. Wu S, Duan B, Qin X, Butcher JT. Living nano-micro fibrous woven fabric/hydrogel composite scaffolds for heart valve engineering. *Acta Biomater* (2017) 51:89–100. doi: 10.1016/j.actbio.2017.01.051
10. Puperi DS, Kishan A, Punske ZE, Wu Y, Cosgriff-Hernandez E, West JL, et al. Electrospun polyurethane and hydrogel composite scaffolds as biomechanical mimics for aortic valve tissue engineering. *ACS Biomater Sci Eng*. (2016) 2:1546–58. doi: 10.1021/acsbomaterials.6b00309
11. Hinderer S, Seifert J, Votteler M, Shen N, Rheinlaender J, Schäffer TE, et al. Engineering of a bio-functionalized hybrid off-the-shelf heart valve. *Biomaterials* (2014) 35:2130–9. doi: 10.1016/j.biomaterials.2013.10.080
12. Mol A, Smits AIPM, Bouten CVC, Baaijens FPT. Tissue engineering of heart valves: advances and current challenges. *Expert Rev Med Devices* (2009) 6:259–75. doi: 10.1586/erd.09.12
13. Wissing TB, Bonito V, Bouten CVC, Smits AIPM. Biomaterial-driven *in situ* cardiovascular tissue engineering—a multi-disciplinary perspective. *Regen Med*. (2017) 2:18. doi: 10.1038/s41536-017-0023-2
14. Mendelson K, Schoen FJ. Heart valve tissue engineering: concepts, approaches, progress, and challenges. *Ann Biomed Eng*. (2006) 34:1799–819. doi: 10.1007/s10439-006-9163-z
15. Iop L, Bonetti A, Naso F, Rizzo S, Cagnin S, Bianco R, et al. Decellularized allogeneic heart valves demonstrate self-regeneration potential after a long-term preclinical evaluation. *PLoS ONE* (2014) 9:e99593. doi: 10.1371/journal.pone.0099593
16. Tudorache I, Theodoridis K, Baraki H, Sarikouch S, Bara C, Meyer T, et al. Decellularized aortic allografts versus pulmonary autografts for aortic valve replacement in the growing sheep model: haemodynamic and morphological results at 20 months after implantation. *Eur J Cardiothorac Surg*. (2016) 49:1228–38. doi: 10.1093/ejcts/ezv362
17. Leyh RG, Wilhelm M, Rebe P, Fischer S, Kofidis T, Haverich A, et al. *In vivo* repopulation of xenogeneic and allogeneic acellular valve matrix conduits in the pulmonary circulation. *Ann Thorac Surg*. (2003) 75:1457–63, discussion:1463. doi: 10.1016/S0003-4975(02)04845-2
18. Sarikouch S, Horke A, Tudorache I, Beerbaum P, Westhoff-Bleck M, et al. Decellularized fresh homografts for pulmonary valve replacement: a decade of clinical experience. *Eur J Cardio-Thoracic Surg*. (2016) 50:281–90. doi: 10.1093/ejcts/ezw050
19. Weber B, Dijkman PE, Scherman J, Sanders B, Emmert MY, Grünfelder J, et al. Off-the-shelf human decellularized tissue-engineered heart valves in a non-human primate model. *Biomaterials* (2013) 34:7269–80. doi: 10.1016/j.biomaterials.2013.04.059
20. Driessen-Mol A, Emmert MY, Dijkman PE, Frese L, Sanders B, Weber B, et al. Transcatheter implantation of homologous “off-the-shelf” tissue-engineered heart valves with self-repair capacity: long-term functionality and rapid *in vivo* remodeling in sheep. *J Am Coll Cardiol*. (2014) 63:1320–9. doi: 10.1016/j.jacc.2013.09.082
21. Spriestersbach H, Prudlo A, Bartosch M, Sanders B, Radtke T, Baaijens FPT, et al. First percutaneous implantation of a completely tissue-engineered self-expanding pulmonary heart valve prosthesis using a newly developed delivery system: a feasibility study in sheep. *Cardiovasc Interv Ther*. (2017) 32:36–47. doi: 10.1007/s12928-016-0396-y
22. Reimer J, Syedain Z, Haynie B, Lahti M, Berry J, Tranquillo R. Implantation of a tissue-engineered tubular heart valve in growing lambs. *Ann Biomed Eng*. (2017) 45:439–51. doi: 10.1007/s10439-016-1605-7
23. Syedain Z, Reimer J, Schmidt J, Lahti M, Berry J, Bianco R, et al. 6-Month aortic valve implantation of an off-the-shelf tissue-engineered valve in sheep. *Biomaterials* (2015) 73:175–84. doi: 10.1016/j.biomaterials.2015.09.016
24. Kluijn J, Talacua H, Smits AIPM, Emmert MY, Brugmans MCP, et al. *In situ* heart valve tissue engineering using a bioresorbable elastomeric implant - From material design to 12 months follow-up in sheep. *Biomaterials* (2017) 125:101–17. doi: 10.1016/j.biomaterials.2017.02.007
25. Bennink G, Torii S, Brugmans M, Cox M, Svanidze O, Ladich E, et al. A novel restorative pulmonary valved conduit in a chronic sheep model: mid-term hemodynamic function and histologic assessment. *J Thorac Cardiovasc Surg*. (2017) 155:2591–601.e3. doi: 10.1016/j.jtcvs.2017.12.046
26. MacGrogan D, Luxán G, Driessen-Mol A, Bouten C, Baaijens F, de la Pompa JL. How to make a heart valve: from embryonic development to bioengineering of living valve substitutes. *Cold Spring Harb Perspect Med*. (2014) 4:a013912. doi: 10.1101/cshperspect.a013912
27. Schoen FJ. Evolving concepts of cardiac valve dynamics: the continuum of development, functional structure, pathobiology, and tissue engineering. *Circulation* (2008) 118:1864–80. doi: 10.1161/CIRCULATIONAHA.108.805911
28. Smits AIPM, Bouten CVC. Tissue Engineering meets immunoengineering: prospective on personalized *in situ* tissue engineering strategies. *Curr Opin Biomed Eng*. (2018) 6:17–26. doi: 10.1016/j.cobme.2018.02.006
29. van Loon SLM, Smits AIPM, Driessen-Mol A, Baaijens FPT, Bouten CVC. The immune response in *in situ* tissue engineering of aortic heart valves. In: Aikawa E. *Calcific Aortic Disease*. (Rijeka: InTech). p. 207–45.
30. Franz S, Rammelt S, Scharnweber D, Simon JC. Immune responses to implants - a review of the implications for the design of immunomodulatory biomaterials. *Biomaterials* (2011) 32:6692–709. doi: 10.1016/j.biomaterials.2011.05.078
31. Roh JD, Sawh-Martinez R, Brennan MP, Jay SM, Devine L, Rao DA, et al. Tissue-engineered vascular grafts transform into mature blood vessels via an inflammation-mediated process of vascular remodeling. *Proc Natl Acad Sci USA*. (2010) 107:4669–74. doi: 10.1073/pnas.0911465107
32. Talacua H, Smits AIPM, Muylaert DEP, van Rijswijk JW, Vink A, Verhaar MC, et al. *In situ* tissue engineering of functional small-diameter blood vessels by host circulating cells only. *Tissue Eng Part A* (2015) 21:2583–94. doi: 10.1089/ten.TEA.2015.0066
33. Mol A, van Lieshout MI, Dam-de Veen CG, Neuschwander S, Hoerstrup SP, Baaijens FPT, Bouten CVC. Fibrin as a cell carrier in cardiovascular tissue engineering applications. *Biomaterials* (2005) 26:3113–21. doi: 10.1016/j.biomaterials.2004.08.007
34. Blum KM, Drews JD, Breuer CK. Tissue-engineered heart valves: a call for mechanistic studies. *Tissue Eng Part B Rev*. (2018) 24:240–53. doi: 10.1089/ten.TEB.2017.0425
35. Rashid ST, Salacinski HJ, Hamilton G, Seifalian AM. The use of animal models in developing the discipline of cardiovascular tissue engineering: a review. *Biomaterials* (2004) 25:1627–37. doi: 10.1016/S0142-9612(03)00522-2
36. Barnhart G, Jones M, Ishihara T, Rose D, Chavez A, Ferrans V. Degeneration and calcification of bioprosthetic cardiac valves.: bioprosthetic tricuspid valve implantation in sheep. *Am J Pathol*. (1982) 106:136–9.
37. Ali ML, Bjornstad K, Duran CMG, Cardiovascular S. The sheep as an animal model for heartvalve research. *Cardiovasc Surg*. (1996) 4:543–9.
38. Hoerstrup SP, Cummings Mrcs I, Lachat M, Schoen FJ, Jenni R, Leschka S, et al. Functional growth in tissue-engineered living, vascular grafts: follow-up at 100 weeks in a large animal model. *Circulation* (2006) 114:1159–66. doi: 10.1161/CIRCULATIONAHA.105.001172
39. Aikawa E, Whittaker P, Farber M, Mendelson K, Padera RF, Aikawa M, et al. Human semilunar cardiac valve remodeling by activated cells from fetus to adult: implications for postnatal adaptation, pathology, and tissue engineering. *Circulation* (2006) 113:1344–52. doi: 10.1161/CIRCULATIONAHA.105.591768
40. van Geemen D, Soares ALF, Oomen PJA, Driessen-Mol A, Janssen-van den Broek MWJT, et al. Age-dependent changes in geometry, tissue composition

- and mechanical properties of fetal to adult cryopreserved human heart valves. *PLoS ONE* (2016) 11:e0149020. doi: 10.1371/journal.pone.0149020
41. Votteler M, Berrio DAC, Horke A, Sabatier L, Reinhardt DP, Nsair A, et al. Elastogenesis at the onset of human cardiac valve development. *Development* (2013) 140:2345–53. doi: 10.1242/dev.093500
 42. Stephens EH, Post AD, Laucirica DR, Grande-Allen KJ. Perinatal changes in mitral and aortic valve structure and composition. *Pediatr Dev Pathol.* (2010) 13:447–58. doi: 10.2350/09-11-0749-OA.1
 43. Russell HK. A modification of Movat's pentachrome stain. *Arch Pathol.* (1972) 94:187–91.
 44. Syedain Z, Reimer J, Lahti M, Berry J, Johnson S, Tranquillo RT. Tissue engineering of acellular vascular grafts capable of somatic growth in young lambs. *Nat Commun.* (2016) 7:12951. doi: 10.1038/ncomms12951
 45. De Visscher G, Plusquin R, Mesure L, Flameng W. Selection of an immunohistochemical panel for cardiovascular research in sheep. *Appl Immunohistochem Mol Morphol.* (2010) 18:382–91. doi: 10.1097/PAI.0b013e3181cd32e7
 46. Della Rocca F, Sartore S, Guidolin D, Bertiplaglia B, Gerosa G, Casarotto D, et al. Cell composition of the human pulmonary valve: a comparative study with the aortic valve—the VESALIO Project. *Vitalitate Exornatum Succedaneum Aorticum labore Ingegnoso Obtinebitur. Ann Thorac Surg.* (2000) 70:1594–600. doi: 10.1016/S0003-4975(00)01979-2
 47. Tseng H, Grande-Allen KJ. Elastic fibers in the aortic valve spongiosa: a fresh perspective on its structure and role in overall tissue function. *Acta Biomater.* (2011) 7:2101–8. doi: 10.1016/j.actbio.2011.01.022
 48. Rabkin E, Aikawa M, Stone JR, Fukumoto Y, Libby P, Schoen FJ. Activated interstitial myofibroblasts express catabolic enzymes and mediate matrix remodeling in myxomatous heart valves. *Circulation* (2001) 104:2525–32. doi: 10.1161/hc4601.099489
 49. Oomen PJA, Loerakker S, van Geemen D, Neggers J, Goumans M-JTH, van den Bogaerd AJ, et al. Age-dependent changes of stress and strain in the human heart valve and their relation with collagen remodeling. *Acta Biomater.* (2016) 29:161–9. doi: 10.1016/j.actbio.2015.10.044
 50. van Geemen D, Driessen-Mol A, Grootzwagers LGM, Soekhradj-Soechit RS, Riem Vis PW, Baaijens FPT, et al. Variation in tissue outcome of ovine and human engineered heart valve constructs: relevance for tissue engineering. *Regen Med.* (2012) 7:59–70. doi: 10.2217/rme.11.100
 51. Kudo A. Periostin in fibrillogenesis for tissue regeneration: periostin actions inside and outside the cell. *Cell Mol Life Sci.* (2011) 68:3201–7. doi: 10.1007/s00018-011-0784-5
 52. Norris RA, Potts JD, Yost MJ, Junor L, Brooks T, Tan H, et al. Periostin promotes a fibroblastic lineage pathway in atrioventricular valve progenitor cells. *Dev Dyn.* (2009) 238:1052–63. doi: 10.1002/dvdy.21933
 53. Monaghan MG, Linneweh M, Liebscher S, Van Handel B, Layland SL, Schenke-Layland K. Endocardial-to-mesenchymal transformation and mesenchymal cell colonization at the onset of human cardiac valve development. *Development* (2016) 143:473–82. doi: 10.1242/dev.133843
 54. Snider P, Hinton RB, Moreno-Rodriguez RA, Wang J, Rogers R, Lindsley A, et al. Periostin is required for maturation and extracellular matrix stabilization of noncardiomyocyte lineages of the heart. *Circ Res.* (2008) 102:752–60. doi: 10.1161/CIRCRESAHA.107.159517
 55. Stephens EH, Chu CK, Grande-Allen KJ. Valve proteoglycan content and glycosaminoglycan fine structure are unique to microstructure, mechanical load and age: relevance to an age-specific tissue-engineered heart valve. *Acta Biomater.* (2008) 4:1148–60. doi: 10.1016/j.actbio.2008.03.014
 56. Reed CC, Iozzo RV. The role of decorin in collagen fibrillogenesis and skin homeostasis. *Glycoconj J.* (2002) 19:249–55. doi: 10.1023/A:1025383913444
 57. Schönherr E, Witsch-Prehm P, Harrach B, Robenek H, Rauterberg J, Kresse H. Interaction of biglycan with type I collagen. *J Biol Chem.* (1995) 270:2776–83.
 58. Liu X, Wu H, Byrne M, Krane S, Jaenisch R. Type III collagen is crucial for collagen I fibrillogenesis and for normal cardiovascular development. *Proc Natl Acad Sci USA.* (1997) 94:1852–6.
 59. Kang I, Yoon DW, Braun KR, Wight TN. Expression of versican V3 by arterial smooth muscle cells alters tumor growth factor β (TGF β)-, epidermal growth factor (EGF)-, and nuclear factor κ B (NF κ B)-dependent signaling pathways, creating a microenvironment that resists monocyte adhesion. *J Biol Chem.* (2014) 289:15393–404. doi: 10.1074/jbc.M113.544338
 60. Dreger SA, Taylor PM, Allen SP, Yacoub MH. Profile and localization of matrix metalloproteinases (MMPs) and their tissue inhibitors (TIMPs) in human heart valves. *J Heart Valve Dis.* (2002) 11:875–80, discussion 880.
 61. Wagenseil JE, Mecham RP. New insights into elastic fiber assembly. *Birth Defects Res C Embryo Today* (2007) 81:229–40. doi: 10.1002/bdrc.20111
 62. Horiguchi M, Inoue T, Ohbayashi T, Hirai M, Noda K, Marmorstein LY, et al. Fibulin-4 conducts proper elastogenesis via interaction with cross-linking enzyme lysyl oxidase. *Proc Natl Acad Sci USA* (2009) 106:19029–34. doi: 10.1073/pnas.0908268106
 63. Nakamura T, Lozano PR, Ikeda Y, Iwanaga Y, Hinek A, Minamisawa S, et al. Fibulin-5/DANCE is essential for elastogenesis *in vivo*. *Nature* (2002) 415:171–5. doi: 10.1038/415171a
 64. Yanagisawa H, Davis EC, Starcher BC, Ouchi T, Yanagisawa M, Richardson JA, et al. Fibulin-5 is an elastin-binding protein essential for elastic fibre development *in vivo*. *Nature* (2002) 415:168–71. doi: 10.1038/415168a
 65. Sabatier L, Chen D, Fagotto-Kaufmann C, Hubmacher D, McKee MD, Annis DS, et al. Fibrillin assembly requires fibronectin. *Mol Biol Cell* (2009) 20:846–58. doi: 10.1091/mbc.E08-08-0830
 66. Nakasaki M, Hwang Y, Xie Y, Kataria S, Gund R, Hajam EY, et al. The matrix protein Fibulin-5 is at the interface of tissue stiffness and inflammation in fibrosis. *Nat Commun.* (2015) 6:8574. doi: 10.1038/ncomms9574
 67. Sugiura T, Agarwal R, Tara S, Yi T, Lee YU, Breuer CK, Weiss AS, Shinoka T. Tropoelastin inhibits intimal hyperplasia of mouse bioresorbable arterial vascular grafts. *Acta Biomater.* (2017) 52:74–80. doi: 10.1016/j.actbio.2016.12.044
 68. Rabkin-Aikawa E, Aikawa M, Farber M, Kratz JR, Garcia-Cardena G, Kouchoukos NT, et al. Clinical pulmonary autograft valves: pathologic evidence of adaptive remodeling in the aortic site. *J Thorac Cardiovasc Surg.* (2004) 128:552–61. doi: 10.1016/j.jtcvs.2004.04.016
 69. Schenke-Layland K, Riemann I, Opitz F, König K, Halbhuber KJ, Stock UA. Comparative study of cellular and extracellular matrix composition of native and tissue engineered heart valves. *Matrix Biol.* (2004) 23:113–25. doi: 10.1016/j.matbio.2004.03.005
 70. Carthy JM, Boroomand S, McManus BM. Versican and CD44 in *in vitro* valvular interstitial cell injury and repair. *Cardiovasc Pathol.* 21:74–82. doi: 10.1016/j.carpath.2011.03.003
 71. Butcher JT, Nerem RM. Valvular endothelial cells regulate the phenotype of interstitial cells in co-culture: effects of steady shear stress. *Tissue Eng.* (2006) 12:905–15. doi: 10.1089/ten.2006.12.905
 72. Hjortnaes J, Shapero K, Goettsch C, Hutcheson JD, Keegan J, Kluin J, et al. Valvular interstitial cells suppress calcification of valvular endothelial cells. *Atherosclerosis* (2015) 242:251–60. doi: 10.1016/j.atherosclerosis.2015.07.008
 73. Latif N, Sarathchandra P, Chester AH, Yacoub MH. Expression of smooth muscle cell markers and co-activators in calcified aortic valves. *Eur Heart J.* (2015) 36:1335–45. doi: 10.1093/eurheartj/ehf547
 74. Bowen CJ, Zhou J, Sung DC, Butcher JT. Cadherin-11 coordinates cellular migration and extracellular matrix remodeling during aortic valve maturation. *Dev Biol.* (2015) 407:145–57. doi: 10.1016/j.ydbio.2015.07.012
 75. Zhou J, Bowen C, Lu G, Knapp C III, Recknagel A, Norris RA, Butcher JT. Cadherin-11 expression patterns in heart valves associate with key functions during embryonic cushion formation, valve maturation and calcification. *Cells Tissues Organs* (2013) 198:300–10. doi: 10.1159/000356762
 76. Sung DC, Bowen CJ, Vaidya KA, Zhou J, Chapurin N, Recknagel A, et al. Cadherin-11 overexpression induces extracellular matrix remodeling and calcification in mature aortic valves. *Arterioscler Thromb Vasc Biol.* (2016) 36:1627–37. doi: 10.1161/ATVBAHA.116.307812
 77. Goettsch C, Hutcheson JD, Aikawa M, Iwata H, Pham T, Nykjaer A, et al. Sortilin mediates vascular calcification via its recruitment into extracellular vesicles. *J Clin Invest.* (2016) 126:1323–36. doi: 10.1172/JCI80851
 78. Reilkoff RA, Bucala R, Herzog EL. Fibrocytes: emerging effector cells in chronic inflammation. *Nat Rev Immunol.* (2011) 11:427–35. doi: 10.1038/nri2990
 79. Bischoff J, Aikawa E. Progenitor cells confer plasticity to cardiac valve endothelium. *J Cardiovasc Transl Res.* (2011) 4:710–9. doi: 10.1007/s12265-011-9312-0

80. Mahler GJ, Farrar EJ, Butcher JT. Inflammatory cytokines promote mesenchymal transformation in embryonic and adult valve endothelial cells. *Arterioscler Thromb Vasc Biol.* (2013) 33:121–30. doi: 10.1161/ATVBAHA.112.300504
81. Mahler GJ, Butcher JT. Inflammatory regulation of valvular remodeling: the good(?), the bad, and the ugly. *Int J Inflamm.* (2011) 2011:721419. doi: 10.4061/2011/721419
82. Moghaddam AS, Mohammadian S, Vazini H, Taghadosi M, Esmaili S-A, Mardani F, et al. Macrophage plasticity, polarization and function in health and disease. *J Cell Physiol.* (2018) 233:6425–440. doi: 10.1002/jcp.26429
83. Brown BN, Londono R, Tottey S, Zhang L, Kukla KA, Wolf MT, et al. Macrophage phenotype as a predictor of constructive remodeling following the implantation of biologically derived surgical mesh materials. *Acta Biomater.* (2012) 8:978–87. doi: 10.1016/j.actbio.2011.11.031
84. Mosser D, Edwards J. Exploring the full spectrum of macrophage activation. *Nat Rev Immunol.* (2008) 8:958–69. doi: 10.1038/nri2448.Exploring
85. Griebel PJ, Entrican G, Rocchi M, Beskorwayne T, Davis WC. Cross-reactivity of mAbs to human CD antigens with sheep leukocytes. *Vet Immunol Immunopathol.* (2007) 119:115–22. doi: 10.1016/j.vetimm.2007.06.015
86. Hamann J, Koning N, Pouwels W, Ulfman LH, van Eijk M, Stacey M, et al. EMR1, the human homolog of F4/80, is an eosinophil-specific receptor. *Eur J Immunol.* (2007) 37:2797–802. doi: 10.1002/eji.200737553
87. Pridans C, Davis GM, Sauter KA, Lisowski ZM, Corripio-Miyar Y, Raper A, et al. A Csf1r-EGFP transgene provides a novel marker for monocyte subsets in sheep. *J Immunol.* (2016) 197:2297–305. doi: 10.4049/jimmunol.1502336
88. Cui W, Ke JZ, Zhang Q, Ke H-Z, Chalouni C, Vignery A. The intracellular domain of CD44 promotes the fusion of macrophages. *Blood* (2006) 107:796–805. doi: 10.1182/blood-2005-05-1902
89. Sadtler K, Allen BW, Estrellas K, Housseau F, Pardoll DM, Elisseeff JH. The scaffold immune microenvironment: biomaterial-mediated immune polarization in traumatic and nontraumatic applications. *Tissue Eng Part A* (2017) 23:1–42. doi: 10.1089/ten.tea.2016.0304

Conflict of Interest Statement: The authors declare that the research was conducted in the absence of any commercial or financial relationships that could be construed as a potential conflict of interest.

Copyright © 2018 Dekker, van Geemen, van den Bogaardt, Driessen-Mol, Aikawa and Smits. This is an open-access article distributed under the terms of the Creative Commons Attribution License (CC BY). The use, distribution or reproduction in other forums is permitted, provided the original author(s) and the copyright owner(s) are credited and that the original publication in this journal is cited, in accordance with accepted academic practice. No use, distribution or reproduction is permitted which does not comply with these terms.



Stem Cell Cytoskeletal Responses to Pulsatile Flow in Heart Valve Tissue Engineering Studies

Glenda Castellanos, Sana Nasim, Denise M. Almora, Sasmita Rath and Sharan Ramaswamy*

Tissue Engineered Mechanics Imaging and Materials Laboratory, Biomedical Engineering, Florida International University, Miami, FL, United States

OPEN ACCESS

Edited by:

Julie A. Phillippi,
University of Pittsburgh, United States

Reviewed by:

Cécile Oury,
University of Liège, Belgium
Philippe Sucofsky,
Wright State University, United States

*Correspondence:

Sharan Ramaswamy
sramaswa@fiu.edu

Specialty section:

This article was submitted to
Atherosclerosis and Vascular
Medicine,
a section of the journal
Frontiers in Cardiovascular Medicine

Received: 03 January 2018

Accepted: 15 May 2018

Published: 05 June 2018

Citation:

Castellanos G, Nasim S, Almora DM,
Rath S and Ramaswamy S (2018)
Stem Cell Cytoskeletal Responses to
Pulsatile Flow in Heart Valve Tissue
Engineering Studies.
Front. Cardiovasc. Med. 5:58.
doi: 10.3389/fcvm.2018.00058

Heart valve replacement options remain exceedingly limited for pediatric patients because they cannot accommodate somatic growth. To overcome this shortcoming, heart valve tissue engineering using human bone marrow stem cells (HBMSCs) has been considered a potential solution to the treatment of critical congenital valvular defects. The mechanical environments during *in vitro* culture are key regulators of progenitor cell fate. Here, we report on alterations in HBMSCs, specifically in their actin cytoskeleton and their nucleus under fluid-induced shear stresses of relevance to heart valves. HBMSCs were seeded in microfluidic channels and were exposed to the following conditions: pulsatile shear stress (PSS), steady shear stress (SS), and no flow controls ($n = 4/\text{group}$). Changes to the actin filament structure were monitored and subsequent gene expression was evaluated. A significant increase ($p < 0.05$) in the number of actin filaments, filament density and angle (between 30° and 84°), and conversely a significant decrease ($p < 0.05$) in the length of the filaments were observed when the HBMSCs were exposed to PSS for 48 h compared to SS and no flow conditions. No significant differences in nuclear shape were observed among the groups ($p > 0.05$). Of particular relevance to valvulogenesis, *klf2a*, a critical gene in valve development, was significantly expressed only by the PSS group ($p < 0.05$). We conclude that HBMSCs respond to PSS by alterations to their actin filament structure that are distinct from SS and no flow conditions. These changes coupled with the subsequent gene expression findings suggest that at the cellular level, the immediate effect of PSS is to initiate a unique set of quantifiable cytoskeletal events (increased actin filament number, density and angle, but decrease in filament length) in stem cells, which could be useful in the fine-tuning of *in vitro* protocols in heart valve tissue engineering.

Keywords: pulsatile shear stress, HBMSCs, actin filaments, cytoskeleton, nuclear, tissue engineering, *klf2a*, heart valves

INTRODUCTION

Congenital heart defects occur in four to six infants out of every 1,000 births (1). Approximately 24.5% of neonatal mortality is attributed to congenital heart defects (2). Among the plethora of cardiovascular defects, one of the more common, yet life-threatening conditions, is critical aortic valve stenosis (AVS), which results in high mortality and morbidity despite early interventions

(3). The developmental mechanisms that lead to critical AVS are unknown. However, AVS is characterized by poor or missing valve commissures in fetal development, as well as abnormal leaflet fusion; infection, specifically endocarditis *in utero* has been proposed as one of the causal factors (4–9). The most severe forms of congenital heart disease have an incidence rate of ~20,000 live births/year (10), and of these, ~1/3 of cases present problems associated with the aortic heart valve.

Under normal circumstances, valve leaflet composition and structure permits endurance of demanding mechanical forces as they function under a complex, coupled loading state of cyclic tensile, cyclic flexure, and fluid-induced shear stresses, including oscillatory shear stresses (PSS) (11–13). However, in AVS, significant systolic transvalvular pressure gradients with a mean > 60 mmHg, resulting from narrowing of the aortic root, imposes considerable workload on the left ventricle, leading to rapid heart failure if left untreated (14–16).

Over the last 20 years, tissue engineered heart valves (TEHVs) derived from stem cells have been investigated to overcome the shortcomings associated with treatment of critical valve anomalies in children (17–20). Recent studies have applied mechanical stimuli to formulate tissue structures with enhanced extracellular matrix (ECM) properties resembling native heart valves, in particular, using human bone marrow-derived stem cells (HBMSCs) seeded onto biodegradable scaffolds (18, 21). These mechanical stimuli are sensed by the cell membrane receptors, later transferred to the cytoskeleton; consequently, these stimuli initiate a biochemical signaling cascade (22). In HBMSCs, the cytoskeletal structure has shown to be altered after exposure to fluid-induced shear stress (23). The actin filaments of the cell cytoskeleton serve as structural contributors to modulation of subsequent cell biological responses, including gene expression, cellular, and ECM synthesis (24). In general, it has been shown that the application of mechanical stress on actin filaments causes cytoskeleton reorganization, leading to tissue remodeling affecting stem cell viability, self-renewal, and differentiation (25). Although, detailed characterization of intracellular structures, specifically in response to fluid-induced shear stress, is not known. In addition, other cellular components such as focal adhesions, integrin, and the nucleus collectively play important roles in modulating cellular biological responses (18).

Our laboratory has previously demonstrated that HBMSC-derived tissue formation and flow-responsive differential regulation is robust when cell-seeded constructs are cultured under fluid-induced PSS environments. Spatial distribution of HBMSCs that differentiated to the endothelial phenotype (CD31+) were largely found on the tissue surfaces, while cells with an activated myofibroblast phenotype (α SMA +) were mostly aggregated in the interstitial space, similar to the native heart valve cellular-makeup (12, 13, 26, 27). Specifically, PSS regulates HBMSCs structure and has been shown to be highly relevant to both native heart valve development and to TEHVs (27–29). Yet, identifying alterations in the HBMSCs cytoskeleton during PSS exposure may lead to a deeper understanding of specific changes at the cell structural-level. Our underlying hypothesis is that cytoskeletal changes, primarily with actin filaments can be quantified as they can be monitored during

culture. Such quantification can serve as early indicators of *in vitro* differential HBMSCs regulation for functional TEHV development and optimization. Thus, in this investigation we applied PSS to growing HBMSCs to understand fundamental cellular structural responses that precede the resulting gene expression, in the context of the heart valve tissue engineering.

METHODS

Culture and Expansion of HBMSCs

Approximately 5×10^5 HBMSCs/mL (ThermoFisher Scientific, Pittsburgh, PA) were cultured in T75 vented cell culture flasks using AdvanceStem Mesenchymal Stem Cell Medium (GE Healthcare Hyclone, Logan, UT) with 10% mesenchymal stem cell growth supplement (GE Healthcare, Malborough, MA) and 1% penicillin and streptomycin (ThermoFisher Scientific) for growth and expansion. Cells were grown in a standard cell culture incubator operating with 5% CO₂ at 37°C with 95% humidity. HBMSCs culture expanded to passages 4–6 were utilized for subsequent studies.

HBMSCs Transfection

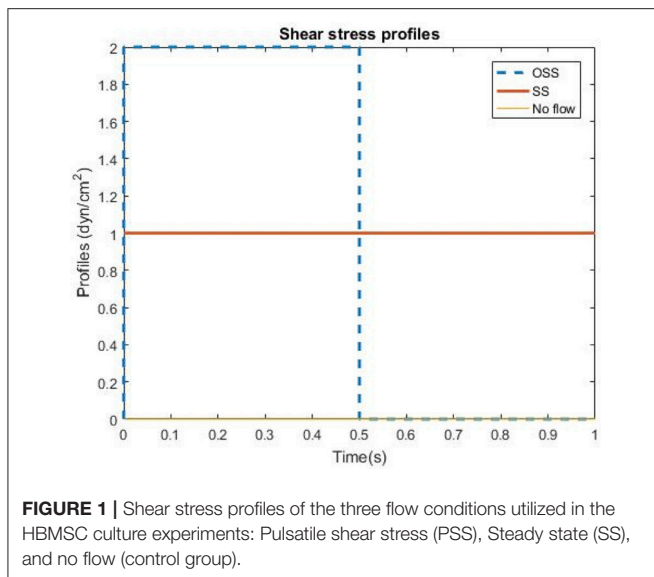
As previously described, HBMSCs were transfected for purposes of cell visualization with green fluorescent protein (GFP) via electroporation (30). In brief, a density of 1×10^6 HBMSCs were transfected using electroporation (Gene Pulser Xcell Electroporation System BIO-RAD, Hercules, CA) and plasmid-delivery of 60 μ g pTAGGFP-actin, a vector encoding TagGFP fusion with actin used for labeling actin filaments in living cells (Evrogen, Moscow, Russia). The following settings were used for electroporation: Exponential Decay Pulse, Voltage of 350 V, capacitance of 950 μ F, and Resistance: of 200 ohms (30).

Transfection Efficiency

Cell viability and cell apoptosis were assessed using Propidium iodide (PI) solution and Annexin protein respectively following manufacturer supplied instructions (Biolegend, San Diego, CA). In brief, 2 days following transfection, HBMSCs were re-suspended in Annexin V Binding Buffer at a concentration of 2.5×10^5 cells/mL. PI was added to 100 μ L of cell suspension. After 15 min of incubation without light exposure, they were evaluated by flow cytometry (BD Bioscientific, San Jose, CA).

Fluid-Induced Mechanobiology Experiments

Transfected HBMSCs were plated in Collagen Type I (ThermoFisher Scientific), coated micro-fluidic channels in which HBMSCs were subjected to flow exposure (Fluxion Biosciences, South San Francisco, CA). Three groups were evaluated in this study: pulsatile shear stress (PSS), steady shear stress (SS) and no flow ($n = 8$ wells/group). The SS was set to 1 dyne/cm² whereas the PSS group consisted of a square waveform, which was applied for 48 h (Figure 1). The time-averaged shear stress in the PSS group was the same magnitude as the shear stress used in the SS condition, i.e., 1 dyne/cm². Additionally, the flow



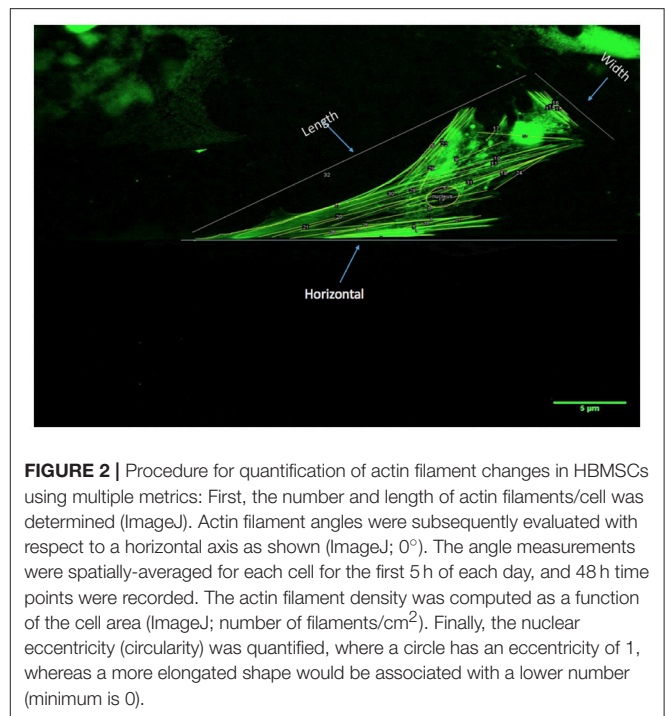
groups included an initial 3 days of gradual increase in shear stresses before applying the PSS or SS profiles (0.50—Day 1, 0.75—Day 2, 1—Day 3 dynes/cm²). HBMSCs in the no flow, SS and PSS flow groups were cultured for a total of 5 days.

Cell Structure Quantification

Images of the cells under the three different flow environments were acquired using fluorescent microscopy (Olympus IX81, CA) every 5 h for the first 2 days, and 48 h time points at the end of the gradual increase of shear stress for a period of 3 days. Cell actin filaments and nuclear changes using multiple metrics were quantified by analyses of images acquired during the time course of the cell culture experiments (ImageJ, NIH Image, Bethesda, MD). The initial quantification was based on the number of actin filaments and their length, illustrated in **Figure 2**. Next, the angle of inclination, the angle measured clockwise between 0° and 180°, of each actin filament within each cell was measured with respect to the horizontal axis, and subsequently spatially-averaged (**Figure 2**) for the first 5 h of each day and 48 h time point. Nuclear eccentricity (circularity), a measure of cell nucleus elongation, was determined in the range of 0–1, where a circle has an eccentricity of one whereas a more elongated shape would be associated with a lower number (31). Moreover, filament density was defined as the number of filaments per unit area (cm²), where the number of filaments and the area of the cell were quantified via Image analysis software (ImageJ). This metric (filaments/area) for each cell that was counted was divided to obtain the average filament density/cell. Additionally, cell length and width quantification was utilized to determine the area as well as the number of filaments per cell (**Figure 2**).

Gene Expression Analysis

HBMSCs were plated in microfluidic channels (Fluxion Biosciences) coated with fibronectin from bovine plasma (Sigma



Aldrich, St. Louis, MO). After 5 days of culture HBMSCs under the conditions of SS, PSS and No Flow, cells were trypsinized from the channels ($n = 4$ samples, where each sample was pooled from 2 to 3 microfluidic channels).

Gene expression analysis on a selected list of genes (**Table 1**) was subsequently conducted as previously described (32). In brief, total RNA was isolated according to the manufacturer's protocol (RNeasy Micro kit, Qiagen) and was eluted in 15 μ L nuclease-free water. Isolated RNA quantity and concentration was verified using NanoDrop 2000c spectrophotometer (ThermoFisher Scientific). 0.5 μ g of total RNA was used for the reverse transcription using the GoScript™ Reverse Transcription System (Promega, Madison, WI). The cDNA was synthesized using the Oligo (dT)₁₅ primer according to the manufacturer's protocol. Quantitative real-time polymerase reaction (RT-PCR) was performed using a commercially available kit Maxima SYBER Green/ROX qPCR Master Mix (ThermoFisher Scientific). The primer (**Table 1**) sequences were previously obtained from Rath et al. (12). Signals were detected using a Step-One Real-Time PCR System (Applied Biosystems, Grand Island, NY). In brief, the PCR tubes (Applied Biosystems) were incubated at 95°C for 10 min before initiating the cycle for Taq polymerase activation. The cycling parameters were as follows: 95°C for 5 s; 60°C for 45 s; 95°C for 15 s. Finally, the change in cycle threshold (Δ Ct) values were averaged and normalized with *GAPDH*, an endogenous housekeeping gene using the $\Delta\Delta$ Ct method (32). Fold changes were calculated as 2^{-Ct} to calculate the relative gene expression occurring after treatment, i.e., after HBMSC exposure to No Flow, SS and PSS culture conditions.

TABLE 1 | Quantitative Real time -polymerase chain reaction primer sequences.

	Gene name	Forward primers (5'-3')	Reverse primers (5'-3')
1	GAPDH	AGCCACATCGCTCAGACAC	GCCCAATACGACCAAATCC
2	α -SMA	TCAATGTCCCAGCCATGTAT	CAGCACGATGCCAGTTGT
3	Klf2a	CCGTCTGCTTTCCGGTAGTG	AAGAGTTCGCATCTGAAGGC
4	FzD2	CGGCCCCGACGCGCCCTGCC	ACACGAACCCAGGAGGACGCAGGCC
5	Osteocalcin	CACTCCTCGCCCTATTGGC	CCCTCCTGCTTGGACACAAG
6	CD31	CCAAGGTGGGATCGTGAGG	TCGGAAGGATAAACGCGGTC

All sequences were obtained using the BLAST program, National Center for Biotechnology (NCBI).

Statistical Analysis

Since cell cytoskeletal organization varies considerably, even from cell to cell, results were interpreted in terms of the overall increase or decrease in the mean nuclear eccentricity and mean actin filament metrics (number, length, angle, and density) between the zero and 48 h cell culture time points. A one-way ANOVA followed by a Tukey's *post-hoc* test was conducted to test for any significant differences among the three groups: no flow, SS and PSS ($n = 8$ wells/groups; SPSS, V16, IBM, Armonk, NY). A statistically significant result was interpreted to have occurred when $p < 0.05$. Quantification of actin filament and nuclear eccentricity metrics were presented in terms of the mean values \pm standard error of the mean (33).

RESULTS

Transfection Efficiency

Successful GFP Transfection was found to occur in 77.4% of the cells (Figure 3A). However, of all the cells transfected, ~50% were found to also be viable (Figure 3B).

Number of Actin Filaments

HBMSC actin filaments increased in number by 122.6% after 48 h of PSS (Figure 4A). On the other hand, cells exposed to SS demonstrated only an 18.2% increase in the average number of filaments/cell after 48 h of exposure, while the no flow group displayed marginal changes. The average increase in the number of filaments in cells exposed to PSS compared to both SS and no flow groups was found to be $p < 0.05$. However, $p > 0.05$ was found in comparing the average number of filaments/cells between cells exposed to SS and no flow.

F-Actin Filament Length

There was a 53.8% decrease in the average length of the filaments after 48 h in the cells exposed to PSS (Figure 4B). On the other hand, there was a 37.5% increase in average filament length on cells exposed to SS, and marginal changes in cells in the no flow group. $p < 0.05$ was observed in the average actin filament length in HBMSCs exposed to PSS, compared to cells in both the SS and no flow groups.

Nuclear Eccentricity

We observed noticeable short-term changes in cell nuclear shape in the SS and PSS groups during the first 5 h after treatment, compared to the no flow group, where there were negligible

alterations (Figure 4C). However, after 48 h, nuclear eccentricity was found to only reduce by ~5% and 1.7% for SS and PSS respectively; thus $p > 0.05$ was found amongst the no flow, SS and PSS groups.

Actin Filament Angle

There was a 40% increase in actin filament angle after 48 h of PSS conditioning applied on HBMSCs (Figure 4D). Conversely, SS and no flow conditions on the cells yielded a 21 and 60% decrease in cytoskeletal angle respectively. The actin filament angles of HBMSCs under PSS treatment were found to be $p < 0.05$ in comparison to no flow environments. However, there was no statistical difference found between the SS and PSS groups ($p > 0.05$).

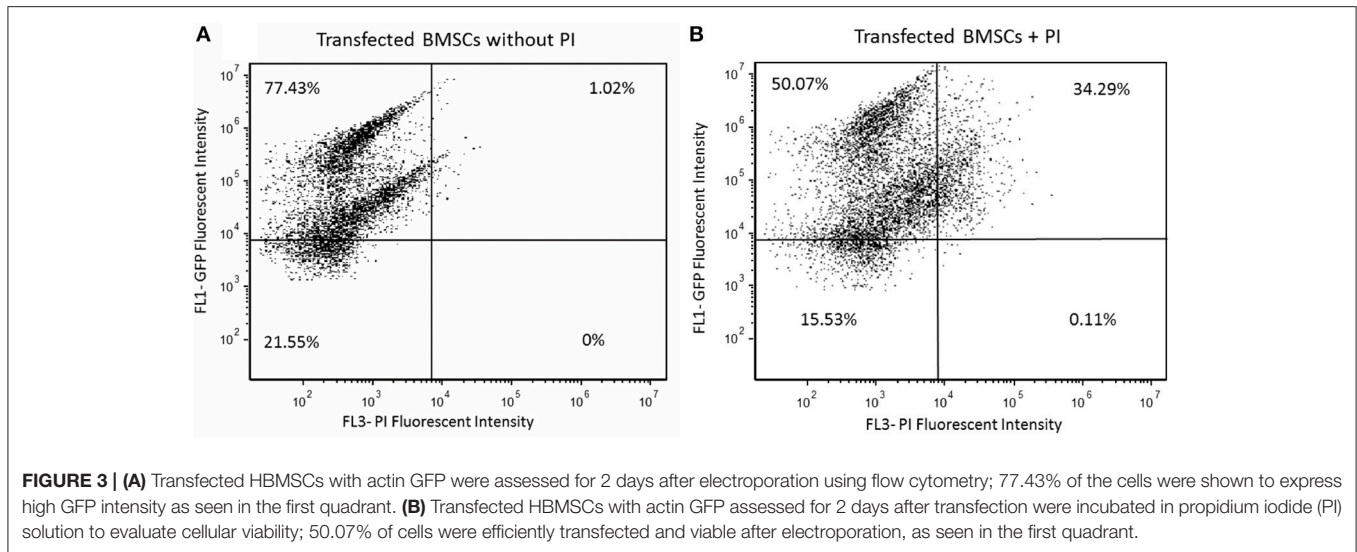
Density of Actin Filaments

HBMSCs actin filament density after PSS exposure was observed to be $p < 0.05$ in comparison to the no flow and SS group, with an increase of 53.2% in filament density after 48 h of treatment (Figure 4E). The SS-treated group had a slight increase in filament density of 10.9%, while no changes were observed in the no flow group after 48 h of HBMSC culture (SS vs. no flow, $p > 0.05$).

Gene Expression

PSS application on the surface of HBMSCs resulted in $p < 0.05$ of the endothelial cell marker, *CD31* in comparison to SS and no flow groups (Figure 5). The α -SMA gene marker, which is indicative of an activated interstitial cell phenotype as well as the bone gene marker, *Osteocalcin*, were $p < 0.05$ in the PSS-treated HBMSCs group compared to the corresponding SS and no flow groups. No statistical differences ($p > 0.05$) were observed between the SS and no flow groups in the expression of α -SMA, *CD31*; however, the SS flow group did exhibit a $p < 0.05$ of *osteocalcin* expression compared to the no flow groups.

A $p < 0.05$ of *klf2a*, a critical transcription factor for valvulogenesis in the PSS-treated samples, was found in comparison to the SS and no flow groups. Finally, the absence of robust expression of *FZD2*, a gene that is developmentally regulated and is found to be uniquely expressed in the heart valve, skin, and pericardium, were observed in all three groups (34). However, the expression of *FZD2* was $p < 0.05$ in the no flow control group in comparison to the SS and PSS-treated groups. Note that the SS and PSS cases had similar levels of expression ($p > 0.05$).



DISCUSSION

HBMSCs remain a promising cell source for TEHV, promoting tissue repair and differentiating along cardiovascular and valvular pathways (20, 35). A fundamental response to mechanical stimuli can thus be observed within the cell cytoskeletal structure. In the current study, our primary goal was to quantify fundamental changes in HBMSC actin filaments after PSS exposure. A priori knowledge of HBMSCs structural events may facilitate optimization of *in vitro* grown TEHV intended for subsequent animal studies or clinical translation. Such optimization is important in the context of enhancing mechanical and biological resilience of the engineered construct when subjected to the *in vivo* environment.

Shear stresses derived from pulsatile blood flow are innate mechanical stress states present on the surfaces of native heart valves (36). Specifically, on the ventricularis-side, the shear stresses are relatively higher in magnitude and uni-directional, while on the fibrosa-side, blood flow is more disturbed, resulting in lower magnitude but high-OSS. Moreover, we previously have shown that pulsatile flow leading to shear stress oscillations within a narrow physiological range augments the gene expression of several key genes of relevance to valve development (27).

Here the HBMSCs exposed to PSS and SS were found to orient themselves in the direction of flow (unpublished observations) in a similar manner to ECs (37). Moreover, after 48 h of culture, we found an increase ($p < 0.05$) in the average number of actin filaments, filament angle, and filament density, i.e., number of filaments/unit area in HBMSCs while exposed to PSS in comparison to the other two groups (SS and no flow). It has been previously demonstrated that specific forces exerted on cells can result in the generation of additional actin filaments (38), which was observed here for the HBMSCs exposed to PSS. This finding therefore suggests that PSS may uniquely trigger stem cell differentiation compared to uni-directional shear stress. The immediate effects that can be specifically observed at the HBMSC

cytoskeletal level are augmentation of the actin filament number, angle, and density.

PSS-treated HBMSCs samples were found to have shorter actin filament lengths ($p < 0.05$) in comparison to SS and no flow-treated cells. The cause for the reduction in filament length is not known and could be due to several factors such as actin-binding proteins which lead to actin filament disassembly (23). However, the resulting disassociation of actin filaments in endothelial cells to fluid shear stress has been shown to permit cellular alignment to flow (23). Therefore, we speculate that a decrease in actin filament length under PSS states to be a triggering event for mesenchymal to endothelial transformation, an important process in the formation of an endothelium in the TEHVs. Specifically, here we demonstrated that concomitant differential regulation of HBMSCs toward the valve lineage under pulsatile flow conditions was evidenced by significantly higher ($p < 0.05$) levels of *CD31* and α -SMA expression, indicative of their heterogeneity. Note that on the other hand, SS conditions resulted in an increase in filament length, which may indicate reduced actin disassembly and hence, more restrictive differential regulation of HBMSCs compared to PSS. Collectively these findings are consistent with our previous work at the tissue-scale, wherein pulsatile flow-induced environments directed expression of *CD31* on HBMSC-derived engineered tissue surfaces and α -SMA within the ECM interstitium in a robust manner (12).

A sub-set of valve-relevant genes that we previously reported on (12, 27, 34) were repeated for analysis in the current study after 48 h of cell culture media flow-induced shear stresses derived from a physiologically-relevant pulsatile flow waveform. A higher expression of *klf2a* was found in the pulsatile flow-treated HBMSCs in comparison to the SS and no flow groups. *Klf2a* is a critical gene that is modulated by oscillatory shear stresses during the valve developmental process; without *Klf2a* expression, valves have been shown to form with defects (28). Even though the augmented expression of *Osteocalcin* by HBMSCs exposed to pulsatile flow is a

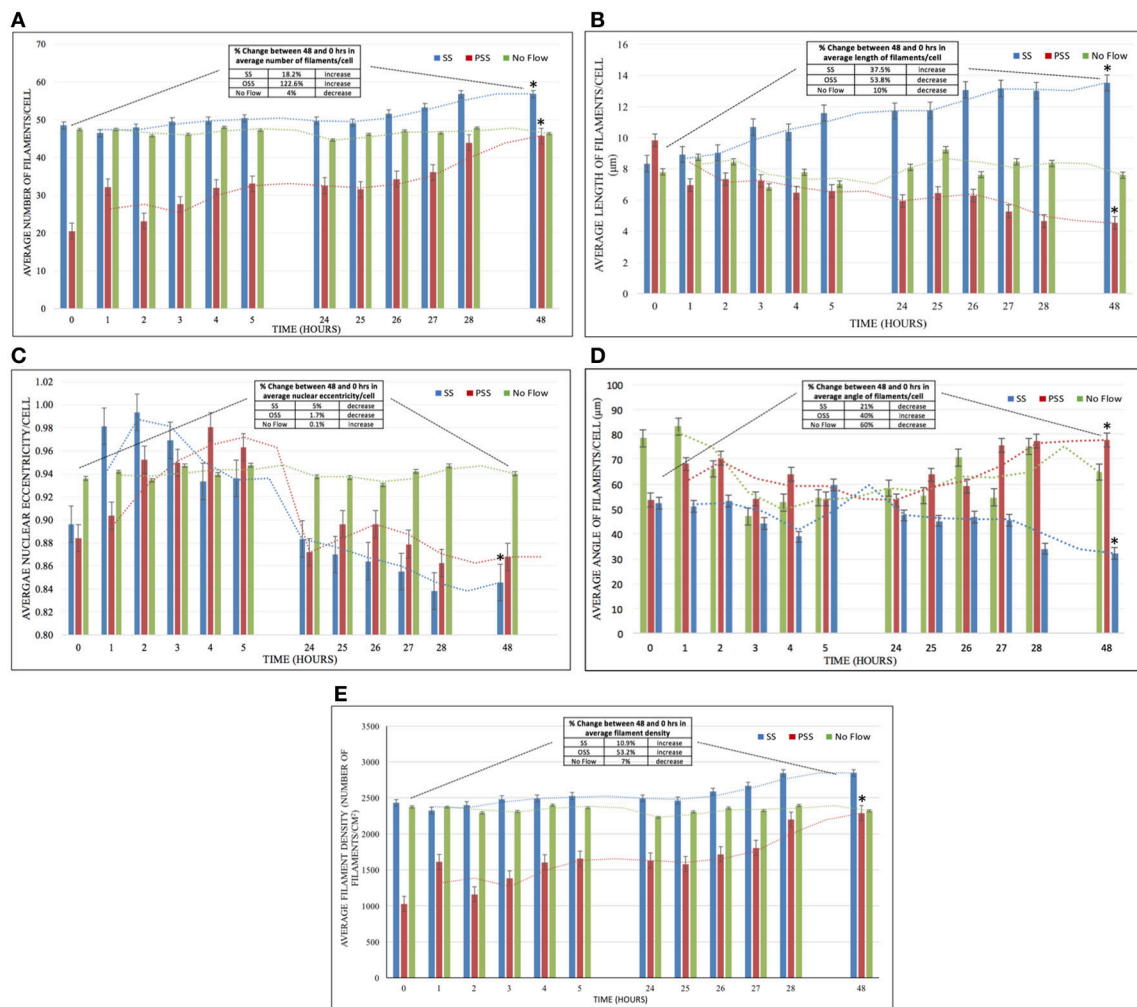


FIGURE 4 | (A) The effect of HBMSCs when exposed to PSS, SS, and No Flow (static) groups on the *average number of filaments/cell* ($n = 8$ wells/group). There was a significantly higher number of actin filaments ($p < 0.05$) found in HBMSCs exposed to PSS compared to SS and no flow groups; however, no significant difference ($p > 0.05$) was observed between SS and no flow groups. **(B)** The PSS, SS, and No Flow (static) groups on average HBMSCs *average length of filaments/cell* ($n = 8$ wells/group). There was a significant decrease ($p < 0.05$) in comparing the average number of filaments in cells exposed to PSS compared to SS and no flow groups. **(C)** *Average nuclear eccentricity/cell* (circularity) in HBMSCs while being exposed to PSS, SS, and No Flow (static) groups ($n = 8$ wells/group). Noticeable changes in nuclear shape (unpublished observations) in the first 5 h of exposure were seen. However, at 48 h, cells in all groups seemed to have reverted to their original configuration (at 0 h), and thus no significant differences ($p > 0.05$) were observed among the three groups. **(D)** *Average angle of filaments/cell* ($n = 8$ wells/group) for the exposure of PSS, SS, and No Flow (static) groups. Actin filament angles were found to be significantly higher ($p < 0.05$) in HBMSCs exposed to PSS compared to corresponding SS and no flow groups over the 48 h period. **(E)** *Average filament density* (Number of filaments/cm²; $n = 8$ wells/group) for the exposure of PSS, SS and No Flow (static) conditions. Actin filament density was found to be significantly higher ($p < 0.05$) in HBMSCs exposed to PSS compared to SS and no flow conditions over the 48 h period; on the other hand, there were no significant differences found ($p > 0.05$) between the SS and no flow groups. Error bars are displayed as \pm SEM; ($n = 8$ samples/group). Note that the table in each figure shows the percentage difference as well as the increase/decrease/unchanged status between the 48 and 0-h time-points for the corresponding metric being quantified. *indicates a significant difference ($p < 0.05$) in that group (PSS, SS or no flow) at 48 hrs compared to 0 hrs.

concern, i.e., an osteogenic pathway, it is not surprising given the documented upregulation of bone markers to PSS (39, 40). It is possible that demonstration of the bone phenotype can be minimized if the specific range of pulsatile flows conducive for valvulogenesis can be identified; this range is likely to be physiologically-relevant. We were able to recently demonstrate (27) that, under a physiologically-relevant PSS condition, *BMP 2* and *NOTCH 1* were significantly upregulated

by HBMSCs in comparison to SS-environments. There were no significant differences in the expression of the inflammatory marker *VCAM* and calcification-inducing *TGF β 1* between the two conditions.

The current study has many limitations. We acknowledge that the mean magnitude of shear stress (1 dynes/cm²) utilized may only be relevant to a few selected regions on the fibrosa side [0.1 to 2.5 dynes/cm² (36)] of the native aortic heart

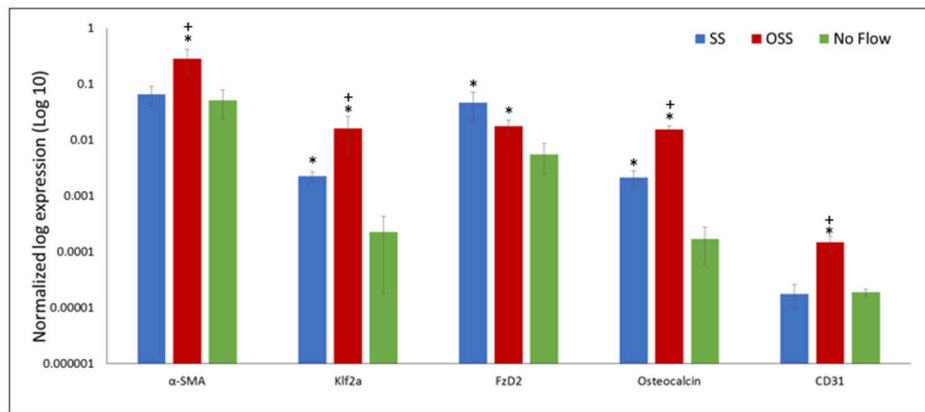


FIGURE 5 | Gene expression follows 48 h of HBMSCs exposure to PSS, SS, and no flow groups. Error bars are displayed as \pm SEM; ($n = 4$). Of particular importance is the significantly greater ($p < 0.05$) expression of *klf2a* found in the PSS-treated cells compared to SS and no flow groups; *klf2a*, a critical gene regulated by PSS, is required for normal valve development and whose absence results in valvular defects. *indicates a significant difference ($p < 0.05$) between the flow groups (SS and/or PSS) and the no flow controls. +indicates the PSS flow group is significantly different ($p < 0.05$) compared to the SS flow group.

valve and does not elucidate the much higher shear stresses experienced by the ventricularis layer [0.1 to 14 dynes/cm² (36)]. Indeed, more recent computational investigations (41–44), including selected works with highly accurate computational fluid-structure approaches (43, 44), as well as direct *in vitro* (45, 46) and *in vivo* (47) evaluations suggest that the dynamic range of shear stresses on leaflet surfaces are much larger than originally thought, extending up to 20 and 90 dynes/cm² on the fibrosa and ventricularis sides of the leaflet respectively. Therefore, the actin filament dynamics that were observed in the current study are solely limited to the one shear stress setting that was chosen (time-averaged shear stress of 1 dynes/cm²), thereby restricting the physiological-context and especially does not represent the kinematics of HBMSC actin filaments at higher aortic valve-relevant shear stress magnitudes. Moreover, exhaustive temporal gene expression analysis, i.e., not solely after 48 h of cell culture, at shorter as well as at longer time points are required to provide conclusive findings.

Another distinct limitation is that a square waveform was utilized to generate PSS which only fluctuated within the positive shear stress range and was thus not fully oscillatory, as would occur regionally on the native valve fibrosa surface. Additionally, in the current study, we did not make any attempts to further optimize gene expression findings by using a physiologically-relevant pulsatile flow profile. Furthermore, the PSS and SS conditions were only matched under time-averaged conditions, while the effects of instantaneous shear stress exposure during pulsatile flow conditioning of HBMSCs, which have previously shown to trigger unique cellular responses (48), were not investigated.

Finally, the current study is limited in that we neither attempted to uncover secretion of valvular ECM components, nor address fundamental mechanisms in cell signaling pathways (e.g., leading to *klf2a* gene expression) as a function of the changes to the HBMSCs cytoskeleton or nucleus. While this

is important and needs to be eventually determined, our initial attempts here were to primarily quantify flow-responsive HBMSC actin filament changes that occurred under shear stress and which were observed to be distinct under PSS conditions (compared to SS and No Flow). Thus, despite the several study constraints, our current findings do suggest at least very preliminarily that HBMSCs exposed to pulsatility effects in culture media, i.e., temporal flow acceleration and deceleration events, partially promote the heart valve-relevant gene expression following distinct actin filament changes in comparison to flow that is solely unidirectional.

In summary, we presented the changes in F-actin filaments and nuclear deformation responses of HBMSCs to PSS, SS, and no flow groups over a period of 48 h. Structural changes and differences were clearly observed between the groups. Specifically, over a 48-h culture period, PSS-conditioned cells responded with a $p < 0.05$ in the actin filament number, angle and density but a decrease of $p < 0.05$ in the length of the filaments. These events could serve as structural precursors that may be monitored and manipulated in culture to enhance differential regulation of HBMSCs for engineered valve tissue growth. In conclusion, the procedures described herein provide a simple yet quantifiable assessment of specific cytoskeletal changes, particularly under PSS states that could regulate stem cell fate in a manner conducive for engineering valvular tissues.

AUTHOR CONTRIBUTIONS

GC conceived the study, performed the cell culture experiments, wrote the paper, and prepared figures pertaining to actin filament structure and nuclear shape quantification. SN also helped with writing the paper and conducted statistical analysis, the gene expression experiments, and prepared its related figure. DA carried out actin filament and nuclear shape quantification using image analysis. SRAT provided technical assistance with gene

expression analysis. SRAM conceived and coordinated the study, interpreted the results and wrote the paper. All authors reviewed the results and approved the final version of the manuscript.

ACKNOWLEDGMENTS

We acknowledge that the topic of this manuscript and parts of its content were derived from the Master's Degree Thesis (49) of the first author GC. Research funding through a Coulter Seed Grant, Department of Biomedical Engineering at Florida International University (FIU) is gratefully acknowledged. The authors thank Dr. Erasmo Perera for assistance with cell transfection and

Christopher Chin for guidance with flow cytometry. We would like to thank the MBRS-RISE program at FIU for providing additional funding through the Biomedical Research Initiative award to conduct this research. A Latin American and Caribbean fellowship to support GC, by the FIU graduate school is gratefully acknowledged. SN received funding through a NSF FGLSAMP FIU Bridge to the Doctorate fellowship award HRD#1301998. DA was partially funded through a Pressley and Mauise Vinson McPhail Undergraduate Research Fellowship in Biomedical Engineering Award. Finally, we would like to thank the FIU writing center for their assistance with proofreading the manuscript.

REFERENCES

1. Ferencz C, Rubin JD, McCarter RJ, Brenner JI, Neill CA, Perry LW, et al. Congenital heart disease: prevalence at livebirth. The Baltimore-Washington Infant Study. *Am J Epidemiol.* (1985) **121**:31–6. doi: 10.1093/oxfordjournals.aje.a113979
2. Centers for Disease and Prevention. Racial differences by gestational age in neonatal deaths attributable to congenital heart defects — United States, 2003–2006. *MMWR Morb Mortal Wkly Rep.* (2010) **59**:1208–11.
3. Nava MM, Raimondi MT, Pietrabissa R. Controlling self-renewal and differentiation of stem cells via mechanical cues. *J Biomed Biotechnol.* (2012) **2012**:797410. doi: 10.1155/2012/797410
4. Osler W. The bicuspid condition of the aortic valves. *Trans Assoc Am Phys.* (1886) **1**:185–92.
5. Farfar S, Hubbard J. Fetal endomyocarditis: intrauterine infection as the cause of congenital cardiac anomalies. *Am J Med Sci.* (1933) **186**:705–13. doi: 10.1097/00000441-193311000-00013
6. Oka M, Angrist A. Mechanism of cardiac valvular fusion and stenosis. *Am Heart J.* (1967) **74**:37–47. doi: 10.1016/0002-8703(67)90038-5
7. Van Mierop L. Pathology and pathogenesis of the common cardiac malformations. *Cardiovasc Clin.* (1970) **2**:28–59.
8. Peacock TB. Malformations which do not interfere with the functions of the heart, but may lay the foundation of disease in after life. Irregularities of the valves. In: Peacock TB, editor. *On malformations, and C., of the human heart. With original cases [1858]*. Boston, MA: Milford House (1973). p. 93–102.
9. Moore GW, Hutchins GM, Brito JC, Kang H. Congenital malformations of the semilunar valves. *Hum Pathol.* (1980) **11**:367–72. doi: 10.1016/S0046-8177(80)80033-5
10. Hoffman JI. Incidence of congenital heart disease: I. Postnatal incidence. *Pediatr Cardiol.* (1995) **16**:103–13. doi: 10.1007/BF00801907
11. Butcher JT, Penrod AM, Garcia AJ, Nerem RM. Unique morphology and focal adhesion development of valvular endothelial cells in static and fluid flow environments. *Arterioscler Thromb Vasc Biol.* (2004) **24**:1429–34. doi: 10.1161/01.ATV.0000130462.50769.5a
12. Rath S, Salinas M, Villegas AG, Ramaswamy S. Differentiation and distribution of marrow stem cells in flex-flow environments demonstrate support of the valvular phenotype. *PLoS ONE* (2015) **10**:e0141802. doi: 10.1371/journal.pone.0141802
13. Salinas M, Rath S, Villegas A, Unnikrishnan V, Ramaswamy S. Relative effects of fluid oscillations and nutrient transport in the *in vitro* growth of valvular tissues. *Cardiovasc Eng Technol.* (2016) **7**:170–81. doi: 10.1007/s13239-016-0258-x
14. Hasan A, Ragaert K, Swieszkowski W, Selimovic S, Paul A, Camci-Unal G, et al. Biomechanical properties of native and tissue engineered heart valve constructs. *J Biomech.* (2014) **47**:1949–63. doi: 10.1016/j.jbiomech.2013.09.023
15. Butcher JT, Nerem RM. Valvular endothelial cells regulate the phenotype of interstitial cells in co-culture: effects of steady shear stress. *Tissue Eng.* (2006) **12**:905–15. doi: 10.1089/ten.2006.12.905
16. Bates ER. Treatment options in severe aortic stenosis. *Circulation* (2011) **124**:355–9. doi: 10.1161/CIRCULATIONAHA.110.974204
17. Neidert MR, Tranquillo RT. Tissue-engineered valves with commissural alignment. *Tissue Eng.* (2006) **12**:891–903. doi: 10.1089/ten.2006.12.891
18. Sutherland FW, Perry TE, Yu Y, Sherwood MC, Rabkin E, Masuda Y, et al. From stem cells to viable autologous semilunar heart valve. *Circulation* (2005) **111**:2783–91. doi: 10.1161/CIRCULATIONAHA.104.498378
19. Freed LE, Guilak F, Guo XE, Gray ML, Tranquillo R, Holmes JW, et al. Advanced tools for tissue engineering: scaffolds, bioreactors, and signaling. *Tissue Eng.* (2006) **12**:3285–305. doi: 10.1089/ten.2006.12.3285
20. Vander Roest MJ, Merryman WD. A developmental approach to induced pluripotent stem cells-based tissue engineered heart valves. *Future Cardiol.* (2017) **13**:1–4. doi: 10.2217/fca-2016-0071
21. Engelmayr GC Jr, Sales VL, Mayer JE Jr, Sacks MS. Cyclic flexure and laminar flow synergistically accelerate mesenchymal stem cell-mediated engineered tissue formation: Implications for engineered heart valve tissues. *Biomaterials* (2006) **27**:6083–95. doi: 10.1016/j.biomaterials.2006.07.045
22. Liu YS, Lee OK. In search of the pivot point of mechanotransduction: mechanosensing of stem cells. *Cell Transplant.* (2014) **23**:1–11. doi: 10.3727/096368912X659925
23. Osborn EA, Rabodzey A, Dewey CF Jr, Hartwig JH. Endothelial actin cytoskeleton remodeling during mechanostimulation with fluid shear stress. *Am J Physiol Cell Physiol.* (2006) **290**:C444–52. doi: 10.1152/ajpcell.00218.2005
24. Ito K, Sakamoto N, Ohashi T, Sato M. Effects of frequency of pulsatile flow on morphology and integrin expression of vascular endothelial cells. *Technol Health Care* (2007) **15**:91–101.
25. Jones TD, Naimipour H, Sun S, Cho M, Alapati SB. Mechanical changes in human dental pulp stem cells during early odontogenic differentiation. *J Endod.* (2015) **41**:50–5. doi: 10.1016/j.joen.2014.07.030
26. Rath S, Salinas M, Bhattacharjee S, Ramaswamy S. Marrow stem cell differentiation for valvulogenesis via oscillatory flow and nicotine agonists: unusual suspects? *J Long Term Eff Med Implants* (2015) **25**:147–160. doi: 10.1615/JLongTermEffMedImplants.2015011695
27. Williams A, Nasim S, Salinas M, Moshkforoush A, Tsoukias N, Ramaswamy S. A “sweet-spot” for fluid-induced oscillations in the conditioning of stem cell-based engineered heart valve tissues. *J Biomech.* (2017) **65**:40–8. doi: 10.1016/j.jbiomech.2017.09.035
28. Vermot J, Forouhar AS, Liebling M, Wu D, Plummer D, Gharib M, et al. Reversing blood flows act through *klf2a* to ensure normal valvulogenesis in the developing heart. *PLoS Biol.* (2009) **7**:e1000246. doi: 10.1371/journal.pbio.1000246
29. Salinas M, Ramaswamy S. Computational simulations predict a key role for oscillatory fluid shear stress in de novo valvular tissue formation. *J Biomech.* (2014) **47**:3517–23. doi: 10.1016/j.jbiomech.2014.08.028
30. Helledie T, Nurcombe V, Cool SM. A simple and reliable electroporation method for human bone marrow mesenchymal stem cells. *Stem Cells Dev.* (2008) **17**:837–48. doi: 10.1089/scd.2007.0209

31. Mahler GJ, Frenzl CM, Cao Q, Butcher JT. Effects of shear stress pattern and magnitude on mesenchymal transformation and invasion of aortic valve endothelial cells. *Biotechnol Bioeng.* (2014) **111**:2326–37. doi: 10.1002/bit.25291
 32. Vandesompele J, De Preter K, Pattyn F, Poppe B, Van Roy N, De Paep A, et al. Accurate normalization of real-time quantitative RT-PCR data by geometric averaging of multiple internal control genes. *Genome Biol.* (2002) **3**: RESEARCH0034. doi: 10.1186/gb-2002-3-7-research0034
 33. Padang R, Bagnall RD, Semsarian C. Genetic basis of familial valvular heart disease. *Circ Cardiovasc Genet.* (2012) **5**:569–80. doi: 10.1161/CIRCGENETICS.112.962894
 34. Martinez C, Rath S, Van Gulden S, Pelaez D, Alfonso A, Fernandez N, et al. Periodontal ligament cells cultured under steady-flow environments demonstrate potential for use in heart valve tissue engineering. *Tissue Eng Part A* (2013) **19**:458–66. doi: 10.1089/ten.tea.2012.0149
 35. Kalinina NI, Sysoeva VY, Rubina KA, Parfenova YV, Tkachuk VA. Mesenchymal stem cells in tissue growth and repair. *Acta Nat.* (2011) **3**:30–7.
 36. Sacks MS, Yoganathan AP. Heart valve function: a biomechanical perspective. *Philos Trans R Soc Lond B Biol Sci.* (2007) **362**:1369–91. doi: 10.1098/rstb.2007.2122
 37. Butcher JT, Nerem RM. Valvular endothelial cells and the mechanoregulation of valvular pathology. *Phil Trans R Soc Lond B Biol Sci.* (2007) **362**:1445–57. doi: 10.1098/rstb.2007.2127
 38. Sewell-Loftin MK, Chun YW, Khademhosseini A, Merryman WD. EMT-inducing biomaterials for heart valve engineering: taking cues from developmental biology. *J Cardiovasc Transl Res.* (2011) **4**:658–71. doi: 10.1007/s12265-011-9300-4
 39. Li YJ, Batra NN, You L, Meier SC, Coe IA, Yellowley CE, et al. Oscillatory fluid flow affects human marrow stromal cell proliferation and differentiation. *J Orthop Res.* (2004) **22**:1283–9. doi: 10.1016/j.orthres.2004.04.002
 40. Arnsdorf EJ, Tummala P, Kwon RY, Jacobs CR. Mechanically induced osteogenic differentiation—the role of RhoA, ROCKII and cytoskeletal dynamics. *J Cell Sci.* (2009) **122**:546–53. doi: 10.1242/jcs.036293
 41. Ge L, Sotiropoulos F. Direction and magnitude of blood flow shear stresses on the leaflets of aortic valves: is there a link with valve calcification? *J Biomech Eng.* (2010) **132**:014505. doi: 10.1115/1.4000162
 42. Chandra S, Rajamannan NM, Sucusky P. Computational assessment of bicuspid aortic valve wall-shear stress: implications for calcific aortic valve disease. *Biomech Model Mechanobiol.* (2012) **11**:1085–96. doi: 10.1007/s10237-012-0375-x
 43. Cao K, Bukac M, Sucusky P. Three-dimensional macro-scale assessment of regional and temporal wall shear stress characteristics on aortic valve leaflets. *Comput Methods Biomech Biomed Eng.* (2016) **19**:603–13. doi: 10.1080/10255842.2015.1052419
 44. Cao K, Sucusky P. Aortic valve leaflet wall shear stress characterization revisited: impact of coronary flow. *Comput Methods Biomech Biomed Eng.* (2017) **20**:468–70. doi: 10.1080/10255842.2016.1244266
 45. Yap CH, Saikrishnan N, Tamilselvan G, Yoganathan AP. Experimental measurement of dynamic fluid shear stress on the aortic surface of the aortic valve leaflet. *Biomech Model Mechanobiol.* (2012) **11**:171–182. doi: 10.1007/s10237-011-0301-7
 46. Yap CH, Saikrishnan N, Yoganathan AP. Experimental measurement of dynamic fluid shear stress on the ventricular surface of the aortic valve leaflet. *Biomech Model Mechanobiol.* (2012) **11**:231–44. doi: 10.1007/s10237-011-0306-2
 47. Kilner PJ, Yang GZ, Wilkes AJ, Mohiaddin RH, Firmin DN, Yacoub MH. Asymmetric redirection of flow through the heart. *Nature* (2000) **404**:759–61. doi: 10.1038/35008075
 48. Sun L, Rajamannan NM, Sucusky P. Defining the role of fluid shear stress in the expression of early signaling markers for calcific aortic valve disease. *PLoS ONE* (2013) **8**:e84433. doi: 10.1371/journal.pone.0084433
 49. Castellanos GL. Cellular events under flow states pertinent to heart valve function. In: *FIU electronic theses and Dissertations 2285* (2015). Available online at: <http://digitalcommons.fiu.edu/etd/2285>
- Conflict of Interest Statement:** The authors declare that the research was conducted in the absence of any commercial or financial relationships that could be construed as a potential conflict of interest.
- Copyright © 2018 Castellanos, Nasim, Almora, Rath and Ramaswamy. This is an open-access article distributed under the terms of the Creative Commons Attribution License (CC BY). The use, distribution or reproduction in other forums is permitted, provided the original author(s) and the copyright owner are credited and that the original publication in this journal is cited, in accordance with accepted academic practice. No use, distribution or reproduction is permitted which does not comply with these terms.



Mechanotransduction Mechanisms in Mitral Valve Physiology and Disease Pathogenesis

Leah A. Pagnozzi and Jonathan T. Butcher*

Meinig School of Biomedical Engineering, Cornell University, Ithaca, NY, United States

OPEN ACCESS

Edited by:

Joshua D. Hutcheson,
Florida International University,
United States

Reviewed by:

Mary Kathryn Sewell-Loftin,
Washington University Medical
Center, United States
Mark C. Blaser,
Brigham and Women's Hospital,
United States

*Correspondence:

Jonathan T. Butcher
jtb47@cornell.edu

Specialty section:

This article was submitted to
Atherosclerosis and Vascular
Medicine,
a section of the journal
Frontiers in Cardiovascular Medicine

Received: 15 October 2017

Accepted: 07 December 2017

Published: 22 December 2017

Citation:

Pagnozzi LA and Butcher JT (2017)
Mechanotransduction Mechanisms
in Mitral Valve Physiology and
Disease Pathogenesis.
Front. Cardiovasc. Med. 4:83.
doi: 10.3389/fcvm.2017.00083

The mitral valve exists in a mechanically demanding environment, with the stress of each cardiac cycle deforming and shearing the native fibroblasts and endothelial cells. Cells and their extracellular matrix exhibit a dynamic reciprocity in the growth and formation of tissue through mechanotransduction and continuously adapt to physical cues in their environment through gene, protein, and cytokine expression. Valve disease is the most common congenital heart defect with watchful waiting and valve replacement surgery the only treatment option. Mitral valve disease (MVD) has been linked to a variety of mechano-active genes ranging from extracellular components, mechanotransductive elements, and cytoplasmic and nuclear transcription factors. Specialized cell receptors, such as adherens junctions, cadherins, integrins, primary cilia, ion channels, caveolae, and the glycocalyx, convert mechanical cues into biochemical responses *via* a complex of mechanoresponsive elements, shared signaling modalities, and integrated frameworks. Understanding mechanosensing and transduction in mitral valve-specific cells may allow us to discover unique signal transduction pathways between cells and their environment, leading to cell or tissue specific mechanically targeted therapeutics for MVD.

Keywords: mitral valve, valve disease, mechanotransduction, pathogenesis, biomechanics

INTRODUCTION

The mitral valve is a bicuspid valve that facilitates the flow of blood from the left atrium to the left ventricle. Mitral valve disease (MVD) affects 2.4% of the population and is a common congenital heart defect (1, 2). In adults, the most common disorders of the valve are mitral insufficiency (i.e., regurgitation), mitral stenosis, myxomatous degeneration, and mitral valve prolapse, with broad disease likely to include several of these effects.

The mitral valve leaflets consist of four layers that differ in extracellular matrix (ECM) composition and mechanical properties. The thickest layer of the valve, the fibrosa, is the main load bearing layer. It provides the majority of leaflet tensile strength through a thick layer of dense, aligned collagen fibers while a looser collagen network with increased glycosaminoglycan (GAG) and proteoglycan content provides compressive strength. The mitral valve is mechanically supported through the GAG-rich chordae tendinae which attach the mitral leaflets to the papillary muscles along the ventricular wall and maintain valve closure during systole. MVD results in altered mechanical and structural properties of the valve. Myxomatous mitral valves are characterized by leaflet enlargement, annular dilation, thickened and elongated chordae, GAG accumulation, loss of structure, increased compliance, and myxoid lesions. Disorganization and remodeling of the ECM and weakening of the chordae result in a loss of most of the valve's mechanical properties and an overall thickened and

enlarged leaflet. This in turn prevents the valve from fully closing causing symptoms of mitral regurgitation and prolapse.

The mitral valve is a dynamic structure which changes mechanically during the cardiac cycle; the constant flow of blood and opening and shutting of the valves exposes the tissue to a complex and demanding environment. The valve is subjected to bending, deformation, large area changes, shear stress, and heterogeneous strains in response to myocardial contraction, transvalvular pressure, and hemodynamic flow. The mitral valve exhibits a non-linear stress-strain relationship with complex viscoelastic and axial coupling behaviors (3, 4). These dynamic and adaptive interactions between the myocardial wall and valve leaflets ultimately impact the mechanical stress and strain experienced by cells through the ECM (5).

Cells and their ECM exhibit dynamic reciprocity, continuous, bidirectional interaction between cells and their ECM, in the growth and formation of tissue through mechanotransduction, the conversion of mechanical signals into biochemical responses (6). Cells and their ECM reorganize *via* a complex of mechanoresponsive elements (6) to physically regulate the spatiotemporal distribution of biochemical components maintaining homeostasis. MVD has been linked to a variety of mechano-active genes, such as extracellular components, mechanotransductive elements, and transcription factors. Mechanical stimulus in the microenvironment provides inductive signals of homeostasis and remodeling to the native cells—valve interstitial cells (VICs), and endothelial cells (VECs).

Valve endothelial cells reside on the exterior of the valve, maintain a non thrombogenic surface layer, and regulate immune and inflammatory reactions. The majority of valve cells are the VICs, a mesenchymal population that resides in all layers of the valve, distinct in their ability to differentiate into multiple phenotypes. There are five known phenotypes of VICs: embryonic progenitor endothelial/mesenchymal, quiescent, activated, progenitor, and osteoblastic VICs which may convert from one form to another. Most VICs in the healthy adult valve are quiescent with a small population of activated VICs to maintain base ECM remodeling. In pathological states, there is an increase in activated VICs which regulate repair and remodeling, which may lead to fibrosis and calcification. Inflammation, biochemical, and mechanical stimuli can induce activation of quiescent fibroblasts into myofibroblasts. VICs and VECs continuously remodel their environment by secreting and degrading ECM, and adapting their gene, protein, and cytokine expression to alter phenotype and function. These dynamic and adaptive interactions between the myocardial wall, flowing blood, and valve leaflets ultimately impact the mechanical stress and strain experienced by cells through the ECM. The movement, anisotropic deformation, and complex geometries of the mitral valve create a variety of ever changing mechanical cues between the cells and their matrix. ECM composition, fiber alignment, and compaction regulate cell deformation and thus mechanotransductive response. By focusing on broad classes of mechanosensing pathways as well as their integration in mechanotransduction, this review will explore the biomechanical mechanisms at play in the mitral valve microenvironment and mediators of mechanotransduction in this tissue.

MECHANOBIOLOGY OF MITRAL VALVULOGENESIS

During valve development, the embryonic heart transforms from a myocardial tube into a complex, four chambered, mature structure. Valve cells differentiate from endocardial cells during gastrulation and by E9.5 valvulogenesis begins when the heart tube loops creating the primitive ventricle and atria. In these early embryos position sensing (7, 8) and force transduction instruct lineage allocation. Endothelial cells (ECs) of the endocardium form valve cushions in a GAG-rich cardiac jelly where, in response to growth factors, such as Transforming Growth Factor- β (TGF- β), they undergo endothelial to mesenchymal transition (EMT). ECs reorganize their actin architecture to permit migration, adhesion, and morphogenesis in the embryo. Knockout of cytoskeletal adaptors in ECs causes disorganized cytoskeletal organization, cell morphology, impaired focal adhesion development, and actin signaling, inhibiting EMT in embryonic mice (9). Atrioventricular endocardial cells adopt a cuboidal morphology prior to EMT which seems mediated by cardiac contraction- in mutants which lack heart contraction, endocardial cells fail to change shape and initiate EMT (10).

During EMT cell-cell contacts are downregulated and processes governing cell-matrix adhesions and cytoskeleton reorganization are upregulated (11). Cells acquire an invasive phenotype, allowing them to migrate into the cardiac jelly, degrade hyaluronan, and deposit collagen, versican, and proteoglycans to form mature leaflets. Cushion mesenchymal cells give rise to VICs post-EMT which organize their surrounding matrix into a fibrous, rigid tissue able to withstand the hemodynamic loading of the beating heart. Contractile VICs condense the ECM by pulling on it, creating cell-matrix alignment in response to mechanical cues (12, 13). During valvulogenesis, tension points are created which may promote the secretion and alignment of collagen fibrils from VICs in a manner similar to that seen during tendon development (14).

Mechanotransduction of hemodynamic shear and strain are crucial to valvulogenesis. In zebrafish embryos knockdown of oscillatory flow sensitive gene *klf2a* results in dysfunctional or absent leaflet formation despite no change in retrograde flow (15). *klf2a* is related to signaling through mechano-sensitive ion channels, which is discussed later in the Ion Channel section. Physical occlusion of the inflow or outflow tract in zebrafish embryos results in hearts with an abnormal third chamber, looping defects, and impaired valve formation. In the embryo, red blood cells themselves generate important shear fluctuations different than that of normal hemodynamic shear which may mechanically influence ECs (16). Zebrafish with transvalvular flow alterations fail to undergo atrioventricular valve maturation from two to four leaflets despite no alterations in contractility (17). Tissue strain from variations in pressure and cardiac contraction also mechanically drive valve formation in a similar fashion to cell-cell and cell-matrix contacts. Mutations that inhibit myocardial contractility in the embryo fail to form cushions with chemical inhibition of contraction inhibiting endocardial ring formation in a dose dependent fashion (18). Cytoskeletal adaptors in embryonic ECs mediate actin dynamics, and mutations in

them disrupt EMT and valvulogenesis (19). The impact of strain alterations are time dependent as altered cardiac preload results in morphological defects in zebrafish embryos treated in earlier and later developmental stages without impacting groups treated at 30–36 h post fertilization (20). Alterations in cell–matrix homeostasis later in life may reactivate physical or chemical cues of valvulogenesis, particularly EMT, causing aberrant elongation, remodeling, and stiffening (21, 22).

ADHERENS JUNCTIONS AND CADHERINS

Adherens junctions are located at cell–cell contact points where they mediate cell adhesion, force, and signal transduction. Cells send out a finger-like lamellipodia to neighboring cells, which are stabilized by the acceptor lamellae with actin-myosin contractility. This actin finger determines the location and shape of the adherens junction and is co-localized with stress fibers in the neighboring cells. Adhesions are formed through integrin and cadherin interactions in both VECs and VICs at cell–cell and cell–integrin junctions, respectively. At adhesions, adhesion receptors interact with F-actin and adhesion proteins to regulate signaling, junction assembly, and maintenance. While traditionally recognized as distinct structures, adherens junctions and focal adhesions are intracellularly linked to the actin cytoskeleton, and activate the same signaling proteins and actin regulators (23).

Vinculin is a cytoplasmic actin binding protein, enriched at both cell–cell and cell–matrix adhesions, which regulates integrin dynamics and adhesion, stimulating polymerization, and remodeling through actin binding. Vinculin arranges itself in three domains: an integrin signaling layer, actin binding and force transducing layer, and actin regulatory layer. Vinculin is in an open active form in focal adhesions and a closed, inhibited form within the cytoplasm. In this inhibited form, the vinculin head domain interacts extensively with its tail in the integrin signaling layer and when these head–tail interactions are relieved (24), it migrates to the actin binding layer where it recruits proteins to regulate focal adhesion dynamics and cell migration (25).

Cadherins are calcium-dependent cell adhesion proteins composed of an extracellular region, a transmembrane domain, and cytoplasmic region. Cadherins connect the cortical actin cytoskeleton of neighboring cells and create zipper-like structures to maintain stable intercellular adhesion by regulating cortical tension and maintaining mechanical coupling between cells (26). In confluent monolayers, VICs with strong cell–cell contacts show weak expression of myofibroblastic marker α -smooth muscle actin (α SMA), suggesting cell contact inhibits myofibroblastic activation (27). In these conditions, cadherin protein complexes β -catenin and N-cadherin expression are decreased or absent (27). In aortic valve disease and development cell junction protein cadherin-11 (Cad-11) has been implicated in a variety of mechano-active defects and similar mechanisms may be at play in MVD. Cad-11, a known mediator of dystrophic calcification in calcific aortic valve disease, is strongly expressed in human calcified aortic leaflets with nodule formation dependent on strong cell–cell contacts (28) while cyclic strain upregulates Cad-11 and α SMA expression (29) in aortic VICs (AVICs). In canines

with myxomatous valve disease, VE-cadherin was significantly decreased (30). Downregulation of VE-cadherin results in endothelial migration and EMT in zebrafish valvulogenesis (31) so similar expression in canines suggests a pathological proliferative and migratory endothelial phenotype (30).

Plakophilin-2 links cadherins to intermediate filaments in the cytoskeleton. In prolapsed mitral valves, increased Cad-11, N-cadherin, and aberrant presence of plakophilin-2 at the adherens junction, promotes latent TGF- β activation and pathological ECM remodeling (32). Cad-11 is expressed in chick mitral valves during development at the leaflet tips in endocardial cushion mesenchymal cells (31) and throughout the leaflets of remodeling valves in adults. In hyperlipidemic mice, Cad-11 expression was significantly increased in the aortic and mitral valves (33) inducing ECM remodeling and calcific nodule formation (34).

INTEGRINS

Integrins regulate and respond to force by connecting the ECM to the cytoskeleton. Composed of an α and β subunit which combine to approximately 24 unique heterodimers (35, 36), integrins bind to different ECM proteins and interact with cell-surface ligands, transmembrane proteins, proteases, and growth factors (37). Integrins receive and transmit signals from both sides of the plasma membrane (38, 39). Cytoskeletal contractions pull on integrin links to the matrix, deforming binding proteins that connect actin to focal adhesion proteins and integrin to arginine–glycine–aspartate (RGD) containing proteins, altering gene and protein expression (40). RGD is the main integrin binding domain in ECM proteins common to the mitral valve: collagens, laminin, fibrillin, and fibronectin (41, 42).

Several adhesive peptides control integrin-mediated cell adhesion. VICs strongly express the α 2 and β 1 subunits and α 5 β 1 integrin (43, 44) Collagen I mimetic DGEA binds integrin α 2 β 1 and promotes adhesion and ECM deposition in VICs (45). The α 2 β 1 integrin is necessary in coupling VICs to collagen I, propagating VIC contraction into leaflet force generation (46). In combination with RGD, peptide VAPG with affinity to laminin and elastin, along with DGEA downregulate myofibroblastic and osteogenic differentiation in VICs (45). Blocking integrin receptor 67LR, with affinities to laminin and elastin, resulted in formation of calcific nodules (47) suggesting an anticalcific effect in binding. Disruption of VIC binding *via* the α 5 β 1 integrin or the 67-kDa laminin receptor had a dramatic calcification-stimulating effect. Binding *via* the α 2 β 1 integrin did not alter calcification or VIC phenotype; blocking α 5 β 1 resulted in calcification in AVICs (43) and is likely to have similar pathology in mitral valves.

Integrins bind to and activate TGF- β , which modulates cell growth, adhesion, migration, and ECM synthesis (48, 49). TGF- β secretion consists of three proteins: TGF- β , latency-associated protein (LAP), and latent TGF- β binding protein (LTBP), an ECM-binding protein. Several integrins activate latent TGF- β through binding to an RGD integrin binding site on LAP (50). Under high stress, TGF- β controls expression of α SMA, stress fiber formation, and differentiates quiescent fibroblasts into contractile myofibroblasts creating a positive feedback cycle (51). Mechanically conditioning ECM releases active TGF β 1

(52) demonstrating the role of force in fibroblast activation. VICs grown on stiff surfaces have strong cell-ECM adhesions, contractility, and myofibroblast differentiation (53). Shear flow induces TGF β 1 production and myofibroblast differentiation of fibroblasts in collagen gels (54). In both embryonic and adult VICs, a quiescent phenotype is maintained in unstressed collagen hydrogels; however, contractile expression, TGF- β , and matrix remodeling are upregulated in response to tension (55).

Latent TGF- β binding proteins interact with fibrillin, a large structural protein that polymerizes into extracellular microfibrils and contributes to the functional integrity of connective tissue (56). Mutations in fibrillin-1 cause Marfan Syndrome (MFS) and related disorders from dysregulated TGF- β activity. TGF- β cytokines act through various small GTPases such as RhoA and Rac1, which are implicated in valve disease and development (**Figure 1**). RhoA is a mechano-sensitive GTPase that acts complementary to Rac to control cell migration, differentiation, and proliferation. Filamin-A (FlnA) point mutations in mice, responsible for X-linked myxomatous valve disease (57), deregulate the balance between RhoA and Rac1 in favor of RhoA, altering downstream trafficking of β 1 integrins (58) resulting in a myxomatous phenotype by 2 months of age. For more information on GTPases, see section on Integrated Mechanotransduction at the end. FlnA mutations increase Erk signaling, a non canonical TGF- β driven kinase, which is present in mouse models of MFS (59). In murine aortic valves with an elastogenic defect, mice had latent hemodynamic AV disease from increased Erk1/2 activation, ECM disorganization, and inflammation (60). Both these mutant mice and aged mice display stiffened ECM, fibrosis, cell adhesion and fibronectin alterations, increased collagen expression, and decreased LTBP signaling (60) suggesting a similar mechanism may be driving integrin signaling in MVD.

CILIA

Primary cilia are solitary microtubule structures consisting of a basal body and projecting axoneme “antenna.” The axoneme

senses the external environment and coordinates various signaling pathways, such as TGF- β (61) and calcium sinks (62), indicating a mechanosensory role (63). Primary cilia defects have been linked to various congenital cardiovascular diseases, such as heterotaxy and atrioventricular septal defects (64–66). Cilia are strongly expressed between stages E11.5 and E17.5 on the outflow tract cushions in aortic valvulogenesis, while they are lost in adult VICs (67).

Primary cilia restrain ECM expression during development and remodeling such that ablation of primary cilia during aortic valvulogenesis results in highly penetrant bicuspid valve phenotype (67). Primary cilia loss in arterial ECs sensitizes them toward BMP mediated osteogenic differentiation (68), inflammatory gene expression, and decreased eNOS activity (69). Exome sequencing of chemically mutagenized mice revealed mutations in 61 recessive congenital heart disease genes, 34 of them cilia related (66); cilia axoneme mutants caused outflow tract and atrioventricular septation (70). In polycystic kidney disease (PKD), a genetic disorder with TGF- β mediated abnormalities, there is a 10-fold increase of mitral valve prolapse tied to defective protein localization in the primary cilia (71–73). Mitral insufficiency has been seen in infantile nephronophthisis (74), structural defects in Ellis–van Creveld syndrome (75, 76), severe mitral regurgitation and structural defects in Kartagener’s syndrome (77, 78), and rheumatic valvular insufficiency in Bardet–Biedl syndrome (79).

ION CHANNELS

Mechano-sensitive channels (MCs) are a class of membrane ion channels that detect and respond to force, converting it into electrical or biochemical signals (80, 81). There is increasing evidence MCs play a key role in regulating endothelial response to shear flow (82–84). Cilia coupled with calcium channels (**Figure 2**) transduce shear stress during zebrafish valvulogenesis; endothelial cilia deflect with blood flow correlating to expression of calcium channel gene polycystin-2 (PKD2), increasing endothelial calcium levels, and altering vascular formation (85).

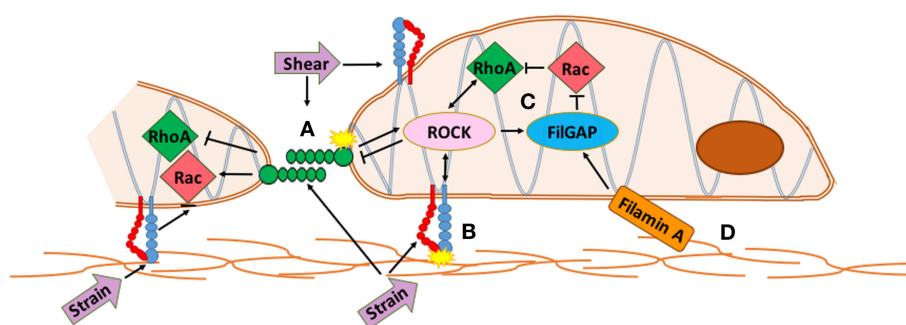
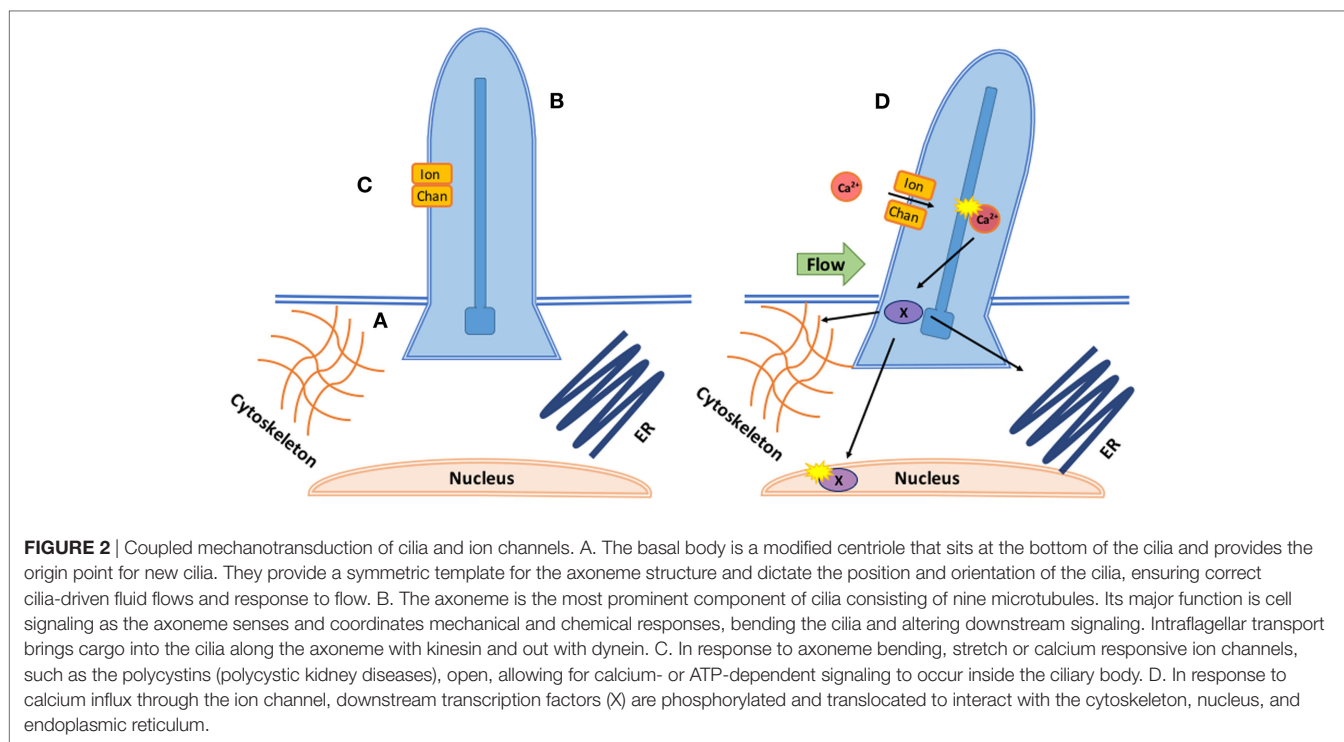


FIGURE 1 | Integrated mechanotransduction of cadherins and integrins through the cytoskeleton and small GTPases. A. At cell–cell adhesion points coupled cadherins transduce strain and shear force into cytoskeletal remodeling and downstream signaling pathways. B. At cell–extracellular matrix (ECM) adhesions, strain is transduced through integrins into cytoskeletal remodeling and downstream signaling pathways. C. RhoA and Rac are mechano-sensitive small GTPases common to multiple methods of mechanotransduction in the mitral valve that act opposite and complementary to control cell migration, differentiation, and proliferation. RhoA regulates actin cytoskeleton and stress fiber formation while Rac1 regulates cell–cell adhesion, actin polymerization, lamellae protrusion, and cytoskeletal polarity. ROCK interacts with integrins and cadherins to mediate RhoA and Rac activity while FilGAP binds to filamin-A to control actin at cytoskeletal interfaces. D. The extracellular matrix interacts with the actin network directly through specific ECM components or through integrins and cadherins. See Section “Integrated Mechanotransduction” for more information.



Cilia response is mediated by transient receptor channels such as Trpv4 and Trpp2 which are expressed during valve development (86). mRNA expression of Piezo1, a mechanically activated cation channel, has been seen in murine hearts (87) while its loss in ECs causes stress fiber and cell orientation (88) deficits in response to shear stress, profound vascular defects, and embryonic lethality within days of the heart beating (89).

Malfunction of MCs results in broad cardiovascular pathology such as arrhythmias (90), hypertension (91), and PKD (92). PKD2 is localized to the cilia in vascular ECs. In mouse embryos it is required for right-left axis determination with knockouts displaying severe cardiac structural defects by E18 (93). PKD2 is mutated in PKD and murine mutants lose the ability to generate nitric oxide (NO) in response to shear flow which may promote high blood pressure (94). PKD2 defects may prolong channel activity by preventing calcium from leaving small compartments, such as cilia (95). Prolongation of the QT interval has been associated with myxomatous mitral valve related sudden cardiac death (96, 97). Mutations in sodium voltage-gated channel V account for 5–10% of long QT cases and have been comorbid with desmoplakin mutations, a protein responsible for mechanical coupling of cardiac myocytes with known overlap in channelopathies (97, 98). Oscillatory flow stimulates *klf2a* expression, a key transcription factor in valvulogenesis, and knockdown results in dysfunctional or absent leaflet formation (15). Oscillatory flow through Trpv4 and Trpp2 (99) modulate the endocardial calcium response and control *klf2a* expression in zebrafish, with absence of either resulting in severe valve defects. *klf2a* misexpression during angiogenesis occurs in the absence of flow, with downregulation of $\beta 1$ integrin rescuing overgrowth and maintaining endothelial quiescence (100).

CAVEOLAE

Caveolae are small plasma membrane invaginations made up of Caveolin (Cav) and Cavin proteins, glycosphingolipids, and cholesterol. Caveolae respond to mechanical stress by flattening into the membrane, increasing surface area to relieve tension, while confining receptors and signaling molecules (101, 102). Caveolae participate in a dynamic cycle of flattening and reassembly in response to mechanical stress independent of the actin cytoskeleton. In vascular smooth muscle cells (103), cardiomyocytes (104), and aortic ECs, translocation of Cav1 to non-caveolar membrane domains during flattening is required for strain and flow induced Erk expression (105). Rho and Rac GTPases (104), Src (106) and MAP kinases (107), and calcium (108) expression are also modulated by caveolae mechanotransduction.

Genomic analysis in canine myxomatous valve disease identified caveolar mediated endocytosis as a canonical pathway relevant to MVD (12). This pathway controls EC growth and migration through endocytosis of cholesterol-enriched membrane microdomain (CEMM) internalization when integrins are uncoupled during cell detachment from the ECM. Integrins target Rac to CEMMs where it interacts with downstream effectors to induce signaling (109, 110). In caveolin-1 knockdowns, TGF- β , fibroblast activation, and collagen gene expression increases in human lung fibroblasts (111). In canines with chordal rupture induced mitral regurgitation, caveolar invagination decreased Erk signaling, regulating hypertrophic remodeling in response to volume overload (112). Positive caveolin staining and caveolae structures have been seen on aortic VECs (113) and may be conserved in mitral valves.

GLYCOCALYX

The glycocalyx (GC) are abundant proteoglycan complexes that cover the surface of ECs and maintain endothelial barrier integrity. They are composed of the syndecan, a transmembrane core protein, and membrane anchored GAGs (114). GC control NO production (115) in vascular ECs by transducing shear stress to the cytoskeleton (116, 117) resulting in intracellular signaling and NO production (118, 119). Breakdown of the GC results in dissolution of tight junctions (120) and production of NO is dependent on calcium intake from TRP channels (121).

Syndecans (Sdcs) are members of a proteoglycan family of adhesion transmembrane receptors (122, 123). There are four mammalian Sdcs that bind to ECM, cell adhesion molecules, and growth factors (43). While no Sdcs are expressed in healthy aortic or mitral VICs (43), Sdc1 is strongly expressed on the vascular EC surface (124) and GCs are broadly expressed on the mitral endothelium in hypercholesterolemic rabbits (125). GCs and Sdcs are implicated in inflammatory (126, 127) and vascular diseases in the context of heart failure (128–130), myocardial dysfunction (131), and myocardial infarct (132). Sdc1-null mice with myocardial infarction display enhanced endothelial adhesion, trans endothelial migration of inflammatory cells, matrix remodeling, and fibrosis (133) as well as attenuated angiotensin II-induced dysfunction (134). Oxidized LDL cholesterol degrades GCs and enhances adherence of leukocytes to the endothelial surface in mouse vascular models (135). Immune involvement provides a potential avenue to MVD given the autoimmune role in rheumatic valve disease.

NUCLEAR

Many mechanosensing modalities are physically coupled to the cytoskeleton filaments which in turn link to nuclear scaffolds, chromatin, and nuclear DNA (136–138). Forces applied to the cell surface cause structural changes to the nucleus (139, 140). As such, the nuclear aspect ratio (NAR) can be used as an index of cellular deformation due to the correlating deformation and directionality of the nucleus to the cell. In the mitral valve, NAR analysis determined VICs in the fibrosa and ventricularis layers deform more than the atrialis and spongiosa (141). MVICs also display cytoplasmic uncoupling from nuclear deformation under hyper-physiological strain levels (142) which may have phenotype and ECM remodeling consequences.

Lamins, nuclear intermediate filaments, are dense protein networks capable of forming stable structures within the nucleoplasm and have a crucial role in DNA/RNA synthesis and transcription (137). Dilated cardiomyopathy (143, 144) a laminopathy, causes volume overload and functional mitral regurgitation. Lamin A/C mutant mouse cells have impaired activation of mechano-sensitive transcription factor MRTF-A which causes cardiac myofibroblastic differentiation (145, 146) and activates vinculin and actin (147). Linker Nucleoskeleton and Cytoskeleton (LINC) proteins are key mechanotransductive structures between the cytoskeleton and nucleus. They include nesprin which connects LINC to the cytoskeleton and SUN which anchors LINC in the nucleus through lamin interactions and chromatin binding proteins (148). Nesprin

is subject to actin-myosin mediated tension in adherent fibroblasts, which is reduced in fibroblasts from Hutchinson–Gilford progeria patients, a multisystem laminopathy (149). Nesprin also interacts with common intracellular signaling pathways such as Erk1/2 (67) and β catenin (150). Nesprin knockdown in ECs cripples nuclear deformation and cell orientation during cyclic strain, but increases focal adhesions (151). Nesprin knockout cells have altered morphology, polarization, and migration (152).

5-HT SEROTONIN

Multi-valve pathology (153) is seen after exposure to serotonergic drugs fenfluramine, dexfenfluramine, ergotamine, and methysergide (154) as well as ergot-derived dopamine agonists pergolide (155), cabergoline (156), and bromocriptine (157). Fenfluramine binds to serotonin or 5-hydroxytryptamine (5-HT) receptors 5-HT_{2A}, 5-HT_{2B}, and 5-HT_{2C} with porcine aortic and mitral VICs expressing 5-HT_{2A} and 5-HT_{2B} receptor transcripts, suggesting valve fibrosis (158) after exposure to fenfluramine, ergot drugs, and 5-HT is a result of 5-HT_{2A} and 5-HT_{2B} stimulation. In ligand screening studies 5-HT_{2B} is the commonly activated serotonin receptor of drugs associated with valvular heart disease (159) with myxomatous canine valves upregulating 5-HT_{2B} receptor mRNA (160) and proteins (161). The 5-HT_{2B} receptor is required for heart development (162) regulating differentiation and proliferation of cardiac tissue; 5-HT transporter deficient mice develop cardiac fibrosis, and valvulopathy (163).

5-HT_{2B} increases MVIC proliferation and ECM production through common mechano-active signaling modalities. 5-HT_{2B} receptor activation increases MAPK activity through Erk1/2 (164, 165) as well as Src family kinases (166), resulting in cell proliferation, while addition of 5-HT to canine MVIC cultures increases collagen and GAG synthesis through H-proline and H-glucosamine incorporation respectively (164). Cross-talk may occur between the TGF- β and 5-HT pathways under elevated mechanical stresses. During atrioventricular valve development in chick embryos, 5-HT induces pathological modeling effects through a TGF- β 3-dependent mechanism causing tissue stiffening, contractile gene expression, and collagen expression (167). In myxomatous mitral valves, 5-HT_{2B} receptor expression is co-localized with α SMA expression (168); neonatal rat cardiac fibroblasts treated with 5-HT upregulated α SMA expression marking fibroblast differentiation and TGF- β signaling (169). AVICs treated with 5-HT show increased TGF- β 1 and 5-HT_{2A} (170) expression while serotonin transporter (SERT) knockout embryonic mice increased expression of TGF- β 1, α SMA, and 5-HT_{2A} in the whole heart (171). At the tissue scale, treating an AVIC seeded construct with a 5-HT_{2B} agonist acutely decreases tone generation of the cells, tissue alignment, and increases the tensile modulus along the primary fiber alignment axis (172). Similar mechanisms may be at play in 5-HT-related MVD.

While 5-HT alters the MV microenvironment and global valve mechanics, it may also be a direct mechanomodulator as proposed in **Figure 3** below. In both aortic banded rats and neonatal rat cardiomyocytes, mechanical stress enhances 5-HT_{2B} signaling in ventricular models of pressure induced cardiomyopathy (173). Serotonin induced a positive inotropic response in the papillary

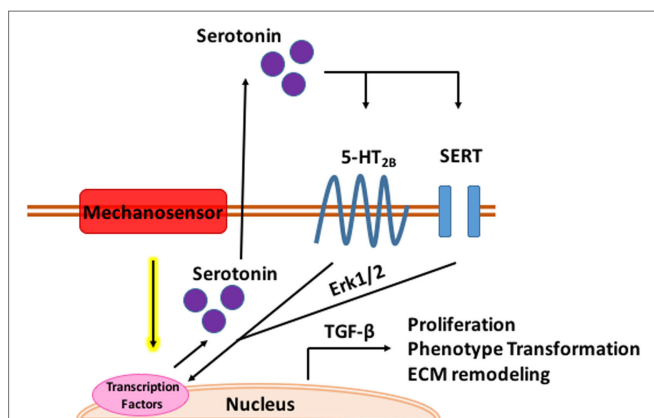


FIGURE 3 | Mechanomodulation of mitral valve disease through serotonin. Tensile strain upregulates serotonin synthesis through a mechanosensory mechanism. Serotonin interacts with the serotonin type 2B receptor and serotonin transporter (SERT) in the mitral valve activating Erk1/2 through G-protein stimulation. Erk1/2 is phosphorylated in the nucleus where it induces TGF- β signaling and transcription of genes mediating myxomatous disease.

muscles and increased 5-HT_{2B} receptor expression in hypertrophic rats with post infarction heart failure which correlated to degree of hypertrophy (174). Cyclic stretch upregulates 5-HT_{2A} and 5-HT_{2B} receptor expression in porcine aortic valve cusps causing AVIC proliferation and ECM remodeling (175). Cell proliferation, collagen synthesis, and tissue stiffness in response to cyclic stretch seem to be specifically modulated by the 5-HT_{2A} receptor in the aortic valve (176) while unstrained *in vitro* experiments in MVs implicate the 5-HT_{2B} receptor. Static and cyclic strain increase expression of myxomatous effector proteins, chondrogenic markers, and markers of the myofibroblastic phenotype compared to unstrained controls in myxomatous canine MVs (177). Interestingly, in both strain conditions, expression of serotonin synthetic enzymes increased with higher serotonin levels in the media of cyclically strained valves suggesting mitral valves are capable of local serotonin synthesis and may be mechanically modulated (177). Myofibroblastic phenotype markers, matrix catabolic enzymes, cathepsins, matrix metalloproteases, and GAGS increased with increasing cyclic strain in cultured sheep MVs with serotonin present in the media of cyclically strained valves with concentration correlating to percent strain; inhibition of serotonin reduced these strain mediated protein expression patterns (178).

INTEGRATED MECHANOTRANSDUCTION

It is likely individual methods of mechanotransduction work in concert through common signaling pathways. Multi faceted proteins such as small GTPases coupled with an integrated framework, such as the cytoskeleton, implicate a coordinated sensing and transduction network of shared, simultaneous components as illustrated in **Figure 4**.

Both RhoA and Rac GTPases mediate endothelial–mesenchymal transition during valvulogenesis (179, 180), while in adult VICs RhoA regulates actin cytoskeleton and stress fiber formation as Rac regulates cell–cell adhesion, actin polymerization, lamellae

protrusion, and cytoskeletal polarity (181). Altering the actin network geometry by overexpressing Rac1 GTPase so precursor actin bundles are suppressed at free borders, changes adherens junction shape, and increases lamellae protrusions (182, 183). RhoA signaling couples cadherin based adhesion with actinomyosin contractility (184). Rac1 and RhoA interact in a spatiotemporal manner with adherens junction proteins to coordinate opening and closing of endothelial junctions (185). FilGAP, a Rac GTPase-activating Protein, binds FlnA to control actin remodeling (186) and is present at focal adhesions but more directly present at cytoskeletal interfaces where FlnA and the β integrin cytoplasmic tail interact to form a binding pocket for opposing β strands (187, 188). FlnA is an actin binding protein widely expressed during valvulogenesis, which anchors transmembrane proteins to the cytoskeleton and mediates remodeling events in response to stimulus.

In both embryonic and adult VICs, a quiescent phenotype is maintained when they are cultured in unstrained collagen hydrogels; however, contractile expression, TGF- β , and matrix remodeling are upregulated in response to mechanical tension (55, 189). During development, this quiescent phenotype transition is governed by decreasing α SMA following decreased RhoA-GTPase expression (11, 190). Cyclic stretch of embryonic valve progenitor cells activates RhoA in acute response to the mechanical stimulus and is later switched to chronic Rac1 activation through FilGAP (191). RhoA mediates myofibroblastic activation during this acute signaling while chronic cyclic strain deactivates RhoA, enabling Rac1 to compact the matrix. Mutations in FlnA are responsible for X-linked myxomatous valve disease (192) by weakening FilGAP binding (193) and disrupting GTPase regulation (58) which alters cytoskeletal remodeling ability. Rac-1 knockdown in embryonic kidney cells abrogated PKD1-mediated signaling suggesting a critical role for small GTPases in PKD, providing insight into ciliary and voltage-gated signaling (194). In Bardet–Biedl syndrome, RhoA levels are upregulated but treatment of mutant cells with RhoA inhibitors restores cilia length and number as well as actin cytoskeleton integrity (195). In vascular SMC, 5-HT induced mitogenesis relies on Rho-mediated translocation of Erk1/2 (196) and induces Smad activation in bovine and human pulmonary artery SMCs *via* RhoA (197). 5-HT potentiates TGF- β expression in cushions which then induces contractile gene expression through RhoA (167).

The cytoskeleton provides an integrated framework for communication by physically connecting distant parts of the cell (145), rapidly transmitting mechanical information and modulating signal transduction through posttranslational modification, remodeling, and reorganization. Mechanical activation of Src 50 μ m from the point of force application in vascular smooth muscle cells takes less than 300 ms through actin stress fibers, orders of magnitude faster than reaction-diffusion signaling cascades (145, 198). Disrupting actin filaments (199) as well as relieving stress fiber prestress (200) impairs rapid long distance mechanotransduction. Association with cadherins and integrins produces a critical interface through which actin filaments are exposed to forces from the ECM. Integrins and cadherins share similar mechanotransductive mechanisms in their interactions with the actin cytoskeleton, recruitment of common adhesion components, and extensive cross-talk (200, 201). Both integrins

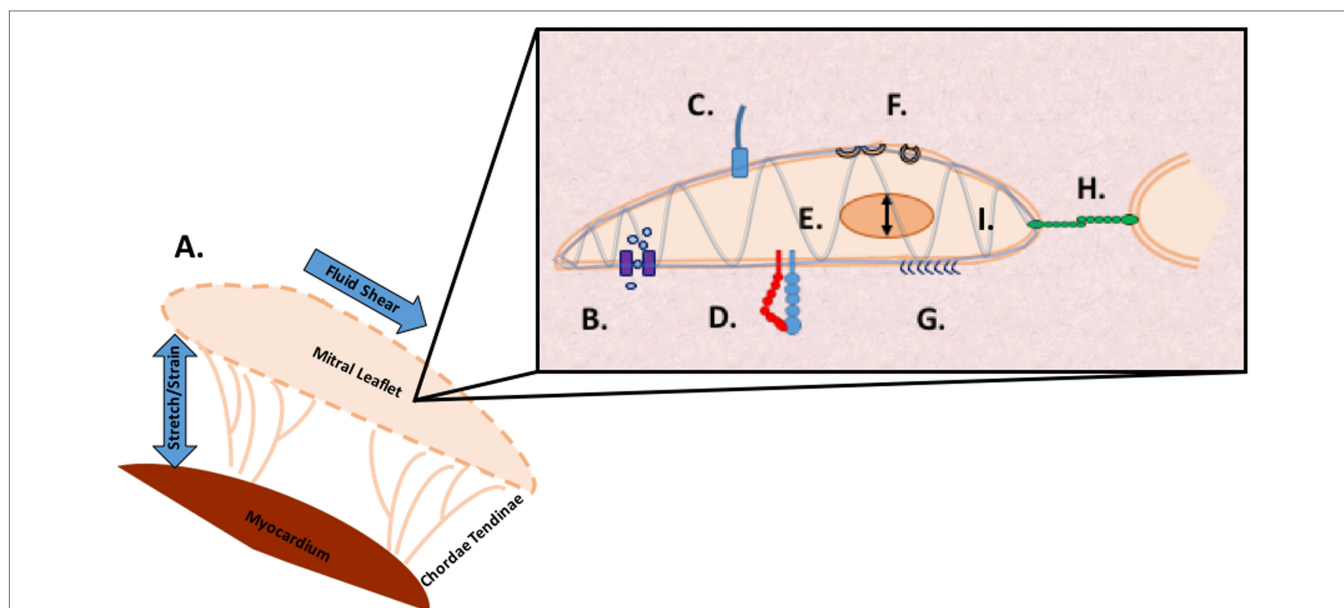


FIGURE 4 | Methods of mechanosensing in the mitral valve. A. At a global level, the valve is subjected to flexure as the valve opens, shear as the blood flows through the valve, flexure as the valve closes, and tension as the valve seals shut to prevent regurgitation. At a microscopic level, mechanotransduction converts these extracellular forces into intracellular signaling through multiple cellular apparatuses. B. Mechano-sensitive ion channels convert mechanical force exerted on the cell membrane into electrical or biochemical signals. C. The axoneme of primary cilia convert extracellular cues into various signaling pathways as well as coupling transduction with voltage-gated channels D. Integrins are the main receptors connecting the cytoskeleton to the extracellular matrix (ECM) and transmit mechanical stress across the plasma membrane E. In nuclear deformation physical force is transmitted across the nuclear envelope to the nuclear interior where they modulate gene expression from physical deformation of genetic material F. Caveolae flatten into the plasma membrane when stimulated by cell-surface tension, relieving tension and physically sequestering proteins, growth hormones, and cytokines G. The glycocalyx transmits fluid shear stress to the cell through core proteins which connect to the actin cytoskeleton and cell membrane mediating cell signaling H. Cadherins are cell adhesion proteins that create zipper like structures at cell junctions to maintain stable intercellular adhesion and mechanical coupling between cells and the adherens junction to transform mechanical to chemical signals as well as interacting with integrins through actin filaments I. Directly or indirectly, the load bearing cytoskeleton is common to the various mechanosensing modalities. Often clustering at focal adhesions, the cytoskeleton rapidly transmits ECM stimulus into cellular response through actin filament reorganization.

and cadherins stimulate Rho and Rac GTPases resulting in cytoskeleton remodeling in response to adhesion (201, 202).

The actin cytoskeleton provides structural stability to GC in ECs under shear stress (203). Depolymerizing actin weakens the anchoring strength of core proteins that support the GC such that the GC layer is ablated under shear stress; this is potentially due to altered mechanotransduction (203). Caveolae associate and align with stress fibers (204, 205) through FlnA actin binding domains. Knock down of FlnA increases the lateral movement of Cav1 and reduces stress fiber alignment of the caveolae (206). Inhibiting actin polymerization increases the abundance of caveolar rosettes and increases Cav1 (207, 208) clustering while increasing stress fiber formation decreases caveolar rosettes (209). Caveolae, specifically Cav1 interactions (210, 211), regulate RhoA-mediated actomyosin contractility (209). Cav1 and RhoA are localized to the same membrane invaginations (212), physically interacting to induce cytoskeletal reorganization in response to force (104). Like FlnA mutations, alterations to the ECM change cytoskeletal structure and function which can result in pathological signaling and remodeling. Erk activity specifically localizes to regions of matrix metalloproteinase 2 expression (213), an ECM degrading enzyme, which is significantly increased in clinical patients with floppy mitral valves and mitral valve prolapse (214). A variety of collagen mutations result in mitral valve prolapse, aortic root dilation, and a host of structural defects (215, 216).

The mitral valve exists in a complex environment where global mechanical deformation alters cell phenotype and ECM remodeling (217) in the microenvironment in a synergistic and reciprocating fashion. It is increasingly apparent that multiple mechanobiological regulatory modalities exist and are interconnected through shared components. Much like our five senses, multiple methods of mechanosensing coexist in the same cell, interacting with each other and the environment. In cells with a disrupted sense, mechanical stimulus may seem preferentially potent in one sense compared to a wild-type cell, causing pathological signaling and remodeling. The interconnected pathways and frameworks of mechanotransduction can be thought of as a network in search of homeostasis; superior treatments may seek to rebalance the network instead of focusing on a solitary gene or protein defect. Increasing our understanding of how cells interact with their environment through mechanosensing and mechanotransduction provides potential therapeutic targets in valve disease by altering the environment, cellular perception of the environment, or communication with the environment in a profound and regenerative manner.

AUTHOR CONTRIBUTIONS

JB suggested the subject of the review, recommended resources, direction of the review, suggested types of figures to include,

and provided extensive editing. LP is a Ph.D. candidate in JB's group and based on the recommendations of JB did an extensive literature review, drafted the article, created figures, and charted the direction and subject matter contained in the review.

REFERENCES

- Go A, Mozaffarian D, Roger V, Benjamin E, Berry J, Borden W, et al. Heart disease and stroke statistics – 2013 update: a report from the American Heart Association. *Circulation* (2012) 127(1):e6–245. doi:10.1161/CIR.0b013e31828124ad
- Chehab G, El-Rassi I, Chokor I, Hammoud C, Saliba Z. Epidemiology of mitral valve disease in pediatrics: a Lebanese study. *J Med Liban* (2011) 59(4):197–201.
- Fung Y. *Biomechanics*. 3rd ed. New York: Springer (2011).
- Sacks MS. Biaxial mechanical evaluation of planar biological materials. *J Elast* (2000) 61:199–246. doi:10.1023/A:1010917028671
- Wang J, Thampatty B. An introductory review of cell mechanobiology. *Biomech Model Mechanobiol* (2006) 5(1):1–16. doi:10.1007/s10237-005-0012-z
- Wang N, Butler J, Ingber D. Mechanotransduction across the cell surface and through the cytoskeleton. *Science* (1993) 260(5111):1124–7. doi:10.1126/science.7684161
- Tarkowski A, Wroblewska J. Development of blastomeres of mouse eggs isolated at the 4- and 8-cell stage. *J Embryol Exp Morphol* (1968) 18(1):155–80.
- Hillman N, Sherman M, Graham C. The effect of spatial arrangement on cell determination during mouse development. *J Embryol Exp Morphol* (1972) 28(2):263–78.
- Hove J, Köster R, Forouhar A, Acevedo-Bolton G, Fraser S, Gharib M. Intracardiac fluid forces are an essential epigenetic factor for embryonic cardiogenesis. *Nature* (2003) 421(6919):172–7. doi:10.1038/nature01282
- Beis D, Bartman T, Jin SW, Scott IC, D'Amico LA, Ober EA, et al. Genetic and cellular analyses of zebrafish atrioventricular cushion and valve development. *Development* (2005) 132(18):4193–204. doi:10.1242/dev.01970
- Nakajima Y, Mironov V, Yamagishi T, Nakamura H, Markwald R. Expression of smooth muscle alpha-actin in mesenchymal cells during formation of avian endocardial cushion tissue: a role for transforming growth factor β 3. *Dev Dyn* (1997) 209(3):296–309. doi:10.1002/(SICI)1097-0177(199707)209:3<296::AID-AJA5>3.0.CO;2-D
- Butcher J, McQuinn T, Sedmera D, Turner D, Markwald R. Transitions in early embryonic atrioventricular valvular function correspond with changes in cushion biomechanics that are predictable by tissue composition. *Circ Res* (2007) 100(10):1503–11. doi:10.1161/CIRCRESAHA.107.148684
- Butcher J, Norris R, Hoffman S, Mjaatvedt C, Markwald R. Periostin promotes atrioventricular mesenchyme matrix invasion and remodeling mediated by integrin signaling through Rho/PI 3-kinase. *Dev Biol* (2007) 302(1):256–66. doi:10.1016/j.ydbio.2006.09.048
- Kapacee Z, Richardson S, Lu Y, Starborg T, Holmes D, Baar K, et al. Tension is required for fibripositor formation. *Matrix Biol* (2008) 27(4):371–5. doi:10.1016/j.matbio.2007.11.006
- Vermot J, Forouhar A, Liebling M, Wu D, Plummer D, Gharib M, et al. Reversing blood flows act through *klf2a* to ensure normal valvulogenesis in the developing heart. *PLoS Biol* (2009) 7(11):e1000246. doi:10.1371/journal.pbio.1000246
- Freund J, Vermot J. The wall-stress footprint of blood cells flowing in microvessels. *Biophys J* (2014) 106(3):752–62. doi:10.1016/j.bpj.2013.12.020
- Kalogirou S, Malissovass N, Moro E, Argenton F, Stainier D, Beis D. Intracardiac flow dynamics regulate atrioventricular valve morphogenesis. *Cardiovasc Res* (2014) 104(1):49–60. doi:10.1093/cvr/cvu186
- Bartman T, Walsh E, Wen K, McKane M, Ren J, Alexander J, et al. Early myocardial function affects endocardial cushion development in zebrafish. *PLoS Biol* (2004) 2(5):E129. doi:10.1371/journal.pbio.0020129
- Clouthier D, Harris C, Harris R, Martin C, Puri M, Jones N. Requisite role for Nck adaptors in cardiovascular development, endothelial-to-mesenchymal transition, and directed cell migration. *Mol Cell Biol* (2015) 35(9):1573–87. doi:10.1128/MCB.00072-15
- Johnson B, Bark D, Van Herck I, Garrity D, Dasi L. Altered mechanical state in the embryonic heart results in time-dependent decreases in cardiac function. *Biomech Model Mechanobiol* (2015) 14(6):1379–89. doi:10.1007/s10237-015-0681-1
- Balachandran K, Alford P, Wylie-Sears J, Goss J, Grosberg A, Bischoff J, et al. Cyclic strain induces dual-mode endothelial-mesenchymal transformation of the cardiac valve. *Proc Natl Acad Sci U S A* (2011) 108(50):19943–8. doi:10.1073/pnas.1106954108
- Maleki S, Kjellqvist S, Paloschi V, Magné J, Branca R, Du L, et al. Mesenchymal state of intimal cells may explain higher propensity to ascending aortic aneurysm in bicuspid aortic valves. *Sci Rep* (2016) 6(1):35712. doi:10.1038/srep35712
- Mui K, Chen C, Assoian R. The mechanical regulation of integrin-cadherin crosstalk organizes cells, signaling and forces. *J Cell Sci* (2016) 129(6):1093–100. doi:10.1242/jcs.183699
- Case L, Baird M, Shtengel G, Campbell S, Hess H, Davidson M, et al. Molecular mechanism of vinculin activation and nanoscale spatial organization in focal adhesions. *Nat Cell Biol* (2015) 17(7):880–92. doi:10.1038/ncb3180
- Humphries J, Wang P, Streuli C, Geiger B, Humphries M, Ballestrem C. Vinculin controls focal adhesion formation by direct interactions with talin and actin. *J Cell Biol* (2007) 179(5):1043–57. doi:10.1083/jcb.200703036
- Sheetz M, Dai J. Modulation of membrane dynamics and cell motility by membrane tension. *Trends Cell Biol* (1996) 6(3):85–9. doi:10.1016/0962-8924(96)80993-7
- Xu S, Liu A, Kim H, Gotlieb A. Cell density regulates in vitro activation of heart valve interstitial cells. *Cardiovasc Pathol* (2012) 21(2):65–73. doi:10.1016/j.carpath.2011.01.004
- Hutcheson J, Chen J, Sewell-Loftin M, Ryzhova L, Fisher C, Su Y, et al. Cadherin-11 regulates cell-cell tension necessary for calcific nodule formation by valvular myofibroblasts. *Arterioscler Thromb Vasc Biol* (2012) 33(1):114–20. doi:10.1161/ATVBAHA.112.300278
- Chen J, Ryzhova L, Sewell-Loftin M, Brown C, Huppert S, Baldwin H, et al. Notch1 mutation leads to valvular calcification through enhanced myofibroblast mechanotransduction. *Arterioscler Thromb Vasc Biol* (2015) 35(7):1597–605. doi:10.1161/ATVBAHA.114.305095
- Lu C, Liu M, Culshaw G, Clinton M, Argyle D, Corcoran B. Gene network and canonical pathway analysis in canine myxomatous mitral valve disease: a microarray study. *Vet J* (2015) 204(1):23–31. doi:10.1016/j.tvjl.2015.02.021
- Armstrong E, Bischoff J. Heart valve development: endothelial cell signaling and differentiation. *Circ Res* (2004) 95(5):459–70. doi:10.1161/01.RES.0000141146.95728.da
- Rizzo S, Basso C, Lazzarini E, Celeghin R, Paolin A, Gerosa G, et al. TGF-beta1 pathway activation and adherens junction molecular pattern in nonsyndromic mitral valve prolapse. *Cardiovasc Pathol* (2015) 24(6):359–67. doi:10.1016/j.carpath.2015.07.009
- Zhou J, Bowen C, Lu G, Knapp C III, Recknagel A, Norris R, et al. Cadherin-11 expression patterns in heart valves associate with key functions during embryonic cushion formation, valve maturation and calcification. *Cells Tissues Organs* (2013) 198(4):300–10. doi:10.1159/000356762
- Sung D, Bowen C, Vaidya K, Zhou J, Chapurin N, Recknagel A, et al. Cadherin-11 overexpression induces extracellular matrix remodeling and calcification in mature aortic ValvesHighlights. *Arterioscler Thromb Vasc Biol* (2016) 36(8):1627–37. doi:10.1161/ATVBAHA.116.307812
- Hynes RO. Integrins: bidirectional, allosteric signaling machines. *Cell* (2002) 110:673–87.
- Luo B, Carman C, Springer T. Structural basis of integrin regulation and signaling. *Annu Rev Immunol* (2007) 25(1):619–47. doi:10.1146/annurev.immunol.25.022106.141618

FUNDING

This work was supported by funding from the National Institutes of Health (HL110328 and HL128745) and the National Science Foundation (DGE-1650441).

37. Van der Flier A, Sonnenberg A. Function and interactions of integrins. *Cell Tissue Res* (2001) 305(3):285–98. doi:10.1007/s004410100417
38. Calderwood DA, Yan B, de Pereda JM, Alvarez BG, Fujioka Y, Liddington RC, et al. The phosphotyrosine binding-like domain of talin activates integrins. *J Biol Chem* (2002) 277(24):21749–58. doi:10.1074/jbc.M111996200
39. Schwartz M. Integrin signaling revisited. *Trends Cell Biol* (2001) 11(12):466–70. doi:10.1016/S0962-8924(01)02152-3
40. Wipff B, Hinz B. Integrins and the activation of latent transforming growth factor β 1 – an intimate relationship. *Eur J Cell Biol* (2008) 87(8–9):601–15. doi:10.1016/j.ejcb.2008.01.012
41. Plow E, Haas T, Zhang L, Loftus J, Smith J. Ligand binding to integrins. *J Biol Chem* (2000) 275(29):21785–8. doi:10.1074/jbc.R000003200
42. Midwood K, Schwarzbauer J. Elastic fibers: building bridges between cells and their matrix. *Curr Biol* (2002) 12(8):R279–81. doi:10.1016/S0960-9822(02)00800-X
43. Latif N, Sarathchandra P, Taylor P, Antoniow J, Yacoub M. Molecules mediating cell-ECM and cell-cell communication in human heart valves. *Cell Biochem Biophys* (2005) 43(2):275–88. doi:10.1385/CBB:43:2:275
44. Danen E, Sonnenberg A. Integrins in regulation of tissue development and function. *J Pathol* (2003) 200(4):471–80. doi:10.1002/path.1416
45. Wu Y, Jane Grande-Allen K, West J. Adhesive peptide sequences regulate valve interstitial cell adhesion, phenotype and extracellular matrix deposition. *Cell Mol Bioeng* (2016) 9(4):479–95. doi:10.1007/s12195-016-0451-x
46. Stephens E, Durst C, Swanson J, Grande-Allen K, Ingels N, Miller D. Functional coupling of valvular interstitial cells and collagen via α 2 β 1 integrins in the mitral leaflet. *Cell Mol Bioeng* (2010) 3(4):428–37. doi:10.1007/s12195-010-0139-6
47. Gu X, Masters K. Regulation of valvular interstitial cell calcification by adhesive peptide sequences. *J Biomed Mater Res A* (2010) 93(4):1620–30. doi:10.1002/jbm.a.32660
48. McCartney-Francis N, Frazier-Jessen M, Wahl S. TGF- β : a balancing act. *Int Rev Immunol* (1998) 16(5–6):553–80. doi:10.3109/08830189809043009
49. Massagué J. TGF- β signal transduction. *Annu Rev Biochem* (1998) 67(1):753–91. doi:10.1146/annurev.biochem.67.1.753
50. Munger J, Sheppard D. Cross talk among TGF-signaling pathways, integrins, and the extracellular matrix. *Cold Spring Harb Perspect Biol* (2011) 3(11):a005017–005017. doi:10.1101/cshperspect.a005017
51. Hinz B, Celetta G, Tomasek J, Gabbiani G, Chaponnier C. Alpha-smooth muscle actin expression upregulates fibroblast contractile activity. *Mol Biol Cell* (2001) 12(9):2730–41. doi:10.1091/mbc.12.9.2730
52. Klingberg F, Chow M, Koehler A, Boo S, Buscemi L, Quinn T, et al. Prestress in the extracellular matrix sensitizes latent TGF- β 1 for activation. *J Cell Biol* (2014) 207(2):283–97. doi:10.1083/jcb.201402006
53. Tomasek J, Gabbiani G, Hinz B, Chaponnier C, Brown R. Myofibroblasts and mechano-regulation of connective tissue remodelling. *Nat Rev Mol Cell Biol* (2002) 3(5):349–63. doi:10.1038/nrm809
54. Ng C, Hinz B, Swartz MA. Interstitial fluid flow induces myofibroblast differentiation and collagen alignment in vitro. *J Cell Sci* (2005) 118(20):4731–9. doi:10.1242/jcs.02605
55. Gould R, Chin K, Santisakultarm T, Dropkin A, Richards J, Schaffer C, et al. Cyclic strain anisotropy regulates valvular interstitial cell phenotype and tissue remodeling in three-dimensional culture. *Acta Biomater* (2012) 8(5):1710–9. doi:10.1016/j.actbio.2012.01.006
56. Sakai L, Keene D, Renard M, De Backer J. FBN1: the disease-causing gene for Marfan syndrome and other genetic disorders. *Gene* (2016) 591(1):279–91. doi:10.1016/j.gene.2016.07.033
57. Alberts J, van Tintelen J, Oomen T, Bergman J, Halley D, Jongbloed J, et al. Screening of TGFBR1, TGFBR2, and FLNA in familial mitral valve prolapse. *Am J Med Gen A* (2013) 164(1):113–9. doi:10.1002/ajmg.a.36211
58. Duval D, Lardeux A, Le Tourneau T, Norris R, Markwald R, Sauzeau V, et al. Valvular dystrophy associated filamin A mutations reveal a new role of its first repeats in small-GTPase regulation. *Biochim Biophys Acta* (2014) 1843(2):234–44. doi:10.1016/j.bbamcr.2013.10.022
59. Holm T, Habashi J, Doyle J, Bedja D, Chen Y, van Erp C, et al. Noncanonical TGF signaling contributes to aortic aneurysm progression in Marfan syndrome mice. *Science* (2011) 332(6027):358–61. doi:10.1126/science.1192149
60. Angel P, Narmoneva D, Sewell-Loftin M, Munjal C, Dupuis L, Landis B, et al. Proteomic alterations associated with biomechanical dysfunction are early processes in the Emilin1 deficient mouse model of aortic valve disease. *Ann Biomed Eng* (2017) 45(11):2548–62. doi:10.1007/s10439-017-1899-0
61. Clement C, Ajbrou K, Koefoed K, Vestergaard M, Veland I, Henriques de Jesus M, et al. TGF- β signaling is associated with endocytosis at the pocket region of the primary cilium. *Cell Rep* (2013) 3(6):1806–14. doi:10.1016/j.celrep.2013.05.020
62. Delling M, DeCaen P, Doerner J, Febvay S, Clapham D. Primary cilia are specialized calcium signalling organelles. *Nature* (2013) 504(7479):311–4. doi:10.1038/nature12833
63. Jin X, Muntean B, Aal-Aaboda M, Duan Q, Zhou J, Nauli S. L-type calcium channel modulates cystic kidney phenotype. *Biochim Biophys Acta* (2014) 1842(9):1518–26. doi:10.1016/j.bbadis.2014.06.001
64. Hoffmann A, Peterson M, Friedland-Little J, Anderson S, Moskowitz I. Sonic hedgehog is required in pulmonary endoderm for atrial septation. *Development* (2009) 136(10):1761–70. doi:10.1242/dev.034157
65. Hoffmann A, Yang X, Burnicka-Turek O, Bosman J, Ren X, Steimle J, et al. Foxf genes integrate Tbx5 and Hedgehog pathways in the second heart field for cardiac septation. *PLoS Genet* (2014) 10(10):e1004604. doi:10.1371/journal.pgen.1004604
66. Li Y, Klena N, Gabriel G, Liu X, Kim A, Lemke K, et al. Global genetic analysis in mice unveils central role for cilia in congenital heart disease. *Nature* (2015) 521(7553):520–4. doi:10.1038/nature14269
67. Toomer K, Fulmer D, Guo L, Drohan A, Peterson N, Swanson P, et al. A role for primary cilia in aortic valve development and disease. *Dev Dyn* (2017) 246(8):625–34. doi:10.1002/dvdy.24524
68. Sánchez-Duffhues G, de Vinuesa A, Lindeman J, Mulder-Stapel A, DeRuiter M, Van Munsteren C, et al. SLUG is expressed in endothelial cells lacking primary cilia to promote cellular calcification. *Arterioscler Thromb Vasc Biol* (2015) 35(3):616–27. doi:10.1161/ATVBAHA.115.305268
69. Dinsmore C, Reiter J. Endothelial primary cilia inhibit atherosclerosis. *EMBO Rep* (2016) 17(2):156–66. doi:10.15252/embr.201541019
70. Willaredt M, Gorgas K, Gardner H, Tucker K. Multiple essential roles for primary cilia in heart development. *Cilia* (2012) 1(1):23. doi:10.1186/2046-2530-1-23
71. Kathem SH, Mohieldin AM, Nauli SM. The roles of primary cilia in polycystic kidney disease. *AIMS Mol Sci* (2013) 1(1):27–46. doi:10.3934/molsci.2013.1.27
72. Sessa A, Righetti M, Battini G. Autosomal recessive and dominant polycystic kidney diseases. *Minerva Urol Nefrol* (2004) 56(4):329–38.
73. Lumiaho A, Ikäheimo R, Miettinen R, Niemitukia L, Laitinen T, Rantala A, et al. Mitral valve prolapse and mitral regurgitation are common in patients with polycystic kidney disease type 1. *Am J Kidney Dis* (2001) 38(6):1208–16. doi:10.1053/ajkd.2001.29216
74. Tory K, Rousset-Rouvière C, Gubler M, Morinière V, Pawtowski A, Becker C, et al. Mutations of NPHP2 and NPHP3 in infantile nephronophthisis. *Kidney Int* (2009) 75(8):839–47. doi:10.1038/ki.2008.662
75. Hills C, Kochilas L, Schimmenti L, Moller J. Ellis-van Creveld syndrome and congenital heart defects: presentation of an additional 32 cases. *Pediatr Cardiol* (2011) 32(7):977–82. doi:10.1007/s00246-011-0006-9
76. O'Connor M, Rider N, Thomas Collins R, Hanna B, Holmes Morton D, Strauss K. Contemporary management of congenital malformations of the heart in infants with Ellis-van Creveld syndrome: a report of nine cases. *Cardiol Young* (2010) 21(02):145–52. doi:10.1017/S1047951110001587
77. Thiam M, Gning S, Faye M, Fall P, Mbaye A, Charpentier P. Kartagener's syndrome: a case report. *Dakar Med* (2002) 47(1):100–2.
78. Kim S, Sir J, Lee B, Kwak C, Kim S, Cho W, et al. Severe mitral regurgitation in a young female with pansinusitis and bronchiectasis. *Respir Med CME* (2008) 1(2):185–7. doi:10.1016/j.rjmedc.2008.04.007
79. Purkait R, Roy B, Samanta T, Mallick A, Sinhamahapatra T. Rheumatic valvular insufficiency in Bardet-Biedl syndrome: a case report. *J Indian Med Assoc* (2012) 110(9):651–2.
80. Baumgarten CM. Origin of mechanotransduction: stretch-activated ion channels. *Madame Curie Bioscience Database*. Austin, TX: Landes Bioscience (2000).
81. Kung C. A possible unifying principle for mechanosensation. *Nature* (2005) 436(7051):647–54. doi:10.1038/nature03896
82. Barakat A, Lieu D, Gojova A. Secrets of the code: do vascular endothelial cells use ion channels to decipher complex flow signals? *Biomaterials* (2006) 27(5):671–8. doi:10.1016/j.biomaterials.2005.07.036

83. Ohno M, Cooke J, Dzau V, Gibbons G. Fluid shear stress induces endothelial transforming growth factor beta-1 transcription and production. Modulation by potassium channel blockade. *J Clin Invest* (1995) 95(3):1363–9. doi:10.1172/JCI117787
84. Malek A, Izumo S. Molecular aspects of signal transduction of shear stress in the endothelial cell. *J Hypertens* (1994) 12(9):989–1000. doi:10.1097/00004872-199409000-00001
85. Goetz J, Steed E, Ferreira R, Roth S, Ramsbacher C, Boselli F, et al. Endothelial cilia mediate low flow sensing during zebrafish vascular development. *Cell Rep* (2014) 6(5):799–808. doi:10.1016/j.celrep.2014.01.032
86. Warren D, Tajsic T, Porter L, Minisah R, Cobb A, Jacob A, et al. Nesprin-2-dependent ERK1/2 compartmentalisation regulates the DNA damage response in vascular smooth muscle cell ageing. *Cell Death Differ* (2015) 22(9):1540–50. doi:10.1038/cdd.2015.12
87. Coste B, Mathur J, Schmidt M, Earley T, Ranade S, Petrus M, et al. Piezo1 and Piezo2 are essential components of distinct mechanically activated cation channels. *Science* (2010) 330(6000):55–60. doi:10.1126/science.1193270
88. Ranade S, Qiu Z, Woo S, Hur S, Murthy S, Cahalan S, et al. Piezo1, a mechanically activated ion channel, is required for vascular development in mice. *Proc Natl Acad Sci U S A* (2014) 111(28):10347–52. doi:10.1073/pnas.1409233111
89. Li J, Hou B, Tumova S, Muraki K, Bruns A, Ludlow M, et al. Piezo1 integration of vascular architecture with physiological force. *Nature* (2014) 515(7526):279–82. doi:10.1038/nature13701
90. Peyronnet R, Nerbonne J, Kohl P. Cardiac mechano-gated ion channels and arrhythmias. *Circ Res* (2016) 118(2):311–29. doi:10.1161/CIRCRESAHA.115.305043
91. Köhler R, Distler A, Hoyer J. Increased mechanosensitive currents in aortic endothelial cells from genetically hypertensive rats. *J Hypertens* (1999) 17(3):365–71. doi:10.1097/00004872-199917030-00009
92. Grieben M, Pike A, Shintre C, Venturi E, El-Ajouz S, Tessitore A, et al. Structure of the polycystic kidney disease TRP channel polycystin-2 (PC2). *Nat Struct Mol Biol* (2016) 24(2):114–22. doi:10.1038/nsmb.3343
93. Pennekamp P, Karcher C, Fischer A, Schweickert A, Skryabin B, Horst J, et al. The ion channel polycystin-2 is required for left-right axis determination in mice. *Curr Biol* (2002) 12(11):938–43. doi:10.1016/S0960-9822(02)00869-2
94. AbouAlaiwi W, Takahashi M, Mell B, Jones T, Ratnam S, Kolb R, et al. Ciliary polycystin-2 is a mechanosensitive calcium channel involved in nitric oxide signaling cascades. *Circ Res* (2009) 104(7):860–9. doi:10.1161/CIRCRESAHA.108.192765
95. DeCaen P, Liu X, Abiria S, Clapham D. Atypical calcium regulation of the PKD2-L1 polycystin ion channel. *Elife* (2016) 5:e13413. doi:10.7554/eLife.13413
96. Piori S. Task force on sudden cardiac death of the European Society of Cardiology. *Eur Heart J* (2001) 22(16):1374–450. doi:10.1053/euhj.2001.2824
97. Missov E, Cogswell R. Sudden cardiac death, mitral valve prolapse, and long QT syndrome. *Am J Med* (2015) 128:e37–8. doi:10.1016/j.amjmed.2015.05.030
98. Haas J, Frese K, Peil B, Kloos W, Keller A, Nietsch R, et al. Atlas of the clinical genetics of human dilated cardiomyopathy. *Eur Heart J* (2014) 36(18):1123–35. doi:10.1093/eurheartj/ehu301
99. Heckel E, Boselli F, Roth S, Krudewig A, Belting HG, Charvin G, et al. Oscillatory flow modulates mechanosensitive *klf2a* expression through *trpv4* and *trpp2* during heart valve development. *Curr Biol* (2015) 25:1354–61. doi:10.1016/j.cub.2015.03.038
100. Renz M, Otten C, Faurobert E, Rudolph F, Zhu Y, Boulday G, et al. Regulation of $\beta 1$ integrin-Klf2-mediated angiogenesis by CCM proteins. *Dev Cell* (2015) 32(2):181–90. doi:10.1016/j.devcel.2014.12.016
101. Simons K, Toomre D. Lipid rafts and signal transduction. *Nat Rev Mol Cell Biol* (2000) 1:31–9. doi:10.1038/35036052
102. Patel H, Murray F, Insel P. Caveolae as organizers of pharmacologically relevant signal transduction molecules. *Annu Rev Pharmacol Toxicol* (2008) 48(1):359–91. doi:10.1146/annurev.pharmtox.48.121506.124841
103. Boyd N, Park H, Yi H, Boo Y, Sorescu G, Sykes M, et al. Chronic shear induces caveolae formation and alters ERK and Akt responses in endothelial cells. *Am J Physiol Heart Circ Physiol* (2003) 285(3):H1113–22. doi:10.1152/ajpheart.00302.2003
104. Kawamura S, Miyamoto S, Brown J. Initiation and transduction of stretch-induced RhoA and Rac1 activation through caveolae. *J Biol Chem* (2003) 278(33):31111–7. doi:10.1074/jbc.M300725200
105. Kawabe J, Okumura S, Lee MC, Sadoshima J, Ishikawa Y. Translocation of caveolin regulates stretch-induced ERK activity in vascular smooth muscle cells. *Am J Physiol Heart Circ Physiol* (2004) 286(5):H1845–52. doi:10.1152/ajpheart.00593.2003
106. Sawada Y, Tamada M, Dubin-Thaler B, Cherniavskaya O, Sakai R, Tanaka S, et al. Force sensing by mechanical extension of the Src family kinase substrate p130Cas. *Cell* (2006) 127(5):1015–26. doi:10.1016/j.cell.2006.09.044
107. Furuchi T, Anderson R. Cholesterol depletion of caveolae causes hyperactivation of extracellular signal-related kinase (ERK). *J Biol Chem* (1998) 273(33):21099–104. doi:10.1074/jbc.273.33.21099
108. Ishiki M, Anderson R. Function of caveolae in Ca²⁺ entry and Ca²⁺-dependent signal transduction. *Traffic* (2003) 4(11):717–23. doi:10.1034/j.1600-0854.2003.00130.x
109. Del Pozo M, Kiosses W, Alderson N, Meller N, Hahn K, Schwartz M. Integrins regulate GTP-Rac localized effector interactions through dissociation of Rho-GDI. *Nat Cell Biol* (2002) 4(3):232–9. doi:10.1038/ncb759
110. Del Pozo M, Price LS, Alderson NB, Ren XD, Schwartz MA. Adhesion to the extracellular matrix regulates the coupling of the small GTPase Rac to its effector PAK. *EMBO J* (2000) 19(9):2008–14. doi:10.1093/emboj/19.9.2008
111. Del Galdo F, Lisanti M, Jimenez S. Caveolin-1, transforming growth factor- β receptor internalization, and the pathogenesis of systemic sclerosis. *Curr Opin Rheumatol* (2008) 20(6):713–9. doi:10.1097/BOR.0b013e3283103d27
112. Liu Y, Dillon A, Tillson M, Makarewich C, Nguyen V, Dell'Italia L, et al. Volume overload induces differential spatiotemporal regulation of myocardial soluble guanylyl cyclase in eccentric hypertrophy and heart failure. *J Mol Cell Cardiol* (2013) 60:72–83. doi:10.1016/j.yjmcc.2013.03.019
113. Rajamannan N, Springett M, Pederson L, Carmichael S. Localization of caveolin 1 in aortic valve endothelial cells using antigen retrieval. *J Histochem Cytochem* (2002) 50(5):617–27. doi:10.1177/002215540205000503
114. Kim Y, Nijst P, Kiefer K, Tang W. Endothelial glycocalyx as biomarker for cardiovascular diseases: mechanistic and clinical implications. *Curr Heart Fail Rep* (2017) 14(2):117–26. doi:10.1007/s11897-017-0320-5
115. Bartosch A, Mathews R, Tarbell J. Endothelial glycocalyx-mediated nitric oxide production in response to selective AFM pulling. *Biophys J* (2017) 113(1):101–8. doi:10.1016/j.bpj.2017.05.033
116. Siegel G, Malmsten M, Ermilov E. Anionic biopolyelectrolytes of the syndecan/perlecan superfamily: physicochemical properties and medical significance. *Adv Colloid Interface Sci* (2014) 205:275–318. doi:10.1016/j.cis.2014.01.009
117. Korte S, Wiesinger A, Straeter A, Peters W, Oberleithner H, Kusche-Vihrog K. Firewall function of the endothelial glycocalyx in the regulation of sodium homeostasis. *Pflugers Arch* (2011) 463(2):269–78. doi:10.1007/s00424-011-1038-y
118. Weinbaum S, Zhang X, Han Y, Vink H, Cowin S. Mechanotransduction and flow across the endothelial glycocalyx. *Proc Natl Acad Sci U S A* (2003) 100(13):7988–95. doi:10.1073/pnas.1332808100
119. Florian J, Kosky JR, Ainslie K, Pang Z, Dull RO, Tarbell JM. Heparan sulfate proteoglycan is a mechanosensor on endothelial cells. *Circ Res* (2003) 93(10):e136–42. doi:10.1161/01.RES.0000101744.47866.D5
120. Radeva MY, Waschke J. Mind the gap: mechanisms regulating the endothelial barrier. *Acta Physiol* (2017). doi:10.1111/apha.12860
121. Dragovich M, Chester D, Zhang X. Mechanotransduction of the endothelial glycocalyx mediates nitric oxide production through activation of TRP channels. *Biophys J* (2016) 110(3):23a. doi:10.1152/ajpcell.00288.2015
122. Carey D. Syndecans: multifunctional cell-surface co-receptors. *Biochem J* (1997) 327(1):1–16. doi:10.1042/bj3270001
123. Tumova S, Woods A, Couchman J. Heparan sulfate proteoglycans on the cell surface: versatile coordinators of cellular functions. *Int J Biochem Cell Biol* (2000) 32(3):269–88. doi:10.1016/S1357-2725(99)00116-8
124. Becker B, Jacob M, Leipert S, Salmon A, Chappell D. Degradation of the endothelial glycocalyx in clinical settings: searching for the sheddases. *Br J Clin Pharmacol* (2015) 80(3):389–402. doi:10.1111/bcp.12629
125. Sarphie T. A cytochemical study of the surface properties of aortic and mitral valve endothelium from hypercholesterolemic rabbits. *Exp Mol Pathol* (1986) 44(3):281–96. doi:10.1016/0014-4800(86)90042-0

126. Chignalia A, Yetimakman F, Christiaans S, Unal S, Bayrakci B, Wagener B, et al. The glycocalyx and trauma. *Shock* (2016) 45(4):338–48. doi:10.1097/SHK.0000000000000513
127. Johansson P, Stensballe J, Rasmussen L, Ostrowski S. A high admission syndecan-1 level, a marker of endothelial glycocalyx degradation, is associated with inflammation, protein C depletion, fibrinolysis, and increased mortality in trauma patients. *Ann Surg* (2011) 254(2):194–200. doi:10.1097/SLA.0b013e318226113d
128. Bielecka-Dabrowa A, Gluba-Brzózka A, Michalska-Kasiczak M, Misztal M, Rysz J, Banach M. The multi-biomarker approach for heart failure in patients with hypertension. *Int J Mol Sci* (2015) 16(5):10715–33. doi:10.3390/ijms160510715
129. Tromp J, van der Pol A, Klip I, de Boer R, Jaarsma T, van Gilst W, et al. Fibrosis marker syndecan-1 and outcome in patients with heart failure with reduced and preserved ejection fraction. *Circ Heart Fail* (2014) 7(3):457–62. doi:10.1161/CIRCHEARTFAILURE.113.000846
130. Meyer S, van der Meer P, van Deursen V, Jaarsma T, van Veldhuisen D, van der Wal M, et al. Neurohormonal and clinical sex differences in heart failure. *Eur Heart J* (2013) 34(32):2538–47. doi:10.1093/eurheartj/eh1152
131. Bielecka-Dabrowa A, Michalska-Kasiczak M, Gluba A, Ahmed A, Gerds E, von Haehling S, et al. Biomarkers and echocardiographic predictors of myocardial dysfunction in patients with hypertension. *Sci Rep* (2015) 5(1):8916. doi:10.1038/srep08916
132. Ostrowski S, Pedersen S, Jensen J, Mogelvang R, Johansson P. Acute myocardial infarction is associated with endothelial glycocalyx and cell damage and a parallel increase in circulating catecholamines. *Crit Care* (2013) 17(1):R32. doi:10.1186/cc12532
133. Vanhoutte D, Schellings M, Gotte M, Swinnen M, Herias V, Wild M, et al. Increased expression of syndecan-1 protects against cardiac dilatation and dysfunction after myocardial infarction. *Circulation* (2007) 115(4):475–82. doi:10.1161/CIRCULATIONAHA.106.644609
134. Schellings M, Vanhoutte D, van Almen G, Swinnen M, Leenders J, Kubben N, et al. Syndecan-1 amplifies angiotensin II-induced cardiac fibrosis. *Hypertension* (2010) 55(2):249–56. doi:10.1161/HYPERTENSIONAHA.109.137885
135. Constantinescu A, Vink H, Spaan JA. Endothelial cell glycocalyx modulates immobilization of leukocytes at the endothelial surface. *Arterioscler Thromb Vasc Biol* (2003) 23(9):1541–7. doi:10.1161/01.ATV.0000085630.24353.3D
136. Ingber D. The riddle of morphogenesis: a question of solution chemistry or molecular cell engineering? *Cell* (1993) 75(7):1249–52. doi:10.1016/0092-8674(93)90612-T
137. Mattout-Drubezki A, Gruenbaum Y. Dynamic interactions of nuclear lamina proteins with chromatin and transcriptional machinery. *Cell Mol Life Sci* (2003) 60(10):2053–63. doi:10.1007/s00018-003-3038-3
138. Booth-Gauthier E, Alcoser T, Yang G, Dahl K. Force-induced changes in subnuclear movement and rheology. *Biophys J* (2012) 103(12):2423–31. doi:10.1016/j.bpj.2012.10.039
139. Fey E, Wan KM, Penman S. Epithelial cytoskeletal framework and nuclear matrix-intermediate filament scaffold: three-dimensional organization and protein composition. *J Cell Biol* (1984) 98(6):1973–84. doi:10.1083/jcb.98.6.1973
140. Maniotis A, Chen C, Ingber D. Demonstration of mechanical connections between integrins, cytoskeletal filaments, and nucleoplasm that stabilize nuclear structure. *Proc Natl Acad Sci U S A* (1997) 94(3):849–54. doi:10.1073/pnas.94.3.849
141. Lee C, Carruthers C, Ayoub S, Gorman R, Gorman J, Sacks M. Quantification and simulation of layer-specific mitral valve interstitial cells deformation under physiological loading. *J Theor Biol* (2015) 373:26–39. doi:10.1016/j.jtbi.2015.03.004
142. Lee C, Amini R, Gorman R, Gorman J, Sacks M. An inverse modeling approach for stress estimation in mitral valve anterior leaflet valvuloplasty for in-vivo valvular biomaterial assessment. *J Biomech* (2014) 47(9):2055–63. doi:10.1016/j.jbiomech.2013.10.058
143. Muchir A, Wu W, Choi J, Iwata S, Morrow J, Homma S, et al. Abnormal p38 mitogen-activated protein kinase signaling in dilated cardiomyopathy caused by lamin A/C gene mutation. *Hum Mol Genet* (2012) 21(19):4325–33. doi:10.1093/hmg/dd265
144. Emerson L, Holt M, Wheeler M, Wehnert M, Parsons M, Ellis J. Defects in cell spreading and ERK1/2 activation in fibroblasts with lamin A/C mutations. *Biochim Biophys Acta* (2009) 1792(8):810–21. doi:10.1016/j.bbdis.2009.05.007
145. Wang N, Tytell J, Ingber D. Mechanotransduction at a distance: mechanically coupling the extracellular matrix with the nucleus. *Nat Rev Mol Cell Biol* (2009) 10(1):75–82. doi:10.1038/nrm2594
146. Small E, Thatcher J, Sutherland L, Kinoshita H, Gerard R, Richardson J, et al. Myocardin-related transcription factor-A controls myofibroblast activation and fibrosis in response to myocardial infarction. *Circ Res* (2010) 107(2):294–304. doi:10.1161/CIRCRESAHA.110.223172
147. Olson E, Nordheim A. Linking actin dynamics and gene transcription to drive cellular motile functions. *Nat Rev Mol Cell Biol* (2010) 11(5):353–65. doi:10.1038/nrm2890
148. Chang W, Worman H, Gundersen G. Accessorizing and anchoring the LINC complex for multifunctionality. *J Cell Biol* (2015) 208(1):11–22. doi:10.1083/jcb.201409047
149. Arsenovic P, Ramachandran I, Bathula K, Zhu R, Narang J, Noll N, et al. Nesprin-2G, a component of the nuclear LINC complex, is subject to myosin-dependent tension. *Biophys J* (2016) 110(1):34–43. doi:10.1016/j.bpj.2015.11.014
150. Zhang Q, Minaisah R, Ferraro E, Li C, Porter L, Zhou C, et al. N-terminal nesprin-2 variants regulate β -catenin signalling. *Exp Cell Res* (2016) 345(2):168–79. doi:10.1016/j.yexcr.2016.06.008
151. Chancellor T, Lee J, Thodeti C, Lele T. Actomyosin tension exerted on the nucleus through nesprin-1 connections influences endothelial cell adhesion, migration, and cyclic strain-induced reorientation. *Biophys J* (2010) 99(1):115–23. doi:10.1016/j.bpj.2010.04.011
152. Isermann P, Lammerding J. Nuclear mechanics and mechanotransduction in health and disease. *Curr Biol* (2013) 23(24):R1113–21. doi:10.1016/j.cub.2013.11.009
153. Connolly H, Crary J, McGoon M, Hensrud D, Edwards B, Edwards W, et al. Valvular heart disease associated with fenfluramine-phentermine. *N Engl J Med* (1997) 337(9):581–8. doi:10.1056/NEJM199708283370901
154. Redfield M. Valve disease associated with ergot alkaloid use: echocardiographic and pathologic correlations. *Ann Intern Med* (1992) 117(1):50. doi:10.7326/0003-4819-117-1-50
155. Zanettini R, Antonini A, Gatto G, Gentile R, Tesei S, Pezzoli G. Valvular heart disease and the use of dopamine agonists for Parkinson's disease. *N Engl J Med* (2007) 356:39–46. doi:10.1056/NEJMoa054830
156. Pinero A, Marcos-Alberca P, Fortes J. Cabergoline-related severe restrictive mitral regurgitation. *N Engl J Med* (2005) 353(18):1976–7. doi:10.1056/NEJM200511033531822
157. Serratrice J, Disdier P, Habib G, Viallet F, Weiller P. Fibrotic valvular heart disease subsequent to bromocriptine treatment. *Cardiol Rev* (2002) 10(6):334–6. doi:10.1097/00045415-200211000-00005
158. Fitzgerald L, Burn T, Brown B, Patterson J, Corjay M, Valentine P, et al. Possible role of valvular serotonin 5-HT_{2B} receptors in the cardiopathy associated with fenfluramine. *Mol Pharmacol* (2000) 57(1):75–81.
159. Rothman R, Baumann M, Savage J, Rausler L, McBride A, Hufeisen S, et al. Evidence for possible involvement of 5-HT_{2B} receptors in the cardiac valvulopathy associated with fenfluramine and other serotonergic medications. *Circulation* (2000) 102(23):2836–41. doi:10.1161/01.CIR.102.23.2836
160. Oyama M, Chittur S. Genomic expression patterns of mitral valve tissues from dogs with degenerative mitral valve disease. *Am J Vet Res* (2006) 67(8):1307–18. doi:10.2460/ajvr.67.8.1307
161. Disatani S, Orton EC. Autocrine serotonin and transforming growth factor beta 1 signaling mediates spontaneous myxomatous mitral valve disease. *J Heart Valve Dis* (2009) 19(1):71–8.
162. Nebigil C, Choi D, Dierich A, Hickel P, Le Meur M, Messaddeq N, et al. Serotonin 2B receptor is required for heart development. *Proc Natl Acad Sci U S A* (2000) 97(17):9508–13. doi:10.1073/pnas.97.17.9508
163. Mekontso-Dessap A, Brouri F, Pascal O, Lechat P, Hanoun N, Lanfumey L, et al. Deficiency of the 5-hydroxytryptamine transporter gene leads to cardiac fibrosis and valvulopathy in mice. *Circulation* (2005) 113(1):81–9. doi:10.1161/CIRCULATIONAHA.105.554667
164. Connolly JM, Bakay MA, Fulmer JT, Gorman RC, Gorman JH III, Oyama MA, et al. Fenfluramine disrupts the mitral valve interstitial cell response to serotonin. *Am J Pathol* (2017) 175:988–97. doi:10.2353/ajpath.2009.081101

165. Launay J, Birraux G, Bondoux D, Callebert J, Choi D, Loric S, et al. Ras involvement in signal transduction by the serotonin 5-HT_{2B} receptor. *J Biol Chem* (1996) 271(6):3141–7. doi:10.1074/jbc.271.6.3141
166. Nebigil C, Launay J, Hickel P, Tournois C, Maroteaux L. 5-Hydroxytryptamine 2B receptor regulates cell-cycle progression: cross-talk with tyrosine kinase pathways. *Proc Natl Acad Sci U S A* (2000) 97(6):2591–6. doi:10.1073/pnas.050282397
167. Buskohl P, Sun M, Thompson R, Butcher J. Serotonin potentiates transforming growth factor-beta3 induced biomechanical remodeling in avian embryonic atrioventricular valves. *PLoS One* (2012) 7(8):e42527. doi:10.1371/journal.pone.0042527
168. Cremer S, Moesgaard S, Rasmussen C, Zois N, Falk T, Reimann M, et al. Alpha-smooth muscle actin and serotonin receptors 2A and 2B in dogs with myxomatous mitral valve disease. *Res Vet Sci* (2015) 100:197–206. doi:10.1016/j.rvsc.2015.03.020
169. Yabanoglu S, Akkiki M, Seguelas M, Mialet-Perez J, Parini A, Pizzinat N. Platelet derived serotonin drives the activation of rat cardiac fibroblasts by 5-HT_{2A} receptors. *J Mol Cell Cardiol* (2009) 46(4):518–25. doi:10.1016/j.yjmcc.2008.12.019
170. Jian B, Xu J, Connolly J, Savani R, Narula N, Liang B, et al. Serotonin mechanisms in heart valve disease I: serotonin-induced up-regulation of transforming growth factor- β 1 via G-protein signal transduction in aortic valve interstitial cells. *Am J Pathol* (2002) 161(6):2111–21. doi:10.1016/S0002-9440(10)64489-6
171. Pavone L, Spina A, Rea S, Santoro D, Mastellone V, Lombardi P, et al. Serotonin transporter gene deficiency is associated with sudden death of newborn mice through activation of TGF- β 1 signalling. *J Mol Cell Cardiol* (2009) 47(5):691–7. doi:10.1016/j.yjmcc.2009.07.021
172. Capulli A, MacQueen L, O'Connor B, Dauth S, Parker K. Acute pergolide exposure stiffens engineered valve interstitial cell tissues and reduces contractility in vitro. *Cardiovasc Pathol* (2016) 25(4):316–24. doi:10.1016/j.carpath.2016.04.004
173. Liang Y, Lai L, Wang B, Juang S, Chang C, Leu J, et al. Mechanical stress enhances serotonin 2B receptor modulating brain natriuretic peptide through nuclear factor- κ B in cardiomyocytes. *Cardiovasc Res* (2006) 72(2):303–12. doi:10.1016/j.cardiores.2006.08.003
174. Brattelid T, Qvigstad E, Birkeland J, Swift F, Bekkevold S, Krobert K, et al. Serotonin responsiveness through 5-HT_{2A} and 5-HT₄ receptors is differentially regulated in hypertrophic and failing rat cardiac ventricle. *J Mol Cell Cardiol* (2006) 40(6):944–5. doi:10.1016/j.yjmcc.2006.03.081
175. Balachandran K, Bakay M, Connolly J, Zhang X, Yoganathan A, Levy R. Aortic valve cyclic stretch causes increased remodeling activity and enhanced serotonin receptor responsiveness. *Ann Thorac Surg* (2011) 92(1):147–53. doi:10.1016/j.athoracsur.2011.03.084
176. Balachandran K, Hussain S, Yap C, Padala M, Chester A, Yoganathan A. Elevated cyclic stretch and serotonin result in altered aortic valve remodeling via a mechanosensitive 5-HT_{2A} receptor-dependent pathway. *Cardiovasc Pathol* (2012) 21(3):206–13. doi:10.1016/j.carpath.2011.07.005
177. Lacerda C, MacLea H, Kisiday J, Orton E. Static and cyclic tensile strain induce myxomatous effector proteins and serotonin in canine mitral valves. *J Vet Cardiol* (2012) 14(1):223–30. doi:10.1016/j.jvc.2011.12.002
178. Lacerda C, Kisiday J, Johnson B, Orton E. Local serotonin mediates cyclic strain-induced phenotype transformation, matrix degradation, and glycosaminoglycan synthesis in cultured sheep mitral valves. *Am J Physiol Heart Circ Physiol* (2012) 302(10):H1983–90. doi:10.1152/ajpheart.00987.2011
179. Knipe R, Tager A, Liao J. The rho kinases: critical mediators of multiple profibrotic processes and rational targets for new therapies for pulmonary fibrosis. *Pharmacol Rev* (2014) 67(1):103–17. doi:10.1124/pr.114.009381
180. Hartmann S, Ridley A, Lutz S. The function of Rho-associated kinases ROCK1 and ROCK2 in the pathogenesis of cardiovascular disease. *Front Pharmacol* (2015) 6:276. doi:10.3389/fphar.2015.00276
181. Price S, Norwood C, Williams J, McElderry H, Merryman W. Radiofrequency ablation directionally alters geometry and biomechanical compliance of mitral valve leaflets: refinement of a novel percutaneous treatment strategy. *Cardiovasc Eng Technol* (2010) 1(3):194–201. doi:10.1007/s13239-010-0018-2
182. Waterman-Storer C, Worthylake R, Liu B, Burridge K, Salmon E. Microtubule growth activates Rac1 to promote lamellipodial protrusion in fibroblasts. *Nat Cell Biol* (1999) 1(1):45–50. doi:10.1038/9018
183. Brevier J, Montero D, Svitkina T, Riveline D. The asymmetric self-assembly mechanism of adherens junctions: a cellular push–pull unit. *Phys Biol* (2008) 5(1):016005. doi:10.1088/1478-3975/5/1/016005
184. Priya R, Gomez G, Budnar S, Acharya B, Czirok A, Yap A, et al. Bistable front dynamics in a contractile medium: travelling wave fronts and cortical advection define stable zones of RhoA signaling at epithelial adherens junctions. *PLoS Comput Biol* (2017) 13(3):e1005411. doi:10.1371/journal.pcbi.1005411
185. Braga V, Del Maschio A, Machesky L, Dejana E. Regulation of cadherin function by Rho and Rac: modulation by junction maturation and cellular context. *Mol Biol Cell* (1999) 10(1):9–22. doi:10.1091/mbc.10.1.9
186. Ohta Y, Hartwig J, Stossel T. FilGAP, a Rho- and ROCK-regulated GAP for Rac binds filamin A to control actin remodelling. *Nat Cell Biol* (2006) 8(8):803–14. doi:10.1038/ncb1437
187. Nakamura F, Pudas R, Heikkinen O, Permi P, Kilpeläinen I, Munday AD, et al. The structure of the GPIb-filamin A complex. *Blood* (2006) 107(5):1925–32. doi:10.1182/blood-2005-10-3964
188. Kiema T, Lad Y, Jiang P, Oxley C, Baldassarre M, Wegener K, et al. The molecular basis of filamin binding to integrins and competition with Talin. *Mol Cell* (2006) 21(3):337–47. doi:10.1016/j.molcel.2006.01.011
189. Wipff PJ, Rifkin DB, Meister JJ, Hinz B. Myofibroblast contraction activates latent TGF- β 1 from the extracellular matrix. *J Cell Biol* (2007) 179(6):1311–23. doi:10.1083/jcb.200704042
190. Townsend T, Wrana J, Davis G, Barnett J. Transforming growth factor- β -stimulated endocardial cell transformation is dependent on Par6 regulation of RhoA. *J Biol Chem* (2008) 283(20):13834–41. doi:10.1074/jbc.M710607200
191. Gould R, Yalcin H, MacKay J, Sauls K, Norris R, Kumar S, et al. Cyclic mechanical loading is essential for Rac1-mediated elongation and remodeling of the embryonic mitral valve. *Curr Biol* (2016) 26(1):27–37. doi:10.1016/j.cub.2015.11.033
192. Kyndt F, Gueffert J, Probst V, Jaafar P, Legendre A, Le Bouffant F, et al. Mutations in the gene encoding filamin A as a cause for familial cardiac valvular dystrophy. *Circulation* (2006) 115(1):40–9. doi:10.1161/CIRCULATIONAHA.106.622621
193. Nakamura F, Heikkinen O, Pentikäinen O, Osborn T, Kasza K, Weitz D, et al. Molecular basis of filamin A-FilGAP interaction and its impairment in congenital disorders associated with filamin A mutations. *PLoS One* (2009) 4(3):4928. doi:10.1371/journal.pone.0004928
194. Arnould T, Kim E, Tsiokas L, Jochimsen F, Grüning W, Chang J, et al. The polycystic kidney disease 1 gene product mediates protein kinase C α -dependent and c-Jun N-terminal kinase-dependent activation of the transcription factor AP-1. *J Biol Chem* (1998) 273(11):6013–8. doi:10.1074/jbc.273.11.6013
195. Hernandez V, Pravin Kumar P, Diaz-Font A, May-Simera H, Jenkins D, Knight M, et al. Bardet-Biedl syndrome proteins control cilia length through regulation of actin polymerisation. *Cilia* (2012) 1(Suppl 1):88. doi:10.1186/2046-2530-1-S1-P88
196. Liu Y, Suzuki YJ, Day RM, Fanburg BL. Rho kinase-induced nuclear translocation of Erk1/Erk2 in smooth muscle cell mitogenesis caused by serotonin. *Circ Res* (2004) 95(6):579–86. doi:10.1161/01.RES.0000141428.53262.a4
197. Liu Y, Ren W, Warburton R, Toksoz D, Fanburg B. Serotonin induces Rho/ROCK-dependent activation of Smads 1/5/8 in pulmonary artery smooth muscle cells. *FASEB J* (2009) 23(7):2299–306. doi:10.1096/fj.08-127910
198. Na S, Collin O, Chowdhury F, Tay B, Ouyang M, Wang Y, et al. Rapid signal transduction in living cells is a unique feature of mechanotransduction. *Proc Natl Acad Sci U S A* (2008) 105(18):6626–31. doi:10.1073/pnas.0711704105
199. Watanabe T, Sato K, Kaibuchi K. Cadherin-mediated intercellular adhesion and signaling cascades involving small GTPases. *Cold Spring Harb Perspect Biol* (2009) 1(3):a003020. doi:10.1101/cshperspect.a003020
200. Burridge K. Focal adhesions: transmembrane junctions between the extracellular matrix and the cytoskeleton. *Annu Rev Cell Dev Biol* (1988) 4(1):487–525. doi:10.1146/annurev.cb.04.110188.002415
201. Parsons J, Horwitz A, Schwartz M. Cell adhesion: integrating cytoskeletal dynamics and cellular tension. *Nat Rev Mol Cell Biol* (2010) 11(9):633–43. doi:10.1038/nrm2957
202. Hu S, Wang N. Control of stress propagation in the cytoplasm by prestress and loading frequency. *Mol Cell Biomech* (2006) 3:49–60.

203. Li W, Wang W. Structural alteration of the endothelial glycocalyx: contribution of the actin cytoskeleton. *Biomech Model Mechanobiol* (2017). doi:10.1007/s10237-017-0950-2
204. Röhlich P, Allison A. Oriented pattern of membrane-associated vesicles in fibroblasts. *J Ultrastruct Res* (1976) 57(1):94–103. doi:10.1016/S0022-5320(76)80059-7
205. Rothberg K, Heuser J, Donzell W, Ying Y, Glenney J, Anderson R. Caveolin, a protein component of caveolae membrane coats. *Cell* (1992) 68(4):673–82. doi:10.1016/0092-8674(92)90143-Z
206. Muriel O, Echarri A, Hellriegel C, Pavon D, Beccari L, Del Pozo M. Phosphorylated filamin A regulates actin-linked caveolae dynamics. *J Cell Sci* (2011) 124(16):2763–76. doi:10.1242/jcs.080804
207. Mundy D, Machleidt T, Ying YS, Anderson RG, Bloom GS. Dual control of caveolar membrane traffic by microtubules and the actin cytoskeleton. *J Cell Sci* (2002) 115(22):4327–39. doi:10.1242/jcs.00117
208. Fujimoto T, Nakade S, Miyawaki A, Mikoshiba K, Ogawa K. Localization of inositol 1,4,5-trisphosphate receptor-like protein in plasmalemmal caveolae. *J Cell Biol* (1992) 119(6):1507–13. doi:10.1083/jcb.119.6.1507
209. Echarri A, Muriel O, Pavon D, Azegrouz H, Escolar F, Terron M, et al. Caveolar domain organization and trafficking is regulated by Abl kinases and mDia1. *J Cell Sci* (2012) 125(18):4413–4413. doi:10.1242/jcs.090134
210. Grande-García A, Echarri A, de Rooij J, Alderson N, Waterman-Storer C, Valdivielso J, et al. Caveolin-1 regulates cell polarization and directional migration through Src kinase and Rho GTPases. *J Cell Biol* (2007) 177(4):683–94. doi:10.1083/jcb.200701006
211. Ogata T, Ueyama T, Isodono K, Tagawa M, Takehara N, Kawashima T, et al. MURC, a muscle-restricted coiled-coil protein that modulates the Rho/ROCK pathway, induces cardiac dysfunction and conduction disturbance. *Mol Cell Biol* (2008) 28(10):3424–36. doi:10.1128/MCB.02186-07
212. Peng F, Wu D, Ingram A, Zhang B, Gao B, Krepinsky J. RhoA activation in mesangial cells by mechanical strain depends on caveolae and caveolin-1 interaction. *J Am Soc Nephrol* (2006) 18(1):189–98. doi:10.1681/ASN.2006050498
213. Sauls K, Toomer K, Williams K, Johnson A, Markwald R, Hajdu Z, et al. Increased infiltration of extra-cardiac cells in myxomatous valve disease. *J Cardiovasc Dev Dis* (2015) 2(3):200–13. doi:10.3390/jcdd2030200
214. Lima SM, Pitsis AA, Kelpis TG, Shahin MH, Langaee TY, Cavallari LH, et al. Matrix metalloproteinase polymorphisms in patients with floppy mitral valve/mitral valve prolapse (FMV/MVP) and FMV/MVP syndrome. *Cardiology* (2017) 138:179–85. doi:10.1159/000477656
215. Ahmad N, Richards A, Murfett H, Shapiro L, Scott J, Yates J, et al. Prevalence of mitral valve prolapse in Stickler syndrome. *Am J Med Genet* (2002) 116A(3):234–7. doi:10.1002/ajmg.a.10619
216. Malfait F, Wenstrup R, De Paepe A. Clinical and genetic aspects of Ehlers-Danlos syndrome, classic type. *Genet Med* (2010) 12(10):597–605. doi:10.1097/GIM.0b013e3181eed412
217. Ayoub S, Lee C, Driesbaugh K, Anselmo W, Hughes C, Ferrari G, et al. Regulation of valve interstitial cell homeostasis by mechanical deformation: implications for heart valve disease and surgical repair. *J R Soc Interface* (2017) 14(135):20170580. doi:10.1098/rsif.2017.0580

Conflict of Interest Statement: The authors declare that the research was conducted in the absence of any commercial or financial relationships that could be construed as a potential conflict of interest.

Copyright © 2017 Pagnozzi and Butcher. This is an open-access article distributed under the terms of the Creative Commons Attribution License (CC BY). The use, distribution or reproduction in other forums is permitted, provided the original author(s) or licensor are credited and that the original publication in this journal is cited, in accordance with accepted academic practice. No use, distribution or reproduction is permitted which does not comply with these terms.



Cell Sources for Tissue Engineering Strategies to Treat Calcific Valve Disease

Eva Jover[†], Marco Fagnano[†], Gianni Angelini and Paolo Madeddu^{*}

Bristol Medical School (Translational Health Sciences), Bristol Heart Institute, University of Bristol, Bristol, United Kingdom

OPEN ACCESS

Edited by:

Joshua D. Hutcheson,
Florida International University,
United States

Reviewed by:

Mark C. Blaser,
Brigham and Women's Hospital,
United States
Carlijn V. Bouten,
Eindhoven University of Technology,
Netherlands

*Correspondence:

Paolo Madeddu
mdpmm@bristol.ac.uk

[†]These authors have contributed
equally to this work

Specialty section:

This article was submitted to
Atherosclerosis and Vascular
Medicine,
a section of the journal
Frontiers in Cardiovascular Medicine

Received: 17 May 2018

Accepted: 10 October 2018

Published: 06 November 2018

Citation:

Jover E, Fagnano M, Angelini G and
Madeddu P (2018) Cell Sources for
Tissue Engineering Strategies to Treat
Calcific Valve Disease.
Front. Cardiovasc. Med. 5:155.
doi: 10.3389/fcvm.2018.00155

Cardiovascular calcification is an independent risk factor and an established predictor of adverse cardiovascular events. Despite concomitant factors leading to atherosclerosis and heart valve disease (VHD), the latter has been identified as an independent pathological entity. Calcific aortic valve stenosis is the most common form of VHD resulting of either congenital malformations or senile “degeneration.” About 2% of the population over 65 years is affected by aortic valve stenosis which represents a major cause of morbidity and mortality in the elderly. A multifactorial, complex and active heterotopic bone-like formation process, including extracellular matrix remodeling, osteogenesis and angiogenesis, drives heart valve “degeneration” and calcification, finally causing left ventricle outflow obstruction. Surgical heart valve replacement is the current therapeutic option for those patients diagnosed with severe VHD representing more than 20% of all cardiac surgeries nowadays. Tissue Engineering of Heart Valves (TEHV) is emerging as a valuable alternative for definitive treatment of VHD and promises to overcome either the chronic oral anticoagulation or the time-dependent deterioration and reintervention of current mechanical or biological prosthesis, respectively. Among the plethora of approaches and established techniques for TEHV, utilization of different cell sources may confer of additional properties, desirable and not, which need to be considered before moving from the bench to the bedside. This review aims to provide a critical appraisal of current knowledge about calcific VHD and to discuss the pros and cons of the main cell sources tested in studies addressing *in vitro* TEHV.

Keywords: valve heart disease, calcification, tissue engineering heart valves, *in vitro*, heterotopic bone formation

INTRODUCTION

Cardiovascular calcification (CVC) is an independent risk factor and an established predictor of adverse and disabling cardiovascular events (**Figure 1**) (1–3). Histopathological studies have demonstrated hydroxyapatite deposits in vulnerable atherosclerotic plaques (4) and aortic valves (5). No longer considered a passive age-related disease, CVC is identified as the active, progressive and multifactorial ectopic bone-like calcification of blood vessels, myocardium or heart valves, leading to the “degeneration”/deterioration and dysfunction of the affected tissue (5, 6). Although there is an overlap between the risk factors leading to atherosclerosis and valvular calcification, only 40–50% of patients diagnosed with atherosclerosis concomitantly develop calcific valvular heart disease (VHD), thus suggesting that VHD is an independent pathological entity (7, 8).

VHD is the third most common cardiovascular pathology after hypertension and coronary artery disease in developed nations (9). Specifically, aortic valve stenosis (AVS) is the most common primary valvulopathy because of either congenital malformation (such as bicuspid aortic valve or BAV) or senile “degeneration.” The result is an increased stiffness and impaired leaflet motion and calcification, lately leading to the left ventricle outflow obstruction (10). Moreover, aging, male gender, cigarette smoking, hypertension, hyperlipidaemia, metabolic syndrome or kidney dysfunction are frequent independent risk factors for calcific VHD and significantly impair the outcome and prognosis of patients (11). The progression of calcific VHD consists of a valve sclerosis prestadium affecting more than 25% of the general population over 65 years old and associated to a 50% increased cardiovascular risk over 5 years (2). The prevalence of calcification and stenosis is reported in ~2% or 2.5% in a population aged over 65 or 75 years, respectively, representing a major cause of morbidity and mortality in the elderly (11, 12). Stenotic aortic valves are also found in congenital bicuspid valves and may require valve replacement even two decades earlier than valves anatomically normal (13). VHD is predicted to become a new cardiovascular epidemic in the next 20 years because of the increase of life expectancy in industrialized nations (9, 12, 14). No specific pharmacological strategy has been developed to retard, halt or revert the progression of VHD. Valve replacement represents the gold standard method to treat VHD through either mechanical or biological prosthesis implantation (15), but it is not suitable or definitive for all patients. New therapeutic solutions are claimed from the clinic to overcome the limitations of current therapeutic options including the chronic oral anticoagulation required for mechanical valves implantation or the degeneration, calcification, and failure of the biological counterparts. A plethora of novel tissue engineering-based approaches has emerged promising a definitive solution. Between the two main tissue engineered heart valves (TEHV) approaches, *in vitro* TEHV may provide, among others, a “native-like” extracellular matrix (ECM) surrogate and promote a “physiologic-like” regeneration in a pathologic environment with a deteriorated reparative system. Implantation of those devices is appealing for pediatric patients with congenital VHD as it might circumvent the failure of growth, repair, and remodeling required after somatic growth. In this review, we assess the current knowledge in the clinical relevance and mechanisms of valvular calcification and critically discuss the benefits and limitations of different cell sources currently used for the development of *in vitro* TEHV.

DETECTION, RISK AND PREVALENCE OF VALVULAR CALCIFICATION

Calcific VHD of anatomically normal valves is a slow and active process driving to degeneration and dysfunction, with a long preclinical and asymptomatic phase. The onset of symptomatology is a general sign of advanced and severe disease associated with a high event rate, rapid valve deterioration and malfunctioning, thus being a poor prognostic indicator

and elective for valve replacement surgery (15). However, the management of patients with asymptomatic valve disease is challenging. The real prevalence of unsuspected VHD is unsure, and a significant proportion of patients remain asymptomatic and undiagnosed until late stages when the long-term benefits of intervention are ambiguous due to increased postoperative complications and further mortality (8, 14). Large European and North American observational studies have provided most of the valuable insights on the overall VHD prevalence and the effect on overall survival (8, 14, 16, 17). In 2001, the Euro Heart Survey study (8) evidenced “degeneration” as the dominant etiological cause of VHD, with AVS (43%), mitral regurgitation (32%), and aortic regurgitation (13%) representing the commonest forms of adult valvopathies. AVS progression occurring in up to 5% of elderly patients (11, 14) carries an 80% 5-year risk of developing heart failure, valve replacement requirement, or death (18). Moreover, a US population-based study in more than 28,000 adults demonstrated the age-dependent VHD prevalence, rising from 0.7% in subjects aged 18–44 to 13% in those over 75 years old (16), significantly impacting the survival rates and emphasizing its significance as a health care issue. A more recent publication showed that general population aged ≥ 60 years across 37 advanced economies (16.1 million people) has a whole prevalence of 4.5% VHD (2.8 and 13.1% in individuals aged 60–74 and ≥ 75 years, respectively) (19). Only in the UK, VHD might account for approximately 1 million people aged over 65 years, and trend predictions suggest a significant raise due to increased life expectancy and the continuum of population aging in industrialized countries. The degeneration of anatomically normal valves is more often and rapid in people over 70 years because of progressive fibrosis and calcification of the valve cusps (www.bcs.com). A population aged over 75 years is projected to rise around 50% by 2025 resulting in a substantial VHD impact (www.statistics.gov.uk) recently estimated in $\approx 331,300$ new cases of severe aortic stenosis per year including 65,600 patients (19). Thereby, VHD may become the next imminent and real cardiac epidemic (9, 12, 20). Genetic background and structural valve differences due to congenital malformations, such as BAV may be considered separately and are not deeply discussed in this review.

The presence and extent of CVC are generally acknowledged as strong predictors of future adverse clinical events including cardiovascular and all-cause mortality (21–23). The latter is highlighted by the up to 73% all-cause survival rate reduction estimated in patients diagnosed with high coronary artery calcification score (21). Importantly, 5–20% of the atherosclerotic lesions contain calcium deposits (24, 25), and it is alarming the potential underestimation of affected tissues due to the presence of chondrogenic intermediates, asymptomatic phases, or the lack of more powerful calcification screening methods. Additionally, the extent of valvular calcification correlates with the severity of stenosis (26). Therefore, a comprehensive and early understanding of the cardiovascular risk associated with calcification is critical for patient management and long-term prognosis (15, 27, 28).

Echocardiography is the mainstay for diagnosis, assessment and follow-up of VHD (15). It allows the calculation of the continuity equation-based aortic valve area both for predicting

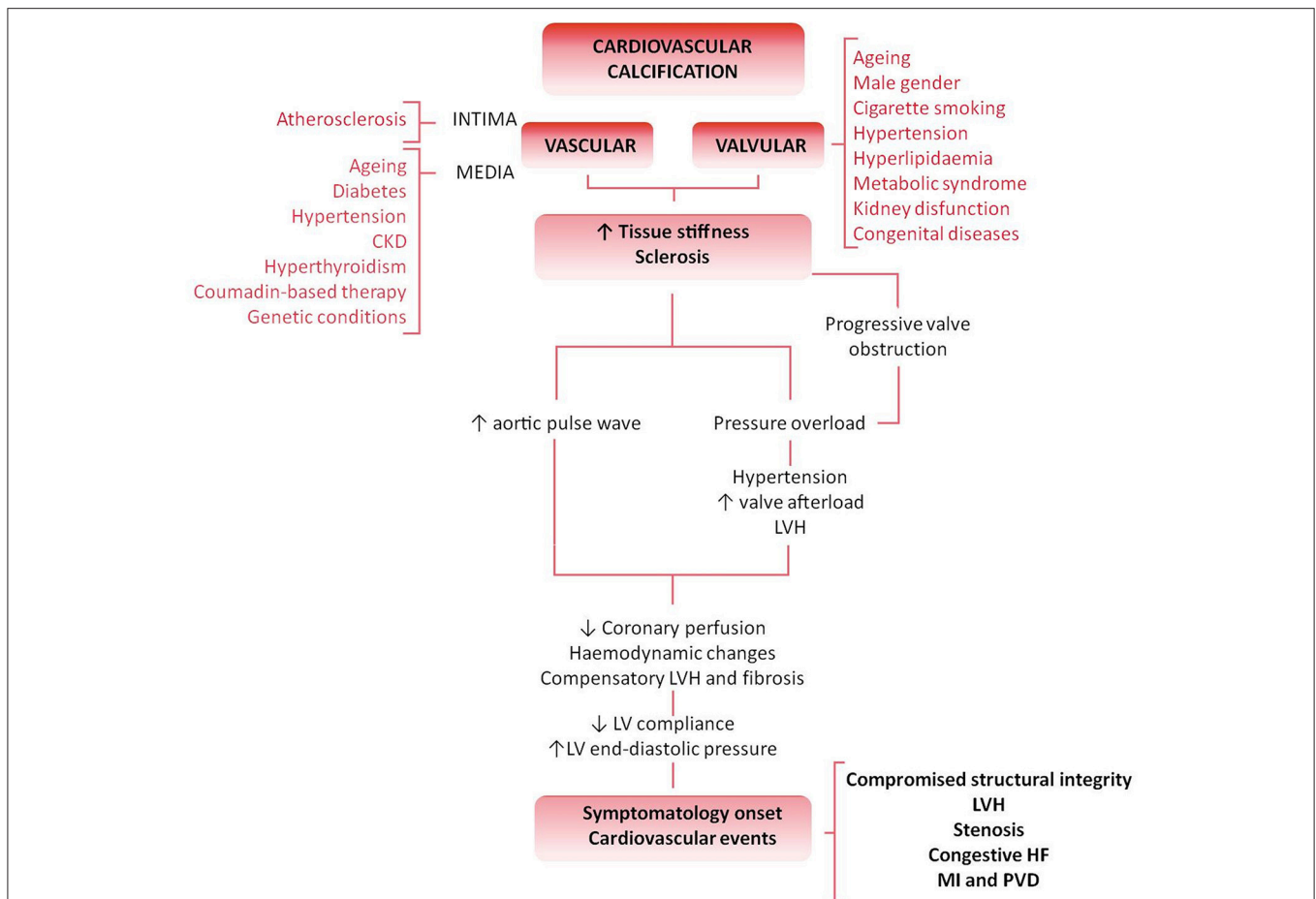


FIGURE 1 | Differential pathology and clinical impact of valvular vs. vascular calcification flowchart. Cardiovascular calcification is an active and degenerative bone-like process affecting the cardiovascular tissues. Both vessels and valves show an athero-inflammatory background and, despite the commonalities and overlap of several risk factors (such as aging, hyperlipidaemia or kidney disease), both atherosclerosis and calcific VHD are two independent pathologic entities. The biological progression of the disease, tissue characteristics and clinical impact stand those differences. The result is the independent plaque rupture primary outcome found in the progression of VHD. An increased stiffness or sclerosis induces an increased aortic pulse wave, triggering hypertension, and a reduction in coronary perfusion. Besides, the pressure overload caused by a sclerotic pre-stadium and observed in the progression of the VHD leads to LV structural and hemodynamic changes. Symptomatology onset and calcification burden are poor prognosis predictors associated with multiple adverse cardiovascular complications, such as left ventricular hypertrophy (LVH), aortic valve stenosis, congestive heart failure (HF), ascending aorta aneurysm, myocardial infarction (MI), and peripheral vascular disease (PVD).

the clinical outcome and for clinical decisions making as well as aortic jet velocity and leaflet calcification (5, 29). However, visualizing abnormal valve anatomy becomes difficult once severe calcification is established. Moreover, concomitant hypertension increases the systemic vascular resistance in addition to the valvular obstruction, thus imposing a double over-load on the left ventricle which may lead to underestimate the assessment of the stenosis severity (30).

Other imaging methods, notably cardiac magnetic resonance imaging (MRI) and coronary computed tomography (CCT), are used if echocardiographic imaging is not satisfactory. Three-dimensional time-resolved, phase contrast cardiac magnetic resonance, otherwise referred as 4-dimensional (4D) flow MRI, is an innovative and appealing method for studying cardiovascular diseases. Dataset integration of 4D-Flow MRI can be retrospectively quantified providing a comprehensive

evaluation of complex secondary vascular parameters, such as mechanical wall shear stress (WSS) on the vessels and heart valves (31) but also flow energy loss and flow displacements (32, 33). BAV is frequently associated with the progression of ascending thoracic aorta aneurysm (AsAo). Intrinsic wall abnormalities cannot fully explain the differential aneurysm progression resulting from different aortic leaflet fusion patterns and asymmetry (34). Echocardiography findings have suggested that abnormal blood flow could potentially trigger those differences in AsAo progression. In the context of VHD, 4D-Flow MRI has demonstrated to be a powerful tool to determine the association of flow hemodynamic, especially in those situations in which eccentric systolic blood flow jets result in abnormal helical systolic flow. The latter has highlighted the potential application of 4D-Flow MRI to study the progression and stratify/predict the risk of AsAo development specially in BAV

patients (34), while echocardiography is not a reliable method. Moreover, recent studies have demonstrated the association of WSS and aortic peak velocity with parameters of left ventricle remodeling, allowing to distinguish BAV patients with or without aortic stenosis or regurgitation (35). Post-operative follow-up of reparative surgery of tetralogy of Fallot is another potential application of 4D-Flow MRI (36). However, long acquisition times, lack of blood pressure determination, susceptibility to motion artifacts, poor spatial resolution and the need of massive data post-processing are the main drawbacks of this technique. In addition, aberrant hemodynamic changes are seen only in advanced stenotic VHD and that represents a limitation for hemodynamic analysis techniques. Earlier phases of the VHD, such as asymptomatic sclerosis pre-stadium of well-functional anatomically normal valves, may not be detected by echocardiography or 4D-Flow MRI. Complementary imaging techniques such as CCT may provide substantial information on the detection and risk assessment of VHD. Multi-slice CCT together with the implementation of new acquisition techniques including ECG synchronization, retrospective image reconstruction and application of algorithms such as Agatston score (37), permit a direct, real-time and easy assessment of calcium content in coronary arteries (38). It has substantially improved the detection of early CVC stages. The high sensitivity of CCT has improved the screening for CVC, evidencing a progressive increment on CVC in patients over 60 years, which is especially relevant in patients diagnosed with VHD. Moreover, CCT combined with coronary angiography (gold-standard for coronary lesion evaluation) has demonstrated a good correlation between coronary calcium content and coronary artery disease (39, 40). The suitability of CCT to screen early stages of valve calcification in sclerotic valves with no hemodynamic obstruction has been also demonstrated (41). Moreover, CCT screening has proved to be a superior and more trustable method than carotid-intima-media thickness or ankle-brachial index for identifying patients at high risk (42). Finally, MRI and CCT can also provide complementary information to improve assessment of the valve lesion and cardiac function to aid the timing of surgery and determine risk (43).

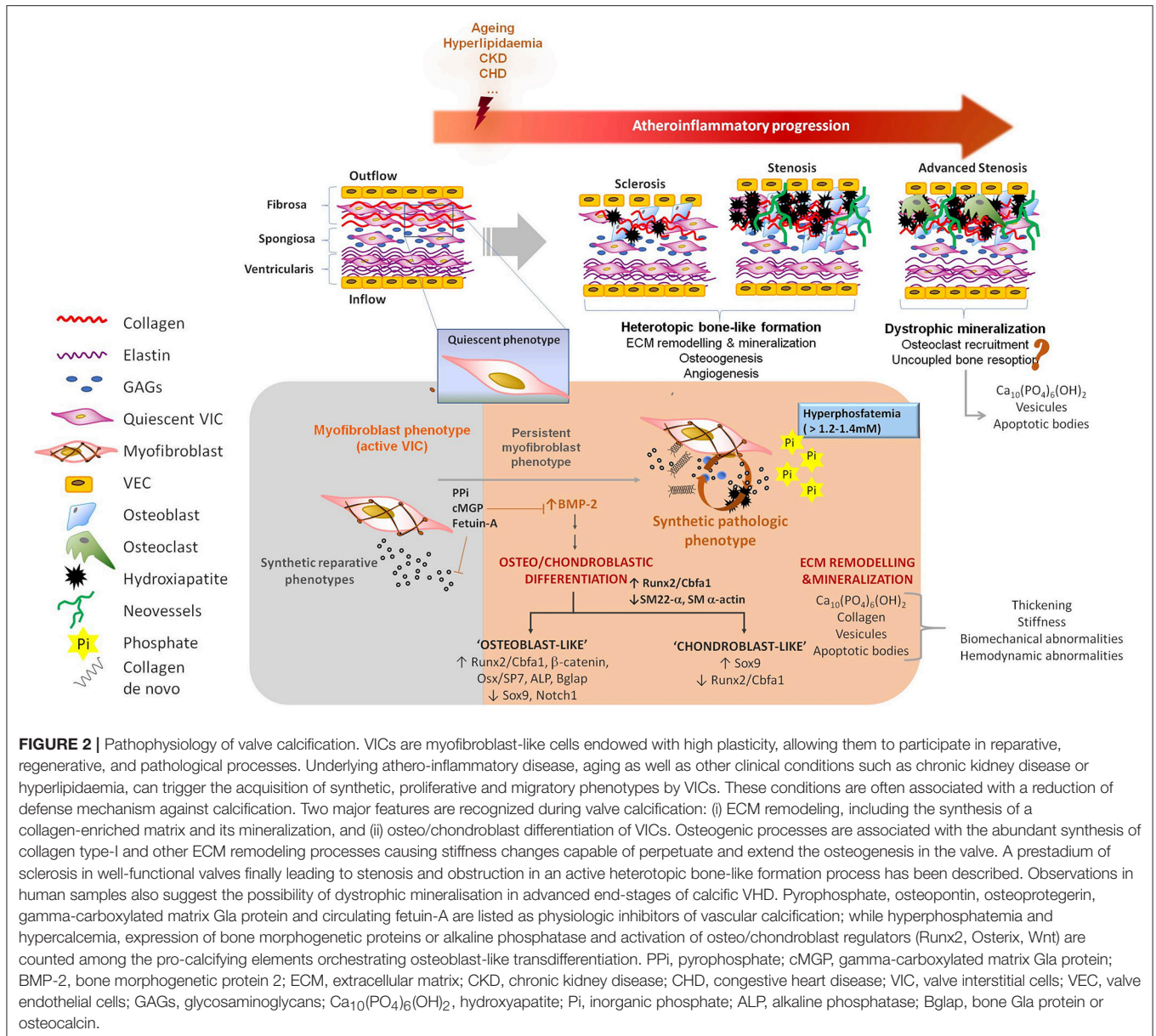
PATHOPHYSIOLOGY OF VALVULAR CALCIFICATION

Over the past four decades, experimental and clinical research has elucidated the pathophysiology of CVC. Ectopic calcification is an active and tightly organized process, which recapitulates several molecular mechanisms orchestrating physiologic chondro/osteogenesis (44–46). Both the phenotypic trans-differentiation into osteo/chondroblast-like cells and the active ECM remodeling, including its mineralization, represent the two hallmarks of ectopic calcifications (47) (**Figure 2**). In particular, calcific VHD has been described as a multifactorial, complex and active heterotopic endochondral lamellar bone-like formation process, driving heart valve calcification, degeneration and dysfunction (5, 6) toward integration of ECM remodeling, osteogenesis, and angiogenesis. Heterotopic bone exhibits

morphological and biochemical features of orthotopic bone, and it is capable of generating bone marrow (48). Higher remodeling rates have been reported in calcified valves than in physiologic bone formation (48) though, thus suggesting uncoupling of bone formation and resorption activities (49). However, histological observations in human specimens of calcific valves have evidenced an 83% prevalence of dystrophic calcification with only a 13% of active bone remodeling (5) and a 92% prevalence of microfractures, which are the main site of active bone remodeling. One could interpret valve calcification as a senile degeneration leading to cellular aging and death, and hydroxyapatite deposition on cellular degradation products rather than an active osteogenic-derived mineralization occurring on collagen and elastin fibers. Further research on this regard will significantly contribute to the understanding of the calcific VHD pathophysiology in the next years and it is currently cause of controversy. Observation of advanced end-stage phases in dystrophic human specimens could lead to misinterpretation of the underlying pathology in which a “preliminary” heterotopic bone-like tissue demonstrated by both *in vitro* and *in vivo* studies, might lately be replaced toward a misbalanced bone resorption (49) leading to an increased presence of dystrophic mineralisation.

Mature valves have an avascular (50) trilaminar organization including the upper surface of the valve or fibrosa (outflow), the central spongiosa and the inflow-orientated ventricularis. Those layers differ with each other by distinct ECM organization, composition and mechanical properties [a detailed description of the valve anatomy and function has been provided by Schoen (44)]. Moreover, two major resident cells are found in the valve: valve endothelial cells (VEC) and valve interstitial cells (VIC). Although VECs are not fully characterized, differential phenotypes and expressional profiles have been identified (51, 52). Biological functions of the VEC may include regulation of permeability, mediate immune responses and establish a paracrine signaling with VICs (53). The VIC represents a heterogenous population of mesenchymal cell type which shares several commonalities with vascular smooth muscle cells (VSMC) and fibroblasts, acts as mechanical sensor thorough complex cell-to-ECM interactions and shows highly dynamic phenotype plasticity (54). The latter allows the VIC to contribute to the permanent ECM turnover and reparative processes guarantying the maintenance of the valve integrity and function (44), but also contributes to the development of valve stenosis (55, 56).

Calcific VHD is regarded as an active athero-inflammatory disease associated with a damaged endothelium and an unresolved immunological inflammation resulting from such insult. The pathogenic role of hyperlipidaemia in the valve was recognized toward the introduction of dyslipidaemia experimental models (57, 58). Early studies in human aortic valve lesions demonstrated the association among atherogenic oxidized low-density lipoproteins (oxLDL) risk factor and the expression of signaling molecules promoting osteogenic processes (57). Moreover, inflammation plays a key role on the pathogenesis of VHD with superimposed calcification (59). Numerous histological studies have suggested inflammation to



trigger ECM remodeling, fibrosis, and valve thickening leading to the structural changes of VHD (60) and the subsequent differentiation of VICs into osteoblast-like phenotypes (55). Despite the commonalities and overlap of several risk factors, both atherosclerosis and calcific VHD are currently considered two independent pathologic entities mainly due to differences in the biological progression of the disease, tissue characteristics, clinical impact and resulting outcomes independent of plaque rupture (8). Among other differences, a CD8 T cell-based inflammatory background has been evidenced in valve calcification instead of the polyclonal lymphocytes reported in atherosclerotic lesions (59, 61).

The discovery of genetic modifications such as Notch1 mutations and their association with dysfunctional tissue structure of BAV and the spectrum of VHD has increased the

current knowledge of these abnormalities through congenital cardiology (62). Signaling components of embryonic valvular development, such as Notch1 as well as bone morphogenetic protein (Bmp) members, transforming growth factor beta 1 (TGF-β1) or Wnt/β-catenin participate in the onset of AVS by contributing to ECM remodeling, osteogenesis and angiogenesis [further reviewed in (47, 63, 64)].

OSTEOGENESIS

Several cell types have been involved in the development and progression of CVC and that includes vascular resident cells (VSMCs, VICs, or VECs) and circulating cells, such as mesenchymal stromal cells (MSCs), endothelial progenitor cells (EPCs) or calcifying vascular cells (CVC) (47). A

dysfunctional valvular endothelium together with an imbalance between activators and natural inhibitors may promote the calcification of neighboring VICs (**Figure 2**) (65–67). Different VICs sub-populations have been identified in the heart valve and may differentially contribute to the pathology of calcific VHD (54). Multiple signaling molecules (such as Bmp2, TGF- β , Wnt/b-catenin, VEGF, or Notch1) are integrated in what resembles a pathologic post-natal recapitulation of fetal valvulogenesis, including the acquisition of quiescent-to-active phenotypes, an active ECM remodeling, cytokine release and promoting *in situ* osteoblast/chondroblast-like differentiation as an environmentally maladaptation (68, 69). Bmp2 is a strong morphogen inducing osteoblast-like phenotypes, and it plays a key role in the pathogenesis of VHD (47). Bmp2 signaling triggers nuclear translocation of Smad proteins and the activation of osteogenic-regulators such as Runx2/Cbfa1. Runx2 is an early master gene of osteoblast differentiation and chondroblast maturation during heterotopic endochondral bone formation (5, 6, 70). Active Runx2 can bind to the SP7 promoter to induce the expression of Osterix, a master transcription factor of differentiated osteoblasts. Both Runx2 and Osterix bind to BGLAP promoter to induce osteocalcin, a marker for differentiated osteoblasts, which contributes to maturation of the mineralised ECM and it is present in calcified heart valves (69). Moreover, ECM synthesis is induced directly by Osterix and its binding to the *COL1A1* promoter or indirectly by Runx2 through the activation of *ATF6* and subsequent *COL1A1*, *COL1A2*, and *BGLAP* expression (66, 67, 70). In addition, Osterix triggers the expression of alkaline phosphatase (ALP), a pyrophosphatase capable of releasing inorganic phosphate from PPI, thus inducing local hyperphosphatemia and PPI deprivation. ALP also inhibits osteopontin phosphorylation and thus its protective biological function. Finally, Wnt/ β -catenin pathway mainly perpetuates osteoblastic phenotype by further induction of Runx2 and Osterix toward Bmp2-dependent signaling (57).

It is now appreciated that VECs, under certain circumstances, may undergo endothelial-to-mesenchymal transition, which is reminiscent of the early formation of the endocardial cushions (71, 72). The result might be an increase in the number of VICs susceptible to display an osteoblast phenotype (45). Dysfunctional VECs also manifest an altered secretome (73). VEC-derived nitric oxide (NO) is a regulator of Notch1 signaling in calcifying VICs (74), and a decreased Notch signaling has been found in AVC (45). Moreover, genetic studies in BAV have identified eNOS and Notch1 as candidate genes contributing to the valve anatomy and the development of VHD (62). Notch signaling leads to the cleavage and nuclear internalization of the Notch1 intracellular domain. One of the target genes of the Notch1 intracellular domain is the Hairy/enhancer-of-split (Hes)-related with YPRW motif (Hey) element, which is involved in early valve development. Both the nuclear location of the Notch1 intracellular domain and the expression of Hey1 are regulated by the VEC-derived NO (74). Furthermore, Notch1-dependent signaling is transduced through Bmp2/Runx2 axis, which directly regulates Sox9 in chondrogenesis and is an important mediator of AVS (75). Hey1 activated by Notch1

signaling forms a complex with Runx2/Cbfa1 and inhibits its transcriptional activation (64).

Pluripotent resident cells, EPCs, MSCs, and MSC-like pericytes have been found in calcified lesions suggesting a role of progenitor cells in the development and progression of ectopic calcification (45, 76, 77). The athero-inflammation associated with the release of multiple cytokines and chemokines may contribute to the recruitment of stem/progenitor cells into an environment whose homeostasis has been hampered by pro-calcifying factors and the depletion of physiologic calcification inhibitors. Finally, bone marrow (BM)-derived cells may contribute to replenishing the VIC population, modifying the proportion of VIC subpopulations yielding increased susceptibility to calcification. By using chimeric mice whose BM was repopulated with enhanced green fluorescent protein expressing total nucleated BM cells, Hajdu et al. documented the engraftment of BM-derived cells occurs as part of normal valve homeostasis (78).

ECM Remodeling

Besides providing biomechanical support, valvular ECM participates in a plethora of biological functions, such as cell communication and differentiation. In addition, the ECM may contribute to ectopic CVC (74, 79, 80). Differentiation of VICs toward myofibroblast or osteoblast phenotype is highly dependent on the complex and unique VIC-to-ECM components interactions (81). Therefore, a loss of the valve ECM integrity causes malfunction and results in VHD. In line with this, propagation of the inflammation-dependent calcification of the heart valves is associated with the active ECM remodeling resulting from the proteolytic and synthetic activities of active macrophages, VICs and mast cells (82). Moreover, substrate stiffness elicits the myofibroblast activation of VICs which remaining persistent can lead to osteoblast differentiation although the exact molecular mechanisms remain unclear (83, 84).

Regulatory factors, such as thrombospondins, have been found characteristically up-regulated in calcific valves (47). Moreover, microstructural changes in collagen fiber number, width, length, density or alignment may regulate pathogenic processes compromising the mechanical properties of the valve, in particular, and most frequently at the level of the spongiosa, chondrogenic-like layer (80). Mechanistically, cartilage-specific ECM genes are downregulated in calcifying VICs because of Sox9 downregulation (74). Moreover, ECM influences VEC function and it is involved in VEC-to-myofibroblast transformation toward EMT processes (85).

Angiogenesis

Heart valves have a sparse vascularity at the proximal part (50) being considered mainly avascular. That valve avascularity is seemingly abrogated in VHD (86), and the extent of neovascularisation correlates well with the burden of the disease (87). The expression of pro- and anti-angiogenic factors in stenotic valves or calcifying VICs (74, 88) has reinforced the idea that angiogenesis in the valve may promote calcific VHD, which calls for the use of modulators of angiogenesis

in the therapy of valve degeneration (86, 88, 89). Accordingly, anti-angiogenic therapy has shown a protective effect on the valvular cusp endothelium (86). Immunohistochemical studies have revealed the co-localization of micro-vascularization with actively proliferating VICs, bone-related proteins, and heavy calcification (90). In addition, during calcific VHD, expression of osteonectin (pro-angiogenic and chondrogenic factor) and Lect1/chondromodulin-1 (Chm-I) (anti-angiogenic factor) is disrupted (74). In human calcified valves, the expression of vascular endothelial growth factor (VEGF), matrix metalloproteinases (MMPs) and angiogenesis is concomitant with a downregulated expression of Chm-I.

Revisiting the physiology of bone formation, one could speculate that valve angiogenesis is not the cause, but the consequence of the osteogenesis perpetuation described for endochondral bone formation or that may provide of support to the thickened tissue produced *de novo* and resulting in a hypoxic microenvironment requiring of oxygen supply (50). An angiogenic switch of cartilage allows neovascular invasion and triggers the replacement of cartilage by bone (91). Resting chondrocytes become active and proliferative to differentiate into pre-hypertrophic chondrocytes, which can then secrete the cartilage matrix (92). Angiogenic factors such as TGF- β or VEGF are normally expressed in the cartilage and Chm-I has been proposed as an inhibitor during avascular phases of chondrogenesis. Chm-I plays divergent biological functions including chondrocyte growth and angiogenesis inhibition, stimulation of osteoblast proliferation and differentiation with a reduction of ALP activity (92, 93) and contribution to bone remodeling (92). Accordingly, Chm-I expression is upregulated by Sox9 during chondrogenesis in the avascular cartilage, but it is not present in the late hypertrophic and calcified zones leading to final osteogenesis (88, 91). In line with this, Chm-I deficient mice showed a significant increase in bone mineral density and lowered resorption (92). Moreover, the basal cartilage-like profile of the normal and mature valve is lost during AVS, though *in vitro* assays have shown an early up-regulation of Sox9 followed by Runx2 and ALP up-regulation (94). This may indicate an early chondroblast intermediate stage before the down-regulation of Sox9 and Chm-I. Noteworthy, angiogenic factors and abundant vascularization have been mostly co-localized in late-stage heavy calcified plaques (87, 94) with the presence of osteopontin and osteocalcin suggesting a mature mineralised ECM (90, 95) but also coinciding with the thickest remodeled tissue. Importantly, VEGF induces osteoblast proliferation and differentiation and osteoclast recruitment (96) but also inhibits calcification of ovine VICs in the presence of particular ECM compositions (97), highlighting again the regulatory importance of the ECM in modulating the action of growth factors.

According to another theory, VHD recapitulates the signaling pathways that control developmental valvulogenesis (98). For instance, Bmp2, canonical Wnt, TGF- β 1, and Notch signaling occurs during the endothelial-to-mesenchymal transition (99, 100) which may induce a myofibroblast phenotype on VECs and the subsequent calcification if the signaling network activation persists in time.

CURRENT THERAPEUTIC APPROACHES FOR CALCIFIC AORTIC VALVE STENOSIS

Several pharmacological attempts have been made for establishing a medical treatment of CVC. The regression observed by *in vivo* calcification models suggests the existence of endogenous mechanisms capable of dismantling the extremely insoluble and stable calcium phosphate deposits (101). Potential strategies to revert CVC have been proposed during the last few years and reviewed by O'Neill et al. (101). Preliminary evidence suggests a beneficial effect of treating calcific VHD, but frequently in association with bone mass weakening (101). Therefore, preventing or reverting the ectopic bone-like formation in the cardiovascular territory may boost bone resorption and increase the risk of fractures, which represents a serious concern for extensive use in the elderly population. To date, surgical valve replacement (SVR) represents the only available therapeutic approach for treating VHD.

Valve replacement, specifically aortic valve replacement, represents the second commonest cardiovascular surgical procedure (102) and accounts for 10 to 20% of all cardiac surgical procedures in the US (9). A 26% increase in the number of patients undergoing aortic SVR was calculated over a 5-year period comprising 2004–2009 in Great Britain and Ireland (103). It is anticipated that the number of patients requiring SVR will be 2.93-fold increased by 2050, in less than 50 years' time. Refusing to undergo SVR is associated with poor prognosis, a significant morbidity (104, 105) and >12-fold the risk of mortality (105). More than half of the patients will die within the next 12–18 months of symptom onset (106). Risk factors, co-morbidities and patient denial are common exclusion criteria for valve replacement. According to a recent survey, about 40% of patients with severe symptomatic VHD and 70% of patients with asymptomatic VHD were not eligible for SVR (19). This heterogeneous population require therefore alternative approaches.

The introduction of SVR has improved the outcome of patients with VHD. Mechanical or biological prosthesis are the two main options for current SVR (107). Mechanical valves last longer and are still the gold standard for patients under 60 years (108), but may come with a high inherent risk of thrombosis and therefore a requirement for chronic oral anticoagulation, based on coumadin derivatives. More frequent use of biological prostheses (mainly porcine or bovine-derived), introduction of minimally-invasive implantation techniques, and better control of risk factors and complications (109, 110) have considerably improved the clinical outcome of people undergoing SVR (111). Geometrical, nano-structural and material features of the bioprosthetic valve are more similar to the native tissue. Moreover, recent bioprosthetic valve improvements have significantly lowered the age for recommended mechanical valve replacement (111, 112). Nevertheless, biological prosthesis has a relatively poor long-term durability; thus, it does not provide a definitive cure. Instead, owing to the progressive deterioration and failure of current valve substitutes, native VHD is traded for “*bioprosthetic valve disease*,” which entails expensive treatments, hospital

readmission and reintervention (110). Structural prosthetic valve deterioration represents a major limit for durability, independently the substitute is a homograft or xenograft. Several factors contribute to this phenomenon. Animal-derived prostheses, now prevalently used because of the shortage of human valve substitutes, are subjected to decellularization procedures to prevent recipient's immune response, and are cross-linked with glutaraldehyde, to provide tensile strength and elasticity, and render them further non-immunogenic. However, improvements in pliability and tolerogenicity come at a price. In fact, elimination of VICs, which synthesize ECM proteins and possess contractile properties, deprive the valves of their unique function in such a mechanically demanding environment and makes prostheses more susceptible to degeneration. Moreover, residual fragments of devitalized VICs and VECs may act as hydroxyapatite nucleation sites and induce activation of immune responses. Atherosclerotic processes also participate in prosthetic valve remodeling, with initial accumulation of oxLDL, followed by monocyte recruitment, generation of a pro-inflammatory milieu, collagen disruption and osteogenic differentiation of resident endothelial cells (ECs) and precursor cells recruited from the circulation (113, 114). Damage of the ECM is cumulative: calcium deposits enlarge and merge, forming nodules that interfere with the bioprosthesis function. Manufacture protocols preserving ECM integrity and encouraging *in vivo* recellularization prolong durability (115, 116). Anti-calcifying agents are also effective (117). However, ECM disorganization and degradation remains the ultimate limiting factor in durability (118).

Pediatric or adolescent patients diagnosed with congenital valve diseases are specially challenging. The risk of prosthetic valve failure becomes relevant in these populations with a 10% rate of failure within 4 years after implantation (117) and usage of mechanical valves linked to chronic oral anticoagulation does not fit with their active lifestyle. Failure of somatic growth, repair and remodeling are also common problems of both mechanical and biological prosthesis. The ideal valve prosthesis has yet to be developed.

FUTURE SOLUTIONS FROM REGENERATIVE MEDICINE AND TISSUE ENGINEERING OF HEART VALVES

Landmark experimental and clinical work has demonstrated the potential of tissue engineering, which combines cells from the body with template materials, to guide the somatic growth of new tissue and correction of organ defects (119). Application of this approach has been proposed to improve the durability of cardiac prostheses and thereby optimize long-term outcomes in patients with congenital or acquired valve defects. Therefore, Tissue Engineering of Heart Valves (TEHV) has emerged as a valuable alternative for definitive treatment of VHD promising to overcome either the chronic oral anticoagulation or the time-dependent deterioration and reintervention of current mechanical or biological prosthesis, respectively and to offer a valve substitute capable to grow in a "physiologic-like"

manner. In the past few decades, two main strategies have been developed to generate TEHV. The underpinning concept for both TEHV approaches is that patient's own cells will generate a viable and physiologically competent tissue able to withstand hemodynamic forces before (*in vitro*) or after (*in situ*) implantation. Briefly, *in vitro* TEHV uses various types of autologous cells, including stem/progenitor cells, that are expanded in culture, seeded on decellularized biological (120, 121) or synthetic scaffolds (122, 123) (see below), and may be conditioned in a bioreactor to ensure fast and competent "natural-like" matrix production before implantation (124). The underlying concept is that *in vitro* incorporation of cells shall confer prosthetic grafts with the characteristics of a living tissue that remodel in a physiologic manner and concert with cardiac and whole-body needs, withstanding the impact of degeneration and calcification. Implantation of *in vitro* TEHV is an appealing alternative for pediatric patients with congenital VHD requiring of SVR even two decades earlier than VHD patients with anatomically normal valves. On the other hand, *in situ* TEHV, aims to create an acellular biodegradable scaffold which gradually transforms into a living valve by recruiting endogenous cells upon orthotopic implantation (125–127). An interesting combination of the *in vitro* and *in situ* approaches is represented by tissue-engineered matrixes (TEMs), which are usually made of autologous vascular cell- or fibroblast-derived ECM/fibrin gel sheets undergoing a decellularization process before implantation. TEMs are supposed to provide a more natural substrate for homing of the recipient's cells (128, 129). A similar strategy to produce a natural ECM graft is the *in vivo* TEHV by which synthetic non-degradable molds are implanted at sub-cutaneous level and expected to produce a collagen-rich, non-immunogenic, harvestable, and implantable fibrotic capsule (108). In the *in vitro* procedures and TEM, a balance between the extent of decellularization and conservation of the native properties of the ECM must be reached to avoid undesired alterations of biomechanical and hydrodynamic properties. The *in situ* approach is instead totally reliant on the endogenous capacity of the hosting organism to mobilize and incorporate the *right cells*, which may be negated by a disease-associated alteration in cell behavior (130–133). The two main strategies, *in vitro* vs. *in situ*, are briefly summarized in Table 1.

A three-dimensional scaffold and the correct choice of cells are the cornerstone elements to consider generating a living valve substitute. A plethora of approaches and techniques have been established on TEHV and that has been recently and extensively reviewed elsewhere (134–136). Unique valve mechanobiology features and implications in the development and design of TEHV has been nicely reviewed by Schoen (137). Furthermore, utilization of different cell sources may confer of additional properties to the valve substitute which may, or may not, be desirable in the VHD environment. The cell of choice to be seeded in *in vitro* TEHV should sense and perform optimal adaptive responses to environmental changes. All that must be considered before moving from the bench to the bedside and is further discussed below.

TABLE 1 | Advantages and disadvantages of *in vitro* and *in situ* TEHV.

	<i>In vitro</i> TEHV	<i>In situ</i> TEHV
Advantages	<ul style="list-style-type: none"> • Exogenous delivery of stem/progenitor cells in an environment with a deteriorated endogenous reparative/regenerative system • Promotion of a "physiologic-like" reparation/regeneration of the injured area by the exogenously delivered stem/progenitor cells • Promotion of resident cell recruitment • Phenotype modification of recruited cells through stem/progenitor cell-derived secretome or other mechanisms • Bioprosthetic-derived <i>in vitro</i> TEHV displays a more "native-like" ECM. Alternatives to GA cross-linking may inhibit calcification and there is a lower ECM damage than in decellularized tissue used in many HV implants • A dynamic maturation prior implantation may favor a desired cell profile and ECM remodeling, including collagens as well as non-collagen proteins (e.g., proteoglycans and glycosaminoglycans) • Cell seeding prior implantation reinforce the capability of the TEHV to support cell functions such as viability, proliferation or migration in both static and dynamic conditions • Inhibition of thrombogenic events • Tailored prosthesis according to patient's anatomy • Maintained natural ECM architecture and depending cell signaling • Biodegradable surrogates mimicking the native ECM • Possibility of Tissue Engineered Matrix (TEM) application 	<ul style="list-style-type: none"> • More rapid implantation and possibly non-invasive • Resident cell recruitment • Surrogates mimicking the native ECM • Off-the-shelf scaffold manufacturing. Limitless supply and ready-to-be implanted for urgent implantations • Different and desired growth factor or drugs can be delivered • Tissue Engineered Matrix (TEM)-<i>in vitro</i> synthesis of a natural-like ECM • Mechanical, chemical, and biochemical features of the construct will stimulate and direct the host's native regeneration capabilities • Controlled and tailored properties • Easy, reproducible and less expensive formulation • Less prone to infections or contaminations
Disadvantages	<ul style="list-style-type: none"> • Time-consuming, need of cell harvest, expansion, repeated manipulation, potential infection • Decellularized products, related toxicity and calcium nucleation sites mainly if using GA cross-linking • Multilineage commitment of exogenous stem/progenitor cells can favor undesired phenotypes • Undesired phenotypes in recruited cells including myofibroblast profiles. Leaflet contraction • Possible immunotherapy for allogenic cells. Autologous cells are not ideal for old patients or patients with CVD • Product heterogeneity depending on baseline characteristic of the donor • Potential malignant transformation of derived cells • Immunogenic response if decellularization process not completed • Optimal cell type/s to be determined • Advanced Therapy Medicinal Product-GMP regulations for cell product and scaffold may make more complicate to transfer the results from the bench to the bedside • Potential modification of prosthesis geometry in tailored prosthesis 	<ul style="list-style-type: none"> • TEM limitations-decellularization (and cross-linked) product, related toxicity and creation of calcium nucleation sites. Some could be not cross-linked • Lower capability of stem/progenitor reparative cell recruitment due to underlying impaired mobilization: physiologic reparative and regenerative processes must be lower under certain clinical conditions causing VHD • Thrombogenicity in collagen-based exposed surfaces needing of rapid <i>in vivo</i> re-endothelisation in hypercoagulable diseases • Limited capability to modify diseased phenotype of recruited resident cells, mostly subjected to the physical properties of the scaffold. • Myofibroblast phenotype activation and leaflet contraction • Time-limited delivery of drugs or growth factors • Prosthesis-patient mismatch in off-the-shelf products • Toxicity of degradation products. Induction of inflammatory response • Difficult balance among hydrolytic polymer degradation and tissue formation in a systemic pathological environment which can drastically modify mechanical and biochemical properties

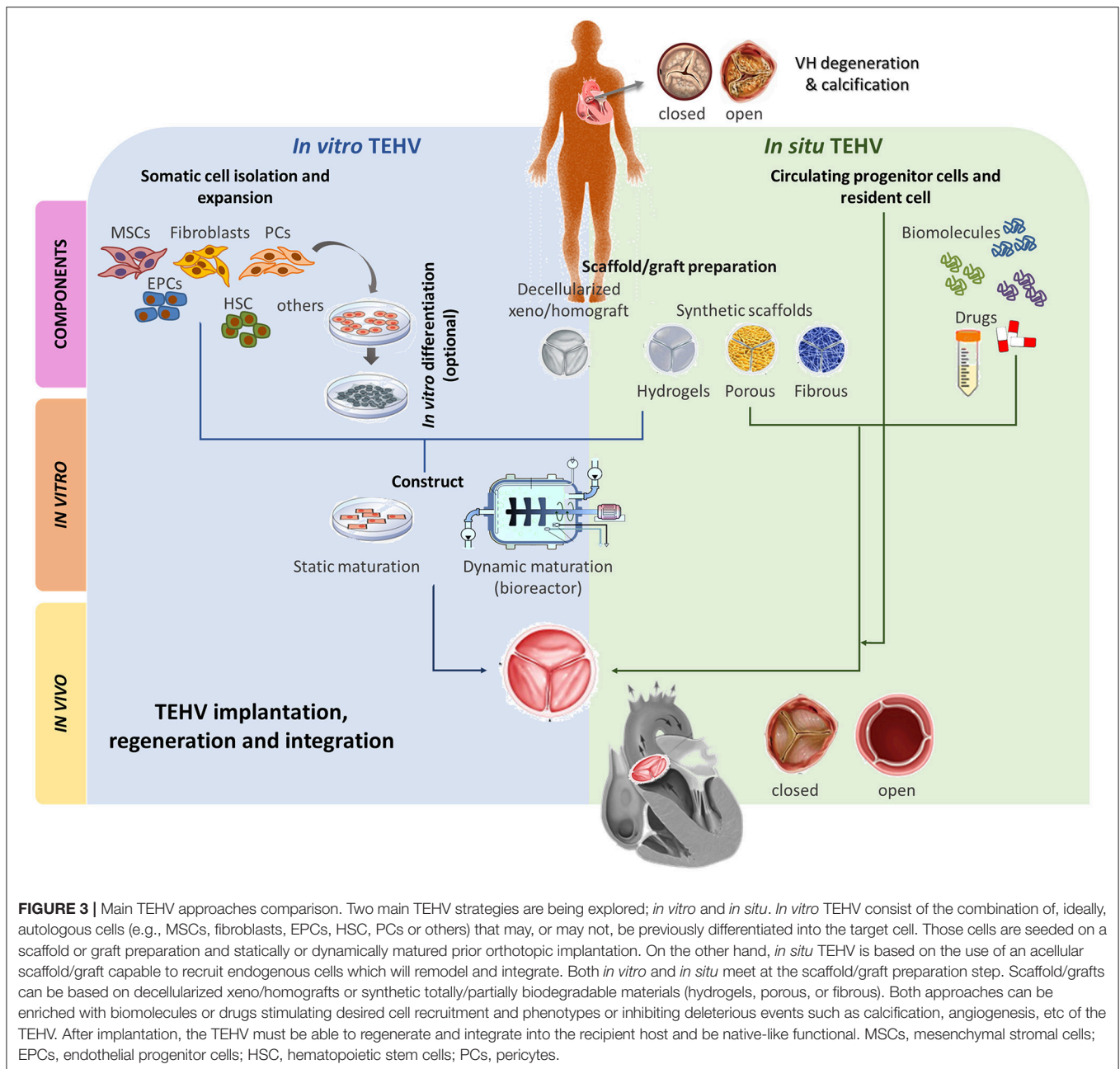
In green color are highlighted the potential advantages; in red color the potential disadvantages. HV, heart valve; ECM, extracellular matrix; GA, glutaraldehyde; TEHV, Tissue Engineered Heart Valve; GMP, good manufacturing practice; CVD, cardiovascular disease.

SCAFFOLDS FOR *IN VITRO* TEHV

Intuitively, the best scaffold/graft to comply with all the requirements of TEHV would be the native aortic valve-derived ECM or similar biological composites. Commercially available bioprostheses are being currently tested as cell carriers thanks to significant improvements in decellularization protocols, which include novel cross-linking procedures to increase pliability while avoiding calcification (138). For instance, glutaraldehyde fixation replaced by heparin has shown to ameliorate valve prosthetic calcification rates probably by blocking calcium phospholipid binding sites as well as to inhibit thrombosis (108, 139). Other cross-linking alternatives are the reduction of free amine groups

and targeting free aldehydes by using reducing agents capable of forming Schiff bases which may allow for glycosaminoglycans and elastin stabilization, avoid collagen deformation and inhibition of calcium binding (138).

As anticipated above, the typical *in vitro* approach is to seed cells on a scaffold, and induce differentiation and ECM synthesis. However, it has been demonstrated that respiring cells on the scaffold periphery and the size of the scaffold can restrict oxygen and nutrients availability at the center of the tissue, leading to areas of necrosis and degeneration(140). Different procedures have been proposed to circumvent this problem, including mechanical compression (141) and flow perfusion (142). The implementation of dynamic systems, such



as use of bioreactors, before implantation into the recipient host may give better results than static systems and considerably contribute to maintain viability of the three-dimensional TEHVs supporting its maturation. Mature grafts/scaffolds might be easier to integrate into the recipient’s heart and to acquire the definitive native features of a living valve (143–145) (Figure 3). However, dynamic culture conditions can also negatively impact cell differentiation and tissue formation. Since two intermediates products are combined in the final Investigational Medicinal Product [definition provided in Directive 2001/20/EC, Article 2 (d)], it is vital the latter is checked for quality and quantity before implantation.

Cell Types for *in vitro* TEHV

Cells represent the biological component of the TEHV, e.g., the ones supposed to confer living properties. The optimal cell type for valve engineering should be non-immunogenic and able to maintain its specialized function or gain such a specialization through differentiation. Autologous cells are the first choice, but they show significant dysfunctions if obtained from old patients or patients with cardiovascular diseases (146), while allogenic cells might be immunogenic (147). Induced pluripotent stem cells (iPSCs) generated by reprogramming somatic cells would be the ultimate solution for patient-tailored therapy but there are still several concerns (148). Hence, differentiated cells or

progenitor cells, including VICs, VECs, MSCs, BM-mononuclear cells (MNCs), fibroblasts or EPCs, remain a safer option thus far. We will go through some examples (144, 149–155) here which are further summarized in **Table 2**.

Two main scopes are followed for graft repopulation: (i) to recreate the internal biologic environment of a valve and (ii) to provide them with an EC coverage. Short-term follow-up studies in sheep and primates showed the potential advantage of repopulating the core of scaffolds/grfts with VICs or MSCs (156, 179–181). However, other aspects such as the prone differentiation into myofibroblast or osteoblast phenotypes must be considered and is discussed below for the main cell sources explored so far.

Mesenchymal Stem Cells (MSC)

MSC with different origins seems to be a consistent choice for the TEHV's cellularization since the VIC represents a heterogeneous population of cells sharing a mesenchymal ancestor. Moreover, the VIC shares phenotypic commonalities with VSMC and fibroblasts, that could be achieved by MSC differentiation as confirmed by antigenic expression (21, 22, 156, 157). In addition, MSCs are easy to be harvested and expanded *in vitro*, and there are multiple tissue sources (e.g., bone marrow, adipose tissue, peripheral blood, umbilical cord blood, umbilical cord, and placenta or amniotic fluid). Both animal and human studies support the immunoprivileged state of the MSC and evidences their unique immunomodulatory characteristics. Accordingly, the MSC is nowadays the preferred cell of choice for *in vitro* TEHV and the several studies in animal models account for that (147, 182). Since MSCs are progenitor stem cells able to differentiate in all the valvular cell phenotypes, they can overcome the issue of primary cells harvested from old and sick patients (147). Finally, unlike other stem cells, MSCs do not develop teratomas and there are not ethical concerns as for the embryonic stem cells (ESCs) (183).

MSC-bioengineered valves differentiated through conditioning in biomimetic and dynamic environments have shown physiologic profiles in terms of ECM composition (e.g., higher amounts of collagen type I and III), mechanical properties and VIC/myofibroblast markers expression (147, 183). These studies have also shown the influence of chemical, flow, and flexural stimuli on the cell phenotype expression and synthesis capabilities, also demonstrating an enhanced outcome of their synergic action. Moreover, MSC preserve their phenotype plasticity, being able to express endothelial or mesenchymal markers in response to different biochemical and mechanical stimuli (157). No evidence of glycosaminoglycans synthesis has been demonstrated by MSCs, but that issue could be circumvented by an additional stimulation with concomitant insulin and hypoxic conditioning (184). *In vivo* experiments performed on rat, sheep, and canine models have confirmed the positive *in vitro* outcomes. MSCs differentiation and different secretion of ECM components were mirroring the native structure (156). Cell labeling of implanted cells has also suggest their active collaboration in tissue regeneration (152, 153). However, performance issues, such as regurgitation and leaflets mobility restriction, have been found in some MSC-bioengineered substitutes (158).

Animal model, mainly pig and sheep, can give some help to test the valve ability to withstand some aspect of the immune reaction and calcification. Sheep model are preferred because of their valve anatomy similarity with humans, and the slower growth pace compared to the pigs. Moreover, juvenile sheep models represent the worst-case scenario to evaluate calcification because of the high level of calcium and phosphorous in the serum. However, they do not consider all the peculiarity of the human immune system. For instance, sheep have reduced platelet activity than the humans (185). Therefore, many *in vivo* studies ended up in failures when translated to clinical practice (186, 187). Comparison studies attempted to determine the superiority of available cells products, in particular, MSCs vs. other cell types, such as BM-mononuclear cells (MNCs) or CD133⁺ aortic-derived cells (144, 154, 188). An interesting report from Vincentelli et al. (154) compared the efficacy of MSC- or MNC-engineered TEHVs implanted in lambs. Both cell groups promoted the re-endothelization of the TEHV through recruitment by the recipient's ECs after 4 months implantation. However, MNC-seeded valves caused leaflet thickening, retraction, inflammation and calcification, while the MSC-seeded valves displayed a α SMA⁺ cellularization with no signs of calcification.

Controversial results have been observed in humans and the therapeutic use of MSCs (188). Modest or null benefit has been documented in clinical trials using BM-MSCs (189, 190). In the context of VHD, experiments are mostly limited to *in vitro*, static or dynamic, TEHV cellularization (185, 186). The experimental results of human *in vitro* studies are aligned with the animal-derived MSCs *in vitro* models. Dynamic culture enhanced the construct mechanical properties, which were comparable to the native valves; tissue formation and organization; endothelialization; and native-like markers patterns (150). Different mechanical stimuli, or different intensity of them, promote several MSC behaviors such as migration or differentiation (144). For example, media enriched with VEGF and high shear stress leads to endothelial phenotype differentiation (191, 192). Concerns also surround the stability of the acquired phenotypes and the potential unwanted fibrotic overgrowth causing retraction and regurgitation of the TEHV. In fact, osteogenic markers (such as alkaline phosphatases, osteopontin, and osteonectin) have been found expressed in the implanted graft, suggesting the susceptibility to prosthetic valve calcification (132, 147). Pro-osteogenic cells may influence resident VICs to acquire similar properties, thus raising concerns about their transplantation into pro-calcifying environments.

Endothelial Progenitor Cells (EPCs)

Similarly to the MSCs, the endothelial progenitor cells (EPCs) have broaden differentiation potential and can be supplied by non-surgical procedures, since they can be isolated from peripheral and umbilical cord blood (147). EPCs are particularly interesting because of their capability to differentiate into EC and to contribute to vascular regeneration and development as well as to neovascularization processes after limb or myocardial ischemia (193). Moreover, EPCs can undergo EMT processes to acquire a VIC-like phenotype under determinate stimuli (e.g., growth factors such as TGF β 1 or mechanical conditioning) and

TABLE 2 | Different cell type candidates for *in vitro* TEHV.

Cell type	Scaffold type	Experiment stages	Therapeutic activity	Outcome	Reference
<p>MSCs</p> <ul style="list-style-type: none"> Autologous BM-MSCs 	<ul style="list-style-type: none"> Nonwoven PGA/PPLA blend melt extruded into sheets assembled to valvular shape 	<ul style="list-style-type: none"> <i>In-vitro</i> dynamic for 4 weeks <i>in-vivo</i> autologous in sheep up to 8 months 	<ul style="list-style-type: none"> Histology resembles the native tissue: elastin on the ventricularis side and collagen on the fibrosa side vimentin expressed throughout the scaffold as native tissue α-SMA expressed only in subendothelial layer (as native t) Continuous layer of vWF+ cells on the surfaces 	<ul style="list-style-type: none"> Closer to native tissue stiffness after 4 weeks. Burst resistance higher than native tissue Extensive remodeling <i>in-vivo</i>, layering and differentiation MSCs phenotype expression and synthesis mirrored the native tissue 	(156)
<p>Autologous BM-MSCs cultured in two different media:</p> <ul style="list-style-type: none"> EGM-2 for ECs differentiation M199 for myofibroblast differentiation 	<ul style="list-style-type: none"> Decellularized porcine pulmonary valves 	<ul style="list-style-type: none"> <i>In-vitro</i> static <i>in-vivo</i> canine model up to 1 week (pulmonary position) and 3 weeks (aortic position) 	<ul style="list-style-type: none"> CD31+ layer on the leaflets surface Sporadic presence of α-SMA+ cells in the interstitial region 	<ul style="list-style-type: none"> Leaflets were intact, with no evidence of thrombus formation. Cellular coverage of leaflet surface and interstitial region repopulation 	(153)
<p>Juvenile sheep BM-MSCs (α-SMA and vimentin +)</p>	<ul style="list-style-type: none"> Nonwoven PGA:PPLA (50:50) scaffold 	<ul style="list-style-type: none"> <i>In-vitro</i> static up to 4 days <i>In-vitro</i> pulsatile flow with flexure stimulus (combined or not) up to 3 weeks 	<ul style="list-style-type: none"> Weak fibronectin and collagen I expression, high collagen III Higher expression of α-SMA, CD31, vWF, and laminin (ECs markers apart α-SMA) on the surface compared with interstitium Significant decrease of DNA content compared to native tissue Higher DNA content in the flexure-flow sample than in the other ones Higher S-GAG content in flex-flow samples 	<ul style="list-style-type: none"> Tissue formation and cellularity was higher in flex-flow samples by three weeks Confirmed positive synergy of flexure and flow stimuli by SEM, H&E, DNA and collagen content assay ECs markers might be the cause of a reduced collagen/cell ratio in the flex-flow samples Phenotype plasticity of MSCs 	(157)
<p>Non-selected lamb BM-MNCs</p> <p>Non-selected lamb BM-MSCs</p>	<ul style="list-style-type: none"> Decellularized porcine pulmonary valves 	<ul style="list-style-type: none"> <i>In-vivo</i> in lambs up to 4 months 	<ul style="list-style-type: none"> In both groups, complete layer of vWF+, and α-actin+ cells demonstrated the presence of a thin ridge of SMCs, more pronounced in the MSC group In adventitia and media of BM-MNCs group the ECM was disorganized with a strong macrophages infiltration (CD68); in adventitia many neo-vessels were present In adventitia of BM-MSCs group the global organization of collagen fibers was preserved, rare neo-vessels were visible No inflammatory cells were found in MSC group 	<ul style="list-style-type: none"> No significant pulmonary regurgitation was recorded at any timepoint BM-MNCs group: wall thickening, calcifications, fibrous pannus covering the suture line; leaflets slightly thickened and retracted BM-MSCs group: no calcifications, wall remained thin and smooth, no fibrotic pannus on the suture lines, thin leaflets 	(154)
<p>Autologous sheep BM-MSCs</p>	<ul style="list-style-type: none"> Nonwoven poly(lactic-co-glycolic acid) PLGA sheets assembled to valvular shape by needle punching 	<ul style="list-style-type: none"> <i>In-vitro</i> dynamic for 1 month <i>In-vivo</i> in sheep up to 20 weeks 	<ul style="list-style-type: none"> No inflammatory cells were found in MSC group 	<ul style="list-style-type: none"> 9 early dead out of 19 animals, mainly due operatory and anesthesia complications Trivial regurgitation at implant, increased with time to sever in some animals Leaflets immobilization, and dimensional decrease at 10 weeks Acquired native conduit curvature Conduit diameter remained stable 	(158)

(Continued)

TABLE 2 | Continued

Cell type	Scaffold type	Experiment stages	Therapeutic activity	Outcome	Reference
<ul style="list-style-type: none"> • Sheep BM-MSCs 	<ul style="list-style-type: none"> • Nonwoven PGA/PLLA 50:50 scaffold sewn around a plastic frame • Basic fibroblast growth factor (bFGF) and ascorbic acid-2-phosphate (AA2P) addition 	<ul style="list-style-type: none"> • <i>In-vitro</i> static up to 3 weeks • <i>In-vitro</i> dynamic (pulsatile flow combined with flexural stimulus-CFF) up to 3 weeks 	<ul style="list-style-type: none"> • Higher collagen I & III for bFGF/AA2P samples • Collagen fibers alignment after 6 weeks static • 4-fold increase in collagen production due to dynamic conditions • 3-fold increase in collagen production due to bFGF/AA2P addition • CFF conditioning increased collagen production by 12% in bFGF/AA2P samples 	<ul style="list-style-type: none"> • Enhanced tissue formation for the bFGF/AA2P samples vs. the basal medium ones • Loss of cellularity (DNA content) with time, possibly due to inefficient cell attachment on absorbed serum proteins, but dynamic condition could keep the DNA level steady • Decreasing of GAG production over time 	(159)
<ul style="list-style-type: none"> • For the scaffold production: ovine vascular-derived cells • Final cellularization: BM-MSCs 	<ul style="list-style-type: none"> • Nonwoven PGA mesh coated with 1.75 % solution of P4HB integrated in nitinol stent 	<ul style="list-style-type: none"> • <i>In-vitro</i> static up to 3 days from MSC seeding 	<ul style="list-style-type: none"> • Abundant amount of crosslinked collagen • 99% of DNA reduction after decellularization • Significant reduction of glycosaminoglycans • No reduction of hydroxyproline • No differences between radial and circumferential direction in the tensile tests • Treated scaffold: uniform luminal WF+, CD34+ under the endothelium (EPCs), large amount of α-SMA in the adventitia, few mononuclear cells and macrophages infiltration (CD45+ and CD68+) • Untreated scaffold: sporadic WF+, no CD34 detected, large amount of α-SMA in the adventitia, few mononuclear cells and macrophages infiltration (CD45+ and CD68+) 	<ul style="list-style-type: none"> • Decellularization of vascular derived cells and MSCs seeding hampered leaflets retraction • Valve dynamic performance improved by decellularization • 18 months storage did not affect histological appearance and mechanical properties • 100% patency and no evidence of stenosis at 4 weeks • Treated scaffold: continuous endothelium, reduced platelet adhesion • Untreated scaffold: no endothelialization 	(160)
<ul style="list-style-type: none"> • Rat BM-MSCs 	<ul style="list-style-type: none"> • Decellularized rat aortic valvular conduit w/w or w/o a multilayer of heparin + SDF-1α 				(152)
<ul style="list-style-type: none"> • Human BM-MSCs 	<ul style="list-style-type: none"> • PGA/P4HB composite 	<ul style="list-style-type: none"> • <i>In-vitro</i> static to <i>in-vitro</i> dynamic (pulse duplicator) conditioning 	<ul style="list-style-type: none"> • H&E showed cellular tissue organized in a layered fashion, with a dense outer layer and lesser cellularity in the deeper portions after 14 days in the pulse duplicator. • Positive staining for collagen types I, III, α-SMA, and vimentin. • No positive staining for desmin, collagen types II and IV. • Myofibroblasts-like actin/myosin filaments, collagen fibrils and elastin fiber networks 	<ul style="list-style-type: none"> • All leaflets were intact, mobile, pliable; and the constructs were competent during valve closure • Static controls showed a loose, less organized tissue formation with irregular cellular ingrowth • <i>In-vitro</i> dynamic conditioned valves comparable to those of native human semilunar valve. Static controls significantly weaker • Confluent endothelial layer in the dynamic <i>in-vitro</i> conditioned samples, static samples with non-confluent endothelial layer • Not achieved typical three-layered structure 	(150)
<ul style="list-style-type: none"> • Human putative BM-MSCs 	<ul style="list-style-type: none"> • Decellularized porcine aortic valve homograft 	<ul style="list-style-type: none"> • <i>In-vitro</i> static 	<ul style="list-style-type: none"> • Homograft seeded cells were α-SMA, vimentin positive and desmin negative • Seeded cells expressed osteopontin, osteonectin, alkaline phosphatases • Leaflets shrank by 85% 	<ul style="list-style-type: none"> • These cells have good potential for tissue engineering because of their plasticity • Osteogenic markers on reseeded cells were attributed to the prolonged static culture without the proper mechanical cues • Good migration rate of the reseeded cells 	(161)

(Continued)

TABLE 2 | Continued

Cell type	Scaffold type	Experiment stages	Therapeutic activity	Outcome	Reference
<ul style="list-style-type: none"> Human mesenchymal progenitors from prenatal chorionic villus specimens Human EPCs from postnatal umbilical cord blood 	<ul style="list-style-type: none"> Sheets of nonwoven mesh PGA dip coated in a 1% (w/v) solution of P4HB shaped in valve fashion 	<ul style="list-style-type: none"> <i>In-vitro</i> dynamic up to 4 weeks 	<ul style="list-style-type: none"> Markers expression (vimentin, α-SMA positive, desmin negative) matching the native tissue TEHV presented collagen on the surfaces and GAG in the interstitium whereas native tissue had more homogeneous distribution GAGs amount comparable, DNA 68%, and hydroxyproline 14% of the native tissue Better mechanical performance of mechanically stimulated constructs 	<ul style="list-style-type: none"> Tissue organization comparable with native neonatal valves Good ingrowth of mesenchymal progenitors from prenatal chorionic villus and complete coverage of EPCs 	(162)
<ul style="list-style-type: none"> Human MSCs 	<ul style="list-style-type: none"> Decellularized ovine aortic valves 	<ul style="list-style-type: none"> Group A: static <i>In-vitro</i> dynamic (pulse duplicator) conditioning with different pressure patterns: <ul style="list-style-type: none"> Group B: cyclic negative pressure up to 72h Group C: cyclic negative pressure up to 72h, cyclic positive pressure up to 10 days 	<ul style="list-style-type: none"> Compared to group A (static conditioning): Group B overexpressed ACTA2 and HSP47/SERPINH2 (VICs), RUNX2 (osteoblast marker), MKI67 (proliferation marker), and BAX (apoptosis marker). Downregulation of ACAN (chondrocytes marker) Group C overexpressed CD90, CD105, and CD29 (MSC marker); and BGLAP (osteoblast marker) in addition to those of group B vWF negative in all groups 	<ul style="list-style-type: none"> MSCs infiltration into the leaflets Mechanical behavior more closely resembled that of the cryopreserved leaflet than that of the decellularized leaflet 	(144)
EPCs					
<ul style="list-style-type: none"> Autologous EPCs from ovine peripheral blood Ovine valve-derived ECs 	<ul style="list-style-type: none"> Sheets of non-woven mesh PGA dip coated in a 1% (w/v) solution of P4HB 	<ul style="list-style-type: none"> <i>In-vitro</i> static 	<ul style="list-style-type: none"> VEGF exposed ECs and EPCs have enhanced proliferation TGF-β1 induces trans-differentiation to mesenchymal phenotype (α-SMA+) Valve-derived ECs have traces of spontaneous trans-differentiation, which attunes them with the trans-differentiation during valvulogenesis 	<ul style="list-style-type: none"> Seeded cells respond (proliferate) to VEGF (valve-derived ECs have attenuated response) TGF-β1 induces trans-differentiation to mesenchymal phenotype 	(163)
<ul style="list-style-type: none"> Autologous EPCs from ovine peripheral blood Ovine vascular ECs Ovine SMCs as control 	<ul style="list-style-type: none"> Sheets of nonwoven mesh PGA dip coated in a 1% (w/v) solution of P4HB sewed to form valvular conduit shape 	<ul style="list-style-type: none"> <i>In-vitro</i> dynamic up to 21 days 	<ul style="list-style-type: none"> CD31 and VEGF-R2 positive cells on the luminal surface α-SMA+ into the interstitium, sign of trans-differentiation (EMT) vWF positive cells throughout the valve conduit Decrease of DNA and collagen content at 21 days compared with 7 days Increased S-GAG content at 21 days Interstitium with less ECM and more scaffold leftovers Metalloproteinases (MMPs) and their inhibitors (TIMPs) concentration decreased with time, allowing ECM build-up 	<ul style="list-style-type: none"> Cellular ingrowth throughout the scaffold TE valve marker expression similar to native valve, with mesenchymal profile in the interstitium Seeded scaffolds have 4.1-fold greater stiffness than the unseeded constructs CD31+ and α-SMA+ cells have native-like spatial distribution Suspected lack of nutrient diffusion inside the scaffold Arterial-derived cells seeded scaffold showed loss of structural integrity Many of the hallmarks of the initial stage of valvulogenesis are seen in this study The construct underwent a developmental event 	(164)

(Continued)

TABLE 2 | Continued

Cell type	Scaffold type	Experiment stages	Therapeutic activity	Outcome	Reference
<ul style="list-style-type: none"> • Mononuclear bone marrow cells and peripheral blood EPCs cultured in fibroblast and endothelial inducing media respectively • Autologous jugular vein myofibroblasts + carotid artery ECs as a comparison 	<ul style="list-style-type: none"> • P(L,D,L)LA (Poly(L-lactide-co-D,L-lactide)) multifilament fibers using a 3-dimensional valve-shaped cast and thermal fixation. Surfaces coated with P(L,D,L)LA 	<ul style="list-style-type: none"> • <i>In-vitro</i> static sequential seeding; following, <i>in-vitro</i> dynamic; and finally, <i>in-vivo</i> in sheep model up to 8 weeks 	<ul style="list-style-type: none"> • eNOS positive on surface, α-SMA expression detected on the surface and in the interstitium. • Good GAG deposition • No detectable amount of elastin 	<ul style="list-style-type: none"> • Leaflets thickening, lowering pressure gradient with time, and minimal regurgitation • No indication of immune reaction • Discontinuous endothelial with bits of fibrous material deposition • Absence of elastin might have caused reduced pliability 	(151)
<ul style="list-style-type: none"> • Autologous sheep EPCs 	<ul style="list-style-type: none"> • Decellularize porcine pulmonary valves 	<ul style="list-style-type: none"> • <i>In-vitro</i> static seeding; then, <i>in-vitro</i> dynamic conditioning; and finally, <i>in-vivo</i> in sheep model up to 3 months 	<ul style="list-style-type: none"> • EPCs scaffold were let express ECs markers in EGM media before scaffold seeding • MMP9 was found in CD133-conjugated scaffolds 	<ul style="list-style-type: none"> • CD133-conjugated scaffold were repopulated better <i>in-vivo</i> than already seed scaffolds 	(165)
<ul style="list-style-type: none"> • Human EPCs from umbilical cord blood • Human Wharton's jelly-derived myofibroblasts 	<ul style="list-style-type: none"> • Sheets of nonwoven mesh PGA dip coated in a 1% (w/v) solution of P4HB and attached to ring-shaped supports 	<ul style="list-style-type: none"> • <i>In-vitro</i> dynamic with static as control 	<ul style="list-style-type: none"> • Growth factors addition resulted: in GAGs amount comparable with native tissue, DNA 65% of native tissue, hydroxyproline 16% of native tissue • No traces of elastin 	<ul style="list-style-type: none"> • Dense cell coverage and leaflet pliable • Phenotype differentiation and tissue organization just in biochemical stimulated construct • Mechanical stimulation enhanced scaffold mechanical properties • Worthon's jelly-derived myofibroblasts might have enhanced tissue ECM production and organization 	(166)
<ul style="list-style-type: none"> • Human EPCs from venous blood 	<ul style="list-style-type: none"> • Decellularized porcine aortic, valve heparin and VEGF coated 	<ul style="list-style-type: none"> • <i>In-vitro</i> static up to 48h 	<ul style="list-style-type: none"> • Coated valves had higher number of adherent cells • Higher proliferation rate on the coated valves • Higher migration rate on the coated valves 	<ul style="list-style-type: none"> • Coated valves had higher number of adherent cells • Higher proliferation rate on the coated valves • Higher migration rate on the coated valves 	(167)
<ul style="list-style-type: none"> • Autologous human EPCs from peripheral blood (mononuclear fraction) 	<ul style="list-style-type: none"> • Decellularized human pulmonary valves from cadaver 	<ul style="list-style-type: none"> • <i>In-vivo</i> human trial on 2 pediatric patients, follow-up to 42 months 	<ul style="list-style-type: none"> • Peripheral blood mononuclear cells were expressing CD31, vWF, VEGF-R2 	<ul style="list-style-type: none"> • No arrhythmia or any other problems in the follow-up • Somatic growth of both the valves and the patients • Trivial regurgitation after 1 year • No signs of malformation • Normal transvalvular gradient 	(168)
<ul style="list-style-type: none"> • Human mesenchymal progenitors from prenatal chorionic villus specimens • Human EPCs from postnatal umbilical cord blood 	<ul style="list-style-type: none"> • Sheets of nonwoven mesh PGA dip coated in a 1% (w/v) solution of P4HB shaped in valve fashion 	<ul style="list-style-type: none"> • <i>In-vitro</i> dynamic up to 4 weeks 	<ul style="list-style-type: none"> • Markers expression (vimentin, α-SMA positive, desmin negative) matching the native tissue • TEHV presented collagen on the surfaces and GAG in the interstitium whereas native tissue had more homogeneous distribution • GAGs amount comparable, DNA 68%, and hydroxyproline 14% of the native tissue • Better mechanical performance of mechanical stimulated constructs 	<ul style="list-style-type: none"> • Tissue organization comparable with native neonatal valves • Good ingrowth of mesenchymal progenitors from prenatal chorionic villus and complete coverage of EPCs 	(162)

(Continued)

TABLE 2 | Continued

Cell type	Scaffold type	Experiment stages	Therapeutic activity	Outcome	Reference
<ul style="list-style-type: none"> Human amniotic fluid mononuclear cells split in CD133+/- Human CD133+ to differentiate in ECs (VEGF, hFGF, R-3-IGF-1) Human CD133- to differentiate into mesenchymal cells (hFGF, R-3-IGF-1, GA-1000, ascorbic acid, 20% fetal bovine serum) Human EPCs from cord blood 	<ul style="list-style-type: none"> Sheets of nonwoven mesh PGA dip coated in a 1% (w/v) solution of P4HB shaped in valve fashion 	<ul style="list-style-type: none"> Sequential seeding, followed by <i>in-vitro</i> dynamic culture up to 28 days 	<ul style="list-style-type: none"> TEHV presented collagen on the surfaces and GAG in the interstitium DNA amount comparable, GAG 80%, and hydroxyproline 5% of the native tissue 	<ul style="list-style-type: none"> Valve had homogeneous thickness Mechanical properties did not reach the physiological values, probably due to the low amount of hydroxyproline 	(169)
<ul style="list-style-type: none"> Porcine decellularized heart valves functionalized with RGD, VEGF, PEG 	<ul style="list-style-type: none"> Porcine decellularized heart valves functionalized with RGD, VEGF, PEG 	<ul style="list-style-type: none"> <i>In-vitro</i> 		<ul style="list-style-type: none"> Functionalized scaffolds had enhanced early attachment Functionalized scaffold favors the proliferation, a cell spread cell morphology, and a complete endothelialization 	(170)
iPSCs					
<ul style="list-style-type: none"> Human skin fibroblast reprogrammed into iPSCs, then, differentiated into MSCs Human iPSCs differentiated into MSCs 	<ul style="list-style-type: none"> Decellularized human pulmonary valve PEGDA coated dishes and 3D PEGDA hydrogels 	<ul style="list-style-type: none"> <i>In-vitro</i> up to 14 days <i>In-vitro</i> up to 20 days 	<ul style="list-style-type: none"> iPSCs-MSCs have twice the proliferation rate of BM-MSCs iPSCs-MSCs on surface expressed α-SMA, whereas iPSCs-MSCs in the interstitium did not 3D PEGDA cultured iMSCs had similar α-SMA expression to VICs iMSCs had higher level of collagen expression 3D PEGDA cultured iMSCs had lower expression of calponin compared to VICs 	<ul style="list-style-type: none"> iPSCs-MSCs produced ECM (glycosaminoglycans and collagen) iPSCs-MSCs shown several similarities to VICs 3D PEGDA cultured iMSCs had similar α-SMA expression to VICs 	(171) (172)
VICs and VECs					
<ul style="list-style-type: none"> VICs from porcine aortic valve VICs from porcine aortic valve 	<ul style="list-style-type: none"> Fibronectin or collagen or heparin coated wells 	<ul style="list-style-type: none"> <i>In-vitro</i> 	<ul style="list-style-type: none"> VICs seeded on fibronectin coated wells in presence of TGF-β1 are activated and stimulated to produce stress fibers and express α-SMA Heparin increases TGF-β1 production in VIC monolayer culture 5% serum for 12h improved the VICs proliferation on the scaffolds Stiffer surfaces enhanced myofibroblastic activity of VICs MMP1 biodegradable hydrogels allowed migration and cell spreading, higher with less crosslinked hydrogels Good proliferation, 7 days of doubling time 	<ul style="list-style-type: none"> VICs seeded on fibronectin coated wells in presence of TGF-β1 are activated and stimulated to produce stress fibers and express α-SMA Heparin increases TGF-β1 production in VIC monolayer culture 5% serum for 12h improved the VICs proliferation on the scaffolds Stiffer surfaces enhanced myofibroblastic activity of VICs MMP1 biodegradable hydrogels allowed migration and cell spreading, higher with less crosslinked hydrogels Good proliferation, 7 days of doubling time 	(173) (174)
<ul style="list-style-type: none"> VICs from porcine aortic valve VICs from porcine aortic valve 	<ul style="list-style-type: none"> Porcine decellularized leaflets Functionalized PEG hydrogel: four-arm poly(ethylene glycol) (PEG) chains connected with enzymatically degradable peptides and RGD 	<ul style="list-style-type: none"> <i>In-vitro</i> <i>In-vitro</i> 	<ul style="list-style-type: none"> RGD increase the spreading TGF-β1 increases α-SMA and collagen I expression 		(175)

(Continued)

TABLE 2 | Continued

Cell type	Scaffold type	Experiment stages	Therapeutic activity	Outcome	Reference
<ul style="list-style-type: none"> • VICs from porcine aortic valve 	<ul style="list-style-type: none"> • Different ratios Polyacrylamide/bisacrylamide coated wells to have different substrate stiffness 	<ul style="list-style-type: none"> • <i>In-vitro</i> 	<ul style="list-style-type: none"> • TGF-β1 did not impact cell density or morphology. On the other hand, it did influence cell spreading, and α-SMA expression • Bigger cells expressed more α-SMA • VEGF-exposed ECs and EPCs have enhanced proliferation • TGF-β1 induces trans-differentiation to mesenchymal phenotype (α-SMA expression) • Valve-derived ECs have traces of spontaneous trans-differentiation, which attunes with the trans-differentiation during valvulogenesis 	<ul style="list-style-type: none"> • Higher substrate stiffness increased cell spreading (84) and influenced morphology (cytoskeletal organization and focal adhesion arrangement) 	(84)
<ul style="list-style-type: none"> • Autologous EPCs from ovine peripheral blood • Ovine valve-derived ECs 	<ul style="list-style-type: none"> • Sheets of nonwoven PGA mesh dip coated in a 1% (w/v) solution of P4HB 	<ul style="list-style-type: none"> • <i>In-vitro</i> 	<ul style="list-style-type: none"> • VEGF-exposed ECs and EPCs have enhanced proliferation • TGF-β1 induces trans-differentiation to mesenchymal phenotype (α-SMA expression) • Valve-derived ECs have traces of spontaneous trans-differentiation, which attunes with the trans-differentiation during valvulogenesis 	<ul style="list-style-type: none"> • Seeded cells respond (proliferate) to VEGF (valve-derived ECs have attenuated response) • TGF-β1 induces trans-differentiation to mesenchymal phenotype 	(163)
<ul style="list-style-type: none"> • Model 1: porcine aortic VICs • Model 2: porcine aortic VICs + lining of porcine aortic VICs 	<ul style="list-style-type: none"> • Collagen gel 	<ul style="list-style-type: none"> • <i>In-vitro</i> dynamic in a parallel plate flow chamber up to 96 h at shear stress of 20 dyne/cm² 	<ul style="list-style-type: none"> • Change of VICs alignment under the flow • VICs in Model 2 migrated toward the surface, perhaps due to the addition diffusion barrier made by the VECs • Model 2 had lost cells, Model 1 no • Model 2 increased the protein content under flow • Vimentin is maintained in both models • α-SMA was less in Model 2 • VECs maintained their phenotype in Model 2 	<ul style="list-style-type: none"> • VECs downregulates α-SMA in VICs • Model 1 static proliferation can resemble the wound healing process (no VECs) 	(73)
<ul style="list-style-type: none"> • Sheep VICs • Sheep VECs • Sheep CAECs • Sheep EPCs from peripheral blood • Human cord blood EPCs (hcbEPCs) • Human dermal microvascular ECs (hDMECs) 	<ul style="list-style-type: none"> • Flasks 	<ul style="list-style-type: none"> • <i>In-vitro</i> 	<ul style="list-style-type: none"> • VECs in TGF-β1 rich media got mesenchymal-like phenotype (α-SMA upregulated, CD31 downregulated) • Less than above VECs samples were able to express osteogenic markers in differentiating media 	<ul style="list-style-type: none"> • No endothelial cell type, apart from valvular was able to express osteogenic markers • VECs on leaflets expressed osteocalcin after mechanical stretching 	(72)
<ul style="list-style-type: none"> • Porcine aortic VECs 	<ul style="list-style-type: none"> • Silicone with different stiffness levels 	<ul style="list-style-type: none"> • <i>In-vitro</i> with TGF-β1 subadministration to induce EMT 	<ul style="list-style-type: none"> • Stiffer substrates induced EMT in presence of TGF-β1 shown by spindle-like morphology, VE-cadherin downregulation, and α-SMA upregulation • B-catenin inhibition reduces α-SMA upregulation 	<ul style="list-style-type: none"> • Stiffer substrates induced EMT in presence of TGF-β1 	(85)
<ul style="list-style-type: none"> • Both human and porcine VICs 	<ul style="list-style-type: none"> • Electrospun polyglycerol sebacate (PGS) and PCL blends 	<ul style="list-style-type: none"> • <i>In-vitro</i> 	<ul style="list-style-type: none"> • PGS decrease the contact angle and enhance cell attachment and spreading when blended with PCL • PGS makes the scaffold quicker to degrade • No elastin synthesis 	<ul style="list-style-type: none"> • Slower spreading in PCL scaffolds • VICs produce more ECM in PGS-PCL blends 	(176)

(Continued)

TABLE 2 | Continued

Cell type	Scaffold type	Experiment stages	Therapeutic activity	Outcome	Reference
ECs + MYOFIBROBLASTS/FIBROBLASTS/SMCs					
<ul style="list-style-type: none"> Autologous jugular vein myofibroblasts Carotid artery ECs 	<ul style="list-style-type: none"> Poly (glycolic acid)-(PGA)-Poly-4-hydroxybutyrate(P4HB) stented scaffold 	<ul style="list-style-type: none"> <i>In-vitro</i> dynamic; then, <i>in-vivo</i> in sheep model up to 8 weeks 	<ul style="list-style-type: none"> DNA content 49 ± 24%, GAG content 39 ± 9%, hydroxyproline content 15 ± 6% that of native t. at 4 weeks DNA content 44 ± 18%, GAG content 39 ± 6%, hydroxyproline content 18 ± 3% that of native t. at 8 weeks 	<ul style="list-style-type: none"> Proper opening and closing behavior, minimal regurgitation in 2 animals Leaflet thickening, hosting wall integration Cell attachment and ingrowth Cellular tissue formation and abundant amounts of collagen in the leaflets, no elastin detected, incomplete ECs layer 	(151)
<ul style="list-style-type: none"> Autologous Carotid myofibroblasts Autologous Carotid ECs 	<ul style="list-style-type: none"> PGA/P4HB composite 	<ul style="list-style-type: none"> <i>In-vitro</i> static; then, <i>in-vitro</i> dynamic (pulse duplicator); finally, <i>in-vivo</i> in sheep model up to 20 weeks 	<ul style="list-style-type: none"> Bioreactor conditioning increased organization and layering of the leaflet structure. DNA content (150% that of native t.), collagen (180% that of native t.), GAGs (140% that of native t.), limited elastin traces by 6 weeks. ECs were CD31, vWF positive; myofibroblasts were α-SMA positive 	<ul style="list-style-type: none"> No evidence of thrombus, stenosis, or aneurysm formation up to 20 weeks. Central pulmonary regurgitation (mild to moderate) Increase of the inner diameter of the valve constructs Mechanical properties at 20 weeks were almost indistinguishable from those of native valve tissue 	(149)
<ul style="list-style-type: none"> Autologous iliac crest bone marrow Myofibroblast-like cells Peripheral blood endothelial progenitors 	<ul style="list-style-type: none"> Multi-layered P(L,DL)LA (Poly(L-lactide-co-D,L lactide)) stented scaffold 	<ul style="list-style-type: none"> <i>In-vitro</i> dynamic; then, in sheep model up to 4 weeks 	<ul style="list-style-type: none"> DNA content 86 ± 54%, GAG content 150 ± 11%, hydroxyproline content 26 ± 6% that of native t. at 4 weeks Cellular tissue formation and abundant amounts of collagen in the leaflets, no elastin detected, incomplete ECs layer Cells staining positive for α-SMA were identified mainly in the wall of the explanted valves, but also in the middle of the leaflets On the leaflet surfaces, endothelial nitric oxide synthase (eNOS) expression detected 	<ul style="list-style-type: none"> Proper opening and closing behavior, minimal regurgitation in 2 animals Leaflet thickening, hosting wall integration Cell attachment and ingrowth 	(149)
<ul style="list-style-type: none"> Ovine carotid artery ECs and SMCs Juvenile sheep bone-marrow derived CD133+ cells 	<ul style="list-style-type: none"> Decellularized stented hybrid ovine small intestine submucosa/ porcine pulmonary valve 	<ul style="list-style-type: none"> <i>In-vitro</i> static up to 3 days; then, <i>in-vitro</i> dynamic (pulsatile flow bioreactor); finally, <i>in-vivo</i> in sheep model up to 3 months 	<ul style="list-style-type: none"> A confluent monolayer was demonstrated by CD31-staining in both groups. Immunohistochemistry revealed strong expression of αSMA and an ingrowth into the leaflets in the two groups (higher for CD133+ cells) CD3, CD20, CD45, and CD68 staining confirmed no signs of inflammation in all animals in group 2, whereas in group 1, small amounts of inflammatory tissue were detected in all animals 	<ul style="list-style-type: none"> Valve good opening and closing characteristics in both groups, no or minimal regurgitation, and a low transvalvular gradient (higher in the ECs/SMCs group) Smooth surfaces without any thrombus formation Mild to moderate calcifications in the annular region of the valve stents in group 1, microcalcifications were detected in one of five animals in group 2 	(155)
<ul style="list-style-type: none"> Human foreskin fibroblasts (hFFs) Human adipose derived stem cells (hADSCs) endothelial differentiated (hCFECs) 	<ul style="list-style-type: none"> Decellularized porcine pulmonary valve 	<ul style="list-style-type: none"> <i>In-vitro</i> up to 6 days 	<ul style="list-style-type: none"> hFFs and hCFECs were able to colonize the scaffolds and penetrated at 6 days hCFECs deployed a layer on top 	<ul style="list-style-type: none"> hFFs and hCFECs were able to colonize the scaffolds and penetrated at 6 days hCFECs deployed a layer on top 	(177)

(Continued)

TABLE 2 | Continued

Cell type	Scaffold type	Experiment stages	Therapeutic activity	Outcome	Reference
<ul style="list-style-type: none"> Human vascular ECs and FBs from saphenous vein 	<ul style="list-style-type: none"> Polyurethane PU sheets made with spraying technique 	<ul style="list-style-type: none"> <i>In-vitro</i> sequential static seeding; then, dynamic culture 	<ul style="list-style-type: none"> Increase of cellular adhesion molecules Increase of Collagen 4, VE-Cadherin, and Fibronectin expression after dynamic culture Increase of inflammatory cytokines but the gene expression did not confirm that 	<ul style="list-style-type: none"> Good endothelial lining orientated with the flow Good FBs layer 	(143)
<ul style="list-style-type: none"> Aortic SMCs Aortic adventitial fibroblast/myofibroblast Umbilical vascular endothelial cells (hVECs) in a tri-layered fashion 	<ul style="list-style-type: none"> Nitinol mesh-enclosed leaflets with cell layers embedded in collagen 	<ul style="list-style-type: none"> <i>In-vitro</i> static; then, <i>in-vitro</i> dynamic (pulsatile flow) 	<ul style="list-style-type: none"> SMCs degraded and contracted the collagen but then ECs stopped their action 	<ul style="list-style-type: none"> The leaflets had a correct functioning in the bioreactor 	(178)

ECs, endothelial cells; PGA, polyglycolic-acid; PLLA, poly-L-lactic acid; P4HB, poly-4-hydroxybutyrate; PCL, polycaprolactone; t, tissue; GAGs, glycosaminoglycans; vWF, von Willebrand factor; H&E, haematoxylin eosin; BM, bone marrow; MSCs, mesenchymal stromal cells; PB, peripheral blood; EPCs, endothelial progenitor cells; α -SMA, alpha-smooth muscle actin; eNOS, endothelial Nitric Oxide Synthase; MNCs, mononuclear cells; SMCs, smooth muscle cells; CAECs, coronary artery endothelial cells; SDF-1 α , stromal cell-derived factor-1 α ; VICs, valve interstitial cells; ACTA2, gene codifying for smooth muscle alpha (a)-2 actin; HSP47, SERP1NH2, gene codifying for Serpine (Or Cysteine) Proteinase Inhibitor, Clade H (Heat Shock Protein 47); Member 2; MKI67, gene codifying for marker of proliferation Ki-67; BAX, gene codifying for BCL2 Associated X, Apoptosis Regulator; ACAN, gene codifying for Aggrecan/Chondroitin Sulphate Proteoglycan Core Protein 1; BGLAP, gene codifying for bone Gla protein/osteocalcin; w/w, with; w/o, without; SEM, scanning electron microscope.

therefore offering the possibility of a complete valve regeneration with a single cell type (163, 194, 195). However, EPCs may also contribute to different pathological stages including cancer and diabetes (196, 197) and the ideal antigenic profile remains controversial (165).

In vitro and *in vivo* experiments have demonstrated the ability of the EPCs to colonize the whole TEHV. Importantly, EPCs express both endothelial and mesenchymal lineage markers (CD31 and α -SMA, respectively), spatially arranged in a native-like fashion with a concomitant expression of MMPs and TIMPs, suggesting an active remodeling which recapitulates a developmental-like process (198). The result is a higher mechanical performance than the one achieved by other cell sources (164). No calcification or thrombi were noticed in all the reported studies. Furthermore, EPCs have been implanted on valve leaflets in animal models leading to a reduced infection and discontinuous endothelialization raise concerns about the EPC-based bioengineered devices (151).

In vitro studies conducted on human-derived EPCs show similar results to those found *in vitro* and *in vivo* using animal sources. Human EPCs derived from umbilical cord blood have been co-seeded with Wharton's Jelly-derived myofibroblasts. Biochemical and mechanical stimulations are also necessary to promote the desired native-like mechanical organization, phenotype determination, and functionalization (166, 167, 170). Human EPCs harvested from umbilical cord blood have been also combined with prenatally harvested chorionic villus-derived MSCs to provide a tissue engineered prosthesis for pediatric patients. A good phenotype and mechanical properties of the resulting prosthetic valve was achieved (162).

Clinical studies of re-endothelialization have confirmed the feasibility of correcting pulmonary valve defects using allografts engineered with vein-derived autologous ECs or EPCs (200). To the best of our knowledge, the only one human *in vivo* study took place in Republic of Moldova in 2002 and was published on Circulation in 2006. Two pediatric patients affected by tetralogy of Fallot, underwent a pulmonary valve replacement with decellularized human pulmonary valves which have been repopulated by autologous MNCs from their peripheral blood. After valve recellularization, the cells were characterized as EPCs. Throughout the follow-up duration (3.5 years), the patients recovered well. Themselves and their prosthetic valves had a somatic growth, and there was no complication whatsoever. Only a trivial regurgitation was reported (168).

Induced Pluripotent Stem Cells (iPSC)

In some cases, adult stem cells are not enough proliferative due to diseases or patient old age. A good alternative might be the iPSC, which are autologous reprogrammed fibroblasts, able to differentiate in MSCs and ECs. Using this cell type, ethical or need for compatible stem cells issues are avoided. Simpson et al. managed to reprogram skin fibroblast into iPSC, and then produce iPSC -derived MSCs (iPSC -MSCs) and iPSC -derived ECs (iPSC -ECs). iPSC -MSCs were seeded on decellularized human pulmonary valves, resulting in valve repopulation and ECM production (171). Compared with

MSCs, the iPSC-MSCs have higher proliferation potential and have some expression pattern similarities with VICs (172). However, there are still safety concerns about IPCSs. Recent reports have emphasized the pitfalls of iPSC technology, including the potential for genetic and epigenetic abnormalities, tumorigenicity, and immunogenicity (148).

Native Cell Types: VIC and VEC to Bioengineer TEHV

TEHV seeded with human mitral or aortic VICs can generate a valvular tissue with mechanical properties similar to the naive human aortic valve (176) while retaining native antigenic expression (201, 202). Similar results have been reported for human VICs isolated from sclerotic valves (146). However, several models using native VICs and VECs to produce *in vitro* TEHV aim to model the pathological development of prosthetic degeneration, calcification and fibrosis by mimicking native-like environments rather than to design prosthetic solutions (203, 204). Other studies have used native resident cells to establish tissue engineering and cell culture protocols (147, 176, 205). For instance, VICs seeded on heparin-coated wells in presence of TGF- β 1 undergo to activation into myofibroblast phenotypes with enhanced synthetic and contractile activity, producing stress fibers and expressing α -SMA, all of them typical markers of active VICs (173). Mechanical properties of the scaffolds are also tested on native resident cells to better understand the mechanobiology of the VIC. Stiffer surfaces enhance their myofibroblastic activity, their density, and spreading (84). Conducting those studies is especially relevant to develop methods capable to obtain a temporary myofibroblast phenotype. Myofibroblasts are known to exert wound healing function but its persistence may promote fibrosis and calcification causing prosthetic valve disease (81, 83) as well as prosthetic retraction and regurgitation due to an excessive contractibility (206).

A priori, more interesting for therapeutic applications would be the VEC given the phenotypic peculiarities mentioned above. Those unique properties allow the VEC to provide an antithrombogenic surface, replenish the VIC population toward EMT processes and regulate VIC phenotype, in response to mechanical and biochemical stimuli. Indeed, Butcher et al. described the capability of the VEC to maintain quiescence of bioengineered VICs (73). However, difficult harvest and their degeneration can lead to valve failure due to neo-vascularization, infiltration of inflammatory agents, or lipid deposition, amongst the many (207). In addition, VECs undergoing to EMT can express osteogenic markers, not reported in other EC populations (72, 85). Although VECs can trigger valve dysfunction, providing an endothelial lining is a main concern when designing TEHV. That justify the use of primary endothelial cells (ECs) or EPCs in many studies (147).

Other Native Resident Cells: ECs, Myofibroblasts/Fibroblasts/VSMC

A way to attempt to reproduce the valvular structure is through using cell types whose lineage is close to VICs and VECs including ECs, fibroblasts (FBs) and VSMC. Sequential seeding of FBs and human adipose-MSC-derived endothelial cells were able to colonize and penetrate into animal decellularized heart valves

(177). However, activation of FBs and VSMC into myofibroblasts has been also reported leading to expression of cytokines, and scaffold degradation and contraction (143, 178). Incorporation of ECs lining seems to stop it (178). Those approaches are getting us close to understand the mechanisms to switch off and on undesired phenotypes by controlling the mechanical and biochemical signals of the designed TEHV (208). In line with *in vitro* results, TEHV bioengineered with myofibroblasts and ECs in sheep for 8–20 weeks was associated with leaflet thickening and moderate regurgitation (149, 151). Incipient calcification and regurgitation have been also found in BM-derived SMC valve substitutes implanted in sheep (155).

The utility of using native resident cells stands also in establishing the suitability of scaffolds designated for *in situ* TEHV and their capability to accommodate the recruitment of resident cells and a proper phenotype.

Alternative Cell Sources

There are other cell products with potential application in the *in vitro* TEHV with minor or not assessment so far. For example, two fractions have been differentially characterized among the progenitor cells isolated from the amniotic fluid. It has been shown that CD133⁺ fraction of the mononuclear cells in the amniotic fluid can acquire endothelial phenotype, whereas the CD133⁻ fraction can differentiate into myofibroblast-like cells. Those cells are especially relevant for the preparation of cellularized valves before birth (169). An unexplored alternative for *in vitro* TEHV in the adult is the suitability of heterogeneous perivascular stem/progenitor cells described in the vascular niche by our group and others and considered native ancestors of heterogenous MSCs (179, 209). The therapeutic potential of those perivascular cells in the cardiovascular regenerative medicine has been already demonstrated (210–212). Moreover, adventitial perivascular progenitor cells (APC) derived from cardiac surgery saphenous vein leftovers have properties, which make them a potential candidate for regenerative medicine (145), including the suitability for cellularization of xenografts (213) and application into myocardial ischemic models (214–216). The latter has shown the superiority of the APC to keep their specialized function upon implantation without acquiring undesired phenotypes (214). Importantly, intramyocardially transplanted APCs did not induce calcification, in contrast with BM-MSCs. It remains unclear if these properties are peculiar to APCs. *In vivo* and *in vitro* studies demonstrated the capability of other pericytes to contribute to the pathogenesis of vascular calcification toward osteogenesis and angiogenesis promotion from the adventitial *vasa vasorum* and the intimal layer (217). However, no intact perivascular coat has been described yet around the new vessels irrigating the growing of the advanced plaque-like tissue (87) and BM-MSC-derived endothelial cells and adventitial Sca1⁺ cells, rather than derived from adventitial *vasa vasorum*, have been described in association with atheromatous plaque progression (218, 219). Further evidences are needed to state that the APC is a cell of choice for *in vitro* TEHV. Adding new cell sources may bear the risk of adding more approaches to the several techniques and approaches found in the literature.

ADDITIONAL CONSIDERATION TO CHOOSE THE PROPER CELL TYPE FOR IN VITRO TEHV

In order to improve graft durability, additional aspects must be considered. (A) *Cell-graft interactions*. These features are inherent to the cells, but also depend on proper interactions between the “right cell” and “right prosthesis.” For instance, VEGF significantly inhibits the formation of calcium nodules when ovine VICs are grown on collagen, fibronectin, and laminin (97), while may confer osteoblast-like phenotypes using other substrates, suggesting that providing “right” specific ECM and/or growth factors may protect VICs from calcification and degeneration. Combining cells and prostheses already available in a clinical format may provide the means for swift exploitation. Thus it may be advantageous to test them first. (B) *Cell accessibility and scalability*. Tissues that are easily accessible as a source of candidate cell products represent the ideal solution. However, thanks to advances in cardiac imaging, it is now possible to obtain tissue specimens for cardiac cell harvesting with minimally invasive procedures. Additionally, expansion and storage protocols of various cell types are well established, thus allowing potential use of diverse cell populations for TE. (C) *Tissue specificity*. It is thought that progenitor cells and differentiated cells maintain an epigenetic memory of the source tissue. In line with this concept, cardiac progenitor cells, VICs and VECs may represent the logic solution for disease conditions that require reparative cardiomyogenesis or valve replacements. (D) *Paracrine activity*. As discussed above, cells seeded onto the graft/scaffold represent a source of biomolecules, favoring re-endothelialization, new native-like ECM (138). In addition, the presence of cells can decrease the degradation rate of the constituent scaffold ECM resulting in enhanced preservation of its mechanical properties (176) and eventually against prosthetic calcification. (E) *Cell retention on the implanted scaffolds*. This important aspect has not been extensively assessed, because of the difficulties in tracking cells incorporated into the graft. A study investigating TEHVs made by autologous canine BM-MSCs, seeded on allogenic or porcine-derived xenogeneic pulmonary valves demonstrated cell retention of 1 and 3 weeks, respectively (153). It remains uncertain whether the pathologic and pro-calcifying environment found in the aortic wall contiguous to the prosthetic valve implantation site may affect the retention and “right” phenotype preservation of cells used for TEHV and that needs to be studied.

CONCLUSIONS

A wide range of approaches is still being explored in the manufacture of TEHVs, based on established technologies and

REFERENCES

1. Madhavan MV, Tarigopula M, Mintz GS, Maehara A, Stone GW, Genereux P. Coronary artery calcification: pathogenesis and prognostic implications. *J Am Coll Cardiol*. (2014) 63:1703–14. doi: 10.1016/j.jacc.2014.01.017

novel cutting-edge techniques. Due to many patients targeted by TE for substitution of cardiac valves, the financial volume for these technologies/products is substantial. A market forecast for tissue engineered products indicates the total value will surpass \$4.8 billion by 2028.

Several publications with promising *in vivo* and *in vitro* results have underestimated the effects of the “minor outcomes” reported and that could lead to valve substitute degeneration in a next generation of the current “*biologic prosthetic valve disease*.” Active native-like ECM deposition and even valvulogenesis-like events must be desirable during the process of valve substitute production, but those must be abolished thereafter to avoid excessive fibrosis, contraction, retraction, degeneration, and calcification of the valve substitute. On this regard, the ideal cell type of choice has yet to be determined and more research is needed to provide the best therapeutic alternative to both adult and congenital VHD. Besides, results from experimental modeling performed with resident native cells seeded on different types of scaffolds, show that scaffold compositions or designs still need to be substantially improved to achieve the correct cell behavior in a diseased environment. Further research on this regard, combined with a better knowledge of the pathology, including the factors triggering myofibroblast phenotype perpetuation, osteoclast recruitment in the calcific valve or the exquisite behavior of the VEC, will significantly contribute to successfully develop valve substitutes. Innovative technologies are required to meet specific, quantitative standards of safety and performance. Similar standards will have to be developed to enable routine clinical use and customized fabrication of TEHVs. While a large number of options have been tested in animal models, more work is warranted before the use of TEHVs can be proposed as a better therapeutic option than available prostheses.

AUTHOR CONTRIBUTIONS

EJ reviewed the literature, drafted the manuscript, and prepared the figures and tables. MF reviewed the literature, drafted the manuscript, and prepared the tables. GA critically revised the manuscript. PM reviewed the literature, drafted, and critically revised the manuscript. All the authors have approved the final submission of the manuscript.

ACKNOWLEDGMENTS

EJ holds a postdoctoral grant funded by British Heart Foundation (BHF) (Grant number PG/15/95/31853). MF also holds a PhD studentship funded by BHF. The Bristol Heart Institute is part of the BHF Centre of Excellence in Vascular Regeneration.

2. Otto CM, Lind BK, Kitzman DW, Gersh BJ, Siscovick DS. Association of aortic-valve sclerosis with cardiovascular mortality and morbidity in the elderly. *N Engl J Med*. (1999) 341:142–7. doi: 10.1056/NEJM199907153410302

3. Maganti K, Rajamannan N. Slowing the progression of aortic stenosis. *Curr Treat Options Cardiovasc Med.* (2008) 10:18–26. doi: 10.1007/s11936-008-0003-3
4. Cheng GC, Loree HM, Kamm RD, Fishbein MC, Lee RT. Distribution of circumferential stress in ruptured and stable atherosclerotic lesions. A structural analysis with histopathological correlation. *Circulation* (1993) 87:1179–87. doi: 10.1161/01.CIR.87.4.1179
5. Mohler ER 3rd, Gannon F, Reynolds C, Zimmerman R, Keane MG, Kaplan FS. Bone formation and inflammation in cardiac valves. *Circulation* (2001) 103:1522–8. doi: 10.1161/01.CIR.103.11.1522
6. Caira FC, Stock SR, Gleason TG, McGee EC, Huang J, Bonow RO, et al. Human degenerative valve disease is associated with up-regulation of low-density lipoprotein receptor-related protein 5 receptor-mediated bone formation. *J Am Coll Cardiol.* (2006) 47:1707–12. doi: 10.1016/j.jacc.2006.02.040
7. Otto CM. Calcific aortic stenosis—time to look more closely at the valve. *N Engl J Med.* (2008) 359:1395–8. doi: 10.1056/NEJMe0807001
8. Iung B, Baron G, Butchart EG, Delahaye F, Gohlke-Barwolf C, Levang OW, et al. A prospective survey of patients with valvular heart disease in Europe: the Euro heart survey on valvular heart disease. *Eur Heart J.* (2003) 24:1231–43. doi: 10.1016/S0195-668X(03)00201-X
9. Iung B, Vahanian A. Epidemiology of valvular heart disease in the adult. *Nat Rev Cardiol.* (2011) 8:162–72. doi: 10.1038/nrcardio.2010.202
10. O'Brien KD. Epidemiology and genetics of calcific aortic valve disease. *J Investig Med.* (2007) 55:284–91. doi: 10.2310/6650.2007.00010
11. Stewart BF, Siscovick D, Lind BK, Gardin JM, Gottdiener JS, Smith VE, et al. Clinical factors associated with calcific aortic valve disease. Cardiovascular health study. *J Am Coll Cardiol.* (1997) 29:630–4. doi: 10.1016/S0735-1097(96)00563-3
12. Supino PG, Borer JS, Preibisz J, Bornstein A. The epidemiology of valvular heart disease: a growing public health problem. *Heart Fail Clin.* (2006) 2:379–93. doi: 10.1016/j.hfc.2006.09.010
13. Rajamannan NM. Bicuspid aortic valve disease: the role of oxidative stress in Lrp5 bone formation. *Cardiovasc Pathol.* (2011) 20:168–76. doi: 10.1016/j.carpath.2010.11.007
14. Lindroos M, Kupari M, Heikkilä J, Tilvis R. Prevalence of aortic valve abnormalities in the elderly: an echocardiographic study of a random population sample. *J Am Coll Cardiol.* (1993) 21:1220–5. doi: 10.1016/0735-1097(93)90249-Z
15. Rosenhek R, Zilberszac R, Schemper M, Czerny M, Mundigler G, Graf S, et al. Natural history of very severe aortic stenosis. *Circulation* (2010) 121:151–6. doi: 10.1161/CIRCULATIONAHA.109.894170
16. Nkomo VT, Gardin JM, Skelton TN, Gottdiener JS, Scott CG, Enriquez-Sarano M. Burden of valvular heart diseases: a population-based study. *Lancet* (2006) 368:1005–11. doi: 10.1016/S0140-6736(06)69208-8
17. Marciniak A, Glover K, Sharma R. Cohort profile: prevalence of valvular heart disease in community patients with suspected heart failure in UK. *BMJ Open* (2017) 7:e012240. doi: 10.1136/bmjopen-2016-012240
18. Otto CM, Burwash IG, Legget ME, Munt BI, Fujioka M, Healy NL, et al. Prospective study of asymptomatic valvular aortic stenosis. Clinical, echocardiographic, and exercise predictors of outcome. *Circulation* (1997) 95:2262–70. doi: 10.1161/01.CIR.95.9.2262
19. De Sciscio P, Brubert J, De Sciscio M, Serrani M, Stasiak J, Moggridge GD. Quantifying the shift toward transcatheter aortic valve replacement in low-risk patients: a meta-analysis. *Circ Cardiovasc Qual Outcomes* (2017) 10:e003287. doi: 10.1161/CIRCOUTCOMES.116.003287
20. d'Arcy JL, Prendergast BD, Chambers JB, Ray SG, Bridgewater B. Valvular heart disease: the next cardiac epidemic. *Heart* (2011) 97:91–3. doi: 10.1136/hrt.2010.205096
21. Blacher J, Guerin AP, Pannier B, Marchais SJ, London GM. Arterial calcifications, arterial stiffness, and cardiovascular risk in end-stage renal disease. *Hypertension* (2001) 38:938–42. doi: 10.1161/hy1001.096358
22. McClelland RL, Jorgensen NW, Budoff M, Blaha MJ, Post WS, Kronmal RA, et al. 10-year coronary heart disease risk prediction using coronary artery calcium and traditional risk factors: derivation in the MESA (multi-ethnic study of atherosclerosis) with validation in the HNR (Heinz Nixdorf Recall) study and the DHS (Dallas Heart Study). *J Am Coll Cardiol.* (2015) 66:1643–53. doi: 10.1016/j.jacc.2015.08.035
23. Budoff MJ, McClelland RL, Nasir K, Greenland P, Kronmal RA, Kondos GT, et al. Cardiovascular events with absent or minimal coronary calcification: the Multi-Ethnic Study of Atherosclerosis (MESA). *Am Heart J.* (2009) 158:554–61. doi: 10.1016/j.ahj.2009.08.007
24. Seemayer TA, Thelmo WL, Morin J. Cartilaginous transformation of the aortic valve. *Am J Clin Pathol.* (1973) 60:616–20. doi: 10.1093/ajcp/60.5.616
25. Hunt JL, Fairman R, Mitchell ME, Carpenter JP, Golden M, Khalapyan T, et al. Bone formation in carotid plaques: a clinicopathological study. *Stroke* (2002) 33:1214–9. doi: 10.1161/01.STR.0000013741.41309.67
26. Ferda J, Linhartova K, Kreuzberg B. Comparison of the aortic valve calcium content in the bicuspid and tricuspid stenotic aortic valve using non-enhanced 64-detector-row-computed tomography with prospective ECG-triggering. *Eur J Radiol.* (2008) 68:471–5. doi: 10.1016/j.ejrad.2007.09.011
27. Nishimura RA, Otto CM, Bonow RO, Carabello BA, Erwin JP, 3rd, Guyton RA, et al. 2014 AHA/ACC guideline for the management of patients with valvular heart disease: executive summary: a report of the American college of cardiology/American heart association task force on practice guidelines. *J Am Coll Cardiol.* (2014) 63:2438–88. doi: 10.1016/j.jacc.2014.02.537
28. Maganti K, Rigolin VH, Sarano ME, Bonow RO. Valvular heart disease: diagnosis and management. *Mayo Clin Proc.* (2010) 85:483–500. doi: 10.4065/mcp.2009.0706
29. Rosenhek R, Binder T, Porenta G, Lang I, Christ G, Schemper M, et al. Predictors of outcome in severe, asymptomatic aortic stenosis. *N Engl J Med.* (2000) 343:611–7. doi: 10.1056/NEJM200008313430903
30. Kadem L, Rieu R, Dumesnil JG, Durand LG, Pibarot P. Flow-dependent changes in Doppler-derived aortic valve effective orifice area are real and not due to artifact. *J Am Coll Cardiol.* (2006) 47:131–7. doi: 10.1016/j.jacc.2005.05.100
31. Stankovic Z, Allen BD, Garcia J, Jarvis KB, Markl M. 4D flow imaging with MRI. *Cardiovasc Diagn Ther.* (2014) 4:173–92. doi: 10.3978/j.issn.2223-3652.2014.01.02
32. Burris NS, Hope MD. 4D flow MRI applications for aortic disease. *Magn Reson Imaging Clin N Am.* (2015) 23:15–23. doi: 10.1016/j.mric.2014.08.006
33. Itatani K, Miyazaki S, Furusawa T, Numata S, Yamazaki S, Morimoto K, et al. New imaging tools in cardiovascular medicine: computational fluid dynamics and 4D flow MRI. *Gen Thorac Cardiovasc Surg.* (2017) 65:611–21. doi: 10.1007/s11748-017-0834-5
34. Hope MD, Hope TA, Crook SE, Ordovas KG, Urbania TH, Alley MT, et al. 4D flow CMR in assessment of valve-related ascending aortic disease. *JACC Cardiovasc Imaging* (2011) 4:781–7. doi: 10.1016/j.jcmg.2011.05.004
35. Geiger J, Rahsepar AA, Suwa K, Powell A, Ghasemiesfe A, Barker AJ, et al. 4D flow MRI, cardiac function, and T1 -mapping: association of valve-mediated changes in aortic hemodynamics with left ventricular remodeling. *J Magn Reson Imaging* (2018) 48:121–31. doi: 10.1002/jmri.25916
36. Vasanawala SS, Hanneman K, Alley MT, Hsiao A. Congenital heart disease assessment with 4D flow MRI. *J Magn Reson Imaging.* (2015) 42:870–86. doi: 10.1002/jmri.24856
37. Agatston AS, Janowitz WR, Hildner FJ, Zusmer NR, Viamonte M, Jr., Detrano R. Quantification of coronary artery calcium using ultrafast computed tomography. *J Am Coll Cardiol.* (1990) 15:827–32. doi: 10.1016/0735-1097(90)90282-T
38. Sandfort V, Bluemke DA. CT calcium scoring. History, current status and outlook. *Diagn Interv Imaging* (2017) 98:3–10. doi: 10.1016/j.diii.2016.06.007
39. Masuda Y, Naito S, Aoyagi Y, Yamada Z, Uda T, Morooka N, et al. Coronary artery calcification detected by CT: clinical significance and angiographic correlates. *Angiology* (1990) 41:1037–47. doi: 10.1177/000331979004101203
40. Timins ME, Pinski R, Sider L, Bear G. The functional significance of calcification of coronary arteries as detected on CT. *J Thorac Imaging* (1991) 7:79–82. doi: 10.1097/00005382-199112000-00010
41. Rajamannan NM, Evans FJ, Aikawa E, Grande-Allen KJ, Demer LL, Heistad DD, et al. Calcific aortic valve disease: not simply a degenerative process: a review and agenda for research from the National Heart and lung and blood institute aortic stenosis working group. Executive summary: calcific aortic valve disease-2011 update. *Circulation* (2011) 124:1783–91. doi: 10.1161/CIRCULATIONAHA.110.006767

42. Mahabadi AA, Mohlenkamp S, Moebs S, Dragano N, Kalsch H, Bauer M, et al. The Heinz Nixdorf Recall study and its potential impact on the adoption of atherosclerosis imaging in European primary prevention guidelines. *Curr Atheroscler Rep.* (2011) 13:367–72. doi: 10.1007/s11883-011-0199-7
43. Budoff MJ, Takasu J, Katz R, Mao S, Shavelle DM, O'Brien KD, et al. Reproducibility of CT measurements of aortic valve calcification, mitral annulus calcification, and aortic wall calcification in the multi-ethnic study of atherosclerosis. *Acad Radiol.* (2006) 13:166–72. doi: 10.1016/j.acra.2005.09.090
44. Schoen FJ. Evolving concepts of cardiac valve dynamics: the continuum of development, functional structure, pathobiology, and tissue engineering. *Circulation* (2008) 118:1864–80. doi: 10.1161/CIRCULATIONAHA.108.805911
45. Liu X, Xu Z. Osteogenesis in calcified aortic valve disease: from histopathological observation towards molecular understanding. *Prog Biophys Mol Biol.* (2016) 122:156–61. doi: 10.1016/j.pbiomolbio.2016.02.002
46. Duer MJ, Friscic T, Proudfoot D, Reid DG, Schoppet M, Shanahan CM, et al. Mineral surface in calcified plaque is like that of bone: further evidence for regulated mineralization. *Arterioscler Thromb Vasc Biol.* (2008) 28:2030–4. doi: 10.1161/ATVBAHA.108.172387
47. Leopold JA. Cellular mechanisms of aortic valve calcification. *Circ Cardiovasc Interv.* (2012) 5:605–14. doi: 10.1161/CIRCINTERVENTIONS.112.971028
48. Sawyer JR, Myers MA, Rosier RN, Puzas JE. Heterotopic ossification: clinical and cellular aspects. *Calcif Tissue Int.* (1991) 49:208–15. doi: 10.1007/BF02556120
49. New SE, Aikawa E. Cardiovascular calcification: an inflammatory disease. *Circ J.* (2011) 75:1305–13. doi: 10.1253/circj.CJ-11-0395
50. Weind KL, Ellis CG, Boughner DR. Aortic valve cusp vessel density: relationship with tissue thickness. *J Thorac Cardiovasc Surg.* (2002) 123:333–40. doi: 10.1067/mtc.2002.119696
51. Butcher JT, Penrod AM, Garcia AJ, Nerem RM. Unique morphology and focal adhesion development of valvular endothelial cells in static and fluid flow environments. *Arterioscler Thromb Vasc Biol.* (2004) 24:1429–34. doi: 10.1161/01.ATV.0000130462.50769.5a
52. Butcher JT, Tressel S, Johnson T, Turner D, Sorescu G, Jo H, et al. Transcriptional profiles of valvular and vascular endothelial cells reveal phenotypic differences: influence of shear stress. *Arterioscler Thromb Vasc Biol.* (2006) 26:69–77. doi: 10.1161/01.ATV.0000196624.70507.0d
53. Chen JH, Simmons CA. Cell-matrix interactions in the pathobiology of calcific aortic valve disease: critical roles for matricellular, matricrine, and matrix mechanics cues. *Circ Res.* (2011) 108:1510–24. doi: 10.1161/CIRCRESAHA.110.234237
54. Liu AC, Joag VR, Gotlieb AI. The emerging role of valve interstitial cell phenotypes in regulating heart valve pathobiology. *Am J Pathol.* (2007) 171:1407–18. doi: 10.2353/ajpath.2007.070251
55. Rabkin-Aikawa E, Farber M, Aikawa M, Schoen FJ. Dynamic and reversible changes of interstitial cell phenotype during remodeling of cardiac valves. *J Heart Valve Dis.* (2004) 13:841–7.
56. Rabkin E, Aikawa M, Stone JR, Fukumoto Y, Libby P, Schoen FJ. Activated interstitial myofibroblasts express catabolic enzymes and mediate matrix remodeling in myxomatous heart valves. *Circulation* (2001) 104:2525–32. doi: 10.1161/hc4601.099489
57. Rajamannan NM, Subramaniam M, Caira F, Stock SR, Spelsberg TC. Atorvastatin inhibits hypercholesterolemia-induced calcification in the aortic valves via the Lrp5 receptor pathway. *Circulation* (2005) 112(9 Suppl):I229–34. doi: 10.1161/01.CIRCULATIONAHA.104.524306
58. Rajamannan NM, Subramaniam M, Springett M, Sebo TC, Niekrasz M, McConnell JP, et al. Atorvastatin inhibits hypercholesterolemia-induced cellular proliferation and bone matrix production in the rabbit aortic valve. *Circulation* (2002) 105:2660–5. doi: 10.1161/01.CIR.0000017435.87463.72
59. Wu HD, Maurer MS, Friedman RA, Marboe CC, Ruiz-Vazquez EM, Ramakrishnan R, et al. The lymphocytic infiltration in calcific aortic stenosis predominantly consists of clonally expanded T cells. *J Immunol.* (2007) 178:5329–39. doi: 10.4049/jimmunol.178.8.5329
60. Aikawa E, Nahrendorf M, Sosnovik D, Lok VM, Jaffer FA, Aikawa M, et al. Multimodality molecular imaging identifies proteolytic and osteogenic activities in early aortic valve disease. *Circulation* (2007) 115:377–86. doi: 10.1161/CIRCULATIONAHA.106.654913
61. Stemme S, Rymo L, Hansson GK. Polyclonal origin of T lymphocytes in human atherosclerotic plaques. *Lab Invest.* (1991) 65:654–60.
62. Rusanescu G, Weissleder R, Aikawa E. Notch signaling in cardiovascular disease and calcification. *Curr Cardiol Rev.* (2008) 4:148–56. doi: 10.2174/157340308785160552
63. Yetkin E, Waltenberger J. Molecular and cellular mechanisms of aortic stenosis. *Int J Cardiol.* (2009) 135:4–13. doi: 10.1016/j.ijcard.2009.03.108
64. Hakuno D, Kimura N, Yoshioka M, Fukuda K. Molecular mechanisms underlying the onset of degenerative aortic valve disease. *J Mol Med.* (2009) 87:17–24. doi: 10.1007/s00109-008-0400-9
65. Merryman WD, Youn I, Lukoff HD, Krueger PM, Guilak F, Hopkins RA, et al. Correlation between heart valve interstitial cell stiffness and transvalvular pressure: implications for collagen biosynthesis. *Am J Physiol Heart Circ Physiol.* (2006) 290:H224–31. doi: 10.1152/ajpheart.00521.2005
66. Johnson RC, Leopold JA, Loscalzo J. Vascular calcification: pathobiological mechanisms and clinical implications. *Circ Res.* (2006) 99:1044–59. doi: 10.1161/01.RES.0000249379.55535.21
67. Demer LL, Tintut Y. Vascular calcification: pathobiology of a multifaceted disease. *Circulation* (2008) 117:2938–48. doi: 10.1161/CIRCULATIONAHA.107.743161
68. Aikawa E, Whittaker P, Farber M, Mendelson K, Padera RF, Aikawa M, et al. Human semilunar cardiac valve remodeling by activated cells from fetus to adult: implications for postnatal adaptation, pathology, and tissue engineering. *Circulation* (2006) 113:1344–52. doi: 10.1161/CIRCULATIONAHA.105.591768
69. Rajamannan NM, Subramaniam M, Rickard D, Stock SR, Donovan J, Springett M, et al. Human aortic valve calcification is associated with an osteoblast phenotype. *Circulation* (2003) 107:2181–4. doi: 10.1161/01.CIR.0000070591.21548.69
70. Shanahan CM, Crouthamel MH, Kapustin A, Giachelli CM. Arterial calcification in chronic kidney disease: key roles for calcium and phosphate. *Circ Res.* (2011) 109:697–711. doi: 10.1161/CIRCRESAHA.110.234914
71. Paranya G, Vineberg S, Dvorin E, Kaushal S, Roth SJ, Rabkin E, et al. Aortic valve endothelial cells undergo transforming growth factor-beta-mediated and non-transforming growth factor-beta-mediated transdifferentiation *in vitro*. *Am J Pathol.* (2001) 159:1335–43. doi: 10.1016/S0002-9440(10)62520-5
72. Wylie-Sears J, Aikawa E, Levine RA, Yang JH, Bischoff J. Mitral valve endothelial cells with osteogenic differentiation potential. *Arterioscler Thromb Vasc Biol.* (2011) 31:598–607. doi: 10.1161/ATVBAHA.110.216184
73. Butcher JT, Nerem RM. Valvular endothelial cells regulate the phenotype of interstitial cells in co-culture: effects of steady shear stress. *Tissue Eng.* (2006) 12:905–15. doi: 10.1089/ten.2006.12.905
74. Bosse K, Hans CP, Zhao N, Koenig SN, Huang N, Guggilam A, et al. Endothelial nitric oxide signaling regulates Notch1 in aortic valve disease. *J Mol Cell Cardiol.* (2013) 60:27–35. doi: 10.1016/j.yjmcc.2013.04.001
75. Nigam V, Srivastava D. Notch1 represses osteogenic pathways in aortic valve cells. *J Mol Cell Cardiol.* (2009) 47:828–34. doi: 10.1016/j.yjmcc.2009.08.008
76. Tanaka K, Sata M, Fukuda D, Suematsu Y, Motomura N, Takamoto S, et al. Age-associated aortic stenosis in apolipoprotein E-deficient mice. *J Am Coll Cardiol.* (2005) 46:134–41. doi: 10.1016/j.jacc.2005.03.058
77. Leskela HV, Satta J, Oiva J, Eriksen H, Juha R, Korkiamaki P, et al. Calcification and cellularity in human aortic heart valve tissue determine the differentiation of bone-marrow-derived cells. *J Mol Cell Cardiol.* (2006) 41:642–9. doi: 10.1016/j.yjmcc.2006.07.014
78. Hajdu Z, Romeo SJ, Fleming PA, Markwald RR, Visconti RP, Drake CJ. Recruitment of bone marrow-derived valve interstitial cells is a normal homeostatic process. *J Mol Cell Cardiol.* (2011) 51:955–65. doi: 10.1016/j.yjmcc.2011.08.006
79. Jover E, Silvente A, Marin F, Martinez-Gonzalez J, Orriols M, Martinez CM, et al. Inhibition of enzymes involved in collagen cross-linking reduces vascular smooth muscle cell calcification. *FASEB J.* 2018:fj201700653R. doi: 10.1096/fj.201700653R
80. Hutson HN, Marohl T, Anderson M, Eliceiri K, Campagnola P, Masters KS. Calcific aortic valve disease is associated with layer-specific

- alterations in collagen architecture. *PLoS ONE* (2016) 11:e0163858. doi: 10.1371/journal.pone.0163858
81. Rodriguez KJ, Masters KS. Regulation of valvular interstitial cell calcification by components of the extracellular matrix. *J Biomed Mater Res A*. (2009) 90:1043–53. doi: 10.1002/jbm.a.32187
 82. New SE, Aikawa E. Molecular imaging insights into early inflammatory stages of arterial and aortic valve calcification. *Circ Res*. (2011) 108:1381–91. doi: 10.1161/CIRCRESAHA.110.234146
 83. Kloxin AM, Benton JA, Anseth KS. *In situ* elasticity modulation with dynamic substrates to direct cell phenotype. *Biomaterials* (2010) 31:1–8. doi: 10.1016/j.biomaterials.2009.09.025
 84. Quinlan AM, Billiar KL. Investigating the role of substrate stiffness in the persistence of valvular interstitial cell activation. *J Biomed Mater Res A*. (2012) 100:2474–82. doi: 10.1002/jbm.a.34162
 85. Zhong A, Mirzaei Z, Simmons CA. The roles of matrix stiffness and ss-catenin signaling in endothelial-to-mesenchymal transition of aortic valve endothelial cells. *Cardiovasc Eng Technol*. (2018) 9:158–67. doi: 10.1007/s13239-018-0363-0
 86. Chalajour F, Treede H, Ebrahimnejad A, Lauke H, Reichenspurner H, Ergun S. Angiogenic activation of valvular endothelial cells in aortic valve stenosis. *Exp Cell Res*. (2004) 298:455–64. doi: 10.1016/j.yexcr.2004.04.034
 87. Collett GD, Canfield AE. Angiogenesis and pericytes in the initiation of ectopic calcification. *Circ Res*. (2005) 96:930–8. doi: 10.1161/01.RES.0000163634.51301.0d
 88. Yoshioka M, Yuasa S, Matsumura K, Kimura K, Shiomi T, Kimura N, et al. Chondromodulin-I maintains cardiac valvular function by preventing angiogenesis. *Nat Med*. (2006) 12:1151–9. doi: 10.1038/nm1476
 89. Soini Y, Salo T, Satta J. Angiogenesis is involved in the pathogenesis of nonrheumatic aortic valve stenosis. *Hum Pathol*. (2003) 34:756–63. doi: 10.1016/S0046-8177(03)00245-4
 90. Rajamannan NM, Nealis TB, Subramaniam M, Pandya S, Stock SR, Ignatiev CI, et al. Calcified rheumatic valve neoangiogenesis is associated with vascular endothelial growth factor expression and osteoblast-like bone formation. *Circulation* (2005) 111:3296–301. doi: 10.1161/CIRCULATIONAHA.104.473165
 91. Hiraki Y, Shukunami C. Chondromodulin-I as a novel cartilage-specific growth-modulating factor. *Pediatr Nephrol*. (2000) 14:602–5. doi: 10.1007/s004670000339
 92. Nakamichi Y, Shukunami C, Yamada T, Aihara K, Kawano H, Sato T, et al. Chondromodulin I is a bone remodeling factor. *Mol Cell Biol*. (2003) 23:636–44. doi: 10.1128/MCB.23.2.636-644.2003
 93. Mori Y, Hiraki Y, Shukunami C, Kakudo S, Shiokawa M, Kagoshima M, et al. Stimulation of osteoblast proliferation by the cartilage-derived growth promoting factors chondromodulin-I and -II. *FEBS Lett*. (1997) 406:310–4. doi: 10.1016/S0014-5793(97)00291-3
 94. Acharya A, Hans CP, Koenig SN, Nichols HA, Galindo CL, Garner HR, et al. Inhibitory role of Notch1 in calcific aortic valve disease. *PLoS ONE* (2011) 6:e27743. doi: 10.1371/journal.pone.0027743
 95. Perrotta I, Moraca FM, Sciangula A, Aquila S, Mazzulla S. HIF-1 α and VEGF: immunohistochemical profile and possible function in human aortic valve stenosis. *Ultrastruct Pathol*. (2015) 39:198–206. doi: 10.3109/01913123.2014.991884
 96. Engsig MT, Chen QJ, Vu TH, Pedersen AC, Therkidsen B, Lund LR, et al. Matrix metalloproteinase 9 and vascular endothelial growth factor are essential for osteoclast recruitment into developing long bones. *J Cell Biol*. (2000) 151:879–89. doi: 10.1083/jcb.151.4.879
 97. Gwanmesia P, Ziegler H, Eurich R, Barth M, Kamiya H, Karck M, et al. Opposite effects of transforming growth factor-beta1 and vascular endothelial growth factor on the degeneration of aortic valvular interstitial cell are modified by the extracellular matrix protein fibronectin: implications for heart valve engineering. *Tissue Eng Part A*. (2010) 16:3737–46. doi: 10.1089/ten.tea.2010.0304
 98. Shworak NW. Angiogenic modulators in valve development and disease: does valvular disease recapitulate developmental signaling pathways? *Curr Opin Cardiol*. (2004) 19:140–6. doi: 10.1097/00001573-200403000-00013
 99. Liebner S, Cattelino A, Gallini R, Rudini N, Iurlaro M, Piccolo S, et al. Beta-catenin is required for endothelial-mesenchymal transformation during heart cushion development in the mouse. *J Cell Biol*. (2004) 166:359–67. doi: 10.1083/jcb.200403050
 100. Person AD, Klewer SE, Runyan RB. Cell biology of cardiac cushion development. *Int Rev Cytol*. (2005) 243:287–335. doi: 10.1016/S0074-7696(05)43005-3
 101. O'Neill WC, Lomashvili KA. Recent progress in the treatment of vascular calcification. *Kidney Int*. (2010) 78:1232–9. doi: 10.1038/ki.2010.334
 102. Roberts WC, Ko JM. Frequency by decades of unicuspid, bicuspid, and tricuspid aortic valves in adults having isolated aortic valve replacement for aortic stenosis, with or without associated aortic regurgitation. *Circulation* (2005) 111:920–5. doi: 10.1161/01.CIR.0000155623.48408.C5
 103. Dunning J, Gao H, Chambers J, Moat N, Murphy G, Pagano D, et al. Aortic valve surgery: marked increases in volume and significant decreases in mechanical valve use—an analysis of 41,227 patients over 5 years from the Society for Cardiothoracic Surgery in Great Britain and Ireland National database. *J Thorac Cardiovasc Surg*. (2011) 142:776–82e3. doi: 10.1016/j.jtcvs.2011.04.048
 104. Perera S, Wijesinghe N, Ly E, Devlin G, Pasupati S. Outcomes of patients with untreated severe aortic stenosis in real-world practice. *NZ Med J*. (2011) 124:40–8.
 105. Kojodjojo P, Gohil N, Barker D, Youssefi P, Salukhe TV, Choong A, et al. Outcomes of elderly patients aged 80 and over with symptomatic, severe aortic stenosis: impact of patient's choice of refusing aortic valve replacement on survival. *QJM* (2008) 101:567–73. doi: 10.1093/qjmed/hcn052
 106. American College of Cardiology/American Heart Association Task Force on Practice G, Society of Cardiovascular A, Society for Cardiovascular A, Interventions, Society of Thoracic S, Bonow RO, et al. ACC/AHA 2006 guidelines for the management of patients with valvular heart disease: a report of the American College of Cardiology/American Heart Association Task Force on Practice Guidelines (writing committee to revise the 1998 Guidelines for the Management of Patients With Valvular Heart Disease): developed in collaboration with the society of cardiovascular anesthesiologists; endorsed by the Society for cardiovascular angiography and interventions and the society of thoracic surgeons. *Circulation* (2006) 114:e84–231. doi: 10.1161/CIRCULATIONAHA.106.176857
 107. Butcher JT, Mahler GJ, Hockaday LA. Aortic valve disease and treatment: the need for naturally engineered solutions. *Adv Drug Deliv Rev*. (2011) 63:242–68. doi: 10.1016/j.addr.2011.01.008
 108. Fioretta ES, Dijkman PE, Emmert MY, Hoerstrup SP. The future of heart valve replacement: recent developments and translational challenges for heart valve tissue engineering. *J Tissue Eng Regen Med*. (2016). 12:e323–35. doi: 10.1002/term.2326
 109. Schmitt CA. Interventional cardiology: percutaneous pulmonary valve implantation: 1-year safety and efficacy reported in German study. *Nat Rev Cardiol*. (2011) 8:186. doi: 10.1038/nrcardio.2011.21
 110. Pibarot P, Dumesnil JG. Prosthetic heart valves: selection of the optimal prosthesis and long-term management. *Circulation* (2009) 119:1034–48. doi: 10.1161/CIRCULATIONAHA.108.778886
 111. Rahimtoola SH. Choice of prosthetic heart valve in adults an update. *J Am Coll Cardiol*. (2010) 55:2413–26. doi: 10.1016/j.jacc.2009.10.085
 112. Nishimura RA, Otto CM, Bonow RO, Carabello BA, Erwin JP 3rd, Fleisher LA, et al. 2017 AHA/ACC Focused Update of the 2014 AHA/ACC guideline for the management of patients with valvular heart disease: a report of the American college of cardiology/American heart association task force on clinical practice guidelines. *J Am Coll Cardiol*. (2017) 70:252–89. doi: 10.1016/j.jacc.2017.03.011
 113. Shetty R, Pibarot P, Audet A, Janvier R, Dagenais F, Perron J, et al. Lipid-mediated inflammation and degeneration of bioprosthetic heart valves. *Eur J Clin Invest*. (2009) 39:471–80. doi: 10.1111/j.1365-2362.2009.02132.x
 114. Gossel M, Khosla S, Zhang X, Higano N, Jordan KL, Loeffler D, et al. Role of circulating osteogenic progenitor cells in calcific aortic stenosis. *J Am Coll Cardiol*. (2012) 60:1945–53. doi: 10.1016/j.jacc.2012.07.042
 115. Honge JL, Funder J, Hansen E, Dohmen PM, Konertz W, Hasenkam JM. Recellularization of aortic valves in pigs. *Eur J Cardiothorac Surg*. (2011) 39:829–34. doi: 10.1016/j.ejcts.2010.08.054
 116. Konertz W, Dohmen PM, Liu J, Beholz S, Dushe S, Posner S, et al. Hemodynamic characteristics of the Matrix P decellularized xenograft for

- pulmonary valve replacement during the Ross operation. *J Heart Valve Dis.* (2005) 14:78–81.
117. Schoen FJ, Levy RJ. Calcification of tissue heart valve substitutes: progress toward understanding and prevention. *Ann Thorac Surg.* (2005) 79:1072–80. doi: 10.1016/j.athoracsur.2004.06.033
 118. Sacks MS, Schoen FJ. Collagen fiber disruption occurs independent of calcification in clinically explanted bioprosthetic heart valves. *J Biomed Mater Res.* (2002) 62:359–71. doi: 10.1002/jbm.10293
 119. O'Brien FJ. Biomaterials and scaffolds for tissue engineering. *Mater Today* (2011) 14:88–95. doi: 10.1016/S1369-7021(11)70058-X
 120. Zafar F, Hinton RB, Moore RA, Baker RS, Bryant R, 3rd, Narmoneva DA, et al. Physiological growth, remodeling potential, and preserved function of a novel bioprosthetic tricuspid valve: tubular bioprosthesis made of small intestinal submucosa-derived extracellular matrix. *J Am Coll Cardiol.* (2015) 66:877–88. doi: 10.1016/j.jacc.2015.06.1091
 121. Ruiz CE, Iemura M, Medie S, Varga P, Van Alstine WG, Mack S, et al. Transcatheter placement of a low-profile biodegradable pulmonary valve made of small intestinal submucosa: a long-term study in a swine model. *J Thorac Cardiovasc Surg.* (2005) 130:477–84. doi: 10.1016/j.jtcvs.2005.04.008
 122. Weber B, Dijkman PE, Scherman J, Sanders B, Emmert MY, Grunenfelder J, et al. Off-the-shelf human decellularized tissue-engineered heart valves in a non-human primate model. *Biomaterials* (2013) 34:7269–80. doi: 10.1016/j.biomaterials.2013.04.059
 123. Syedain Z, Reimer J, Lahti M, Berry J, Johnson S, Tranquillo RT. Tissue engineering of acellular vascular grafts capable of somatic growth in young lambs. *Nat Commun.* (2016) 7:12951. doi: 10.1038/ncomms12951
 124. Sacks MS, Schoen FJ, Mayer JE. Bioengineering challenges for heart valve tissue engineering. *Annu Rev Biomed Eng.* (2009) 11:289–313. doi: 10.1146/annurev-bioeng-061008-124903
 125. Kluin J, Talacua H, Smits AI, Emmert MY, Brugmans MC, Fioretta ES, et al. *In situ* heart valve tissue engineering using a bioresorbable elastomeric implant - From material design to 12 months follow-up in sheep. *Biomaterials* (2017) 125:101–17. doi: 10.1016/j.biomaterials.2017.02.007
 126. Capulli AK, Emmert MY, Pasqualini FS, Kehl D, Caliskan E, Lind JU, et al. JetValve: rapid manufacturing of biohybrid scaffolds for biomimetic heart valve replacement. *Biomaterials* (2017) 133:229–41. doi: 10.1016/j.biomaterials.2017.04.033
 127. Serruys PW, Miyazaki Y, Katsikis A, Abdelghani M, Leon MB, Virmani R, et al. Restorative valve therapy by endogenous tissue restoration: tomorrow's world? Reflection on the EuroPCR 2017 session on endogenous tissue restoration. *EuroIntervention* (2017) 13:AA68–77. doi: 10.4244/EIJ-D-17-00509
 128. Reimer J, Syedain Z, Haynie B, Lahti M, Berry J, Tranquillo R. Implantation of a tissue-engineered tubular heart valve in growing lambs. *Ann Biomed Eng.* (2017) 45:439–51. doi: 10.1007/s10439-016-1605-7
 129. Lu T, Li Y, Chen T. Techniques for fabrication and construction of three-dimensional scaffolds for tissue engineering. *Int J Nanomedicine* (2013) 8:337–50. doi: 10.2147/IJN.S38635
 130. Slater SC, Carrabba M, Madeddu P. Vascular stem cells-potential for clinical application. *Br Med Bull.* (2016) 118:127–37. doi: 10.1093/bmb/ldw017
 131. Rocco KA, Maxfield MW, Best CA, Dean EW, Breuer CK. *In vivo* applications of electrospun tissue-engineered vascular grafts: a review. *Tissue Eng Part B Rev.* (2014) 20:628–40. doi: 10.1089/ten.teb.2014.0123
 132. Cheung DY, Duan B, Butcher JT. Current progress in tissue engineering of heart valves: multiscale problems, multiscale solutions. *Expert Opin Biol Ther.* (2015) 15:1155–72. doi: 10.1517/14712598.2015.1051527
 133. Shinoka T, Miyachi H. Current status of tissue engineering heart valve. *World J Pediatr Congenit Heart Surg.* (2016) 7:677–84. doi: 10.1177/2150135116664873
 134. Zhang X, Xu B, Puperi DS, Wu Y, West JL, Grande-Allen KJ. Application of hydrogels in heart valve tissue engineering. *J Long Term Eff Med Implants* (2015) 25:105–34. doi: 10.1615/JLongTermEffMedImplants.2015011817
 135. Zhu AS, Grande-Allen KJ. Heart valve tissue engineering for valve replacement and disease modeling. *Curr Opin Biomed Eng.* (2018) 5:7. doi: 10.1016/j.cobme.2017.12.006
 136. Kheradvar A, Groves EM, Dasi LP, Alavi SH, Tranquillo R, Grande-Allen KJ, et al. Emerging trends in heart valve engineering: part I. Solutions for future. *Ann Biomed Eng.* (2015) 43:833–43. doi: 10.1007/s10439-014-1209-z
 137. Schoen FJ. Morphology, Clinicopathologic correlations, and mechanisms in heart valve health and disease. *Cardiovasc Eng Technol.* (2018) 9:126–40. doi: 10.1007/s13239-016-0277-7
 138. Mosier J, Nancy N, Parker K, Simpson CL. *Calcification of Biomaterials and Diseased States* (2018). doi: 10.5772/intechopen.71594
 139. Yang M, Lin YH, Shi WP, Shi HC, Gu YJ, Shu YS. Surface heparin treatment of the decellularized porcine heart valve: effect on tissue calcification. *J Biomed Mater Res B Appl Biomater.* (2017) 105:400–5. doi: 10.1002/jbm.b.33490
 140. Tristan C, Silke G, Kilian M, Malcolm D, O'Connor AJ, Geoffrey W, et al. Modelling oxygen diffusion and cell growth in a porous, vascularizing scaffold for soft tissue engineering applications. *Chem Eng Sci.* (2005) 60:4924–34. doi: 10.1016/j.ces.2005.03.051
 141. Wernike E, Li Z, Alini M, Grad S. Effect of reduced oxygen tension and long-term mechanical stimulation on chondrocyte-polymer constructs. *Cell Tissue Res.* (2008) 331:473–83. doi: 10.1007/s00441-007-0500-9
 142. Volkmer E, Drosse I, Otto S, Stangelmayer A, Stengele M, Kallukalam BC, et al. Hypoxia in static and dynamic 3D culture systems for tissue engineering of bone. *Tissue Eng Part A.* (2008) 14:1331–40. doi: 10.1089/ten.tea.2007.0231
 143. Aleksieva G, Hollweck T, Thierfelder N, Haas U, Koenig F, Fano C, et al. Use of a special bioreactor for the cultivation of a new flexible polyurethane scaffold for aortic valve tissue engineering. *Biomed Eng Online* (2012) 11:92. doi: 10.1186/1475-925X-11-92
 144. Converse GL, Buse EE, Neill KR, McFall CR, Lewis HN, VeDepo MC, et al. Design and efficacy of a single-use bioreactor for heart valve tissue engineering. *J Biomed Mater Res B Appl Biomater.* (2017) 105:249–59. doi: 10.1002/jbm.b.33552
 145. Avolio E, Caputo M, Madeddu P. Stem cell therapy and tissue engineering for correction of congenital heart disease. *Front Cell Dev Biol.* (2015) 3:39. doi: 10.3389/fcell.2015.00039
 146. Poggio P, Sainger R, Branchetti E, Grau JB, Lai EK, Gorman RC, et al. Noggin attenuates the osteogenic activation of human valve interstitial cells in aortic valve sclerosis. *Cardiovasc Res.* (2013) 98:402–10. doi: 10.1093/cvr/cvt055
 147. Jana S, Tranquillo RT, Lerman A. Cells for tissue engineering of cardiac valves. *J Tissue Eng Regen Med.* (2016) 10:804–24. doi: 10.1002/term.2010
 148. Okano H, Nakamura M, Yoshida K, Okada Y, Tsuji O, Nori S, et al. Steps toward safe cell therapy using induced pluripotent stem cells. *Circ Res.* (2013) 112:523–33. doi: 10.1161/CIRCRESAHA.111.256149
 149. Hoerstrup SP, Sodan R, Daebritz S, Wang J, Bacha EA, Martin DP, et al. Functional living trileaflet heart valves grown *in vitro*. *Circulation* (2000) 102(19 Suppl 3):III44–9. doi: 10.1161/01.CIR.102.suppl_3.III-44
 150. Hoerstrup SP, Kadner A, Melnitchouk S, Trojan A, Eid K, Tracy J, et al. Tissue engineering of functional trileaflet heart valves from human marrow stromal cells. *Circulation* (2002) 106(12 Suppl 1):I143–50. doi: 10.1161/01.cir.0000032872.55215.05
 151. Schmidt D, Dijkman PE, Driessen-Mol A, Stenger R, Mariani C, Puolakka A, et al. Minimally-invasive implantation of living tissue engineered heart valves: a comprehensive approach from autologous vascular cells to stem cells. *J Am Coll Cardiol.* (2010) 56:510–20. doi: 10.1016/j.jacc.2010.04.024
 152. Zhou J, Ye X, Wang Z, Liu J, Zhang B, Qiu J, et al. Development of decellularized aortic valvular conduit coated by heparin-SDF-1 α multilayer. *Ann Thorac Surg.* (2015) 99:612–8. doi: 10.1016/j.athoracsur.2014.09.001
 153. Kim SS, Lim SH, Hong YS, Cho SW, Ryu JH, Chang BC, et al. Tissue engineering of heart valves *in vivo* using bone marrow-derived cells. *Artif Organs* (2006) 30:554–7. doi: 10.1111/j.1525-1594.2006.00258.x
 154. Vincentelli A, Wautot F, Juthier F, Fouquet O, Corseaux D, Marechaux S, et al. *In vivo* autologous recellularization of a tissue-engineered heart valve: are bone marrow mesenchymal stem cells the best candidates? *J Thorac Cardiovasc Surg.* (2007) 134:424–32. doi: 10.1016/j.jtcvs.2007.05.005
 155. Boldt J, Lutter G, Pohanke J, Fischer G, Schoettler J, Cremer J, et al. Percutaneous tissue-engineered pulmonary valved stent implantation: comparison of bone marrow-derived CD133+ cells and cells obtained from carotid artery. *Tissue Eng Part C Methods* (2013) 19:363–74. doi: 10.1089/ten.tec.2012.0078

156. Sutherland FW, Perry TE, Yu Y, Sherwood MC, Rabkin E, Masuda Y, et al. From stem cells to viable autologous semilunar heart valve. *Circulation* (2005) 111:2783–91. doi: 10.1161/CIRCULATIONAHA.104.498378
157. Engelmayer GC Jr, Sales VL, Mayer JE Jr, Sacks MS. Cyclic flexure and laminar flow synergistically accelerate mesenchymal stem cell-mediated engineered tissue formation: Implications for engineered heart valve tissues. *Biomaterials* (2006) 27:6083–95. doi: 10.1016/j.biomaterials.2006.07.045
158. Gottlieb D, Kunal T, Emani S, Aikawa E, Brown DW, Powell AJ, et al. *In vivo* monitoring of function of autologous engineered pulmonary valve. *J Thorac Cardiovasc Surg.* (2010) 139:723–31. doi: 10.1016/j.jtcvs.2009.11.006
159. Ramaswamy S, Gottlieb D, Engelmayer GC Jr., Aikawa E, Schmidt DE, Gaitan-Leon DM, et al. The role of organ level conditioning on the promotion of engineered heart valve tissue development *in-vitro* using mesenchymal stem cells. *Biomaterials* (2010) 31:1114–25. doi: 10.1016/j.biomaterials.2009.10.019
160. Dijkman PE, Driessen-Mol A, Frese L, Hoerstrup SP, Baaijens FP. Decellularized homologous tissue-engineered heart valves as off-the-shelf alternatives to xeno- and homografts. *Biomaterials* (2012) 33:4545–54. doi: 10.1016/j.biomaterials.2012.03.015
161. Knight RL, Booth C, Wilcox HE, Fisher J, Ingham E. Tissue engineering of cardiac valves: re-seeding of acellular porcine aortic valve matrices with human mesenchymal progenitor cells. *J Heart Valve Dis.* (2005) 14:806–13.
162. Schmidt D, Mol A, Breymann C, Achermann J, Odermatt B, Gossi M, et al. Living autologous heart valves engineered from human prenatally harvested progenitors. *Circulation* (2006) 114(1 Suppl):I125–31. doi: 10.1161/CIRCULATIONAHA.105.001040
163. Dvorin EL, Wylie-Sears J, Kaushal S, Martin DP, Bischoff J. Quantitative evaluation of endothelial progenitors and cardiac valve endothelial cells: proliferation and differentiation on poly-glycolic acid/poly-4-hydroxybutyrate scaffold in response to vascular endothelial growth factor and transforming growth factor beta1. *Tissue Eng.* (2003) 9:487–93. doi: 10.1089/107632703322066660
164. Sales VL, Mettler BA, Engelmayer GC Jr, Aikawa E, Bischoff J, Martin DP, et al. Endothelial progenitor cells as a sole source for *ex vivo* seeding of tissue-engineered heart valves. *Tissue Eng Part A* (2010) 16:257–67. doi: 10.1089/ten.tea.2009.0424
165. Wang D, Li LK, Dai T, Wang A, Li S. Adult stem cells in vascular remodeling. *Theranostics* (2018) 8:815–29. doi: 10.7150/thno.19577
166. Schmidt D, Mol A, Odermatt B, Neuenschwander S, Breymann C, Gossi M, et al. Engineering of biologically active living heart valve leaflets using human umbilical cord-derived progenitor cells. *Tissue Eng.* (2006) 12:3223–32. doi: 10.1089/ten.2006.12.3223
167. Ye X, Wang H, Zhou J, Li H, Liu J, Wang Z, et al. The effect of Heparin-VEGF multilayer on the biocompatibility of decellularized aortic valve with platelet and endothelial progenitor cells. *PLoS ONE* (2013) 8:e54622. doi: 10.1371/journal.pone.0054622
168. Cebotari S, Lichtenberg A, Tudorache I, Hilfiker A, Mertsching H, Leyh R, et al. Clinical application of tissue engineered human heart valves using autologous progenitor cells. *Circulation* (2006) 114(1 Suppl):I132–7. doi: 10.1161/CIRCULATIONAHA.105.001065
169. Schmidt D, Achermann J, Odermatt B, Breymann C, Mol A, Genoni M, et al. Prenatally fabricated autologous human living heart valves based on amniotic fluid derived progenitor cells as single cell source. *Circulation* (2007) 116(11 Suppl):I64–70. doi: 10.1161/CIRCULATIONAHA.106.681494
170. Zhou J, Ding J, Nie B, Hu S, Zhu Z, Chen J, et al. Promotion of adhesion and proliferation of endothelial progenitor cells on decellularized valves by covalent incorporation of RGD peptide and VEGF. *J Mater Sci Mater Med.* (2016) 27:142. doi: 10.1007/s10856-016-5750-1
171. Simpson DL, Wehman B, Galat Y, Sharma S, Mishra R, Galat V, et al. Engineering patient-specific valves using stem cells generated from skin biopsy specimens. *Ann Thorac Surg.* (2014) 98:947–54. doi: 10.1016/j.athoracsur.2014.04.075
172. Nachlas ALY, Li S, Jha R, Singh M, Xu C, Davis ME. Human iPSC-derived mesenchymal stem cells encapsulated in PEGDA hydrogels mature into valve interstitial-like cells. *Acta Biomater.* (2018) 71:235–46. doi: 10.1016/j.actbio.2018.02.025
173. Cushing MC, Liao JT, Anseth KS. Activation of valvular interstitial cells is mediated by transforming growth factor-beta1 interactions with matrix molecules. *Matrix Biol.* (2005) 24:428–37. doi: 10.1016/j.matbio.2005.06.007
174. Cushing MC, Jaeggli MP, Masters KS, Leinwand LA, Anseth KS. Serum deprivation improves seeding and repopulation of acellular matrices with valvular interstitial cells. *J Biomed Mater Res A.* (2005) 75:232–41. doi: 10.1002/jbm.a.30412
175. Benton JA, Fairbanks BD, Anseth KS. Characterization of valvular interstitial cell function in three dimensional matrix metalloproteinase degradable PEG hydrogels. *Biomaterials* (2009) 30:6593–603. doi: 10.1016/j.biomaterials.2009.08.031
176. Sant S, Iyer D, Gaharwar AK, Patel A, Khademhosseini A. Effect of biodegradation and de novo matrix synthesis on the mechanical properties of valvular interstitial cell-seeded polyglycerol sebacate-polycaprolactone scaffolds. *Acta Biomater.* (2013) 9:5963–73. doi: 10.1016/j.actbio.2012.11.014
177. Granados M, Morticelli L, Andriopoulou S, Kaloizoumis P, Pflaum M, Iablonskii P, et al. Development and characterization of a porcine mitral valve scaffold for tissue engineering. *J Cardiovasc Transl Res.* (2017) 10:374–90. doi: 10.1007/s12265-017-9747-z
178. Alavi SH, Kheradvar A. A hybrid tissue-engineered heart valve. *Ann Thorac Surg.* (2015) 99:2183–7. doi: 10.1016/j.athoracsur.2015.02.058
179. Crisan M, Yap S, Casteilla L, Chen CW, Corselli M, Park TS, et al. A perivascular origin for mesenchymal stem cells in multiple human organs. *Cell Stem Cell* (2008) 3:301–13. doi: 10.1016/j.stem.2008.07.003
180. Feng J, Mantesso A, De Bari C, Nishiyama A, Sharpe PT. Dual origin of mesenchymal stem cells contributing to organ growth and repair. *Proc Natl Acad Sci USA.* (2011) 108:6503–8. doi: 10.1073/pnas.1015449108
181. Murray IR, West CC, Hardy WR, James AW, Park TS, Nguyen A, et al. Natural history of mesenchymal stem cells, from vessel walls to culture vessels. *Cell Mol Life Sci.* (2014) 71:1353–74. doi: 10.1007/s00018-013-14626
182. Sousa BR, Parreira RC, Fonseca EA, Amaya MJ, Tonelli FM, Lacerda SM, et al. Human adult stem cells from diverse origins: an overview from multiparametric immunophenotyping to clinical applications. *Cytometry* (2014) 85:43–77. doi: 10.1002/cyto.a.22402
183. Hilfiker A, Kasper C, Hass R, Haverich A. Mesenchymal stem cells and progenitor cells in connective tissue engineering and regenerative medicine: is there a future for transplantation? *Langenbecks Arch Surg.* (2011) 396:489–97. doi: 10.1007/s00423-011-0762-2
184. Balguid A, Mol A, van Vlimmeren MA, Baaijens FP, Bouten CV. Hypoxia induces near-native mechanical properties in engineered heart valve tissue. *Circulation* (2009) 119:290–7. doi: 10.1161/CIRCULATIONAHA.107.749853
185. Nachlas ALY, Li S, Davis ME. Developing a clinically relevant tissue engineered heart valve—a review of current approaches. *Adv Healthc Mater.* (2017) 6. doi: 10.1002/adhm.201700918
186. Fioretta ES, von Boehmer L, Motta SE, Lintas V, Hoerstrup SP, Emmert MY. Cardiovascular tissue engineering: from basic science to clinical application. *Exp Gerontol.* (2018) doi: 10.1016/j.exger.2018.03.022. [Epub ahead of print].
187. Ali ML, Kumar SP, Bjornstad K, Duran CM. The sheep as an animal model for heart valve research. *Cardiovasc Surg.* (1996) 4:543–9. doi: 10.1016/0967-2109(95)00142-5
188. VeDepo MC, Detamore MS, Hopkins RA, Converse GL. Recellularization of decellularized heart valves: progress toward the tissue-engineered heart valve. *J Tissue Eng.* (2017) 8:2041731417726327. doi: 10.1177/2041731417726327
189. Gyongyosi M, Wojakowski W, Lemarchand P, Lunde K, Tendra M, Bartunek J, et al. Meta-Analysis of Cell-based CaRdial stUdiEs (ACCRUE) in patients with acute myocardial infarction based on individual patient data. *Circ Res.* (2015) 116:1346–60. doi: 10.1161/CIRCRESAHA.116.304346
190. Liu B, Duan CY, Luo CF, Ou CW, Sun K, Wu ZY, et al. Effectiveness and safety of selected bone marrow stem cells on left ventricular function in patients with acute myocardial infarction: a meta-analysis of randomized controlled trials. *Int J Cardiol.* (2014) 177:764–70. doi: 10.1016/j.ijcard.2014.11.005
191. Yuan L, Sakamoto N, Song G, Sato M. High-level shear stress stimulates endothelial differentiation and VEGF secretion by human mesenchymal stem cells. *Cell Mol Bioeng.* (2013) 6:220–9. doi: 10.1007/s12195-013-0275-x
192. Pankajakshan D, Kansal V, Agrawal DK. *In vitro* differentiation of bone marrow derived porcine mesenchymal stem cells to endothelial

- cells. *J Tissue Eng Regen Med.* (2013) 7:911–20. doi: 10.1002/term.1483
193. Asahara T, Murohara T, Sullivan A, Silver M, van der Zee R, Li T, et al. Isolation of putative progenitor endothelial cells for angiogenesis. *Science* (1997) 275:964–7. doi: 10.1126/science.275.5302.964
 194. Sales VL, Engelmayr GC Jr, Mettler BA, Johnson JA Jr, Sacks MS, Mayer JE, Jr. Transforming growth factor-beta1 modulates extracellular matrix production, proliferation, and apoptosis of endothelial progenitor cells in tissue-engineering scaffolds. *Circulation* (2006) 114(1 Suppl):I193–9. doi: 10.1161/CIRCULATIONAHA.105.001628
 195. Bischoff J, Aikawa E. Progenitor cells confer plasticity to cardiac valve endothelium. *J Cardiovasc Transl Res.* (2011) 4:710–9. doi: 10.1007/s12265-011-9312-0
 196. Yoder MC. Human endothelial progenitor cells. *Cold Spring Harb Perspect Med.* (2012) 2:a006692. doi: 10.1101/cshperspect.a006692
 197. Asahara T, Masuda H, Takahashi T, Kalka C, Pastore C, Silver M, et al. Bone marrow origin of endothelial progenitor cells responsible for postnatal vasculogenesis in physiological and pathological neovascularization. *Circ Res.* (1999) 85:221–8. doi: 10.1161/01.RES.85.3.221
 198. Jordan JE, Williams JK, Lee SJ, Raghavan D, Atala A, Yoo JJ. Bioengineered self-seeding heart valves. *J Thorac Cardiovasc Surg.* (2012) 143:201–8. doi: 10.1016/j.jtcvs.2011.10.005
 199. Hibino N, McGillicuddy E, Matsumura G, Ichihara Y, Naito Y, Breuer C, et al. Late-term results of tissue-engineered vascular grafts in humans. *J Thorac Cardiovasc Surg.* (2010) 139:431–6. doi: 10.1016/j.jtcvs.2009.09.057
 200. Dohmen PM, Lembcke A, Holinski S, Pruss A, Konertz W. Ten years of clinical results with a tissue-engineered pulmonary valve. *Ann Thorac Surg.* (2011) 92:1308–14. doi: 10.1016/j.athoracsur.2011.06.009
 201. Xue Y, Yatsenko T, Patel A, Stolz DB, Phillippi JA, Sant V, et al. PEGylated poly(ester amide) elastomer scaffolds for soft tissue engineering. *Polym Adv Technol.* (2017) 28:1097–106. doi: 10.1002/pat.4002
 202. Mohsen DK, Kakarougkas A, Allam NK. Recent advances on electrospun scaffolds as matrices for tissue-engineered heart valves. *Materials Today Chemistry* (2017) 5:11–23. doi: 10.1016/j.mtchem.2017.05.001
 203. Wang X, Lee J, Ali M, Kim J, Lacerda CMR. Phenotype transformation of aortic valve interstitial cells due to applied shear stresses within a microfluidic chip. *Ann Biomed Eng.* (2017) 45:2269–80. doi: 10.1007/s10439-017-1871-z
 204. Porras AM, Westlund JA, Evans AD, Masters KS. Creation of disease-inspired biomaterial environments to mimic pathological events in early calcific aortic valve disease. *Proc Natl Acad Sci USA.* (2018) 115:E363–71. doi: 10.1073/pnas.1704637115
 205. Masoumi N, Larson BL, Annabi N, Kharaziha M, Zamanian B, Shapero KS, et al. Electrospun PGS:PCL microfibers align human valvular interstitial cells and provide tunable scaffold anisotropy. *Adv Healthc Mater.* (2014) 3:929–39. doi: 10.1002/adhm.201300505
 206. Parvin Nejad S, Blaser MC, Santerre JP, Caldarone CA, Simmons CA. Biomechanical conditioning of tissue engineered heart valves: too much of a good thing? *Adv Drug Deliv Rev.* (2016) 96:161–75. doi: 10.1016/j.addr.2015.11.003
 207. Tao G, Kotick JD, Lincoln J. Heart valve development, maintenance, and disease: the role of endothelial cells. *Curr Top Dev Biol.* (2012) 100:203–32. doi: 10.1016/B978-0-12-387786-4.00006-3
 208. Wang H, Haeger SM, Kloxin AM, Leinwand LA, Anseth KS. Redirecting valvular myofibroblasts into dormant fibroblasts through light-mediated reduction in substrate modulus. *PLoS ONE* (2012) 7:e39969. doi: 10.1371/journal.pone.0039969
 209. Crisan M, Corselli M, Chen WC, Peault B. Perivascular cells for regenerative medicine. *J Cell Mol Med.* (2012) 16:2851–60. doi: 10.1111/j.1582-4934.2012.01617.x
 210. Geevarghese A, Herman IM. Pericyte-endothelial crosstalk: implications and opportunities for advanced cellular therapies. *Transl Res.* (2014) 163:296–306. doi: 10.1016/j.trsl.2014.01.011
 211. Avolio E, Madeddu P. Discovering cardiac pericyte biology: From physiopathological mechanisms to potential therapeutic applications in ischemic heart disease. *Vascul Pharmacol.* (2016) 86:53–63. doi: 10.1016/j.vph.2016.05.009
 212. Gaceb A, Barbariga M, Ozen I, Paul G. The pericyte secretome: Potential impact on regeneration. *Biochimie* (2018). doi: 10.1016/j.biochi.2018.04.015. [Epub ahead of print].
 213. Avolio E, Rodriguez-Arabaolaza I, Spencer HL, Riu F, Mangialardi G, Slater SC, et al. Expansion and characterization of neonatal cardiac pericytes provides a novel cellular option for tissue engineering in congenital heart disease. *J Am Heart Assoc.* (2015) 4:e002043. doi: 10.1161/JAHA.115.002043
 214. Katare R, Riu F, Mitchell K, Gubernator M, Campagnolo P, Cui Y, et al. Transplantation of human pericyte progenitor cells improves the repair of infarcted heart through activation of an angiogenic program involving micro-RNA-132. *Circ Res.* (2011) 109:894–906. doi: 10.1161/CIRCRESAHA.111.251546
 215. Avolio E, Meloni M, Spencer HL, Riu F, Katare R, Mangialardi G, et al. Combined intramyocardial delivery of human pericytes and cardiac stem cells additively improves the healing of mouse infarcted hearts through stimulation of vascular and muscular repair. *Circ Res.* (2015) 116:e81–94. doi: 10.1161/CIRCRESAHA.115.306146
 216. Alvino VV, Fernandez-Jimenez R, Rodriguez-Arabaolaza I, Slater S, Mangialardi G, Avolio E, et al. Transplantation of allogeneic pericytes improves myocardial vascularization and reduces interstitial fibrosis in a swine model of reperfused acute myocardial infarction. *J Am Heart Assoc.* (2018) 7:e006727. doi: 10.1161/JAHA.117.006727
 217. Bujan J, Bellon JM, Sabater C, Jurado F, Garcia-Honduvilla N, Dominguez B, et al. Modifications induced by atherogenic diet in the capacity of the arterial wall in rats to respond to surgical insult. *Atherosclerosis* (1996) 122:141–52. doi: 10.1016/0021-9150(95)05727-7
 218. Hu Y, Zhang Z, Torsney E, Afzal AR, Davison F, Metzler B, et al. Abundant progenitor cells in the adventitia contribute to atherosclerosis of vein grafts in ApoE-deficient mice. *J Clin Invest.* (2004) 113:1258–65. doi: 10.1172/JCI19628
 219. Hu Y, Davison F, Zhang Z, Xu Q. Endothelial replacement and angiogenesis in arteriosclerotic lesions of allografts are contributed by circulating progenitor cells. *Circulation* (2003) 108:3122–7. doi: 10.1161/01.CIR.0000105722.96112.67
- Conflict of Interest Statement:** The authors declare that the research was conducted in the absence of any commercial or financial relationships that could be construed as a potential conflict of interest.

Copyright © 2018 Jover, Fagnano, Angelini and Madeddu. This is an open-access article distributed under the terms of the Creative Commons Attribution License (CC BY). The use, distribution or reproduction in other forums is permitted, provided the original author(s) and the copyright owner(s) are credited and that the original publication in this journal is cited, in accordance with accepted academic practice. No use, distribution or reproduction is permitted which does not comply with these terms.



Can We Grow Valves Inside the Heart? Perspective on Material-based In Situ Heart Valve Tissue Engineering

Carlijn V. C. Bouten^{1,2*}, Anthal I. P. M. Smits^{1,2} and Frank P. T. Baaijens^{1,2}

¹ Soft Tissue Engineering and Mechanobiology, Department of Biomedical Engineering, Eindhoven University of Technology, Eindhoven, Netherlands, ² Institute for Complex Molecular Systems (ICMS), Eindhoven University of Technology, Eindhoven, Netherlands

OPEN ACCESS

Edited by:

Joshua D. Hutcheson,
Florida International University,
United States

Reviewed by:

Sergio Bertazzo,
University College London,
United Kingdom
Katherine Yutzey,
Cincinnati Children's Hospital Medical
Center, United States

*Correspondence:

Carlijn V. C. Bouten
c.v.c.bouten@tue.nl

Specialty section:

This article was submitted to
Atherosclerosis and
Vascular Medicine,
a section of the journal
Frontiers in Cardiovascular Medicine

Received: 31 January 2018

Accepted: 09 May 2018

Published: 29 May 2018

Citation:

Bouten CVC, Smits AIPM and
Baaijens FPT
(2018) Can We Grow Valves Inside
the Heart? Perspective on
Material-based In Situ Heart Valve
Tissue Engineering.
Front. Cardiovasc. Med. 5:54.
doi: 10.3389/fcvm.2018.00054

In situ heart valve tissue engineering using cell-free synthetic, biodegradable scaffolds is under development as a clinically attractive approach to create living valves right inside the heart of a patient. In this approach, a valve-shaped porous scaffold “implant” is rapidly populated by endogenous cells that initiate neo-tissue formation in pace with scaffold degradation. While this may constitute a cost-effective procedure, compatible with regulatory and clinical standards worldwide, the new technology heavily relies on the development of advanced biomaterials, the processing thereof into (minimally invasive deliverable) scaffolds, and the interaction of such materials with endogenous cells and neo-tissue under hemodynamic conditions. Despite the first positive preclinical results and the initiation of a small-scale clinical trial by commercial parties, in situ tissue formation is not well understood. In addition, it remains to be determined whether the resulting neo-tissue can grow with the body and preserves functional homeostasis throughout life. More important yet, it is still unknown if and how in situ tissue formation can be controlled under conditions of genetic or acquired disease. Here, we discuss the recent advances of material-based in situ heart valve tissue engineering and highlight the most critical issues that remain before clinical application can be expected. We argue that a combination of basic science – unveiling the mechanisms of the human body to respond to the implanted biomaterial under (patho)physiological conditions – and technological advancements – relating to the development of next generation materials and the prediction of in situ tissue growth and adaptation – is essential to take the next step towards a realistic and rewarding translation of in situ heart valve tissue engineering.

Keywords: endogenous regeneration, biomaterials, host response, tissue remodeling, clinical translation

INTRODUCTION

Since the introduction of the first artificial aortic heart valve by Hufnagel et al. more than six decades ago (1), heart valve prosthesis design has seen revolutionary changes in the endeavor to reduce prosthesis-related complications and to treat diverse patient groups. These include the development of bio-prostheses consisting of preserved human or animal tissue (2, 3) and the recent introduction of valve designs for transcatheter valve replacement (4). A true paradigm change, however, has been the construction of living valves through the process of tissue engineering. Conventional tissue engineering,

also named *in vitro* tissue engineering, is defined as the culture of cells – preferably from an autologous source – in combination with a degradable scaffold, to create a living implant or a living tissue mimic outside the human body (5). Living heart valve prostheses offer the potential to grow and adapt to changes in physiological demand and, as such, can last a lifetime. This was conceived as the holy grail for pediatric patients and the increasing number of patients with “grown up congenital heart disease” (GUCH), who will need one or more heart valve replacements later in life (6). Despite encouraging exemplary results (7, 8) and numerous modifications to the procedure (9–12), however, clinical translation has proven difficult. This is primarily caused by suboptimal long term *in vivo* results due to cell traction, consequent valve leaflet retraction, and unforeseen host responses to the constructs after

implantation (13–16). In addition, clinical translation is hindered by the logistic and regulatory complexity of the procedures, very limited shelf life, and costly cell and tissue culture in specialized laboratories, restricting the therapy to developed Western countries (17). These drawbacks have led clinicians and scientists to wonder if heart valve tissue engineering (HVTE) will ever make a difference in heart valve replacement therapy (18).

In Situ Heart Valve Tissue Engineering

Inspired by the *in vivo* host response of living tissue engineered valves, and to resolve the issue of cell traction-induced leaflet retraction, the concept of *in situ* HVTE using acellular starter matrices is explored by different groups (See Table 1). For instance, de-cellularized *in vitro*

TABLE 1 | Selection of (pre)clinical studies on *in situ* tissue engineered heart valves.

Material type	Model	Main findings/status	Refs.
Decellularized allografts			
Decell. allografts	PV and AV replacements in ovine and porcine models	Less calcification and improved durability compared to cryopreserved valves. Adequate nctionality demonstrated in juvenile, growing sheep, as well as elderly sheep. Cellularization typically persistent but partial.	(19–25)
Decell. allografts	PV replacement in children and young adults	Improved freedom from reoperations. Partial cellularization of the leaflet. No systemic immune response.	(26–28)
Decell. allografts + collagen conditioning treatment	PV replacement in baboons and growing lambs	Decreased antigenicity and improved somatic growth potential by collagen conditioning treatment.	(29, 30)
Decellularized xenografts			
Decell. xenografts (porcine)	PV replacement in adults and children	Mixed clinical results. Recellularization potential and immunological compatibility seems strongly dependent on decellularization and cryopreservation methods.	(31–34)
Decell. xenografts + various functionalizations	PV replacement in ovine and canine models	Various functionalization treatments to improve <i>in situ</i> recellularization, including CD133ab, HEP/HGF, G-CSF.	(35–37)
Decell. xenografts + PHB coatings	PV and AV replacements in sheep	Hybrid polymer-coated decellularized xenografts to improve mechanical and structural properties.	(38, 39)
Decellularized ECM			
Decell. SIS (CorMatrix)	Various valve replacements (PV, AV, MV) in children and adults	Mixed immunological response of remodeling and inflammation. Reports of severe insufficiency and degeneration. Consistent reporting of no remodeling into the typical 3-layered valve structure.	(40–42)
Decell. SIS (CorMatrix)	TV replacement in pig	<i>In situ</i> cellularization and remodeling reported, with potential for growth. Severe paravalvular regurgitation.	(43, 44)
Decellularized <i>de novo</i> tissue-engineered heart valves			
Decell. homologous TEHV	Minimally-invasively implanted PV in sheep and non-human primates	Decellularized TEHV technology compatible with minimally-invasive valve delivery. Extensive <i>in situ</i> cellularization of leaflets and tissue remodeling, including elastogenesis. Leaflet retraction and regurgitation at >8 weeks follow-up.	(45–47)
Decell. tubular TEHVs	Implantation as AV in sheep and PV in growing lambs	Extensive cellularization of leaflets and tissue remodeling, including elastogenesis. Sustained functionality for 6-months as AV. Progressive regurgitation of PVs in growing lambs.	(48, 49)
Resorbable synthetic valves			
PGA/P4HB, on-the-fly preseeded with BMCs	Transapically delivered AV in sheep and PV in non-human primates	Feasibility of technology demonstrated with acute valve functionality. Rapid polymer resorption	(50, 51)
P4HB/gelatin hybrid	Transapically delivered PV in sheep	Feasibility of technology demonstrated with acute valve functionality.	(52)
Slow-degrading supramolecular elastomers	PV and AV replacements in sheep	Sustained 1-year functionality with extensive <i>in situ</i> cellularization and tissue formation. Proof-of-concept for <i>in situ</i> TEHV using resorbable synthetic valves. Compatible with minimally-invasive delivery in PV and AV positions.	(53–55)
Slow-degrading supramolecular elastomers	PV replacements in pediatric patients	First ongoing clinical trials using resorbable synthetic valves (Xeltis XPlore-I and XPlore-II, NCT numbers: NCT02700100, NCT03022708).	-

AV, aortic valve; BMCs, bone marrow-derived cells.; G-CSF, granulocyte colony stimulating factor; HEP, heparin; HGF, hepatocyte growth factor; MV, mitral valve; P4HB, poly-4-hydroxybutyrate; PGA, polyglycolic acid; PHB, polyhydroxybutyrate; PV, pulmonary valve; SIS, small intestine submucosa; TEHV, tissue-engineered heart valve; TV, tricuspid valve.

engineered heart valves have been developed (56, 57). This approach aims at the creation of a living valve at the site of implantation using a cell-free, yet *in vitro* cultured, extracellular matrix that recruits endogenous cells after implantation. In contrast to de-cellularized xenografts and homografts (19, 27, 28, 58) *de novo* engineered matrix valves do not depend on the availability of a donor valve or tissue. These *de novo* engineered matrices show rapid repopulation with host cells required for growth and remodeling, both in sheep and non-human primates (45, 46, 48, 49). As such, the outlooks for clinical application are promising, but creation of these valves is still laborious and costly.

In recent years the use of biodegradable synthetic starter matrices has emerged as an alternative technology to grow living valves inside the heart (59). This technology offers readily available valvular grafts at substantially reduced costs. Porous synthetic polymer scaffolds are attractive candidates for the procedure as they can be rationally designed to accommodate cell recruitment and orchestrate tissue formation, while maintaining valve functionality. The technology is compatible with current regulatory frameworks for medical devices and artificial heart valves and exquisitely suited for both surgical and transcatheter valve delivery. We have investigated *in situ* HVTE using a slow-degrading electrospun bis-urea-modified polycarbonate elastomeric graft (55). When implanted as a surgical pulmonary valve replacement in sheep, valves maintained hemodynamic performance over a 12-month follow-up period as endogenous cells that produced a native-like, layered extracellular matrix slowly replaced the graft (Figure 1B). Transapically delivered pulmonary valves in Nitinol stents showed similar native-like matrix formation and good hemodynamic performance over a 6-month follow-up period.

Although this concept is widely explored for *in situ* engineered vascular grafts, leading to exciting preclinical and clinical trials (e.g., reviewed by 60 and 61), this was the first long-term pre-clinical proof of concept that *in situ* formation of living valvular tissue is possible without the use of any donor tissue or even *in vitro* cell and tissue culture. In parallel to – and independent of – this scientific proof of concept ongoing commercial developments of biodegradable polymer pulmonary valves have recently led to a small-scale clinical trial in pediatric patients (Xplore-I and Xplore-II trials) as well as the preclinical exploration of transcatheter aortic heart valves (62).

Despite these developments, complete understanding of neo-tissue formation is missing. In addition, growth of *in situ* engineered heart valves has not been demonstrated yet. Next to ongoing long-term *in vivo* investigation of the technology, a number of scientific and technological challenges must be addressed before *in situ* HVTE can be translated into a routine clinical practice. Below, we highlight the most critical issues.

OUTSTANDING CHALLENGES

I Understanding Materials-Driven Regeneration

Regenerative medicine in general – and *in situ* tissue engineering in particular – builds on the intrinsic self-healing and regenerative capacity of the human body. Hence, for *in situ* HVTE to be

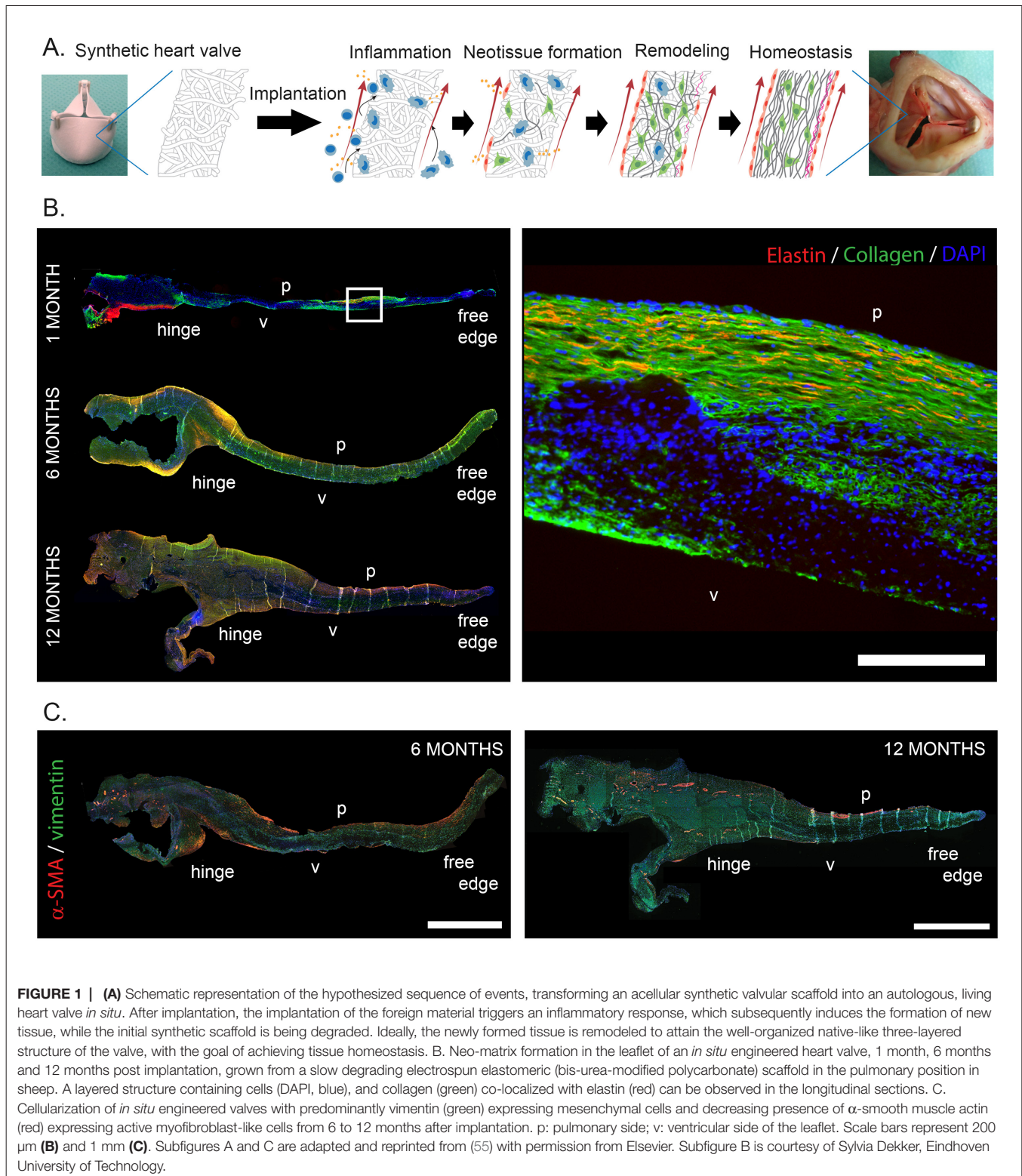
successful and safe, our understanding of the intelligent and diverse ways of human tissue adaptation and regeneration in response to a non-living degrading biomaterial under hemodynamic conditions is critical. Since this knowledge is virtually missing, the prime challenge is to develop a mechanistic understanding of materials-driven valve regeneration and unveil the potential and limitations of *in situ* HVTE under various (patho)physiological circumstances.

The core concept of *in situ* HVTE is that a degradable synthetic heart valve scaffold transforms into viable tissue with growth potential via an inflammatory response to the scaffold (Figure 1A). While little experimental data regarding the fundamental inflammatory and regenerative processes underlying *in situ* HVTE is available, mechanistic data from developmental biology and other *in situ* TE applications may give us more insight into these processes, as reviewed in more detail elsewhere (63). Specifically, studies employing resorbable vascular grafts have demonstrated that the host response to such an implanted grafts in the bloodstream is a cascade of events, initiated by the acute inflammatory response (64).

Upon implantation, the scaffold is first and foremost colonized by immune cells from the bloodstream (e.g., granulocytes, monocytes), followed by recruitment of progenitor cells, macrophages, lymphocytes, and tissue forming cells from blood and adjacent tissue, which are attracted by inflammatory cytokines and chemokines expressed by the immune cells. Next, the scaffold is degraded by foreign body giant cells while endogenous extracellular matrix is produced. Studies on highly regenerative species, such as axolotls, zebrafish and African spiny mice have demonstrated that macrophages are critical for regeneration (65–67). Similarly Hibino et al. demonstrated that systemic macrophage depletion led to a complete abrogation of regeneration of *in situ* TE vascular grafts in mice (68).

By coordinating the initial infiltration and differentiation of innate immune cells into the scaffold, the inflammatory response can potentially be harnessed to avoid chronic inflammation and tissue fibrosis (69). While the role of macrophage polarization in heart valve regeneration remains to be elucidated, it has been postulated that the differentiation of monocytes towards a regenerative macrophage (M2) phenotype should be enhanced early in the process to create the prerequisite initial conditions for stable tissue formation (70, 71). Additionally, recent data on the biomaterial-driven regeneration of skeletal muscle revealed an essential role for T helper 2 cells in the macrophage-driven regeneration (72). Following these initial processes, graft endothelialization and functional matrix organization (i.e., anisotropy, layered-ness) must be achieved, while preventing adverse effects like neo-intima hyperplasia, valvular fibrosis and calcification. The exact origin of the colonizing mature tissue cells remains speculative. With respect to endothelialization, studies in rodents have suggested transanastomotic ingrowth as the primary source of endothelial cells (73). However, the relevance of this suggestion for the human scenario has been contested, and recently transmural capillary ingrowth has been indicated as the primary route of endothelialization (74).

Our own preclinical results have indeed verified the above processes when using macro-porous, degradable electrospun scaffolds. Upon implantation the scaffolds were immediately colonized by immune



cells from the bloodstream, followed by recruitment of macrophages and tissue forming myofibroblast-like α -SMA⁺ and fibroblast-like vimentin⁺ cells from blood and adjacent tissue (valvular root) to eventually achieve a stable, quiescent α -SMA⁻/vimentin⁺ valvular

interstitial-like cell phenotype (**Figure 1C**). In addition, a layered ECM was developed, with mature collagen and elastin fibers, covered by a confluent endothelium weeks to months after implantation (21, 75). It remains to be elucidated if *in situ* tissue development will be

similar under more demanding conditions, such as in case of aortic valve replacement.

Systematic analysis of immune cell recruitment and polarization in preclinical studies, relevant for profound mechanistic understanding, requires the development of species-specific markers (76). More importantly, innate and adaptive immune responses may differ among species (77–79), strongly reducing the impact and translation of preclinical observations for human insights. For translational purposes it should furthermore be noted that the inflammatory host response and subsequent matrix formation is different in young versus old patients (80, 81), and can be affected by common comorbidities, like diabetes or kidney disease, common in older patients requiring heart valve replacements (82–85). Finally, it is far from clear if and how *in situ* tissue regeneration can be controlled under conditions of genetic or acquired disease.

In order to deal with the above-mentioned inter-species and inter-patient variability in the processes of material-driven inflammation and regeneration, the development of dedicated models is paramount. *In vitro* engineered laboratory models, based on human cells (either healthy or diseased) can be exploited to gain an initial understanding of tissue integration and remodeling in response to scaffolds (e.g., reviewed by 86 and 87). Dynamic *in vitro* co-culture platforms are eminently suitable to screen the interactions between human (circulatory) immune cells and valvular scaffolds under physiologically relevant hemodynamic stimuli, such as shear stress (88–90) and cyclic strains (91, 92). By using primary patient-derived cells, the influence of patient-specific characteristics on the cell-scaffold interactions can be assessed (e.g., 93, 94). Accordingly, preclinical animal models are increasingly being tailored to match specific clinical scenarios, for example by considering age (35), induced pathologies (38), or by using humanized animal models (95) or genetically modified animal models e.g., via CRISPR technologies (96, 97). All in all, the development of such refined, more personalized *in vitro* and *in vivo* models enables the fundamental unraveling of materials-driven regeneration for a wide range of patient populations.

II Biomaterial Development and Rational Scaffold Design

Although the use of synthetic degradable materials as valve replacement is attractive from a clinical perspective, the success of this approach fully depends on the generation of sophisticated biomaterials and the processing thereof into valvular scaffolds. For secured valve functionality, these scaffolds should: (i) take over valve functionality immediately upon implantation, thus providing structural and mechanical support; (ii) fully interact and integrate with their biological environment, instructing and guiding neo-tissue formation by providing a microenvironment with the necessary biochemical and biophysical cues for cells to home, stabilize, synthesize, and organize their own load-bearing extracellular matrix. (iii) maintain tissue functionality at all times, thus degrading in pace with neo-tissue formation and permitting matrix homeostasis and remodeling to evolving functional demands; and (iv) result in completely endogenous and well-

structured, layered and endothelialized valves that can adapt to somatic growth.

These demands are relevant across lengths scales. For instance, valve functionality (opening and closing, load-bearing properties) is determined by macroscopic mm-cm scale properties of the valvular scaffold, such as valve geometry, while cell behavior is mainly dependent on microscale properties, like porosity or chemical composition of the scaffold. Degradation profiles, on the other hand, will affect both microscopic and macroscopic properties.

Nowadays, many biomaterials and scaffolds are designed to induce tissue formation or even regeneration through direct interactions with proteins and cells via e.g., chemical function and binding affinity, but also via biophysical properties, like stiffness and nano-, micro- and mesoscale topologies (98–100). Revolutionary improvements in materials science, especially in the area of supramolecular polymers (101, 102) have recently resulted in the development of a new class of biomaterials that can be rendered bioactive and bioresponsive via the appending of functional moieties and tuned with respect to mechanical properties and degradation rate/mechanisms through simple “mix-and-match” assembly. These dynamic materials can interact with the biological system in an almost natural way; instructing and responding to cells and offering full control over the cellular environment. At the same time, they can be used to restore large defects, while providing temporary mechanical and structural support. Recent results with SDF-1 α functionalized scaffolds, for instance, demonstrate the potential of these materials in the cardiovascular system (103).

A main challenge is to develop instructive materials that are capable of harnessing the inevitable host response, for instance by selective recruitment of immune cells or by skewing macrophage polarization. Previous studies indicate that macrophage polarization in cell-free scaffolds can be achieved via the release of specific cytokines and trophic factors (MCP-1, SDF1 α , bFGF; 64, 68, 104). More recent findings, however, demonstrate that the biophysical microenvironment (strain, shear stress, anisotropy) experienced by infiltrating monocytes suffices to modulate macrophage polarization (44, 51, 105). As this would prevent the use of bioactive moieties, the processing of materials into scaffolds with the right initial microstructure might suffice to control the delicate balance between fibrotic and regenerative tissue formation.

Valvular scaffolds have been processed from a wide range of synthetic biomaterials (106, 107) using processing methods like electrospinning (108, 109), 3D printing (110), direct write melt electrospinning (111), jet spinning (52), and double component electrodeposition (112) to control valve macro and microstructure. The outcomes of these studies suggest that controlling leaflet shape and thickness, as well as pore size (for rapid cell repopulation, 113) are among the most critical parameters for ultimate valve function and regeneration.

Still, scaffold development for *in situ* HVTE would benefit greatly from systematic studies on the effects of individual and combined micro and microscale properties on valve function and regeneration. These should include currently unexplored properties like blood-scaffold interactions under anticoagulation therapy (114) and antimicrobial properties (115). The systematic

studies may take advantage from the above-mentioned *in vitro* models for screening candidate materials and even move towards the development of personalized scaffolds. Given the myriad of possible combinations, however, high-throughput analysis techniques combined with data mining may be a faster option (116, 117).

III Predicting Tissue Development and Growth

Computational modeling can also accelerate scaffold design across length scales. A significant example is the development of a predictive computational model to generate new testable hypotheses for scaffold properties that favor tissue engineered neovessel formation and function (118). For HVTE such models are scarce but indispensable. Initially, computational analysis focused at the biomechanics of heart valves and was directed at understanding the stress and strain distribution in the valve leaflets and valve root in relation to the geometry and mechanical properties of the tissues (e.g., reviewed in 119, 120). In particular, the impact of the collagen fiber architecture on the deformation patterns was investigated (121, 122). To this end, constitutive models with increasing complexity were developed to capture the microstructure of the valve. Upon the development of dedicated fluid-structure interaction algorithms, these models could also be used to investigate the impact of the microstructure on the opening and closing behavior of the valve leaflets (123). It was found that collagen fiber architecture not only significantly impact tissue stresses and strains during diastole, their predominant circumferential orientation also has a large effect on valve opening during systole and contribute to the stability of valve motion (124). These observations are likely relevant for valvular scaffolds as well and can be translated into “scaffold leaflets” with a predominantly circumferential anisotropy.

Understanding remodeling of the fibrous collagen network in response to static and dynamic loads – relevant for (neo)tissue adaptation and homeostasis – has evolved significantly over the years. To provide for a mechanistic understanding, these models include collagen synthesis and degradation profiles, as well as the impact of cellular traction forces resulting from intracellular actin stress fibers (125). Recently, these models have been calibrated against a number of experimental observations, demonstrating a remarkably accurate description of the collagen remodeling in native heart valves (126). Yet, they also reveal the complexity of the interplay between valve geometry, the evolving structural and mechanical properties of the tissue, and traction forces generated by the cells, thereby demonstrating the grand challenges in predicting neo-tissue formation and homeostasis in scaffold-driven *in situ* HVTE.

When using a fibrous scaffold as a starter matrix for *in situ* tissue engineering, computational models can provide the *initial* guidelines with respect to the geometry, mechanical properties, and – in particular – the fiber alignment that controls the degree of anisotropy of the leaflets (127). It is the combination of these properties that determines the deformation patterns in the leaflets that, together with the contact guidance provided by the fibers, dictates the alignment of the endogenously synthesized collagen

network (128), and thereby the mechanical functionality of the valve (129).

The next modeling challenge will be the analysis of evolving neo-tissue formation under various scaffold degradation profiles. Our preclinical studies have shown several stages in the process of tissue formation (55). Next to the deposition of collagen and elastin fibers inside the scaffold, significant tissue formation on top of the scaffold is observed, and with time a layered architecture develops. In regions with (near) complete scaffold degradation the tissue composition is markedly different from those with incomplete scaffold degradation. To analyze this staged tissue formation, advanced analysis tools are needed that not only account for mechanical cues, but also for cell signaling mechanisms driven by these cues to describe the complicated processes of growth and remodeling and to predict tissue self organization *in situ*. For example, it has been shown that Notch signaling has a profound impact on the layered architecture in heart valves and new models should incorporate this signaling (130). When established, such models may be extended with more (and even genetically affected) signaling pathways to provide insights in the requirements for scaffolds that drive tissue formation and ultimately tissue stability and functionality in a variety of pathological conditions.

CLINICAL PERSPECTIVE

Today, the question remains whether HVTE will ever make a difference. Yet, significant progress has been made and different concepts are being prepared for translation to the clinic (131). We have no doubt that material-based *in situ* HVTE will leave its footprint on the ongoing quest for a living heart valve replacement. Albeit scientifically and technically extremely challenging, the *in situ* approach may be more attractive to apply in clinic than other tissue engineering approaches as it will eliminate cell and tissue culture, can be easily scaled up to therapeutic needs, and may be developed into personalized therapies, while at the same reducing regulatory complexity. As such, the approach can bring living valve replacement therapy to many patients worldwide and will not just cater to the wealthy.

Obviously, tackling the above challenges will determine whether we reach this goal, or whether *in situ* HVTE will remain an academic exercise. A combination of multidisciplinary research – unveiling the mechanisms, potential and limitations of the postnatal human body to adequately respond to the implanted biomaterial scaffold – and technological advancements – relating to scaffold development and the prediction of tissue adaptation under various conditions – is essential to take the next step en route to clinical application. This step should include rigorous and extensive preclinical evaluation in direct comparison with *in vitro* and *in silico* studies to scrutinize and optimize the technology. Next, a number of reliable, well-regulated randomized clinical trials should be performed for which standardized procedures and endpoints are defined (132). In parallel, simulation models should be developed that estimate the quality of life of patients as well as cost-effectiveness of the new technology compared with existing valvular replacement therapies. These measures will support decision makers in their authorization strategy and will aid patients and doctors in

their choice of a prosthetic valve (133), thereby contributing to a cautious, realistic, and rewarding clinical translation.

AUTHOR CONTRIBUTIONS

CB suggested the subject of the review and drafted the outline of the manuscript. CB, AS, and FB drafted and edited the contents of the manuscript.

FUNDING

This work was supported by the BMM iValve and iValve-II projects, co-funded by the Dutch Ministry of Economic Affairs

REFERENCES

- Hufnagel CA, Harvey WP, Rabil PJ, Mcdermott TF. Surgical correction of aortic insufficiency. *Surgery* (1954) 35:673–83.
- Carpentier A, Lemaigre G, Robert L, Carpentier S, Dubost C. Biological factors affecting long-term results of valvular heterografts. *J Thorac Cardiovasc Surg* (1969) 58:467–83.
- Elkins RC, Dawson PE, Goldstein S, Walsh SP, Black KS. Decellularized human valve allografts. *Ann Thorac Surg* (2001) 71(5):S428–S432. doi: 10.1016/S0003-4975(01)02503-6
- Bonhoeffer P, Boudjemline Y, Saliba Z, Hausse AO, Aggoun Y, Bonnet D, et al. Transcatheter implantation of a bovine valve in pulmonary position : a lamb study. *Circulation* (2000) 102(7):813–6. doi: 10.1161/01.CIR.102.7.813
- Langer R, Vacanti J. Tissue engineering. *Science* (1993) 260(5110):920–6. doi: 10.1126/science.8493529
- Lupinetti FM, Duncan BW, Scifres AM, Fearneyhough CT, Kilian K, Rosenthal GL, et al. Intermediate-term results in pediatric aortic valve replacement. *Ann Thorac Surg* (1999) 68(2):521–5. doi: 10.1016/S0003-4975(99)00642-6
- Shinoka T, Breuer CK, Tanel RE, Zund G, Miura T, Ma PX, Px M, et al. Tissue engineering heart valves: Valve leaflet replacement study in a lamb model. *Ann Thorac Surg* (1995) 60:S513–S516. doi: 10.1016/0003-4975(95)00733-4
- Hoerstrup SP, Sodian R, Daebritz S, Wang J, Bacha EA, Martin DP, et al. Functional living trileaflet heart valves grown in vitro. *Circulation* (2000) 102(19 Suppl 3):III-44–40. doi: 10.1161/01.CIR.102.suppl_3.III-44
- Mol Aet al. Autologous human tissue-engineered heart valves: prospects for systemic application. *Circulation* (2006) 114(1_suppl):I-152–8. doi: 10.1161/CIRCULATIONAHA.105.001123
- Weber B, Scherman J, Emmert MY, Gruenenfelder J, Verbeek R, Bracher M, et al. Injectable living marrow stromal cell-based autologous tissue engineered heart valves: first experiences with a one-step intervention in primates. *Eur Heart J* (2011) 32(22):2830–40. doi: 10.1093/eurheartj/ehr059
- Puperi DS, Kishan A, Punske ZE, Wu Y, Cosgriff-Hernandez E, West JL, et al. Electrospun polyurethane and hydrogel composite scaffolds as biomechanical mimics for aortic valve tissue engineering. *ACS Biomater Sci Eng* (2016) 2(9):1546–58. doi: 10.1021/acsbomaterials.6b00309
- Wu S, Duan B, Qin X, Butcher JT. Living nano-micro fibrous woven fabric/hydrogel composite scaffolds for heart valve engineering. *Acta Biomater* (2017) 51:89–100. doi: 10.1016/j.actbio.2017.01.051
- Schmidt D, Dijkman PE, Driessen-Mol A, Stenger R, Mariani C, Puolakka A, et al. Minimally-invasive implantation of living tissue engineered heart valves: a comprehensive approach from autologous vascular cells to stem cells. *J Am Coll Cardiol* (2010) 56:510–20.
- Gottlieb D, Kunal T, Emani S, Aikawa E, Brown DW, Powell AJ, et al. In vivo monitoring of function of autologous engineered pulmonary valve. *J Thorac Cardiovasc Surg* (2010) 139(3):723–31. doi: 10.1016/j.jtcvs.2009.11.006
- Flanagan TC, Sachweh JS, Frese J, Schnöring H, Gronloh N, Koch S, et al. In vivo remodeling and structural characterization of fibrin-based tissue-

and the Netherlands Heart Foundation. AS received funding from the Netherlands Cardio Vascular Research Initiative: the Netherlands Heart Foundation, Dutch Federation of University Medical Centers, the Netherlands Organization for Health Research and Development and the Royal Netherlands Academy of Arts and Sciences (CVON I Valve). We gratefully acknowledge the financial support by the Ministry of Education, Culture and Science for the Gravitation Program 024.003.103 “Materials Driven Regeneration”.

ACKNOWLEDGMENTS

We acknowledge Dr. E.L. (Leda) Klouda for her critical review of the manuscript.

- engineered heart valves in the adult sheep model. *Tissue Eng Part A* (2009) 15(10):2965–76. doi: 10.1089/ten.tea.2009.0018
- Loerakker S, Ristori T, Baaijens FPT. A computational analysis of cell-mediated compaction and collagen remodeling in tissue-engineered heart valves. *J Mech Behav Biomed Mater* (2016) 58:173–87. doi: 10.1016/j.jmbm.2015.10.001
- Zilla P, Brink J, Human P, Bezuidenhout D. Prosthetic heart valves: Catering for the few. *Biomaterials* (2008) 29(4):385–406. doi: 10.1016/j.biomaterials.2007.09.033
- Yacoub MH, Takkenberg JJM. Will heart valve tissue engineering change the world? *Nat Clin Pract Cardiovasc Med* (2005) 2(2):60–1. doi: 10.1038/ncpcardio0112
- Iop L, Bonetti A, Naso F, Rizzo S, Cagnin S, Bianco R, et al. Decellularized allogeneic heart valves Demonstrate Self-regeneration potential after a long-term preclinical evaluation. *PLoS One* (2014) 9(6):e99593. doi: 10.1371/journal.pone.0099593
- Theodoridis K, Tudorache I, Calistru A, Cebotari S, Meyer T, Sarikouch S, et al. Successful matrix guided tissue regeneration of decellularized pulmonary heart valve allografts in elderly sheep. *Biomaterials* (2015) 52:221–8. doi: 10.1016/j.biomaterials.2015.02.023
- Baraki H, Tudorache I, Braun M, Höffler K, Görlner A, Lichtenberg A, et al. Orthotopic replacement of the aortic valve with decellularized allograft in a sheep model. *Biomaterials* (2009) 30(31):6240–6. doi: 10.1016/j.biomaterials.2009.07.068
- Leyh RG, Wilhelmi M, Rebe P, Fischer S, Kofidis T, Haverich A, et al. In vivo repopulation of xenogeneic and allogeneic acellular valve matrix conduits in the pulmonary circulation. *Ann Thorac Surg* (2003) 75(5):1457–63. doi: 10.1016/S0003-4975(02)04845-2
- della Barbera M, Valente M, Basso C, Thiene G. Morphologic studies of cell endogenous repopulation in decellularized aortic and pulmonary homografts implanted in sheep. *Cardiovasc Pathol* (2015) 24(2):102–9. doi: 10.1016/j.carpath.2014.10.001
- Tudorache I, Theodoridis K, Baraki H, Sarikouch S, Bara C, Meyer T, et al. Decellularized aortic allografts versus pulmonary autografts for aortic valve replacement in the growing sheep model: haemodynamic and morphological results at 20 months after implantation. *Eur J Cardiothorac Surg* (2016) 49(4):1228–38. doi: 10.1093/ejcts/ezv362
- Hopkins RA, Jones AL, Wolfenbarger L, Moore MA, Bert AA, Lofland GK. Decellularization reduces calcification while improving both durability and 1-year functional results of pulmonary homograft valves in juvenile sheep. *J Thorac Cardiovasc Surg* (2009) 137(4):907–13. doi: 10.1016/j.jtcvs.2008.12.009
- Neumann A, Sarikouch S, Breyman T, Cebotari S, Boethig D, Horke A, et al. Early systemic cellular immune response in children and young adults receiving decellularized fresh allografts for pulmonary valve replacement. *Tissue Eng Part A* (2014) 20(5-6):1003–11. doi: 10.1089/ten.tea.2013.0316
- Cebotari S, Tudorache I, Ciubotaru A, Boethig D, Sarikouch S, Goerler A, et al. Use of fresh decellularized allografts for pulmonary valve replacement may reduce the reoperation rate in children and young adults:

- early report. *Circulation* (2011) 124(11_suppl_1):S115–23. doi: 10.1161/CIRCULATIONAHA.110.012161
28. Sarikouch S, Horke A, Tudorache I, Beerbaum P, Westhoff-Bleck M, Boethig D, et al. Decellularized fresh homografts for pulmonary valve replacement: a decade of clinical experience. *Eur J Cardiothorac Surg* (2016) 50(2):281–90. doi: 10.1093/ejcts/ezw050
 29. Hopkins RA, Bert AA, Hilbert SL, Quinn RW, Brasky KM, Drake WB, et al. Bioengineered human and allogeneic pulmonary valve conduits chronically implanted orthotopically in baboons: Hemodynamic performance and immunologic consequences. *J Thorac Cardiovasc Surg* (2013) 145(4):1098–107. doi: 10.1016/j.jtcvs.2012.06.024
 30. Quinn RW, Bert AA, Converse GL, Buse EE, Hilbert SL, Drake WB, et al. Performance of allogeneic bioengineered replacement pulmonary valves in rapidly growing young lambs. *J Thorac Cardiovasc Surg* (2016) 152(4):1156–65. doi: 10.1016/j.jtcvs.2016.05.051
 31. Goecke T, Theodoridis K, Tudorache I, Ciubotaru A, Cebotari S, Ramm R, et al. In vivo performance of freeze-dried decellularized pulmonary heart valve allo- and xenografts orthotopically implanted into juvenile sheep. *Acta Biomater* (2018) 68:41–52. doi: 10.1016/j.actbio.2017.11.041
 32. Rieder E, Kasimir M-T, Silberhumer G, Seebacher G, Wolner E, Simon P, et al. Decellularization protocols of porcine heart valves differ importantly in efficiency of cell removal and susceptibility of the matrix to recellularization with human vascular cells. *J Thorac Cardiovasc Surg* (2004) 127(2):399–405. doi: 10.1016/j.jtcvs.2003.06.017
 33. Schneider M, Stamm C, Brockbank KGM, Stock UA, Seifert M. The choice of cryopreservation method affects immune compatibility of human cardiovascular matrices. *Sci Rep* (2017) 7(1):1–14. doi: 10.1038/s41598-017-17288-z
 34. Vedepo MC, Detamore MS, Hopkins RA, Converse GL. Recellularization of decellularized heart valves: Progress toward the tissue-engineered heart valve. *J Tissue Eng* (2017) 8:2041731417726327. doi: 10.1177/2041731417726327
 35. Juthier F, Vincentelli A, Gaudric J, Corseaux D, Fouquet O, Calet C, et al. Decellularized heart valve as a scaffold for in vivo recellularization: Deleterious effects of granulocyte colony-stimulating factor. *J Thorac Cardiovasc Surg* (2006) 131(4):843–52. doi: 10.1016/j.jtcvs.2005.11.037
 36. Ota T, Sawa Y, Iwai S, Kitajima T, Ueda Y, Coppin C, et al. Fibronectin-hepatocyte growth factor enhances reendothelialization in tissue-engineered heart valve. *Ann Thorac Surg* (2005) 80(5):1794–801. doi: 10.1016/j.athoracsur.2005.05.002
 37. Williams JK, Miller ES, Lane MR, Atala A, Yoo JJ, Jordan JE. Characterization of CD133 Antibody-Directed Recellularized Heart Valves. *J Cardiovasc Transl Res* (2015) 8(7):411–20. doi: 10.1007/s12265-015-9651-3
 38. Stamm C, Khosravi A, Grabow N, Schmohl K, Treckmann N, Drechsel A, et al. Biomatrix/polymer composite material for heart valve tissue engineering. *Ann Thorac Surg* (2004) 78(6):2084–93. doi: 10.1016/j.athoracsur.2004.03.106
 39. Wu S, Liu Y-L, Cui B, Qu X-H, Chen G-Q. Study on decellularized porcine aortic valve/poly (3-hydroxybutyrate-co-3-hydroxyhexanoate) hybrid heart valve in sheep model. *Artif Organs* (2007) 31(9):689–97. doi: 10.1111/j.1525-1594.2007.00442.x
 40. Hofmann M, Schmiady MO, Burkhardt BE, Dave HH, Hübler M, Kretschmar O, et al. Congenital aortic valve repair using CorMatrix®: A histologic evaluation. *Xenotransplantation* (2017) 24(6):1–9. doi: 10.1111/xen.12341
 41. Woo JS, Fishbein MC, Reemtsen B. Histologic examination of decellularized porcine intestinal submucosa extracellular matrix (CorMatrix) in pediatric congenital heart surgery. *Cardiovasc Pathol* (2016) 25(1):12–17. doi: 10.1016/j.carpath.2015.08.007
 42. Zaidi AH, Nathan M, Emani S, Baird C, del Nido PJ, Gauvreau K, et al. Preliminary experience with porcine intestinal submucosa (CorMatrix) for valve reconstruction in congenital heart disease: Histologic evaluation of explanted valves. *J Thorac Cardiovasc Surg* (2014) 148(5):2216–25. doi: 10.1016/j.jtcvs.2014.02.081
 43. Ropcke DM, Ilkjaer C, Tjørnild MJ, Skov SN, Ringgaard S, Hjortdal VE, et al. Small intestinal submucosa tricuspid valve tube graft shows growth potential, remodelling and physiological valve function in a porcine model. *Interact Cardiovasc Thorac Surg* (2017) 24(6):918–24. doi: 10.1093/icvts/ivx017
 44. Ropcke DM, Rasmussen J, Ilkjaer C, Skov SN, Tjørnild MJ, Baandrup UT, et al. Mid-term function and remodeling potential of tissue engineered tricuspid valve: Histology and biomechanics. *J Biomech* (2018) 71:52–8. doi: 10.1016/j.jbiomech.2018.01.019
 45. Driessen-Mol A, Emmert MY, Dijkman PE, Frese L, Sanders B, Weber B, et al. Transcatheter implantation of homologous “off-the-shelf” tissue-engineered heart valves with self-repair capacity: long-term functionality and rapid in vivo remodeling in sheep. *J Am Coll Cardiol* (2014) 63:1320–9.
 46. Weber B, Dijkman PE, Scherman J, Sanders B, Emmert MY, Grünenfelder J, et al. Off-the-shelf human decellularized tissue-engineered heart valves in a non-human primate model. *Biomaterials* (2013) 34(30):7269–80. doi: 10.1016/j.biomaterials.2013.04.059
 47. Spriestersbach H, Prudlo A, Bartosch M, Sanders B, Radtke T, Baaijens FPT, et al. First percutaneous implantation of a completely tissue-engineered self-expanding pulmonary heart valve prosthesis using a newly developed delivery system: a feasibility study in sheep. *Cardiovasc Interv Ther* (2017) 32(1):36–7. doi: 10.1007/s12928-016-0396-y
 48. Syedain Z, Reimer J, Schmidt J, Lahti M, Berry J, Bianco R, et al. 6-Month aortic valve implantation of an off-the-shelf tissue-engineered valve in sheep. *Biomaterials* (2015) 73:175–84. doi: 10.1016/j.biomaterials.2015.09.016
 49. Reimer J, Syedain Z, Haynie B, Lahti M, Berry J, Tranquillo R. Implantation of a Tissue-engineered tubular heart valve in growing lambs. *Ann Biomed Eng* (2017) 45(2):439–51. doi: 10.1007/s10439-016-1605-7
 50. Weber B, Scherman J, Emmert MY, Gruenenfelder J, Verbeek R, Bracher M, et al. Injectable living marrow stromal cell-based autologous tissue engineered heart valves: first experiences with a one-step intervention in primates. *Eur Heart J* (2011) 32(22):2830–40. doi: 10.1093/eurheartj/ehr059
 51. Emmert MY, Weber B, Behr L, Sammut S, Frauenfelder T, Wolint P, et al. Transcatheter aortic valve implantation using anatomically oriented, marrow stromal cell-based, stented, tissue-engineered heart valves: technical considerations and implications for translational cell-based heart valve concepts. *Eur J Cardiothorac Surg* (2014) 45(1):61–8. doi: 10.1093/ejcts/ezt243
 52. Capulli AK, Emmert MY, Pasqualini FS, Kehl D, Caliskan E, Lind JU, et al. JetValve: Rapid manufacturing of biohybrid scaffolds for biomimetic heart valve replacement. *Biomaterials* (2017) 133:229–41. doi: 10.1016/j.biomaterials.2017.04.033
 53. Bennink G, Torii S, Brugmans M, Cox M, Svanidze O, Ladich E, et al. A novel restorative pulmonary valved conduit in a chronic sheep model: Mid-term hemodynamic function and histologic assessment. *J Thorac Cardiovasc Surg* (2017). doi: 10.1016/j.jtcvs.2017.04.033
 54. Serruys P, Miyazaki Y, Katsikis A, Abdelghani M, Leon M, Virmani R, et al. Restorative valve therapy by endogenous tissue restoration: tomorrow's world? Reflection on the EuroPCR 2017 session on endogenous tissue restoration. *EuroIntervention* (2017) 13(AA):AA68–AA77. doi: 10.4244/EIJ-D-17-00509
 55. Kluijn J, Talacua H, Smits AIPM, Emmert MY, Brugmans MCP, Fioretta ES, et al. *In situ* heart valve tissue engineering using a bioresorbable elastomeric implant – From material design to 12 months follow-up in sheep. *Biomaterials* (2017) 125:101–17. doi: 10.1016/j.biomaterials.2017.02.007
 56. Dijkman PE, Driessen-Mol A, Frese L, Hoerstrup SP, Baaijens FPT. Decellularized homologous tissue-engineered heart valves as off-the-shelf alternatives to xeno- and homografts. *Biomaterials* (2012) 33(18):4545–54. doi: 10.1016/j.biomaterials.2012.03.015
 57. Reimer JM, Syedain ZH, Haynie BHT, Tranquillo RT. Pediatric tubular pulmonary heart valve from decellularized engineered tissue tubes. *Biomaterials* (2015) 62:88–94. doi: 10.1016/j.biomaterials.2015.05.009
 58. Jordan JE, Williams JK, Lee S-J, Raghavan D, Atala A, Yoo JJ, et al. Bioengineered self-seeding heart valves. *J Thorac Cardiovasc Surg* (2012) 143(1):201–8. doi: 10.1016/j.jtcvs.2011.10.005
 59. Bouten CVC, Driessen-Mol A, Baaijens FPT. *In situ* heart valve tissue engineering: simple devices, smart materials, complex knowledge. *Expert Rev Med Devices* (2012) 9(5):453–5. doi: 10.1586/erd.12.43
 60. Li S, Sengupta D, Chien S. Vascular tissue engineering: from *in vitro* to *in situ*. *Wiley Interdiscip Rev Syst Biol Med* (2014) 6(1):61–76. doi: 10.1002/wsbm.1246
 61. Pashneh-Tala S, Macneil S, Claeysens F. The Tissue-Engineered Vascular Graft—Past, Present, and Future. *Tissue Eng Part B* (2016) 22:68–100.
 62. Miyazaki Y, Soliman O, Abdelghani M, Katsikis A, Naz C, Lopes S, et al. Acute performance of a novel restorative transcatheter aortic valve: preclinical results. *EuroIntervention* (2017) 13(12):e1410–7. doi: 10.4244/EIJ-D-17-00554

63. Wissing TB, Bonito V, Bouten CVC, Smits AIPM. Biomaterial-driven in situ cardiovascular tissue engineering—a multi-disciplinary perspective. *NPJ Regen Med* (2017) 2(2-171):18. doi: 10.1038/s41536-017-0023-2
64. Roh JD, Sawh-Martinez R, Brennan MP, Jay SM, Devine L, Rao DA, et al. Tissue-engineered vascular grafts transform into mature blood vessels via an inflammation-mediated process of vascular remodeling. *Proc Natl Acad Sci U S A* (2010) 107(10):4669–74. doi: 10.1073/pnas.0911465107
65. Godwin JW, Pinto AR, Rosenthal NA. Macrophages are required for adult salamander limb regeneration. *Proc Natl Acad Sci U S A* (2013) 110(23):9415–20. doi: 10.1073/pnas.1300290110
66. Petrie TA, Strand NS, Tsung-Yang C, Rabinowitz JS, Moon RT. Macrophages modulate adult zebrafish tail fin regeneration. *Development* (2014) 141(13):2581–91. doi: 10.1242/dev.098459
67. Simkin J, Gawriluk TR, Gensel JC, Seifert AW. Macrophages are necessary for epimorphic regeneration in African spiny mice. *eLife* (2017) 6. doi: 10.7554/eLife.24623
68. Hibino N, Yi T, Duncan DR, Rathore A, Dean E, Naito Y, et al. A critical role for macrophages in neovessel formation and the development of stenosis in tissue-engineered vascular grafts. *FASEB J* (2011) 25(12):4253–63. doi: 10.1096/fj.11-186585
69. Wissing TB, Bonito V, Bouten CVC, Smits AIPM. Biomaterial-driven in situ cardiovascular tissue engineering—a multi-disciplinary perspective. *NPJ Regen Med* (2017) 2(2-171):18. doi: 10.1038/s41536-017-0023-2
70. Brown BN, Londono R, Tottey S, Zhang L, Kukla KA, Wolf MT, et al. Macrophage phenotype as a predictor of constructive remodeling following the implantation of biologically derived surgical mesh materials. *Acta Biomater* (2012) 8(3):978–87. doi: 10.1016/j.actbio.2011.11.031
71. Badylak SF, Valentin JE, Ravindra AK, McCabe GP, Stewart-Akers AM. Macrophage phenotype as a determinant of biologic scaffold remodeling. *Tissue Eng Part A* (2008) 14:1835–42.
72. Stadtler K, Estrellas K, Allen BW, Wolf MT, Fan H, Tam AJ, et al. Developing a pro-regenerative biomaterial scaffold microenvironment requires T helper 2 cells. *Science* (2016) 15:366–70.
73. Hibino N, Villalona G, Pietris N, Duncan DR, Schoffner A, Roh JD, et al. Tissue-engineered vascular grafts form neovessels that arise from regeneration of the adjacent blood vessel. *The FASEB Journal* (2011) 25(8):2731–9. doi: 10.1096/fj.11-182246
74. Pennel T, Bezuidenhout D, Koehne J, Davies NH, Zilla P. Transmural capillary ingrowth is essential for confluent vascular graft healing. *Acta Biomater* (2018) 65:237–47. doi: 10.1016/j.actbio.2017.10.038
75. Talacua H, Smits AIPM, Muylaert DEP, van Rijswijk JW, Vink A, Verhaar MC, et al. In Situ tissue engineering of functional small-diameter blood vessels by host circulating cells only. *Tissue Eng Part A* (2015) 21(19-20):2583–94. doi: 10.1089/ten.tea.2015.0066
76. de Visscher G, Plusquin R, Mesure L, Flameng W. Selection of an immunohistochemical panel for cardiovascular research in sheep. *Appl Immunohistochem Mol Morphol* (2010) 18(4):382–91. doi: 10.1097/PAI.0b013e3181cd32e7
77. Seok J, Warren HS, Cuenca AG, Mindrinos MN, Baker HV, Xu W, et al. Genomic responses in mouse models poorly mimic human inflammatory diseases. *Proc Natl Acad Sci U S A* (2013) 110(9):3507–12. doi: 10.1073/pnas.1222878110
78. Spiller KL, Wrona EA, Romero-Torres S, Pallotta I, Graney PL, Witherell CE, et al. Differential gene expression in human, murine, and cell line-derived macrophages upon polarization. *Exp Cell Res* (2016) 347(1):1–13. doi: 10.1016/j.yexcr.2015.10.017
79. Mestas J, Hughes CCW. Of mice and not men: differences between mouse and human immunology. *J Immunol* (2004) 172(5):2731–8. doi: 10.4049/jimmunol.172.5.2731
80. Hachim D, Wang N, Lopresti ST, Stahl EC, Umeda YU, Rege RD, et al. Effects of aging upon the host response to implants. *J Biomed Mater Res A* (2017) 105(5):1281–92. doi: 10.1002/jbm.a.36013
81. Levy O. Innate immunity of the newborn: basic mechanisms and clinical correlates. *Nat Rev Immunol* (2007) 7(5):379–90. doi: 10.1038/nri2075
82. Socarrás TO, Vasconcelos AC, Campos PP, Pereira NB, Souza JPC, Andrade SP. Foreign body response to subcutaneous implants in diabetic rats. *PLoS One* (2014) 9(11):e110945. doi: 10.1371/journal.pone.0110945
83. Wang Z, Zheng W, Wu Y, Wang J, Zhang X, Wang K, et al. Differences in the performance of PCL-based vascular grafts as abdominal aorta substitutes in healthy and diabetic rats. *Biomater Sci* (2016) 4(10):1485–92. doi: 10.1039/C6BM00178E
84. Kooman JP, Dekker MJ, Usvyat LA, Kotanko P, van der Sande FM, Schalkwijk CG, et al. Inflammation and premature aging in advanced chronic kidney disease. *Am J Physiol Renal Physiol* (2017) 313(4):F938–F950. doi: 10.1152/ajprenal.00256.2017
85. Simionescu A, Schulte JB, Fercana G, Simionescu DT. Inflammation in cardiovascular tissue engineering: The challenge to a promise: A Minireview. *Int J Inflammation* (2011) ID 958247. doi: 10.1155/2011/958247
86. Wolf F, Vogt F, Schmitz-Rode T, Jockenhoevel S, Mela P. Bioengineered vascular constructs as living models for in vitro cardiovascular research. *Drug Discov Today* (2016) 21(9):1446–55. doi: 10.1016/j.drudis.2016.04.017
87. Zhu AS, Grande-Allen KJ. Heart valve tissue engineering for valve replacement and disease modeling. *Curr Opin Biomed Eng* (2018) 5:35–41. doi: 10.1016/j.cobme.2017.12.006
88. Smits AI, Driessen-Mol A, Bouten CV, Baaijens FP. A mesofluidics-based test platform for systematic development of scaffolds for in situ cardiovascular tissue engineering. *Tissue Eng Part C Methods* (2012) 18(6):475–85. doi: 10.1089/ten.tec.2011.0458
89. Smits AIPM, Ballotta V, Driessen-Mol A, Bouten CVC, Baaijens FPT. Shear flow affects selective monocyte recruitment into MCP-1-loaded scaffolds. *J Cell Mol Med* (2014) 18(11):2176–88. doi: 10.1111/jcmm.12330
90. Sanders B, Driessen-Mol A, Bouten CVC, Baaijens FPT. The effects of scaffold remnants in decellularized tissue-engineered cardiovascular constructs on the recruitment of blood cells. *Tissue Eng Part A* (2017) 23(19-20):1142–51. doi: 10.1089/ten.tea.2016.0503
91. Battiston KG, Labow RS, Simmons CA, Santerre JP. Immunomodulatory polymeric scaffold enhances extracellular matrix production in cell co-cultures under dynamic mechanical stimulation. *Acta Biomater* (2015) 24:74–86. doi: 10.1016/j.actbio.2015.05.038
92. Ballotta V, Driessen-Mol A, Bouten CVC, Baaijens FPT. Strain-dependent modulation of macrophage polarization within scaffolds. *Biomaterials* (2014) 35(18):4919–28. doi: 10.1016/j.biomaterials.2014.03.002
93. Boersema GSA, Utomo L, Bayon Y, Kops N, van der Harst E, Lange JE, et al. Monocyte subsets in blood correlate with obesity related response of macrophages to biomaterials in vitro. *Biomaterials* (2016) 109:32–9. doi: 10.1016/j.biomaterials.2016.09.009
94. Simionescu D, Jaeggli M, Liao J, Simionescu A. Translational personalized regenerative medicine; scaffolds and stem cells for patient-tailored aortic heart valve tissue engineering. *Cardiology* (2012) 121:138.
95. Wang RM, Johnson TD, He J, Rong Z, Wong M, Nigam V, et al. Humanized mouse model for assessing the human immune response to xenogeneic and allogeneic decellularized biomaterials. *Biomaterials* (2017) 129:98–110. doi: 10.1016/j.biomaterials.2017.03.016
96. Yang H, Wang H, Jaenisch R. Generating genetically modified mice using CRISPR/Cas-mediated genome engineering. *Nat Protoc* (2014) 9(8):1956–68. doi: 10.1038/nprot.2014.134
97. Zhang W, Wang G, Wang Y, Jin Y, Zhao L, Xiong Q, et al. Generation of complement protein C3 deficient pigs by CRISPR/Cas9-mediated gene targeting. *Sci Rep* (2017) 7(1):5009. doi: 10.1038/s41598-017-05400-2
98. Langer R, Tirrell DA. Designing materials for biology and medicine. *Nature* (2004) 428(6982):487–92. doi: 10.1038/nature02388
99. Murphy WL, Mcdevitt TC, Engler AJ. Materials as stem cell regulators. *Nat Mater* (2014) 13(6):547–57. doi: 10.1038/nmat3937
100. Huebsch N, Mooney DJ. Inspiration and application in the evolution of biomaterials. *Nature* (2009) 462(7272):426–32. doi: 10.1038/nature08601
101. Dankers PY, Harmsen MC, Brouwer LA, van Luyn MJ, Meijer EW. A modular and supramolecular approach to bioactive scaffolds for tissue engineering. *Nat Mater* (2005) 4(7):568–74. doi: 10.1038/nmat1418
102. Webber MJ, Appel EA, Meijer EW, Langer R. Supramolecular biomaterials. *Nat Mater* (2016) 15(1):13–26. doi: 10.1038/nmat4474
103. Muylaert DE, van Almen GC, Talacua H, Flederius JO, Kluin J, Hendrikse SI, et al. Early in-situ cellularization of a supramolecular vascular graft is modified by synthetic stromal cell-derived factor-1 α derived peptides. *Biomaterials* (2016) 76:187–95. doi: 10.1016/j.biomaterials.2015.10.052

104. Ballotta V, Smits AI, Driessen-Mol A, Bouten CV, Baaijens FP. Synergistic protein secretion by mesenchymal stromal cells seeded in 3D scaffolds and circulating leukocytes in physiological flow. *Biomaterials* (2014) 35(33):9100–13. doi: 10.1016/j.biomaterials.2014.07.042
105. Garg K, Pullen NA, Oskeritzian CA, Ryan JJ, Bowlin GL. Macrophage functional polarization (M1/M2) in response to varying fiber and pore dimensions of electrospun scaffolds. *Biomaterials* (2013) 34(18):4439–51. doi: 10.1016/j.biomaterials.2013.02.065
106. Bouten CV, Dankers PY, Driessen-Mol A, Pedron S, Brizard AM, Baaijens FP. Substrates for cardiovascular tissue engineering. *Adv Drug Deliv Rev* (2011) 63(4-5):221–41. doi: 10.1016/j.addr.2011.01.007
107. Nachlas ALY, Li S, Davis ME. Developing a review of Current Approaches. *Adv Healthc Mater* (2017) 6(24):1700918. doi: 10.1002/adhm.201700918
108. Simonet M, Driessen – Mol A, Baaijens FPT, Bouten CVC. Heart valve tissue regeneration. In: *Bosworth L, Downes S, editors. Electrospinning for tissue regeneration*. Cambridge: Woodhead Publishing Limited (2011). p. 202–24.
109. del Gaudio C, Grigioni M, Bianco A, de Angelis G. Electrospun bioresorbable heart valve scaffold for tissue engineering. *Int J Artif Organs* (2008) 31(1):68–75. doi: 10.1177/039139880803100110
110. Hockaday LA, Kang KH, Colangelo NW, Cheung PY, Duan B, Malone E, et al. Rapid 3D printing of anatomically accurate and mechanically heterogeneous aortic valve hydrogel scaffolds. *Biofabrication* (2012) 4(3):035005. doi: 10.1088/1758-5082/4/3/035005
111. Ristovski N, Bock N, Liao S, Powell SK, Ren J, Kirby GT, Gilles TS, et al. Improved fabrication of melt electrospun tissue engineering scaffolds using direct writing and advanced electric field control. *Biointerphases* (2015) 10(1):011006. doi: 10.1116/1.4914380
112. D'Amore A, Luketich SK, Raffa GM, Ollia S, Menallo G, Mazzola A, et al. Heart valve scaffold fabrication: Bioinspired control of macro-scale morphology, mechanics and micro-structure. *Biomaterials* (2018) 150:25–37. doi: 10.1016/j.biomaterials.2017.10.011
113. Balgud A, Mol A, van Marion MH, Bank RA, Bouten CV, Baaijens FP. Tailoring fiber diameter in electrospun poly(epsilon-caprolactone) scaffolds for optimal cellular infiltration in cardiovascular tissue engineering. *Tissue Eng Part A* (2009) 15(2):437–44. doi: 10.1089/ten.tea.2007.0294
114. Gross L, Sibbing D, Eickhoff M, Baquet M, Orban M, Krieg A, et al. Impact of the bioresorbable vascular scaffold surface area on on-treatment platelet reactivity. *Platelets* (2016) 27(5):446–51. doi: 10.3109/09537104.2016.1143918
115. Riool M, de Breij A, Drijfhout JW, Nibbering PH, Zaat SAJ. Antimicrobial peptides in biomedical device manufacturing. *Frontiers Chem* (2017) 5:63. doi: 10.3389/fchem.2017.00063
116. Unadkat HV, Hulsman M, Cornelissen K, Papenburg BJ, Truckenmüller RK, Carpenter AE, et al. An algorithm-based topographical biomaterials library to instruct cell fate. *Proc Natl Acad Sci U S A* (2011) 108(40):16565–70. doi: 10.1073/pnas.1109861108
117. Vasilevich AS, Carlier A, de Boer J, Singh S. How not to drown in data: a guide for biomaterial engineers. *Trends Biotechnol* (2017) 35(8):743–55. doi: 10.1016/j.tibtech.2017.05.007
118. Miller KS, Khosravi R, Breuer CK, Humphrey JD. A hypothesis-driven parametric study of effects of polymeric scaffold properties on tissue engineered neovessel formation. *Acta Biomater* (2015) 11:283–94. doi: 10.1016/j.actbio.2014.09.046
119. Sacks MS, Yoganathan AP. Heart Valve Function: A Biomechanical Perspective. *Philosophical Transactions: R Soc Lond B Biol Sci* (2007) 362(1484):1369–91. doi: 10.1098/rstb.2007.2122
120. Weinberg EJ, Shahmirzadi D, Mofrad MR. On the multiscale modeling of heart valve biomechanics in health and disease. *Biomech Model Mechanobiol* (2010) 9(4):373–87. doi: 10.1007/s10237-009-0181-2
121. Driessen NJB, Boerboom RA, Huyghe JMR, Bouten CVC, Baaijens FPT. Computational analyses of mechanically induced collagen fibre remodeling in the aortic heart valve. *J Biomech Eng* (2003) 125(4):549–57. doi: 10.1115/1.1590361
122. Loerakker S, Argento G, Oomens CW, Baaijens FP. Effects of valve geometry and tissue anisotropy on the radial stretch and coaptation area of tissue-engineered heart valves. *J Biomech* (2013) 46(11):1792–800. doi: 10.1016/j.jbiomech.2013.05.015
123. de Hart J, Peters GW, Schreurs PJ, Baaijens FP. A three-dimensional computational analysis of fluid-structure interaction in the aortic valve. *J Biomech* (2003) 36(1):103–12. doi: 10.1016/S0021-9290(02)00244-0
124. de Hart J, Peters GW, Schreurs PJ, Baaijens FP. Collagen fibers reduce stresses and stabilize motion of aortic valve leaflets during systole. *J Biomech* (2004) 37(3):303–11. doi: 10.1016/S0021-9290(03)00293-8
125. Loerakker S, Obbink-Huizer C, Baaijens FP. A physically motivated constitutive model for cell-mediated compaction and collagen remodeling in soft tissues. *Biomech Model Mechanobiol* (2014) 13(5):985–1001. doi: 10.1007/s10237-013-0549-1
126. Oomen PJA, Loerakker S, van Geemen D, Negggers J, Goumans MTH, van den Bogaerd AJ, et al. Age-dependent changes of stress and strain in the human heart valve and their relation with collagen remodeling. *Acta Biomater* (2016) 29:161–9. doi: 10.1016/j.actbio.2015.10.044
127. Argento G, Simonet M, Oomens CW, Baaijens FP. Multi-scale mechanical characterization of scaffolds for heart valve tissue engineering. *J Biomech* (2012) 45(16):2893–8. doi: 10.1016/j.jbiomech.2012.07.037
128. de Jonge N, Kanters FM, Baaijens FP, Bouten CV. Strain-induced collagen organization at the micro-level in fibrin-based engineered tissue constructs. *Ann Biomed Eng* (2013) 41(4):763–74. doi: 10.1007/s10439-012-0704-3
129. Argento G, de Jonge N, Söntjens SH, Oomens CW, Bouten CV, Baaijens FP. Modeling the impact of scaffold architecture and mechanical loading on collagen turnover in engineered cardiovascular tissues. *Biomech Model Mechanobiol* (2015) 14(3):603–13. doi: 10.1007/s10237-014-0625-1
130. Luna-Zurita L, Prados B, Grego-Bessa J, Luxán G, del Monte G, Benguria A, et al. Integration of a Notch-dependent mesenchymal gene program and Bmp2-driven cell invasiveness regulates murine cardiac valve formation. *J Clin Invest* (2010) 120(10):3493–507. doi: 10.1172/JCI42666
131. Chester AH. Tissue Engineering—Bridging the Gap. *J Cardiovasc Transl Res* (2017) 10(2):91–2. doi: 10.1007/s12265-017-9749-x
132. Cossu G, Birchall M, Brown T, de Coppi P, Culme-Seymour E, Gibbon S, et al. Lancet Commission: Stem cells and regenerative medicine. *Lancet* (2018) 391(10123):883–910. doi: 10.1016/S0140-6736(17)31366-1
133. Huygens SA, Rutten-van Molken MP, Bekkers JA, Bogers AJ, Bouten CV, Chamuleau SA, et al. Conceptual model for early health technology assessment of current and novel heart valve interventions. *Open Heart* (2016) 3(2):e000500. doi: 10.1136/openhrt-2016-000500

Conflict of Interest Statement: CB and FB are non-voting shareholders of XELTIS AG based on intellectual property licensed to XELTIS. The authors declare that the research and the work related to the preparation of this manuscript was performed in the absence of any commercial or financial relationships.

Copyright © 2018 Bouten, Smits and Baaijens. This is an open-access article distributed under the terms of the Creative Commons Attribution License (CC BY). The use, distribution or reproduction in other forums is permitted, provided the original author(s) and the copyright owner are credited and that the original publication in this journal is cited, in accordance with accepted academic practice. No use, distribution or reproduction is permitted which does not comply with these terms.



Case Study: Intra-Patient Heterogeneity of Aneurysmal Tissue Properties

Giampaolo Martufi^{1,2}, Arianna Forneris³, Samaneh Nobakht³, Kristina D. Rinker^{4,5}, Randy D. Moore⁶ and Elena S. Di Martino^{1,5*}

¹ Department of Civil Engineering, University of Calgary, Calgary, AB, Canada, ² Unit for Health Innovation, School for Technology and Health, Royal Institute of Technology, KTH, Huddinge, Sweden, ³ Biomedical Engineering Graduate Program, University of Calgary, Calgary, AB, Canada, ⁴ Department of Chemical and Petroleum Engineering, University of Calgary, Calgary, AB, Canada, ⁵ Centre for Bioengineering Research and Education and Libin Cardiovascular Institute of Alberta, University of Calgary, Calgary, AB, Canada, ⁶ Department of Surgery, University of Calgary, Calgary, AB, Canada

OPEN ACCESS

Edited by:

Julie A. Phillippi,
University of Pittsburgh, United States

Reviewed by:

Dennis Kusters,
University of Michigan Health System,
United States
Vladimir Makaloski,
University Children's Hospital Bern,
Switzerland

*Correspondence:

Elena S. Di Martino
edimarti@ucalgary.ca

Specialty section:

This article was submitted to
Atherosclerosis and Vascular
Medicine,
a section of the journal
Frontiers in Cardiovascular Medicine

Received: 19 January 2018

Accepted: 11 June 2018

Published: 03 July 2018

Citation:

Martufi G, Forneris A, Nobakht S,
Rinker KD, Moore RD and Di
Martino ES (2018) Case Study:
Intra-patient Heterogeneity of
Aneurysmal Tissue Properties.
Front. Cardiovasc. Med. 5:82.
doi: 10.3389/fcvm.2018.00082

Introduction: Current recommendations for surgical treatment of abdominal aortic aneurysms (AAAs) rely on the assessment of aortic diameter as a marker for risk of rupture. The use of aortic size alone may overlook the role that vessel heterogeneity plays in aneurysmal progression and rupture risk. The aim of the current study was to investigate intra-patient heterogeneity of mechanical and fluid mechanical stresses on the aortic wall and wall tissue histopathology from tissue collected at the time of surgical repair.

Methods: Finite element analysis (FEA) and computational fluid dynamics (CFD) simulations were used to predict the mechanical wall stress and the wall shear stress fields for a non-ruptured aneurysm 2 weeks prior to scheduled surgery. During open repair surgery one specimen partitioned into different regions was collected from the patient's diseased aorta according to a pre-operative map. Histological analysis and mechanical testing were performed on the aortic samples and the results were compared with the predicted stresses.

Results: The preoperative simulations highlighted the presence of altered local hemodynamics particularly at the proximal segment of the left anterior area of the aneurysm. Results from the post-operative assessment on the surgical samples revealed a considerable heterogeneity throughout the aortic wall. There was a positive correlation between elastin fragmentation and collagen content in the media. The tensile tests demonstrated a good prediction of the locally varying constitutive model properties predicted using geometrical variables, i.e., wall thickness and thrombus thickness.

Conclusions: The observed large regional differences highlight the local response of the tissue to both mechanical and biological factors. Aortic size alone appears to be insufficient to characterize the large degree of heterogeneity in the aneurysmal wall. Local assessment of wall vulnerability may provide better risk of rupture predictions.

Keywords: abdominal aortic aneurysm, histology, mechanical properties, FEA, CFD

INTRODUCTION

An abdominal aortic aneurysm (AAA) is a localized dilatation of the abdominal aorta most often found in the infrarenal region of the artery above the iliac bifurcation. Both open and endovascular surgeries—the only treatments available—carry a significant risk of complications and should be reserved for cases that are at risk for rupture. The ideal diagnostic tool should reliably identify and rank the risk for rupture of an individual aorta, helping the design of clinical/surgical interventions and the selection of patients. Current clinical guidelines rely on the assessment of maximum aortic diameter as indication for surgical repair, overlooking the role played by wall heterogeneity and localized weakening (1).

Studies show that irreversible pathological remodeling of the extracellular matrix and structural degradation of the aortic wall trigger aortic dilatation, while inflammation and imbalance between elastin and collagen turnover are thought to be important biological processes involved in aneurysmal progression and rupture (2–4). There is growing evidence in the literature that abnormal blood flow patterns (5, 6) and high stresses (7) experienced by the diseased wall are important factors in the development of an aneurysm. Several investigations associated thrombus formation to disturbed hemodynamics, with regions of expansion and rupture characterized by low wall shear stress ($WSS < 0.4$ Pa) and intraluminal thrombus (ILT) accumulation (8, 9). Increased mechanical stress and ILT deposition, degradation of the elastic fibers and loss of integrity through inflammatory processes may lead to a reduction in the wall strength and, eventually, to rupture.

The present study aims at investigating intra-patient heterogeneity of mechanical and fluid mechanical stresses on the aortic wall and wall tissue histopathology on corresponding aneurysmal regions collected at the time of surgical repair. Specifically, the mechanical stress and the time-averaged wall shear stress (TAWSS) were predicted 2 weeks before surgical repair by employing finite element stress analysis (FEA) and computational fluid dynamics (CFD) simulations, respectively. The derived stress maps allowed for an informed collection of regional samples from the patient diseased aorta at the time of surgery. Finally, in the post-operative setting, histological analysis, and mechanical testing were performed on the harvested tissue and compared to the predicted fluid-mechanical stresses.

METHODS

One patient (age range 52–58 years) presenting with a non-ruptured infra-renal AAA with maximum diameter of 56.70 mm was included in the study after obtaining informed consent. The patient underwent routine contrast-enhanced computed tomography-angiography (CTA) examination 2 weeks prior to the scheduled surgery for aortic resection, following informed consent according to institutional ethical guidelines.

The three-dimensional AAA geometry was reconstructed from the stack of CTA images and pre-operative FEA and CFD simulations were performed to evaluate the patient-specific state of mechanical and fluid dynamic stresses. Tissue samples from

different regions of the aneurysm were obtained fresh from the operating room according to an approved ethical protocol and used for post-operative assessment that included mechanical testing and histological analysis.

Pre-operative Simulations

CFD Analysis

Computational model

The three-dimensional patient-specific aneurysmal lumen was reconstructed using an image-processing and model generation software (ScanIP; Simpleware Ltd., Exeter, UK). The mesh generating module (ScanFE; Simpleware Ltd., Exeter, UK) was used to discretize the reconstructed vessel geometry into a grid of tetrahedral elements with boundary layer to refine the mesh at the wall. The model was then imported in the commercial software Fluent (Ansys, Canonsburg, PA, USA) for CFD simulations. A sensitivity analysis was performed to assess the spatial resolution, in terms of mesh size, and temporal resolution, in terms of time step size. An isotropic, incompressible, Newtonian fluid was adopted to model the blood assuming a constant density of 1050 Kg/m^3 and a constant dynamic viscosity of 0.00319 Pa·s.

A velocity inlet and two pressure outlets, corresponding to the iliac arteries, were imposed as boundary conditions. No-slip conditions were applied to the luminal surface. The pressure waveform applied at the outlets was computed by using a coupled 3-element Windkessel 0D model of the downstream vasculature.

The aortic wall was assumed to be rigid, although some of the features of wall elasticity were captured by coupling the Windkessel model to the 3D geometry.

Hemodynamic wall descriptors

Wall shear stress-based hemodynamic descriptors, namely the TAWSS, the oscillatory shear index (OSI) and relative residence time (RRT) were computed to characterize the blood flow patterns and quantify the hemodynamic disturbances. The TAWSS is the wall shear stress magnitude averaged over the cardiac cycle T :

$$TAWSS = \frac{1}{T} \int_0^T |WSS(s, t)| dt$$

s identifies the position on the vessel wall at time instant t .

The OSI provides a measurement of the WSS vector deviation from the main direction of the flow over the cardiac cycle:

$$OSI = 0.5 \left[1 - \frac{\left| \int_0^T WSS(s, t) dt \right|}{\int_0^T |WSS(s, t)| dt} \right]$$

Finally, the RRT is defined as a combination of the previous parameters and provides an information about the time spent by the blood particles near the vessel wall:

$$RRT = \frac{1}{(1 - 2 \cdot OSI) \cdot TAWSS}$$

Stress Analysis

Constitutive model of aneurysmal wall

The aneurysmal wall was modeled as a fibrous collagenous tissue, where bundles of collagen fibrils mutually cross-linked by proteoglycans (CFPG-complex) reinforce an isotropic matrix material (elastin and ground matrix). The matrix material was described by an isotropic Neo-Hookean constitutive model. The CFPG-complex was described by a virtually linear stress-strain response and a triangular probability density function that defines the relative amount of engaged collagen fibrils when the collagen fiber is exposed to stretch λ . An isotropic constitutive model was used for the fibril and a constant collagen fiber density $\frac{\rho(N)=\rho_0=1.35}{4\pi} sr^{-1}$ was adopted in all directions. The model integrates two mechanical parameters (μ and k), and one structural parameter (λ_{\max}). In details, the mechanical parameters μ and k quantify the matrix material shear modulus and the stiffness of the CFPG-complex, respectively, while the value of λ_{\max} characterizes the degree of waviness of the collagen fibrils. The detailed model and its numerical implementation are reported in Martufi and Gasser (10).

Geometry, load, and boundary conditions

The aortic geometry was reconstructed from the CTA data (A4research, VASCOPS GmbH) acquired prior to elective repair.

A suite of custom-written routines (MATLAB 2014a, The MathWorks, Inc., Natick, Massachusetts, USA) was used to segment the lumen, the outer and inner wall of the vessel. The minimum distances between the inner and outer wall and between the inner wall and the lumen were used to estimate the AAA wall thickness and the ILT thickness, respectively (11, 12). These estimates were used to redefine the hexahedral elements that discretize the aortic wall segmented in VASCOPS in order to account for the local wall thickness (13).

The top and bottom surfaces of the Finite Element model were fixed, no contact with the surrounding organs was considered and peak systolic blood pressure of 120 mmHg (16 kPa) was applied.

The maximum principal stress (MPS) field was predicted by means of finite element analysis (FEA) using FEAP (vs. 8.2, University of California at Berkeley, CA, USA) considering non-homogeneous population-averaged material properties (13) and using the described constitutive model. In details, each element was considered as belonging to one of four categories with their constitutive parameters assigned according to a discrete categorization of the material properties, i.e., thin wall-thin ILT ($\mu = 50$ kPa, $k = 7,800$ kPa, $\lambda_{\max} = 1.04$), thin wall-thick ILT ($\mu = 5$ kPa, $k = 3,600$ kPa, $\lambda_{\max} = 1.04$), thick wall-thin ILT ($\mu = 40$ kPa, $k = 7,400$ kPa, $\lambda_{\max} = 1.12$), and thick wall-thick ILT ($\mu = 5$ kPa, $k = 3,900$ kPa, $\lambda_{\max} = 1.12$) (13). Finally, ILT tissue was modeled using a one parameter Ogden-like strain energy function, with 2.11 kPa as constitutive parameter (14).

Intra-Operative Tissue Collection

Surgery Map Definition

Twenty-five different regions were identified on the aneurysmal sac, i.e., 12 left lateral regions (six left anterior and six left posterior), 12 right lateral regions (six anterior and six posterior) and the neck region. Region-averaged maximum principal

stress (MPS_{ra}), region-averaged time averaged wall shear stress ($TAWSS_{ra}$), region-averaged oscillatory shear index (OSI_{ra}), region-averaged relative residence time (RRT_{ra}), region-averaged ILT (ILT_{ra}), and wall thickness (WT_{ra}) were computed and used as global descriptors of the geometrical and mechanical characteristics for each region.

The defined regions served as a guide to collect tissue from the patient resected aorta corresponding to areas with different global descriptors (Figure 1A and Table 1).

Tissue Collection

From the intra-operative tissue specimen, ten regions ($\sim 20 \times 15$ mm) were obtained; each was $\sim 20 \times 15$ mm in size with one edge parallel to the circumferential orientation with respect to the intact aorta and the other one perpendicular to it. Tissues that were selected for histology were fixed in 10% buffered formalin immediately after collection. Tissues destined for mechanical analysis were placed in saline solution and refrigerated at 4°C.

Post-operative Assessment

Mechanical Tensile Tests

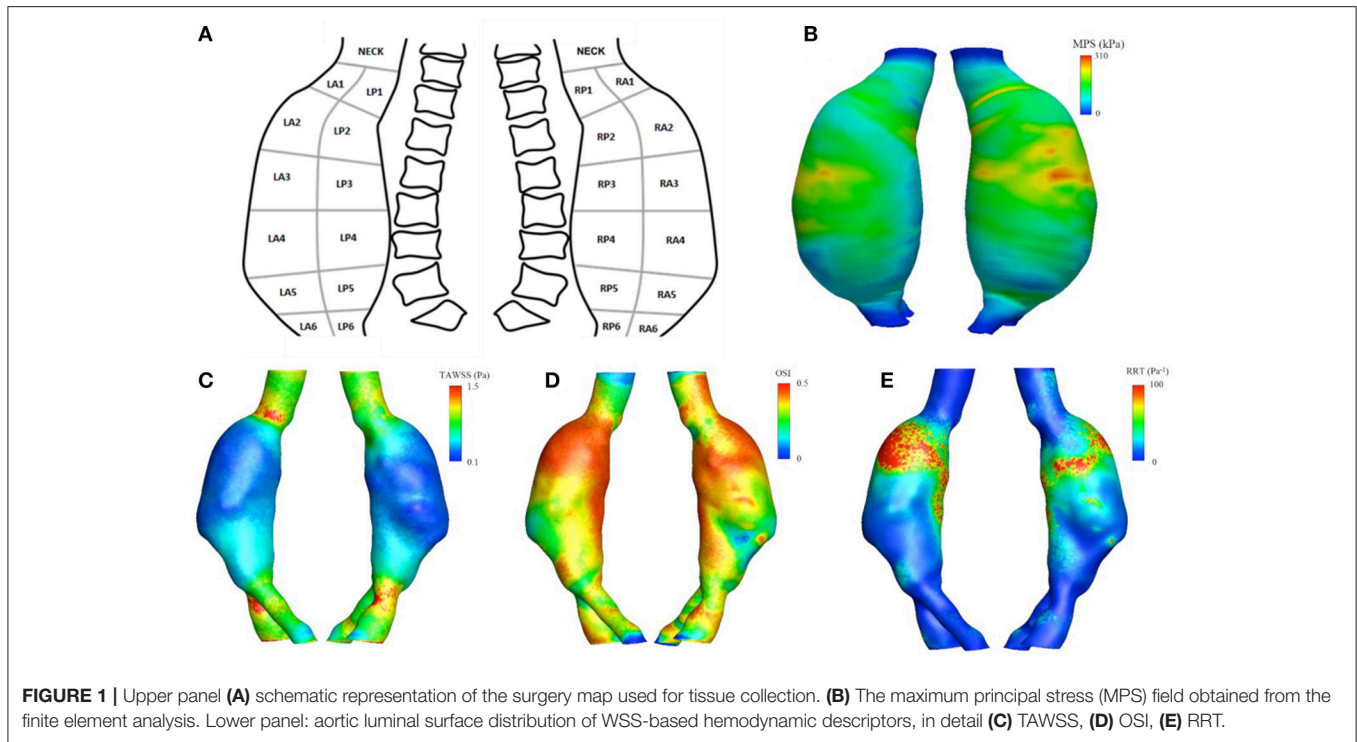
Four regions $\sim 10 \times 10$ mm in size were tested within 48 h of procurement: one from the neck, two from the right anterior region and one from the left anterior region. Width, length, and thickness were measured for each sample with a manual caliper. Tissues were tested using a planar biaxial system (ElectroForce, TA Instruments, MO, USA) with displacement-controlled protocol reaching a maximum stretch of 40% on both axes while being continuously irrigated with saline solution at 37°C. After a short thermal equilibration period, a frequency of 0.333 Hz and 10 cycles count were used for each experiment. If the tissue sample was not wide enough to perform biaxial tensile tests, uniaxial tensile test at the same strain rate and with the same maximum stretch was performed. From the acquired data, the first Piola-Kirchhoff stress was calculated normalizing the recorded force by the cross-sectional area in the undeformed configuration, while the stretch was computed as the deformed length normalized by the original specimen length.

Constitutive Model for the Individual Specimen Properties

A computational model representing a single cubic element of tissue was used to estimate the mechanical parameters μ , k , and the structural parameter λ_{\max} of the constitutive model from the tensile experimental data. The clear physical meaning of the model parameters allowed their straightforward identification by manual adjustments as described previously (10). For each specimen, the stress values obtained in the physiological strain range for an aneurysm [$\sim 7\%$, see Satriano et al. (15)] using the optimized *ex-vivo* material parameters were compared with stresses obtained using our previously published population-averaged material properties (7). The root-mean-square error (RMSE) was employed to measure differences.

Histological Analysis

Samples for histology were fixed in 10% buffered formalin and then stained with Movat and Picrosirius red to assess elastin



fragmentation and quantify the percentage of total area occupied by collagen fibers. Slides were observed and imaged at 2X and 20X magnification using an Olympus BX53 DP73 microscope.

Visual inspection was used to identify the tunica media from Movat images at 2X magnification. The pixels identified as belonging to the media were then used to estimate the percentage of area occupied by collagen in the corresponding Picrosirius red-stained slides (16). The original images were first converted into grayscale images, i.e., the luminance (luminous intensity per unit area) of the original image was retained while information about hue and saturation were eliminated. In order to highlight the collagen structure, brightness and contrast were automatically optimized according to the histograms and the images were finally converted into binary images. The percentage area of collagen in the media was computed as the percentage of pixels identified as collagen material.

Elastin fragmentation in the media was visually inspected from Movat stained images at 20X magnification and scored as (1) minor, (2) moderate, or (3) high. A score of (4) was assigned if no elastin was detected in the sample and N/A if the media was entirely disrupted.

RESULTS

Pre-operative Simulations

Figure 1 (lower panels) show the luminal distribution of WSS-based hemodynamic descriptors allowing for a visual inspection of flow patterns within the vessel. The aneurysmal region presented lower values of TAWSS (**Figure 1C**), compared to those observed in the areas upstream and downstream the dilatation, between 0.1 and 0.4 vs. 0.8 and 1.5 Pa.

The values for the OSI (**Figure 1D**) ranged between 0 and 0.5, while the RRT (**Figure 1E**) varied between 10 and 100 Pa⁻¹ within the aneurysmal region, with higher values located in the proximal segment of the left lateral region.

The MPS field, computed accounting for locally varying wall thickness and non-homogenous material properties, is plotted in **Figure 1B**. The predicted macroscopic stress was distributed non-uniformly over the aneurysmal wall. High stresses were located at ILT-free regions with thin wall and regions with thick wall covered with thin ILT.

There was a statistically significant negative correlation between region-averaged maximum principal stress (MPS_{ra}) and ILT_{ra} (Pearson's $\rho = -0.51$, $p = 0.009$), between MPS_{ra} and $TAWSS_{ra}$ (Pearson's $\rho = -0.55$, $p = 0.005$), and between MPS_{ra} and RRT_{ra} (Pearson's $\rho = -0.41$, $p = 0.04$). The maximum MPS_{ra} of 202.9 kPa was recorded in the RA3 region, where an ILT-free wall 1.4 ± 0.1 mm thick was measured. In contrast, the lowest $TAWSS_{ra}$ (0.09 Pa) was observed in region RA4, where a thick wall of 1.7 ± 0.2 mm covered by 7.0 ± 2.0 mm of ILT_{ra} was recorded. The maximum OSI_{ra} and RRT_{ra} were 0.47 and 109.8 Pa⁻¹, respectively, and were both localized in the LA2 region ($WT_{ra} = 1.4 \pm 0.1$ mm and $ILT_{ra} = 7.3 \pm 0.9$ mm). Finally, the maximum $TAWSS_{ra}$ (0.60 Pa) and minimum MPS_{ra} (36.0 kPa) were located in the neck region (see **Table 1**).

Post-operative Assessment

Mechanical Properties

Tissue samples harvested from the neck and right anterior region RA4 were subject to uniaxial tensile testing. Samples collected from regions RA2 and LA4 underwent biaxial tensile tests. Following the categorization based on wall and ILT thickness

TABLE 1 | Summary of geometrical and mechanical parameters of the different aneurysmal regions.

Region ID	WT _{ra} (mm)	ILT _{ra} (mm)	TAWSS _{ra} (Pa)	OSI _{ra}	RRT _{ra} (Pa ⁻¹)	MPS _{ra} (kPa)
NECK	1.3 ± 0.1	0	0.60	0.25	5.1	36.0
RP1	1.5 ± 0.2	4.5 ± 1.0	0.45	0.44	25.4	120.5
RA1	1.4 ± 0.1	3.1 ± 1.4	0.49	0.34	6.0	117.4
RP2	1.3 ± 0.1	3.8 ± 0.5	0.41	0.40	14.4	149.2
RA2	1.3 ± 0.1	5.5 ± 1.3	0.32	0.45	54.7	153.6
RP3	1.4 ± 0.1	6.3 ± 1.8	0.16	0.46	59.6	145.7
RA3	1.4 ± 0.1	0	0.18	0.40	36.7	202.9
RP4	1.4 ± 0.1	10.4 ± 1.0	0.13	0.44	47.1	115.0
RA4	1.7 ± 0.2	7.0 ± 2.0	0.09	0.31	16.4	138.4
RP5	1.4 ± 0.1	10.0 ± 1.3	0.19	0.43	24.8	79.4
RA5	1.3 ± 0.1	8.7 ± 1.1	0.15	0.22	8.4	91.1
RP6	1.4 ± 0.1	6.5 ± 0.7	0.40	0.35	5.4	87.2
RA6	1.2 ± 0.1	6.5 ± 0.9	0.31	0.29	4.9	86.6
LA1	1.5 ± 0.2	6.4 ± 1.4	0.41	0.43	38.5	101.6
LP1	1.4 ± 0.1	4.5 ± 0.5	0.55	0.24	2.3	85.7
LA2	1.4 ± 0.1	7.3 ± 0.9	0.17	0.47	109.8	100.4
LP2	1.3 ± 0.1	7.0 ± 1.2	0.43	0.46	45.9	143.6
LA3	1.4 ± 0.1	4.6 ± 1.8	0.15	0.41	42.4	166.7
LP3	1.4 ± 0.1	8.6 ± 1.1	0.18	0.46	67.9	89.9
LA4	1.6 ± 0.1	4.7 ± 2.6	0.12	0.31	12.0	158.4
LP4	1.5 ± 0.2	10.2 ± 0.7	0.16	0.46	64.1	82.0
LA5	1.4 ± 0.1	8.8 ± 1.8	0.18	0.29	7.1	91.7
LP5	1.4 ± 0.1	10.8 ± 0.9	0.19	0.42	19.8	76.1
LA6	1.5 ± 0.1	8.0 ± 1.0	0.23	0.35	10.9	74.2
LP6	1.5 ± 0.1	7.9 ± 0.6	0.38	0.36	5.8	74.6

Region-averaged intraluminal thrombus (ILT_{ra}); region-averaged wall thickness (WT_{ra}); region-averaged time average wall shear stress (TAWSS_{ra}); region-averaged oscillatory shear index (OSI_{ra}); region-averaged relative residence time (RRT_{ra}); region-averaged maximum principal stress (MPS_{ra}).

(13), sample from RA4 was labeled as tissue with thick wall and thick ILT ($WT_{ra} > 1.4$ mm, $ILT_{ra} > 6.5$ mm), RA2 belonged to the category with thin wall and thin ILT and LA4 was classified as thick wall, thin ILT. Because the neck region was ILT-free no category was assigned.

Figure 2 shows the experimental mechanical response, the FE model best fit and the stress-stretch predictions using a population based mean material properties according to the above defined subgroups (13).

The fitted values for the matrix shear modulus (μ) of the samples collected from the right-anterior region, were 60 kPa for RA2 and 10 kPa for RA4, with a CFPG-complex stiffness (k) of 3,500 and 1,000 kPa, respectively. The estimated μ and k parameters of the constitutive model were 32 and 2,900 kPa, respectively for the specimen harvested from the left-anterior region LA4, and 8 and 2,500 kPa for the neck tissue sample. **Table 2** reports a summary of the mechanical parameters found. Neighboring regions are reported to facilitate comparison with histological results. It must be noted that comparisons between neighboring regions are indicative due to the high variability.

Specimen RA2 showed the highest CFPG-complex stiffness and is adjacent to RA1 that shows high collagen content. The neck specimen allowed a direct comparison and showed the lowest elastin fragmentation, the lowest matrix material shear modulus and the highest λ_{max} suggesting high elastin content.

Pre-operative Mechanical Properties Assumptions and specimen Individual Tissue Properties

For the three samples tested, a total RMSE of 8.8 kPa was recorded between the actual stress values and those estimated in the preoperative setting using population-averaged material properties. RA2 exhibited the largest RMSE (13.7 kPa). The RMSE decreased to the values of 6.8 and 0.95 kPa, for LA4 and RA4, respectively. No comparison was performed for neck tissue because population-averaged parameters were not available.

Histology

Movat and Picrosirius red stained samples at 2X magnification are showed in **Figure 3**.

Figures 4, 5 show Movat's stain at 20X magnification for four regions to demonstrate the degree of elastin fragmentation in the media. There was a strong positive correlation between elastin fragmentation score and percentage of collagen content in the media (Pearson's $\rho = 0.94$, $p = 0.019$). RP4 and LA5 resulted in score 4 for elastin fragmentation due to the complete disruption of the medial layer. The two highest collagen contents were measured in RA5 (65.8%) and RA1 (38.2%) where a score of 4 and 3 for elastin fragmentation was recorded, respectively. Both LA1 and LA3 exhibited moderate elastin disruption (score 2); however, collagen content was higher for LA1 (19.7%) than LA3 (10.8%). Finally, low elastin fragmentation (score 1) with collagen content of 12.4% was observed for the neck sample (see **Table 3** and **Figures 3, 4**).

Comparisons

Statistically non-significant negative correlations were found between TAWSS_{ra} and elastin fragmentation (Pearson's $\rho = -0.62$, $p = 0.18$). A complete media disruption (N/A for elastin fragmentation) was observed for RP4 where low TAWSS_{ra} (0.13 Pa), high OSI_{ra} (0.44), and RRT_{ra} (47.14 Pa⁻¹) and thick ILT (10.4 ± 1.0 mm) were measured. A TAWSS_{ra} of 0.15 Pa was associated with both moderate elastin fragmentation (score 2) and entirely degraded elastin (score 4) in LA3 and RA5, respectively.

Despite exhibiting the same TAWSS_{ra}, RA5 presented an OSI_{ra} almost half than the one measured for LA3 (0.22 vs. 0.41) and five times smaller RRT_{ra} (8.42 vs. 42.44 Pa⁻¹). Additionally, RA5 showed an ILT deposition almost double than the one measured for LA3, i.e., $ILT_{ra} = 8.7 \pm 1.1$ mm for RA5 vs. $ILT_{ra} = 4.6 \pm 1.8$ mm for LA3, and six times higher collagen content, i.e., 65.8% for RA5 vs. 10.8% for LA3. LA5 presented a ILT_{ra} of 8.8 ± 1.8 mm similar to RA5 that was associated with a TAWSS_{ra} of 0.18 Pa (OSI_{ra} = 0.29; RRT_{ra} = 7.11 Pa⁻¹), and a complete disruption of the media layer (N/A for elastin fragmentation). LA1 showed a moderate elastin fragmentation (score 2) with TAWSS_{ra} of 0.41 Pa, OSI_{ra} of 0.43 and RRT_{ra} of 38.46 Pa while, for RA1 the TAWSS_{ra} of 0.49 Pa (OSI_{ra} = 0.34; RRT_{ra} = 6.04 Pa)

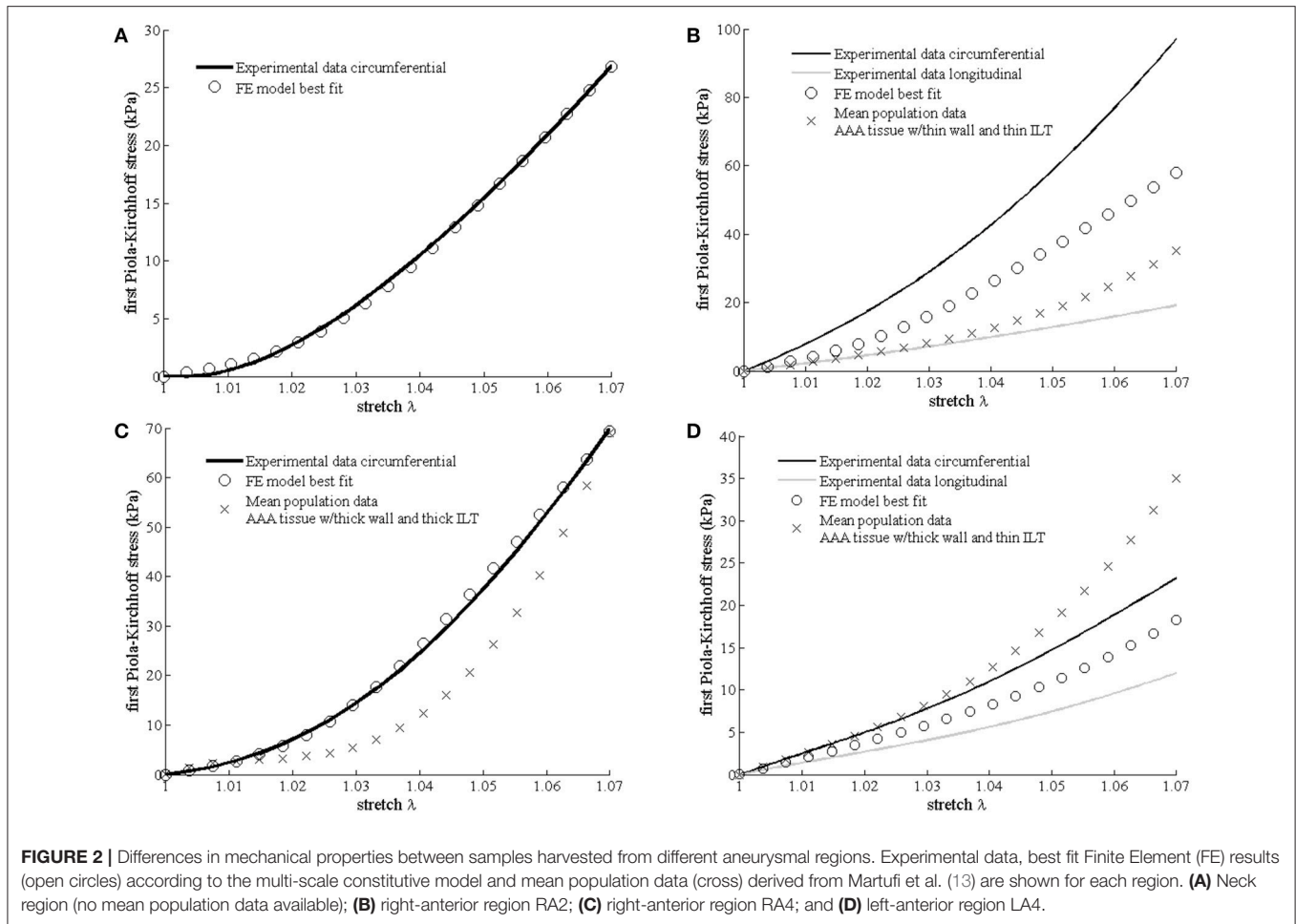


TABLE 2 | Summary of structural and mechanical parameters of the constitutive model for different aneurysmal regions.

Region ID	Matrix material shear modulus μ (kPa)	CFPG-complex stiffness k (kPa)	λ_{max}	Adjacent regions (refer to Table 3 for histology)
NECK	8	2,500	1.27	NECK
RA2	60	3,500	1.04	RA1
RA4	10	1,000	1.06	RP4, RA5
LA4	32	2,900	1.13	LA5, LA3

Adjacent regions are reported to facilitate comparisons with histological results in Table 3.

was related to higher elastin fragmentation (score 3). Finally, the neck region displayed the lowest elastin fragmentation score (1) with the lowest RRT_{ra} (Pa^{-1}) and the highest $TAWSS_{ra}$ (0.60 Pa).

There was no correlation between MPS_{ra} and collagen content (Pearson's $\rho = -0.08$, $p = 0.9$). The neck region exhibited the lowest values of MPS_{ra} (36.0 ± 35.2 kPa) and the lowest score for elastin fragmentation (score 1) with relatively low percentage of collagen in the media (12.4%). RA5 and LA5 showed similar stress level (RA5: $MPS_{ra} = 91.1$ kPa; LA5: $MPS_{ra} = 91.6$ kPa) and similar ILT thickness deposited (RA5: $ILT_{ra} = 8.7 \pm 1.1$ mm;

LA5: $ILT_{ra} = 8.8 \pm 1.8$ mm) that were associated with high elastin fragmentation or complete media destruction in both the samples, and with the highest collagen content (65.8%) for RA5. RA1 and RP4 were exposed to similar stress level (RA1: $MPS_{ra} = 117.40$ kPa; RP4: $MPS_{ra} = 114.99$ kPa) but presented different ILT coverage (RA1: $ILT_{ra} = 3.1 \pm 1.4$ mm; RP4: $ILT_{ra} = 10.4 \pm 1.0$ mm) that was associated with a score of 3 for elastin fragmentation and a collagen content of 38.2% for RA1, while RP4 had complete media destruction.

LA1 and LA3 showed a moderate fragmentation of elastic fibers (score 2) that was associated with different stress levels and different ILT thickness; i.e., LA1: $ILT_{ra} = 6.4 \pm 1.4$ mm and $MPS_{ra} = 101.64$ kPa; LA3: $ILT_{ra} = 4.6 \pm 1.8$ mm and $MPS_{ra} = 166.67$ kPa (see Table 3 and Figures 3, 4).

DISCUSSION AND CONCLUSION

An aortic aneurysm is the final result of a multifactorial process that involves pathological remodeling and degradation of the aortic wall leading to its weakening.

Early publications have reported potential correlation between mechanical stress and metabolism in the aneurysmal wall supporting the hypothesis of a stress mediated process that

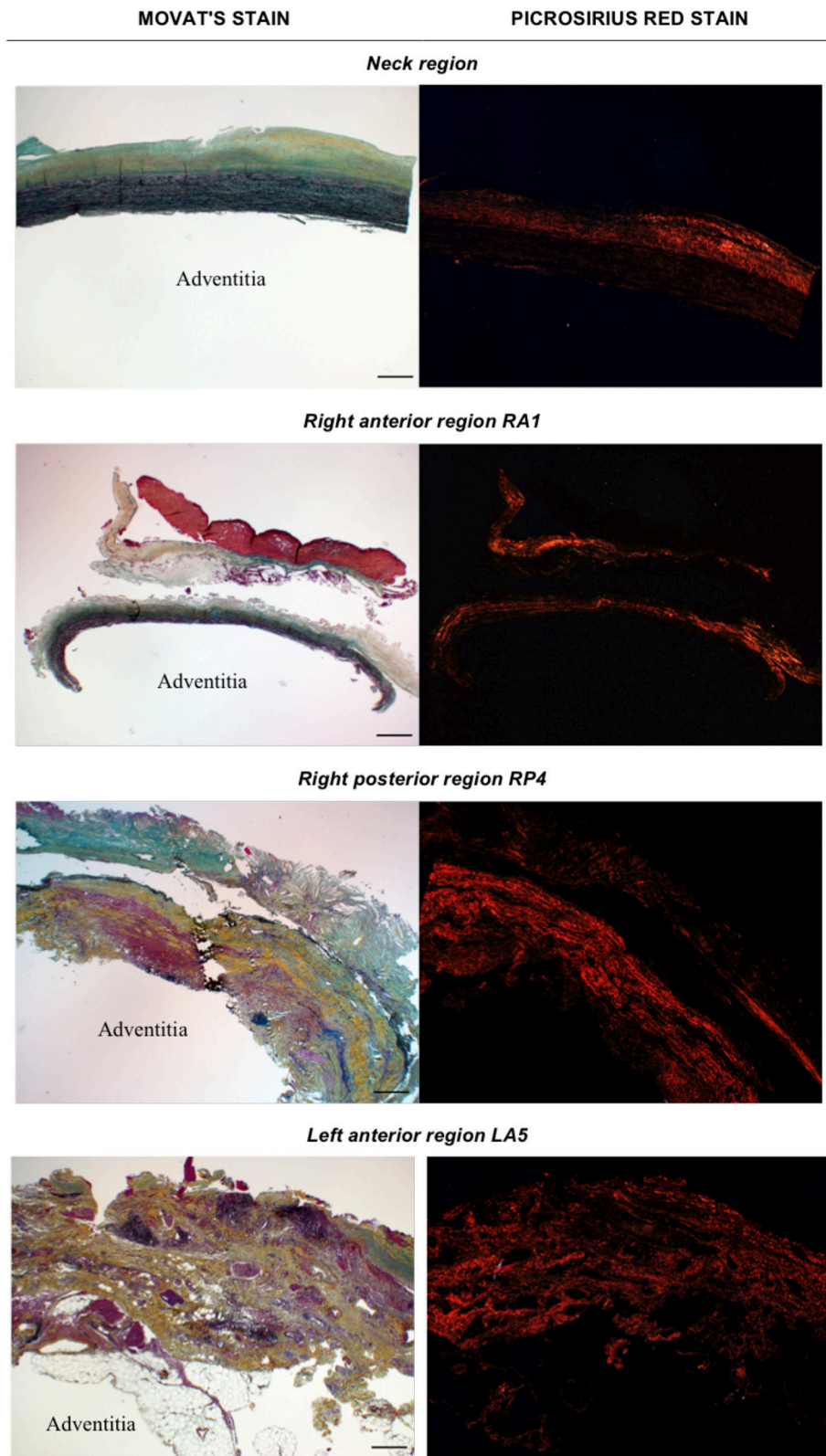


FIGURE 3 | Histological images obtained with Movat stain (left) and Picosirius red stain (right) at 2X magnification. The adventitia layer of the aortic wall is labeled as reference in each image. Scale bar is 0.5 mm (located bottom right).

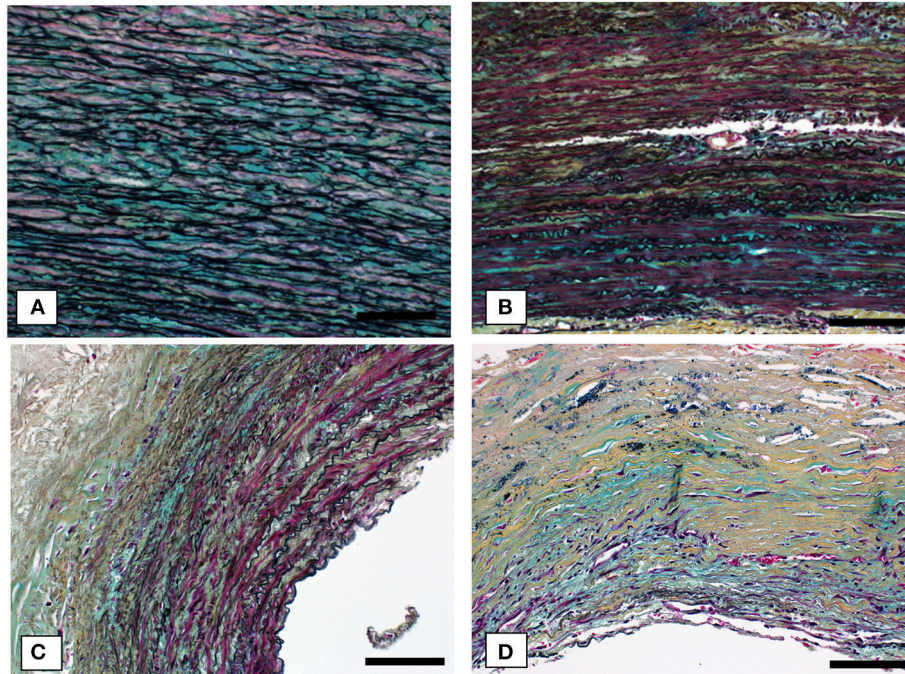


FIGURE 4 | Representative cases of elastin fragmentation in the media. Movat images at 20X magnification: **(A)** Neck region with low elastin fragmentation (score 1); **(B)** LA3 region with moderate elastin fragmentation (score 2); **(C)** RA1 region with high elastin fragmentation (score 3) and **(D)** RA5 region with no elastin content (score 4). Scale bar 0.1 mm.

weakens the vessel (7, 17). However, evidences on the correlation between mechanical environment and underlying histological structure are currently very limited. This study focused on intrapatient variability of local mechanical and fluid dynamic stresses and on histological and mechanical properties of corresponding aneurysmal regions evaluated from one *ex-vivo* specimen.

The preoperative simulations provided insight on the stresses acting on the wall. Both MPS and WSS-based hemodynamic descriptors were distributed non-uniformly over the aneurysmal wall. The entire aneurysmal lumen generally presented disturbed flow conditions characterized by low oscillatory wall shear stress and high relative residence time pointing to recirculation and poor wash out associated with adverse remodeling of the extracellular matrix and ILT deposition. The effect of altered local hemodynamics was particularly evident in the proximal segment of the left anterior region, where LA2 and LA3 showed high OSI_{ra} , high RRT_{ra} , and low $TAWSS_{ra}$ and were characterized by thick ILT.

The tensile tests on tissues collected demonstrated that constitutive parameters estimated non-invasively from geometric variables—ILT thickness and wall thickness, according to Martufi et al. (13)—produce a fairly accurate prediction of the *ex-vivo* constitutive model obtained fitting the experimental tensile tests data directly, suggesting a relationship between geometric macroscopic parameters and tissue properties.

The seven histological samples collected cover distal, central, and proximal regions and showed very heterogeneous features in terms of elastin degradation and collagen content. Higher

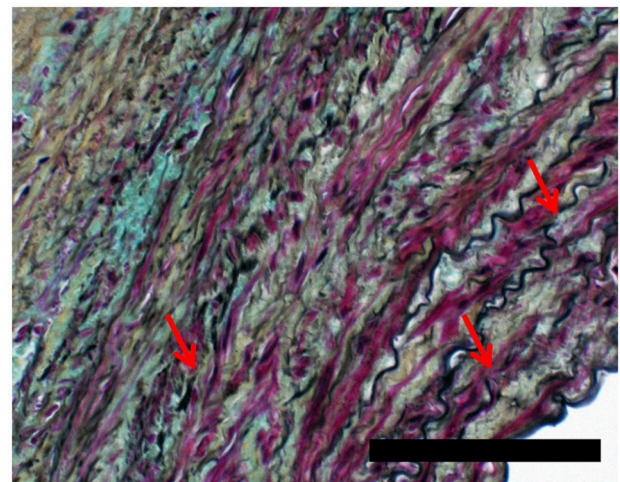


FIGURE 5 | Detail of RA1 sample (20x) showing elastin fragmentation (red arrows). Scale bar 0.1 mm.

degrees of medial disruption were found in the distal regions of the aneurysmal expansion.

Findings from the histological analysis showed a positive correlation between elastin fragmentation and collagen content in the media, suggesting a compensatory process that involves progressive increase in collagen synthesis and wall remodeling. It is hypothesized that as the aneurysm grows, the elastic

TABLE 3 | Summary of geometrical, mechanical and histological features for different aneurysmal regions.

Region ID	WT _{ra} (mm)	ILT _{ra} (mm)	TAWSS _{ra} (Pa)	OSI _{ra}	RRT _{ra} (Pa ⁻¹)	MPS _{ra} (kPa)	Collagen content (%)	Elastin fragmentation
NECK	1.3	0	0.60	0.25	5.06	36.05	12.4	1
RA1	1.4 ± 0.1	3.1 ± 1.4	0.49	0.34	6.04	117.4	38.2	3
RP4	1.4 ± 0.1	10.4 ± 1.0	0.13	0.44	47.14	115.0	N/A	N/A
RA5	1.3 ± 0.1	8.7 ± 1.1	0.15	0.22	8.42	91.1	65.8	4 (no elastin)
LA1	1.5 ± 0.2	6.4 ± 1.4	0.41	0.43	38.46	101.6	19.7	2
LA3	1.4 ± 0.1	4.6 ± 1.8	0.15	0.41	42.44	166.7	10.8	2
LA5	1.4 ± 0.1	8.8 ± 1.8	0.18	0.29	7.11	91.6	N/A	N/A

fibers are distributed over a bigger area and elastin synthesis further decreases due to inflammatory processes and muscle cells apoptosis (18, 19). Elastin fragmentation was generally associated with low TAWSS_{ra} and high MPS_{ra}, but no statistically significant correlation was found.

The first limitation is that the analysis encompasses one aneurysmal specimen from one patient. This study was designed as a feasibility study to investigate the presence of significant heterogeneity in the aneurysm wall, even intra-patient.

The second limitation, pertaining the pre-operative stress analysis, is the use of population average parameters for the constitutive equations of both wall and ILT. The constitutive parameters were modulated locally based on Martufi et al. (13) and reasonable agreement was found between pre-operative and *ex-vivo* parameters as confirmed by the experimental tensile tests on explanted tissues.

Third, ILT was modeled as a non-porous material overlooking the complex role of the intraluminal thrombus as a biomechanically active component (20).

The constitutive model of the wall also presents limiting assumptions: the isotropic matrix model does not account directly for elastin degradation and smooth muscle cells (SMCs) are not directly modeled. However, the relative contribution of the isotropic component is reduced in the presence of elastin degradation. It should also be noted that SMCs are almost absent in the diseased aneurysmal wall at late stages (21).

Finally, the velocity boundary conditions at the inlet of the fluid dynamic model were not patient-specific and the aortic wall was assumed to be rigid during the simulation. Despite a typically stiffer wall, a compliant effect is still observable in aneurysmal patients; accordingly, some of the features of a compliant wall were captured by coupling the 3-element Windkessel model of the downstream vasculature.

Our findings point to the importance of the local mechanical environment in promoting intra-patient wall heterogeneity that is observable in the analysis of adjacent regions, such as RA3 and RA4. RA3 is an ILT-free region exhibiting the maximum MPS_{ra}, while RA4, labeled as tissue with thick wall and thick ILT, presents the lowest TAWSS_{ra}. The heterogeneity of the wall is confirmed by the postoperative assessment carried out by mean of mechanical tensile tests and histological analysis on the surgical specimen.

It is interesting to note that altered hemodynamics, and low TAWSS values appeared to be co-localized with wall exhibiting

disrupted elastin and generally thicker ILT. While the low TAWSS values were computed at the interface between lumen and ILT, and not at the aneurysmal wall surface, it appears that altered fluid dynamics at the luminal surface co-localizes with disrupted wall constituents even in the presence of a thrombus layer, pointing to a remodeling mechanism that may be mediated by matrix proteinases secreted in the thrombus. This may help explain why altered hemodynamics and low TAWSS have been reported at sites of aneurysms rupture regardless of the presence of intraluminal thrombus (9).

The large variability observed at the local level in terms of mechanical properties and disruption of wall constituents suggests that local, rather than global, variables should be considered in the future for better risk of rupture prediction. Each individual aneurysmal region may have very different susceptibility to rupture depending on the combination of wall vulnerability and local fluid-mechanics conditions. True patient- and location-specific indicators of wall vulnerability are needed to increase the reliability of clinical outcomes prediction and consequent risk stratification as a mean for selective surgical repair.

ETHICS STATEMENT

This study was carried out in accordance with the recommendations of the Conjoint Health Research Ethics Board at the University of Calgary. All subjects gave written informed consent in accordance with the Declaration of Helsinki. The protocol was approved by the Conjoint Health Research Ethics Board.

AUTHOR CONTRIBUTIONS

GM: FEA, tensile test analysis, histology, results comparison, manuscript preparation; AF: CFD simulation, CFD indices, and results, results comparison and discussion, manuscript preparation; SN: Windkessel model for CFD, CFD simulation; KR: conception and design of the study; RM: study design, patient selection, specimen collection; ED: conception and design of the study, critical evaluation of results, histology analysis, manuscript preparation. All authors contributed to manuscript revision, read, and approved the submitted version.

FUNDING

This work was supported by Discovery Grants #RGPIN/04043-2014, RGPIN/327488-2012 and RGPIN/04870-2017 from the Natural Sciences and Engineering Research Council (NSERC) of Canada, Heart, and Stroke Foundation Grant G 17 0019141, MITACS Postdoctoral Elevate Award, NSERC CREATE Postdoctoral Fellowship Award, NSERC CREATE I3T Doctoral Award, and the Graupe Doctoral Scholarship award.

REFERENCES

- Vallabhaneni SR, Gilling-Smith GL, How TV, Carter SD, Brennan JA, Harris PL. Heterogeneity of tensile strength and matrix metalloproteinase activity in the wall of abdominal aortic aneurysms. *J Endovasc Ther.* (2004) 11:494–502. doi: 10.1583/04-1239.1
- Michel JB, Thanaud O, Houard X, Meilhac O, Caligiuri G, Nicoletti A. Topological determinants and consequences of adventitial responses to arterial wall injury. *Arterioscler Thromb Vasc Biol.* (2007) 27:1259–68. doi: 10.1161/ATVBAHA.106.137851
- Fontaine V, Jacob MP, Houard X, Rossignol P, Plissonnier D, Angles-Cano E, et al. Involvement of the mural thrombus as a site of protease release and activation in human aortic aneurysms. *Am J Pathol.* (2002) 161:1701–10. doi: 10.1016/S0002-9440(10)64447-1
- Sakalihan N, Limet R, Defawe OD. Abdominal aortic aneurysm. *Lancet* (2005) 365:1577–89. doi: 10.1016/S0140-6736(05)66459-8
- Ailawadi G, Knipp BS, Lu G, Roelofs KJ, Ford JW, Hannawa KK et al. A nonintrinsic regional basis for increased infrarenal aortic MMP-9 expression and activity. *J Vasc Surg.* (2003) 37:1059–66. doi: 10.1067/mva.2003.163
- Chiu JJ, Chien S. Effects of disturbed flow on vascular endothelium: pathophysiological basis and clinical perspectives. *Physiol Rev.* (2011) 91:327–87. doi: 10.1152/physrev.00047.2009
- Martufi G, Lindquist Liljeqvist M, Sakalihan N, Panuccio G, Hultgren R, Roy J, et al. Local diameter, wall stress, and thrombus thickness influence the local growth of abdominal aortic aneurysms. *J Endovasc Ther.* (2016) 23:957–96. doi: 10.1177/1526602816657086
- Zambrano BA, Gharahi H, Lim C, Jaber FA, Choi J, Lee W, et al. Association of intraluminal thrombus, hemodynamic forces, and abdominal aortic aneurysm expansion using longitudinal CT images. *Ann Biomed Eng.* (2016) 44:1502–14. doi: 10.1007/s10439-015-1461-x
- Boyd AJ, Kuhn DC, Lozowy RJ, Kulbisky GP. Low wall shear stress predominates at sites of abdominal aortic aneurysm rupture. *J Vasc Surg.* (2016) 63:1613–9. doi: 10.1016/j.jvs.2015.01.040
- Martufi G, Gasser TC. A constitutive model for vascular tissue that integrates fibril, fiber and continuum levels with application to the isotropic and passive properties of the infrarenal aorta. *J Biomech.* (2011) 44:2544–50. doi: 10.1016/j.jbiomech.2011.07.015
- Martufi G, Di Martino ES, Amon CH, Muluk SC, Finol EA. Three-dimensional geometrical characterization of abdominal aortic aneurysms: image image-based wall thickness distribution. *J Biomech Eng.* (2009) 131:061015. doi: 10.1115/1.3127256
- Shum J, Martufi G, Di Martino ES, Washington CB, Grisafi J, Muluk SC, et al. Quantitative assessment of abdominal aortic aneurysm shape. *Ann Biomed Eng.* (2011) 39:277–86. doi: 10.1007/s10439-010-0175-3
- Martufi G, Satriano A, Moore RD, Vorp DA, Di Martino ES. Local quantification of wall thickness and intraluminal thrombus offer insight into the mechanical properties of the aneurysmal aorta. *Ann Biomed Eng.* (2015) 43:1759–71. doi: 10.1007/s10439-014-1222-2
- Gasser TC, Gorgulu G, Folkesson M, Swedenborg J. Failure properties of intra-luminal thrombus in abdominal aortic aneurysm under static and pulsating mechanical loads. *J Vasc Surg.* (2008) 48:179–88. doi: 10.1016/j.jvs.2008.01.036
- Satriano A, Rivolo S, Martufi G, Finol EA, Di Martino ES. *In vivo* strain assessment of the abdominal aortic aneurysm. *J Biomech.* (2015) 48:354–60. doi: 10.1016/j.jbiomech.2014.11.016
- Abramoff MD, Magalhaes PJ, Ram SJ. Image processing with ImageJ. *Biophotonics Internat.* (2004) 11:36–42.
- Nchimi A, Cheramy-Bien JB, Gasser TC, Namur G, Gomez P, Seidel L, et al. Multifactorial relationship between 18f-fluoro-deoxy-glucose positron emission tomography signaling and biomechanical properties in unruptured aortic aneurysms. *Circ Cardiovasc Imaging* (2014) 7:82–9. doi: 10.1161/CIRCIMAGING.112.000415
- Davies MJ. Aortic aneurysm formation: lessons from human studies and experimental models. *Circulation* (1998) 98:193–5. doi: 10.1161/01.CIR.98.3.193
- Choke E, Cockerill G, Wilson WR, Sayed S, Dawson J, Loftus I, et al. A review of biological factors implicated in abdominal aortic aneurysm rupture. *Eur J Vasc Endovasc Surg.* (2005) 30:227–44. doi: 10.1016/j.ejvs.2005.03.009
- Adolph R, Vorp DA, Steed DL, Webster MW, Kameneva MV, Watkins SC. Cellular content and permeability of intraluminal thrombus in abdominal aortic aneurysm. *J Vasc Surg.* (1997) 25:916–26. doi: 10.1016/S0741-5214(97)70223-4
- Lopez-Candales A, Holmes DR, Liao S, Scott MJ, Wickline SA, Thompson RW. Decreased vascular smooth muscle cell density in medial degeneration of human abdominal aortic aneurysms. *Am J Pathol.* (1997) 150:993–1007.

Conflict of Interest Statement: The authors declare that the research was conducted in the absence of any commercial or financial relationships that could be construed as a potential conflict of interest.

Copyright © 2018 Martufi, Forneris, Nobakht, Rinker, Moore and Di Martino. This is an open-access article distributed under the terms of the Creative Commons Attribution License (CC BY). The use, distribution or reproduction in other forums is permitted, provided the original author(s) and the copyright owner(s) are credited and that the original publication in this journal is cited, in accordance with accepted academic practice. No use, distribution or reproduction is permitted which does not comply with these terms.



Medial Hypoxia and Adventitial Vasa Vasorum Remodeling in Human Ascending Aortic Aneurysm

Marie Billaud^{1,2,3}, Jennifer C. Hill¹, Tara D. Richards¹, Thomas G. Gleason^{1,2,3,4} and Julie A. Phillippi^{1,2,3,4*}

¹ Department of Cardiothoracic Surgery, University of Pittsburgh, Pittsburgh, PA, United States, ² McGowan Institute for Regenerative Medicine, University of Pittsburgh, Pittsburgh, PA, United States, ³ Department of Bioengineering, University of Pittsburgh, Pittsburgh, PA, United States, ⁴ Center for Vascular Remodeling and Regeneration, University of Pittsburgh, Pittsburgh, PA, United States

OPEN ACCESS

Edited by:

Alan Daugherty,
University of Kentucky, United States

Reviewed by:

Xinchun Pi,
Baylor College of Medicine,
United States
Yuqing Huo,
Augusta University, United States

*Correspondence:

Julie A. Phillippi
phillippija@upmc.edu

Specialty section:

This article was submitted to
Atherosclerosis and Vascular
Medicine,
a section of the journal
Frontiers in Cardiovascular Medicine

Received: 09 May 2018

Accepted: 20 August 2018

Published: 17 September 2018

Citation:

Billaud M, Hill JC, Richards TD,
Gleason TG and Phillippi JA (2018)
Medial Hypoxia and Adventitial Vasa
Vasorum Remodeling in Human
Ascending Aortic Aneurysm.
Front. Cardiovasc. Med. 5:124.
doi: 10.3389/fcvm.2018.00124

Human ascending aortic aneurysms characteristically exhibit cystic medial degeneration of the aortic wall encompassing elastin degeneration, proteoglycan accumulation and smooth muscle cell loss. Most studies have focused on the aortic media and there is a limited understanding of the importance of the adventitial layer in the setting of human aneurysmal disease. We recently demonstrated that the adventitial ECM contains key angiogenic factors that are downregulated in aneurysmal aortic specimens. In this study, we investigated the adventitial microvascular network (vasa vasorum) of aneurysmal aortic specimens of different etiology and hypothesized that the vasa vasorum is disrupted in patients with ascending aortic aneurysm. Morphometric analyses of hematoxylin and eosin-stained human aortic cross-sections revealed evidence of vasa vasorum remodeling in aneurysmal specimens, including reduced density of vessels, increased lumen area and thickening of smooth muscle actin-positive layers. These alterations were inconsistently observed in specimens of bicuspid aortic valve (BAV)-associated aortopathy, while vasa vasorum remodeling was typically observed in aneurysms arising in patients with the morphologically normal tricuspid aortic valve (TAV). Gene expression of hypoxia-inducible factor 1 α and its downstream targets, metallothionein 1A and the pro-angiogenic factor vascular endothelial growth factor, were down-regulated in the adventitia of aneurysmal specimens when compared with non-aneurysmal specimens, while the level of the anti-angiogenic factor thrombospondin-1 was elevated. Immunodetection of glucose transporter 1 (GLUT1), a marker of chronic tissue hypoxia, was minimal in non-aneurysmal medial specimens, and locally accumulated within regions of elastin degeneration, particularly in TAV-associated aneurysms. Quantification of GLUT1 revealed elevated levels in the aortic media of TAV-associated aneurysms when compared to non-aneurysmal counterparts. We detected evidence of chronic inflammation as infiltration of lymphoplasmacytic cells in aneurysmal specimens, with a higher prevalence of lymphoplasmacytic infiltrates in aneurysmal specimens from patients with TAV compared to that of patients with BAV. These data highlight differences

in vasa vasorum remodeling and associated medial chronic hypoxia markers between aneurysms of different etiology. These aberrations could contribute to malnourishment of the aortic media and could conceivably participate in the pathogenesis of thoracic aortic aneurysm.

Keywords: vasa vasorum, aneurysm, hypoxia, angiogenesis, adventitia

INTRODUCTION

The tunica adventitia of large blood vessels includes extracellular matrix and diverse cell types constituting a unique microenvironment distinct from the neighboring tunica media. In elastic conduit arteries, this outer layer provides substantial biomechanical support and is thought to be critically important in maintaining vascular homeostasis (1, 2). However, the biological mechanisms by which the adventitia influences large blood vessels' functions are less understood. Despite this gap in knowledge, a growing body of evidence supports a critical role for adventitia in vascular wall physiology and pathophysiology (3–6).

In addition to luminal flow, large blood vessels require their own external access to a blood supply to maintain vascular health. The *vasa vasorum* (Latin: “vessels of the vessels”) serves this vital role in large blood vessels. During his research on anatomy in the seventeenth century, Willis was purportedly the first to report the existence of vasa vasorum in the aorta (7). Since this first acquaintance, the purpose and functionality of this extensive microvascular network have barely begun to be understood. In human, the ascending thoracic aorta has an expansive network of vasa vasorum that originates from the coronary and brachiocephalic arteries (7, 8). The vasa vasorum infiltrates the blood vessel wall from the abluminal side and weaves extensively through the adventitial layer. The arteries of the vasa vasorum supply oxygen and nutrients to the outer two-thirds of larger blood vessels (>0.5 mm thick) comprised of at least 29 elastic lamellae at birth (e.g., thoracic aorta, pulmonary artery, and saphenous vein of humans, sheep and dogs) while the veins remove waste products (9, 10). Blood vessels with fewer than 29 elastic lamellae, with the exception of coronary arteries or certain disease states, are devoid of vasa vasorum in the outer media such as those of small rodents, and are adequately nourished from the lumen (9). Nearly half a century ago, the importance of the vasa vasorum was realized from observations of ischemic medial necrosis in the canine ascending aorta following occlusion of the vasa vasorum (11). Other investigators have reproduced these findings in other animal models and corroborated the remodeling of the aortic wall, which is reminiscent of the histopathological hallmark of cystic medial degeneration in human thoracic aortic aneurysm (10, 12–14). These studies raised important questions on the role of the vasa vasorum in human aortic disease.

Our laboratory focuses on ascending thoracic aortic aneurysm (TAA), the main pathology known to affect the ascending aorta. TAAs can arise in patients with the morphologically normal tricuspid aortic valve (TAV), but patients with the most common

congenital anomaly of the aortic valve (bicuspid aortic valve, BAV) have a heightened risk of developing aneurysm in the proximal ascending aorta (15, 16). Our work has centered on understanding the cellular and molecular mechanisms involved in TAAs arising in both patient populations (17–20). We have uncovered mechanisms distinctly involved in BAV aortopathy, such as altered response to oxidative stress (17), unique medial matrix architecture (21), and altered biomechanical strength (22). Considering these findings mostly focused on the aortic media, we extended our interests to the adventitia as an important neighboring microenvironment in the setting of aortic disease. We concentrated on the vasa vasorum network specifically and hypothesized that this microvascular network is disrupted in patients with TAA. Here, we describe remodeling of vasa vasorum vessels and note aberrations in size, abundance and wall thickness in TAA specimens associated with down-regulation of angiogenic and hypoxia-related gene targets in the adventitial layer while the medial layer displayed evidence of hypoxia. These aberrations uncover a new view of the pathophysiology of human thoracic aortic disease from the perspective of the adventitia.

MATERIALS AND METHODS

Tissue Collection and Processing

Human ascending thoracic aortic specimens ($n = 91$) were collected during elective aortic valve and ascending aortic replacement operations or during heart transplantation with informed patient consent and approval of the Institutional Review Board of the University of Pittsburgh and through the Center for Organ Recovery and Education. All patient-related procedures were carried out in accordance with principles outlined in the Declaration of Helsinki. The aortic specimens were obtained within 1–2 cm of the sinotubular junction. Upon excision, tissue specimens were placed in saline on ice and transported to the laboratory. Specimens were categorized according to their aortic valve morphology: tricuspid (TAV) or bicuspid (BAV). Patient demographics, aortic dimensions, and comorbidities, (e.g., hypertension) were carefully recorded (Table 1). None of the included patients had diagnosed Marfan, Ehlers-Danlos or Loeys-Dietz syndromes or chronic or acute dissection. Patients are otherwise relatively healthy. Maximal orthogonal aortic diameter was measured via intraoperative trans-esophageal echocardiography. The non-aneurysmal cohorts included patients with maximal orthogonal diameters of ≤ 42 mm. The aneurysmal patient cohorts included patients undergoing ascending aortic replacement due to ascending TAA and exhibited a maximal orthogonal aortic diameter > 42 mm.

TABLE 1 | Patient demographics.

	TAV		BAV	
	NA	TAA	NA	TAA
N (M/F)	40 (23/16) ^a	39 (22/17)	31 (20/11)	44 (35/9)
Age (year)	56 ± 16.9	67 ± 8.7*	57 ± 11.2 [^]	56 ± 10.6 [^]
Diameter (mm)	32 ± 3.4 ^b	52 ± 5.8*	38 ± 3.8 ^c	51 ± 3.9 [^]
AI				
1+	5.3%	23.1%	16.7%	20.9%
2–3+	15.8%	35.9%	6.7% [^]	18.6%
4+	5.3%	20.5%	26.9%	11.6%
AS				
Mild	0%	0%	0%	23.1% [^] #
Mod	0%	0%	3.3%	15.4% [^] #
Severe	25.0%	7.7%	76.7% [^] ^	30.7% [^] #
HTN	50.0%	76.9%*	61.3%	70.5%
Diabetes	17.5%	13.5%	12.9%	23.3%
Smoking	47.5%	43.2%	43.4%	45.5%
ARB	0%	17.9%*	38.7% [^] ^	9.1% [^] ^
ACE-inhibitor	35%	10.8%*	12.1%	37.2% [^] #
Statins	27.5%	53.8%*	64.5%*	43.2%*

Quantitative data are presented as median ± SD.

*, #, and ^ indicate significance vs. TAV-NA, BAV-NA, and TAV-TAA, respectively and were obtained using a Chi-squared or a Kruskal-Wallis test.

HTN, hypertension; S.D., standard deviation; ARB, angiotensin-receptor blocker; ACE, angiotensin-converting enzyme; AS, aortic stenosis, AI, aortic insufficiency.

^aSex of one patient was not recorded.

^{b,c}Calculated from data from 17 and 22 patients, respectively.

Histology and Immunofluorescence

Portions (~0.5 cm²) of human aortic specimens were fixed in 10% buffered formalin overnight or 4% paraformaldehyde for 30 min and paraffin-embedded. Cross-sections (5 μm) were stained with hematoxylin and eosin (H&E) to reveal aortic layers and vasa vasorum structures (McGowan Institute for Regenerative Medicine Histology Core, University of Pittsburgh). Sections were reviewed by two authors (MB and JP). Before immunolabeling, paraffin was removed using xylene followed by an ethanol dehydration series, rehydration in water and phosphate buffer saline (PBS) and antigen retrieval (Target Retrieval Solution, pH 6, Dako #S1700). Blocked slides (0.5% bovine serum albumin) were incubated in primary unconjugated antibody (α-SMA, 1:1000, DAKO, # M0851, GLUT1, 1:500, Millipore #07-1401) in blocking solution overnight at 4°C. Secondary labeling was accomplished with Alexa Fluor-conjugated secondary antibodies (anti-mouse Alexa Fluor 594, # 715-585-150, anti-rabbit Alexa Fluor 594, # 711-585-152, all from Jackson ImmunoResearch) for 2 h at room temperature. A FITC-conjugated antibody targeting Von Willebrand Factor was added to the secondary labeling step (1:100, US Biological, # V2700-01C). Sections were mounted with coverslips using Prolong Gold with DAPI (Invitrogen, # P-36931) and allowed to dry overnight. Slides were visualized using a TE-2000-E inverted microscope (Nikon) using bright field or epi-fluorescence microscopy and captured using a DS-Fi1 5MP color camera (Nikon) or an Imaging Array CoolSNAP ES2 Monochrome 1,394 × 1,040 High Resolution Camera (Photometrics) and NIS Elements Software

TABLE 2 | Primer set details.

Gene name	Gene symbol	Assay ID #
Hypoxia-inducible factor 1α	<i>Hif-1α</i>	Hs00936366_m1
Metallothionein IA	<i>Mt-1A</i>	Hs00831826_s1
Vascular endothelial growth factor	<i>Vegf-A</i>	Hs00900055_m1

3.2 (Nikon). Vasa vasorum morphometrics were independently calculated from the entirety of each section using NIS Elements Software by two researchers (MB and JP) and similar outcomes were observed for each. Reported vessel diameters and lumen areas were calculated from vessel perimeter measurements. Vessel thickness was calculated by normalizing the vessel wall area to the lumen diameter. Vasa vasorum density was calculated from the total number of vessels observed on aortic cross sections and divided by the adventitial area. To limit the influence of potential histological embedding and sectioning artifacts, a binary thresholding method was employed to quantify adventitial tissue area. Inflammatory infiltrates were described by a clinical pathologist of the University of Pittsburgh Medical Center.

RNA Isolation and Quantitative Real-Time PCR

Portions of aortic adventitial specimens were swiftly placed in RNAlater solution (Life Technologies) and stored at –20°C until use. Specimens (15–20 mg) were homogenized in RLT buffer (QIAGEN) containing β-mercaptoethanol (1/100, Fisher Scientific BP176-100) using the gentleMACS Tissue Dissociator (Miltenyi, Auburn, CA). Further homogenization was achieved using the QIAshredder kit (Qiagen). Total RNA was isolated from adventitial tissue extracts using the RNeasy Plus Mini kit (QIAGEN) according to the manufacturer's instructions. Gene expression of hypoxia-inducible factor 1 alpha (*Hif-1α*), vascular endothelial growth factor (*Vegf*), and metallothionein (*Mt*)-1A were quantified from 5 to 25 ng of template RNA using inventoried Taqman[®] Gene Expression Assays and 1-step RNA-to-CT[™] kit (Life Technologies). Primer set details can be found in **Table 2**. Thermocycling conditions were as follows: RNA was reverse-transcribed at 48°C for 15 min followed by *Taq* activation at 95°C for 10 min, and 40 cycles of denaturation for 15 s at 95°C, and primer and probe annealing at 60°C for 1 min. All target gene probes were labeled with FAM as the 5' reporter dye and TAMRA as the 3' quencher dye. Assays were carried out in triplicate on an ABI Prism 7900HT sequence detection system in the Genomics and Proteomics Core Laboratories of the University of Pittsburgh. Data was analyzed using SDS 2.2.2 Software (Applied Biosystems). Relative gene expression levels were calculated using the ΔC_T and reported as relative gene expression normalized to *PPIA* as the endogenous control.

Western Blotting

Ascending aortic media specimens were mechanically processed to remove the adventitial and the intimal layers.

The resulting aortic medial specimens were homogenized in RIPA buffer (Pierce) containing phosphatase and protease inhibitor cocktails (ThermoFisher and Sigma, respectively) and phenylmethanesulfonylfluoride (PMSF, Sigma) using the gentleMACS Tissue Dissociator. Following a low-speed centrifugation (1,500 g for 5 min at 4°C), samples were placed on ice for 30 min. Samples were then centrifuged at high speed (12,000 g) for 20 min at 4°C and protein concentration of the supernatant was determined using the bicinchoninic acid (BCA) assay (Pierce).

Western blotting was performed using standard procedure as previously described (18). Briefly, samples were mixed with Laemmli buffer and boiled at 100°C for 5 min. Electrophoresis was performed on SDS-PAGE containing 10% acrylamide and proteins were transferred to polyvinylidene fluoride membrane. After blocking for 1 h in blotting-grade blocker (BioRad), membranes were incubated overnight at 4°C with an anti-GLUT1 antibody (1:500, Millipore #07-1401), rinsed in PBS-Tween-20 0.1% and incubated for 2 h at room temperature with an anti-goat antibody coupled to horseradish peroxidase (Santa Cruz Biotechnology, #sc-2020). Protein bands were visualized using enhanced chemiluminescence Western Blotting Substrate (Pierce), captured using a ChemiDoc imager (BioRad) and quantified using ImageLab software (BioRad). Membranes were stripped in Re-Blot Plus Strong Solution (EMD Millipore) and re-probed with an anti- β -actin antibody (1:5,000, Abcam, #ab8227) for normalization. Relative GLUT1 expression was calculated as the ratio of GLUT1 band density over β -actin band density for each sample.

Thrombospondin-1 ELISA

Aortic adventitial specimens were placed in RIPA buffer supplemented with protease and phosphatase inhibitors and protein lysates were prepared as described above for aortic medial samples. The BCA assay was employed to determine the protein concentration of each sample and 25 μ g of adventitial lysates were used to determine TSP1 levels via ELISA following the manufacturer's instructions (R&D).

Statistical Analyses

Quantitative data are reported in the text as mean \pm standard error of the mean and are represented in figures in hanging box plot format, where median and interquartile ranges are shown, and error bars represent 90 and 10th percentile (SigmaPlot 12.5). Outliers were excluded using the Outlier Labeling Rule according to Hoaglin and Iglewicz (23) and using SPSS Statistic software version 24.0 (IBM Corp.) Prevalence of hypertension, aortic stenosis and aortic insufficiency were compared between patient groups using a Chi-Squared test. All other data were compared using the non-parametric Mann-Whitney test or the Kruskal-Wallis followed by a Dunn's *post-hoc* test, as indicated in each figure legend. A *p*-value of <0.05 was considered significant. When indicated, variables were evaluated for correlation using the bivariate Pearson correlation analysis.

RESULTS

Decreased Density of Vasa Vasorum in Thoracic Aortic Aneurysm

We histologically evaluated the adventitia of aneurysmal aortic specimens and examined the abundance of vasa vasorum in comparison to their non-aneurysmal counterparts (Figures 1A–H). Inspection of H&E stained aortic cross sections revealed less density of vessels in aneurysmal TAV patients when compared with non-aneurysmal aortas from TAV patients (11.9 ± 1.53 vs. 24.7 ± 3.04 vessels/mm², respectively, $p = 0.004$, Figure 1I). The density of vasa vasorum in aneurysmal and non-aneurysmal BAV specimens was similar to that of non-aneurysmal TAV specimens (19.8 ± 2.45 and 24.7 ± 3.26 vs. 24.7 ± 3.04 vessels/mm², $p = 0.224$ and $p = 0.922$, respectively, Figure 1I). Interestingly, when data from aneurysmal BAV and TAV specimens were compared, the density of vasa vasorum was higher in aneurysmal BAV specimens (19.8 ± 2.45 vs. 11.9 ± 1.53 vessels/mm², $p = 0.009$). Of note, when normalized to the total section area, we found that the adventitial area was larger in aneurysmal specimens when compared to non-aneurysmal specimens (11.1 ± 1.0 vs. $8.1 \pm 0.8\%$ of total section area, $p = 0.002$). Normalized adventitial area was highest in TAV-TAA specimens when compared to all other groups (14.7 ± 1.7 vs. 7.8 ± 1.2 (TAV-NA), $8.6 \pm 1.1\%$ (BAV-NA) and $9.6 \pm 0.8\%$ (BAV-TAA), $p < 0.02$). Analysis of vasa vasorum density as a function of the ascending aortic diameter revealed a negative correlation in specimens from TAV patients only (Pearson's $\rho = -0.544$, $p = 0.002$, Figure 1J). There was no correlation between vasa vasorum density and aortic diameter in specimens from BAV patients ($p = 0.913$, Figure 1H). There was no correlation of vasa vasorum density with age of the patients.

Increased Vasa Vasorum Lumen Size in Thoracic Aortic Aneurysm

Inspection of the vessel size revealed increased lumen area in aneurysmal aortas from BAV patients compared to specimens from non-aneurysmal BAV patients ($1,338 \pm 230$ vs. 691 ± 126 mm², $p = 0.022$, Figures 2A–E). However, the lumen area in aneurysmal TAV and BAV patients was similar when compared to non-aneurysmal TAV specimens ($1,093 \pm 174$ mm² and $1,338 \pm 230$ vs. 866 ± 132 mm², $p = 0.329$ and $p = 0.128$, respectively, Figure 2E). The lumen area of all aneurysmal specimens (BAV and TAV combined) were collectively larger than the lumen area of all the non-aneurysmal specimens combined ($1,524 \pm 263$ vs. 789 ± 92.3 , $p = 0.013$, Figure 2E). While there was no correlation found between lumen area of vasa vasorum and patients' age for TAV or BAV cohorts, the lumen area was positively correlated with maximal orthogonal aortic diameter in BAV specimens only (Pearson's $\rho = 0.351$, $p = 0.036$, Figure 2F).

We further compared the relative distribution of vessel size according to the classification described by Giannoni et al. (24). Aneurysmal aortic specimens from both TAV and BAV patients displayed less small vessels (lumen diameter $<50 \mu$ m) when compared to non-aneurysmal TAV specimens (8.49 ± 1.17 and 10.6 ± 1.41 vs. 19.6 ± 2.55 , $p < 0.001$ and $p = 0.005$, respectively, Figure 3A). The density of small size vessels

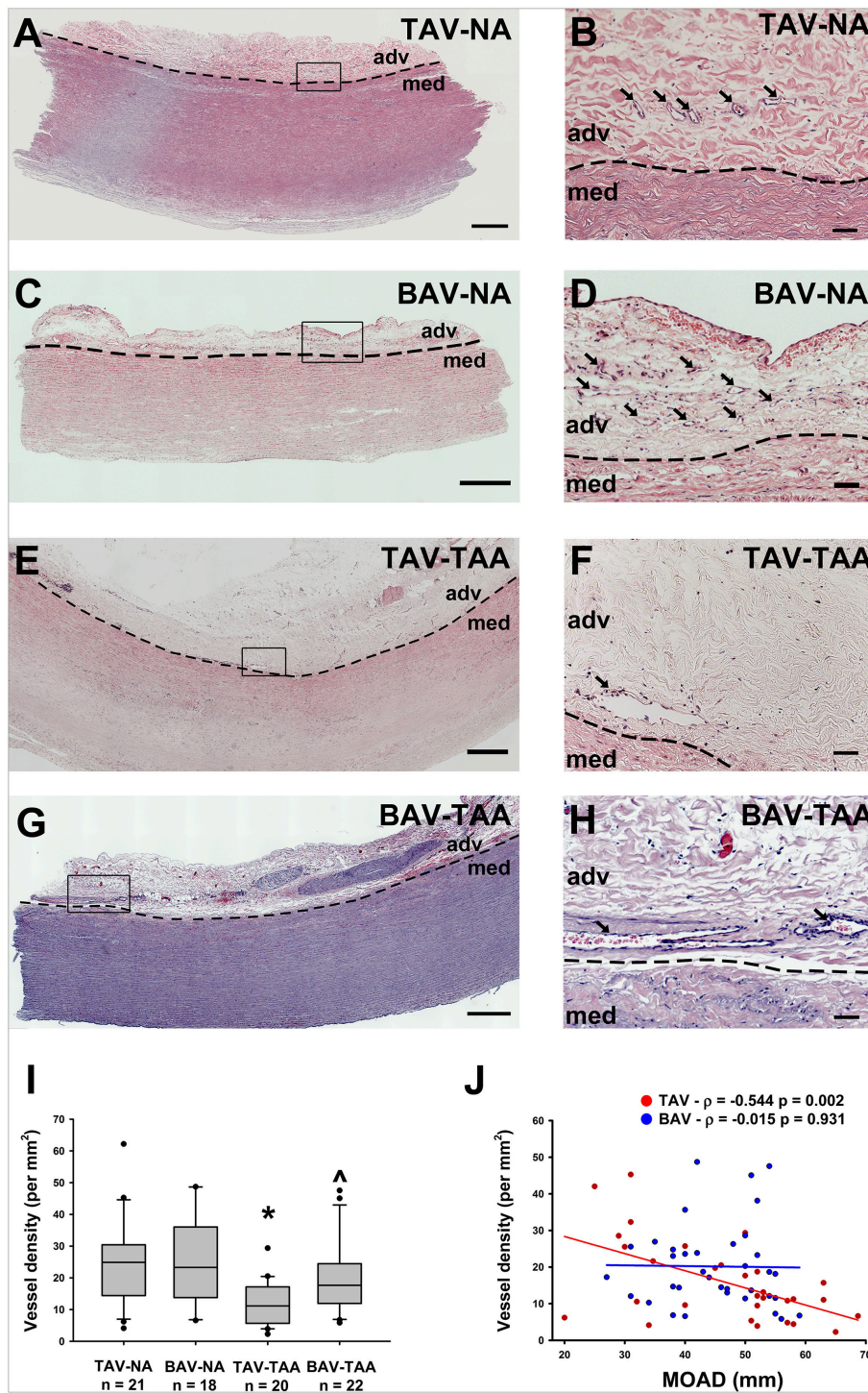


FIGURE 1 | Reduced vasa vasorum density in human ascending aortic adventitia of aneurysmal TAV patients. Representative H&E staining of specimens from a non-aneurysmal (NA) patient with a morphologically normal tricuspid aortic valve (TAV) (A, B) or with a bicuspid aortic valve (BAV) (C, D). Images in (E, F) show representative H&E staining of aneurysmal (TAA) specimens from a TAV patient and in (G, H), from a BAV patient. Images in (A, C, E, G) depict an aortic specimen that were captured with a 20X objective and tiled to comprise the entire section, scale bar = 500 μm. Panels (B, D, F, H) represent magnification of insets denoted in the corresponding image in the left panel and are representative of the observed reduced density of vasa vasorum (arrows) in aneurysmal specimens. Images were captured with a 20X objective, scale bar = 50 μm. Images of vasa vasorum in the adventitia (adv) were captured adjacent to the tunica media (med). Dashed line = adv-med border. (I) Quantification of vessel density as number of vessels per mm² of adventitia. * and ^ indicates $p < 0.05$ vs. TAV-NA and TAV-TAA, respectively and assessed with the Kruskal-Wallis test. (J) Graphical representation of vessel density as a function of the maximal orthogonal aortic diameter (MOAD) in TAV (red) and BAV (blue) specimens. ρ indicates the coefficient of correlation and p indicates the p -value obtained using a bivariate Pearson correlation analysis.

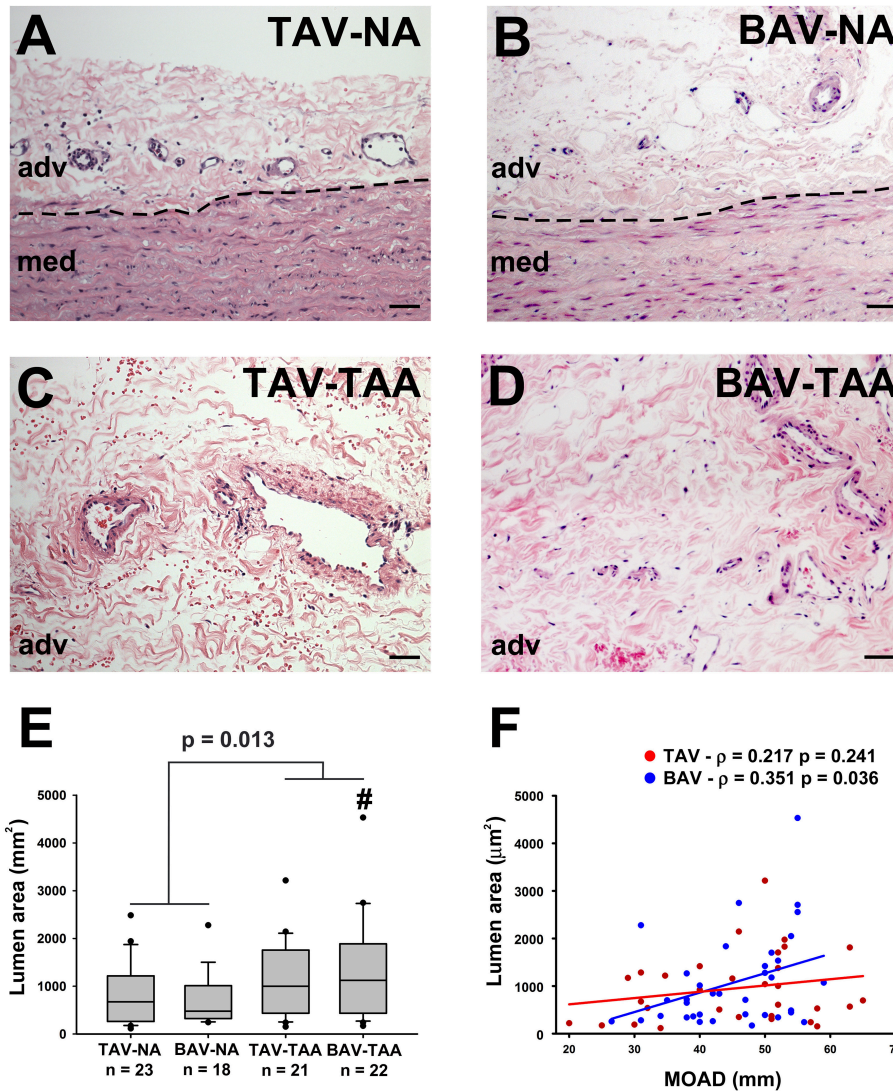
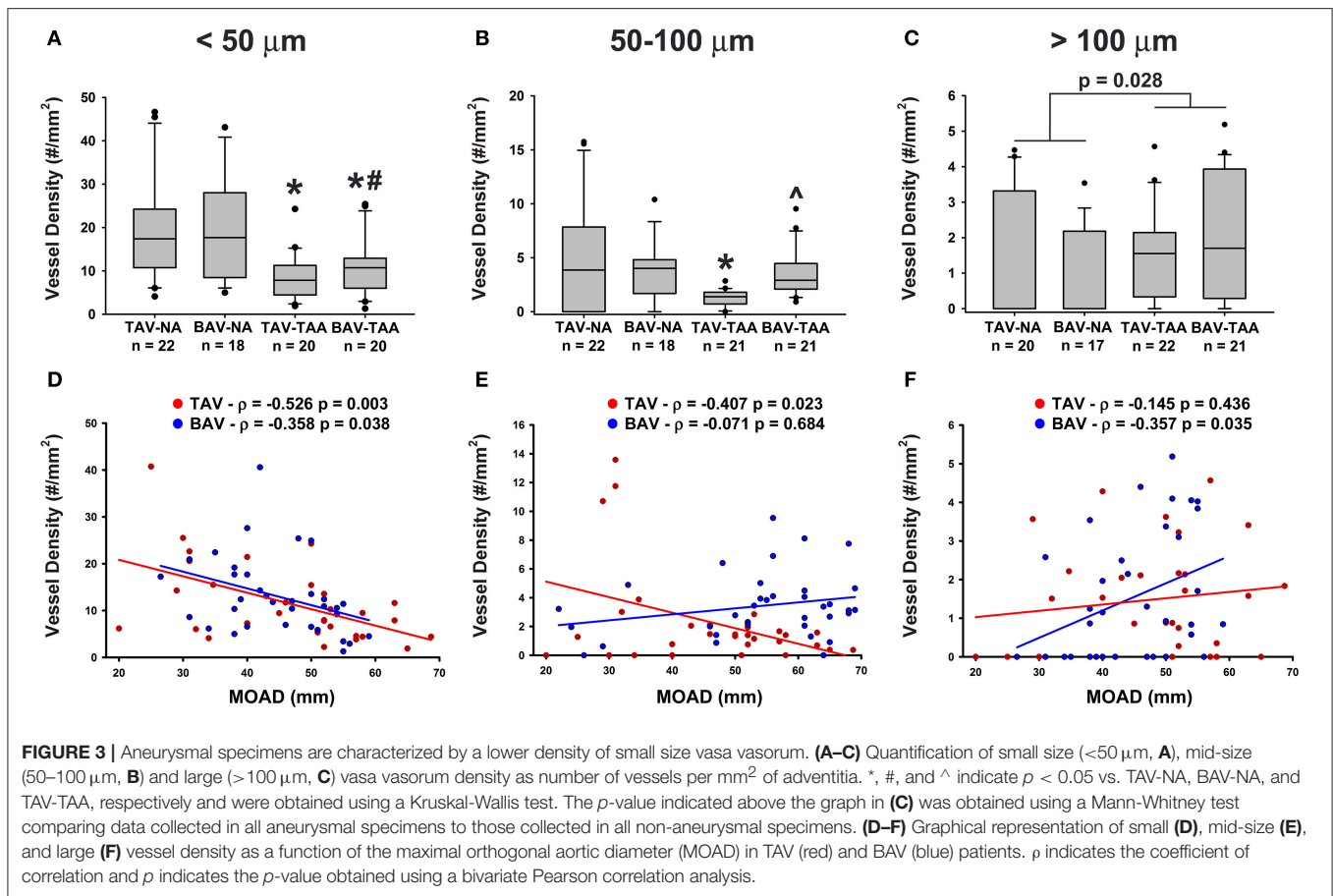


FIGURE 2 | Increased vasa vasorum lumen area in human ascending aortic adventitia of aneurysmal patients. Representative images of aortic specimens stained with H&E collected from non-aneurysmal (NA) or aneurysmal (TAA) patients with a morphologically normal tricuspid aortic valve (TAV) (A,C) or with a bicuspid aortic valve (BAV) (B,D). Specimens were imaged with a 20X objective, scale bar = 50 μm. The border between the adventitia (adv) and the media (med) is denoted by a dashed line. Quantification of vasa vasorum lumen area (mm²) in the four patient cohorts is shown in (E). # indicates *p* < 0.05 vs. BAV-NA and was obtained using a Kruskal-Wallis test. The *p*-value indicated above the graph was determined using a Mann-Whitney test comparing data collected in all aneurysmal specimens to those collected in all non-aneurysmal specimens. Vessel density was expressed as a function of the maximal orthogonal aortic diameter (MOAD) in TAV (red) and BAV (blue) specimens (F). ρ indicates the coefficient of correlation and *p* indicates the *p*-value obtained using a bivariate Pearson correlation analysis.

was also lower in aneurysmal BAV specimens when compared to that of non-aneurysmal BAV specimens (10.6 ± 1.41 vs. 19.3 ± 2.79 , $p = 0.022$, **Figure 3A**). With respect to mid-size vessels (50–100 μm), their density was lower in aneurysmal TAV specimens when compared to non-aneurysmal TAV specimens (1.26 ± 0.16 vs. 5.12 ± 1.14 , $p = 0.037$, **Figure 3B**). In contrast, aneurysmal BAV specimens displayed a similar density of mid-size vessels when compared to non-aneurysmal BAV specimens (3.50 ± 0.47 vs. 3.93 ± 0.64 , $p = 0.929$, **Figure 3B**), but a higher number of mid-size vessels were observed when compared to aneurysmal TAV specimens (3.50 ± 0.47 vs. 1.26 ± 0.16 ,

$p = 0.027$, **Figure 3B**). Quantification of large vasa vasorum (>100 μm of diameter) showed that all aneurysmal specimens displayed more numerous large vasa vasorum when compared to all non-aneurysmal specimens (1.79 ± 0.24 vs. 1.16 ± 0.25 , $p = 0.028$, **Figure 3C**). We identified negative correlations between small vessel density and ascending aortic diameter in both BAV- and TAV-associated aortopathy ($\rho = -0.358$, $p = 0.038$ for BAV specimens and $\rho = -0.526$, $p = 0.003$ for TAV specimens **Figure 3D**). While mid-size density was negatively correlated with ascending aortic diameter in TAV specimens ($\rho = -0.407$, $p = 0.023$, **Figure 3E**), there was no correlation between large



size vessels and ascending aortic diameter. Conversely, mid-size vessels displayed no correlation with ascending aortic diameter in BAV specimens, while the density of large vessels increased with ascending aortic diameter ($\rho = 0.357, p = 0.035$, Figure 3F). Pearson's correlation tests on the density of the different sizes of vasa vasorum and age of the patients were not significant.

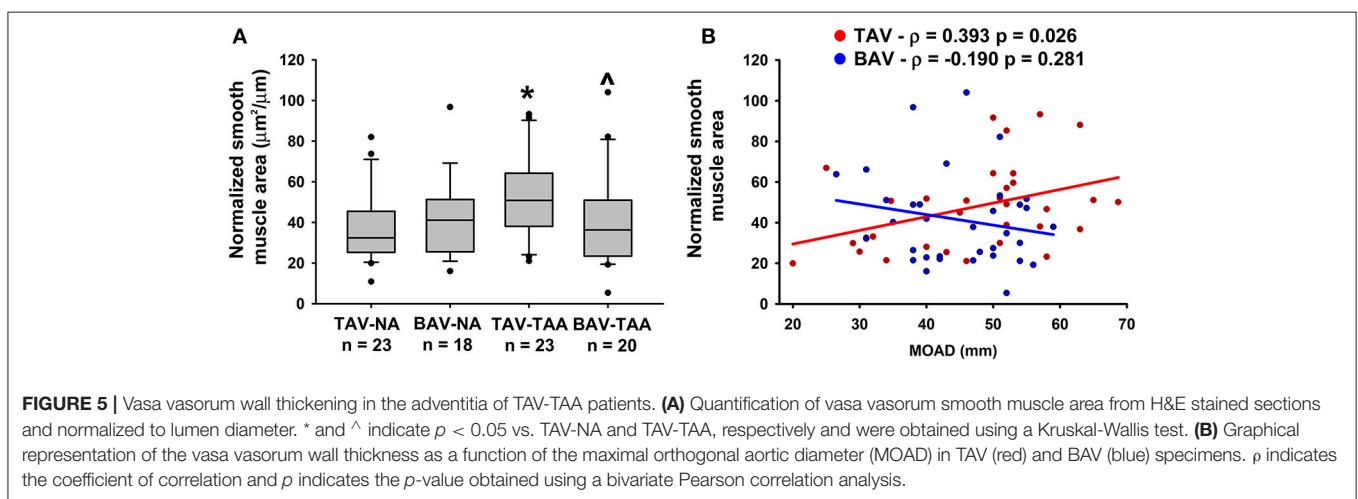
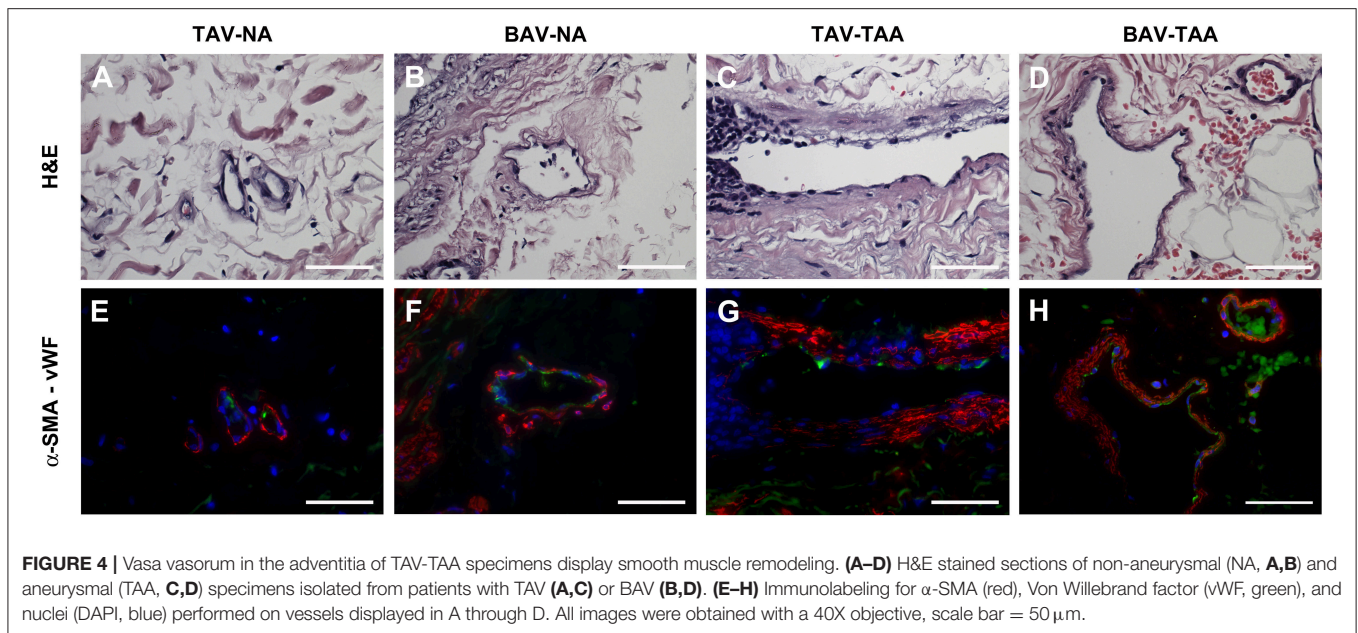
Vasa Vasorum Wall Remodeling in Thoracic Aortic Aneurysm

Qualitative inspection of vasa vasorum structures revealed disparity in the thickness of the vessel wall (Figures 4A–D). Immunolabeling revealed more numerous α -SMA positive and vWF negative cells in the thickened vasa vasorum walls (Figures 4E–H). Measurement of vasa vasorum wall area normalized to the lumen diameter revealed increased vessel wall thickness in aneurysmal TAV aorta when compared with non-aneurysmal TAV aorta (52.8 ± 4.39 vs. $37.0 \pm 3.83, p = 0.07$, Figure 5A). The vasa vasorum wall thickness was similar among all non-aneurysmal specimens and aneurysmal BAV specimens, and aneurysmal BAV specimens displayed less thick vasa vasorum when compared to aneurysmal TAV specimens (40.5 ± 5.28 vs. $52.8 \pm 4.39, p = 0.031$). Comparison of vasa vasorum thickness and ascending aortic diameter revealed a positive correlation between the two variables in TAV specimens

only ($\rho = 0.393, p = 0.026$, Figure 5B). The vasa vasorum thickness was not correlated with age of the patients.

Decreased Expression of Pro-angiogenic and Hypoxia Gene Targets in the Adventitia of Aneurysmal Patients

To investigate possible reasons for altered vasa vasorum density, we examined expression of gene targets associated with angiogenic and hypoxic signaling. Real-time PCR experiments on total mRNA from adventitial specimens revealed that expression of *hypoxia-inducible factor-1 alpha (Hif-1 α)* was down-regulated in adventitial specimens from aneurysmal BAV specimens when compared with specimens from non-aneurysmal TAV and BAV specimens (0.022 ± 0.005 vs. $0.069 \pm 0.018, p = 0.008$, and vs. $0.041 \pm 0.006, p = 0.037$, Figure 6A). Down-regulation of *Hif-1 α* downstream gene targets *vascular endothelial growth factor (Vegf)* and *metallothionein (Mt-1A)* was also noted in the adventitia of aneurysmal specimens when compared with non-aneurysmal specimens TAV patients (0.024 ± 0.003 vs. $0.059 \pm 0.014, p = 0.049$, Figure 6B and 0.0077 ± 0.0015 vs. $0.048 \pm 0.016, p = 0.018$, Figure 6C). Additionally, the adventitia of BAV-TAA specimens contained lower amounts of *Mt-1A* mRNA in comparison to TAV-NA specimens (0.0109 ± 0.0016 vs. $0.048 \pm 0.016, p = 0.046$, Figure 6C). When gene expression from



all aneurysmal specimens was compared to all non-aneurysmal specimens, *Hif-1 α* and *Mt-1A* expression level were found to be lower (0.028 ± 0.004 vs. 0.055 ± 0.010 , $p = 0.013$, **Figure 6A** and 0.033 ± 0.008 vs. 0.009 ± 0.001 , $p = 0.019$, **Figure 6C**). Protein expression level of the anti-angiogenic factor thrombospondin-1 (TSP1) was elevated in TAV-TAA specimens when compared to TAV-NA specimens (227 ± 67 vs. 62 ± 14 ng/ml, $p = 0.022$, **Figure 6D**). Lastly, all aneurysmal specimens contained higher amounts of TSP1 when compared to all non-aneurysmal specimens (183 ± 40 vs. 81 ± 14 ng/ml, $p = 0.038$, **Figure 6D**).

Chronic Hypoxia in the Media of Aneurysmal Specimens

To explore the potential effects of adventitial vasa vasorum remodeling on the aortic media, we probed for evidence of chronic hypoxia using immuno-based detection of the glucose transporter GLUT1 (**Figure 7**). We found that GLUT1 was

abundantly present within the aortic media of aneurysmal specimens and primarily localized to areas of elastin degeneration in TAV-TAA specimens (**Figure 7A**). In contrast, qualitative inspection of non-aneurysmal aortic media revealed visibly lower levels of GLUT1 expression. Quantification of GLUT1 expression in lysates of aortic media specimens confirmed elevated levels of expression in aneurysmal aorta when compared to non-aneurysmal aorta for specimens from patients with TAV (1.08 ± 0.16 vs. 0.58 ± 0.08 , $p = 0.006$, **Figure 7B**). Similarly, aneurysmal aortic specimens from BAV patients exhibited increased GLUT1 protein expression when compared to non-aneurysmal specimens from patients with TAV (0.99 ± 0.12 vs. 0.58 ± 0.08 , $p = 0.011$, **Figure 7B**). GLUT1 expression was higher in all aneurysmal specimens when compared with all non-aneurysmal specimens (1.04 ± 0.10 vs. 0.66 ± 0.06 , $p = 0.004$). Expression levels of *Glut1* were positively correlated with ascending aortic

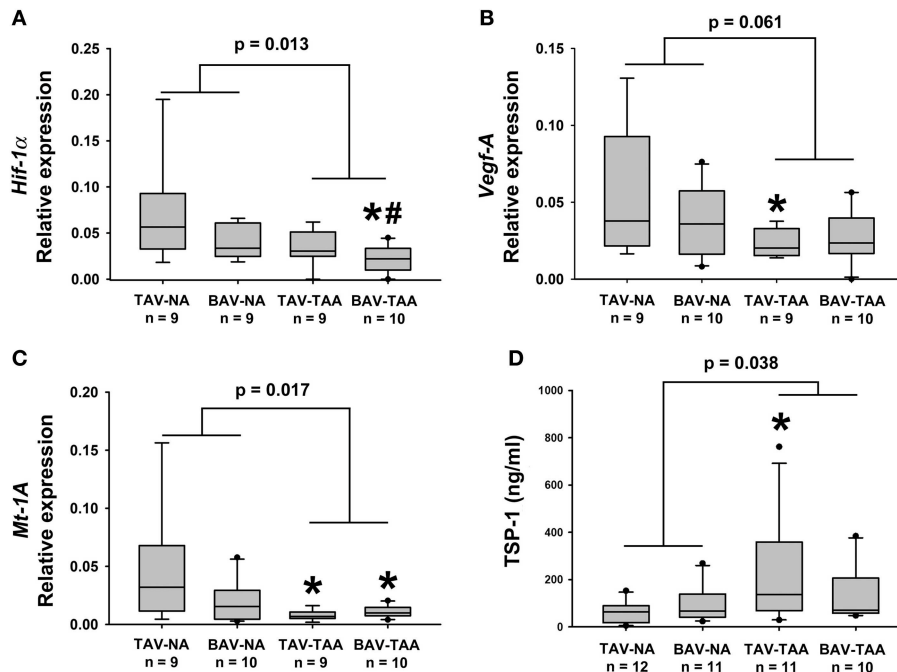


FIGURE 6 | Expression of angiogenesis and hypoxia-related target genes in human ascending aortic adventitia. Quantitative real-time PCR was employed to measure expression of *Hif-1α* (A), *Vegf-A* (B) and *Mt-1A* (C) in total mRNA isolated from adventitia of human ascending aortic specimens. Thrombospondin 1 (TSP1) levels were quantified via ELISA in 25 μg of adventitial lysates (D). * and # indicate $p < 0.05$ vs. TAV-NA and BAV-NA, respectively and were obtained using a Kruskal-Wallis test. The p -values indicated above the graphs were obtained using a Mann-Whitney test comparing data collected in all aneurysmal specimens to those collected in all non-aneurysmal specimens.

diameter in TAV specimens only ($\rho = 0.513$, $p = 0.036$, Figure 7C).

Adventitial Inflammation in Specimens of Degenerative Thoracic Aortic Aneurysm

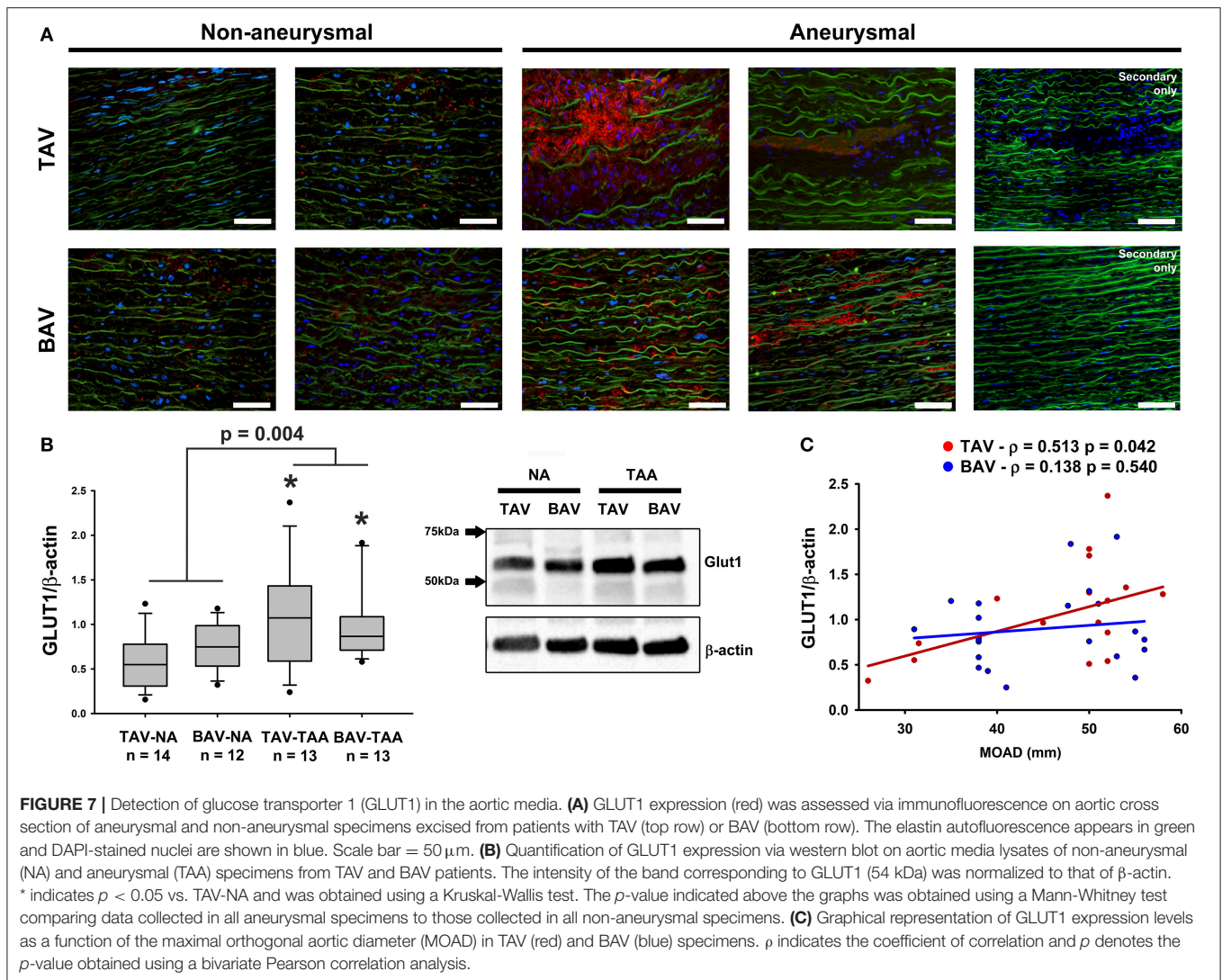
While there was no evidence of an inflammatory infiltrate in specimens from non-aneurysmal patients (Figures 8A,B), we noted an extensive chronic inflammatory component in the adventitia of aneurysmal patients. Evidence of a lymphoplasmacytic infiltrate was found in the majority of aneurysmal specimens from patients with TAV (92%, Figures 8C,D) and was observed only in 25% of aneurysmal specimens from patients with BAV (Figures 8E,F). Images representative of specimens from aneurysmal TAV patients (Figures 8C,D) and BAV patients (Figures 8E,F) reveal infiltration of lymphocytes and plasma cells (arrowheads) localized to smaller vessels of the vasa vasorum within the adventitia.

DISCUSSION

In large vessels such as the aorta, blood perfusion from the aortic lumen is the principal source of nutrients and oxygen for the cells located on the luminal side, while the vasa vasorum provides nourishment to cells located on the abluminal side (25, 26). Specifically, work in animals uncovered that this microvascular network supplies the adventitia and the smooth muscle cells

located in the outer third of the medial layer with oxygen and nutrients (10). Because medial degeneration, which includes loss of smooth muscle cells, is characteristic of ascending aortic aneurysms, we reasoned that alterations in the adventitial vasa vasorum network may play a role in aneurysm pathophysiology. In support of this concept, we reveal adventitial vasa vasorum remodeling and down-regulation of angiogenic signaling in the adventitia of specimens of human ascending aortic aneurysm, along with evidence of chronic hypoxia in the medial layer.

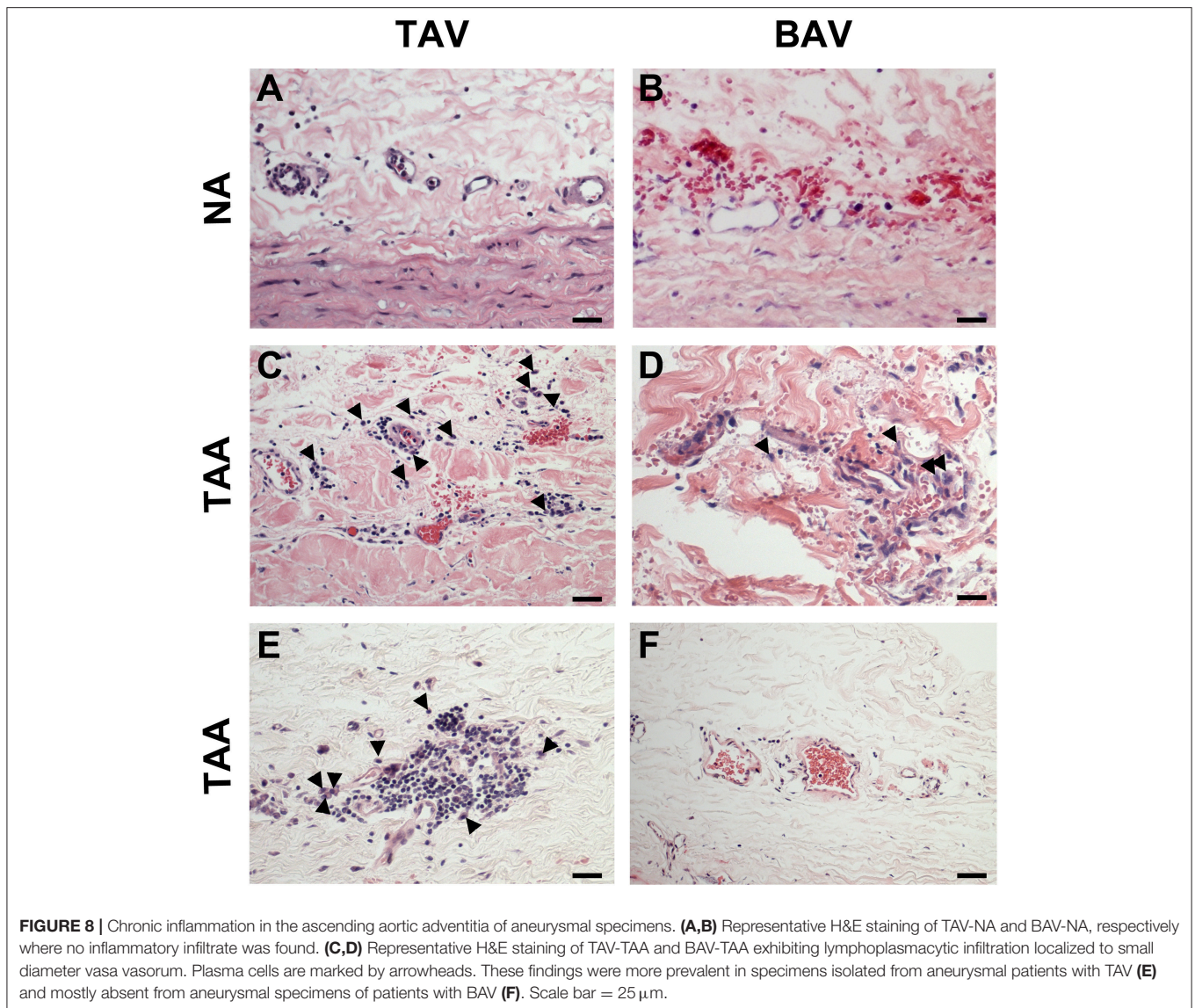
In our study of human aortic specimens, the decreased density of vasa vasorum and their significant remodeling in TAA, along with the altered distribution of vessel size could all lead to reduced blood flow to the medial layer. While our findings of increased lumen area of the vasa vasorum might be presumed to deliver a larger blood volume, a “paradoxical decrease” in blood flow through a dilated vasa vasorum has been documented following angioplasty in the canine (27). Nevertheless, our results reveal evidence of chronic hypoxia in the media with increased expression levels of GLUT1, a gene target of HIF1α (28). Increased expression of GLUT1 occurs during anaerobic glycolysis and is indicative of a state of chronic hypoxia. Our results are suggestive of a chronic hypoxic environment in the media of aneurysmal ascending aortic specimens alongside intense remodeling of vasa vasorum in the neighboring adventitia. A recent study by Niinimaki et al. corroborates this notion, since the authors described higher expression of another player in the hypoxic



pathway, carbonic anhydrase IX, in the media of aneurysmal ascending aortic specimens (29). The adventitia of aneurysmal specimens coincided with down-regulation of hypoxia-related genes, including *Hif-1 α* and its signaling targets *Vegf* and *Mt1a*. Interestingly, we previously demonstrated reduced levels of *Mt-1a* gene expression, while *Vegf* gene expression was unchanged in the media of aneurysmal ascending aortic specimens from BAV patients compared to that of non-aneurysmal patients with TAV (17, 30). Although hypoxia-triggered signaling typically involves post-translational activation of HIF-1 α and induction of downstream targets, including *Mt-1a* (31) and *Vegf* (32), chronic local tissue hypoxia has been shown to decrease VEGF signaling and angiogenic response via a HIF1 α -dependent mechanism in human endothelial cells (33). Furthermore, since MT has been shown to rescue HIF-1 α transcriptional activity in other systems (34), the reduction of *Mt-1A* in the adventitia could further limit transcription of hypoxia gene targets such as *Vegf* as we demonstrated here. This theory of hypoxia-mediated down-regulation of VEGF signaling agrees with our observation

of a less dense vasa vasorum network and less small vessels (<50 μm) in the adventitia of aneurysmal specimens. Taken together, down-regulation of key gene targets of angiogenesis and hypoxic signaling in the adventitia of aneurysmal thoracic aorta might be a consequence of the chronic hypoxia in the media and could have been initially triggered by reduced perfusion of the adventitia due to alterations in the vasa vasorum network. These findings collectively underscore the complexity of thoracic aortic disease and additional studies will address how adventitial hypoperfusion relates to medial hypoxia.

Our findings of thickened walls of vasa vasorum in the adventitia of aneurysmal aortic specimens agree with those reported by Osada et al. who described evidence of intimal sclerotic thickening in dissected human aorta (35). Furthermore, TAA arising in patients with mutations in the genes encoding the smooth muscle cytoskeletal proteins *Acta2* and *Myh11* also displayed local SMC hyperplasia and occlusion of the vasa vasorum (36, 37). While hyperplastic thickening of the vasa vasorum has been reported in cases of syphilitic aortitis, causing



restricted blood flow to the media with resultant ischemia (38), none of the patients in our study had a history of syphilis. Rather, the vasa vasorum thickening noted in our study was presumably due to outward remodeling of their smooth muscle layer, which is likely to be associated with alterations of the vasa vasorum contractility. In the healthy aortic wall, blood flow regulation in the vasa vasorum network is complex. While sympathetic innervation contributes to adventitial blood flow regulation, vasa vasorum react to several contractile and dilatory agonists *ex vivo* (39, 40). The effect of microvessel thickening and smooth muscle hyperplasia on vasa vasorum contractility and blood flow regulation warrant further considerations in the context of aortic diseases.

Despite a few observations in aneurysmal diseases, the contribution of vasa vasorum in diseases of large vessels has been primarily examined in the setting of atherosclerosis, where multiple inflammatory pathways drive vasa vasorum

expansion from the adventitia to the neointima (26). These inflammatory pathways are thought to be stimulated by an increase in oxygen demand as the wall thickness of the diseased vessel increases and consequently leads to hypoxia (41–45). This hypoxic state activates the HIF-1 signaling pathway and its gene targets, including the angiogenic factor VEGF, which drives neovascularization during neointimal and plaque formation (40, 46). Interestingly, our findings suggest that the mechanisms of vasa vasorum remodeling in the setting of human ascending aortic aneurysm markedly differ from those observed in atherosclerosis. In our study, the presence of lymphoplasmacytic infiltration near small-diameter vessels in the adventitia of degenerative TAA might contribute to poor expansion of the vasa vasorum in these patients. This observation of an inflammatory process in the adventitia is consistent with prior work by others in cases of thoracic aortic aneurysm (47) and related to IgG4 in aortic dissection (48) though these studies did

not include inspection of specimens from patients with BAV. In our study, there was no history or suspicion of arteritis in patients from which aortic specimens revealing evidence of chronic inflammation in the adventitia were obtained, thus implicating an inflammatory component in degenerative aneurysmal disease prior to, or in the absence of dissection and patients without BAV.

In the setting of ascending aortic aneurysms, we characterized vasa vasorum remodeling by a depletion of small vessels ($\leq 50 \mu\text{m}$) with an associated decrease in the pro-angiogenic factors *Hif-1 α* and *Vegf-A* gene expression and increased levels of the antiangiogenic factor TSP1, together pointing to decreased angiogenic capacity. These observations are consistent with our recent work revealing decreased levels of angiogenic factors in the adventitial extracellular matrix of aneurysmal ascending aortic specimens when compared to non-aneurysmal specimens, determined utilizing an angiogenic array (49). Our data corroborate the study by Kessler et al. which reported a decrease in VEGF at the mRNA level in the adventitia of human TAA specimens and found no difference at the protein level using ELISA (50). Information on adventitial microvessel prevalence or morphometrics was not previously reported (50). Our study adds new knowledge on adventitial vasa vasorum and confirms elevated TSP1 in the adventitia of aneurysmal aorta (50). Interestingly, Kessler et al. reported increased density of microvessels in the media of aneurysmal ascending aortic specimens from patients with TAV associated with increased expression of key pro-angiogenic factors in the medial layer, such as angiopoietin-1 and -2, and FGF1 (50). Moreover, we observed wall thickening of vasa vasorum observed in our aneurysmal specimens, which could be an indication of arteriogenesis. While we can neither rule out nor confirm involvement of arteriogenesis in the observed changes in the vasa vasorum network of human TAA, possible mechanisms underlying wall thickening include microvascular shear stress and changes in fluid dynamics or pressure. Altered hemodynamics are known to occur in the aorta itself in the setting of TAA (51) but whether the vasa vasorum also experiences shear stress and changes in fluid dynamics and pressure or is affected by hemodynamic changes in the parent vessel remains unknown. Nevertheless, our observations highlight alterations in pro- and anti-angiogenic signals, and their specific impact on the vasa vasorum network in the pathophysiology of ascending aortic aneurysms warrants further study.

Based on our study and others, it appears that TAAs exhibit remodeling of vasa vasorum and dysregulation of hypoxia- and angiogenesis-related factors. These data in human aorta are supported by several earlier studies in animal models that demonstrate the importance of adventitial vasa vasorum in medial homeostasis of the host. The study by Wilens et al. in canine was the first to show a direct link between interruption of blood flow through the vasa vasorum of the descending aorta and necrosis of the aortic media (11). These observations demonstrating the importance of vasa vasorum in aortic wall homeostasis were corroborated by other investigators studying the impact of vasa vasorum occlusion in porcine and rabbit models who described medial necrosis evidenced by localized areas of SMC loss, and sparse and discontinuous

elastin fibers (10, 13, 14). These histopathologic phenomena are reminiscent of the hallmarks of human TAA known as cystic medial degeneration. Although these studies did not establish a direct link between blood flow in the vasa vasorum and aneurysm development, a recent study in rat by Tanaka et al. showed that hypoperfusion of adventitial vasa vasorum led to medial hypoxia associated with aneurysmal development in the abdominal aorta (52). Determination of remodeled vessel function including endothelial-dependent vasoreactivity and NO signaling capacity and the influence of extracellular cues in the setting of aneurysmal disease could offer insights on how vasa vasorum remodeling affects media biology and biomechanics.

Whether or not vasa vasorum remodeling directly influences the risk of aneurysm and subsequent dissection in human ascending aortic aneurysms is unclear. Pursuit of this notion is supported by knowledge that human Type A aortic dissection commonly propagates in the adventitia-media border and reports of dissection alongside the vasa vasorum pathway (35). Furthermore, Niinimäki et al. found that expression level of the hypoxia marker carbonic anhydrase IX increased with the diameter of aortic aneurysms, supporting our own findings in specimens from TAV patients, where we revealed a positive correlation between Glut1 expression and ascending aortic diameter. In this same study, specimens from patients presenting with acute aortic dissection displayed carbonic anhydrase IX positive staining (29). These observations suggest a possible connection between hypoxic levels and TAA disease progression into aortic dissection. Lastly, the possible role of altered vasa vasorum in the risk of dissection is further supported by the observation of leaky neovessels and accumulation of plasma proteins in the media of TAA specimens (50). Based on these observations, Mallat et al. proposed that dysfunctional vasa vasorum may be key in the initiation of aortic dissection (53). While these observations collectively point to a possible association between vasa vasorum dysfunction in the progression of TAA toward dissection, the impact of not only microvascular remodeling and possible dysfunction but also medial and adventitial integrity in the setting of TAA deserve further consideration.

Our study revealed a few differences between aortopathy related to the presence of BAV and in patients with the morphologically normal TAV. Specifically, aneurysms in patients with TAV displayed lower vasa vasorum density when compared to that of patients with BAV, and the density of vasa vasorum was inversely related to increasing aortic diameter. Additionally, thickening of the vasa vasorum wall and locally increased GLUT1 expression were only found in aneurysmal specimens from patients with TAV. Gaining acceptance is the concept that aneurysms arising in patients with BAV are mechanistically distinct from those arising in TAV patients (21, 54), others have started to consider differences in the adventitial layer (50). Collectively, these observations add to a growing body of literature describing the distinctions in the mechanisms involved in the pathophysiology of BAV- and TAV-related TAA and could help explain why patients with BAV seem no more likely to dissect than patients with TAV (55, 56). Because we noted distinct differences in the adventitia of aortic specimens from BAV and

TAV patients, we continue to pursue understanding how the extracellular cues influence cell behavior in all layers of the aortic wall.

In conclusion, we describe here several interesting anomalies in vasa vasorum size, abundance, and thickness in the setting of ascending thoracic aortic aneurysm. Wall thickening, SMC hyperplasia and lumen dilatation of the vasa vasorum are all changes that could limit nutrient delivery in the host vessel. Furthermore, our observations of down-regulated expression of angiogenic and hypoxia-related gene targets in the adventitia associated with evidence of chronic hypoxia in the media suggest a complex interplay among hypoxic signaling, microvascular function, and ascending aortic aneurysm pathophysiology. These findings have wide-spread implications for increasing our understanding of perivascular influence of vascular homeostasis and mechanisms of aortic disease.

LIMITATIONS AND FUTURE PERSPECTIVES

The focus of our study on resected samples of human aorta imposes a few limitations on the extent to which our results can be interpreted. Whether the noted vasa vasorum remodeling is a cause or a consequence of the aneurysmal pathology requires further study. The subject of our ongoing work includes developing appropriate human cell and tissue-based disease models to study microvascular physiology in the setting of human aortic disease. New animal models might prove useful in deciphering mechanisms of putative microvascular dysfunction related to human aortic disease that could be distinct from mechanisms at play in the abdominal aorta. Likewise, the influence of adventitial biology on media homeostasis may be both anatomically and etiologically-specific. Inspection of vasa vasorum physiology in smaller aneurysm (<45 mm) might offer additional insights into pathways of early disease and provide new information of what factors dictate progressive degeneration

of the aortic media, leading to biomechanical failure. These areas collectively shape the focus of our ongoing trajectory toward a comprehensive multi-layer understanding of human aortic pathophysiology.

AUTHOR CONTRIBUTIONS

MB, JH, TR, and JP participated in experimental data collection. MB and JP performed morphometric analyses, while qPCR data were analyzed by JH. MB completed all additional analyses. MB and JP generated the manuscript with input from TG. JP supervised the entire study.

FUNDING

This work was supported by the National Heart, Lung and Blood Institute of the National Institutes of Health under Award Number HL127214 and HL131632 to JP and Award Number HL109132 to TG and by the University of Pittsburgh Medical Center Health System Competitive Medical Research Fund award to JP.

ACKNOWLEDGMENTS

The authors are grateful to the patients and their families for the generous gift of their tissue which allowed us to perform this work. We thank Kristin Konopka, Amanda Urosek, and Julie Schreiber for their assistance with IRB protocols and obtaining informed patient consent. We thank Benjamin Green, Michael Eskay and Trevor Weis for assistance with tissue processing and histological analysis and Bradley Ellis for help with RNA isolations and qPCR. We express our gratitude to Dr. Jeffrey Nine for his expert advice in evaluating our histological specimens. We are grateful to our surgical colleagues of the Department of Cardiothoracic Surgery, University of Pittsburgh Medical Center and to the Center for Organ Recovery & Education for their assistance with aortic specimen acquisition.

REFERENCES

- Cabrera Fischer EI, Bia D, Camus JM, Zocalo Y, de Forteza E, Armentano RL. Adventitia-dependent mechanical properties of brachiocephalic ovine arteries in *in vivo* and *in vitro* studies. *Acta Physiol (Oxf)*. (2006) 188:103–11. doi: 10.1111/j.1748-1716.2006.01614.x
- Stenmark KR, Yeager ME, El Kasmi KC, Nozik-Grayck E, Gerasimovskaya EV, Li M, et al. The adventitia: essential regulator of vascular wall structure and function. *Annu Rev Physiol*. (2013) 75:23–47. doi: 10.1146/annurev-physiol-030212-183802
- Dutertre CA, Clement M, Morvan M, Schakel K, Castier Y, Alsac JM, et al. Deciphering the stromal and hematopoietic cell network of the adventitia from non-aneurysmal and aneurysmal human aorta. *PLoS ONE* (2014) 9:e89983. doi: 10.1371/journal.pone.0089983
- Li N, Cheng W, Huang T, Yuan J, Wang X, Song M. Vascular adventitia calcification and its underlying mechanism. *PLoS ONE* (2015) 10:e0132506. doi: 10.1371/journal.pone.0132506
- Majesky MW. Adventitia and perivascular cells. *Arterioscler Thromb Vasc Biol*. (2015) 35:e31–35. doi: 10.1161/ATVBAHA.115.306088
- Bersi MR, Bellini C, Wu J, Montaniel KR, Harrison DG, Humphrey JD. Excessive adventitial remodeling leads to early aortic maladaptation in angiotensin-induced *Hypertension* (2016) 67:890–6. doi: 10.1161/HYPERTENSIONAHA.115.06262
- Clarke JA. An X-ray microscopic study of the vasa vasorum of the normal human ascending aorta. *Br Heart J*. (1965) 27:99–104. doi: 10.1136/hrt.27.1.99
- Mulligan-Kehoe MJ. The vasa vasorum in diseased and nondiseased arteries. *Am J Physiol Heart Circ Physiol*. (2010) 298:H295–305. doi: 10.1152/ajpheart.00884.2009
- Wolinsky H, Glagov S. Nature of species differences in the medial distribution of aortic vasa vasorum in mammals. *Circ Res*. (1967) 20:409–21. doi: 10.1161/01.RES.20.4.409
- Heistad DD, Marcus ML, Larsen GE, Armstrong ML. Role of vasa vasorum in nourishment of the aortic wall. *Am J Physiol*. (1981) 240:H781–787. doi: 10.1152/ajpheart.1981.240.5.H781
- Wilens SL, Malcolm JA, Vazquez JM. Experimental infarction (medial necrosis) of the dog's aorta. *Am J Pathol*. (1965) 47:695–711.
- Heistad DD, Marcus ML. Role of vasa vasorum in nourishment of the aorta. *Blood Vessels* (1979) 16:225–38. doi: 10.1159/000158209

13. Stefanadis C, Vlachopoulos C, Karayannacos P, Boudoulas H, Stratos C, Filippides T, et al. Effect of vasa vasorum flow on structure and function of the aorta in experimental animals. *Circulation* (1995) 91:2669–78. doi: 10.1161/01.CIR.91.10.2669
14. Angouras D, Sokolis DP, Dostos T, Kostomitsopoulos N, Boudoulas H, Skalkeas G, et al. Effect of impaired vasa vasorum flow on the structure and mechanics of the thoracic aorta: implications for the pathogenesis of aortic dissection. *Eur J Cardiothorac Surg.* (2000) 17:468–73. doi: 10.1016/S1010-7940(00)00382-1
15. Edwards WD, Leaf DS, Edwards JE. Dissecting aortic aneurysm associated with congenital bicuspid aortic valve. *Circulation* (1978) 57:1022–5. doi: 10.1161/01.CIR.57.5.1022
16. Hoffman JJ, Kaplan S. The incidence of congenital heart disease. *J Am Coll Cardiol.* (2002) 39:1890–900. doi: 10.1016/S0735-1097(02)01886-7
17. Phillippi JA, Klyachko EA, Kenny JP IV, Eskay MA, Gorman RC, Gleason TG. Basal and oxidative stress-induced expression of metallothionein is decreased in ascending aortic aneurysms of bicuspid aortic valve patients. *Circulation* (2009) 119:2498–506. doi: 10.1161/CIRCULATIONAHA.108.770776
18. Kotlarczyk MP, Billaud M, Green BR, Hill JC, Shiva S, Kelley EE, et al. Regional disruptions in endothelial nitric oxide pathway associated with bicuspid aortic valve. *Ann Thorac Surg.* (2016) 102:1274–81. doi: 10.1016/j.athoracsur.2016.04.001
19. Billaud M, Phillippi JA, Kotlarczyk MP, Hill JC, Ellis BW, St Croix CM, et al. Elevated oxidative stress in the aortic media of patients with bicuspid aortic valve. *J Thorac Cardiovasc Surg.* (2017) 154:1756–62. doi: 10.1016/j.jtcvs.2017.05.065
20. Phillippi JA, Hill JC, Billaud M, Green BR, Kotlarczyk MP, Gleason TG. Bicuspid aortic valve morphotype correlates with regional antioxidant gene expression profiles in the proximal ascending aorta. *Ann Thorac Surg.* (2017) 104:79–87. doi: 10.1016/j.athoracsur.2016.10.039
21. Phillippi JA, Green BR, Eskay MA, Kotlarczyk MP, Hill MR, Robertson AM, et al. Mechanism of aortic medial matrix remodeling is distinct in patients with bicuspid aortic valve. *J Thorac Cardiovasc Surg.* (2014) 147:1056–64. doi: 10.1016/j.jtcvs.2013.04.028
22. Pichamuthu JE, Phillippi JA, Cleary DA, Chew DW, Hempel J, Vorp DA, et al. Differential tensile strength and collagen composition in ascending aortic aneurysms by aortic valve phenotype. *Ann Thorac Surg.* (2013) 96:2147–54. doi: 10.1016/j.athoracsur.2013.07.001
23. Hoaglin DC, Iglewicz B. Fine-tuning some resistant rules for outlier labeling. *J Am Stat Assoc.* (1987) 82:1147–9. doi: 10.1080/01621459.1987.10478551
24. Giannoni MF, Vicenzini E, Citone M, Ricciardi MC, Itrace L, Laurito A, et al. Contrast carotid ultrasound for the detection of unstable plaques with neoangiogenesis: a pilot study. *Eur J Vasc Endovasc Surg.* (2009) 37:722–7. doi: 10.1016/j.ejvs.2008.12.028
25. Santilli SM, Fiegel VD, Knighton DR. Changes in the aortic wall oxygen tensions of hypertensive rabbits. Hypertension and aortic wall oxygen. *Hypertension* (1992) 19:33–9. doi: 10.1161/01.HYP.19.1.33
26. Mulligan-Kehoe MJ, Simons M. Vasa vasorum in normal and diseased arteries. *Circulation* (2014) 129:2557–66. doi: 10.1161/CIRCULATIONAHA.113.007189
27. Cragg AH, Einzig S, Rysavy JA, Castaneda-Zuniga WR, Borgwardt B, Amplatz K. The vasa vasorum and angioplasty. *Radiology* (1983) 148:75–80. doi: 10.1148/radiology.148.1.6222396
28. Ebert BL, Firth JD, Ratcliffe PJ. Hypoxia and mitochondrial inhibitors regulate expression of glucose transporter-1 via distinct Cis-acting sequences. *J Biol Chem.* (1995) 270:29083–9. doi: 10.1074/jbc.270.49.29083
29. Niinimäki E, Muola P, Parkkila S, Kholova I, Haapasalo H, Pastorekova S, et al. Carbonic anhydrase IX deposits are associated with increased ascending aortic dilatation. *Scand Cardiovasc J.* (2016) 50:162–6. doi: 10.3109/14017431.2016.1158416
30. Phillippi JA, Eskay MA, Kubala AA, Pitt BR, Gleason TG. Altered oxidative stress responses and increased type I collagen expression in bicuspid aortic valve patients. *Ann Thorac Surg.* (2010) 90:1893–8. doi: 10.1016/j.athoracsur.2010.07.069
31. Murphy BJ, Kimura T, Sato BG, Shi Y, Andrews GK. Metallothionein induction by hypoxia involves cooperative interactions between metal-responsive transcription factor-1 and hypoxia-inducible transcription factor-1alpha. *Mol Cancer Res.* (2008) 6:483–90. doi: 10.1158/1541-7786.MCR-07-0341
32. Damert A, Machein M, Breier G, Fujita MQ, Hanahan D, Risau W, et al. Up-regulation of vascular endothelial growth factor expression in a rat glioma is conferred by two distinct hypoxia-driven mechanisms. *Cancer Res.* (1997) 57:3860–4.
33. Olszewska-Pazdrak B, Hein TW, Olszewska P, Carney DH. Chronic hypoxia attenuates VEGF signaling and angiogenic responses by downregulation of KDR in human endothelial cells. *Am J Physiol Cell Physiol.* (2009) 296:C1162–70. doi: 10.1152/ajpcell.00533.2008
34. Feng W, Wang Y, Cai L, Kang YJ. Metallothionein rescues hypoxia-inducible factor-1 transcriptional activity in cardiomyocytes under diabetic conditions. *Biochem Biophys Res Commun.* (2007) 360:286–9. doi: 10.1016/j.bbrc.2007.06.057
35. Osada H, Kyogoku M, Ishidou M, Morishima M, Nakajima H. Aortic dissection in the outer third of the media: what is the role of the vasa vasorum in the triggering process? *Eur J Cardio Thorac Surg.* (2013) 43:e82–8. doi: 10.1093/ejcts/ezs640
36. Guo DC, Pannu H, Tran-Fadulu V, Papke CL, Yu RK, Avidan N, et al. Mutations in smooth muscle alpha-actin (ACTA2) lead to thoracic aortic aneurysms and dissections. *Nat Genet.* (2007) 39:1488–93. doi: 10.1038/ng.2007.6
37. Pannu H, Tran-Fadulu V, Papke CL, Scherer S, Liu Y, Presley C, et al. MYH11 mutations result in a distinct vascular pathology driven by insulin-like growth factor 1 and angiotensin II. *Hum Mol Genet.* (2007) 16:2453–62. doi: 10.1093/hmg/ddm201
38. du Toit DF, McCormich M, Laker L. Syphilitic aortitis. A case report. *S Afr Med J.* (1985) 67, 778–9.
39. Scotland RS, Vallance PJ, Ahluwalia A. Endogenous factors involved in regulation of tone of arterial vasa vasorum: implications for conduit vessel physiology. *Cardiovasc Res.* (2000) 46:403–11. doi: 10.1016/S0008-6363(00)00023-7
40. Moreno PR, Purushothaman KR, Sirol M, Levy AP, Fuster V. Neovascularization in human atherosclerosis. *Circulation* (2006) 113:2245–52. doi: 10.1161/CIRCULATIONAHA.105.578955
41. Bjornheden T, Levin M, Ewaldsson M, Wiklund O. Evidence of hypoxic areas within the arterial wall *in vivo*. *Arterioscler Thromb Vasc Biol.* (1999) 19:870–6. doi: 10.1161/01.ATV.19.4.870
42. Vorp DA, Lee PC, Wang DH, Makaroun MS, Nemoto EM, Ogawa S, et al. Association of intraluminal thrombus in abdominal aortic aneurysm with local hypoxia and wall weakening. *J Vasc Surg.* (2001) 34:291–9. doi: 10.1067/mva.2001.114813
43. Doyle B, Caplice N. Plaque neovascularization and antiangiogenic therapy for atherosclerosis. *J Am Coll Cardiol.* (2007) 49:2073–80. doi: 10.1016/j.jacc.2007.01.089
44. Luque A, Turu M, Juan-Babot O, Cardona P, Font A, Carvajal A, et al. Overexpression of hypoxia/inflammation markers in atherosclerotic carotid plaques. *Front Biosci.* (2008) 13:6483–90. doi: 10.2741/3168
45. Sluimer JC, Gasc JM, van Wanroij JL, Kisters N, Groeneweg M, Sollewijn Gelpke MD, et al. Hypoxia, hypoxia-inducible transcription factor, and macrophages in human atherosclerotic plaques are correlated with intraplaque angiogenesis. *J Am Coll Cardiol.* (2008) 51:1258–65. doi: 10.1016/j.jacc.2007.12.025
46. Kwon HM, Sangiorgi G, Ritman EL, Lerman A, McKenna C, Virmani R, et al. Adventitial vasa vasorum in balloon-injured coronary arteries: visualization and quantitation by a microscopic three-dimensional computed tomography technique. *J Am Coll Cardiol.* (1998) 32:2072–9. doi: 10.1016/S0735-1097(98)00482-3
47. Agaimy A, Weyand M, Strecker T. Inflammatory thoracic aortic aneurysm (lymphoplasmacytic thoracic aortitis): a 13-year-experience at a German Heart Center with emphasis on possible role of IgG4. *Int J Clin Exp Pathol.* (2013) 6:1713–22.
48. Wu D, Choi JC, Sameri A, Minard CG, Coselli JS, Shen YH, et al. Inflammatory cell infiltrates in acute and chronic thoracic aortic dissection. *Aorta* (2013) 1:259–67. doi: 10.12945/j.aorta.2013.13-044
49. Fercana GR, Yerneni S, Billaud M, Hill JC, VanRyzin P, Richards TD, et al. Perivascular extracellular matrix hydrogels mimic native matrix microarchitecture and promote angiogenesis via

- basic fibroblast growth factor. *Biomaterials* (2017) 123:142–54. doi: 10.1016/j.biomaterials.2017.01.037
50. Kessler K, Borges LF, Ho-Tin-Noe B, Jondeau G, Michel JB, Vranckx R. Angiogenesis and remodelling in human thoracic aortic aneurysms. *Cardiovasc Res.* (2014) 104:147–59. doi: 10.1093/cvr/cvu196
51. Mahadevia R, Barker AJ, Schnell S, Entezari P, Kansal P, Fedak PW, et al. Bicuspid aortic cusp fusion morphology alters aortic three-dimensional outflow patterns, wall shear stress, and expression of aortopathy. *Circulation* (2014) 129:673–82. doi: 10.1161/CIRCULATIONAHA.113.003026
52. Tanaka H, Zaima N, Sasaki T, Sano M, Yamamoto N, Saito T, et al. Hypoperfusion of the adventitial vasa vasorum develops an abdominal aortic aneurysm. *PLoS ONE* (2015) 10:e0134386. doi: 10.1371/journal.pone.0134386
53. Mallat Z, Tedgui A, Henrion D. Role of microvascular tone and extracellular matrix contraction in the regulation of interstitial fluid: implications for aortic dissection. *Arterioscler Thromb Vasc Biol.* (2016) 36:1742–7. doi: 10.1161/ATVBAHA.116.307909
54. Della Corte A, Body SC, BoherAM, Schaefer HJ, Milewski RK, Michelena HI, et al. Surgical treatment of bicuspid aortic valve disease: knowledge gaps and research perspectives. *J Thorac Cardiovasc Surg.* (2014) 147:1749–57, 1757 e1741. doi: 10.1016/j.jtcvs.2014.01.021
55. Michelena HI, Khanna AD, Mahoney D, Margaryan E, Topilsky Y, Suri RM, et al. Incidence of aortic complications in patients with bicuspid aortic valves. *JAMA* (2011) 306:1104–12. doi: 10.1001/jama.2011.1286
56. Kim JB, Spotnitz M, Lindsay ME, MacGillivray TE, Isselbacher EM, Sundt TM III. Risk of aortic dissection in the moderately dilated ascending aorta. *J Am Coll Cardiol.* (2016) 68:1209–19. doi: 10.1016/j.jacc.2016.06.025

Conflict of Interest Statement: The authors declare that the research was conducted in the absence of any commercial or financial relationships that could be construed as a potential conflict of interest.

Copyright © 2018 Billaud, Hill, Richards, Gleason and Phillippi. This is an open-access article distributed under the terms of the Creative Commons Attribution License (CC BY). The use, distribution or reproduction in other forums is permitted, provided the original author(s) and the copyright owner(s) are credited and that the original publication in this journal is cited, in accordance with accepted academic practice. No use, distribution or reproduction is permitted which does not comply with these terms.



Cell Phenotype Transitions in Cardiovascular Calcification

Luis Hortells[†], Swastika Sur[†] and Cynthia St. Hilaire^{*}

Division of Cardiology, Department of Medicine, and the Pittsburgh Heart, Lung, and Blood Vascular Medicine Institute, University of Pittsburgh, Pittsburgh, PA, United States

OPEN ACCESS

Edited by:

Joshua D. Hutcheson,
Florida International University,
United States

Reviewed by:

Vicky E. MacRae,
University of Edinburgh,
United Kingdom
Jose Javier Fuster,
Boston University, United States

*Correspondence:

Cynthia St. Hilaire
sthilaire@pitt.edu

[†]These authors have contributed
equally to this work

Specialty section:

This article was submitted to
Atherosclerosis and
Vascular Medicine,
a section of the journal
Frontiers in Cardiovascular Medicine

Received: 01 January 2018

Accepted: 14 March 2018

Published: 26 March 2018

Citation:

Hortells L, Sur S and St. Hilaire C
(2018) Cell Phenotype Transitions in
Cardiovascular Calcification.
Front. Cardiovasc. Med. 5:27.
doi: 10.3389/fcvm.2018.00027

Cardiovascular calcification was originally considered a passive, degenerative process, however with the advance of cellular and molecular biology techniques it is now appreciated that ectopic calcification is an active biological process. Vascular calcification is the most common form of ectopic calcification, and aging as well as specific disease states such as atherosclerosis, diabetes, and genetic mutations, exhibit this pathology. In the vessels and valves, endothelial cells, smooth muscle cells, and fibroblast-like cells contribute to the formation of extracellular calcified nodules. Research suggests that these vascular cells undergo a phenotypic switch whereby they acquire osteoblast-like characteristics, however the mechanisms driving the early aspects of these cell transitions are not fully understood. Osteoblasts are true bone-forming cells and differentiate from their pluripotent precursor, the mesenchymal stem cell (MSC); vascular cells that acquire the ability to calcify share aspects of the transcriptional programs exhibited by MSCs differentiating into osteoblasts. What is unknown is whether a fully-differentiated vascular cell directly acquires the ability to calcify by the upregulation of osteogenic genes or, whether these vascular cells first de-differentiate into an MSC-like state before obtaining a “second hit” that induces them to re-differentiate down an osteogenic lineage. Addressing these questions will enable progress in preventative and regenerative medicine strategies to combat vascular calcification pathologies. In this review, we will summarize what is known about the phenotypic switching of vascular endothelial, smooth muscle, and valvular cells.

Keywords: vascular calcification, valvular calcification, cell phenotype transition, vascular smooth muscle cell, endothelial cell, valve interstitial cell

INTRODUCTION

In bone formation, there are two different ossification processes, intramembranous ossification and endochondral ossification (1). During intramembranous ossification, the mineral hydroxyapatite is produced by osteoblasts and secreted into the dense network of extracellular matrix (ECM) proteins, together which harden to form a mineralized bone structure. Endochondral ossification involves hyaline cartilage and chondrocytes as a precursor for the hydroxyapatite nesting. Calcification in areas other than bone or tooth formation is pathologic, developing in the ECM of soft tissues, where osteoblasts do not reside. Ectopic calcification was once considered a passive and degenerative process, but it is now recognized as an active biological process which shares many features of physiological bone formation and remodeling, however the precise mechanisms inducing and propagating pathological

calcification are not completely understood. The resulting pathology from ectopic calcification can induce or exacerbate a variety of disease states.

Calcification of the cardiovascular system is one of the most frequent expressions of ectopic calcification, and the sites exhibiting calcification include the myocardium, heart valves, and the large and small arteries of the body (2–4). Myocardial calcification presents in two main forms: metastatic and dystrophic. The former is associated with aberrations in calcium homeostasis and is commonly found in patients with chronic kidney disease or kidney failure, as well as hyperparathyroidism (5, 6). Dystrophic myocardial calcification is more prevalent than metastatic, and occurs as a result of injury due to events such as myocardial infarction or infection (7, 8). Calcification of the aortic valve, termed calcific aortic valve disease (CAVD), encompasses a wide spectrum of pathology, from the stiffening of the leaflets (aortic sclerosis) to the presence of calcification that impairs leaflet movement and reduces blood flow (aortic stenosis). CAVD represents an ever-growing health burden associated with substantial costs (9, 10). Aortic valves are composed of three leaflets made up of three layers: the collagen-rich fibrosa lines the aortic side, the proteoglycan and glycosaminoglycan-rich spongiosa in the middle layer, and the elastin and collagen-rich ventricularis on the side of the left ventricle (3). Valve endothelial cells (VECs) cover the surface of the leaflets while valve interstitial cells (VICs) reside in all three layers. While both VECs and VICs can calcify, nodules of calcification originate in the fibrosa along the aortic side (11). In the arteries, calcification is divided in two main forms: intimal and medial. While the advanced stages of calcification in either arterial layer can invade into the other, the origin and course of these pathologies is distinct. Calcification of the intima is derived from atheroma plaque formation and is driven in part by necrosis, inflammation, and changes in endothelial cells (12), while early stages of medial calcification are not driven by inflammation but rather a breakdown of extracellular matrix, vascular smooth muscle cell (VSMC) phenotypic change (13), as well as an accumulation of extracellular matrix vesicles that are loaded with a variety of proteins, microRNAs, and the calcium and phosphate building blocks necessary for mineralization (14). In the field of vascular calcification, atherosclerotic intimal calcification is more widely recognized and better studied, while non-atherosclerotic medial calcification, which commonly occurs in patients with diabetes, renal disease, or hypertension, and several genetic diseases, has been less studied and therefore the processes that drive this pathology are less understood (4).

In this review, we will focus on the contribution of cellular fate, and how fully differentiated cells can revert to an immature state and then acquire an osteoblastic phenotype that drives calcification pathogenesis in cardiac tissues, aortic valves, and medial-layer calcification. Similar to osteogenic transitions, chondrocytic phenotype changes have also been identified during cardiovascular ossification pathobiology (15, 16). Recently, various studies have focused on the role of cell phenotype switching. In addition to changes in cell function, this phenomenon implies global transcriptional modifications that lead to the aberrant activation of genes involved in the calcification process.

FIBROBLAST TO MYOFIBROBLAST TO OSTEOBLAST-LIKE CELL

Studies in murine models have identified that cardiac fibroblasts make up close to 25% of the heart tissue (17). While not possessing electrical or contractile functions themselves, cardiac fibroblasts can couple to cardiomyocytes to aid in the propagation of electrical signals, maintain extracellular matrix homeostasis, and secrete cytokines and chemokines to modulate the immune system (18, 19). After injury, these fibroblasts exhibit functions to remodel the ECM, alter chemical and mechanical signals, participate in angiogenesis, and contribute to fibrosis (20, 21). Cardiac fibroblasts, like fibroblasts of other tissues, can acquire a “myofibroblast” phenotype, a state which shares some of the features seen in smooth muscle cells, including the ability to contract, the acquisition of smooth muscle cell markers such as α -smooth muscle actin (SMA- α), and secretion of ECM components (21, 22). It is well known that ectopic calcification in soft-tissue occurs at sites of injury, near the resulting scar tissue generated from fibrotic remodeling (23). Considering this, elegant experiments by Pillai et al. sought to determine whether cardiac fibroblasts are the source of cardiac calcifications (24). *In vitro* studies showed that with treatment of medium that differentiates mesenchymal stem cells into osteoblasts (often referred to as osteogenic media) both murine and human cardiac fibroblasts, but not endothelial cells, could be induced to calcify. *In vivo* lineage tracing experiments in a murine line prone to develop myocardial calcification show that cardiac fibroblasts reside amongst the hydroxyapatite minerals in fibrotic areas, and further analysis identified osteogenic signatures, such as the master osteogenic transcription factor *Runx2* (24). This work also highlights the important and complex role of inorganic phosphate (Pi) and pyrophosphate (PPi) homeostasis. Pi is a building block of mineralization, while PPi is generally considered an endogenous calcification inhibitor. Enzymes regulating this homeostasis include tissue non-specific alkaline phosphatase (TNAP), which metabolizes PPi into Pi, and ectonucleotide pyrophosphatase/phosphodiesterase-1 (ENPP1) which breaks down ATP into AMP and PPi (25). The disease Generalized Arterial Calcification of Infancy (GACI) is caused by homozygous inactivating mutations in this gene (26, 27). However, Pillai et al noticed that injured hearts presenting with calcification also showed increased expression of ENPP1. While hydroxyapatite is the most common chemical formulation found in ectopic calcification, other chemical formulations exist (4), including calcium pyrophosphate dihydrate (CPPD) (28). Indeed, the authors found CPPD minerals in calcified cardiac tissue (24), suggesting that perhaps ENPP1 was driving pathogenesis. A small molecule ENPP1 inhibitor was used and prevented this cardiac calcification (24). These results highlight the complicated dynamics of Pi/PPi homeostasis and the importance of knowing the chemical content of ectopic calcification when considering therapeutics. The study also clearly illustrates the ability of a fibroblast cell to acquire an osteogenic phenotype, but further work is needed to detail the step-wise progression that triggers differentiation from a myofibroblast-state down an osteogenic lineage.

The aortic valve also contains a fibroblast-like cell, called the valve interstitial cell (VIC). VICs populate all three layers of the valve and reside in a quiescent state. The aortic valve is a dynamic structure that controls the unidirectional flow of blood from the left ventricle to the aorta. In systole, valves open against the wall of the aorta, and the reverse pressure gradient in diastole induces them to unfurl and stretch out toward the center of the aortic annulus, forming a seal to prevent regurgitation. Every heartbeat induces this movement which exposes the valve cells and their surrounding extracellular matrix to an array of stresses (e.g., mechanical, shear, inflammatory). Mechanical and inflammatory stresses alone can induce a transcriptionally permissive chromatin structure (29, 30). These stresses are also thought to contribute to the early events that drive VICs to transition from a quiescent state to the activated myofibroblast state, which can go on to become calcifying osteoblast-like VICs (3, 11, 31–34).

It is well-established that osteogenic genes such as *Runx2*, *osteocalcin*, and *TNAP* are all upregulated in calcifying cells (32, 35, 36). The induction of these osteogenic genes in myofibroblasts is reminiscent of the differentiation of a mesenchymal stem cell (MSC) into an osteoblast (37–39). When MSCs themselves are seeded onto valve scaffolds and cultured under pulsatile flow conditions they acquire a myofibroblast-like phenotype, suggesting that exposure to mechanical and flow forces can drive progenitor cells to differentiate down the osteogenic lineage (40). In line with myofibroblast plasticity, VICs can exhibit the MSC/pericyte-like function of providing structural support to valve endothelial networks (41). *In vitro* co-culture assays in matrigel found that VICs possess chemo-attractive properties and wrap around sprouts of valve endothelial cells (VECs). Together these observations suggest that activated myofibroblasts can behave and respond to stimuli like MSC-like cells that are then further induced to upregulate expression of osteogenic genes (32, 34, 37, 42).

In vitro VICs acquire an activated myofibroblast-like state in part via increasing expression of TGF- β , which drives their proliferation, migration, and expression of the myofibroblast marker SMA- α (43). Activated VICs themselves alter the mechanical properties of the valve, creating a stiffer environment (44, 45). Elastic properties of the ECM also influence valve cell biology as stiffness promotes a calcific phenotype (33). Culturing VICs on a stiffer matrix promotes osteogenic differentiation, and specific substrates such as fibrin, heparin, and laminin induce the osteogenic transition of VICs into calcifying cells. In osteoblasts, ENPP1 generates PPI, which when hydrolyzed generates Pi with subsequent formation of hydroxyapatite (46), yet interestingly and similar to what was found in cardiac calcification, ENPP1 has also been found to be highly expressed in calcific aortic valve disease and in VICs (47). This release ATP promotes VICs survival, but in disease tissues upregulation of ENPP1 depletes the extracellular pool of ATP and thus promotes mineralization in VICs by promoting apoptosis (47, 48).

Inflammation also contributes to calcification pathogenesis, and inflammatory cells are found within and surrounding the calcified areas in the valve and heart (7, 49). Murine studies show that recruitment of immune cells is an early event in CAVD pathogenesis (50). And like the effects of mechanical stretch, inflammatory cells, such as mast cells, can also contribute to

remodeling the ECM via the release of proteases and growth factors known to drive both physiological and pathophysiological calcification (15). The contribution of inflammation to the early progression of osteogenesis on vascular cells was illustrated *in vivo* in the valves and arteries in the atherosclerotic *ApoE* knockout model (51). This study followed the temporal association of inflammation and calcification in atherosclerosis and found that inflamed areas exhibited high levels of the key mineralization enzyme, alkaline phosphatase, before microscopic evidence of calcification. PET imaging techniques found a similar temporal association in calcified foci in human thoracic aortas (52). The inflammatory cytokines TNF- α induced early differentiation of human bone marrow-derived MSCs into calcifying osteoblast-like cells, illustrating that inflammatory pathway activation can prime a cell to become osteogenic (53). Additionally, TNF- α signals stimulated by high fat diet-induced obesity and type II diabetes mellitus promotes aortic *Msx2* expression, a transcription factor in the BMP signaling pathway, and enhances pro-calcific arterial *Msx2-Wnt* cascades (54). Together this data suggests that in atherosclerotic calcification, inflammation precedes calcification; subsequent studies should delineate the role of inflammation and inflammatory signaling pathways in driving pro-osteogenic transcriptional and epigenetic changes.

ENDOTHELIAL TO MESENCHYMAL TRANSITION

Cells of various developmental origins come together to create the tissues that comprise the adult vasculature. Angioblasts are the developmental precursors to endothelial cells. Once endothelial cells are specified *de novo* vasculogenesis can occur, though the precise molecular cues regulating these early processes *in vivo* have not yet been fully characterized (55). During development, some structures are derived from the de-differentiation of endothelial cells, a process referred to as endothelial-to-mesenchymal transition (EndMT). For example the endocardial cushion tissue, which is the precursor of the semilunar valves of the heart, are derived from cells that undergo EndMT (56). Endothelial cells form a barrier along the lumen of vessels that is held intact by endothelial-specific proteins which form tight junctions and connections between adjacent endothelial cells (57). In EndMT, expression of these markers diminishes and endothelial cells lose cell-to-cell connections, enabling their migration and proliferation, as well as trans-differentiation. The TGF- β superfamily of cytokines, which includes both TGF- β s and BMPs, has several important and broad roles such as regulating cell growth and multiplication, differentiation or apoptosis, and EndMT. Embryonic EndMT processes are regulated by TGF- β signaling (58) via the upregulation of transcription factors such as Snail, which drives the detachment of the endothelial cells, promoting their phenotype switch (59).

While EndMT is a developmental program, it is also activated after vascular injury and stress, such as vein-graft remodeling and neointima formation (60), or in disease states such as atherosclerotic plaque development and progression (61), cardiac fibrosis (62) and CAVD pathogenesis (63). In developmental and pathogenic

EndMT, endothelial cells not only lose their markers, but gain expression of mesenchymal progenitor cell genes such as *Snail1*, *Twist1*, *Msx1/2*, and *Sox9*, indicative of phenotypic transition (64), suggesting that they are switching from their fully differentiated phenotype into a pluripotent-like state that has the ability to then de-differentiate down another mesenchymal-derived lineage.

The clearest evidence that EndMT contributes to vascular calcification is found in the disease fibrodysplasia ossificans progressive (FOP), where patients develop calcification in the microvasculature in the soft tissue. FOP stems from mutations that cause constitutive activation of the TGF- β superfamily receptor *ALK2* (65), which propagates BMP4 signaling. Calcified lesions in FOP patients exhibit evidence of EndMT, as both endothelial (vWF, VE-Cadherin), mesenchymal (*Sox9*), and osteoblast (osteocalcin) proteins are co-expressed on cells. This pattern mimics a mouse model of the disease. *In vitro* experiments using endothelial cells treated with TGF- β or BMP4 showed these signals induce expression of mesenchymal cell markers and allow these cells to behave like true MSCs, differentiating down the adipogenic, chondrogenic, and osteogenic lineages (66). Thus, in FOP patients the constitutively active *ALK2* primes vascular endothelial cells to transition and acquire mesenchymal-like properties, enabling them to differentiate into osteoblast-like calcifying cells. This would suggest a step-wise progression from fully-differentiated cell to a cell with a progenitor-like state that is then directed down an osteogenic lineage.

Aberrant BMP signaling and EndMT also contribute to medial calcification in larger conduit vessels. Keutel syndrome, a rare autosomal recessive disease, stems from mutations in the gene *Matrix GLA Protein (MGP)*, and these patients develop ectopic calcification in soft tissue throughout the body, including the vasculature (67). MGP acts as a potent inhibitor of vascular calcification via binding to and quenching BMP signaling (68, 69). The importance of MGP's inhibitory activities is clearly apparent in the *MGP*-knockout mouse model, which develops extensive and severe medial-layer calcification in the large arteries and results in death a few months after birth (70). The endothelium of *MGP*-knockout mice exhibits endothelial specific markers (CD31, vWF) as well as markers of multipotency (*Sox2*, *Nanog*, *Oct4*) and osteogenesis (*Osterix*). Specifically, this study found that expression of multipotent markers occurred before expression of osteogenic genes (71). Key to these trans-differentiation events is the Yamanaka factor *Sox9*, as endothelial-specific deletion of this gene inhibits calcification on both the *MGP* and diabetic *Ins2^{Akit1/+}* backgrounds (72). This further suggests that in the transition of cells from their fully-differentiated state to an osteogenic state, cells pass through a multipotent stem cell-like state.

EndMT also contributes to CAVD pathobiology (73). During embryogenesis, valve endothelial cells (VECs) sit atop a layer of matrix referred to as the cardiac jelly. A subset of VECs are stimulated to undergo EndMT and migrate into this jelly which forms the cardiac cushions. By processes that are still not thoroughly understood, cardiac cushions morph into the leaflets, and the cells within these new structures differentiate into VICs (73). As mentioned above, the layers of the valve are rich with collagens, elastin, proteoglycans, and glycosaminoglycans, and it is well-established that these ECM proteins can initiate and propagate

signaling events. For example, the glycosaminoglycans chondroitin sulfate and hyaluronic acid can drive EndMT in healthy adult VECs in a 3D *in vitro* culture system (74). The constant movement of the valves exposes the leaflets to both mechanical and shear forces. VECs are directly exposed to these stresses, which are sufficient to induce a healthy VEC to undergo EndMT in 3D *in vitro* models (75). The severity of these mechanical forces can elicit differential effects; low levels of strain induced Wnt signaling in a 2D model using sheep VECs, while high levels of cyclic strain induced TGF- β signaling (76). While TGF- β is known to drive EndMT in the development of the valves, a study looking for the early drivers of EndMT identified that inflammatory cytokines induce EndMT via Akt/NF- κ B activation in both embryonic and adult VECs, but that TGF- β signaling only induced EndMT in the embryonic cells (77). Mechanical stress signals may trigger the initiation of EndMT, and with the acquisition of an MSC-like state a cell may be more readily primed to transdifferentiate into a calcifying cell.

SYNTHETIC SMOOTH MUSCLE CELLS TO OSTEOBLAST-LIKE CELLS

Vascular smooth muscle cells (VSMCs) comprise the medial-layer of blood vessels. They are organized in concentric circular layers along the elastic lamina, and are surrounded by the extracellular matrix and contractile fibers. In healthy adult tissues VSMCs reside in a quiescent, contractile state, commonly referred to as a contractile phenotype (78), but in diseased or damaged arterial beds, VSMCs can switch from this fully-differentiated state to a proliferative one, referred to as the synthetic phenotype. Synthetic VSMCs have diminished expression of contractile proteins such as smooth muscle α -actin (*ACTA2*) or smooth muscle myosin heavy chain (*Myh11*) (79, 80); this dedifferentiation also occurs in the development of ectopic vascular calcification (81). With higher proliferative capacity and protein synthesis, as well as a progressive loss of contractile proteins, synthetic VSMCs seem to have features resembling myofibroblasts and MSCs (82). Indeed, an *in vitro* study that compared the gene expression profile of calcifying VSMCs and MSCs differentiating into osteoblasts found that while the overall transcriptional program differed between these groups, a sub-set of genes that make ECM proteins and catalyze biomineralization were shared between the two cell types (83). While this demonstrates that VSMCs undergo a transcriptional shift, this study was performed at the time point when both VSMCs and MSCs produced calcified matrix (after 25 days of osteogenic stimulation), and it remains unclear if in this process VSMCs undergo a stepwise process where they acquire a pluripotent MSC-like state before further differentiating into a calcifying cell.

VSMCs in the various vascular beds are derived from different embryonic origins. Fate mapping was first used to identify that the abdominal aorta SMCs come from splanchnic mesoderm, thoracic aorta SMCs from somatic mesoderm, aortic arch SMCs from neural crest, and coronary artery SMCs from the proepicardium (84). More recently, elegant fate-mapping was performed in murine models and found that VSMCs derived from the cardiac neural crest extended from the aortic root through

the aortic arch, while VSMCs derived from the second heart field localized to the ascending aorta (85). More importantly, this study identified heterogeneity in the developmental origin of VSMCs in the ascending aorta; VSMCs of the inner laminar regions close to the intima are derived from cardiac neural crest, while cells along the outer laminar area along the adventitial side of the vessel wall are derived from the second heart field (85). The different developmental origins of VSMCs may be an important key to understanding cardiovascular disease pathogenesis. In the case of vascular calcification, VSMCs in atherosclerotic lesions from the coronaries have a higher propensity to calcify than VSMCs of the aortic wall (86). Indeed, our independent studies using primary human VSMCs isolated from the coronary and aorta of the same patient show that coronary VSMCs readily calcify but aortic VSMCs do not (unpublished). Additionally, under similar calcifying conditions, Leroux-Berger et al. showed that the VSMCs in the aortic arch region, which are neural crest derivatives, calcify earlier than the VSMCs in the regions flanking both sides of the aortic arch, which are of mesodermal origin. This supports the idea that the embryonic origin influences the ability of a cells to calcify (87). Further highlighting the distinctions in the calcification potential of VSMCs residing in different vascular beds is the genetic disease Arterial Calcification due to Deficiency of CD73 (ACDC; also, called CALJA) (88). Patients with ACDC develop medial-layer vascular calcification that is localized to their lower-extremity arteries and is dependent on the upregulation of the mineralizing enzyme, TNAP (89). Pathological samples showed that calcification appears to initiate along the internal elastic lamina, which is fragmented and duplicated (88, 90). This data is highly suggestive that the ability of healthy VSMCs to transdifferentiate into calcifying cells is influenced by the developmental origin. Further exploration of this hypothesis could uncover novel epigenetic signatures that prime cells to transdifferentiate into osteoblast-like cells capable of producing calcified matrix.

Factors such as high concentrations of extracellular phosphate and calcium, oxidized lipoproteins and reactive oxygen species, and inflammatory cytokines help drive VSMCs toward a calcifying phenotype in both atherosclerotic and non-atherosclerotic calcification (91–96). The role of TGF- β superfamily signaling, which includes TGF- β as well as bone morphogenic protein (BMP) cytokines, is well characterized in the regulation of skeletal development and bone homeostasis (97), and not surprisingly, these pathways are also upregulated in the calcification of VSMCs. Advanced atherosclerotic lesions exhibit increased levels of TGF- β and bone-like structures (98, 99), and can induce osteogenic differentiation and calcification of VSMCs *in vitro* (100, 101). As in endothelial cells mentioned above, in VSMCs, TGF- β signaling is kept in check by MGP (70). MGP exerts its anti-calcific effects via repressing TGF- β signaling and allowing Wnt/Notch signaling to keep VSMCs in their fully-contractile state (16). Another TGF- β family member, BMP2, stimulates VSMCs to uptake inorganic phosphate and induces transcription of the osteogenic transcription factor *RUNX2* (102). In addition to activation of osteogenic transcriptional programs, TGF- β signaling contributes to the secretion of calcifying extracellular vesicles that accumulate in the extracellular matrix of VSMCs (103). While TGF- β family

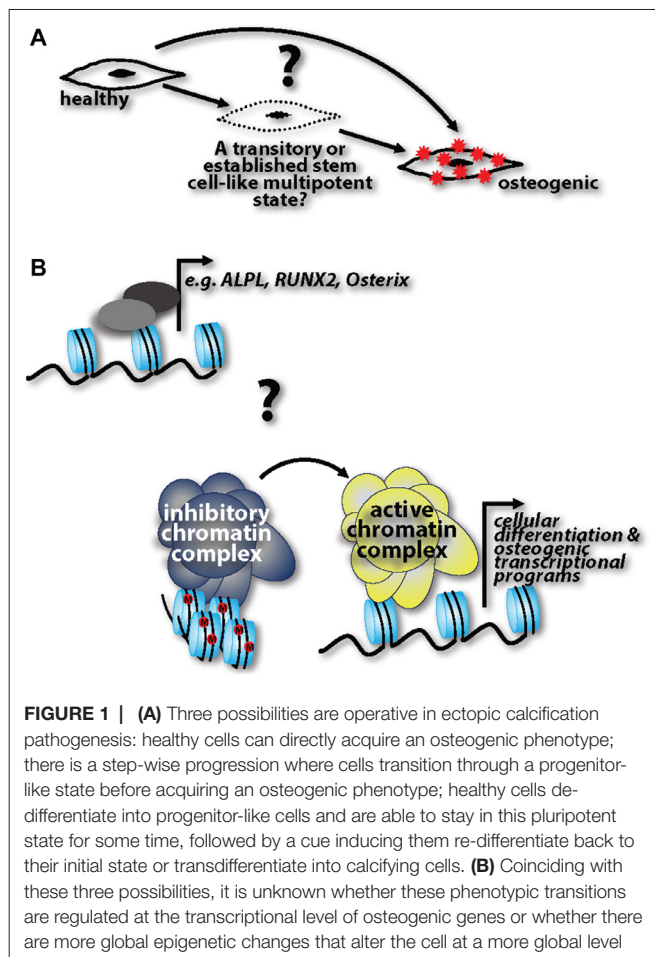
cytokines, as well as other stimuli, induce VSMCs to calcify, it is still not clear if the phenotypic switch to a calcifying cell happens directly from the mature, fully differentiated state, or if there is an intermediate MSC-like cell that requires the proper signal to acquire an osteoblast-like phenotype (104, 105).

Murine knockout models have shown that Wnt signaling may help to drive the osteogenic-like and chondrogenic-like differentiation of VSMCs. Conditional deletion of *Msx1* and *Msx2* reduces calcification of VSMCs in atherosclerotic murine models via reducing Wnt7b, Wnt5a, and Wnt2 signaling (106). And VSMC-specific deletion of the Wnt receptor, LRP6, protects against atherosclerotic calcification of VSMCs (107).

VSMCs can also differentiate into a chondrocyte-like state. Mice with loss of MGP develop extensive calcification in the large vessels and die a few months after birth due to rupture. These mice exhibit osteochondrogenic precursors that have the ability to differentiate into osteoblast-like and chondrocyte-like cells (108). Osteochondrogenic precursors exhibit decreased expression of SMC-specific genes such as *SM22 α* and *myocardin*, and increased expression of *Runx2*. Osteogenesis is driven by increased activity of *osterix*, *Msx2*, and Wnt/b-catenin, while chondrogenesis is driven by decreased activity of *Msx2* and increased activity of *Sox9*, a master regulator of chondrogenesis (109). Importantly, VSMCs have been shown to express both *Runx2* and *Sox9* *in vitro* and *in vivo*. While the expression of *Runx2* appears to correlate with the onset of calcification *in vivo*, *Sox9* expression is more widespread, which suggests *Sox9* may regulate expression of several ECM genes shared by both VSMCs and cartilage (110).

A COMMON DENOMINATOR IN THE CELL FATE SWITCH

The phenotypic switch of a healthy vascular cell into a calcifying one requires the upregulation of genes and proteins that participate and regulate the calcification process. A common denominator in all forms of ectopic calcification is the enzyme tissue non-specific alkaline phosphatase (TNAP, in reference to the protein; *ALPL* is the gene encoding TNAP; NM_000478), which is both necessary and sufficient for the mineralization in physiological and pathological calcification (111, 112). *ALPL* has also been shown to be one of the earliest calcification-related genes upregulated during ectopic calcification *in vivo* (13). TNAP breaks down pyrophosphate (PPi), an endogenous inhibitor of calcification, to Pi, a building block necessary for mineralization; the extracellular PPi/Pi ratio drives the ectopic calcification process and TNAP is the key enzyme that regulates this balance (113). A sophisticated murine model was developed which specifically overexpresses *ALPL* in an X-linked manner in VSMCs using the *TAGLN* promoter, enabling a dose-effect of TNAP to be studied (114). In this model, medial-layer calcification occurred in a dose-dependent manner and was independent of alteration in serum levels of calcium, phosphate, or renal function in the mice, highlighting that TNAP activity alone can induce calcification. Similarly, this same group used a *Tie2* system to overexpress *ALPL* in endothelial cells and found



a similar, though less severe, vascular calcification phenotype (115). Together, these *in vivo* models solidify the idea that TNAP activity alone is sufficient to promote ectopic calcification. Less well-defined are the various factors that induce the transcription of *ALPL* in the cells of the vasculature. Indeed, a large question

REFERENCES

- Bilezikian JP, Raisz LG, Martin TJ. *Principles of bone biology*. San Diego, California: Academic Press/Elsevier (2008).
- Nance JW, Crane GM, Halushka MK, Fishman EK, Zimmerman SL. Myocardial calcifications: pathophysiology, etiologies, differential diagnoses, and imaging findings. *J Cardiovasc Comput Tomogr* (2015) 9(1):58–67. doi: 10.1016/j.jcct.2014.10.004
- Rajamannan NM, Evans FJ, Aikawa E, Grande-Allen KJ, Demer LL, Heistad DD, et al. Calcific aortic valve disease: not simply a degenerative process: A review and agenda for research from the National Heart and Lung and Blood Institute Aortic Stenosis Working Group * Executive summary: Calcific aortic valve disease- 2011 update. *Circulation* (2011) 124(16):1783–91. doi: 10.1161/CIRCULATIONAHA.110.006767
- Lanzer P, Boehm M, Sorribas V, Thiriet M, Janzen J, Zeller T, et al. Medial vascular calcification revisited: review and perspectives. *Eur Heart J* (2014) 35(23):1515–25. doi: 10.1093/eurheartj/ehu163
- Rostand SG, Sanders C, Kirk KA, Rutsky EA, Fraser RG. Myocardial calcification and cardiac dysfunction in chronic renal failure. *Am J Med* (1988) 85(5):651–7. doi: 10.1016/S0002-9343(88)80237-7
- Zaidi AN, Ceneviva GD, Phipps LM, Dettorre MD, Mart CR, Thomas NJ. Myocardial calcification caused by secondary hyperparathyroidism due to dietary deficiency of calcium and vitamin D. *Pediatr Cardiol* (2005) 26(4):460–3. doi: 10.1007/s00246-004-0765-7
- van Kruijsdijk RC, van der Heijden JJ, Uijlings R, Otterspoor LC. Sepsis-related myocardial calcification. *Circulation* (2011) 4(5):e16–18. doi: 10.1161/CIRCHEARTFAILURE.111.962183
- El-Bialy A, Shenoda M, Saleh J, Tilkian A. Myocardial calcification as a rare cause of congestive heart failure: a case report. *J Cardiovasc Pharmacol Ther* (2005) 10(2):137–43. doi: 10.1177/107424840501000208
- Nishimura RA, Otto CM, Bonow RO, Carabello BA, Erwin JP, Guyton RA, et al. 2014 AHA/ACC Guideline for the Management of Patients With Valvular Heart Disease: executive summary: a report of the American College of Cardiology/American Heart Association Task Force on

remaining in the switch of a healthy to a calcifying cell is whether these shifts occur at the transcriptional level, or whether more large-scale epigenetic changes occur.

Other key questions remain (Figure 1): Do fully differentiated cells de-differentiate into progenitor-like cells and then readily acquire an osteogenic phenotype, or are de-differentiated cells able to stay in this pluripotent state for some time, and then depending on the cue, re-differentiate back to their initial state or transdifferentiate into calcifying cells? If the latter is the case, what are the cues that influence re-differentiation or transdifferentiation, respectively? This “MSC-like” window could be specifically targeted to halt disease progression. Cell lineage tracking genetic models specific to calcification processes are lacking. Harnessing these technologies would help to capture cells in the de-differentiated state and track their progression into a fully calcifying cell. And lastly, while evidence cited herein shows the ability of healthy cells to transition into calcifying cells, it is unclear whether these transitions happen at the transcriptional level of specific genes, such as *Runx2*, and *ALPL*, or whether there are more global epigenetic changes that are at play in this pathogenesis. Future studies addressing these questions with help identify druggable targets to harness, halt, or possibly even reverse ectopic calcification in the vasculature.

AUTHOR CONTRIBUTIONS

CS recommended the review topic, developed the direction and an outline of the review, provided content as well as extensive editing. LH and SS are postdoctoral fellows in CS’s group and performed extensive literature review and drafted the article. CS created the figure.

FUNDING

This work was supported by funding from National Institutes of Health (K22HL117917).

- Practice Guidelines. *Circulation* (2014) 129(23):2440–92. doi: 10.1161/CIR.0000000000000029
10. Clark MA, Duhay FG, Thompson AK, Keyes MJ, Svensson LG, Bonow RO, et al. Clinical and economic outcomes after surgical aortic valve replacement in Medicare patients. *Risk Manag Healthc Policy* (2012) 5:117–26. doi: 10.2147/RMHP.S34587
 11. Wang H, Leinwand LA, Anseth KS. Cardiac valve cells and their microenvironment—insights from in vitro studies. *Nat Rev Cardiol* (2014) 11(12):715–27. doi: 10.1038/nrcardio.2014.162
 12. Yahagi K, Kolodgie FD, Otsuka F, Finn AV, Davis HR, Joner M, et al. Pathophysiology of native coronary, vein graft, and in-stent atherosclerosis. *Nat Rev Cardiol* (2015).
 13. Hortells L, Sosa C, Guillen N, Lucea S, Millan A, Sorribas V. Identifying early pathogenic events during vascular calcification in uremic rats. *Kidney Int* (2017).
 14. New SEP, Aikawa E. Role of extracellular vesicles in de novo mineralization: an additional novel mechanism of cardiovascular calcification. *Arterioscler Thromb Vasc Biol* (2013) 33(8):1753–8. doi: 10.1161/ATVBAHA.112.300128
 15. Mohler ER, Gannon F, Reynolds C, Zimmerman R, Keane MG, Kaplan FS. Bone formation and inflammation in cardiac valves. *Circulation* (2001) 103(11):1522–8. doi: 10.1161/01.CIR.103.11.1522
 16. Beazley KE, Nurminsky D, Lima F, Gandhi C, Nurminskaya MV. Wnt16 attenuates TGF β -induced chondrogenic transformation in vascular smooth muscle. *Arterioscler Thromb Vasc Biol* (2015) 35(3):573–9. doi: 10.1161/ATVBAHA.114.304393
 17. Banerjee I, Fuseler JW, Price RL, Borg TK, Baudino TA. Determination of cell types and numbers during cardiac development in the neonatal and adult rat and mouse. *Am J Physiol Heart Circ Physiol* (2007) 293(3):H1883–91. doi: 10.1152/ajpheart.00514.2007
 18. Furtado MB, Hasham M. Properties and Immune Function of Cardiac Fibroblasts. *Adv Exp Med Biol* (2017) 1003:35–70. doi: 10.1007/978-3-319-57613-8_3
 19. Kohl P, Camelliti P, Burton FL, Smith GL. Electrical coupling of fibroblasts and myocytes: relevance for cardiac propagation. *J Electrocardiol* (2005) 38(4):45–50. doi: 10.1016/j.jelectrocard.2005.06.096
 20. Souders CA, Bowers SLK, Baudino TA. Cardiac fibroblast: the renaissance cell. *Circ Res* (2009) 105(12):1164–76. doi: 10.1161/CIRCRESAHA.109.209809
 21. Lighthouse JK, Small EM. Transcriptional control of cardiac fibroblast plasticity. *J Mol Cell Cardiol* (2016) 91:52–60. doi: 10.1016/j.yjmcc.2015.12.016
 22. Gabbiani G. The cellular derivation and the life span of the myofibroblast. *Pathol Res Pract* (1996) 192(7):708–11. doi: 10.1016/S0344-0338(96)80092-6
 23. Pugashetti R, Shinkai K, Ruben BS, Grossman ME, Maldonado J, Fox LP. Calcium may preferentially deposit in areas of elastic tissue damage. *J Am Acad Dermatol* (2011) 64(2):296–301. doi: 10.1016/j.jaad.2010.01.046
 24. Pillai ICL, Li S, Romay M, Lam L, Lu Y, Huang J, et al. Cardiac Fibroblasts Adopt Osteogenic Fates and Can Be Targeted to Attenuate Pathological Heart Calcification. *Cell Stem Cell* (2017) 20(2):e215–. doi: 10.1016/j.stem.2016.10.005
 25. Goding JW, Grobden B, Slegers H. Physiological and pathophysiological functions of the ecto-nucleotide pyrophosphatase/phosphodiesterase family. *Biochim Biophys Acta* (2003) 1638(1):1–19. doi: 10.1016/S0925-4439(03)00058-9
 26. Lorenz-Depiereux B, Schnabel D, Tiosano D, Häusler G, Strom TM. Loss-of-function ENPP1 mutations cause both generalized arterial calcification of infancy and autosomal-recessive hypophosphatemic rickets. *Am J Hum Genet* (2010) 86(2):267–72. doi: 10.1016/j.ajhg.2010.01.006
 27. Rutsch F, Ruf N, Vaingankar S, Toliat MR, Suk A, Höhne W, et al. Mutations in ENPP1 are associated with 'idiopathic' infantile arterial calcification. *Nat Genet* (2003) 34(4):379–81. doi: 10.1038/ng1221
 28. Ferrone C, Andracco R, Cimmino MA. Calcium pyrophosphate deposition disease: clinical manifestations. *Reumatismo* (2012) 63(4):246–52. doi: 10.4081/reumatismo.2011.246
 29. Arnsdorf EJ, Tummala P, Castillo AB, Zhang F, Jacobs CR. The epigenetic mechanism of mechanically induced osteogenic differentiation. *J Biomech* (2010) 43(15):2881–6. doi: 10.1016/j.jbiomech.2010.07.033
 30. Khyzha N, Alizada A, Wilson MD, Fish JE. Epigenetics of Atherosclerosis: Emerging Mechanisms and Methods. *Trends Mol Med* (2017) 23(4):332–47. doi: 10.1016/j.molmed.2017.02.004
 31. Paranya G, Vineberg S, Dvorin E, Kaushal S, Roth SJ, Rabkin E, et al. Aortic valve endothelial cells undergo transforming growth factor-beta-mediated and non-transforming growth factor-beta-mediated transdifferentiation in vitro. *Am J Pathol* (2001) 159(4):1335–43. doi: 10.1016/S0002-9440(10)62520-5
 32. Yutzey KE, Demer LL, Body SC, Huggins GS, Towler DA, Giachelli CM, et al. Calcific aortic valve disease: a consensus summary from the Alliance of Investigators on Calcific Aortic Valve Disease. *Arterioscler Thromb Vasc Biol* (2014) 34(11):2387–93. doi: 10.1161/ATVBAHA.114.302523
 33. Chen JH, Simmons CA. Cell-matrix interactions in the pathobiology of calcific aortic valve disease: critical roles for matricellular, matricrine, and matrix mechanics cues. *Circ Res* (2011) 108(12):1510–24. doi: 10.1161/CIRCRESAHA.110.234237
 34. Leopold JA. Cellular mechanisms of aortic valve calcification. *Circ Cardiovasc Interv* (2012) 5(4):605–14. doi: 10.1161/CIRCINTERVENTIONS.112.971028
 35. Rajamannan NM, Subramaniam M, Rickard D, Stock SR, Donovan J, Springett M, et al. Human aortic valve calcification is associated with an osteoblast phenotype. *Circulation* (2003) 107(17):2181–4. doi: 10.1161/01.CIR.0000070591.21548.69
 36. Aikawa E, Libby P. A rock and a hard place: chiseling away at the multiple mechanisms of aortic stenosis. *Circulation* (2017) 135:1951–5.
 37. Liu AC, Joag VR, Gotlieb AI. The emerging role of valve interstitial cell phenotypes in regulating heart valve pathobiology. *Am J Pathol* (2007) 171(5):1407–18. doi: 10.2353/ajpath.2007.070251
 38. Wu SS, Lin X, Yuan LQ, Liao EY. The Role of epigenetics in arterial calcification. *Biomed Res Int* (2015) 2015(1):320849–. doi: 10.1155/2015/320849
 39. Song R, Fullerton DA, Ao L, Zhao K-Seng, Meng X. An epigenetic regulatory loop controls pro-osteogenic activation by TGF- β 1 or bone morphogenetic protein 2 in human aortic valve interstitial cells. *J Biol Chem* (2017) 292(21):8657–66. doi: 10.1074/jbc.M117.783308
 40. Hoerstrup SP, Kadner A, Melnitchouk S, Trojan A, Eid K, Tracy J, et al. Tissue engineering of functional trileaflet heart valves from human marrow stromal cells. *Circulation* (2002) 106:1143–50.
 41. Arevalos CA, Berg JM, Nguyen JMV, Godfrey EL, Iriondo C, Grande-Allen KJ. Valve interstitial cells act in a pericyte manner promoting angiogenesis and invasion by valve endothelial cells. *Ann Biomed Eng* (2016) 44(9):2707–23. doi: 10.1007/s10439-016-1567-9
 42. Wirrig EE, Yutzey KE. Conserved transcriptional regulatory mechanisms in aortic valve development and disease. *Arterioscler Thromb Vasc Biol* (2014) 34(4):737–41. doi: 10.1161/ATVBAHA.113.302071
 43. Liu AC, Gotlieb AI. Transforming growth factor-beta regulates in vitro heart valve repair by activated valve interstitial cells. *Am J Pathol* (2008) 173(5):1275–85. doi: 10.2353/ajpath.2008.080365
 44. Liu AC, Gotlieb AI. Characterization of cell motility in single heart valve interstitial cells in vitro. *Histol Histopathol* (2007) 22:873–82.
 45. Yip CYY, Chen J-H, Zhao R, Simmons CA. Calcification by valve interstitial cells is regulated by the stiffness of the extracellular matrix. *Arterioscler Thromb Vasc Biol* (2009) 29(6):936–42. doi: 10.1161/ATVBAHA.108.182394
 46. Nam HK, Liu J, Li Y, Kragor A, Hatch NE. Ectonucleotide pyrophosphatase/phosphodiesterase-1 (ENPP1) protein regulates osteoblast differentiation. *J Biol Chem* (2011) 286(45):39059–71. doi: 10.1074/jbc.M111.221689
 47. Côté N, El Hussein D, Pépin A, Gouaque-Orlarte S, Ducharme V, Bouchard-Cannon P, et al. ATP acts as a survival signal and prevents the mineralization of aortic valve. *J Mol Cell Cardiol* (2012) 52(5):1191–202. doi: 10.1016/j.yjmcc.2012.02.003
 48. El Hussein D, Boulanger M-C, Fournier D, Mahmut A, Bossé Y, Pibarot P, et al. High expression of the Pi-transporter SLC20A1/Pit1 in calcific aortic valve disease promotes mineralization through regulation of Akt-1. *PLoS One* (2013) 8(1):e53393. doi: 10.1371/journal.pone.0053393
 49. Dweck MR, Jones C, Joshi NV, Fletcher AM, Richardson H, White A, et al. Assessment of valvular calcification and inflammation by positron emission tomography in patients with aortic stenosis. *Circulation* (2012) 125(1):76–86. doi: 10.1161/CIRCULATIONAHA.111.051052
 50. Aikawa E, Nahrendorf M, Sosnovik D, Lok VM, Jaffer FA, Aikawa M, et al. Multimodality molecular imaging identifies proteolytic and osteogenic activities in early aortic valve disease. *Circulation* (2007) 115(3):377–86. doi: 10.1161/CIRCULATIONAHA.106.654913

51. Aikawa E, Nahrendorf M, Figueiredo J-L, Swirski FK, Shtatland T, Kohler RH, et al. Osteogenesis associates with inflammation in early-stage atherosclerosis evaluated by molecular imaging in vivo. *Circulation* (2007) 116(24):2841–50. doi: 10.1161/CIRCULATIONAHA.107.732867
52. Abdelbaky A, Corsini E, Figueroa AL, Fontanez S, Subramanian S, Ferencik M, et al. Focal arterial inflammation precedes subsequent calcification in the same location: a longitudinal FDG-PET/CT study. *Circulation* (2013) 127(12):1477–84. doi: 10.1161/CIRCIMAGING.113.000382
53. Croes M, Oner FC, Kruyt MC, Blokhuis TJ, Bastian O, Dhert WJA, et al. Proinflammatory Mediators Enhance the Osteogenesis of Human Mesenchymal Stem Cells after Lineage Commitment. *PLoS One* (2015) 10(7):e0132781. doi: 10.1371/journal.pone.0132781
54. Al-Aly Z, Shao J-S, Lai C-F, Huang E, Cai J, Behrmann A, et al. Aortic Msx2-Wnt calcification cascade is regulated by TNF-alpha-dependent signals in diabetic Ldlr-/- mice. *Arterioscler Thromb Vasc Biol* (2007) 27(12):2589–96. doi: 10.1161/ATVBAHA.107.153668
55. Udan RS, Culver JC, Dickinson ME. Understanding vascular development. *WIREs Dev Biol* (2013) 2(3):327–46. doi: 10.1002/wdev.91
56. Kovacic JC, Mercader N, Torres M, Boehm M, Fuster V. Epithelial-to-mesenchymal and endothelial-to-mesenchymal transition: from cardiovascular development to disease. *Circulation* (2012) 125(14):1795–808. doi: 10.1161/CIRCULATIONAHA.111.040352
57. Dejana E. Endothelial cell–cell junctions: happy together. *Nat Rev Mol Cell Biol* (2004) 5(4):261–70. doi: 10.1038/nrm1357
58. Camenisch TD, Molin DGM, Person A, Runyan RB, Gittenberger-de Groot AC, McDonald JA, et al. Temporal and distinct TGFβ ligand requirements during mouse and avian endocardial cushion morphogenesis. *Dev Biol* (2002) 248(1):170–81. doi: 10.1006/dbio.2002.0731
59. Cano A, Pérez-Moreno MA, Rodrigo I, Locascio A, Blanco MJ, del Barrio MG, et al. The transcription factor snail controls epithelial–mesenchymal transitions by repressing E-cadherin expression. *Nat Cell Biol* (2000) 2(2):76–83. doi: 10.1038/35000025
60. Cooley BC, Nevado J, Mellad J, Yang D, St. Hilaire C, Negro A, et al. TGF-beta signaling mediates endothelial-to-mesenchymal transition (EndMT) during vein graft remodeling. *Sci Transl Med* (2014) 6(227):ra234. doi: 10.1126/scitranslmed.3006927
61. Chen P-Y, Qin L, Baeyens N, Li G, Afolabi T, Budatha M, et al. Endothelial-to-mesenchymal transition drives atherosclerosis progression. *J Clin Invest* (2015) 125(12):4514–28. doi: 10.1172/JCI82719
62. Zeisberg EM, Tarnavski O, Zeisberg M, Dorfman AL, McMullen JR, Gustafsson E, et al. Endothelial-to-mesenchymal transition contributes to cardiac fibrosis. *Nat Med* (2007) 13(8):952–61. doi: 10.1038/nm1613
63. Hjortnaes J, Shapero K, Goettsch C, Hutcheson JD, Keegan J, Kluin J, et al. Valvular interstitial cells suppress calcification of valvular endothelial cells. *Atherosclerosis* (2015) 242(1):251–60. doi: 10.1016/j.atherosclerosis.2015.07.008
64. Wrigg EE, Yutzey KE. Developmental Pathways in CAVD. In: Aikawa E, editor. *Calcific Aortic Valve Disease*. Ch. 03. Rijeka: InTech (2013).
65. Shore EM, Kaplan FS. Insights from a rare genetic disorder of extra-skeletal bone formation, fibrodysplasia ossificans progressiva (FOP). *Bone* (2008) 43(3):427–33. doi: 10.1016/j.bone.2008.05.013
66. Medici D, Shore EM, Lounev VY, Kaplan FS, Kalluri R, Olsen BR. Conversion of vascular endothelial cells into multipotent stem-like cells. *Nat Med* (2010) 16(12):1400–6. doi: 10.1038/nm.2252
67. Munroe PB, Olgunturk RO, Fryns J-P, Maldergem LV, Ziereisen F, Yuksel B, et al. Mutations in the gene encoding the human matrix Gla protein cause Keutel syndrome. *Nat Genet* (1999) 21(1):142–4. doi: 10.1038/5102
68. Wallin R, Cain D, Hutson SM, Sane DC, Loeser R. Modulation of the binding of matrix Gla protein (MGP) to bone morphogenetic protein-2 (BMP-2). *Thromb Haemost* (2000) 84:1039–44.
69. Yao Y, Shahbazian A, Bostrom KI. Proline and gamma-carboxylated glutamate residues in matrix Gla protein are critical for binding of bone morphogenetic protein-4. *Circ Res* (2008) 102(9):1065–74. doi: 10.1161/CIRCRESAHA.107.166124
70. Luo G, Ducey P, Mckee MD, Pinero GJ, Loyer E, Behringer RR, et al. Spontaneous calcification of arteries and cartilage in mice lacking matrix GLA protein. *Nature* (1997) 386(6620):78–81. doi: 10.1038/386078a0
71. Yao Y, Jumabay M, Ly A, Radparvar M, Cubberly MR, Bostrom KI. A role for the endothelium in vascular calcification. *Circ Res* (2013) 113(5):495–504. doi: 10.1161/CIRCRESAHA.113.301792
72. Yao J, Guihard PJ, Blazquez-Medela AM, Guo Y, Moon JH, Jumabay M, et al. Serine protease activation essential for endothelial–mesenchymal transition in vascular calcification novelty and significance. *Circ Res* (2015) 117(9):758–69. doi: 10.1161/CIRCRESAHA.115.306751
73. Armstrong EJ, Bischoff J. Heart valve development: endothelial cell signaling and differentiation. *Circ Res* (2004) 95(5):459–70. doi: 10.1161/01.RES.0000141146.95728.da
74. Dahal S, Huang P, Murray BT, Mahler GJ. Endothelial to mesenchymal transformation is induced by altered extracellular matrix in aortic valve endothelial cells. *J Biomed Mater Res A* (2017).
75. Mahler GJ, Frenzl CM, Cao Q, Butcher JT. Effects of shear stress pattern and magnitude on mesenchymal transformation and invasion of aortic valve endothelial cells. *Biotechnol Bioeng* (2014) 111(11):2326–37. doi: 10.1002/bit.25291
76. Balachandran K, Alford PW, Wylie-Sears J, Goss JA, Grosberg A, Bischoff J, et al. Cyclic strain induces dual-mode endothelial–mesenchymal transformation of the cardiac valve. *Proc Natl Acad Sci U S A* (2011) 108(50):19943–8. doi: 10.1073/pnas.1106954108
77. Mahler GJ, Farrar EJ, Butcher JT. Inflammatory cytokines promote mesenchymal transformation in embryonic and adult valve endothelial cells. *Arterioscler Thromb Vasc Biol* (2013) 33(1):121–30. doi: 10.1161/ATVBAHA.112.300504
78. Mosse PR, Campbell GR, Wang ZL, Campbell JH. Smooth muscle phenotypic expression in human carotid arteries. I. Comparison of cells from diffuse intimal thickenings adjacent to atheromatous plaques with those of the media. *Lab Invest* (1985) 53:556–62.
79. Shanahan CM, Weissberg PL. Smooth muscle cell heterogeneity: patterns of gene expression in vascular smooth muscle cells in vitro and in vivo. *Arterioscler Thromb Vasc Biol* (1998) 18(3):333–8. doi: 10.1161/01.ATV.18.3.333
80. Grainger DJ, Metcalfe JC, Grace AA, Mosedale DE. Transforming growth factor-beta dynamically regulates vascular smooth muscle differentiation in vivo. *J Cell Sci* (1998) 111(Pt 19):2977–88.
81. Lacolley P, Regnault V, Nicoletti A, Li Z, Michel J-B. The vascular smooth muscle cell in arterial pathology: a cell that can take on multiple roles. *Cardiovasc Res* (2012) 95(2):194–204. doi: 10.1093/cvr/cvs135
82. Tintut Yet al. Multilineage potential of cells from the artery wall. *Circulation* (2003) 108(20):2505–10. doi: 10.1161/01.CIR.0000096485.64373.C5
83. Alves RDAM, Eijken M, van de Peppel J, van Leeuwen JPTM. Calcifying vascular smooth muscle cells and osteoblasts: independent cell types exhibiting extracellular matrix and biomineralization-related mimics. *BMC Genomics* (2014) 15(1):965. doi: 10.1186/1471-2164-15-965
84. Majesky MW. Developmental basis of vascular smooth muscle diversity. *Arterioscler Thromb Vasc Biol* (2007) 27(6):1248–58. doi: 10.1161/ATVBAHA.107.141069
85. Sawada H, Rateri DL, Moorleggen JJ, Majesky MW, Daugherty A. Smooth muscle cells derived from second heart field and cardiac neural crest reside in spatially distinct domains in the media of the ascending aorta—brief report. *Arterioscler Thromb Vasc Biol* (2017) 37(9):1722–6. doi: 10.1161/ATVBAHA.117.309599
86. Gu X, He Y, Li Z, Kontos MC, Paulsen WH, Arrowood JA, et al. Relation between the incidence, location, and extent of thoracic aortic atherosclerosis detected by transesophageal echocardiography and the extent of coronary artery disease by angiography. *Am J Cardiol* (2011) 107(2):175–8. doi: 10.1016/j.amjcard.2010.09.003
87. Leroux-Berger M, Queguiner I, Maciel TT, Ho A, Relaix F, Kempf H. Pathologic calcification of adult vascular smooth muscle cells differs on their crest or mesodermal embryonic origin. *J Bone Miner Res* (2011) 26(7):1543–53. doi: 10.1002/jbmr.382
88. St Hilaire C, Ziegler SG, Markello TC, Brusco A, Groden C, Gill F, et al. NT5E mutations and arterial calcifications. *N Engl J Med* (2011) 364(5):432–42. doi: 10.1056/NEJMoa0912923
89. Jin H, St Hilaire C, Huang Y, Yang D, Dmitrieva NI, Negro A, et al. Increased activity of TNAP compensates for reduced adenosine production and promotes ectopic calcification in the genetic disease ACDC. *Sci Signal* (2016) 9(458):ra121. doi: 10.1126/scisignal.aaf9109

90. Markello TC, Pak LK, St. Hilaire C, Dorward H, Ziegler SG, Chen MY, et al. Vascular pathology of medial arterial calcifications in NT5E deficiency: implications for the role of adenosin in pseudoxanthoma elasticum. *Mol Genet Metab* (2011) 103(1):44–50. doi: 10.1016/j.ymgme.2011.01.018
91. Yang H, Curinga G, Giachelli CM. Elevated extracellular calcium levels induce smooth muscle cell matrix mineralization in vitro. *Kidney Int* (2004) 66:2293–9.
92. Crouthamel MH, Lau WL, Leaf EM, Chavkin NW, Wallingford MC, Peterson DF, et al. Sodium-dependent phosphate cotransporters and phosphate-induced calcification of vascular smooth muscle cells: redundant roles for PiT-1 and PiT-2. *Arterioscler Thromb Vasc Biol* (2013) 33:2625–32.
93. Parhami F, Morrow AD, Balucan J, Leitinger N, Watson AD, Tintut Y, et al. Lipid oxidation products have opposite effects on calcifying vascular cell and bone cell differentiation. A possible explanation for the paradox of arterial calcification in osteoporotic patients. *Arterioscler Thromb Vasc Biol* (1997) 17(4):680–7. doi: 10.1161/01.ATV.17.4.680
94. Tang Y, Xu Q, Peng H, Liu Z, Yang T, Yu Z, et al. The role of vascular peroxidase 1 in ox-LDL-induced vascular smooth muscle cell calcification. *Atherosclerosis* (2015) 243(2):357–63. doi: 10.1016/j.atherosclerosis.2015.08.047
95. Tintut Y, Patel J, Parhami F, Demer LL. Tumor necrosis factor- α promotes in vitro calcification of vascular cells via the cAMP pathway. *Circulation* (2000) 102(21):2636–42. doi: 10.1161/01.CIR.102.21.2636
96. Agharazii M, St-Louis R, Gautier-Bastien A, Ung R-V, Mokas S, Larivière R, et al. Inflammatory cytokines and reactive oxygen species as mediators of chronic kidney disease-related vascular calcification. *Am J Hypertens* (2015) 28(6):746–55. doi: 10.1093/ajh/hpu225
97. Wu M, Chen G, Li Y-P. TGF- β and BMP signaling in osteoblast, skeletal development and bone formation, homeostasis and disease. *Bone Res* (2016) 4(1):16009. doi: 10.1038/boneres.2016.9
98. Jeziorska M. Transforming growth factor- β s and CD105 expression in calcification and bone formation in human atherosclerotic lesions. *Z Kardiol* (2001) 90(Suppl 3):23–6. doi: 10.1007/s003920170037
99. Jeziorska M, Mccollum C, Wooley DE. Observations on bone formation and remodelling in advanced atherosclerotic lesions of human carotid arteries. *Virchows Arch* (1998) 433(6):559–65. doi: 10.1007/s004280050289
100. Simionescu A, Philips K, Vyavahare N. Elastin-derived peptides and TGF- β 1 induce osteogenic responses in smooth muscle cells. *Biochem Biophys Res Commun* (2005) 334(2):524–32. doi: 10.1016/j.bbrc.2005.06.119
101. Demer LL, Watson KE, Boström K. Mechanism of calcification in atherosclerosis. *Trends Cardiovasc Med* (1994) 4(1):45–9. doi: 10.1016/1050-1738(94)90025-6
102. Li X, Yang H-Y, Giachelli CM. BMP-2 promotes phosphate uptake, phenotypic modulation, and calcification of human vascular smooth muscle cells. *Atherosclerosis* (2008) 199(2):271–7. doi: 10.1016/j.atherosclerosis.2007.11.031
103. Krohn JB, Hutcheson JD, Martínez-Martínez E, Irvin WS, Bouten CV, Bertazzo S, et al. Discoidin Domain Receptor-1 Regulates Calcific Extracellular Vesicle Release in Vascular Smooth Muscle Cell Fibrocalcific Response via Transforming Growth Factor- β Signaling. *Arterioscler Thromb Vasc Biol* (2016) 36(3):525–33. doi: 10.1161/ATVBAHA.115.307009
104. Demer LL, Tintut Y. Vascular calcification: pathobiology of a multifaceted disease. *Circulation* (2008) 117(22):2938–48. doi: 10.1161/CIRCULATIONAHA.107.743161
105. Mizobuchi M, Towler D, Slatopolsky E. Vascular calcification: the killer of patients with chronic kidney disease. *J Am Soc Nephrol* (2009) 20(7):1453–64. doi: 10.1681/ASN.2008070692
106. Cheng SL, Behrmann A, Shao JS, Ramachandran B, Krchma K, Bello Arredondo Y, et al. Targeted reduction of vascular Mx1 and Mx2 mitigates arteriosclerotic calcification and aortic stiffness in LDLR-deficient mice fed diabetogenic diets. *Diabetes* (2014) 63(12):4326–37. doi: 10.2337/db14-0326
107. Cheng SL, Ramachandran B, Behrmann A, Shao JS, Mead M, Smith C, et al. Vascular smooth muscle LRP6 limits arteriosclerotic calcification in diabetic LDLR-/- mice by restraining noncanonical Wnt signals. *Circ Res* (2015) 117(2):142–56. doi: 10.1161/CIRCRESAHA.117.306712
108. Speer MY, Yang HY, Brabb T, Leaf E, Look A, Lin WL, et al. Smooth muscle cells give rise to osteochondrogenic precursors and chondrocytes in calcifying arteries. *Circ Res* (2009) 104(6):733–41. doi: 10.1161/CIRCRESAHA.108.183053
109. Hino K, Saito A, Kido M, Kanemoto S, Asada R, Takai T, et al. Master regulator for chondrogenesis, Sox9, regulates transcriptional activation of the endoplasmic reticulum stress transducer BBF2H7/CREB3L2 in chondrocytes. *J Biol Chem* (2014) 289(20):13810–20. doi: 10.1074/jbc.M113.543322
110. Iyemere VP, Proudfoot D, Weissberg PL, Shanahan CM. Vascular smooth muscle cell phenotypic plasticity and the regulation of vascular calcification. *J Intern Med* (2006) 260(3):192–210. doi: 10.1111/j.1365-2796.2006.01692.x
111. Narisawa S, Yadav MC, Millán JL. In vivo overexpression of tissue-nonspecific alkaline phosphatase increases skeletal mineralization and affects the phosphorylation status of osteopontin. *J Bone Miner Res* (2013) 28(7):1587–98. doi: 10.1002/jbmr.1901
112. Hortells L, Sosa C, Millán A, Sorribas V. Critical Parameters of the In Vitro Method of Vascular Smooth Muscle Cell Calcification. *PLoS One* (2015) 10(11):e0141751. doi: 10.1371/journal.pone.0141751
113. Picher M, Burch LH, Hirsh AJ, Spychala J, Boucher RC. Ecto 5'-nucleotidase and nonspecific alkaline phosphatase. Two AMP-hydrolyzing ectoenzymes with distinct roles in human airways. *J Biol Chem* (2003) 278(15):13468–79. doi: 10.1074/jbc.M300569200
114. Sheen CR, Kuss P, Narisawa S, Yadav MC, Nigro J, Wang W, et al. Pathophysiological role of vascular smooth muscle alkaline phosphatase in medial artery calcification. *J Bone Miner Res* (2015) 30(5):824–36. doi: 10.1002/jbmr.2420
115. Savinov AY, Salehi M, Yadav MC, Radichev I, Millan JL, Savinova OV. Transgenic Overexpression of Tissue-Nonspecific Alkaline Phosphatase (TNAP) in Vascular Endothelium Results in Generalized Arterial Calcification. *J Am Heart Assoc* (2015) 4(12):e002499. doi: 10.1161/JAHA.115.002499

Conflict of Interest Statement: The authors declare that the research was conducted in the absence of any commercial or financial relationships that could be construed as a potential conflict of interest.

Copyright © 2018 Hortells, Sur and St. Hilaire. This is an open-access article distributed under the terms of the Creative Commons Attribution License (CC BY). The use, distribution or reproduction in other forums is permitted, provided the original author(s) and the copyright owner are credited and that the original publication in this journal is cited, in accordance with accepted academic practice. No use, distribution or reproduction is permitted which does not comply with these terms.



Future Perspectives on the Role of Stem Cells and Extracellular Vesicles in Vascular Tissue Regeneration

Eoghan M. Cunnane^{1,2,3}, Justin S. Weinbaum^{1,2,4}, Fergal J. O'Brien^{3,5,6} and David A. Vorp^{1,2,7,8,9*}

¹ Department of Bioengineering, University of Pittsburgh, Pittsburgh, PA, United States, ² McGowan Institute for Regenerative Medicine, University of Pittsburgh, Pittsburgh, PA, United States, ³ Tissue Engineering Research Group, Department of Anatomy, Royal College of Surgeons in Ireland, Dublin, Ireland, ⁴ Department of Pathology, University of Pittsburgh, Pittsburgh, PA, United States, ⁵ Trinity Centre for Bioengineering, Trinity College Dublin, Dublin, Ireland, ⁶ Advanced Materials and Bioengineering Research Centre, Royal College of Surgeons in Ireland and Trinity College Dublin, Dublin, Ireland, ⁷ Department of Surgery, University of Pittsburgh, Pittsburgh, PA, United States, ⁸ Department of Cardiothoracic Surgery, University of Pittsburgh, Pittsburgh, PA, United States, ⁹ Department of Chemical and Petroleum Engineering, University of Pittsburgh, Pittsburgh, PA, United States

OPEN ACCESS

Edited by:

Joshua D. Hutcheson,
Florida International University,
United States

Reviewed by:

Chris A. Bashur,
Florida Institute of Technology,
United States
Willi Jahnen-Dechent,
RWTH Aachen Universität, Germany

*Correspondence:

David A. Vorp
vorp@pitt.edu

Specialty section:

This article was submitted to
Atherosclerosis and Vascular
Medicine,
a section of the journal
Frontiers in Cardiovascular Medicine

Received: 25 April 2018

Accepted: 13 June 2018

Published: 03 July 2018

Citation:

Cunnane EM, Weinbaum JS,
O'Brien FJ and Vorp DA (2018) Future
Perspectives on the Role of Stem
Cells and Extracellular Vesicles in
Vascular Tissue Regeneration.
Front. Cardiovasc. Med. 5:86.
doi: 10.3389/fcvm.2018.00086

Vascular tissue engineering is an area of regenerative medicine that attempts to create functional replacement tissue for defective segments of the vascular network. One approach to vascular tissue engineering utilizes seeding of biodegradable tubular scaffolds with stem (and/or progenitor) cells wherein the seeded cells initiate scaffold remodeling and prevent thrombosis through paracrine signaling to endogenous cells. Stem cells have received an abundance of attention in recent literature regarding the mechanism of their paracrine therapeutic effect. However, very little of this mechanistic research has been performed under the aegis of vascular tissue engineering. Therefore, the scope of this review includes the current state of TEVGs generated using the incorporation of stem cells in biodegradable scaffolds and potential cell-free directions for TEVGs based on stem cell secreted products. The current generation of stem cell-seeded vascular scaffolds are based on the premise that cells should be obtained from an autologous source. However, the reduced regenerative capacity of stem cells from certain patient groups limits the therapeutic potential of an autologous approach. This limitation prompts the need to investigate allogeneic stem cells or stem cell secreted products as therapeutic bases for TEVGs. The role of stem cell derived products, particularly extracellular vesicles (EVs), in vascular tissue engineering is exciting due to their potential use as a cell-free therapeutic base. EVs offer many benefits as a therapeutic base for functionalizing vascular scaffolds such as cell specific targeting, physiological delivery of cargo to target cells, reduced immunogenicity, and stability under physiological conditions. However, a number of points must be addressed prior to the effective translation of TEVG technologies that incorporate stem cell derived EVs such as standardizing stem cell culture conditions, EV isolation, scaffold functionalization with EVs, and establishing the therapeutic benefit of this combination treatment.

Keywords: tissue engineered vascular grafts, stem cells, autologous, allogeneic, conditioned media, extracellular vesicles, exosomes

INTRODUCTION

Vascular tissue engineering is an area of regenerative medicine that attempts to restore defective segments of the vascular network. One approach to vascular tissue engineering is to implant biodegradable tubular scaffolds seeded with appropriate cells. Research has focused on lining the lumen of the scaffold with endothelial progenitor cells (1–5), self-assembly of vascular grafts by *in vitro* culture of fused vascular cell sheets (6–12), seeding scaffolds with native vascular cells (13–16), progenitor cells pre-differentiated into vascular phenotypes (17–22) using biomechanical/biochemical stimuli [as reviewed in Maul et al. (23)], and pluripotent stem cells pre-differentiated into vascular phenotypes (24, 25). However, employing native vascular cells, terminally differentiated progenitor/pluripotent cells, or self-assembled cell sheets requires extended culture periods and the use of expensive culture media that is often derived from xenogeneic sources. Seeding biodegradable scaffolds with undifferentiated stem (and/or progenitor) cells initiates scaffold remodeling through paracrine signaling to endogenous cells (26, 27). Seeding vascular scaffolds with stem cells also bypasses many of the aforementioned limitations due to the fact that a sufficient number of implant-ready cells can be acquired from a single harvest, therefore eliminating the time and resources spent culturing or differentiating cells. *The motivation for this review is that stem/progenitor cells have received an abundance of attention in recent literature regarding the mechanism of their paracrine therapeutic effect. However, this parallel research has yet to translate fully to the field of vascular tissue engineering. Therefore, the scope of this review includes the current state of TEVGs generated using the incorporation of stem cells in biodegradable scaffolds and potential cell-free directions for TEVGs based on stem cell secreted products (Figure 1).*

STEM CELL BASED TEVG STUDIES

Numerous studies have demonstrated that implanting biodegradable vascular scaffolds, seeded with stem cells from a variety of sources, triggers the development of functional, immuno-compatible, native-like vascular replacements (Table 1). Bone marrow mononuclear cells (BM-MNCs) have been employed in numerous preclinical (26, 28–31, 33, 36–38, 43, 44) and clinical studies (28, 32, 51, 52). BM-MNCs are a heterogeneous population comprised of mesenchymal stem cells (MSCs), endothelial precursor cells, mature endothelial cells, hematopoietic stem cells, monocytes, CD4+ T cells, CD8+ T cells, B cells, and natural killer cells (26). Recently, it has been shown that BM-MNCs have a dose dependent effect on scaffold development when implanted as an inferior vena cava interposition in a mouse model whereby increasing BM-MNC number increased graft patency and decreased the number of infiltrated macrophages (42). Purified MSCs have also been employed in vascular tissue engineering and are obtained from various sources. MSCs are adherent adult progenitor cells with the ability to self-renew and differentiate into a variety of cells with a more specialized function [as reviewed in Huang and Li

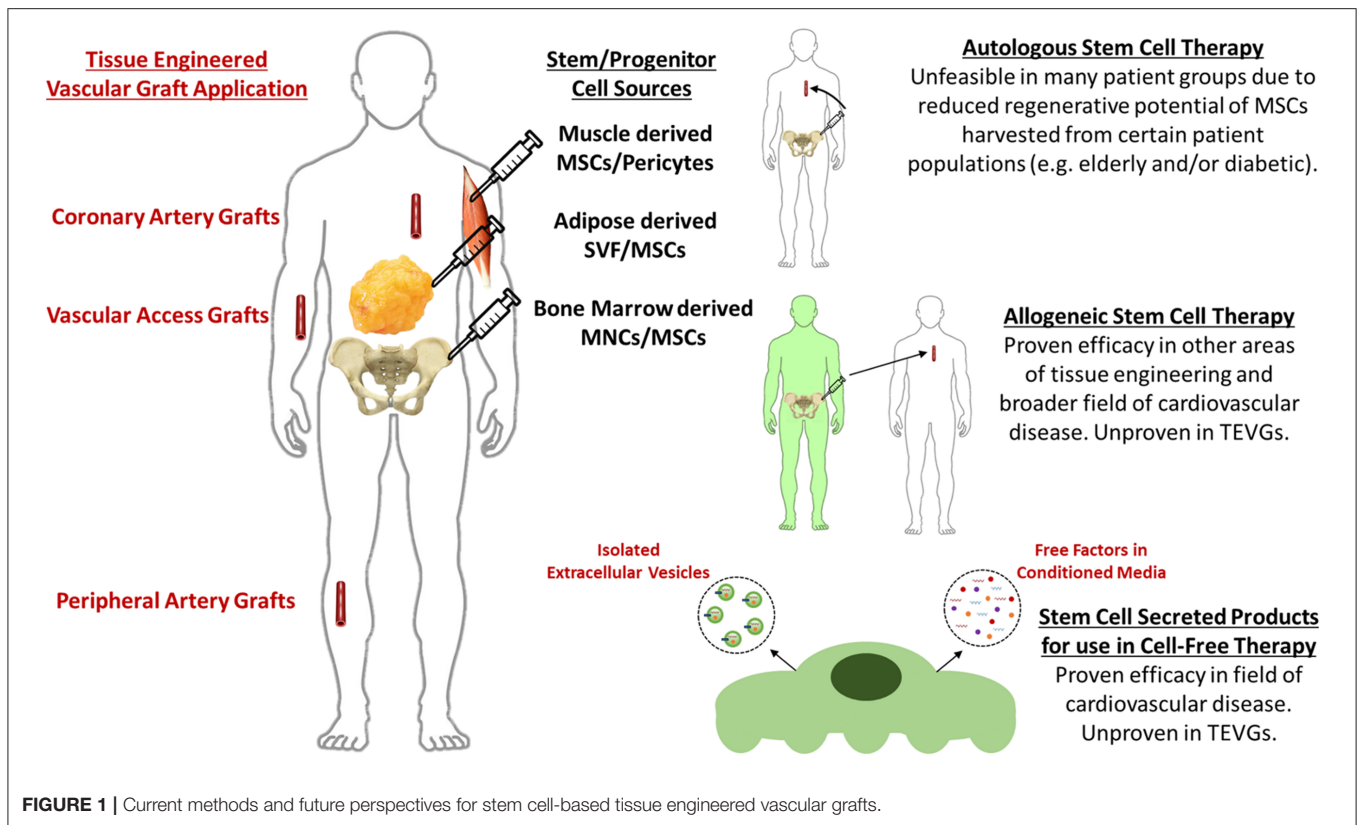
(53)]. Furthermore, MSCs secrete a variety of angiogenic and arteriogenic growth factors and cytokines (as discussed in section Allogeneic MSCs). Recent literature suggests that MSCs could be renamed Medicinal Signaling Cells to emphasize that MSCs do not differentiate at the site of injury (and are therefore not true stem cells), but rather signal to endogenous cells to regenerate and/or replace the injured/absent tissue (54). Bone marrow derived MSCs (BM-MSCs), purified from BM-MNCs, have demonstrated favorable preclinical findings in TEVGs (45–47). Similarly, adipose derived MSCs (ADMSCs) (48, 55) and muscle derived MSCs (49, 56) have been used in TEVG studies. Studies employing pericytes are also included in this review (50) as they have been shown to express MSC markers and display the capacity for tri-lineage differentiation [as reviewed in Crisan et al. (57)].

AUTOLOGOUS STEM CELLS

Numerous preclinical (28–31, 38) and clinical studies (32, 51, 52, 58) have used autologous stem cells as a cellular base for vascular scaffolds. Autologous stem cell studies have focused on restoring vascular integrity in pediatric/young patients with congenital heart defects and have demonstrated favorable long term clinical results (32). However, a combination of *in vitro* and *in vivo* studies has demonstrated the diminished regenerative potential of stem cells in vascular tissue engineering when harvested from elderly or diabetic patients (Figure 2). The ability of ADMSCs to prevent acute thrombosis and encourage graft remodeling in a murine model is reduced when cells are harvested from elderly or diabetic patient groups and seeded on a PEUU scaffold (48) using established methods (60, 61). Furthermore, the ability of ADMSCs from elderly or diabetic patients to encourage smooth muscle cell migration and secrete factors that promote fibrinolysis is also decreased (48, 59). The work of Krawiec et al. therefore highlights the limitations of an autologous stem cell approach as many of the patient groups in need of regenerative therapies are elderly and/or diabetic e.g., coronary/peripheral bypass patients and end stage renal disease patients. Furthermore, the diminished regenerative potential of elderly/diabetic stem cells may expand to include more degenerative conditions. However, the inherent limitations of an autologous stem cell approach can be largely bypassed by using allogeneic MSCs harvested from young healthy donors.

ALLOGENEIC MSCs

MSCs are an appropriate candidate for allogeneic stem cell therapies as they are immune evasive. MSC immune evasion can be partially attributed to their low expression of major histocompatibility complex (MHC) class I antigens and freedom from expression of MHC class II antigens which are both associated with immune rejection (62, 63). Similarly, the MSC secretome has been shown to suppress immune response by inhibiting T cell proliferation and monocyte maturation and also by promoting regulatory T cells and M2 macrophages (64). Although allogeneic MSCs have not yet been investigated as a



cellular base for TEVGs, the use of allogeneic fibroblasts for generating vascular grafts by self-assembly has been proven safe for use in humans as arteriovenous fistulas following devitalization (12). The use of allogeneic fibroblasts highlights the premise of employing allogeneic cells in vascular tissue engineering. Furthermore, other fields of tissue engineering have employed allogeneic MSCs to safely and effectively regenerate bone (65–67), cartilage (68–70), skin (71, 72), and nerve (73).

Clinical studies of allogeneic MSCs in the broader field of cardiovascular disease have also presented convincing evidence to suggest that allogeneic MSCs are minimally immunogenic and induce an equivalent therapeutic response when compared to autologous MSCs. The POSEIDON randomized trial compared the safety and efficacy of allogeneic MSCs to autologous MSCs in patients with ischemic cardiomyopathy. The trial results found that transendocardial delivery of allogeneic MSCs did not stimulate significant donor-specific immune reactions and was also associated with a reduction in left ventricle volume and an increase in ejection fraction comparable to treatment with autologous MSCs (74). It has also been demonstrated that transendocardial injections of allogeneic MSCs produce a dose dependent reduction in major adverse events in chronic heart failure patients (75). Furthermore, adventitial administration of commercially available allogeneic MSCs to the coronary arteries of myocardial infarction (MI) patients showed that allogeneic MSCs were well tolerated, with no serious adverse events, and significantly increased both ejection fraction and ventricular stroke volume (76).

The safety and therapeutic efficacy of administering allogeneic MSCs to treat MI has also been demonstrated separately in both large (77) and small animal preclinical models (78). Combined, the preceding evidence supports the premise of employing allogeneic vascular cells as a cellular base for developing TEVGs and also the safety and efficacy of administering allogeneic MSCs to treat cardiovascular conditions. The use of allogeneic MSCs is therefore one potential future direction for stem cell based TEVGs that has yet to be fully investigated.

REMODELING PROCESS OF STEM CELL SEEDED VASCULAR SCAFFOLDS

Despite the great success of directly incorporating stem cells in vascular tissue engineered scaffolds, evidence supporting a paracrine mechanism as the main effector of stem cell therapy indicates the potential of employing stem cell secreted products as a more straightforward, cell-free therapeutic base for tissue engineering (Figure 1). Compelling evidence for the paracrine effect of stem cells in vascular tissue engineering is that remodeling of implanted vascular scaffolds is mediated by an inflammatory process (26, 27, 42), and that seeded stem cells signal the recruitment and moderation of the immune cells that trigger the required inflammatory process in a paracrine manner (26, 27, 35).

TABLE 1 | Studies that have implanted scaffolds seeded with stem cells as vascular grafts.

References	Type	Origin	Model	Source	Implant	Duration	Patency
(28)	BM-MNC	Canine	Beagle dog	Auto	IVC	2 years	100%
(29)	BM-MNC	Canine	Beagle dog	Auto	IVC	4 weeks	100%
(30)	BM-MNC	Canine	Beagle dog	Auto	IVC	6 months	100%
(31)	BM-MNC	Ovine	Lamb	Auto	IVC	6 months	100%
(32)	BM-MNC	Human	Human	Auto	CPC	5.8 years	100%
(33)	BM-MNC	Human	Immunodeficient mouse	Xeno	IVC	6 months	100%
(26)	BM-MNC	Human	Immunodeficient mouse	Xeno	IVC	24 weeks	100%
(27)	BM-MNC	Murine	C57BL/6 mouse	Syng	IVC	2 weeks	68%
(34)	BM-MNC	Human	SCID/bg mouse	Xeno	IVC	10 weeks	100%
(35)	BM-MNC	Murine	C57BL/6 mouse	Syng	IVC	6 months	100%
(36)	BM-MNC	Murine	C57BL/6 mouse	Syng	IVC	4 weeks	100%
(37)	BM-MNC	Murine	C57BL/6 mouse	Syng	IVC	7 months	72% Survival
(38)	BM-MNC	Ovine	Lamb	Auto	IVC	6 months	100%
(39)	BM-MNC	Ovine	Lamb	Auto	IVC	6 months	100%
(40)	BM-MNC	Murine	C57BL/6 mouse	Syng	IVC	2 weeks	78% (Filter Group)
(41)	BM-MNC	Unclear	C57BL/6 mouse	Unclear	IVC	8 weeks	Unclear
(42)	BM-MNC	Murine	C57BL/6 mouse	Syng	IVC	2 weeks	95% (10×10^6 cells Group)
(43)	BM-MNC	Murine	C57BL/6 mouse	Syng	IVC	2 weeks	88.9%
(44)	BM-MNC	Ovine	Lamb	Syng/Auto	CaVC	6 months	25%
(45)	BM-MSC	Canine	Beagle dog	Auto	AA	6 months	100%
(46)	BM-MSC	Human	Nude mouse	Xeno	CA	35 days	100%
(47)	BM-MSC	Human	Athymic rat	Xeno	CA	60 days	100%
(48)	ADMSC	Human	Lewis rat	Xeno	AA	8 weeks	100%
(48)	ADMSC	Human	Lewis rat	Xeno	AA	8 weeks	100%
(49)	MD-MSC	Rat	Lewis rat	Syng	AA	8 weeks	65%
(50)	Pericytes	Human	Lewis rat	Xeno	AA	8 weeks	100%

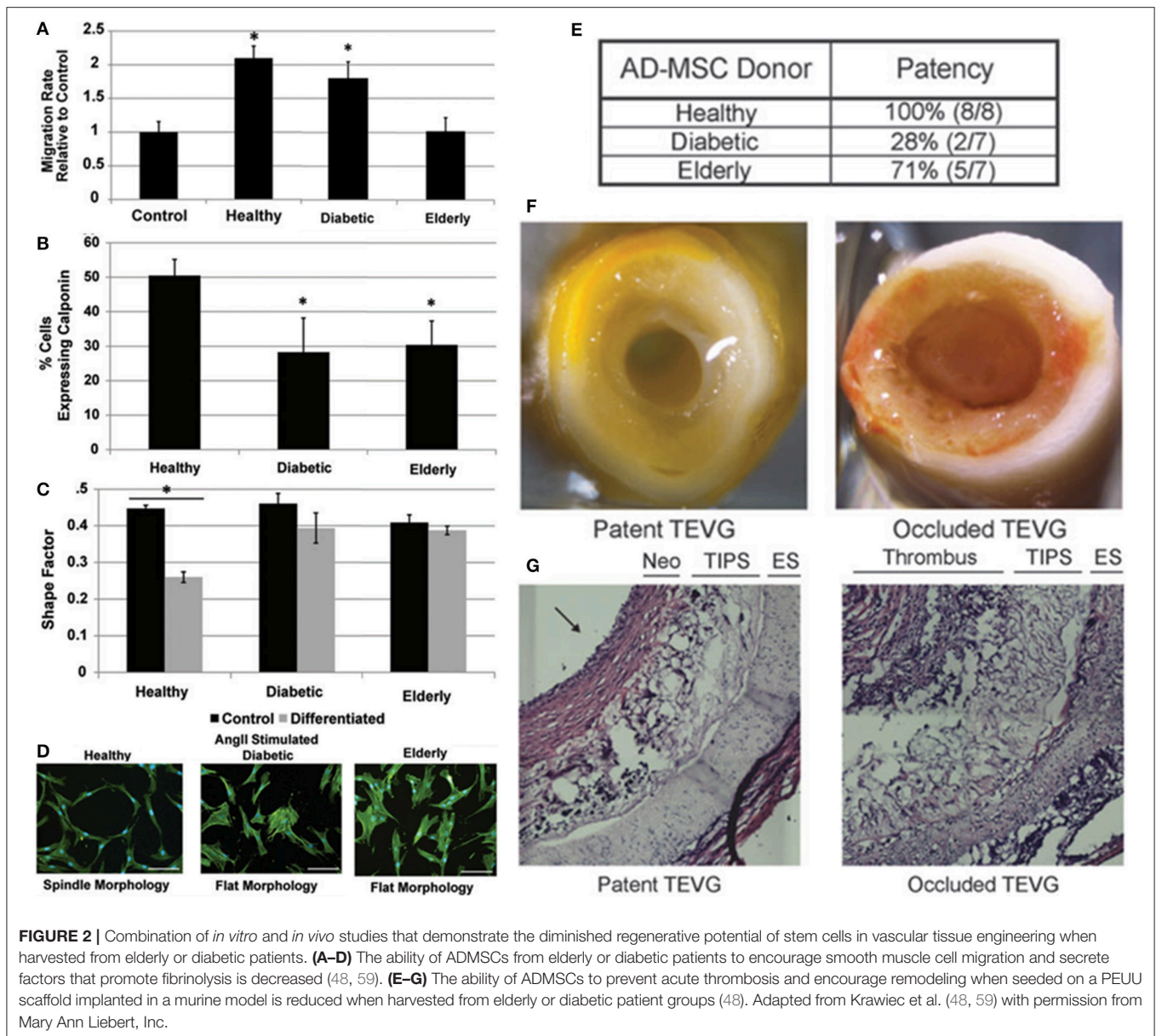
BM-MNC, Bone Marrow Mononuclear Cells; Auto, Autologous; IVC, Inferior Vena Cava; CPC, Cavopulmonary connection; Xeno, Xeogeneic; Syng, Syngeneic; CaVC, Caudal Vena Cava; AA, Abdominal Aorta; CA, Carotid Artery.

The role of inflammation in vascular graft remodeling was initially demonstrated through observations that host monocyte and macrophage infiltration precedes the repopulation of scaffolds with vascular cells (26). Subsequently, it was demonstrated that peak macrophage infiltration coincides with the formation of functional vascular tissue and that depleting the host of macrophages completely inhibits the formation of neo-tissue (27). Furthermore, the role of modulating host immune cells was demonstrated by preventing host monocytes from secreting pro-inflammatory factors, through inhibition of TGF- β receptor 1, which significantly increased unseeded scaffold patency relative to untreated controls (79). Functionalization of vascular scaffolds to locally release TGF- β 1 inhibitor was proven to be as effective as seeding BM-MNCs in promoting graft patency (41). Therefore, both recruitment and modulation of host immune cells are required to ensure the formation of a functional neo-vessel.

Evidence for the paracrine role of seeded stem cells in vascular scaffold remodeling is that seeded BM-MNCs reside in the scaffold for <7 days *in vivo* and are not incorporated

into the developing neo-vessel (26, 35). Rather, the transient presence of BM-MNCs significantly increases the recruitment of host immune cells (monocytes and macrophages) compared to unseeded controls, partially through the secretion of MCP-1 (26). Subsequently, functionalization of vascular scaffolds to locally release MCP-1 was proven to be significantly more effective than seeded BM-MNCs in recruiting host monocytes (26). Furthermore, BM-MNCs have been shown to suppress the expression of M1 macrophage phenotype, the presence of which has been shown to decrease graft patency and remodeling (27). Seeded stem cells therefore modulate both the infiltration and phenotype of the host immune cells that mediate the vascular remodeling process in a paracrine manner through the secretion of bioactive products.

The concept of moving toward a cell-free approach by employing stem cell secreted products is to preserve the formation of neo-tissue while also removing the potential safety, regulatory, and practicality issues of cellular incorporation such as the use of stem cells with damaged/mutated DNA, undesirable trans-differentiation of persistent stem cells, and



micro-vessel clotting in the case of stem cell relocation (80). It is important to note that TEVGs formed using cell secreted products may be better described as Tissue Regenerative Vascular Grafts to reflect the departure from the traditional cell based paradigm.

MSC SECRETED FACTORS/CONDITIONED MEDIA

Stem cells, particularly MSCs, secrete a range of bioactive products that have an indirect or trophic effect on surrounding cells (81) and it has been proposed that these MSC-secreted bioactive products could replace MSCs as a therapeutic base for cell-free vascular tissue

engineering (26, 41). One such manner of moving toward a cell-free approach is to utilize MSC conditioned media (MSC-CM) as it has been frequently demonstrated that MSCs secrete trophic factors into their surrounding media. However, the use of MSC-CM in vascular tissue engineering has demonstrated poor initial results. Scaffolds incubated over-night in BM-MNC-CM, following over-night incubation of the cells in serum-free media at 5% O₂, exhibited poor patency rates *in vivo* which were comparable to PBS incubated scaffolds (patent: 2/10 vs. 6/25) (43).

Despite the discouraging results observed by Best et al, free injections of MSC-CM to treat MI have exhibited pre-clinical success. Intracardial administration of CM from BM-MSCs, under hypoxic conditions, and overexpressing the

survival gene Akt1, significantly decreased infarct size and apoptosis in a murine model of MI (82). Intravenous and intracoronary administration of CM harvested from human embryonic stem cell (hESC) derived MSC was associated with a 60% reduction in infarct size, improvements in systolic and diastolic cardiac performance and increased capillary density in an infarct porcine model (83, 84). Furthermore, co-administration of MSC-CM and the parent ADMSCs synergistically increased neovascularization of infarcted myocardium compared to saline control in a porcine model of MI (77).

Culture conditions of MSCs can greatly alter the content of MSC-CM (85), therefore optimization of culture conditions could generate a more effective therapeutic. Exposing BM-MSCs to hypoxic conditions has been shown to induce a >1.5 fold increase in an array of angiogenic/arteriogenic cytokine genes; furthermore, administering the same MSC-CM to a murine model of hind limb ischemia enhanced collateral flow, improved limb function, reduced auto-amputation, and attenuated muscle atrophy when compared with control media (86). Forming spheroids of BM-MSCs (25k cells) using the hanging drop method has been shown to increase the production of anti-inflammatory agents TSG-6 and PGE2 compared to dissociated MSCs, and the administration of the resulting MSC-CM attenuated macrophage phenotype *in vitro* and significantly lowered inflammation in a mouse model of peritonitis (87, 88). Exposing MSC spheroids to hypoxic conditions and inflammatory stimuli further enhanced the

secretion of PGE2 and VEGF (85) and encapsulating MSC spheroids in unmodified or RGD modified fibrin gels has also been shown to increase MSC secretion of VEGF and PGE2 (89–91). However, recent findings suggest that MSCs seeded onto macroporous scaffolds secrete significantly higher levels of pro-angiogenic factors compared to MSCs encapsulated in fibrin gels (92). Furthermore, culturing ADMSCs on electrospun fibers produces significantly higher levels of anti-inflammatory and pro-angiogenic cytokines compared to those cultured on plates (93). Combined, the preceding evidence suggests that culturing MSC spheroids in 3D hypoxic environments, and exposing cells to an inflammatory stimulus, enhances the anti-inflammatory and pro-angiogenic potential of the resulting MSC-CM.

Providing a therapeutic effect using MSC secreted factors or MSC-CM is limited by the difficulties in delivering these products to the intended cell type and also by their short residence time *in vivo* which necessitates high initial concentrations. These limitations can largely be overcome by employing only the extracellular vesicles (EVs) secreted by stem cells. EVs offer many benefits as a therapeutic base for functionalizing vascular scaffolds such as cell specific targeting via the presentation of surface/membrane proteins (94, 95), physiological delivery of cargo to target cells (96, 97), reduced immunogenicity and stability under physiological conditions including protection of cargo from enzymatic degradation (98) and bypass of complement activation (95, 99, 100). The potential of employing EVs as a therapeutic base for

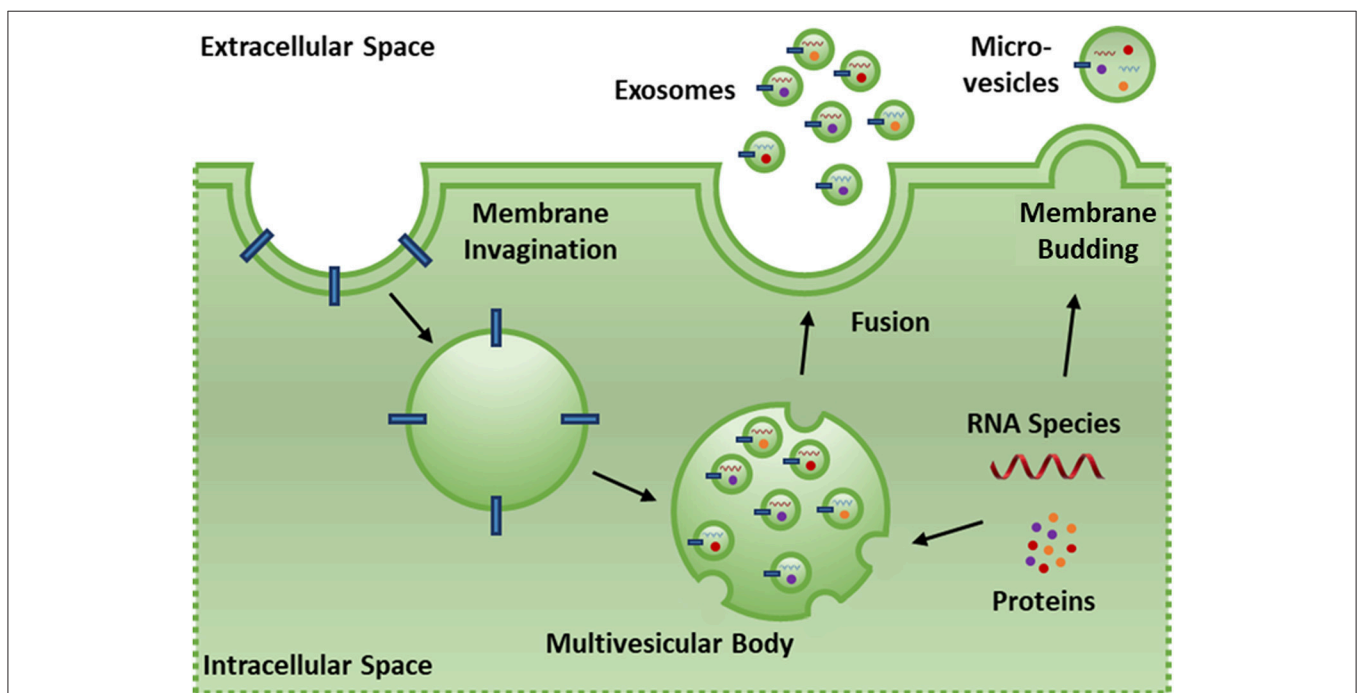


FIGURE 3 | Exosomes (30–200 nm) are released by cells when intracellular multi-vesicle bodies form via invaginations of the cell membrane and are selectively loaded with endosomes containing protein, mRNA and miRNA. Fusion of the multi-vesicle body with the cell membrane releases these endosomes as exosomes. Micro-vesicles (200–1,000 nm) are released via direct outward budding of the cell membrane and contain protein, mRNA and miRNA. The loading of microvesicle cargo is less selective than exosomes and membrane proteins are more reflective of the parent cell membrane due to direct budding.

functionalizing vascular scaffolds is explored in the following section.

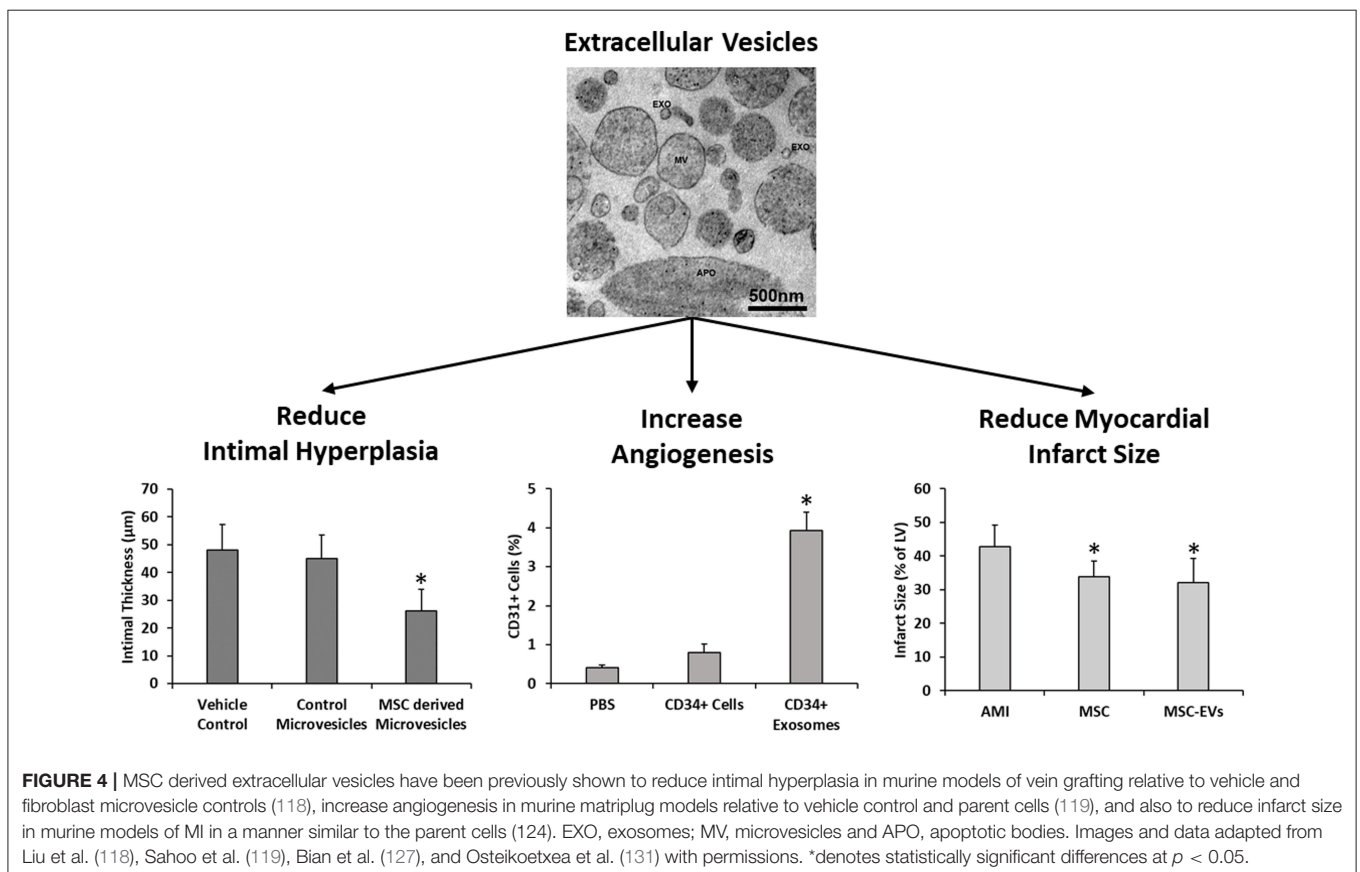
MSC DERIVED EXTRACELLULAR VESICLES

EVs are cell-derived phospholipid membrane based nanoparticles that present with functional surface/membrane proteins and contain protein and RNA species that dynamically reflect the state of the parent cell and tissue (101). EVs are produced by most cells in the body (102, 103) and serve to transmit biological signals, transfer proteins/nucleic acids, and induce biological effects on target cells via surface receptor interactions, membrane fusion or endocytosis of the EVs by the target cell (96, 97). EVs can be categorized into three classes based on their cellular origins. Exosomes (30–200 nm) are released by cells when intracellular multi-vesicle bodies form via invagination of the cell membrane and are selectively loaded with endosomes containing protein, mRNA and miRNA. Fusion of the multi-vesicle body with the cell membrane releases these endosomes as exosomes (104). Micro-vesicles (200–1,000 nm) are released via direct outward budding of the cell membrane and contain protein, mRNA, and miRNA (Figure 3). The loading of microvesicle cargo is less selective than exosomes and membrane proteins are more reflective of the parent cell membrane due to direct budding

(103). Apoptotic bodies (1,000–5,000 nm) are released by cells upon fragmentation of the plasma membrane during apoptosis (105). The term EV is used here to refer exclusively to exosomes and microvesicles as apoptotic bodies are distinct in activity and content (106).

EVs can be isolated from cell culture supernatant via density-based, size-based, precipitation, immunoaffinity, and microfluidic based techniques [as reviewed in Li et al. (107)]. Although ultracentrifugation remains the gold standard, each technique has inherent advantages and limitations regarding process speed/cost and EV yield/functionality. Once isolated, guidelines have been published by the International Society for EVs regarding minimum standards for EV characterization. These guidelines require that EV size, concentration and morphology be determined in addition to screening for EV enriched markers and quantifying the co-precipitating protein levels to assess the purity of the EV isolate (108).

MSC-EVs have already shown regenerative potential and have also been credited with many of the therapeutic effects seen during the treatment of cells and tissues with MSC-CM (109, 110). Furthermore, MSCs are regarded as the optimal source for obtaining therapeutic EVs due to their immunomodulatory properties (111), their high expansion capacity/potential for immortalization (112) and the large numbers of EVs that they secrete relative to other cells (100). Although not yet employed in the field of vascular tissue engineering, other



areas of tissue engineering have begun to utilize EVs such as bone regeneration (113), adipose tissue regeneration (114), and wound healing (115, 116). Furthermore, the functional relevance of EVs in regenerative medicine (such as promoting cell viability, angiogenesis, extracellular matrix interactions, and immunomodulation) has already been highlighted [as reviewed in De Jong et al. (117)].

Numerous studies have examined the effects of free EV injections in other areas of cardiovascular research such as vein grafting, angiogenesis and MI. Liu et al. demonstrated that the degree of intimal hyperplasia was significantly decreased following vein graft implantation in a murine model with multiple intraperitoneal injections of human ADMSC-EVs. Macrophage presence was also found to be reduced and significantly decreased expression levels of IL-6 and MCP-1 were found in ADMSC-EV treated mice compared to controls (118). MSC derived exosomes have been shown to induce angiogenesis *in vitro* through increased endothelial cell migration and tube formation (119, 120), and also *in vivo* through increased vessel formation in murine Matrigel plugs, corneal assays, and cerebral artery occlusion relative to controls (119, 121–124). Furthermore, administration of hESC derived exosomes (125), hESC-MSCs derived exosomes (109, 112, 126), BM-MSC derived EVs (127), and BM-MSC derived exosomes (128–130) have all been shown to significantly reduce infarct size in murine models of MI compared to controls (Figure 4). Interestingly, only intact and not lysed exosomes demonstrated a therapeutic effect, therefore suggesting that both exosome mediated delivery, in addition to exosome cargo, are required to successfully treat cardiovascular conditions (126).

In an attempt to elucidate the therapeutic mechanism of MSC-EVs, extensive transcriptomic and proteomic characterization of ADMSC-EVs has been performed and the results compared to those obtained from the parent MSCs. It has been shown that ADMSC-EVs contain a similar yet distinct protein, miRNA and mRNA cargo compared to their parent cells. Specifically, ADMSC-EVs are enriched for the mi-RNAs miR-183, miR-378, miR-140, and miR-222; for 255 genes including TRPS1, ELK4, KLF7, and NR1P1; and for 277 proteins that play important biological roles including glycoproteins, extracellular matrix remodeling, blood coagulation, inflammatory response, TGF- β signaling pathway, and angiogenic proteins. The ADMSC-EV cargo is therefore enriched to support a range of functions important to vascular tissue engineering including extracellular matrix remodeling, angiogenesis, inflammation, blood coagulation, and apoptosis (132–134). Consequently, MSC-derived EVs are worthy of future research/therapeutic focus in this context.

FUTURE OF MSC-EVs IN VASCULAR TISSUE ENGINEERING

The role of MSC-EVs in vascular tissue engineering is particularly exciting due to the need for a cell-free therapeutic base that can be incorporated into a scaffold and signal to cells in a paracrine manner to prevent acute thrombosis and encourage

appropriate remodeling. However, a number of points must be addressed prior to the effective translation of TEVG technologies that incorporate MSC-EVs:

1. The optimal culture conditions for parent MSCs must be identified to ensure that the optimal yield of EVs is being obtained in a safe and repeatable manner. Although this has been studied extensively for MSC-CM (see section MSC Derived Extracellular Vesicles), the therapeutic effects of free factors and EVs in MSC-CM must be de-coupled and culture conditions optimized to specifically increase the therapeutic efficacy of isolated EVs.

2. A cheap, reliable and EV friendly method of isolating MSC-EVs must be identified and implemented to ensure that the optimal yield of EVs is being obtained in a safe and repeatable manner. Ultimately, a preferred method of isolating intact EVs must be identified and scaled so that EV based TEVGs can be developed into a clinically viable therapy.

3. The optimal method of delivering and retaining MSC-EVs into a tissue engineered vascular scaffold must be identified to ensure that MSC-EVs are present in sufficient numbers and remain intact. Encouraging research has demonstrated that directly incorporating EVs into a decalcified bone matrix scaffold is possible and elicits an equivalent neo-vessel formation response compared to incorporating MSCs alone following subcutaneous murine implants (113). Furthermore, it has been shown that cardiosphere derived EVs remain stable at -80°C for up to 90 days and that both *in vitro* and *in vivo* bioactivity is preserved following lyophilisation (135). This suggests that EVs can be directly incorporated into many forms of scaffold production and therefore exhibit potential as a therapeutic source in off-the-shelf vascular graft applications.

4. The *in vivo* remodeling potential of MSC-EV seeded vascular scaffolds must be assessed using established small and large animal preclinical models to determine if they elicit an appropriate TEVG host remodeling response.

SUMMARY

One approach to vascular tissue engineering is to implant biodegradable tubular scaffolds, seeded with autologous stem cells that trigger the development of functional native-like vascular replacements. However, stem cells harvested from elderly or diabetic patients have diminished regenerative potential in vascular tissue engineering. The inherent limitations of an autologous stem cell approach can be addressed using allogeneic MSCs. However, potential safety, regulatory, and practicality issues of cellular incorporation suggest that a cell-free approach may be more prudent. MSC-EVs present as one such cell-free approach and offer many benefits as a therapeutic base for functionalizing vascular scaffolds such as cell specific targeting, physiological delivery of cargo to target cells, reduced immunogenicity, and stability under physiological conditions. Despite promising findings of EV therapy in the broader field of cardiovascular research, further work is required to explore

the full potential of this promising therapeutic in vascular tissue engineering.

AUTHOR CONTRIBUTIONS

EC: concept generation, literature review, manuscript writing, critical review of manuscript; JW, FO and DV: concept generation, manuscript writing, critical review of manuscript.

REFERENCES

- Kaushal S, Amiel GE, Guleserian KJ, Shapira OM, Perry T, Sutherland FW, et al. Functional small-diameter neovessels created using endothelial progenitor cells expanded *ex vivo*. *Nat Med.* (2001) 7:1035–40. doi: 10.1038/nm0901-1035
- He H, Shirota T, Yasui H, Matsuda T. Canine endothelial progenitor cell-lined hybrid vascular graft with nonthrombogenic potential. *J Thorac Cardiovasc Surg.* (2003) 126:455–64. doi: 10.1016/S0022-5223(02)73264-9
- Zhu C, Ying D, Mi J, Li L, Zeng W, Hou C, et al. Development of anti-atherosclerotic tissue-engineered blood vessel by A20-regulated endothelial progenitor cells seeding decellularized vascular matrix. *Biomaterials* (2008) 29:2628–36. doi: 10.1016/j.biomaterials.2008.03.005
- Neff LP, Tillman BW, Yazdani SK, MacHingal MA, Yoo JJ, Soker S, et al. Vascular smooth muscle enhances functionality of tissue-engineered blood vessels *in vivo*. *J Vasc Surg.* (2011) 53:426–34. doi: 10.1016/j.jvs.2010.07.054
- Quint C, Kondo Y, Manson RJ, Lawson JH, Dardik A, Niklason LE. Decellularized tissue-engineered blood vessel as an arterial conduit. *Proc Natl Acad Sci USA.* (2011) 108:9214–9. doi: 10.1073/pnas.1019506108
- L'Heureux N, Pâquet S, Labbé R, Germain L, Auger FA. A completely biological tissue-engineered human blood vessel. *FASEB J.* (1998) 12:47–56. doi: 10.892-6638/97/0012-0047
- L'Heureux N, Dusserre N, König G, Victor B, Keire P, Wight TN, et al. Human tissue-engineered blood vessels for adult arterial revascularization. *Nat Med.* (2006) 12:361–5. doi: 10.1038/nm1364
- L'Heureux N, McAllister TN, de la Fuente LM. Tissue-engineered blood vessel for adult arterial revascularization. *N Engl J Med.* (2007) 357:1451–3. doi: 10.1056/NEJMc071536
- McAllister TN, Maruszewski M, Garrido SA, Wystrychowski W, Dusserre N, Marini A, et al. Effectiveness of haemodialysis access with an autologous tissue-engineered vascular graft: a multicentre cohort study. *Lancet* (2009) 373:1440–6. doi: 10.1016/S0140-6736(09)60248-8
- Dahl SLM, Kypson AP, Lawson JH, Blum JL, Strader JT, Li Y, et al. Readily available tissue-engineered vascular grafts. *Sci Trans Med.* (2011) 3:68ra9. doi: 10.1126/scitranslmed.3001426
- Wystrychowski W, Cierpka L, Zagalski K, Garrido S, Dusserre N, Radochowski S, et al. Case study: first implantation of a frozen, devitalized tissue-engineered vascular graft for urgent hemodialysis access. *J Vasc Access* (2011) 12:67–70. doi: 10.5301/JVA.2011.6360
- Wystrychowski W, McAllister TN, Zagalski K, Dusserre N, Cierpka L, L'Heureux N. First human use of an allogeneic tissue-engineered vascular graft for hemodialysis access. *J Vasc Surg.* (2014) 60:1353–7. doi: 10.1016/j.jvs.2013.08.018
- Shin'oka T, Shum-Tim D, Ma PX, Tanel RE, Isogai N, Langer R, et al. Creation of viable pulmonary artery autografts through tissue engineering. *J Thorac Cardiovasc Surg.* (1998) 115:536–46. doi: 10.1016/S0022-5223(98)70315-0
- Niklason LE, Gao J, Abbott WM, Hirschi KK, Houser S, Marini R, et al. Functional arteries grown *in vitro*. *Science* (1999) 284:489–93. doi: 10.1126/science.284.5413.489
- Shin'oka T, Imai Y, Ikada Y. Transplantation of a tissue-engineered pulmonary artery. *N Engl J Med.* (2001) 344:532–3. doi: 10.1056/NEJM200102153440717

FUNDING

This work was funded by the European Union's Horizon 2020 research and innovation program under the Marie Skłodowska-Curie grant agreement No 708867 awarded to EC, the Competitive Medical Research Fund, University of Pittsburgh awarded to JW and the National Institute of Health under grant agreement No R01HL130077 awarded to DV.

- Naito Y, Imai Y, Shin'oka T, Kashiwagi J, Aoki M, Watanabe M, et al. Successful clinical application of tissue-engineered graft for extracardiac Fontan operation. *J Thorac Cardiovasc Surg.* (2003) 125:419–420. doi: 10.1067/mtc.2003.134
- Cho SW, Lim SH, Kim IK, Hong YS, Kim SS, Yoo KJ, et al. Small-diameter blood vessels engineered with bone marrow-derived cells. *Ann Surg.* (2005) 241:506–15. doi: 10.1097/01.sla.0000154268.12239.ed
- Cho SW, Lim JE, Chu HS, Hyun HJ, Choi CY, Hwang KC, et al. Enhancement of *in vivo* endothelialization of tissue-engineered vascular grafts by granulocyte colony-stimulating factor. *J Biomed Mater Res.* (2006) 76:252–263. doi: 10.1002/jbm.a.30535
- Cho SW, Kim IK, Kang JM, Song KW, Kim HS, Park CH, et al. Evidence for *in vivo* growth potential and vascular remodeling of tissue-engineered artery. *Tissue Eng A.* (2009) 15:901–912. doi: 10.1089/ten.tea.2008.0172
- Roh JD, Brennan MP, Lopez-Soler RI, Fong PM, Goyal A, Dardik A, et al. Construction of an autologous tissue-engineered venous conduit from bone marrow-derived vascular cells: optimization of cell harvest and seeding techniques. *J Pediatr Surg.* (2007) 42:198–202. doi: 10.1016/j.jpedsurg.2006.09.054
- Lim SH, Cho SW, Park JC, Jeon O, Lim JM, Kim SS, et al. Tissue-engineered blood vessels with endothelial nitric oxide synthase activity. *J Biomed Mater Res.* (2008) 85B:537–46. doi: 10.1002/jbm.b.309770
- Zhao Y, Zhang S, Zhou J, Wang J, Zhen M, Liu Y, et al. The development of a tissue-engineered artery using decellularized scaffold and autologous ovine mesenchymal stem cells. *Biomaterials* (2010) 31:296–307. doi: 10.1016/j.biomaterials.2009.09.049
- Maul TM, Nieponice A, Vorp DA. Chapter 9: Vascular differentiation of stem cells by mechanical forces. *Hemodynamics Mechanobiol Endothelium.* (2010) 247–69. doi: 10.1142/9789814280426_0009
- Gui L, Dash BC, Luo J, Qin L, Zhao L, Yamamoto K, et al. Implantable tissue-engineered blood vessels from human induced pluripotent stem cells. *Biomaterials* (2016) 102:120–9. doi: 10.1016/j.biomaterials.2016.06.010
- Luo J, Qin L, Kural MH, Schwan J, Li X, Bartulos O, et al. Vascular smooth muscle cells derived from inbred swine induced pluripotent stem cells for vascular tissue engineering. *Biomaterials* (2017) 147:116–32. doi: 10.1016/j.biomaterials.2017.09.019
- Roh JD, Sawh-Martinez R, Brennan MP, Jay SM, Devine L, Rao DA, et al. Tissue-engineered vascular grafts transform into mature blood vessels via an inflammation-mediated process of vascular remodeling. *Proc Natl Acad Sci USA.* (2010) 107:4669–74. doi: 10.1073/pnas.0911465107
- Hibino N, Yi T, Duncan DR, Rathore A, Dean E, Naito Y, et al. A critical role for macrophages in neovessel formation and the development of stenosis in tissue-engineered vascular grafts. *Faseb J.* (2011) 25:4253–63. doi: 10.1096/fj.11-186585
- Matsumura G, Miyagawa-Tomita S, Shin'oka T, Ikada Y, Kurosawa H. First evidence that bone marrow cells contribute to the construction of tissue-engineered vascular autografts *in vivo*. *Circulation* (2003) 108:1729–34. doi: 10.1161/01.CIR.0000092165.32213.61
- Hibino N, Shin'oka T, Matsumura G, Ikada Y, Kurosawa H. The tissue-engineered vascular graft using bone marrow without culture. *J Thorac Cardiovasc Surg.* (2005) 129:1064–70. doi: 10.1016/j.jtcvs.2004.10.030
- Matsumura G, Ishihara Y, Miyagawa-Tomita S, Ikada Y, Matsuda S, Kurosawa H, et al. Evaluation of tissue-engineered vascular autografts. *Tissue Eng.* (2006) 12:3075–83. doi: 10.1089/ten.2006.12.3075

31. Brennan MP, Dardik A, Hibino N, Roh JD, Nelson GN, Papademitris X, et al. Tissue-engineered vascular grafts demonstrate evidence of growth and development when implanted in a Juvenile animal model. *Trans Meet Am Surg Assoc.* (2008) 126:20–7. doi: 10.1097/SLA.0b013e318184dcbd
32. Hibino N, McGillicuddy E, Matsumura G, Ichihara Y, Naito Y, Breuer C, et al. Late-term results of tissue-engineered vascular grafts in humans. *J Thorac Cardiovasc Surg.* (2010) 139:431–6, 436.e1–2. doi: 10.1016/j.jtcvs.2009.09.057
33. Mirensky TL, Hibino N, Sawh-Martinez RF, Yi T, Villalona G, Shinoka T, et al. Tissue-engineered vascular grafts: does cell seeding matter? *J Pediatric Surg.* (2010) 45:1299–305. doi: 10.1016/j.jpedsurg.2010.02.102
34. Hibino N, Nalbandian A, Devine L, Martinez RS, McGillicuddy E, Yi T, et al. Comparison of human bone marrow mononuclear cell isolation methods for creating tissue-engineered vascular grafts: novel filter system versus traditional density centrifugation method. *Tissue Eng. Part C Methods* (2011) 17:933–8. doi: 10.1089/ten.tec.2011.0110
35. Hibino N, Villalona G, Pietris N, Duncan DR, Schoffner A, Roh JD, et al. Tissue-engineered vascular grafts form neovessels that arise from regeneration of the adjacent blood vessel. *FASEB J.* (2011) 25:2731–9. doi: 10.1096/fj.11-182246
36. Naito Y, Williams-Fritze M, Duncan DR, Church SN, Hibino N, Madri JA, et al. Characterization of the natural history of extracellular matrix production in tissue-engineered vascular grafts during neovessel formation. *Cells Tissues Organs* (2011) 195:60–72. doi: 10.1159/000331405
37. Udelsman BV, Khosravi R, Miller KS, Dean EW, Bersi MR, Rocco K, et al. Characterization of evolving biomechanical properties of tissue engineered vascular grafts in the arterial circulation. *J Biomech.* (2014) 47:2070–9. doi: 10.1016/j.jbiomech.2014.03.011
38. Stacy MR, Naito Y, Maxfield MW, Kurobe H, Tara S, Chan C, et al. Targeted imaging of matrix metalloproteinase activity in the evaluation of remodeling tissue-engineered vascular grafts implanted in a growing lamb model. *J Thorac Cardiovasc Surg.* (2014) 148:2227–33. doi: 10.1016/j.jtcvs.2014.05.037
39. Kurobe H, Maxfield MW, Naito Y, Cleary M, Stacy MR, Solomon D, et al. Comparison of a closed system to a standard open technique for preparing tissue-engineered vascular grafts. *Tissue Eng. Part C Methods* (2015) 21:88–93. doi: 10.1089/ten.tec.2014.0160
40. Kurobe H, Tara S, Maxfield MW, Rocco KA, Bagi PS, Yi T, et al. Comparison of the biological equivalence of two methods for isolating bone marrow mononuclear cells for fabricating tissue-engineered vascular grafts. *Tissue Eng. Part C Methods* (2015) 21:597–604. doi: 10.1089/ten.tec.2014.0442
41. Duncan DR, Chen PY, Patterson JT, Lee YU, Hibino N, Cleary M, et al. TGF β R1 inhibition blocks the formation of stenosis in tissue-engineered vascular grafts. *J Am College Cardiol.* (2015) 512–4. doi: 10.1016/j.jacc.2014.08.057
42. Lee YU, Mahler N, Best CA, Tara S, Sugiura T, Lee AY, et al. Rational design of an improved tissue-engineered vascular graft: determining the optimal cell dose and incubation time. *Regener Med.* (2016) 11:159–67. doi: 10.2217/rme.15.85
43. Best C, Tara S, Wiet M, Reinhardt J, Pepper V, Ball M, et al. Deconstructing the Tissue engineered vascular graft: evaluating scaffold pre-wetting, conditioned media incubation, and determining the optimal mononuclear cell source. *ACS Biomater Sci Eng.* (2017) 3:1972–9. doi: 10.1021/acsbomaterials.6b00123
44. Pepper VK, Clark ES, Best CA, Onwuka EA, Sugiura T, Heuer ED, et al. Intravascular Ultrasound characterization of a tissue-engineered vascular graft in an ovine model. *J Cardiovasc Trans Res.* (2017) 10:128–38. doi: 10.1007/s12265-016-9725-x
45. Zhang L, Zhou J, Lu Q, Wei Y, Hu S. A novel small-diameter vascular graft: *in vivo* behavior of biodegradable three-layered tubular scaffolds. *Biotechnol Bioeng.* (2008) 99:1007–15. doi: 10.1002/bit.21629
46. Hjortnaes J, Gottlieb D, Figueiredo JL, Melero-Martín J, Kohler RH, Bischoff J, et al. Intravital molecular imaging of small-diameter tissue-engineered vascular grafts in mice: a feasibility study. *Tissue Eng.* (2010) 16:597–607. doi: 10.1089/ten.tec.2009.0466
47. Hashi CK, Zhu Y, Yang GY, Young WL, Hsiao BS, Wang K, et al. Antithrombotic property of bone marrow mesenchymal stem cells in nanofibrous vascular grafts. *Proc Natl Acad Sci USA.* (2007) 104:11915–20. doi: 10.1073/pnas.0704581104
48. Krawiec JT, Weinbaum JS, Liao HT, Ramaswamy AK, Pezzone DJ, Josowitz AD, et al. *In vivo* functional evaluation of tissue-engineered vascular grafts fabricated using human adipose-derived stem cells from high cardiovascular risk populations. *Tissue Eng.* (2016) 22:765–75. doi: 10.1089/ten.tea.2015.0379
49. Nieponice A, Soletti L, Guan J, Deasy BM, Huard J, Wagner WR, et al. Development of a tissue-engineered vascular graft combining a biodegradable scaffold, muscle-derived stem cells and a rotational vacuum seeding technique. *Biomaterials* (2008) 29:825–33. doi: 10.1016/j.biomaterials.2007.10.044
50. He W, Nieponice A, Soletti L, Hong Y, Gharaibeh B, Crisan M, et al. Pericyte-based human tissue engineered vascular grafts. *Biomaterials* (2010) 31:8235–44. doi: 10.1016/j.biomaterials.2010.07.034
51. Shin'oka T, Matsumura G, Hibino N, Naito Y, Watanabe M, Konuma T, et al. Midterm clinical result of tissue-engineered vascular autografts seeded with autologous bone marrow cells. *J Thorac Cardiovasc Surg.* (2005) 129:1330–8. doi: 10.1016/j.jtcvs.2004.12.047
52. Shin'oka T, Breuer C. Tissue-engineered blood vessels in pediatric cardiac surgery. *Yale J Biol Med.* (2008) 81:161–6.
53. Huang NF, Li S. Mesenchymal stem cells for vascular regeneration. *Regener Med.* (2008) 3:877–92. doi: 10.2217/17460751.3.6.877
54. Caplan AI. Mesenchymal stem cells: time to change the name!. *Stem Cells Trans Med.* (2017) 6:1445–51. doi: 10.1002/sctm.17-0051
55. Krawiec JT, Liao HT, Kwan LY, D'Amore A, Weinbaum JS, Rubin JP, et al. Evaluation of the stromal vascular fraction of adipose tissue as the basis for a stem cell-based tissue-engineered vascular graft. *J Vasc Surg.* (2017) 66:883.e1–90.e1. doi: 10.1016/j.jvs.2016.09.034
56. Nieponice A, Soletti L, Guan J, Hong Y, Gharaibeh B, Maul TM, et al. *In vivo* assessment of a tissue-engineered vascular graft combining a biodegradable elastomeric scaffold and muscle-derived stem cells in a rat model. *Tissue Eng.* (2010) 16:1215–23. doi: 10.1089/ten.TEA.2009.0427
57. Crisan M, Corselli M, Chen WCW, Pêault B. Perivascular cells for regenerative medicine. *J Cell Mol Med.* (2012) 16:2851–60. doi: 10.1111/j.1582-4934.2012.01617.x
58. Matsumura G, Hibino N, Ikada Y, Kurosawa H, Shin'oka T. Successful application of tissue engineered vascular autografts: clinical experience. *Biomaterials* (2003) 24:2303–8. doi: 10.1016/S0142-9612(03)00043-7
59. Krawiec JT, Weinbaum JS, St Croix CM, Phillippi JA, Watkins SC, Peter Rubin J, et al. A cautionary tale for autologous vascular tissue engineering: impact of human demographics on the ability of adipose-derived mesenchymal stem cells to recruit and differentiate into smooth muscle cells. *Tissue Eng.* (2015) 21:426–37. doi: 10.1089/ten.tea.2014.0208
60. Soletti L, Nieponice A, Guan J, Stankus JJ, Wagner WR, Vorp DA. A seeding device for tissue engineered tubular structures. *Biomaterials* (2006) 27:4863–70. doi: 10.1016/j.biomaterials.2006.04.042
61. Soletti L, Hong Y, Guan J, Stankus JJ, El-Kurdi MS, Wagner WR, et al. A bilayered elastomeric scaffold for tissue engineering of small diameter vascular grafts. *Acta Biomater.* (2010) 6:110–22. doi: 10.1016/j.actbio.2009.06.026
62. Le Blanc K, Tammik C, Rosendahl K, Zetterberg E, Ringdén O. HLA expression and immunologic properties of differentiated and undifferentiated mesenchymal stem cells. *Exp Hematol.* (2003) 31:890–6. doi: 10.1016/S0301-472X(03)00110-3
63. Le Blanc K, Tammik L, Sundberg B, Haynesworth SE, Ringdén O. Mesenchymal stem cells inhibit and stimulate mixed lymphocyte cultures and mitogenic responses independently of the major histocompatibility complex. *Scand. J Immunol.* (2003) 57:11–20. doi: 10.1046/j.1365-3083.2003.01176.x
64. François M, Romieu-Mourez R, Li M, Galipeau J. Human MSC suppression correlates with cytokine induction of indoleamine 2,3-dioxygenase and bystander m2 macrophage differentiation. *Mol Ther.* (2012) 20:187–95. doi: 10.1038/mt.2011.189
65. Tsuchida H, Hashimoto J, Crawford E, Manske P, Lou J, Louis S, et al. Engineered allogeneic mesenchymal stem cells repair femoral segmental defect in rats.pdf. *J Orthopaedic Res.* (2003) 21:44–53. doi: 10.1016/S0736-0266(02)00108-0

66. Liu G, Zhang Y, Liu B, Sun J, Li W, Cui L. Bone regeneration in a canine cranial model using allogeneic adipose derived stem cells and coral scaffold. *Biomaterials* (2013) 34:2655–64. doi: 10.1016/j.biomaterials.2013.01.004
67. Wu J, Wang Q, Fu X, Wu X, Gu C, Bi J, et al. Influence of immunogenicity of allogeneic bone marrow mesenchymal stem cells on bone tissue engineering. *Cell Trans.* (2016) 25:229–42. doi: 10.3727/096368915X687967
68. Vega A, Martín-Ferrero MA, Del Canto F, Alberca M, García V, Munar A, et al. Treatment of knee osteoarthritis with allogeneic bone marrow mesenchymal stem cells. *Transplantation* (2015) 99:1681–90. doi: 10.1097/TP.0000000000000678
69. Harman R, Carlson K, Gaynor J, Gustafson S, Dhupa S, Clement K, et al. A prospective, randomized, masked, and placebo-controlled efficacy study of intraarticular allogeneic adipose stem cells for the treatment of osteoarthritis in dogs. *Front Vet Sci.* (2016) 3:81. doi: 10.3389/fvets.2016.00081
70. Feng C, Luo X, He N, Xia H, Lv X, Zhang X, et al. Efficacy and persistence of allogeneic adipose-derived mesenchymal stem cells combined with hyaluronic acid in osteoarthritis after intra-articular injection in a sheep model. *Tissue Eng.* (2017) 24:219–33. doi: 10.1089/ten.tea.2017.0039
71. Chen L, Tredget EE, Liu C, Wu Y. Analysis of allogenicity of mesenchymal stem cells in engraftment and wound healing in mice. *PLoS ONE* (2009) 4: e7119. doi: 10.1371/journal.pone.0007119
72. Hanson SE, Kleinbeck KR, Cantu D, Kim J, Bentz ML, Faucher LD, et al. Local delivery of allogeneic bone marrow and adipose tissue-derived mesenchymal stromal cells for cutaneous wound healing in a porcine model. *J Tissue Eng Regen Med.* (2016) 10:E90–E100. doi: 10.1002/term.1700
73. Ryu HH, Lim JH, Byeon YE, Park JR, Seo MS, Lee YW, et al. Functional recovery and neural differentiation after transplantation of allogenic adipose-derived stem cells in a canine model of acute spinal cord injury. *J Vet Sci.* (2009) 10:273–84. doi: 10.4142/jvs.2009.10.4.273
74. Hare JM, Fishman JE, Gerstenblith G, DiFede Velazquez DL, Zambrano JP, Suncion VY, et al. Comparison of allogeneic vs autologous bone marrow-derived mesenchymal stem cells delivered by transcatheter injection in patients with ischemic cardiomyopathy. *JAMA* (2012) 308:2369. doi: 10.1001/jama.2012.25321
75. Perin EC, Borow KM, Silva GV, DeMaria AN, Marroquin OC, Huang PP, et al. A Phase II dose-escalation study of allogeneic mesenchymal precursor cells in patients with ischemic or nonischemic heart failure. *Circ Res.* (2015) 117:576–84. doi: 10.1161/CIRCRESAHA.115.306332
76. Penn MS, Ellis S, Gandhi S, Greenbaum A, Hodes Z, Mendelsohn FO, et al. Adventitial delivery of an allogeneic bone marrow-derived adherent stem cell in acute myocardial infarction: phase I clinical study. *Circ Res.* (2012) 110:304–11. doi: 10.1161/CIRCRESAHA.111.253427
77. Vilahur G, Oñate B, Cubedo J, Béjar MT, Arderiu G, Peña E, et al. Allogenic adipose-derived stem cell therapy overcomes ischemia-induced microvessel rarefaction in the myocardium: systems biology study. *Stem Cell Res Ther.* (2017) 8:52. doi: 10.1186/s13287-017-0509-2
78. Huang XP, Sun Z, Miyagi Y, Kinkaid HM, Zhang L, Weisel RD, et al. Differentiation of allogeneic mesenchymal stem cells induces immunogenicity and limits their long-term benefits for myocardial repair. *Circulation* (2010) 122:2419–29. doi: 10.1161/CIRCULATIONAHA.110.955971
79. Lee YU, De Dios Ruiz-Rosado J, Mahler N, Best CA, Tara S, Yi T, et al. TGF- β receptor 1 inhibition prevents stenosis of tissue-engineered vascular grafts by reducing host mononuclear phagocyte activation. *FASEB J.* (2016) 30:2627–36. doi: 10.1096/fj.201500179R
80. Phinney DG, Pittenger MF. Concise review: MSC-derived exosomes for cell-free therapy. *Stem Cells* (2017) 35:851–8. doi: 10.1002/stem.2575
81. Caplan AI, Dennis JE. Mesenchymal stem cells as trophic mediators. *J Cell Biochem.* (2006) 98:1076–84. doi: 10.1002/jcb.20886
82. Gneccchi M, He H, Liang OD, Melo LG, Morello F, Mu H, et al. Paracrine action accounts for marked protection of ischemic heart by Akt-modified mesenchymal stem cells. *Nat Med.* (2005) 11:367–8. doi: 10.1038/nm0405-367
83. Timmers L, Lim SK, Arslan E, Armstrong JS, Hofer IE, Doevendans PA, et al. Reduction of myocardial infarct size by human mesenchymal stem cell conditioned medium. *Stem Cell Res.* (2008) 1:129–37. doi: 10.1016/j.scr.2008.02.002
84. Timmers L, Lim SK, Hofer IE, Arslan F, Lai RC, van Oorschot AAM, et al. Human mesenchymal stem cell-conditioned medium improves cardiac function following myocardial infarction. *Stem Cell Res.* (2011) 6:206–14. doi: 10.1016/j.scr.2011.01.001
85. Murphy KC, Whitehead J, Falahee PC, Zhou D, Simon SI, Leach JK. Multifactorial experimental design to optimize the anti-inflammatory and proangiogenic potential of mesenchymal stem cell spheroids. *Stem Cells* (2017) 35:1493–504. doi: 10.1002/stem.2606
86. Kinnaird T, Stabile E, Burnett MS, Lee CW, Barr S, Fuchs S, et al. Marrow-derived stromal cells express genes encoding a broad spectrum of arteriogenic cytokines and promote *in vitro* and *in vivo* arteriogenesis through paracrine mechanisms. *Circ Res.* (2004) 94:678–85. doi: 10.1161/01.RES.0000118601.37875.AC
87. Bartosh TJ, Ylöstalo JH, Mohammadipoor A, Bazhanov N, Coble K, Claypool K, et al. Aggregation of human mesenchymal stromal cells (MSCs) into 3D spheroids enhances their anti-inflammatory properties. *Proc Natl Acad Sci USA.* (2010) 107:13724–9. doi: 10.1073/pnas.1008117107
88. Ylöstalo JH, Bartosh TJ, Coble K, Prockop DJ. Human mesenchymal stem/stromal cells cultured as spheroids are self-activated to produce prostaglandin E2 that directs stimulated macrophages into an anti-inflammatory phenotype. *Stem Cells* (2012) 30:2283–96. doi: 10.1002/stem.1191
89. Murphy KC, Fang SY, Leach JK. Human mesenchymal stem cell spheroids in fibrin hydrogels exhibit improved cell survival and potential for bone healing. *Cell Tissue Res.* (2014) 357:91–9. doi: 10.1007/s00441-014-1830-z
90. Ho SS, Murphy KC, Binder BYK, Vissers CB, Leach JK. Increased survival and function of mesenchymal stem cell spheroids entrapped in instructive alginate hydrogels. *Stem Cells Trans Med.* (2016) 5:773–81. doi: 10.5966/sctm.2015-0211
91. Murphy KC, Whitehead J, Zhou D, Ho SS, Leach JK. Engineering fibrin hydrogels to promote the wound healing potential of mesenchymal stem cell spheroids. *Acta Biomater.* (2017) 64:176–186. doi: 10.1016/j.actbio.2017.10.007
92. Qazi TH, Mooney DJ, Duda GN, Geissler S. Biomaterials that promote cell-cell interactions enhance the paracrine function of MSCs. *Biomaterials* (2017) 140:103–14. doi: 10.1016/j.biomaterials.2017.06.019
93. Su N, Gao PL, Wang K, Wang JY, Zhong Y, Luo Y. Fibrous scaffolds potentiate the paracrine function of mesenchymal stem cells: a new dimension in cell-material interaction. *Biomaterials* (2017) 141:74–85. doi: 10.1016/j.biomaterials.2017.06.028
94. Mittelbrunn M, Gutiérrez-Vázquez C, Villarroya-Beltri C, González S, Sánchez-Cabo F, González MÁ, et al. Unidirectional transfer of microRNA-loaded exosomes from T cells to antigen-presenting cells. *Nat Commun.* (2011) 2:282. doi: 10.1038/ncomms1285
95. Kooijmans SAA, Vader P, van Dommelen SM, van Solinge WW, Schifferers RM. Exosome mimetics: a novel class of drug delivery systems. *Int J Nanomed.* (2012) 7:1525–41. doi: 10.2147/IJN.S296661
96. Théry C, Zitvogel L, Amigorena S. Exosomes: composition, biogenesis and function. *Nat Rev Immunol.* (2002) 2:569–79. doi: 10.1038/nri855
97. Valadi H, Ekström K, Bossios A, Sjöstrand M, Lee JJ, Lötvall JO. Exosome-mediated transfer of mRNAs and microRNAs is a novel mechanism of genetic exchange between cells. *Nat Cell Biol.* (2007) 9:654–9. doi: 10.1038/ncb1596
98. Biancone L, Bruno S, Deregibus MC, Tetta C, Camussi G. Therapeutic potential of mesenchymal stem cell-derived microvesicles. *Nephrol Dialysis Trans.* (2012) 27:3037–42. doi: 10.1093/ndt/gfs168
99. Clayton A, Harris CL, Court J, Mason MD, Morgan BP. Antigen-presenting cell exosomes are protected from complement-mediated lysis by expression of CD55 and CD59. *Eur J Immunol.* (2003) 33:522–31. doi: 10.1002/immu.200310028
100. Yeo RWY, Lai RC, Zhang B, Tan SS, Yin Y, Teh BJ, et al. Mesenchymal stem cell: An efficient mass producer of exosomes for drug delivery. *Adv Drug Deliv Rev.* (2013) 65:336–341. doi: 10.1016/j.addr.2012.07.001
101. Van Dommelen SM, Vader P, Lakhal S, Kooijmans SAA, Van Solinge WW, Wood MJA, et al. Microvesicles and exosomes: opportunities for cell-derived membrane vesicles in drug delivery. *J Control Release* (2012) 161:635–44. doi: 10.1016/j.jconrel.2011.11.021
102. Théry C, Ostrowski M, Segura E. Membrane vesicles as conveyors of immune responses. *Nat Reviews Immunol.* (2009) 9:581–93. doi: 10.1038/nri2567

103. El Andaloussi S, Mäger I, Breakefield XO, Wood MJA. Extracellular vesicles: biology and emerging therapeutic opportunities. *Nat Rev Drug Discov.* (2013) 12:347–57. doi: 10.1038/nrd3978
104. Mathivanan S, Ji H, Simpson RJ. Exosomes: extracellular organelles important in intercellular communication. *J Proteom.* (2010) 73:1907–20. doi: 10.1016/j.jprot.2010.06.006
105. Akers JC, Gonda D, Kim R, Carter BS, Chen CC. Biogenesis of extracellular vesicles (EV): exosomes, microvesicles, retrovirus-like vesicles, and apoptotic bodies. *J Neuro-oncol.* (2013) 113:1–11. doi: 10.1007/s11060-013-1084-8
106. Bruno S, Porta S, Bussolati B. Extracellular vesicles in renal tissue damage and regeneration. *Eur J Pharmacol.* (2016) 790:83–91. doi: 10.1016/j.ejphar.2016.06.058
107. Li P, Kaslan M, Lee SH, Yao J, Gao Z. Progress in exosome isolation techniques. *Theranostics* (2017) 7:789–804. doi: 10.7150/thno.18133
108. Lotvall J, Hill AE, Hochberg F, Buzas EI, Vizio D, Di G, Thery C, et al. Minimal experimental requirements for definition of extracellular vesicles and their functions: a position statement from the International Society for extracellular vesicles. *J Extracell Vesicles* (2014) 3:26913. doi: 10.3402/jev.v3.26913
109. Lai RC, Arslan F, Lee MM, Sze NSK, Choo A, Chen TS, et al. Exosome secreted by MSC reduces myocardial ischemia/reperfusion injury. *Stem Cell Res.* (2010) 4:214–22. doi: 10.1016/j.scr.2009.12.003
110. Wang K, Jiang Z, Webster K, Chen J, Hu H, Zhou Y, et al. Enhanced cardioprotection by human endometrium mesenchymal stem cells driven by exosomal MicroRNA-21. *Stem Cells Trans Med.* (2016) 6:209–22. doi: 10.5966/sctm.2015-0023
111. Puissant B, Barreau C, Bourin P, Clavel C, Corre J, Bousquet C, et al. Immunomodulatory effect of human adipose tissue-derived adult stem cells: comparison with bone marrow mesenchymal stem cells. *Br J Haematol.* (2005) 129:118–29. doi: 10.1111/j.1365-2141.2005.05409.x
112. Chen T, Arslan F, Yin Y, Tan S, Lai R, Choo A, et al. Enabling a robust scalable manufacturing process for therapeutic exosomes through oncogenic immortalization of human ESC-derived MSCs. *J Trans Med.* (2011) 9:47. doi: 10.1186/1479-5876-9-47
113. Xie H, Wang Z, Zhang L, Lei Q, Zhao A, Wang H, et al. Extracellular vesicle-functionalized decalcified bone matrix scaffolds with enhanced pro-angiogenic and pro-bone regeneration activities. *Sci Rep.* (2017) 7:1–13. doi: 10.1038/srep45622
114. Dai M, Yu M, Zhang Y, Tian W. Exosome-like vesicles derived from adipose tissue provide biochemical cues for adipose tissue regeneration. *Tissue Eng.* (2017) 23: 1221–30. doi: 10.1089/ten.tea.2017.0045
115. Hu L, Wang J, Zhou X, Xiong Z, Zhao J, Yu R, et al. Exosomes derived from human adipose mesenchymal stem cells accelerates cutaneous wound healing via optimizing the characteristics of fibroblasts. *Sci Rep.* (2016) 6:32993. doi: 10.1038/srep32993
116. Wang L, Hu L, Zhou X, Xiong Z, Zhang C, Shehada HMA, et al. Exosomes secreted by human adipose mesenchymal stem cells promote scarless cutaneous repair by regulating extracellular matrix remodelling. *Sci Rep.* (2017) 7:13321. doi: 10.1038/s41598-017-12919-x
117. De Jong OG, Van Balkom BWM, Schiffelers RM, Bouten CVC, Verhaar MC. Extracellular vesicles: potential roles in regenerative medicine. *Front Immunol.* (2014) 5:608. doi: 10.3389/fimmu.2014.00608
118. Liu R, Shen H, Ma J, Sun L, Wei M. Extracellular vesicles derived from adipose mesenchymal stem cells regulate the phenotype of smooth muscle cells to limit intimal hyperplasia. *Cardiovasc Drugs Ther.* (2016) 30:111–8. doi: 10.1007/s10557-015-6630-5
119. Sahoo S, Klychko E, Thorne T, Misener S, Schultz KM, Millay M, et al. Exosomes from human CD34+ stem cells mediate their proangiogenic paracrine activity. *Circ Res.* (2011) 109:724–28. doi: 10.1161/CIRCRESAHA.111.253286
120. Salomon C, Ryan J, Sobrevia L, Kobayashi M, Ashman K, Mitchell M, et al. Exosomal signaling during hypoxia mediates microvascular endothelial cell migration and vasculogenesis. *PLoS ONE* (2013) 8:e68451. doi: 10.1371/journal.pone.0068451
121. Zhang PE, Su HJ, Zhang M, Li JF, Liu CX, Ding SF, et al. Atherosclerotic plaque components characterization and macrophage infiltration identification by intravascular ultrasound elastography based on b-mode analysis: validation *in vivo*. *Int J Cardiovasc Imaging* (2011) 27:39–49. doi: 10.1007/s10554-010-9659-3
122. Xin H, Li Y, Cui Y, Yang JJ, Zhang ZG, Chopp M. Systemic administration of exosomes released from mesenchymal stromal cells promote functional recovery and neurovascular plasticity after stroke in rats. *J Cerebral Blood Flow Metab.* (2013) 33:1711–5. doi: 10.1038/jcbfm.2013.152
123. Doeppner TR, Herz J, Gorgens A, Schlechter J, Ludwig AK, Radtke S, et al. Extracellular vesicles improve post-stroke neuroregeneration and prevent postischemic immunosuppression. *Stem Cells Trans Med.* (2015) 4:1131–43. doi: 10.5966/sctm.2013-0118
124. Liang X, Zhang L, Wang S, Han Q, Zhao RC. Exosomes secreted by mesenchymal stem cells promote endothelial cell angiogenesis by transferring miR-125a. *J Cell Sci.* (2016) 129:2182–9. doi: 10.1242/jcs.170373
125. Khan M, Nickoloff E, Abramova T, Johnson J, Verma SK, Krishnamurthy P, et al. Embryonic stem cell-derived exosomes promote endogenous repair mechanisms and enhance cardiac function following myocardial infarction. *Circ Res.* (2015) 117:52–64. doi: 10.1161/CIRCRESAHA.117.305990
126. Arslan F, Lai RC, Smeets MB, Akeroyd L, Choo A, Aguior ENE, et al. Mesenchymal stem cell-derived exosomes increase ATP levels, decrease oxidative stress and activate PI3K/Akt pathway to enhance myocardial viability and prevent adverse remodeling after myocardial ischemia/reperfusion injury. *Stem Cell Res.* (2013) 10:301–12. doi: 10.1016/j.scr.2013.01.002
127. Bian S, Zhang L, Duan L, Wang X, Min Y, Yu H. Extracellular vesicles derived from human bone marrow mesenchymal stem cells promote angiogenesis in a rat myocardial infarction model. *J Mol Med.* (2014) 92:387–97. doi: 10.1007/s00109-013-1110-5
128. Feng Y, Huang W, Wani M, Yu X, Ashraf M. Ischemic preconditioning potentiates the protective effect of stem cells through secretion of exosomes by targeting Mecp2 via miR-22. *PLoS ONE* (2014) 9:e0088685. doi: 10.1371/journal.pone.0088685
129. Teng X, Chen L, Chen W, Yang J, Yang Z, Shen Z. Mesenchymal stem cell-derived exosomes improve the microenvironment of infarcted myocardium contributing to angiogenesis and anti-inflammation. *Cell Physiol Biochem.* (2015) 37:2415–24. doi: 10.1159/000438594
130. Yu B, Kim HW, Gong M, Wang J, Millard RW, Wang Y, et al. Exosomes secreted from GATA-4 overexpressing mesenchymal stem cells serve as a reservoir of anti-apoptotic microRNAs for cardioprotection. *Int J Cardiol.* (2015) 182:349–360. doi: 10.1016/j.ijcard.2014.12.043
131. Osteikoetxea X, Sódar B, Németh A, Szabó-Taylor K, Pálóczi K, Vukman KV, et al. Differential detergent sensitivity of extracellular vesicle subpopulations. *Org Biomol Chem R Soc Chem.* (2015) 13:9775–82. doi: 10.1039/C5OB01451D
132. Eirin A, Riestler SM, Zhu XY, Tang H, Evans JM, O'Brien D, et al. MicroRNA and mRNA cargo of extracellular vesicles from porcine adipose tissue-derived mesenchymal stem cells. *Gene* (2014) 551:55–64. doi: 10.1016/j.gene.2014.08.041
133. Eirin A, Zhu, XY, Puranik AS, Woollard JR, Tang H, Dasari S, et al. Comparative proteomic analysis of extracellular vesicles isolated from porcine adipose tissue-derived mesenchymal stem/stromal cells. *Sci Rep.* (2016) 6:36120. doi: 10.1038/srep36120
134. Eirin A, Zhu, XY, Puranik AS, Woollard JR, Tang H, Dasari S, et al. Integrated transcriptomic and proteomic analysis of the molecular cargo of extracellular vesicles derived from porcine adipose tissue-derived mesenchymal stem cells. *Plos ONE* (2017) 12:e0174303. doi: 10.1371/journal.pone.0174303
135. Kreke M, Smith R, Hanscome P, Peck K, Ibrahim A. (2016). *Processes for Producing Stable Exosome Formulations*. United States Patent application US 14/958,804.

Conflict of Interest Statement: The authors declare that the research was conducted in the absence of any commercial or financial relationships that could be construed as a potential conflict of interest.

Copyright © 2018 Cunnane, Weinbaum, O'Brien and Vorp. This is an open-access article distributed under the terms of the Creative Commons Attribution License (CC BY). The use, distribution or reproduction in other forums is permitted, provided the original author(s) and the copyright owner(s) are credited and that the original publication in this journal is cited, in accordance with accepted academic practice. No use, distribution or reproduction is permitted which does not comply with these terms.

Advantages of publishing in Frontiers



OPEN ACCESS

Articles are free to read for greatest visibility and readership



FAST PUBLICATION

Around 90 days from submission to decision



HIGH QUALITY PEER-REVIEW

Rigorous, collaborative, and constructive peer-review



TRANSPARENT PEER-REVIEW

Editors and reviewers acknowledged by name on published articles

Frontiers

Avenue du Tribunal-Fédéral 34
1005 Lausanne | Switzerland

Visit us: www.frontiersin.org

Contact us: info@frontiersin.org | +41 21 510 17 00



REPRODUCIBILITY OF RESEARCH

Support open data and methods to enhance research reproducibility



DIGITAL PUBLISHING

Articles designed for optimal readership across devices



FOLLOW US

[@frontiersin](https://twitter.com/frontiersin)



IMPACT METRICS

Advanced article metrics track visibility across digital media



EXTENSIVE PROMOTION

Marketing and promotion of impactful research



LOOP RESEARCH NETWORK

Our network increases your article's readership